Richard M. Steingart
Jennifer E. Liu
Editors

Atlas of Imaging in Cardio-Oncology

Case-Based Study Guide

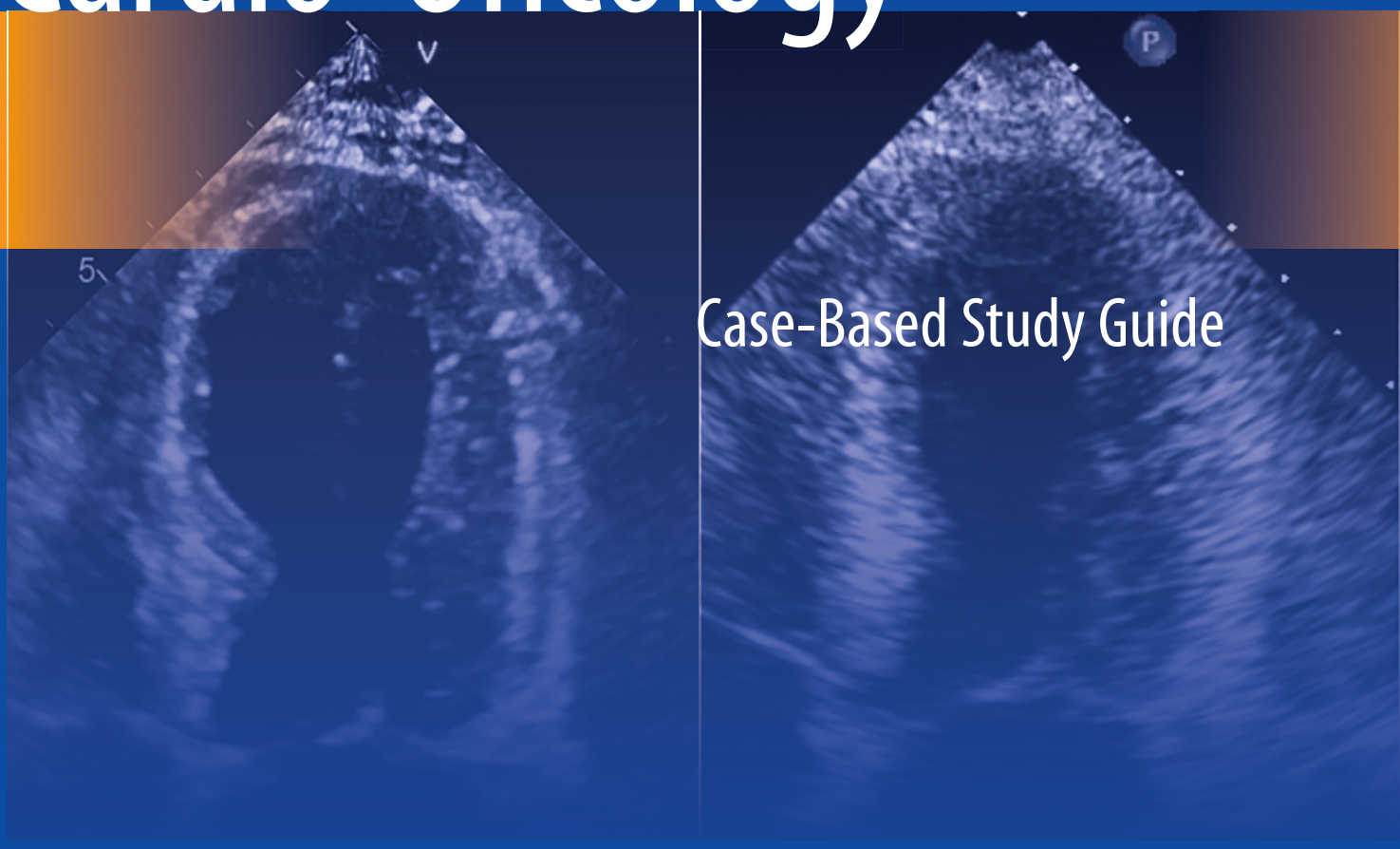

MOREMEDIA
Springer

Atlas of Imaging in Cardio-Oncology

Richard M. Steingart • Jennifer E. Liu
Editors

Atlas of Imaging in Cardio-Oncology

Case-Based Study Guide

Springer

Editors
Richard M. Steingart
Department of Medicine, Cardiology Service
Memorial Sloan Kettering Cancer Center
New York, NY, USA

Jennifer E. Liu
Memorial Sloan Kettering Cancer Center
New York, NY, USA

ISBN 978-3-030-70997-6 ISBN 978-3-030-70998-3 (eBook)
https://doi.org/10.1007/978-3-030-70998-3

This Springer imprint is published by the registered company Springer Nature Switzerland AG
The registered company address is: Gewerbestrasse 11, 6330 Cham, Switzerland

Preface

Advances in cancer treatment have resulted in significant improvements in cancer survival, curing or transforming once-fatal cancers into chronic diseases. However, cancer and its treatments are known for their propensity to cause both early and late cardiac complications. The mechanisms behind those complications have become increasingly more complex with the introduction of novel treatments such as immunotherapy and signaling inhibitors. In addition to the on-treatment toxicities of these therapies, with the increase in cancer survival, patients now live long enough to experience late-onset treatment-related adverse cardiovascular effects and become even more vulnerable to the cardiovascular insults associated with aging and traditional cardiovascular risk factors. Consequently, cardiovascular diseases have emerged as major contributors to the cancer patient's morbidity and mortality, threatening to limit the tremendous gains achieved in cancer survival. Thus, the burgeoning field of cardio-oncology, a joint discipline between oncology and cardiology aimed at optimizing cardiovascular health in cancer patients during and after cancer therapy. Cardiovascular imaging plays a central role in the practice of cardio-oncology. Various imaging modalities and emerging techniques are utilized for the early detection of cardiac injury and to guide treatment strategies.

The goal of this *Atlas of Imaging in Cardio-Oncology* is to use a case-based approach to illustrate the effective application of imaging techniques during and after cancer treatment in the management of patients with cancer. The authors of these chapters are a carefully curated selection of the world's preeminent cardio-oncology clinicians and academicians. They present their experiences with a truly broad range of clinical challenges in cardio-oncology, beautifully illustrated with key diagnostic imaging. A careful reading of this Atlas will take the reader through the equivalent of years of hands-on experience in a busy and diverse cardio-oncology practice. The authors and editors of each chapter have chosen actual cases that were seen in their practice, ranging from community-based settings to large tertiary cancer centers in the US and around the world. We found it inspiring that authors were able to convey their emotional investment in the management of these patients as they recount the clinical course. This was not surprising to us as we know the authors well, having visited with one another in the outpatient clinics and on the wards of our respective institutions, participated jointly in cardio-oncology lectures and symposia, and collaborated on clinical research and other academic projects. We never hesitate to pick up the phone to tap into their particular expertise and to gather their opinions. We hope that reading the work in this Atlas will inspire you to do so as well. The chapters include a discussion on the imaging strategies to address specific clinical problems encountered in clinical practice along with abundant figures and video illustrations incorporated into each case to convey knowledge and enhance the readers' clinical decision making. The Atlas provides a link to the web to see the text, pictures, and videos. A list of key points is provided for each case with emphasis on interpretation of the imaging findings and their impact on clinical management.

We extend our deepest gratitude to our contributors and to our editors. Our thanks go out to the courageously strong patients described in these pages during their battle with cancer and heart disease. They have left us with an indelible impression. We hope that they engage you as

you explore this Atlas of the practice of cardio-oncology. Please do contact the corresponding authors of the individual chapters, or Jennifer E. Liu and Richard M. Steingart, the Atlas' editors, for suggestions, comments, and questions.

New York, USA

Richard M. Steingart
Jennifer E. Liu

Contents

Contributors

Albert A. Akhobekov Clinical Hospital Lapino, Moscow Region, Russia

Jose Alvarez-Cardona Cardio-Oncology Center of Excellence, Washington University in St Louis, St. Louis, MO, USA

Lauren Balkan Department of Internal Medicine, New York Presbyterian Hospital, Weill Cornell Medical Center, New York, NY, USA

Lance Berger Monmouth Cardiology Associates, Eatontown, NJ, USA

Lior Z. Braunstein Department of Radiation Oncology, Memorial Sloan Kettering Cancer Center, New York, NY, USA

Oren Cahlon Department of Radiation Oncology, Memorial Sloan Kettering Cancer Center, New York, NY, USA

Massimiliano Camilli Department of Cardiovascular and Pulmonary Sciences, Catholic University of the Sacred Heart, Rome, Italy

Montserrat Carrillo-Estrada Division of Cardiology, Peter Munk Cardiac Centre, Ted Rogers Program in Cardiotoxicity Prevention, University Health Network, University of Toronto, Toronto, ON, Canada

Angel T. Chan Department of Medicine, Memorial Sloan Kettering Cancer Center, New York, NY, USA

Carol L. Chen Department of Medicine, Memorial Sloan Kettering Cancer Center, New York, NY, USA

Heidi M. Connolly Department of Cardiovascular Medicine, Mayo Clinic, Rochester, Minnesota, United States

Robert S. Copeland-Halperin Department of Cardiology, Northwell Health (Zucker School of Medicine at Hofstra /Northwell), New Hyde Park, NY, USA

Olga A. Drobiazko Department of Radiology, Federal Scientific and Research Center, FMBA Russia, Moscow, Russia

David P. Dundua Cardiology Center, Federal Scientific and Research Center, FMBA Russia, Moscow, Russia

Stephanie Feldman Department of Medicine, Memorial Sloan Kettering Cancer Center, New York, NY, USA

Josef J. Fox Radiology Department, Memorial Sloan Kettering Cancer Center, New York, NY, USA

Luis Hernandez Robert and Suzanne Tomsich Department of Cardiovascular Medicine, Heart and Vascular Institute, Cleveland Clinic Florida, Weston, FL, USA

Joerg Herrmann Department of Cardiovascular Diseases, Mayo Clinic, Rochester, MN, USA

Zaza Iakobishvili Department of Community Cardiology, Tel Aviv Jaffa District, Clalit Health Services, Holon, Israel

Osnat Itzhaki Ben Zadok Cardiology Department, Rabin Medical Center, Petah Tikva, Israel

Mark Iwanochko Division of Cardiology Peter Munk Cardiac Centre, Toronto General Hospital, University Health Network, University of Toronto, Toronto, ON, Canada

Kristine Jang Department of Medicine, Memorial Sloan Kettering Cancer Center, New York, NY, USA

Michelle N. Johnson Department of Medicine, Memorial Sloan Kettering Cancer Center, New York, NY, USA

Yu Kang Hospital of the University of Pennsylvania, Philadelphia, PA, USA

Mahim Kapoor Monmouth Cardiology Associates, Eatontown, NJ, USA

Ana G. Kedrova Department of Oncology, Federal Scientific and Research Center, FMBA Russia, Moscow, Russia

Jacobo Kirsch Robert and Suzanne Tomsich Department of Cardiovascular Medicine, Heart and Vascular Institute, Cleveland Clinic Florida, Weston, FL, USA

Elena V. Kononova P. Hertsen Moscow Oncology Research Institute - branch of the National Medical Research Radiological Centre of the Ministry of Health of Russian Federation, Moscow, Russia

Valeriy V. Kucherov A. Tsyb Medical Radiological Research Centre - branch of the National Medical Research Radiological Centre of the Ministry of Health of Russian Federation, Obninsk, Russia

Katherine Lee Chuy Cook County Health, John H. Stroger Jr. Hospital of Cook County, Chicago, IL, USA

Bénédicte Lefebvre Hospital of the University of Pennsylvania, Philadelphia, PA, USA

Daniel J. Lenihan Cardio-Oncology Center of Excellence, Washington University in St Louis, St. Louis, MO, USA

Kevin Leung Robert and Suzanne Tomsich Department of Cardiovascular Medicine, Heart and Vascular Institute, Cleveland Clinic Florida, Weston, FL, USA

Jennifer E. Liu Department of Medicine, Memorial Sloan Kettering Cancer Center, New York, NY, USA

Shiying Liu Division of Cardiology, Peter Munk Cardiac Centre, Ted Rogers Program in Cardiotoxicity Prevention, University Health Network, University of Toronto, Toronto, ON, Canada

Sushil Allen Luis Department of Cardiovascular Medicine, Mayo Clinic, Rochester, Minnesota, United States

Syed S. Mahmood Cardiology Division, New York Presbyterian Hospital, Weill Cornell Medical Center, New York, NY, USA

Saurabh Malhotra Cook County Health, John H. Stroger Jr. Hospital of Cook County, Chicago, IL, USA

Giorgio Minotti Department of Medicine and Unit of Drug Sciences, Campus Bio-Medico University, Rome, Italy

Dmitriy O. Nadinskiy A. Tsyb Medical Radiological Research Centre - branch of the National Medical Research Radiological Centre of the Ministry of Health of Russian Federation, Obninsk, Russia

Kazuaki Negishi Faculty of Medicine and Health Department of Cardiology, Sydney Medical School Nepean, Charles Perkins Centre Nepean, The University of Sydney, Kingswood, NSW, Australia

Tomas G. Neilan Cardio-Oncology Program, Division of Cardiology, Department of Medicine, Massachusetts General Hospital, Boston, MA, USA

Felix Nguyen Cardio-Oncology Center of Excellence, Washington University in St Louis, St. Louis, MO, USA

Nicolas L. Palaskas Department of Cardiology, Division of Internal Medicine, University of Texas MD Anderson Cancer Center, Houston, TX, USA

Faraz Pathan Faculty of Medicine and Health Department of Cardiology, Sydney Medical School Nepean, Charles Perkins Centre Nepean, The University of Sydney, Kingswood, NSW, Australia

Anna Plitt Department of Medicine, Memorial Sloan Kettering Cancer Center, New York, NY, USA

Ekaterina V. Plokhova Cardiology Center, Federal Scientific and Research Center, FMBA Russia, Moscow, Russia

Maria Poltavskaya Department of Cardiology, Functional and Ultrasound Diagnostics, I.M. Sechenov First Moscow State Medical University (Sechenov University), Moscow, Russia

Olga E. Popovkina A. Tsyb Medical Radiological Research Centre - branch of the National Medical Research Radiological Centre of the Ministry of Health of Russian Federation, Obninsk, Russia

Alexandra V. Potekhina National Medical Research Center of Cardiology, Russian Ministry of Health, Moscow, Russia

Vera I. Potievskaya P. Hertsen Moscow Oncology Research Institute - branch of the National Medical Research Radiological Centre of the Ministry of Health of Russian Federation, Moscow, Russia

Diego Sadler Robert and Suzanne Tomsich Department of Cardiovascular Medicine, Heart and Vascular Institute, Cleveland Clinic Florida, Weston, FL, USA

Wendy Schaffer Department of Medicine, Memorial Sloan Kettering Cancer Center, New York, NY, USA

Marielle Scherrer-Crosbie Director of the Echocardiography Laboratory, Hospital of the University of Pennsylvania, Philadelphia, PA, USA

Dylana Smith Department of Medicine, Memorial Sloan Kettering Cancer Center, New York, NY, USA

Richard M. Steingart Department of Medicine, Memorial Sloan Kettering Cancer Center, New York, NY, USA

Olga V. Stukalova National Medical Research Center of Cardiology, Russian Ministry of Health, Moscow, Russia

Paaladinesh Thavendiranathan Division of Cardiology Peter Munk Cardiac Centre, Toronto General Hospital, University Health Network, University of Toronto, Toronto, ON, Canada

Marina V. Vitsenya National Medical Research Center of Cardiology, Russian Ministry of Health, Moscow, Russia

Jonathan W. Weinsaft Department of Medicine, Weill Cornell Medicine, New York, NY, USA

Howard Weinstein Department of Medicine, Memorial Sloan Kettering Cancer Center, New York, NY, USA

Eric H. Yang Division of Cardiology, Department of Medicine, UCLA Cardio-Oncology Program, University of California at Los Angeles, Los Angeles, CA, USA

Darwin F. Yeung Department of Medicine, Division of Cardiology, University of British Columbia, Vancouver, British Columbia, Canada

Anthony F. Yu Department of Medicine, Memorial Sloan Kettering Cancer Center, New York, NY, USA

Christopher Yu Faculty of Medicine and Health Department of Cardiology, Sydney Medical School Nepean, Charles Perkins Centre Nepean, The University of Sydney, Kingswood, NSW, Australia

Osnat Itzhaki Ben Zadok Cardiology Department, Rabin Medical Center, Petah Tikva, Israel

Lili Zhang Cardio-Oncology Program, Division of Cardiology, Department of Medicine, Montefiore Medical Center, Albert Einstein College of Medicine, Bronx, NY, USA

L. Steven Zukerman Monmouth Cardiology Associates, Eatontown, NJ, USA

Elena A. Zvezdkina Department of Radiology, Federal Scientific and Research Center, FMBA Russia, Moscow, Russia

Multimodality Imaging in Cardio-Oncology

1

Shiying Liu, Montserrat Carrillo-Estrada, Mark Iwanochko, and Paaladinesh Thavendiranathan

Key Points

- Cardiovascular imaging plays a crucial role in the practice of cardio-oncology.
- Echocardiography is the imaging modality of choice for monitoring cardiac function before, during, and after cancer treatment.
- A unique role of cardiac magnetic resonance is to provide tissue characterization, allowing the identification of early myocardial injury and differentiation of cardiac tumors from thrombus.
- Other imaging techniques such as cardiac computed tomography and positron emission tomography provide incremental diagnostic value and serve as useful tools for the evaluation of patients in cardio-oncology.
- Cardiovascular imaging of patients with cancer requires high-quality imaging as the results have a major impact on cancer treatment decisions and long-term cardiovascular follow-up of patients.

Electronic supplementary material
The online version of this chapter (https://doi.org/10.1007/978-3-030-70998-3_1) contains supplementary material, which is available to authorized users.

S. Liu · M. Carrillo-Estrada
Division of Cardiology, Peter Munk Cardiac Centre, Ted Rogers Program in Cardiotoxicity Prevention, University Health Network, University of Toronto, Toronto, ON, Canada
e-mail: shiying.liu@uhn.ca

M. Carrillo-Estrada
e-mail: Montserrat.carrillo-estrada@uhn.ca

M. Iwanochko · P. Thavendiranathan (✉)
Division of Cardiology Peter Munk Cardiac Centre, Toronto General Hospital, University Health Network, University of Toronto, Toronto, ON, Canada
e-mail: Dinesh.Thavendiranathan@uhn.ca

M. Iwanochko
e-mail: Robertmark.iwanochko@uhn.ca

R. M. Steingart et al. (eds.), *Atlas of Imaging in Cardio-Oncology*, https://doi.org/10.1007/978-3-030-70998-3_1

1.1 Introduction

Cardiovascular multimodality imaging plays a crucial role in the identification of cardiovascular disease in patients with cancer [1, 2]. The ultimate goal is to use the imaging data to guide the prevention of cardiovascular-disease-related morbidity and mortality while enabling optimal cancer therapy. Traditional and novel cancer therapies can have various adverse cardiovascular effects that can be identified by cardiovascular imaging [3]. This chapter focuses on the most commonly recognized toxicity, heart failure, the spectrum of toxicities includes myocarditis, arrhythmias, coronary artery disease (CAD), autonomic dysfunction, valvular disease, pericardial disease, and vascular disease [4].

The primary imaging modality that is used should be driven by the clinical question, the availability of imaging techniques, and the expertise at each center [2]. Echocardiography is the imaging modality of choice for monitoring cardiac function before, during, and after cancer treatment [5, 6]. Echocardiography based 3D left ventricular ejection fraction (LVEF) and 2D global longitudinal strain (GLS) offer a reproducible assessment of cardiac function and the possibility for early detection of myocardial dysfunction, respectively [7, 8]. Cardiac magnetic resonance (CMR) is the method of choice to identify subtle myocardial structural and functional changes related to cancer therapy. A unique role of CMR is to identify early myocardial injury (e.g., inflammation, edema, or fibrosis) or to differentiate cardiac tumors from thrombus using tissue characterization techniques. CMR is also a robust modality to investigate myocardial ischemia or pericardial disease. Cardiac computed tomography (CT) plays a complementary role in cardio-oncology aiding with the assessment of CAD, pericardial disease, and cardiac masses [9].

Multigated acquisition (MUGA) scans continue to be used for serial monitoring of LVEF during chemotherapy when echocardiography is unavailable [5]. Another unique role of nuclear imaging in cardio-oncology is the use of bone avid radiotracers (Tc-99 m-PYP/DPD/HMDP) for the noninvasive

Table 1.1 Strengths and limitations of cardiac imaging modalities and clinical application according to cardiac toxicity

Imaging modality	Strengths	Limitations	Clinical application
Echocardiography	- Availability - Low cost - No radiation exposure - Anatomical and hemodynamic assessment - 3D LVEF higher accuracy and reproducibility - Strain allows detection of subclinical cardiac dysfunction - Stress echo allows for functional assessment of CAD	- Inter-, intra-observer and test–re-test variability - Image quality may be influenced by body habitus, surgical interventions, localized pain, and breast expanders - 3DE—lower spatial and temporal resolution - Strain—influenced by preload, afterload, and heart rate	- CTRCD - Pulmonary hypertension - Pericardial disease - Valvular heart disease - Cardiac amyloidosis, assessment of ischemia
Magnetic Resonance Imaging	- No radiation exposure - Identifies small changes in volumes - Accurate LVEF assessment - Tissue characterization - Assessment of myocardial ischemia	- Higher cost - Lack of widespread availability - Risk of nephrogenic systemic fibrosis in patients with renal impairment - Use of GBCA	- CTRCD - ICI-related myocarditis - Cardiac masses - Valvular heart disease - Pericardial disease - Cardiac amyloidosis, assessment of ischemia
Computed Tomography	- Non-invasive method for assessment of CAD - High sensitivity and NPV for CAD - Identification of pericardial, valvular, and anular calcification	- Higher cost - Radiation exposure - Use of IV contrast	- CAD - Pericardial disease - Valvular heart disease
Nuclear imaging Multigated angiocardiography	- Availability - High sensitivity and specificity for LVEF - Measurement reproducibility	- Radiation exposure - Accuracy affected by gating and count quality	- CTRCD
Positron Emission Tomography	- Assessment of myocardial metabolism, ischemia, viability	- Lack of widespread availability - Higher cost - Radiation exposure	- Evaluation of microvascular dysfunction, ischemia, myocardial viability - Cardiac masses, differentiation of benign versus malignant tumors

CAD: Coronary artery disease. CTRCD: Cancer therapeutics-related cardiac dysfunction. GBCA: Gadolinium-based contrast agents. ICI: Immune Checkpoint Inhibitors. LVEF: Left ventricular ejection fraction. NPV: Negative predictive value

diagnosis of transthyretin (ATTR) cardiac amyloidosis [10]. Finally, Positron Emission Tomography (PET) imaging is a noninvasive method for the assessment of myocardial metabolism and has a potential role in the identification of patients with early myocardial injury or vascular inflammation [11]. Table 1.1 provides a summary of the strengths and limitations of the different cardiac imaging modalities that are commonly used in cardio-oncology. This chapter will provide readers the guidance as to the selection of appropriate imaging tests and what local cardiac imaging laboratories may consider to ensure high-quality cardio-oncology imaging services.

1.2 Considerations in the Echocardiography Laboratory

Due to its wide availability and relatively low costs, transthoracic echocardiography (TTE) is the most commonly used noninvasive cardiac imaging modality in cardio-oncology. However, standardization of imaging is crucial to provide high-quality data for the cardio-oncology population where cancer treatment decisions often hinge on imaging data.

1.3 2D Echocardiography

Laboratories continuing to use 2D-LVEF should ensure the acquisition of dedicated apical 4- and 2-chamber views specifically for the purpose of measurement of LVEF with careful attention to apical foreshortening and endocardial drop-out. The biplane disk summation technique (modified Simpson's rule) is the method of choice to measure LVEF and volumes [12]. This method relies on geometrical assumptions of the LV shape, and is sensitive to apical foreshortening and endocardial dropout, resulting in increased inter- and intra-observer and test–re-test variability [7, 12]. The temporal variability of LVEF by 2D biplane Simpson's method is up to 10% [7], which is analogous to the threshold used to define cancer-therapy-related cardiac dysfunction [6], thus making this an imprecise method for serial follow-up of LV systolic function. To reduce test–re-test variability it is critical for sonographers/physicians to review images from prior visits side by side to ensure that views obtained and endocardial contouring (at compacted myocardium) are similar (Figs. 1.1 and 1.2). This comparison can also be used to ensure that any changes in ventricular function are also visually confirmed. Besides LVEF, diastolic function and its change during treatment should also be assessed and reported.

1.4 3D Echocardiography

Laboratories with experience in using 3DE should use this as the preferred method for measurement of LVEF in patients with good image quality. Optimization of 3D image acquisition should follow the American Society of Echocardiography (ASE) guidelines [13]. The ECG-gated multi-beat acquisition of a full-volume dataset is recommended for analysis of LV volumes, LVEF, and regional wall motion as it provides better temporal resolution compared to single-beat acquisition, while maintaining high spatial resolution. Acquisition of 3D full volume dataset should be guided by the simultaneous display of multiple tomographic short-axis views of the LV from apex to base or multiple long-axis views [13]. We recommend this approach to ensure all ventricular segments are included in the volume, there is good endocardial visualization of all segments, and to assess for stitch artifacts (Videos 1.1 and 1.2). Multiple 3D volumes should be obtained to ensure choice in post-processing. During post-processing, care should be taken to ensure LV trabeculae and papillary muscles are included in the ventricular volume (i.e., contours at the compacted myocardium) and that endocardial border tracking is accurate and consistent for all segments in diastole and systole (Video 1.3).

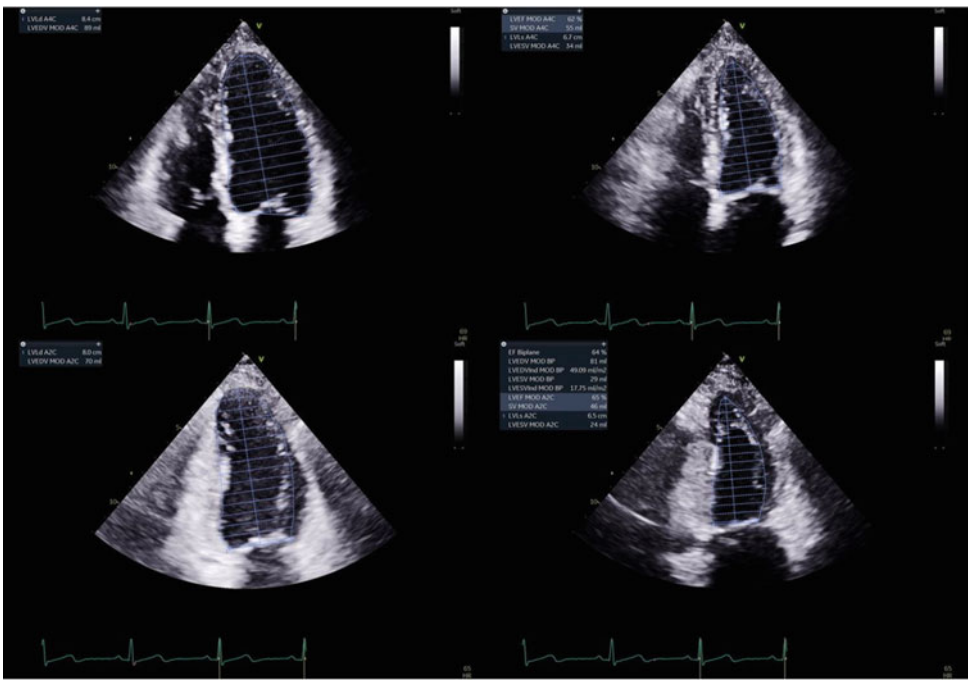

Fig. 1.1 Two-dimensional left ventricular volumes and ejection fraction measurement by biplane disk summation technique (modified Simpson's rule). Endocardial contours should be drawn at the compacted myocardium as demonstrated

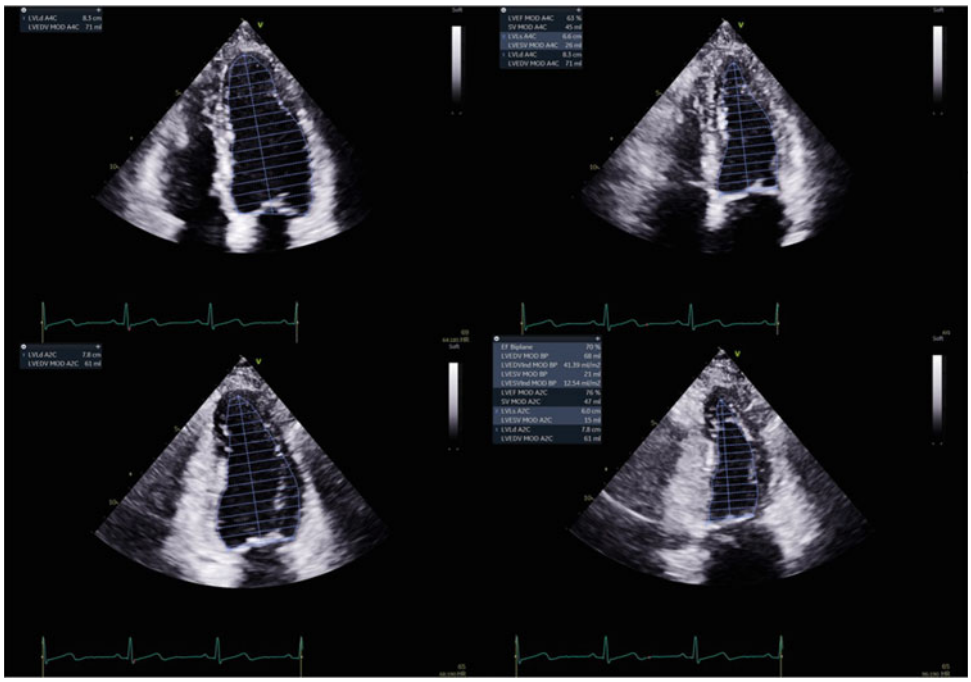

Fig. 1.2 Left ventricular volumes and ejection fraction for the same patient in Fig. 1.1. Contours are drawn incorrectly at the blood pool trabecular border at many locations instead of the compacted myocardial layer. This results in different volumes and LVEF values as compared with Fig. 1.1

Current limitations of 3DE include lower spatial and temporal resolution than 2DE, larger transducer footprint, and the time required for post-processing [13]. Wider experience with 3DE, incorporation of 3DE in sonography schools and fellowship training, and future enhancement of fully automated left heart chamber quantification will allow for broader implementation of this technique within the cardio-oncology population.

1.5 Use of Ultrasound Enhancing Agents

The use of ultrasound enhancing agents (UEAs) for LV opacification is recommended to improve endocardial border delineation when two or more contiguous segments are poorly visualized [12]. Compared to unenhanced 2DE, UEA-enhanced images provide a more accurate and reproducible analysis of LV volume, EF, and regional wall motion [12]. UEA-enhanced images of the LV produce larger volumes than non-UEA enhanced images, irrespective of the 2D or 3D echo techniques used, and have better agreement with the values obtained by CMR [14, 15]. It is estimated that UEA use can convert approximately 75–90% of suboptimal echocardiograms to diagnostic quality [16]. If UEA is used in cardio-oncology studies, it should be used in all subsequent follow-ups to enable comparison of changes. It is important to note that pulmonary hypertension or known/suspected right-to-left cardiac shunts are no longer contraindications to UEA use based on the recent ASE guidelines [14]. Optimization of UEA images is an important skill for all sonographers to acquire and has been outlined in the ASE guidelines [14, 17]. We recommend training of dedicated personnel for UEA administration. Sonographers should also have the opportunity to be trained in intravenous insertion to facilitate the workflow. All echo lab personnel should be trained in the early recognition of UEA-related side effects and effective management strategies [17]. UEAs can interfere with strain imaging, and therefore dedicated images should be acquired and strain analysis performed prior to contrast administration.

1.6 Myocardial Strain Imaging

Myocardial strain measured with speckle tracking echocardiography (STE) is an important clinical tool in the early detection of subclinical LV systolic dysfunction. GLS is the most robust and reproducible strain parameter, with diagnostic and prognostic value [18, 19]. Measurement of GLS is recommended as part of the comprehensive cardio-oncology echocardiogram protocol [6]. Although GLS can be measured using 2D and 3D acquisitions, current clinical applications are limited to 2DE.

Image acquisition: For measurement of GLS, standard LV apical 3-, 4-, and 2-chamber views should be acquired with careful attention to optimizing both temporal and spatial resolution. The ASE recommends a frame rate of 40–90 Hz for strain analysis involving normal heart rates [6]. Higher frame rates are advisable to avoid under-sampling in

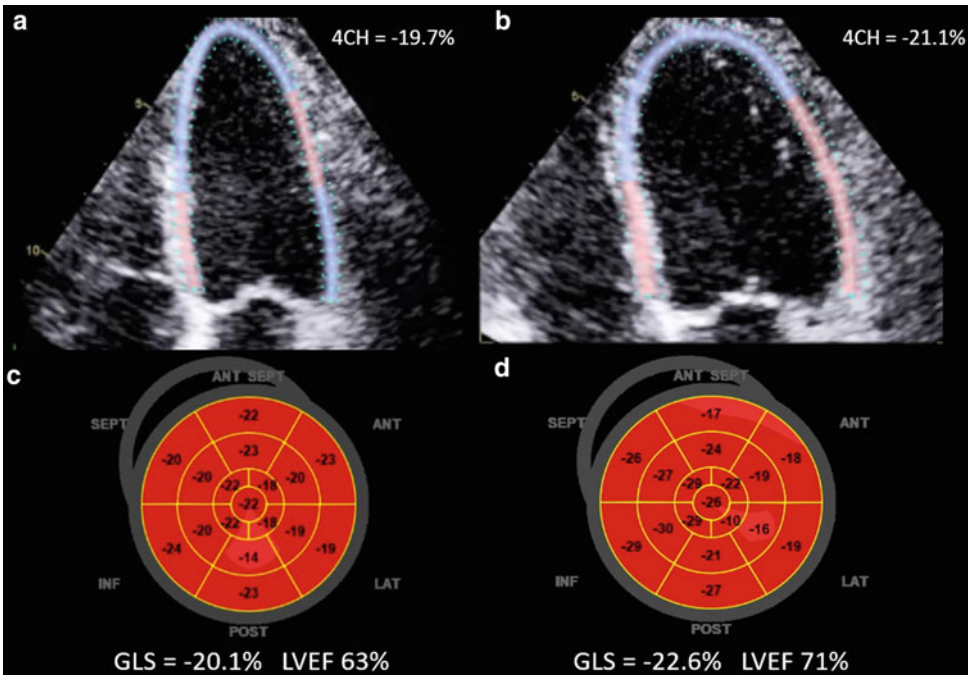

Fig. 1.3 Impact of apical foreshortening on LVEF and GLS values. Panel A and C illustrate the standard 2D apical 4-chamber view and the corresponding longitudinal strain bull's eye plot. Panel B and D illustrate the foreshortened apical 4-chamber view and the bull's eye plot in the same patient. Notice the increase in GLS and LVEF values in the foreshortened views

tachycardia which can be common during cancer therapy [20]. However, a frame rate that is too high is often achieved at the expense of spatial resolution. Good image quality with clear visualization of the endocardial border and myocardium for the entire cardiac cycle is essential. Imaging artifacts such as acoustic shadowing, reverberations and echo drop-outs, and foreshortening of the apex (Fig. 1.3, Videos 1.4 and 1.5) can result in inaccurate strain measurements [20]. During image acquisition, the patient should be instructed to suspend breathing for several heartbeats and the ECG signal should be adequate to ensure appropriate timing. The apical 3 chamber view should clearly demonstrate the LVOT and aortic valve in order to help determine aortic valve closure time (Fig. 1.4). We suggest the heart rate difference between the three apical views used for GLS calculation to be less than 5 bpm. To achieve this, it is best to obtain all 3 apical views together toward the end of the study as dedicated images for strain analysis. Furthermore, it is advisable to obtain 3–5 cardiac cycles and/or 2–3 different acquisitions to ensure that the most optimal images are available for analysis.

Strain post-processing: The best images or cardiac cycle should be chosen for analysis. The definitions of end-diastole (ED) and end-systole (ES) directly influence strain quantification. ED is marked by mitral valve closure (MVC), and is the time point where the strain curve is zeroed [20]. ES is marked by aortic valve closure (AVC), and the time point from ED to ES defines the systolic phase of the strain curve [20]. Laboratories should define consistent ways to define ED/ES and this may be vendor-specific. Systolic strain can refer to either the peak systolic or end-systolic strain. The peak systolic strain is the peak value during systole, while the end-systolic strain is the value that that

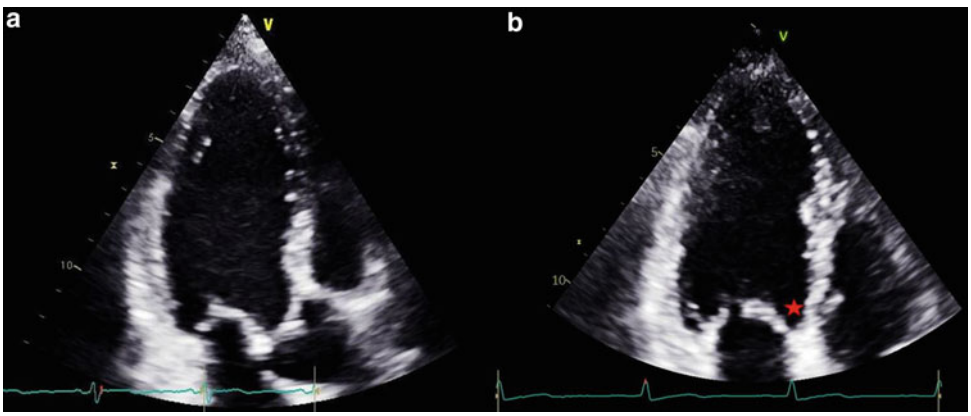

Fig. 1.4 Panel A shows the standard apical 3-chamber view with clear visualization of the LVOT and aortic valve. Panel B shows a suboptimal apical 3-chamber view without visualization of the aortic valve

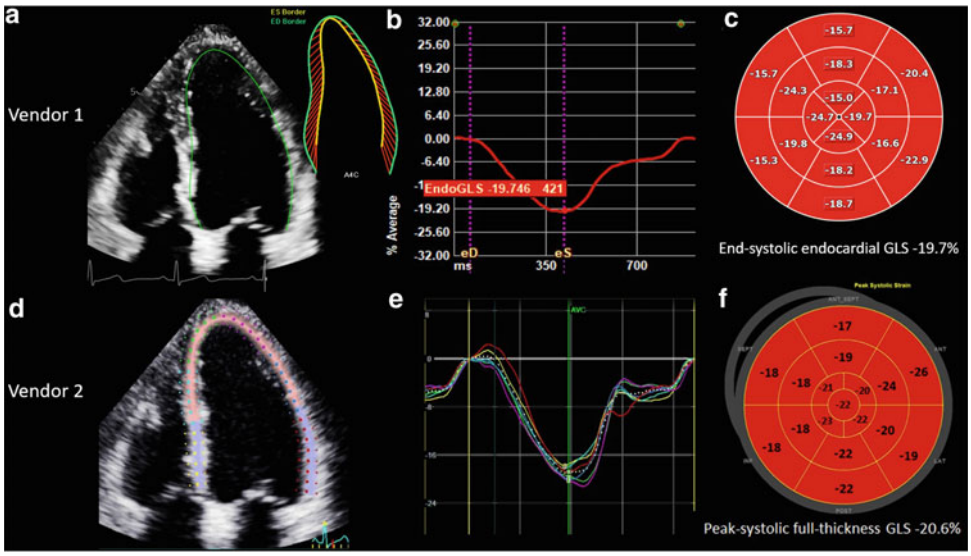

Fig. 1.5 The differences in default settings, with respect to the strain layer, measurement timing, and segmentation model, between two strain vendors are highlighted using the same apical images. With Vendor 1 the endocardial longitudinal strain was measured at end-systole using the entire end-diastolic and end-systolic border length (A–C). With Vendor 1 there is an option of reporting end-systolic or peak systolic strain. In contrast, vendor 2 measures the full-thickness strain, which encompasses the entire thickness of the myocardium (D–F). Vendor 1 uses a 16-segment model (C), while vendor 2 uses a 17-segment model of the left ventricle that includes the apical cap (F). AVC: aortic valve closure; ED: end-diastole; ES: end-systole; GLS: global longitudinal strain

coincides with ES or AVC [21]. The European Association of Cardiovascular Imaging/American Society of Echocardiography (EACVI/ASE) and Industry Task Force recommends the report of end-systolic GLS by default [21]. Selection of region of interest (ROI) for GLS may include endocardial, midwall, epicardial, or full myocardial thickness strain. Some strain software provide the ability to measure layer-specific strain. Each echocardiography laboratory should become familiar with the default settings of their strain package with respect to the automatic ED and ES timing selection, definition of systolic strain, and the default strain layer being measured (Fig. 1.5).

Accurate contouring of the subendocardial and the subepicardial border determines the tracking quality and has repercussions on the strain results. Currently available strain packages rely on a semiautomatic method. Fully automated strain analysis has also become a clinical reality and provides a rapid and reproducible assessment of GLS [22]. However, the operator should still visually inspect all tracking markers to ensure they closely follow the underlying tissue motion. Papillary muscles and trabeculations should be excluded from the endocardial contour as this affects GLS values [23] (Video 1.6). Basal contours should extend down to the mitral annulus but not beyond it (Videos 1.7 and 1.8). Similarly, the contour should not extend into the aortic root [23] (Video 1.9). There is a gradient in the myocardial deformation amplitude, such that strain value is highest in the endocardium and progressively decreases toward the epicardium [24]. The ROI should appropriately cover the myocardium (Video 1.10). If the width of the ROI is too thin (Video 1.11) and does not include the whole myocardium or too thick (Video 1.12) and includes the pericardium then the strain values can be altered with vendors who provide whole myocardial thickness based strain [23]. Once segmental strain curves are generated, they should be carefully examined to ensure good regional tracking and the absence of significant outliers. It is crucial to use the same imaging equipment and software during serial follow-ups of cancer patients to facilitate interpretation and comparison of results.

Strain measurements, similar to that of LVEF, are sensitive to preload, afterload, and heart rate [25] and cancer patients are especially vulnerable to hemodynamic fluctuations [6]. Laboratories should ensure that patients' vitals are documented in each study so that sequential changes in strain can be related back to changes in hemodynamics. The sources of variation in strain measurements are summarized in Table 1.2.

1.7 Workflow Considerations in the Echocardiography Laboratory

A comprehensive cardio-oncology echocardiogram protocol is outlined in Table 1.3 and could be modified as necessary depending on the clinical question. The growing need for high-quality cardio-oncology echocardiograms combined with the need for dedicated technology and personnel can affect the normal workflow of an echocardiography

Table 1.2 Sources of variation in echocardiographic strain assessment

Clinical • Loading conditions, e.g., blood pressure, heart rate, volume status
Operator • Image quality, frame rate, clip selection • Selection of end-diastole and end-systole • Contouring of subendocardium and subepicardium
Vendor • Proprietary tracking algorithms, e.g., spatial and temporal smoothing • Strain computation and default settings: - Calculation of global strain by a mathematical average of segmental strain values or by using the entire myocardial line length - Endocardial vs full-thickness strain - End-systolic vs peak systolic strain - Use of 16, 17, or 18-segmentation model

Table 1.3 Comprehensive **cardio-oncology echocardiography** protocol

Prior to starting the echocardiogram • Review any prior echocardiograms to appreciate the image quality, particularly the apical views, and check if contrast was used previously • Document the patient's blood pressure, heart rate, and the timing of echocardiography with respect to IV cancer therapy infusion (e.g., number of days before or after)
Standard transthoracic echocardiogram (as per ASE/EAE guidelines with highlights below) [6] • Obtain the best apical 2- and 4-chamber views for LV volumes and LVEF assessment by 2D biplane disk summation method • Comprehensive assessment of diastolic function • Assess RV systolic function using TAPSE, S', and FAC
2D strain imaging *Acquisition* • Obtain dedicated apical 3-, 4-, and 2- chamber views of the LV sequentially • Acquire ≥ 3 cardiac cycles for each view • Ask the patient to hold breath • Ensure similar frame rate (40–90 Hz), and imaging depth • Obtain aortic valve spectral Doppler (for determining aortic valve closure) *Analysis* • Analyze the LV apical three-chamber view first and verify the timing of aortic valve closure • Contour the subendocardial and subepicardial (when available) borders consistently • Checking tracking quality • Display the segmental strain curves from apical views in quad format • Display the global strain in a bull's eye plot
3D imaging *Acquisition* • Obtain multi-beat (usually 4 beats) gated LV full-volume using the apical four-chamber view • Ask patient to hold breath • Use 'multi-slice' or multiplanar display to ensure the entire LV is included in the pyramidal volume and to look for stitch artifacts *Analysis* • Semiautomatic contouring of the compacted myocardium • Display in a surface-rendered format with volume-time curve
Contrast (if inadequate visualization of 2 or more contiguous segments in the apical views)[14] • Low mechanical index imaging • Watch for artifacts and adjust the rate of injection accordingly

[*] *Modified from* Table 2 of ASE 2014 guidelines on multimodality imaging in cardio-oncology Plana JC et al. [6], *with permission from Elsevier*; please note that echocardiography plays an important role in the assessment of other toxicities related to cancer therapy including valvular heart disease, pericardial constriction, coronary artery disease, etc., however, specific protocols for this have not been provided as this would follow clinical standards in the echocardiography laboratories

laboratory. Each echocardiography laboratory should develop an effective triage system for transthoracic echocardiography (TTE) scheduling, with flexible imaging slots to accommodate urgent requests. For instance, many cardio-oncology TTEs need to be scheduled in accordance to the timing of cancer therapies. There may also be value to a specialized order set for cardio-oncology TTEs that allow the referring provider to clearly state the indication (e.g., screening, therapeutic monitoring, survivor surveillance), the type and timing of cancer therapies, and urgency of the request. This will lead to more efficient triage, and enable better planning to ensure the availability of dedicated imaging equipment and software. A focused cardio-oncology protocol can be used for follow-up surveillance exams that include assessments of 2D/3D LVEF, GLS, LV volumes, and diastolic function, and RV systolic function. There is also a need to consider room times for cardio-oncology studies as these could require longer times for acquisition and post-processing than the standard TTE. Sonographers and readers need to be trained on the use of novel technology and be familiar with the latest protocols and guidelines. Labs interested in cardio-oncology imaging should engage in concordance activities to ensure all sonographers acquire and analyze images in a similar manner. Concordance activities are also recommended among readers to ensure similar approaches to assessing the quality of EF and strain data and consistency in reporting. Regular educational and quality improvement conferences will facilitate continued learning and high-quality TTE studies.

1.8 Cardio-Oncology Echocardiographic Report

A cardio-oncology echocardiographic report should be comprehensive yet provide critical information in summary that can be readily interpreted by the referring oncologist or used by a cardio-oncology clinician. The technique used to quantify LVEF should be clearly stated (i.e., 2D vs. 3D, use of UEA). If 3D imaging is not feasible the reason should be stated, and the reader should provide the best 2D LVEF estimate. Whenever possible and reliable serial changes in 3D LV volumes should be reported. GLS should be reported along with a clear description of the imaging system, software, and version of the software used for acquisition and analysis. Each echocardiography laboratory may also consider incorporating the normal strain value, in accordance with the patient's age, gender, and vendor software [6]. GLS should be reported as an absolute value. If regional tracking is suboptimal GLS should not be reported [6]. Diastolic function grade and its change compared to baseline should be included in the report as it can have prognostic implications [26, 27]. For all these measures, change relative to baseline should be described. For GLS, this is best described as a relative change.

When a clinician reads a cardio-oncology TTE report, they should pay particular attention to any comment on the image quality or artifacts, and if present, should interpret with caution. The clinician should also compare the vital signs documented on the report, as fluctuations in blood pressure and heart rate can influence the LVEF, diastolic function, and strain measurements. If LVEF is being followed, the clinician should check the modality used (e.g., 2D, 3D, with or without contrast) and ensure that the same metric was used in prior studies. Also, it is important to pay attention to ventricular volume changes. A concerning change in LVEF is more likely to have occurred when there is an associated increase in left ventricular end-systolic volume. While the strain is reported in absolute values, relative changes are more relevant and should be calculated as a difference between the current measurement and the baseline measurement divided by the baseline measurement. The clinician should also look for statements of direct side-by-side comparisons in the report rather than just comparing numbers.

1.9 Considerations in the CMR / CT Laboratory

1.9.1 Ventricular Volume and Function Quantification

Routine use of CMR for monitoring cardiac function during cancer therapy is yet to become common practice. However, when used, acquisition and post- processing of images for measurement of ventricular volumes and function should follow the Society of Cardiovascular Magnetic Resonance (SCMR) recommendations [28, 29]. In order to ensure that changes in ventricular volumes and function represent true changes as opposed to measurement-related variability, standardized contouring practices for basal slice and compacted myocardium should be followed within the laboratory (e.g., inclusion/exclusion of papillary muscles in ventricular volumes). If a significant change in ventricular volume or LVEF occurs during sequential follow-up (Videos 1.13 and 1.14), studies should be compared side by side and prior studies re-contoured to minimize inter-observer variability. It is also important to contextualize changes in LVEF in relationship to changes in ventricular volumes to help understand whether a reduction in contractility is the driver of a decline in LVEF [30]. Changes in right ventricular function appear to follow changes in LVEF [31]. Hence it would be prudent to report right ventricular ejection fraction (RVEF) along with LVEF as a potential

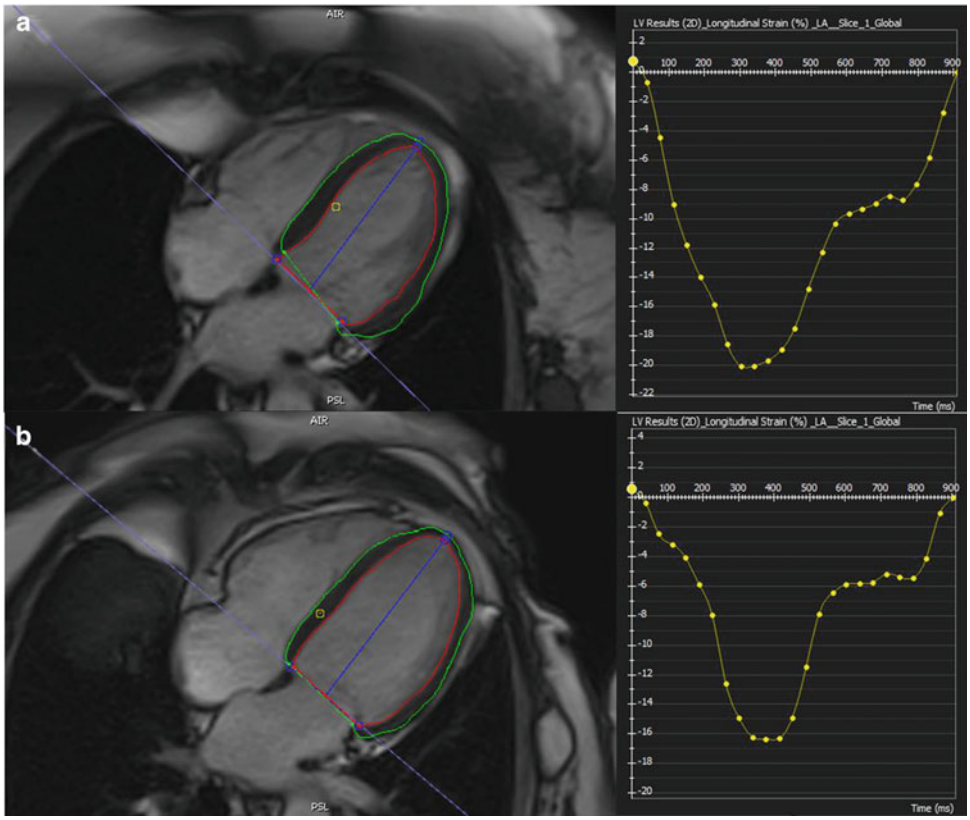

Fig. 1.6 Cardiovascular magnetic resonance imaging feature tracking based strain. Panel A demonstrates 4- chamber global longitudinal strain in a patient prior to anthracycline therapy and Panel B demonstrates measurement in the same patient toward the end of cancer therapy. There is a significant reduction in a 4- chamber longitudinal strain from −20.0 to −16.2%

confirmatory measure of myocardial dysfunction. Strain analysis has not become standard of practice with CMR laboratories in patients receiving cancer therapy. When there is an interest in strain analysis, to minimize the length of the CMR examination, feature tracking methods that use routinely acquired cine images can be considered (Fig. 1.6). Similar to echocardiography, the same technique and post-processing software should be used for sequential follow-up. Suggested CMR protocols and analysis have been summarized in Table 1.4.

1.9.2 Myocardial Tissue Characterization

The value of routine myocardial tissue characterization techniques (e.g., T1 or T2 weighted imaging or mapping, late gadolinium enhancement, and extracellular volume quantification) in patients receiving cancer therapy is unclear. However, these techniques can have a role in the identification of myocarditis due to cancer therapy and in the work-up of cardiac masses. When quantitative CMR tissue characterization techniques are used (e.g., T1, T2 mapping) center-specific normal values should be established as suggested in the SCMR position paper [32]. Ideally, phantoms should be used on a periodic basis to ensure calibration of the quantitative methods. When reporting quantitative mapping data, reports should specify the vendor, magnet strength, specific sequence, and the normal range for the laboratory. It is ideal to use product mapping sequence as opposed to work in progress packages as the latter is subject to change resulting in an alteration in normal values with newer versions of the packages. When sequential imaging is performed, it is important to carefully consider imaging the same slice position at each visit to enable comparability of changes. T1 and T2 mapping values are not directly comparable between vendors and if possible the same magnet should be used for sequential follow-up (Fig. 1.7a, b). When assessing cardiac masses with CMR, it is important to compare other available imaging data to identify location, size, and mobility of the mass. Based on this information, targeted sequences including black and white blood sequences for localization, cine images to identify mobility, tissue characterization to delineate mass composition, and perfusion imaging to identify vascularity should be considered.

1.9.3 Coronary and Pericardial Disease Assessment

Standard cardiac CT protocols for assessment of coronary artery disease can be used for cardiac imaging with the use of prospectively gated acquisitions and narrow acquisition

Table 1.4 Targeted cardio-oncology CMR protocols

General Considerations • Review any prior CMRs to assess the planning of basal slice and tissue characterization slices • Document the patient's blood pressure and heart rate
Assessment of myocardial toxicity *Acquisition* • Standard short-axis cines for assessment of left and right ventricular ejection fraction • Long axis cines (4, 3, 2 chamber) to confirm location short-axis slices while contouring and to potentially measure longitudinal strain using feature tracking methods • Dedicated strain images (e.g., tagged cines) if there is interest in sequential strain follow-up using dedicated strain images (requires extra time during acquisition) • Myocardial T2 weighted imaging, T1 and T2 mapping, and late gadolinium enhancement imaging *Analysis* • Consistent approach within the lab to choose basal short axis slice and contouring of endocardial borders. Careful attention to ventricular volumes. Semi-automated or automated contouring methods are preferred • T1 and T2 mapping analysis should ensure careful attention to the endocardial and epicardial border to ensure avoidance of blood pool and epicardial fat. Use of software features that allows automatic 10–15% offset toward the myocardium from the drawn will ensure minimization of contamination of quantitative values
Assessment of myocarditis *Acquisition* • Standard cine images as above for assessment of volumes, function, regional wall motion abnormalities, strain, and presence of pericardial effusion • Tissue characterization with T2 weighted imaging, T2 mapping, T1 mapping (pre- and post-contrast to allow calculation of extracellular volume fraction), late gadolinium enhancement • If pericarditis present, real-time free-breathing cines in mid short axis view to assess for respiro-phasic septal shift and measure of pericardial constraint *Analysis* • Similar to above
Myocardial masses *Acquisition* • Based on prior images or other modalities, dedicated cine images to assess the size, location, and extent of the mass • In the best imaging planes, T1 and T2 weighted imaging, T1 and T2 mapping, myocardial perfusion imaging, and late gadolinium enhancement *Analysis* • Visual description of location, invasion, tissue characteristics, and quantitative perfusion of mass

*Please note CMR plays an important role in the assessment of other cardiovascular complications related to cancer therapy such as pericardial constriction, vascular disease, myocardial ischemia, etc., however, the CMR protocols for these applications do not differ from clinical routine and hence are not outlined in the list above

windows following the Society of Cardiovascular Computed Tomography (SCCT) guidelines [33]. Especially during cancer treatment, patients may experience high heart rate and lower blood pressure due to volume depletion and hence careful administration of beta-blockers and nitrates is essential to minimize symptomatic hypotension. Outpatient prescription of beta-blockers/calcium channel blockers for a few days prior to CT to improve heart rate control can minimize the need to administer IV medications at the time of image acquisition. CT protocols should ensure that the specific clinical question is addressed and that radiation doses are minimized. Both cardiac CT and CMR can have a complementary role in the assessment of pericardial disease with pericardial calcification (Fig. 1.8) better appreciated on CT while hemodynamic impacts of pericardial disease are better delineated by CMR (Videos 1.15 and 1.16).

1.10 Considerations for the Nuclear Laboratory

1.10.1 Assessment of LVEF

MUGA scan is a well-validated technique for the assessment of LVEF [34–36]. The validity of MUGA for follow-up of patients undergoing cardiotoxic chemotherapy is well established [37]. Validated and established techniques and protocols have been previously published [38–40]. Using MUGA for the assessment of LVEF requires careful adherence to best practices for patient preparation, tracer injection, imaging, and assessment of the final image data. For patients undergoing cancer therapy, the usefulness of MUGA is limited to the assessment of LVEF and for

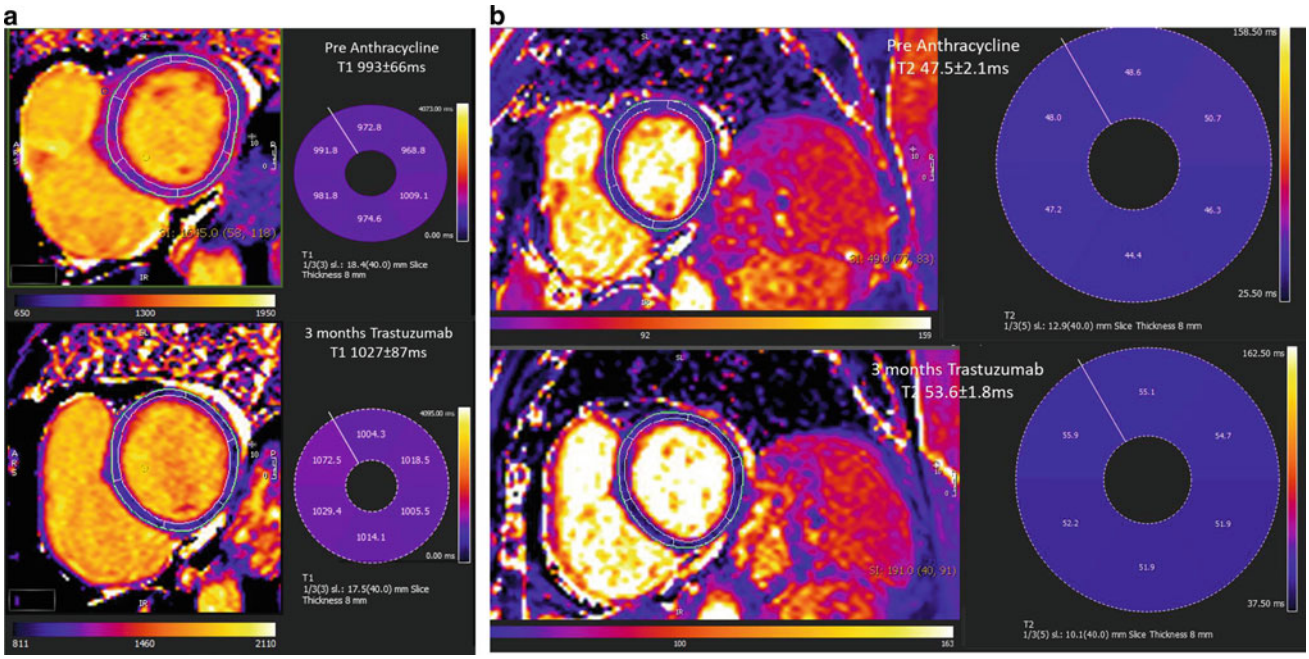

Fig. 1.7 Native myocardial **a** T1 map and **b** T2 map in a short-axis view pre-cancer therapy (top panel) and 3 months into trastuzumab therapy (bottom panel). There was an increase in myocardial native-T1 and T2 values seen early during cancer therapy

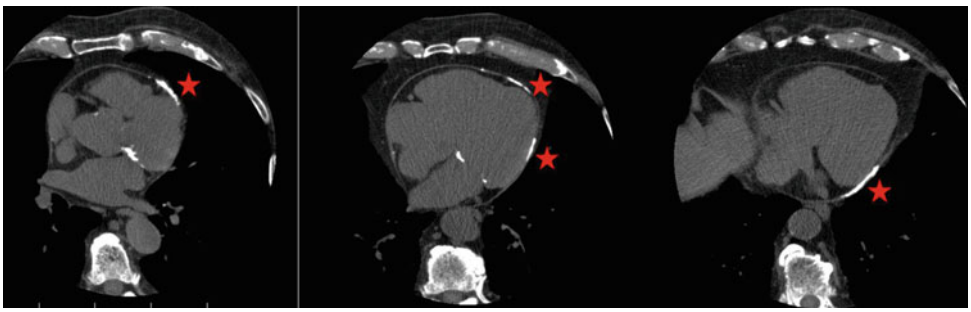

Fig. 1.8 Non-contrast gated cardiac computed tomography showing pericardial calcification (stars) at 3 different positions

accurate assessment of right ventricular ejection fraction using first-pass imaging. The radiation dose is approximately 8 mSv. This is slightly higher than double average background radiation for most patients [41]. The accuracy of MUGA can be affected by several variables.

Gating: The acquisition of MUGA requires accurate gating, this can be an issue in rapid atrial fibrillation or patients with frequent ventricular ectopics. It is always preferable to repeat analysis when the heart rhythm is controlled.

Count quality: There are several medications that can affect red cell labeling. Doxorubicin is of particular concern in oncology patients. If count quality is poor then caution must be taken during reporting to ensure an artifactually low LVEF is not reported [40] (Please also see Table 2 in Reference 41).

Standard assessment of LVEF is performed using the left anterior oblique 45 or best septal view. Care must be taken to ensure optimal separation of the LV and RV cavities when obtaining this view.

LVEF is calculated as follows ($EDCounts_{backgroundcorrected}$-$ESCounts_{backgroundcorrected}$)/($EDCounts_{backgroundcorrected}$). The technique uses counts averaged from 5 min of data. This helps to reduce beat-to-beat variation of LV filing. It is also independent of LV chamber geometry. It is important that the technologist and reading physician carefully assess the ED and ES tracings to ensure appropriate tracking of counts. Background assessment is also critical for accurate values. If the background is placed in an abnormally count poor area such as a pericardial effusion, or a region of left ventricular hypertrophy, background counts will be under subtracted and the LVEF will be artifactually lowered. If the

background is placed in an abnormally count rich area such as over the aorta or enlarged spleen then the background will be over subtracted resulting in an artifactually increased LVEF.

1.10.2 PET Imaging for Inflammation/Metabolism

Cardiac positron emission tomography (PET) is a powerful imaging technique for the assessment of myocardial blood flow and for imaging cardiac inflammation. Although there are several promising imaging tracers that will permit imaging myocardial damage associated with cardiotoxic chemotherapy, the only FDA-approved PET tracer is ^{18}F-FDG [42, 43]. Cardiac PET imaging with ^{18}F-FDG is ideal for assessing coronary flow reserve. Impaired coronary flow reserve (CFR) is a marker of coronary microvascular dysfunction. Studies have demonstrated that PET measures of CFR correlate to microvascular disease associated with thoracic radiation for cancer treatment [44]. Since active inflammatory cells have a high glycolytic activity, imaging with ^{18}F-FDG allows visualization of immune cell activation and infiltration into the myocardium. It is particularly useful for the dynamic assessment of active myocardial inflammation. ^{18}F-FDG PET/CT imaging can be useful in differentiating primary cardiac tumors from metastatic tumors [45] (*see* Figs. 1.9 and 1.10). Recent work by Meng et al.

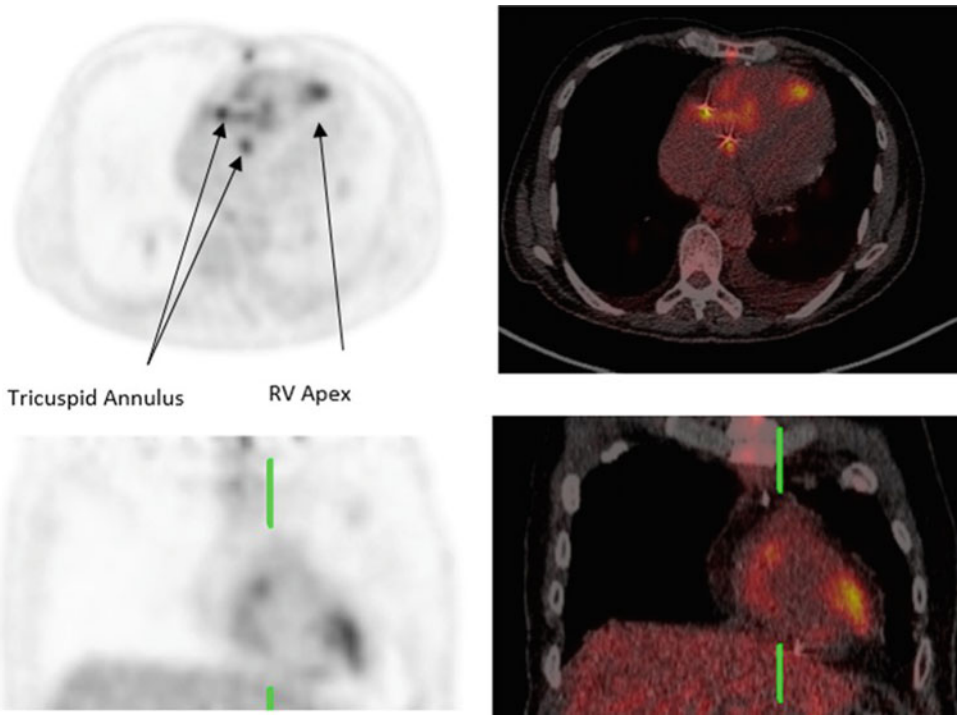

Fig. 1.9 18F-FDG PET/CT axial (upper panel) and coronal images (lower panel) in a patient with metastatic mucinous adenocarcinoma (primary diagnosed and treated 17 years prior), SUVmax, 5.6 and TBRmax, 4.3

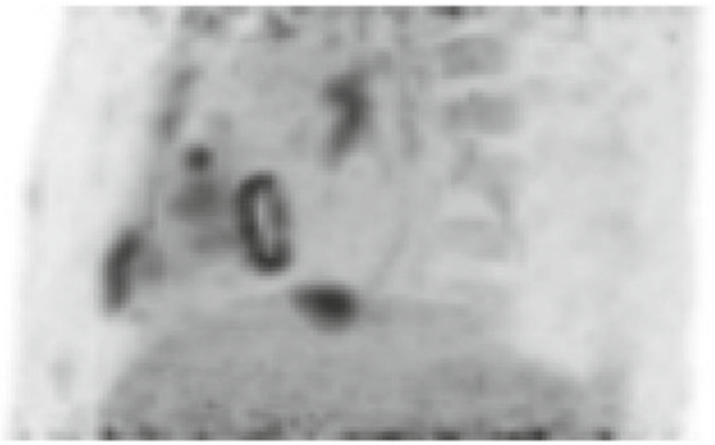

Fig. 1.10 18F-FDG PET, 3D MIP demonstrating tumor infiltration in the tricuspid annulus and right ventricular apex in the same case as Fig. 1.9

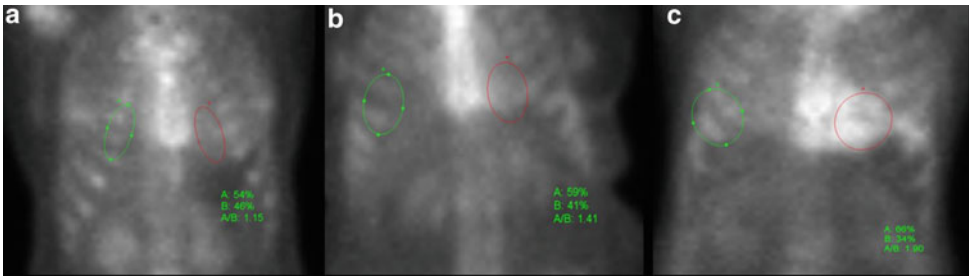

Fig. 1.11 Planar-99mTc-PYP 3 h Images. Panel A shows a negative study, with no appreciable myocardial uptake with HCL < 1.5. Panel B shows an equivocal study with borderline uptake HCL < 1.5. Panel C shows a positive study, with significant myocardial uptake, Grade 3, HCL > 1.5

demonstrated that differentiation can be achieved based on standardized uptake values (SUVmax) and tumor to background ratio (TBRmax) values: benign cardiac tumors (SUVmax 2.35 ± 1.31, TBRmax = 1.05 ± 0.50), primary cardiac tumors (SUVmax = 8.90 ± 4.23, TBRmax = 3.82 ± 1.44) and cardiac metastases (SUVmax = 14.37 ± 8.05, TBRmax = 6.19 ± 3.38) [46]. As expected, a high SUVmax or TBRmax were associated with increased mortality.

An important aspect of ^{18}F-FDG imaging for inflammation is the suppression of physiological cardiomyocyte uptake of glucose. It is critical that the patient adheres to the carbohydrate-free diet for a minimum of 24 h prior to the scan. For patients where endogenous cardiomyocytes are not suppressed with a 24-h diet, successful suppression may occur with a 48–96 h diet [47]. Quantitative assessment of myocardial uptake is essential for sequential follow-up and assessment of response to treatment. Standardized uptake values are used for the routine description of abnormal uptake. Cardiac metabolic volumes provide a better assessment of the burden of abnormal uptake and are useful for assessing response to treatment [48].

1.10.3 Nuclear Imaging for Cardiac Amyloid

The diagnosis of cardiac amyloidosis requires both careful clinical assessment and multimodality imaging. The bone imaging agent 99mTc-pyrophosphate can be used to image transthyretin (ATTR) amyloidosis [49]. The tracers 99mTc-PYP/DPD/HMDP/ and 123I-mIBG/PET have all been demonstrated to be useful in imaging ATTR [50]. 99mTc-pyrophosphate is a common imaging agent in North America. Images are best obtained in an anterior planar view, tomographic images (SPECT) can be useful in difficult cases. It is advised that gating be applied to the planar, and SPECT acquisition.

Images are interpreted using both a visual and semi-quantitative ratio of heart to contralateral chest uptake (H/CL). A ratio of >1.5 is suggestive of ATTR (Fig. 1.11). Visual scoring is obtained using a scale of 0–3, where 0 = no cardiac activity with normal rib uptake, 1 = cardiac activity < rib, 2 = cardiac activity = rib, and 3 = cardiac activity > rib [50] (Fig. 1.11). Common sources of error include:

(1) Previous myocardial infarction which limits myocardium available to take up tracer, tomographic imaging (SPECT) can be helpful in such cases
(2) A dilated LV such that the "Heart region of interest" oversamples the LV cavity with incomplete inclusion of the myocardial uptake
(3) The "CL region of interest" is placed near the mediastinum and can sample myocardial activity in a dilated heart.

Residual blood pool activity can result in a H/CL ratio approaching 1.5. This can easily be detected by looking at the gated anterior planar view. This can be avoided by imaging at 3 h post-injection instead of 1-h post-injection.

1.11 Conclusion

Cardiovascular imaging plays a crucial role in the field of cardio-oncology. Laboratories engaged in the cardiovascular imaging of patients with cancer should ensure high-quality imaging as the results have a major impact on cancer treatment decisions and long-term cardiovascular follow-up of patients.

Acknowledgements The authors gratefully acknowledge Babitha Thampinathan and Dr. Tamar Shalmon for curating some of the images and videos used in this chapter.

References

1. Steingart RM, Chandrashekhar Y, Marwick TH. Imaging in cardio-oncology: where are we and where should we be going? JACC Cardiovasc Imaging. 2018;11:1209–11.
2. Plana JC, Thavendiranathan P, Bucciarelli-Ducci C, Lancellotti P. Multi-modality imaging in the assessment of cardiovascular toxicity in the cancer patient. JACC Cardiovasc Imaging. 2018;11:1173–86.
3. Yeh ET, Chang HM. Oncocardiology-past, present, and future: a review. JAMA Cardiol. 2016;1:1066–72.
4. Biersmith MA, Tong MS, Guha A, Simonetti OP, Addison D. Multimodality cardiac imaging in the era of emerging cancer therapies. J Am Heart Assoc. 2020;9:e013755.
5. Armenian SH, Lacchetti C, Barac A, et al. Prevention and monitoring of cardiac dysfunction in survivors of adult cancers: american society of clinical oncology clinical practice guideline. J Clin Oncol. 2017;35:893–911.
6. Plana JC, Galderisi M, Barac A, et al. Expert consensus for multimodality imaging evaluation of adult patients during and after cancer therapy: a report from the American Society of Echocardiography and the European Association of Cardiovascular Imaging. J Am Soc Echocardiogr. 2014;27:911–39.
7. Thavendiranathan P, Grant AD, Negishi T, Plana JC, Popovic ZB, Marwick TH. Reproducibility of echocardiographic techniques for sequential assessment of left ventricular ejection fraction and volumes: application to patients undergoing cancer chemotherapy. J Am Coll Cardiol. 2013;61:77–84.
8. Thavendiranathan P, Poulin F, Lim KD, Plana JC, Woo A, Marwick TH. Use of myocardial strain imaging by echocardiography for the early detection of cardiotoxicity in patients during and after cancer chemotherapy: a systematic review. J Am Coll Cardiol. 2014;63:2751–68.
9. Pitekova B, Ravi S, Shah SV, Mladosievicova B, Heitner S, Ferencik M. The role of imaging with cardiac computed tomography in cardio-oncology patients. Curr Cardiol Rep. 2016;18:87.
10. Dorbala S, Cuddy S, Falk RH. How to image cardiac amyloidosis: a practical approach. JACC Cardiovasc Imaging. 2020;13:1368–83.
11. Bauckneht M, Ferrarazzo G, Fiz F, et al. Doxorubicin effect on myocardial metabolism as a prerequisite for subsequent development of cardiac toxicity: a translational (18)F-FDG PET/CT observation. J Nucl Med. 2017;58:1638–45.
12. Lang RM, Badano LP, Mor-Avi V, et al. Recommendations for cardiac chamber quantification by echocardiography in adults: an update from the American Society of Echocardiography and the European Association of Cardiovascular Imaging. Eur Heart J Cardiovasc Imaging. 2015;16:233–70.
13. Lang RM, Badano LP, Tsang W, et al. EAE/ASE recommendations for image acquisition and display using three-dimensional echocardiography. J Am Soc Echocardiogr. 2012;25:3–46.
14. Porter TR, Mulvagh SL, Abdelmoneim SS, et al. Clinical applications of ultrasonic enhancing agents in echocardiography: 2018 American Society of Echocardiography Guidelines Update. J Am Soc Echocardiogr. 2018;31:241–74.
15. Hoffmann R, Barletta G, von Bardeleben S, et al. Analysis of left ventricular volumes and function: a multicenter comparison of cardiac magnetic resonance imaging, cine ventriculography, and unenhanced and contrast-enhanced two-dimensional and three-dimensional echocardiography. J Am Soc Echocardiogr. 2014;27:292–301.
16. Mulvagh SL, Rakowski H, Vannan MA, et al. American Society of Echocardiography Consensus Statement on the Clinical Applications of Ultrasonic Contrast Agents in Echocardiography. J Am Soc Echocardiogr 2008;21:1179–201; quiz 1281.
17. Porter TR, Abdelmoneim S, Belcik JT, et al. Guidelines for the cardiac sonographer in the performance of contrast echocardiography: a focused update from the American Society of Echocardiography. J Am Soc Echocardiogr. 2014;27:797–810.
18. Oikonomou EK, Kokkinidis DG, Kampaktsis PN, et al. Assessment of prognostic value of left ventricular global longitudinal strain for early prediction of chemotherapy-induced cardiotoxicity: a systematic review and meta-analysis. JAMA Cardiol. 2019;4:1007–18.
19. Lambert J, Lamacie M, Thampinathan B, et al. Variability in echocardiography and MRI for detection of cancer therapy cardiotoxicity. Heart. 2020;106:817–23.
20. Mor-Avi V, Lang RM, Badano LP, et al. Current and evolving echocardiographic techniques for the quantitative evaluation of cardiac mechanics: ASE/EAE consensus statement on methodology and indications endorsed by the Japanese Society of Echocardiography. J Am Soc Echocardiogr. 2011;24:277–313.
21. Voigt JU, Pedrizzetti G, Lysyansky P, et al. Definitions for a common standard for 2D speckle tracking echocardiography: consensus document of the EACVI/ASE/Industry Task Force to standardize deformation imaging. Eur Heart J Cardiovasc Imaging. 2015;16:1–11.
22. Knackstedt C, Bekkers SC, Schummers G, et al. Fully automated versus standard tracking of left ventricular ejection fraction and longitudinal strain: the FAST-EFs multicenter study. J Am Coll Cardiol. 2015;66:1456–66.
23. Negishi K, Negishi T, Kurosawa K, et al. Practical guidance in echocardiographic assessment of global longitudinal strain. JACC Cardiovasc Imaging. 2015;8:489–92.
24. Nagata Y, Wu VC, Otsuji Y, Takeuchi M. Normal range of myocardial layer-specific strain using two-dimensional speckle tracking echocardiography. PLoS ONE. 2017;12:e0180584.
25. Voigt JU, Cvijic M. 2- and 3-dimensional myocardial strain in cardiac health and disease. JACC Cardiovasc Imaging. 2019;12:1849–63.
26. Nagueh SF, Smiseth OA, Appleton CP, et al. Recommendations for the evaluation of left ventricular diastolic function by echocardiography: an update from the American Society of Echocardiography and the European Association of Cardiovascular Imaging. J Am Soc Echocardiogr. 2016;29:277–314.
27. Upshaw JN, Finkelman B, Hubbard RA, et al. Comprehensive assessment of changes in left ventricular diastolic function with contemporary breast cancer therapy. JACC Cardiovasc Imaging. 2020;13:198–210.
28. Kramer CM, Barkhausen J, Bucciarelli-Ducci C, Flamm SD, Kim RJ, Nagel E. Standardized cardiovascular magnetic resonance imaging (CMR) protocols: 2020 update. J Cardiovasc Magn Reson. 2020;22:17.
29. Schulz-Menger J, Bluemke DA, Bremerich J, et al. Standardized image interpretation and post-processing in cardiovascular magnetic resonance—2020 update: Society for Cardiovascular Magnetic Resonance (SCMR): Board of Trustees Task Force on Standardized Post-Processing. J Cardiovasc Magn Reson. 2020;22:19.
30. Melendez GC, Sukpraphrute B, D'Agostino RB Jr, et al. Frequency of left ventricular end-diastolic volume-mediated declines in ejection fraction in patients receiving potentially cardiotoxic cancer treatment. Am J Cardiol. 2017;119:1637–42.
31. Barthur A, Brezden-Masley C, Connelly KA, et al. Longitudinal assessment of right ventricular structure and function by cardiovascular magnetic resonance in breast cancer patients treated with trastuzumab: a prospective observational study. J Cardiovasc Magn Reson. 2017;19:44.
32. Messroghli DR, Moon JC, Ferreira VM, et al. Clinical recommendations for cardiovascular magnetic resonance mapping of T1,

T2, T2* and extracellular volume: a consensus statement by the Society for Cardiovascular Magnetic Resonance (SCMR) endorsed by the European Association for Cardiovascular Imaging (EACVI). J Cardiovasc Magn Reson. 2017;19:75.
33. Abbara S, Blanke P, Maroules CD, et al. SCCT guidelines for the performance and acquisition of coronary computed tomographic angiography: a report of the society of cardiovascular computed tomography guidelines committee: Endorsed by the North American Society for Cardiovascular Imaging (NASCI). J Cardiovasc Computed Tomogr. 2016;10:435–49.
34. Mitra D, Basu S. Equilibrium radionuclide angiocardiography: Its usefulness in current practice and potential future applications. World J Radiol. 2012;4:421–30.
35. Upton MT, Rerych SK, Newman GE, Bounous EP Jr, Jones RH. The reproducibility of radionuclide angiographic measurements of left ventricular function in normal subjects at rest and during exercise. Circulation. 1980;62:126–32.
36. Romero-Farina G, Aguade-Bruix S. Equilibrium radionuclide angiography: present and future. J Nucl Cardiol. 2019.
37. Schwartz RG, McKenzie WB, Alexander J et al. Congestive heart failure and left ventricular dysfunction complicating doxorubicin therapy. Seven-year experience using serial radionuclide angiocardiography. The Am J Med. 1987;82:1109–18.
38. Mahmarian JJ, Moye L, Verani MS, Eaton T, Francis M, Pratt CM. Criteria for the accurate interpretation of changes in left ventricular ejection fraction and cardiac volumes as assessed by rest and exercise gated radionuclide angiography. J Am Coll Cardiol. 1991;18:112–9.
39. Klocke FJ, Baird MG, Lorell BH, et al. ACC/AHA/ASNC guidelines for the clinical use of cardiac radionuclide imaging–executive summary: a report of the American College of Cardiology/American Heart Association Task Force on Practice Guidelines (ACC/AHA/ASNC Committee to Revise the 1995 Guidelines for the Clinical Use of Cardiac Radionuclide Imaging). J Am Coll Cardiol. 2003;42:1318–33.
40. Corbett JR, Akinboboye OO, Bacharach SL, et al. Equilibrium radionuclide angiocardiography. J Nucl Cardiol. 2006;13:e56-79.
41. Plana JC, Mikati IA, Dokainish H, et al. A randomized cross-over study for evaluation of the effect of image optimization with contrast on the diagnostic accuracy of dobutamine echocardiography in coronary artery disease The OPTIMIZE Trial. JACC Cardiovasc Imaging. 2008;1:145–52.
42. Dreyfuss AD, Bravo PE, Koumenis C, Ky B. Precision cardio-oncology. J Nucl Med. 2019;60:443–50.
43. Tilkemeier PL, Bourque J, Doukky R, Sanghani R, Weinberg RL. ASNC imaging guidelines for nuclear cardiology procedures: standardized reporting of nuclear cardiology procedures. J Nucl Cardiol. 2017;24:2064–128.
44. Groarke JD, Divakaran S, Nohria A, et al. Coronary vasomotor dysfunction in cancer survivors treated with thoracic irradiation. J Nucl Cardiol. 2020.
45. Rahbar K, Seifarth H, Schafers M, et al. Differentiation of malignant and benign cardiac tumors using 18F-FDG PET/CT. J Nucl Med. 2012;53:856–63.
46. Meng J, Zhao H, Liu Y, et al. Assessment of cardiac tumors by (18)F-FDG PET/CT imaging: histological correlation and clinical outcomes. J Nucl Cardiol. 2020.
47. Osborne MT, Hulten EA, Murthy VL, et al. Patient preparation for cardiac fluorine-18 fluorodeoxyglucose positron emission tomography imaging of inflammation. J Nucl Cardiol. 2017;24:86–99.
48. Ahmadian A, Brogan A, Berman J, et al. Quantitative interpretation of FDG PET/CT with myocardial perfusion imaging increases diagnostic information in the evaluation of cardiac sarcoidosis. J Nucl Cardiol. 2014;21:925–39.
49. Bokhari S, Castano A, Pozniakoff T, Deslisle S, Latif F, Maurer MS. (99m)Tc-pyrophosphate scintigraphy for differentiating light-chain cardiac amyloidosis from the transthyretin-related familial and senile cardiac amyloidoses. Circ Cardiovasc Imaging. 2013;6:195–201.
50. Dorbala S, Ando Y, Bokhari S, et al. ASNC/AHA/ASE/EANM/HFSA/ISA/SCMR/SNMMI expert consensus recommendations for multimodality imaging in cardiac amyloidosis: Part 1 of 2-evidence base and standardized methods of imaging. J Nucl Cardiol. 2019;26:2065–123.

Anthracycline/Trastuzumab Cardiac Toxicity

2

Christopher Yu, Faraz Pathan, and Kazuaki Negishi

Key Points

- Two major anti-cancer agents with higher risk for developing cardiac dysfunction: Anthracyclines (often irreversible and dose related myocyte injury) and trastuzumab (often reversible, not dose dependent).
- The risk of trastuzumab-related cardiac dysfunction is increased by sevenfold when trastuzumab is used after an anthracycline-based chemotherapy.
- Medical therapy includes the use of beta blockers (BB) and angiotensin receptor blockers or angiotensin converting enzyme inhibitors (ACEi) derived from the literature supporting their use in heart failure with reduced ejection fraction.
- Echocardiography is the fundamental imaging modality used in the detection of left ventricular impairment in cardio-oncology.
- Global longitudinal strain has been shown to detect left ventricular dysfunction earlier than LVEF in patients receiving cancer therapy and has the potential to guide therapy by minimizing clinically important cardiotoxicity.

Cancer therapy-related cardiac dysfunction (CTRCD) is defined as a decrease in the left ventricular ejection fraction (LVEF) of > 10%, to a value below the institutional lower limit of normal (LLN) (e.g., 50 or 53%) (Table 2.1) [1–3].

The European Society of Cardiology (ESC) position paper recommends that this decrease should be confirmed by repeated cardiac imaging done 2–3 weeks after the diagnostic study showing the initial decrease in LVEF.

Broadly speaking, there are two major anti-cancer agents with higher risk for developing CTRCD: Anthracyclines (often irreversible and dose related myocyte injury) and trastuzumab (often reversible, does not demonstrate typical anthracycline related ultrastructural cellular injury and is not dose dependent). As these agents are often used together or in succession, the resultant myocardial injury and cardiac dysfunction are a result of synergistic injury (Fig. 2.1).

2.1 Anthracycline-Related CTRCD

Anthracyclines are the most extensively investigated agents. This class of chemotherapy incorporates a range of agents, such as doxorubicin, epirubicin, and idarubicin. They are the cornerstone of multiple chemotherapy regimens used to treat different types of cancer such, as breast, sarcoma, lymphoma, and pediatric leukemia.

There are multiple proposed mechanisms of anthracycline cardiotoxicity, however, the two widely accepted theories include excessive reactive oxygen species and topoisomerase 2β inhibition causing cardiomyocyte death [4]. The risk of developing anthracycline-related CTRCD is dependent on many factors including cumulative anthracycline dose, concomitant radiotherapy, sequential cardiotoxic therapy (i.e., trastuzumab), age ≥ 60 years, multiple cardiovascular risk factors, and known baseline cardiac impairment [5]. The frequency of CTRCD exponentially increases with higher anthracycline doses. A pooled analysis of three clinical trials demonstrated the frequency of CTRCD was 9% at a cumulative doxorubicin dose of 250 mg/m^2 and increasing to 18% and 38% at cumulative doses of 350 mg/m^2 and 450 mg/m^2, respectively [6].

Electronic supplementary material
The online version of this chapter (https://doi.org/10.1007/978-3-030-70998-3_2) contains supplementary material, which is available to authorized users.

C. Yu · F. Pathan · K. Negishi (✉)
Faculty of Medicine and Health Department of Cardiology, Sydney Medical School Nepean, Charles Perkins Centre Nepean, The University of Sydney, Kingswood, NSW 2747, Australia
e-mail: kazuaki.negishi@sydney.edu.au

C. Yu
e-mail: christopher.yu@sydney.edu.au

R. M. Steingart et al. (eds.), *Atlas of Imaging in Cardio-Oncology*, https://doi.org/10.1007/978-3-030-70998-3_2

Table 2.1 Definition of Cardiotoxicity/CTRCD

Year	2014	2016	2020
Medical Society	**ASE/EACVI** [1]	**ESC** [2]	**ESMO** [3]
Definition of Cardiotoxicity (or CTRCD)	An LVEF drop of >10 percentage points, to a value <53%	An LVEF drop of >10 percentage points, to a value below the LLN	An LVEF drop $\geq$10 percentage point to a value below the LLN (<50%)

ASE, American Society of Echocardiography; EACVI, European Association of Cardiovascular Imaging; ESC, European Society of Cardiology; ESMO, European Society of Medical Oncology; LLN, lower limit of normal

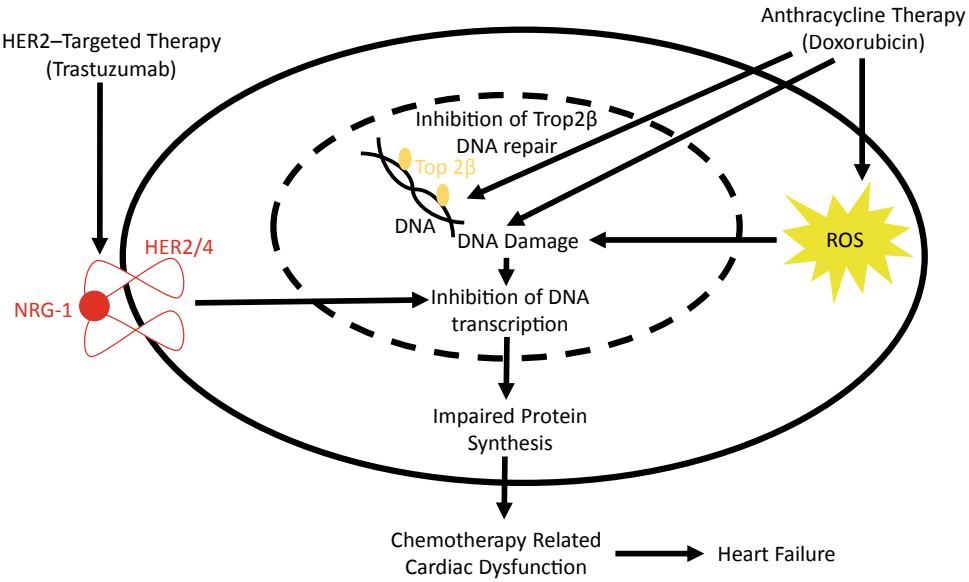

Fig. 2.1 Mechanism of anthracycline/trastuzumab cardiac toxicity. NRG-1, Neuregulin-1; HER2/4, Human epidermal receptor 2/4; Trop2β, Topoisomerase II-beta; ROS, Reactive oxidative species (*Adapted from* Shaw et al. [26]; with permission from Elsevier)

2.2 Trastuzumab-Related CTRCD

Trastuzumab is a monoclonal antibody that targets the human epidermal growth factor receptor 2 (HER2) and is used for the treatment of HER2-positive tumors, such as breast cancer and gastric cancer. The mechanism of cardiotoxicity is due to the disruption in the signaling between the HER2 receptor and neuregulin (a ligand growth factor), which is critical for normal myocyte growth and survival [7]. Trastuzumab-related CTRCD is highly dependent on the concomitant or prior use of anthracyclines. Trastuzumab and anthracyclines are not administered concomitantly in practice because of the very high incidence of CTRCD. The risk of trastuzumab-related CTRCD is increased by sevenfold when trastuzumab is used after an anthracycline-based chemotherapy compared with no anthracycline therapy [8]. The incidence CTRCD after 2 years of trastuzumab is 7.3% post completion of primary therapy [9].

2.3 Treatment for CTRCD

There is a lack of high-quality evidence in the management of CTRCD with expert consensus currently providing the foundation of guidance [2]. The approach to the management of CTRCD is dependent on symptoms and decline in LVEF most commonly based on echocardiography. Medical therapy in CTRCD includes the use of beta blockers (BB) and angiotensin receptor blockers or angiotensin converting enzyme inhibitors (ACEi). The premise for the use of BB and ACEi is derived from the literature supporting their use in heart failure with reduced ejection fraction as well as preventative effects shown in meta-analyses [10]. Patients with asymptomatic reduction in LVEF as a result of cancer therapy should be commenced on one or more guideline-base heart failure therapies as per the ESC Position statement [2]. Enalapril (ACEi) and carvedilol or bisoprolol (BB), having shown positive results in improving LVEF in

an anthracycline-related CRTCD trial [11]. The initiation of cardioprotective medications and/or modification of the cancer therapy should be made by a multidisciplinary cardio-oncology team [12].

2.4 Role of Imaging in Anthracycline/Trastuzumab Cardiotoxicity

The roles of cardiovascular imaging in CTRCD include:

- Screening patients for baseline cardiac function prior to the commencement of therapy.
- Ongoing surveillance at 3/6 monthly intervals for the duration of therapy.
- Identifying pre-existing conditions which may preclude treatment.
- Identifying early biological signatures of CTRCD.

These will enable changes to treatment or chemotherapy to achieve optimal outcome for management of malignancy and cardiac function, including early initiation of cardioprotective therapy.

The ideal imaging modality should be readily available, affordable, sensitive to early changes, minimal radiation exposure given the frequency of repeat investigation and have good test–retest reproducibility. The modalities used to achieve these roles include echocardiography, cardiac magnetic resonance, and nuclear imaging. Each has advantages and disadvantages with respect to use in CTRCD (Table 2.2).

2.5 Echocardiography in Anthracycline/Trastuzumab Cardiotoxicity

Echocardiography is the fundamental imaging modality used in the detection of LV impairment in cardio-oncology. Guidelines emphasize the need for assessment of LV function upon completion of anthracycline therapy, and again 6 months after completing therapy in asymptomatic patients [1]. For those receiving trastuzumab, repeated LVEF assessments should occur 3 months during therapy. The biplane method of disks technique by 2D echocardiography (2DE) is the most commonly used method to assess LVEF. As shown above, CTRCD is defined as decrease in the LVEF of > 10% to a value below the institutional LLN (Table 2.1). 3D echocardiography has greater reproducibility and accuracy than 2DE and can also be used to calculate LVEF, thus is recommended by current guidelines [1, 13]. Despite the ease of determining LVEF on echocardiography, it has a low sensitivity for detecting small changes in LV function. Furthermore, feasibility of high-quality imaging may be influenced by patient body habitus, radiation therapy, or recent surgery (e.g., mastectomy). Contrast enhanced echocardiography may alleviate some of these imaging limitations and provide a more accurate assessment of LVEF [14].

Global longitudinal strain (GLS) has been shown to detect LV dysfunction earlier than LVEF in patients receiving cancer therapy and has the potential to guide therapy by early detection of clinically important cardiotoxicity [15]. 2D GLS and 3D EF have the lowest temporal variability with respect to detection of changes due to

Table 2.2 Summary of imaging modality in Anthracycline/Trastuzumab cardiotoxicity

	Echocardiography	Cardiac Magnetic Resonance (CMR)	Equilibrium Radionuclide Angiocardiography (ERNA)
LVEF	Yes	Yes	Yes
LV GLS	Yes	Yes	No
RV function	Yes*	Yes	No
Valvular heart disease	Yes	Yes	No
Pericardial disease	Yes	Yes	No
LV tissue characterization	Yes$	Yes	No
Additional CV pathology	Yes	Yes	No

CV—Cardiovascular LVEF—Left ventricular ejection fraction; LV GLS—Left ventricular global longitudinal strain; RV—Right ventricle; *Echocardiographic measures of RV function are indirect and less accurate compared to CMR; $integrated backscatter can give limited tissue characterization

CTRCD and 2D GLS has better inter and intraobserver reproducibility than LVEF [16].

In the absence of GLS, adjunctive quantification methods to LVEF can include M-mode measurement of the mitral annular plane systolic excursion and/or the peak systolic velocity (s') of the mitral annulus by pulsed-wave Doppler tissue imaging [1]. Despite the focus of echocardiography being on LV function, it is important to assess other cardiac structures such as the heart valves and the pericardium. There is no established evidence supporting the role of LV diastolic function predicting CRTCD.

2.6 Cardiac Magnetic Resonance (CMR) in Anthracycline/Trastuzumab Cardiotoxicity

CMR is the gold standard technique for anatomical and functional evaluation of the heart (including biventricular size and systolic function) due to its high spatial resolution, reproducibility, and accuracy. However, cost and availability limit the widespread adoption of CMR. CMR is recommended where LVEF cannot be accurately assessed by echocardiography due to poor image acquisition [1]. CMR can also accurately calculate LV mass. Larger declines in LV mass due to anthracycline therapy is associated with increased incidence of adverse cardiovascular events [17]. In addition to low temporal variability of CMR derived ejection fraction, CMR has excellent inter- and intraobserver reproducibility compared to echocardiography [16]. The precision of CMR enables detection of smaller changes in LVEF and right ventricular (RV) EF. GLS can also be calculated in CMR using a feature-tracking technique on traditional apical views, however, its application in cardio-oncology has not been systematically evaluated.

The early biological signatures of cardiotoxicity may manifest as interstitial edema or early diffuse interstitial fibrosis. CMR's ability to accurately characterize myocardial tissue through T1 and T2 weighted imaging enables one to identify both interstitial edema and fibrosis (Fig. 2.2). Unique biological signatures of early inflammatory involvement (raised both native T1 and T2) and interstitial fibrosis and remodeling (raised native T1 but not T2), respectively, may identify susceptible myocardium and guide cardioprotective therapy [18].

T1 mapping also allows for the calculation of extracellular volume fraction (ECV), which is a marker of edema or interstitial fibrosis. Early post anthracycline therapy, myocardial edema can be identified by T2-weighted sequence and is associated with reduced RV function [19]. Additionally, elevated LV T1 mapping and ECV have been identified in post anthracycline therapy patients, independent of cardiovascular comorbidities [20]. The clinical significance of these findings has yet to be determined. Despite the advantages of using CMR-based tissue characterization, in contrast to CMR derived ejection fraction, the significant temporal variability of T1, T2 mapping and ECV for now limit its routine use in CTRCD [21]. Late gadolinium enhancement is not associated with CTRCD from anthracycline/trastuzumab therapy.

2.7 Nuclear Imaging in Anthracycline/Trastuzumab Cardiotoxicity

Traditionally, multiple gated acquisition scanning (MUGA) has been one of the first-line imaging modalities for the assessment of LVEF because of more accurate and reproducible results than echocardiography [22]. However, nuclear imaging techniques have fallen out of favor for LV assessment because of increased radiation exposure (approximately 5–10 mSv) and limited assessment of other cardiac structures or functions. Furthermore, a recent study

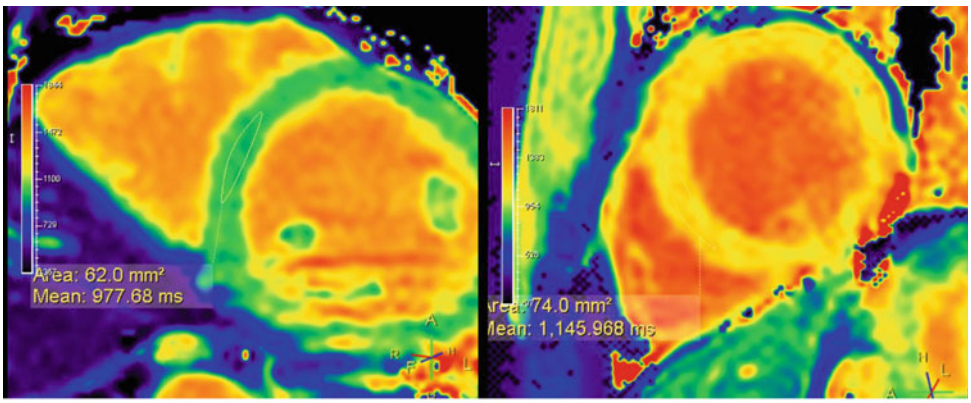

Normal T1- no evidence of inflammation or fibrosis (n 900-1000 msec)

Elevated T1- due to myocardial inflammation/ Fibrosis (900-1000 msec)

Fig. 2.2 CMR myocardial mapping with right panel showing elevated T1 (yellow) in the myocardium

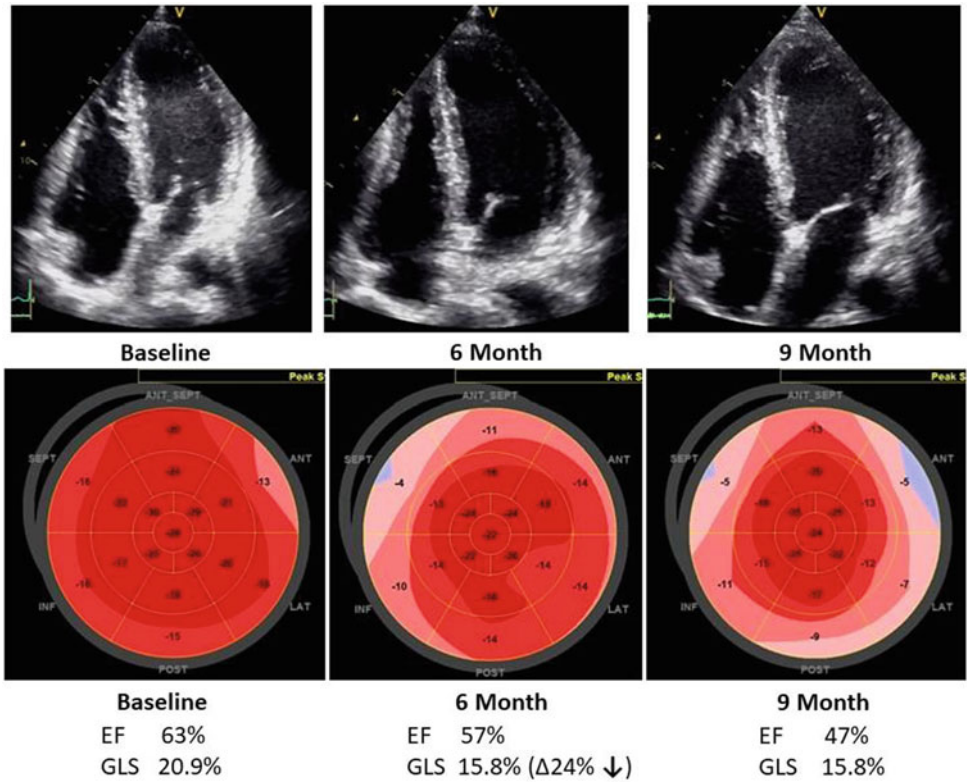

Fig. 2.3 Ejection fraction-guided intervention. GLS declined months before the decline in EF met criteria for CTRCD. EF, Ejection Fraction; GLS, global longitudinal strain

demonstrated that MUGA-derived LVEFs are only modestly accurate when compared with CMR reference LVEFs [23].

PET imaging solely assesses myocardial metabolism. Though of limited use currently, in a small retrospective study, low myocardial fluorodeoxyglucose uptake before doxorubicin chemotherapy in Hodgkin disease patients independently predicted the development of CRTCD [24]. Stress nuclear perfusion studies can be of value when testing is required to exclude ischemic heart disease as a contributing factor to the observed left ventricular dysfunction.

2.8 Case 1: Asymptomatic Cardiotoxicity from Epirubicin and Trastuzumab

- Cardiotoxicity can often be asymptomatic.
- Despite LVEF being the marker for cardiotoxicity, GLS can detect cardiotoxicity earlier.

62-year-old woman was diagnosed with bilateral HER2-positive breast cancer. Baseline echocardiography demonstrated an LVEF of 63%, GLS 20.9%. She commenced EC chemotherapy with epirubicin (90 mg/m^2) and cyclophosphamide for four cycles. She subsequently commenced weekly paclitaxel and had one dose of trastuzumab (8 mg/kg). The patient was asymptomatic from a cardiovascular perspective. On a serial echocardiogram at 6 months, the LVEF and GLS declined to 57% and 15.8% (relative decline [Δ] 15.8–20.9/20.9 = -24%), respectively. Despite the decline in LVEF, no changes were made to medical therapy, as the decline in LVEF was insufficient to be classified as CTRCD according to guidelines. The patient completed chemotherapy and had a further echocardiogram at 9 months that demonstrated CTRCD with an LVEF of 47%. This case highlights the disadvantage of using LVEF as the primary marker of CTRCD. The next case will discuss the role of a GLS-guided cardioprotective strategy (Fig. 2.3, Video 2.1).

2.9 Case 2: GLS-Guided Cardioprotective Therapy during Epirubicin and Trastuzumab

- Cardiotoxicity can be detected with GLS earlier than with LVEF.
- Cardioprotective therapy when initiated appropriately can reverse cardiotoxicity.to prevent overt heart failure and aid completion of planned chemotherapy [25].

A 55-year-old woman was diagnosed with triple positive right-sided breast cancer. She had no past medical history and no cardiovascular risk factors. Her baseline echocardiogram demonstrated an LVEF 62%, GLS 23.6%. She commenced FEC-DH chemotherapy with

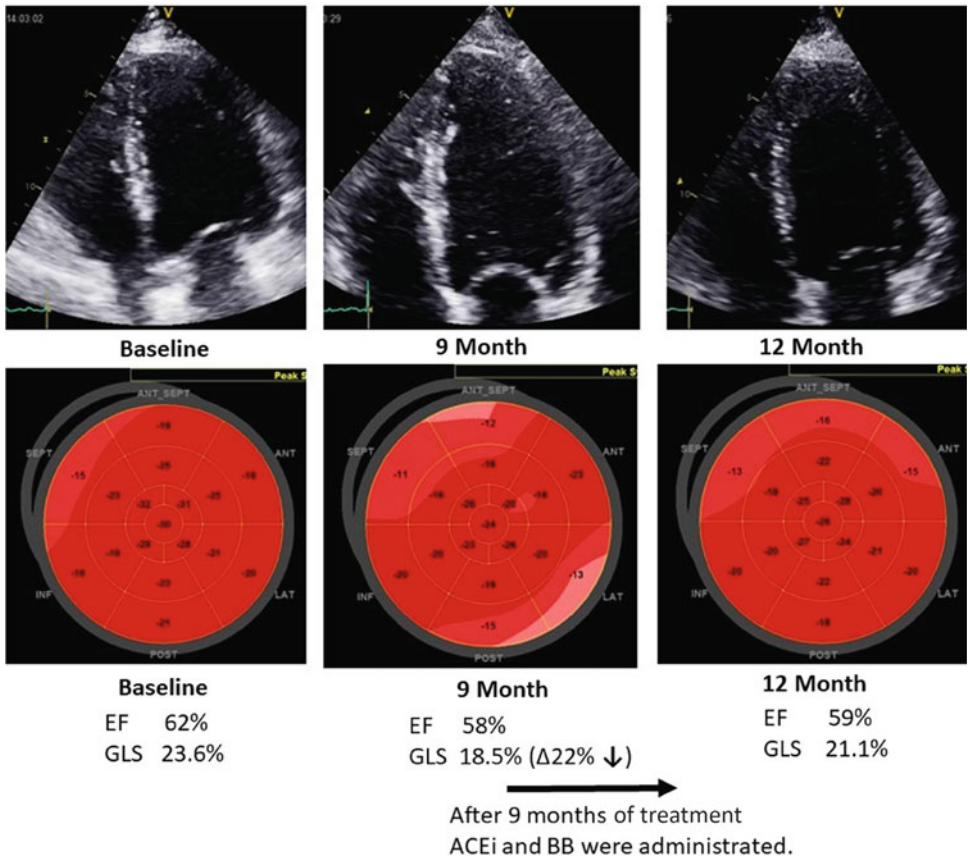

Fig. 2.4 Global Longitudinal strain guided intervention

epirubicin (90 mg/m^2), cyclophosphamide, and 5-fluroracil. She subsequently commenced docetaxel and trastuzumab. The patient was asymptomatic from a cardiovascular perspective. On a serial echocardiogram at 9 months, the LVEF and GLS declined to 58% and 18.5% (relative decline [Δ] 18.5–23.6/23.6 = −22%), respectively. The treating cardio-oncologist used a GLS-guided approach to treating with cardioprotective therapy. GLS-cardiotoxicity is defined as $\geq$12% relative decrease or $\geq$5% absolute decrease as per the latest ESMO consensus recommendations [3]. The patient was started on cardioprotective therapy which was ACEi and BB (ramipril and carvedilol). A repeat echocardiogram 3 months later (12 months from baseline) showed a significant improvement in the GLS from 15.8 to 21.1% while the LVEF remained stable at 59%. This case reinforces the recent 12 months follow-up results from a randomized control trial (SUCCOUR study). It demonstrated at 12 months follow-up, patients with a GLS-guided strategy had a lower incidence of cardiotoxicity compared to those on a LVEF guided strategy, 5 versus 13%, respectively (*presented at ESC and manuscript under review*) (Fig. 2.4, Video 2.2).

2.9.1 Case 3: Symptomatic Cardiotoxicity from Doxorubicin and Trastuzumab for Triple Positive Left-Sided Breast Cancer

- Cardiotoxicity can be missed with near fatal consequences.
- Cardioprotective therapies can be helpful in treating overt cardiotoxicity.

A 71-year-old woman with early stage triple positive left-sided breast cancer. Her treatment involved a left mastectomy, doxorubicin, cyclophosphamide, four cycles of trastuzumab, and taxol. Prior to chemotherapy, the patient had a baseline echocardiogram demonstrating normal LVEF (62%) and mildly impaired GLS (17.9%). She subsequently commenced doxorubicin (405 mg

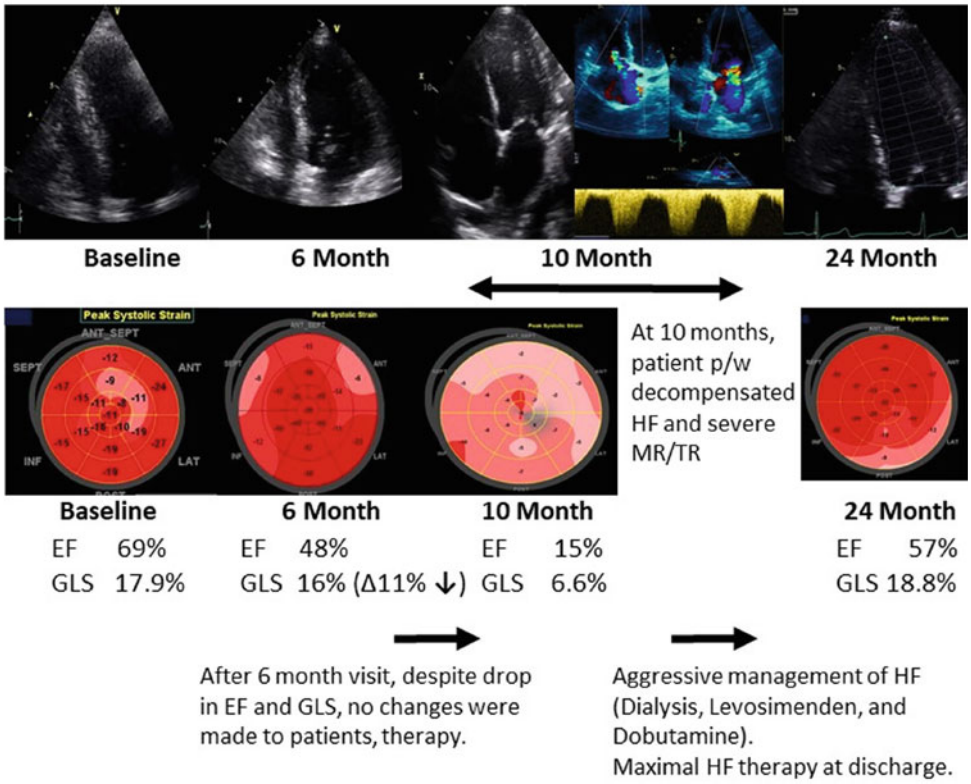

Fig. 2.5 Untreated CTRCD. HF, Heart failure; MR, Mitral regurgitation; TR, Tricuspid regurgitation

[260 g/m^2] cumulative dose) and cyclophosphamide. During chemotherapy, a serial echocardiogram was performed. There was a deterioration of the LVEF (48%) and GLS (16%) (Fig. 2.5). Unfortunately, the significance of the deterioration in the LV function was not appreciated. The patient continued chemotherapy without any changes to cancer therapy and cardioprotective therapy was not initiated. Four months later, the patient presented to the emergency department in acute pulmonary edema requiring non-invasive ventilation. An echocardiogram demonstrated severely impaired LV function (LVEF 15%) with severe mitral and tricuspid regurgitation. Given the potential for reversibility for trastuzumab induced cardiac injury, she was managed aggressively. Her acute treatment in addition to intravenous diuresis included inotropes (levosimenden and dobutamine) and a brief stint of dialysis for aggressive fluid removal. On discharge, her medical therapy consisted of nebivolol 5 mg daily, valsartan 40 mg daily, furosemide 40 mg twice daily, and ivabradine 7.5 mg twice daily. A year after her admission for decompensated heart failure, a follow-up echocardiogram demonstrated the LVEF and GLS improved to 57 and 18.8%, respectively.

2.9.2 Case 4: Surveillance Echocardiography is Important in Detecting Anthracycline and Trastuzumab Therapy. Good Acoustic Windows for Echocardiography of Patients with Breast Cancer can be Difficult Post-Surgery

- Contrast echocardiography can provide a simple solution to accurately calculate the LVEF.

A 75-year-old woman with metastatic breast cancer. Her treatment included trastuzumab, pertuzumab, and previous radiotherapy. She was referred to the Cardio-Oncology clinic as there was a concern that she had developed cardiotoxicity with an LVEF of 44%. Her main symptoms were back pain due to her metastatic

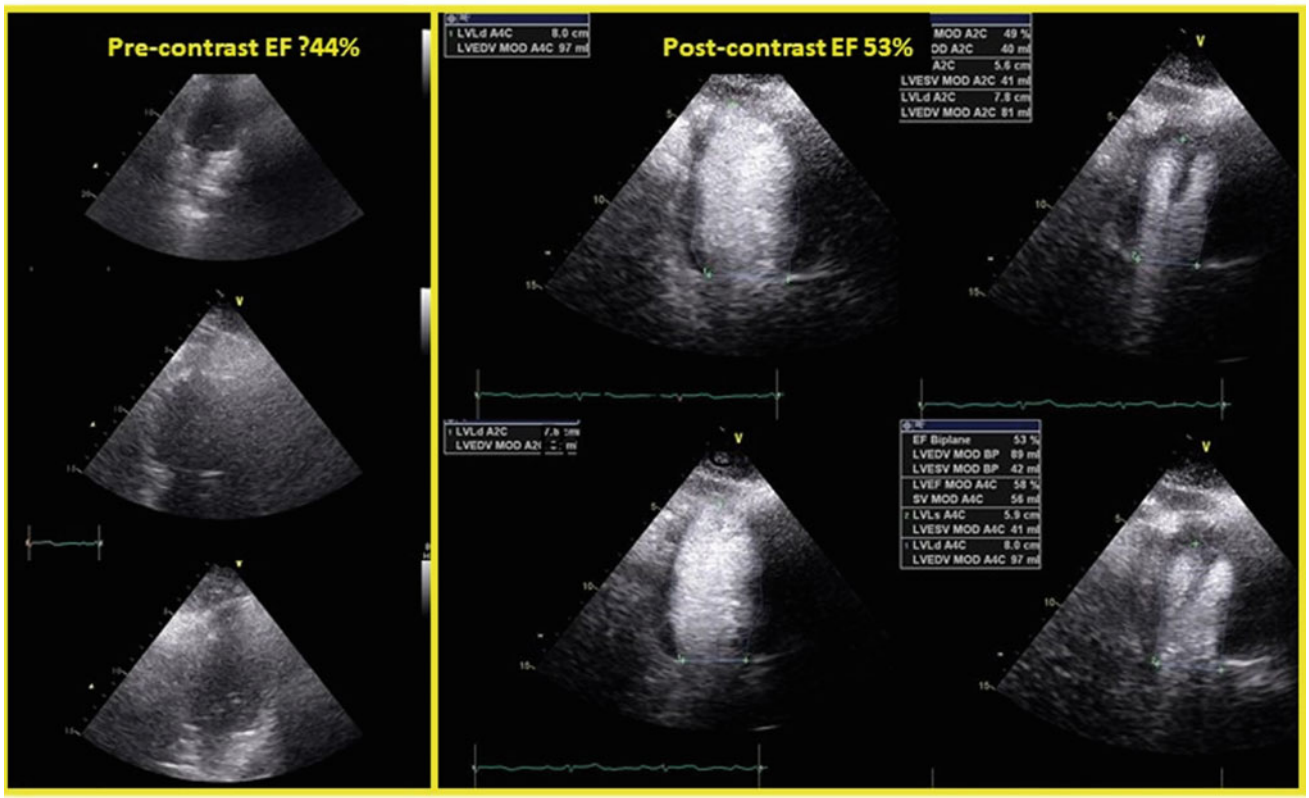

Fig. 2.6 Poor images optimized using contrast. Pre-contrast echo images were technically difficult with suboptimal visualization of the endocardial border, suggesting an estimated LVEF of 44%. Post-contrast echo images showed improved border detection, allowing more accurate quantification with LVEF now at 53%

bone disease. She had no shortness of breath or chest pain. The images were of poor quality and subsequently a contrast echocardiogram was ordered (Fig. 2.6). The contrast echocardiogram revealed an LVEF of 53%.

2.9.3 Case 5: Cardiac Magnetic Resonance Imaging Identifies Additional Unrelated Pathology Including Left Ventricular Thrombus

- CMR can provide additive information to echocardiography and nuclear imaging given its superior spatial resolution, ideal windows, and reduced susceptibility to challenging body habitus.

A 60-year-old obese (BMI 39 kg/m^2) male with a known history of ischemic cardiomyopathy and stage IV diffuse large B-cell lymphoma undergoing radiotherapy. His treatment previously included rituximab, cyclophosphamide, doxorubicin, vincristine, and prednisone. Patient had a gated heart pool scan reporting an EF of 28%. Echocardiogram with poor apical images reported impaired LVEF. Given complex decision about continuing chemotherapy for recurrent cancer and/or revascularizing known left anterior descending coronary artery disease, a viability scan with CMR was performed and demonstrated additional pathology unknown to that point (left ventricular thrombus) (Fig. 2.7). This was not appreciated on the patient's routine transthoracic echocardiogram. The LV thrombus was treated with warfarin with complete resolution.

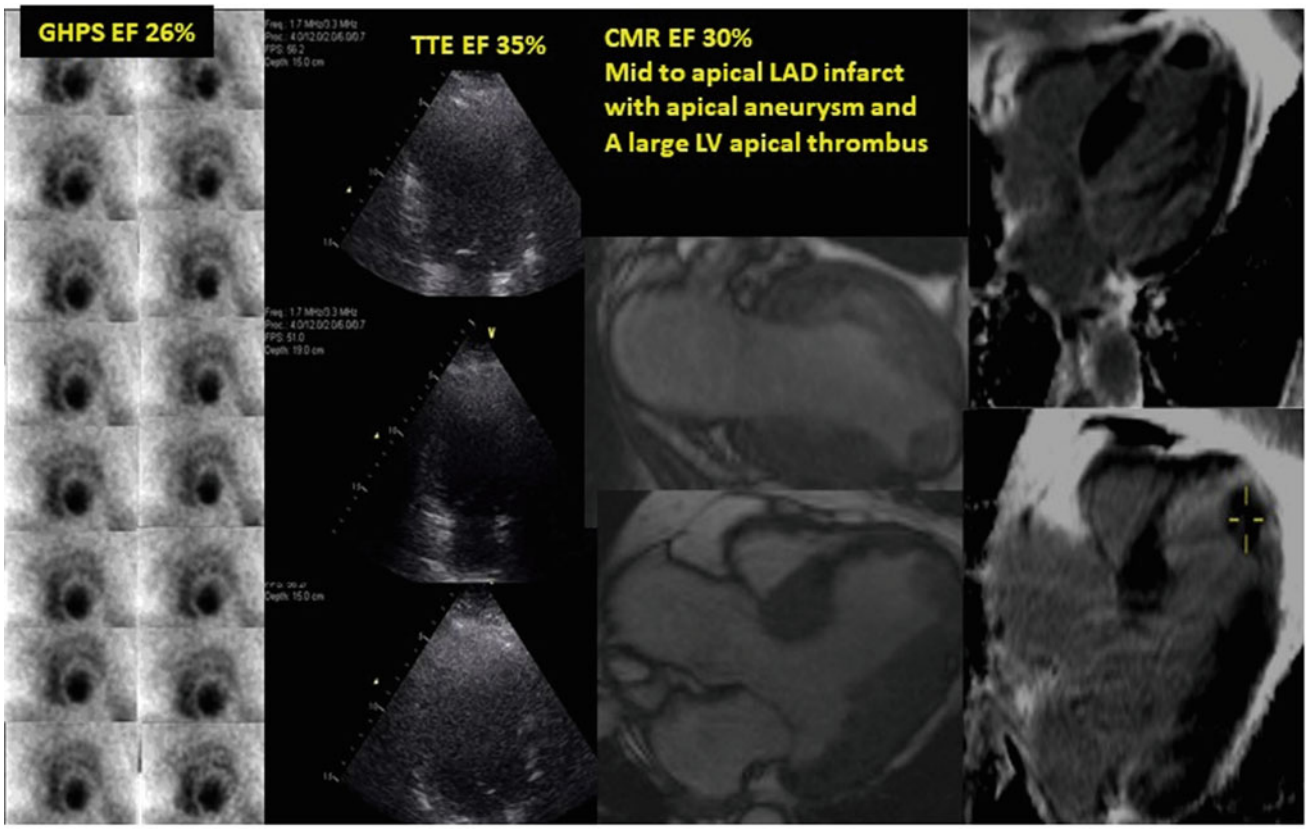

Fig. 2.7 Multi-modality imaging and additional findings using CMR. Left panel gated heart pool scan (GHPS) with EF of 26%. Next panel, transthoracic echocardiogram (TTE) with technically poor images particularly at the apex, EF 35%. Next panels cardiac magnetic resonance scan (CMR) showing apical thrombus, EF 30%. LAD, Left anterior descending; LV, left ventricle. Yellow marker indicates thrombus

References

1. Plana JC, Galderisi M, Barac A, Ewer MS, Ky B, Scherrer-Crosbie M, et al. Expert consensus for multimodality imaging evaluation of adult patients during and after cancer therapy: a report from the American society of echocardiography and the European Association of Cardiovascular Imaging. J Am Soc Echocardiogr. 2014;27(9):911–39.
2. Zamorano JL, Lancellotti P, Rodriguez Muñoz D, Aboyans V, Asteggiano R, Galderisi M, et al. 2016 ESC Position Paper on cancer treatments and cardiovascular toxicity developed under the auspices of the ESC committee for practice guidelines: the task force for cancer treatments and cardiovascular toxicity of the European Society of Cardiology (ESC). Eur Heart J. 2016;37(36):2768–801.
3. Curigliano G, Lenihan D, Fradley M, Ganatra S, Barac A, Blaes A, et al. Management of cardiac disease in cancer patients throughout oncological treatment: ESMO consensus recommendations. Ann Oncol. 2020;31(2):171–90.
4. Vejpongsa P, Yeh ETH. Prevention of anthracycline-induced cardiotoxicity: challenges and opportunities. J Am Coll Cardiol. 2014;64(9):938–45.
5. Armenian SH, Lacchetti C, Barac A, Carver J, Constine LS, Denduluri N, et al. Prevention and monitoring of cardiac dysfunction in survivors of adult cancers: american society of clinical oncology clinical practice guideline. J Clin Oncol. 2017;35(8):893–911.
6. Swain SM, Whaley FS, Ewer MS. Congestive heart failure in patients treated with doxorubicin: a retrospective analysis of three trials. Cancer. 2003;97(11):2869–79.
7. Lenneman CG, Sawyer DB. Cardio-oncology: an update on cardiotoxicity of cancer-related treatment. Circ Res. 2016;118(6):1008–20.
8. Bowles EJ, Wellman R, Feigelson HS, Onitilo AA, Freedman AN, Delate T, et al. Risk of heart failure in breast cancer patients after anthracycline and trastuzumab treatment: a retrospective cohort study. J Natl Cancer Inst. 2012;104(17):1293–305.
9. Cameron D, Piccart-Gebhart MJ, Gelber RD, Procter M, Goldhirsch A, de Azambuja E, et al. 11 years' follow-up of trastuzumab after adjuvant chemotherapy in HER2-positive early breast cancer: final analysis of the HERceptin Adjuvant (HERA) trial. Lancet. 2017;389(10075):1195–205.
10. Kalam K, Marwick TH. Role of cardioprotective therapy for prevention of cardiotoxicity with chemotherapy: a systematic review and meta-analysis. Eur J Cancer (Oxford, England: 1990). 2013;49(13):2900–9.
11. Cardinale D, Colombo A, Bacchiani G, Tedeschi I, Meroni CA, Veglia F, et al. Early detection of anthracycline cardiotoxicity and improvement with heart failure therapy. Circulation. 2015;131(22):1981–8.

12. Lancellotti P, Suter TM, Lopez-Fernandez T, Galderisi M, Lyon AR, Van der Meer P, et al. Cardio-oncology services: rationale, organization, and implementation. Eur Heart J. 2019;40 (22):1756–63.
13. Thavendiranathan P, Grant AD, Negishi T, Plana JC, Popović ZB, Marwick TH. Reproducibility of echocardiographic techniques for sequential assessment of left ventricular ejection fraction and volumes: application to patients undergoing cancer chemotherapy. J Am Coll Cardiol. 2013;61(1):77–84.
14. Senior R, Becher H, Monaghan M, Agati L, Zamorano J, Vanoverschelde JL, et al. Clinical practice of contrast echocardiography: recommendation by the European Association of Cardiovascular Imaging (EACVI) 2017. Eur Heart J Card Imaging. 2017;18(11):1205-af.
15. Negishi K, Negishi T, Hare JL, Haluska BA, Plana JC, Marwick TH. Independent and incremental value of deformation indices for prediction of trastuzumab-induced cardiotoxicity. J Am Soc Echocardiogr. 2013;26(5):493–8.
16. Lambert J, Lamacie M, Thampinathan B, Altaha MA, Esmaeilzadeh M, Nolan M, et al. Variability in echocardiography and MRI for detection of cancer therapy cardiotoxicity. Heart (British Cardiac Society). 2020;106(11):817–23.
17. Neilan TG, Coelho-Filho OR, Pena-Herrera D, Shah RV, Jerosch-Herold M, Francis SA, et al. Left ventricular mass in patients with a cardiomyopathy after treatment with anthracyclines. Am J Cardiol. 2012;110(11):1679–86.
18. Haslbauer JD, Lindner S, Valbuena-Lopez S, Zainal H, Zhou H, D'Angelo T, et al. CMR imaging biosignature of cardiac involvement due to cancer-related treatment by T1 and T2 mapping. Int J Cardiol. 2019;275:179–86.
19. Grover S, Leong DP, Chakrabarty A, Joerg L, Kotasek D, Cheong K, et al. Left and right ventricular effects of anthracycline and trastuzumab chemotherapy: a prospective study using novel cardiac imaging and biochemical markers. Int J Cardiol. 2013;168 (6):5465–7.
20. Jordan JH, Vasu S, Morgan TM, D'Agostino RB, Jr., Meléndez GC, Hamilton CA, et al. Anthracycline-associated T1 mapping characteristics are elevated independent of the presence of cardiovascular comorbidities in cancer survivors. Circ Cardiovasc Imaging. 2016;9(8).
21. Altaha MA, Nolan M, Marwick TH, Somerset E, Houbois C, Amir E, et al. Can quantitative CMR tissue characterization adequately identify cardiotoxicity during chemotherapy?: impact of temporal and observer variability. JACC Cardiovasc Imaging. 2020;13(4):951–62.
22. Bellenger NG, Burgess MI, Ray SG, Lahiri A, Coats AJ, Cleland JG, et al. Comparison of left ventricular ejection fraction and volumes in heart failure by echocardiography, radionuclide ventriculography and cardiovascular magnetic resonance; are they interchangeable? Eur Heart J. 2000;21(16):1387–96.
23. Huang H, Nijjar PS, Misialek JR, Blaes A, Derrico NP, Kazmirczak F, et al. Accuracy of left ventricular ejection fraction by contemporary multiple gated acquisition scanning in patients with cancer: comparison with cardiovascular magnetic resonance. J Cardiovasc Magn Reson. 2017;19(1):34.
24. Bauckneht M, Ferrarazzo G, Fiz F, Morbelli S, Sarocchi M, Pastorino F, et al. Doxorubicin effect on myocardial metabolism as a prerequisite for subsequent development of cardiac toxicity: a translational (18)F-FDG PET/CT observation. J Nucl Med. 2017;58(10):1638–45.
25. Santoro C, Esposito R, Lembo M, Sorrentino R, De Santo I, Luciano F, et al. Strain-oriented strategy for guiding cardioprotection initiation of breast cancer patients experiencing cardiac dysfunction. Eur Heart J Cardiovasc Imaging. 2019;20(12):1345–52.
26. Shaw LJ, Min JK, Hachamovitch R, Peterson ED, Hendel RC, Woodard PK, et al. Cardiovascular imaging research at the crossroads. JACC Cardiovasc Imag. 2010;3(3):316–24.

Immune Checkpoint Inhibitor (ICI)-Associated Myocarditis

3

Nicolas L. Palaskas, Eric H. Yang, and Tomas G. Neilan

Key Points

- ICIs have revolutionized the treatment of cancers, specifically melanoma, lung, and genitourinary malignancies, with significant improvements in oncologic outcomes.
- The most serious of the immune-related adverse events (irAEs) is myocarditis, with a reported mortality of 25–50%. However, ICI-associated myocarditis is uncommon with an incidence of 1–2% in recent publications.
- The only established risk factor is the use of combination ICI therapy.
- The mainstay of treatment for ICI-associated myocarditis is glucocorticoids.
- The presentation may be non-specific, at times insidious, other times fulminant. Multiple imaging modalities, serial biomarkers, myocardial biopsy, and astute clinical judgement in combination with a high index of suspicion are all required to diagnosis and manage these complex patients.

3.1 Introduction

The observation of an association between the use of immune checkpoint inhibitors (ICI) and the development of myocarditis is relatively recent. Despite the presumed low incidence of myocarditis, increasing use and the expansion of ICI for treating different malignancies have led to an increase in the number of cases being seen in academic centers and the community. Any cardio-oncology practice must be equipped to recognize and treat this potentially fatal disease. The diagnosis of ICI-associated myocarditis is complicated and relies on a combination of clinical, laboratory, imaging, and biopsy findings. All patients with suspected ICI myocarditis should be admitted for assessment. Various treatment regimens have been reported with the mainstay of treatment involving cessation of the ICI and the administration of corticosteroids. The three cases presented below will highlight differences in clinical presentations, diagnostic tests, and treatments followed by an in-depth discussion of these differences.

3.2 Cases

3.2.1 Case 1. Relatively Asymptomatic but Troponin is Elevated

An 80-year-old male presented with a history of coronary artery disease, hypertension, and hyperlipidemia. He underwent coronary artery bypass grafting in 2016 for an acute coronary syndrome. He has been free of cardiovascular symptoms since that time and was physically very active. In late 2018, he was diagnosed with metastatic melanoma and was started on a PD-1 inhibitor in January 2019. He received a single dose. Four weeks later, he presented with new onset of fatigue with exertion. He was without chest pain or shortness of breath. On examination, he had a regular rhythm at 78 beats per minute. His blood pressure was

Electronic supplementary material
The online version of this chapter (https://doi.org/10.1007/978-3-030-70998-3_3) contains supplementary material, which is available to authorized users.

N. L. Palaskas
Department of Cardiology, Division of Internal Medicine, University of Texas MD Anderson Cancer Center, Houston, TX, USA
e-mail: nlpalaskas@mdanderson.org

E. H. Yang
Division of Cardiology, Department of Medicine, UCLA Cardio-Oncology Program, University of California at Los Angeles, Los Angeles, CA, USA
e-mail: ehyang@uclahealth.org

T. G. Neilan (✉)
Cardio-Oncology Program, Division of Cardiology, Department of Medicine, Massachusetts General Hospital, 165 Cambridge Street, Suite 400, Boston, MA 02114, USA
e-mail: TNEILAN@mgh.harvard.edu

R. M. Steingart et al. (eds.), *Atlas of Imaging in Cardio-Oncology*, https://doi.org/10.1007/978-3-030-70998-3_3

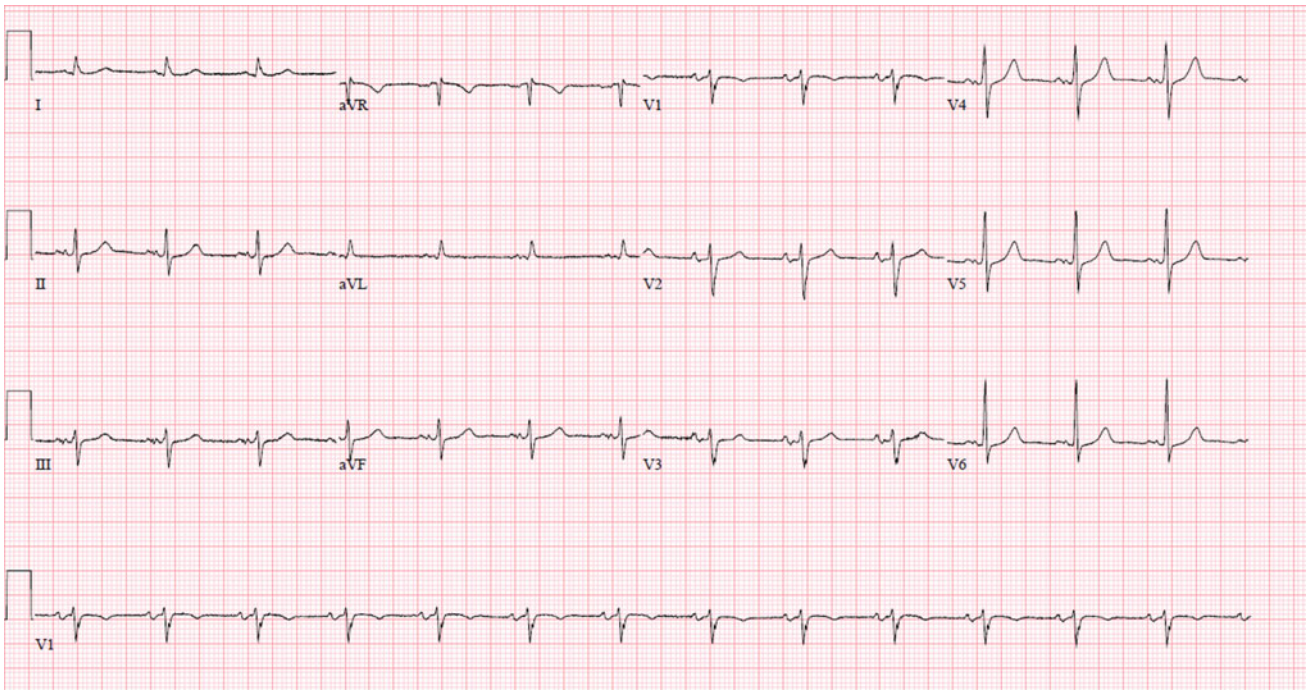

Fig. 3.1 Presentation EKG showing sinus rhythm, a left atrial abnormality, but was otherwise unremarkable

126/72 and he had no signs of heart failure. He had an EKG (Fig. 3.1) which, apart from a left atrial abnormality, was unremarkable. His creatinine kinase was 3,005 U/L (normal <400 U/L). His HsTNT was 369 ng/L (normal <14 ng/L). His ICI was held and he was admitted to the in-patient cardiology service with a consult to the cardio-oncology team. He had a transthoracic echocardiogram (Fig. 3.2, Video 3.1). This echocardiogram showed normal left ventricular (LV) size and ejection fraction (LVEF 72%). There was abnormal interventricular septal motion. The left atrial volume was increased and the pulmonary artery systolic pressure was 42 mmHg. There was no pericardial effusion. He underwent cardiac magnetic resonance imaging. This confirmed normal LV size and EF without significant wall motion abnormality or pericardial effusion. The right ventricle also had a normal volume and function. There was no evidence of myocarditis using late gadolinium enhancement imaging or black blood T2 imaging (Fig. 3.3). Parametric T1

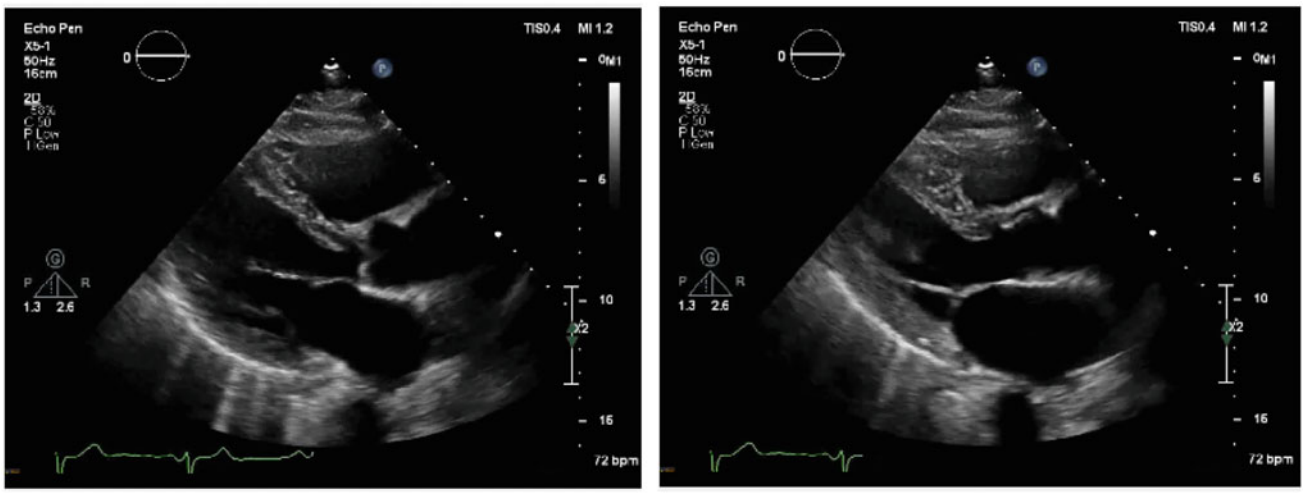

Fig. 3.2 Transthoracic echocardiogram showing normal left ventricular (LV) size and ejection fraction (LVEF 72%). There was abnormal interventricular septal motion. The left atrial volume was increased and the pulmonary artery systolic pressure was 42 mm Hg. There was no pericardial effusion

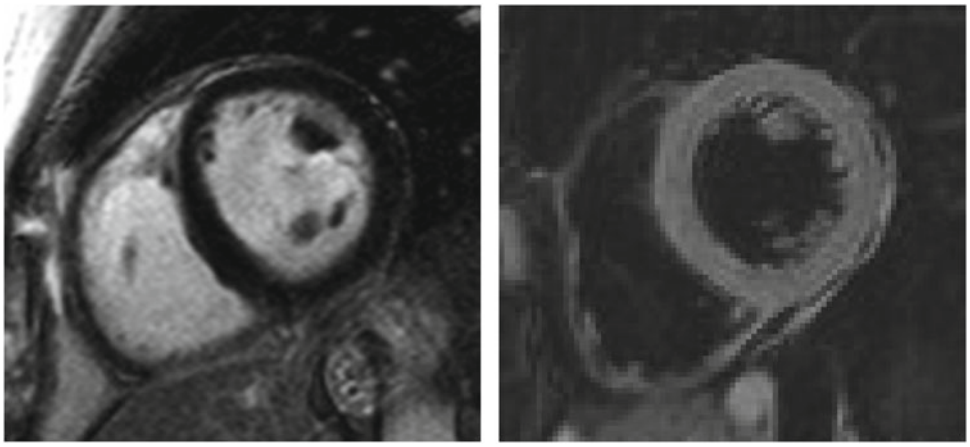

Fig. 3.3 Still images from the cardiac MRI imaging. There was no evidence of myocarditis using late gadolinium enhancement imaging or black blood T2 imaging. Parametric T1 or T2 mapping was not available

or T2 mapping was not available. The troponin-T increased to 563 ng/L on the day of admission while creatine kinase decreased slightly to 2,776 U/L. The patient remained stable but in view of the rising troponin and negative cardiac MRI, an endomyocardial biopsy was performed. This showed focal infiltration by lymphocytes, macrophages, and scattered eosinophils with associated cardiomyocyte injury consistent with myocarditis (Fig. 3.4). He was started on a gram of methylprednisone per day, prophylaxis for pneumocystis pneumonia, and a proton pump inhibitor. His troponin did not decrease. On day 5, he was treated with a single dose of infliximab 5 mg/kg without effect on his serum troponin. On day 7, a repeat dose of infliximab was administered, while he transitioned to 60 mg of oral prednisone per day. The serum troponin increased. The patient remained stable with occasional new frequent episodes of non-sustained ventricular tachycardia (NSVT). Mycophenolate mofetil was added at 750 mg twice a day, rising to 1000 mg twice a day. His troponin began to decline (Fig. 3.5). However, on day 30 of his admission, he developed frequent runs of NSVT and, after a family meeting where several options were presented, it was decided to administer intravenous immunoglobulin. His episodes of NSVT resolved. Six weeks after discharge, he presented with odynophagia, an esophagogastroscopy was performed and biopsies revealed cytomegalovirus esophagitis. His viral load was very elevated and he was treated with ganciclovir and later transitioned to oral valganciclovir. Two weeks after that discharge, he reported bilateral lower extremity edema. He had a lower extremity duplex ultrasound which revealed bilateral deep venous thrombosis and he was started on enoxaparin. One week after that he was admitted with an upper GI bleed. Three weeks later, his oral intake was poor and he was losing weight. He was diagnosed with Candidal esophagitis. He was treated with fluconazole. Thereafter he did well symptomatically, and was ultimately able to exercise for 2 hours daily. He presented eight months later with coffee-ground emesis and was found to have a large submucosal mass in the gastric body with pathology consistent with metastatic melanoma. He had a gastric wedge resection and is well and cancer-free 19 months after his initial presentation.

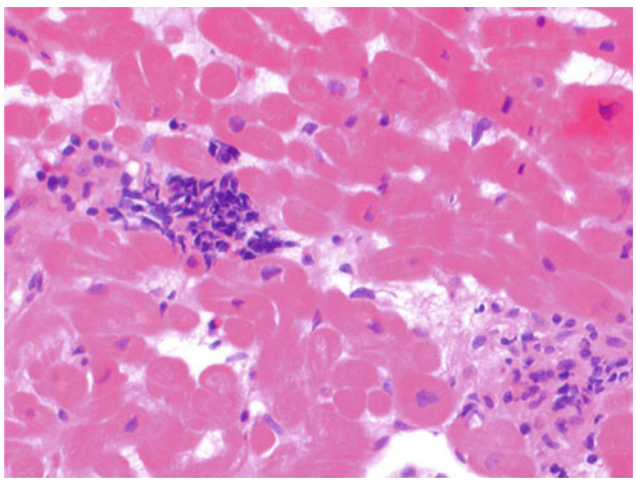

Fig. 3.4 Pathological images from endomyocardial biopsy showing focal infiltration by lymphocytes, macrophages, and scattered eosinophils with associated cardiomyocyte injury consistent with myocarditis

3.2.2 Case 2. Moderately Symptomatic with Abnormal Imaging

A 67-year-old female with a history of metastatic urothelial carcinoma presented to the emergency room with several weeks of worsening pelvic and abdominal pain related to her malignancy, along with fatigue and weakness. She denied any symptoms of chest pain, dyspnea, fevers, chills, nausea, or vomiting and was debilitated due to severe abdominal pain. Her oncologic history was significant for a diagnosis of

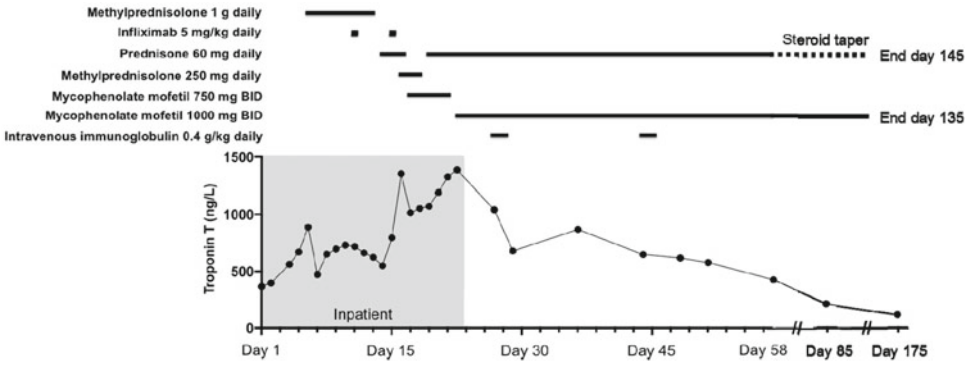

Fig. 3.5 Clinical course of the patient with troponin change over time and each of the treatments that were instituted at each time point and how the troponin responded. The patient was treated with solumedrol, infliximab, mycophenolate, and IVIG at different stages

urothelial cancer with pelvic lymphadenopathy and peritoneal carcinomatosis. She had undergone six cycles of cisplatin and gemcitabine; given a lack of clinical response, she was started on combination immunotherapy with a PD-L1 inhibitor and a T cell immunoreceptor with Ig and ITIM domains (TIGIT) inhibitor. Her first treatment was administered 5 days prior to presentation. Her vital signs were significant for hypotension at 80/63 mm Hg and a heart rate of 116 bpm. She was afebrile with an oxygen saturation of 98% on room air. Her cardiovascular examination was negative for jugular venous distension, peripheral edema, murmurs, rubs, gallops, S3 or S4. Lung auscultation was unremarkable. Her physical examination was only positive for pelvic/abdominal pain on palpation without any signs of acute abdomen. The patient's laboratory results were significant for a leukocytosis of 49.9×10^3/microliter, a hemoglobin level of 14.5 g/dL, and a platelet count of 300×10^3/microliter. Her electrolytes were significant for a potassium of 6.6 mmol/L, and an elevated creatinine of 2.0 mg/dL. Liver enzymes were mildly elevated with an aspartate aminotransferase level of 69 U/L, and an alanine aminotransferase level of 16 U/L. Thyroid-stimulating hormone levels were within normal limits. Her total creatine kinase level was elevated at 596 U/L and troponin-I levels were elevated at 10.4 ng/mL. A 12-lead electrocardiogram (ECG) obtained on admission was significant for sinus tachycardia with diffuse ST segment elevations seen in the precordial and inferior limb leads (Fig. 3.6). A transthoracic echocardiogram (TTE) obtained demonstrated low normal left ventricular ejection fraction (LVEF) of 50–55%, with dyskinetic motion of the mid to distal left ventricle with normal wall motion of all other wall segments (Fig. 3.7, Video 3.2). ECG and TTE prior to ICI treatment were both unremarkable. Coronary angiography and cardiac magnetic resonance imaging were recommended and offered to the patient, but ultimately not performed in line with her goals of care. The wall motion abnormalities noted on TTE were not congruent with the extent of ST segment elevations seen on ECG, nor was it consistent with a myocardial injury pattern with traditional coronary anatomy; thus, the leading diagnosis was stress-induced (Takotsubo) cardiomyopathy (see Chap. 15) and probable perimyocarditis (abnormal cardiac biomarkers and atypical wall motion abnormalities on echocardiography) associated with ICI use. A total of 1 g methylprednisone was given intravenously for 5 days, then switched to oral prednisone 60 mg daily. The patient's troponin-I levels peaked at 26.4 ng/mL on hospital day 2 and down trended afterwards; the patient never had symptoms of myocardial ischemia or heart failure. A repeat TTE done 7 days after admission demonstrated an improved LVEF at 60–65% with resolving—but still present—wall motion abnormalities in the distal left ventricle. Because of the patient's poor prognosis and ongoing severe pain related to her malignancy, and in discussion with the patient and family, the decision was made to transition the patient to hospice and palliative care. The patient passed away on hospital day 17; autopsy was declined by the family.

3.2.3 Case 3. Life-Threatening Myocarditis

A 74-year-old man with metastatic bladder cancer presented with severe fatigue, dyspnea, and lightheadedness 5 days after receiving the second dose of nivolumab (PD-1 inhibitor). The patient had a past medical history of hypertension but notably no history of coronary artery disease, CVA, dyslipidemia, or diabetes. On arrival to the emergency room he had a heart rate of 27 beats per minute and hypotension with blood pressure of 93/61 mmHg. The electrocardiogram revealed complete heart block with a ventricular escape rhythm (Fig. 3.8). A temporary pacemaker was placed at the bedside in the emergency room with improvement in blood pressure and dizziness; however, the patient had continued

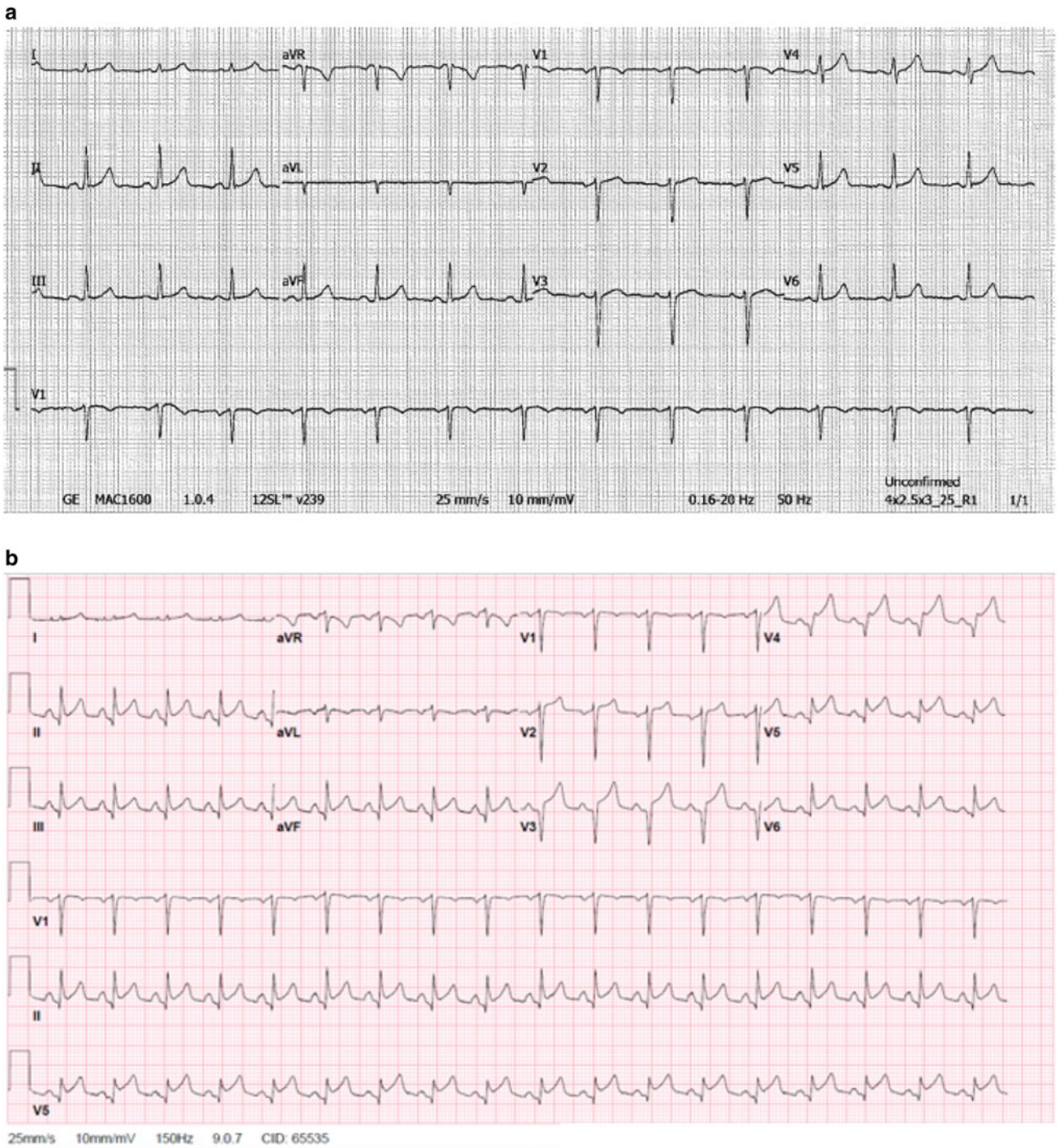

Fig. 3.6. 12-lead electrocardiograms before and during presentation of immune checkpoint inhibitor (ICI) associated myocarditis. Panel A: Normal 12-lead ECG two weeks before ICI treatment. Panel B: 12-lead ECG on admission for suspected ICI-associated myocarditis sinus tachycardia with diffuse ST segment elevations in the precordial and inferior limb leads. PR segment depressions are seen in the precordial leads.

fatigue and dyspnea. The initial troponin-T value was 1085 ng/L and echocardiogram revealed normal left ventricular systolic function with a moderate-sized pericardial effusion (Fig. 3.9). The patient is taken to the catheterization laboratory for left and right heart catheterization with endomyocardial biopsy which ruled out acute coronary syndrome, and biopsy results reveal lymphocytic infiltration with myocyte necrosis consistent with myocarditis

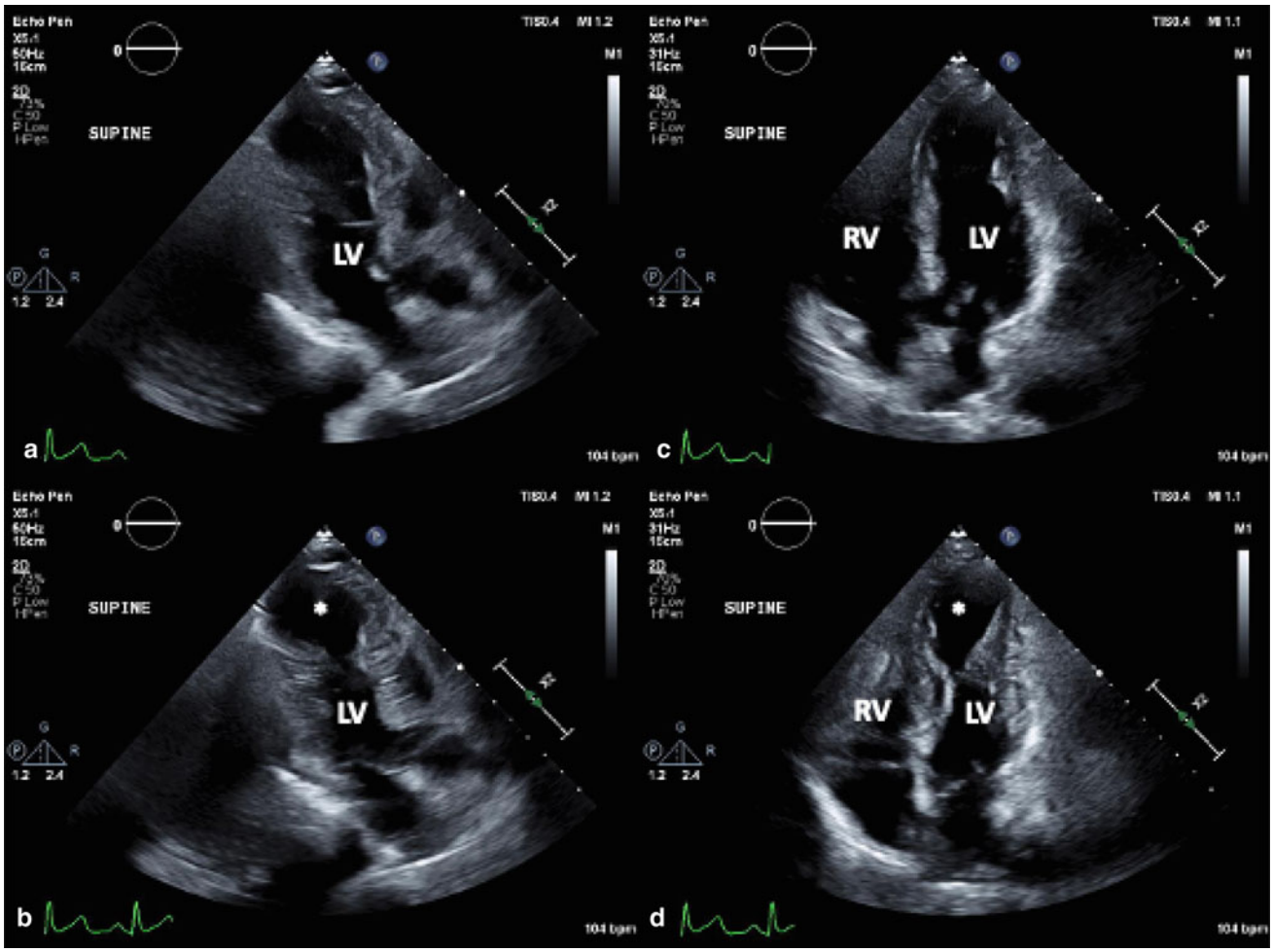

Fig. 3.7 Transthoracic echocardiography on admission. Apical three-chamber views in diastole (Panel A) and systole (Panel B), and apical four-chamber views in diastole (Panel C) and systole (Panel D) demonstrate dyskinesis of the distal left ventricle (*), including the mid to distal lateral, septum, apex, and anterior walls. Because the wall motion abnormalities were incongruous with the extent of the diffuse ST elevations noted on 12-lead electrocardiogram, imaging was suggestive of stress-induced (Takotsubo) cardiomyopathy and peri-myocarditis associated with immune checkpoint inhibitor use. Left ventricular ejection fraction (LVEF) was calculated at 50–55%. Repeat echocardiography 7 days later demonstrated an improvement in LVEF with improved, but persistent distal wall motion abnormalities. LV: left ventricle. RV: right ventricle

(Fig. 3.10). The patient was initiated on high-dose steroids at 1 g solumedrol daily for 3 days followed by 1 mg/kg daily of prednisone with a troponin peak of 1454 ng/L. However, his respiratory status continued to decline and he required intubation for mechanical ventilation. Therefore, second-line therapy was initiated with plasmapheresis (5 sessions) followed by intravenous immunoglobulin for three doses with improvement allowing for extubation. The complete heart block persisted and he required permanent pacemaker implantation. The troponin levels decreased to 291 ng/L but never became normal. He continued a corticosteroid taper over the next 6 weeks. The patient did not have any other therapeutic options for his metastatic bladder cancer, and therefore, a decision was made to pursue hospice and he passed away 6 months after discharge.

3.3 Discussion

3.3.1 Background

ICIs have revolutionized the treatment of cancers, specifically melanoma, lung, and genitourinary malignancies, with significant improvements in oncologic outcomes [1]. They are a form of immunotherapy that is relatively new with the first ICI being approved by the United States Food and Drug Administration (FDA) in 2011. Ipilimumab was the first ICI developed and is a cytotoxic T-lymphocyte associated protein 4 (CTLA-4) inhibitor. Since then, there have been six additional FDA-approved ICI which are all programmed cell death protein 1 (PD1) or programmed death-ligand 1

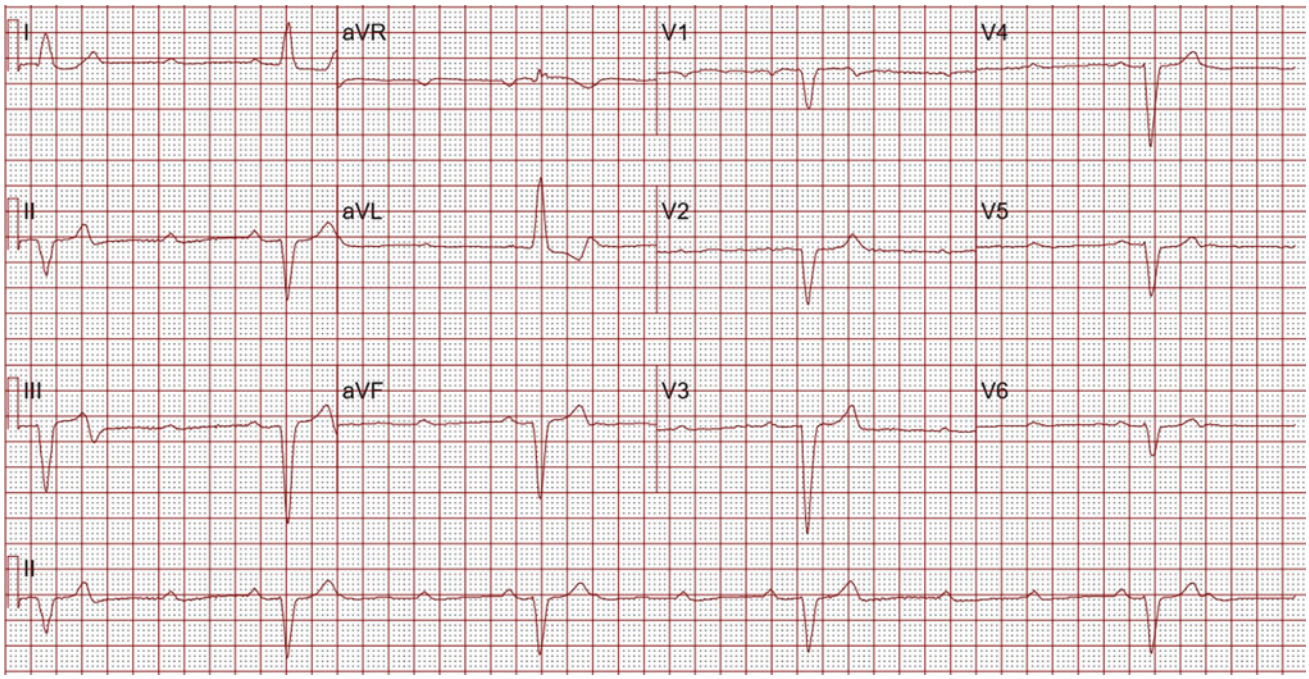

Fig. 3.8 12-lead electrocardiogram showing complete heart block and ventricular escape rhythm at 27 beats per minute

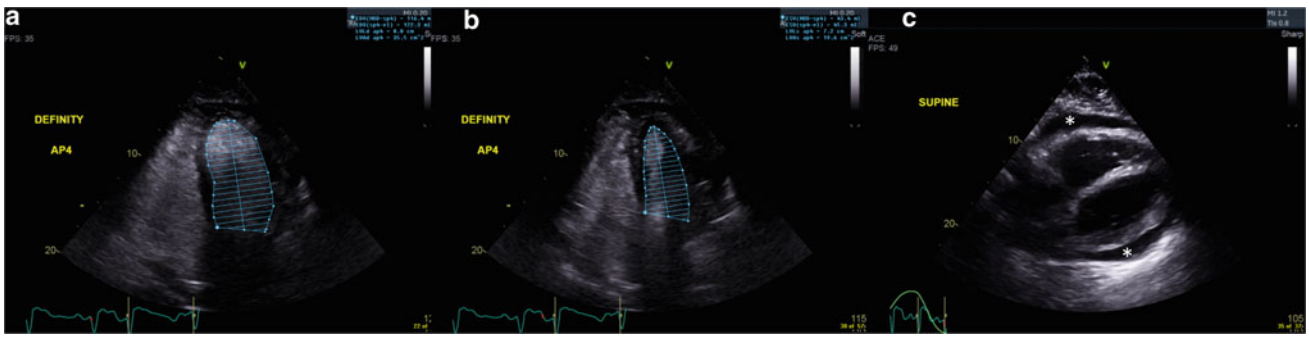

Fig. 3.9 Echocardiographic images showing normal left ventricular ejection fraction, 55% per biplane modified Simpson's, and a moderate-sized pericardial effusion. **a** Apical four-chamber view with micro-bubble-enhanced image showing modified Simpson's end-diastolic volume measurement. **b** Apical four-chamber view with micro-bubble-enhanced image showing modified Simpson's end-systolic volume measurement. **c** Subcostal image showing circumferential moderate-sized pericardial effusion (white asterisks)

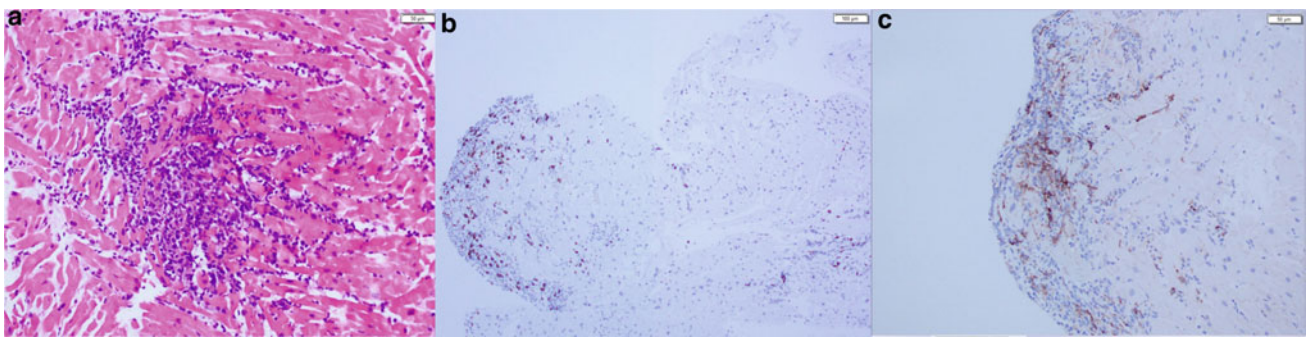

Fig. 3.10 Endomyocardial biopsy pathology slides showing inflammatory infiltrate and myocyte loss consistent with myocarditis. **a** Hematoxylin and eosin stain showing inflammatory infiltrate with myocyte loss. **b** Immunohistochemical stain for CD8+ T cells showing patchy infiltration of the myocardium. **c** Immunohistochemical stain for programmed death ligand 1 (PD-L1) showing increased uptake in the areas of inflammatory infiltrate

(PD-L1) inhibitors. There are numerous other classes of ICI currently in development with notable targets, including lymphocyte activation gene-3 (LAG-3), T cell immunoglobulin, ITIM domain (TIGIT), and V-domain Ig suppressor of T cell activation (VISTA). It was anticipated that leveraging the immune system would be associated with immune-related adverse events (irAEs) affecting multiple parts of the body from the thyroid to the joints [2]. The most serious of the irAEs is myocarditis with a reported mortality of 25–50% [3–6]. However, ICI-associated myocarditis is uncommon with an incidence of 1–2% in recent publications [4]. The cases presented above highlight several important aspects of myocarditis: the varied clinical presentation, various modalities used for diagnosis, and evolving treatments.

3.3.2 Pathophysiology

Malignant cells can evade the immune system by immune checkpoints which abrogate the activation of immune cells [7]. T cell activation requires co-stimulation with both antigen presentation to T cell receptors and activation of CD28 receptors by B7 molecules on antigen presenting cells [8, 9]. Immune checkpoints such as CTLA-4 bind to B7 molecules with higher affinity than CD28 receptors and thus suppress T cell activation [10]. By inhibition of immune checkpoints or of their ligand, PD-L1, T cells can recognize tumor cells and attack the cancer. However, releasing the brakes on the T cell activation can result in unwanted off-target effects such as T cells attacking normal tissues. Endomyocardial biopsies of patients with ICI-associated myocarditis reveal predominantly T cell infiltration of the myocardium that resembles acute cellular rejection in transplanted hearts [3, 11]. The proposed mechanism is via molecular mimicry and shared epitopes between antigens of tumor cells and substructures of the myocardium [3]. Further research is needed to confirm this as the mechanism of ICI cardiotoxicity.

3.3.3 Clinical Presentation

Beyond combination immune therapy, the risk factors for ICI-associated myocarditis are incompletely understood. Additional risk factors suggested include age, pre-existing cardiovascular disease, and hypertension [12, 13]. Patients with ICI-associated myocarditis present with a myriad of symptoms and there is a spectrum of clinical presentations ranging from smoldering to fulminant [3, 14, 15]. Some of the more common symptoms are non-specific, including fatigue, dyspnea, and weakness which makes the diagnosis difficult. Patients may also present in heart failure with orthopnea, paroxysmal nocturnal dyspnea, and volume overload or present with chest pain similar to an acute coronary syndrome [16–19]. The most concerning presentations are those of fulminant myocarditis in which patients present in shock with hemodynamic instability either from hypoperfusion due to cardiac failure, complete heart block, or ventricular tachycardia/sudden cardiac death [3, 18]. Initial reports of myocarditis suggested that this was a rare disease occurring in 0.06% of those with monotherapy and 0.27% of those on combination therapy [3]. It is likely that these were capturing only the fulminant cases of myocarditis [20]. As recognition of this disease entity has improved, less severe clinical presentations have been diagnosed as myocarditis and the incidence has increased to approximately 1% [4]. Most commonly, myocarditis will occur within the first 2 months after initiation of ICI, however, late presentations up to 454 days after starting ICI have been described [4].

The only established risk factor is the use of combination ICI therapy as opposed to monotherapy with smaller reports suggesting the possibility of female sex, obesity, and increased neutrophil to lymphocyte ratio at baseline as potentially additional risk factors [3]. It is worth noting that traditional cardiac risk factors for anthracycline cardiotoxicity such as age, hypertension, diabetes, coronary artery disease, and congestive heart failure do not appear to be risk factors for developing ICI-associated myocarditis. In addition, multiple irAE can occur in patients at the same time. The most common irAE to overlap with ICI-associated myocarditis are myasthenia gravis and myositis [2], with the overlap associated with a higher mortality. It can be difficult to differentiate whether symptoms of dyspnea and fatigue are due to myocardial involvement of myocarditis versus neuromuscular junction or muscle cell involvement of myasthenia gravis or myositis.

3.3.4 Diagnosis

The diagnosis of ICI-associated myocarditis is dependent on a combination of the clinical presentation, laboratory data, non-invasive imaging, and/or endomyocardial biopsy [11, 21]. Each test has its limitations in making a diagnosis of myocarditis which will be discussed below. Therefore, a combination of several tests in addition to the clinical presentation and ruling out more common cardiac conditions such as acute coronary syndrome or ischemic heart disease [19] is necessary prior to making the diagnosis of ICI-associated myocarditis. Bonaca et al. proposed diagnostic criteria for myocarditis in the setting of cancer therapeutics that separated the diagnosis into three categories

(definite myocarditis, probable myocarditis, or possible myocarditis) based on combinations of the clinical presentation and diagnostic tests. The criteria include [22]:

1. Definite Myocarditis: presence of at least one of the following
   a. Pathology consistent with myocarditis
   b. Diagnostic CMR, clinical syndrome of myocarditis, and positive biomarker or EKG
   c. Echo with wall motion abnormality, clinical syndrome of myocarditis, positive biomarker, positive EKG, and negative angiography for CAD
2. Probable Myocarditis:
   a. Diagnostic CMR without clinical syndrome of myocarditis, positive EKG, or positive biomarker OR
   b. Suggestive CMR with one of the following:
      i. Clinical syndrome of myocarditis
      ii. Positive EKG
      iii. Positive biomarker OR
   c. Echo with wall motion abnormality and clinical syndrome of myocarditis with either positive EKG or biomarker OR
   d. Clinical syndrome of myocarditis with PET scan evidence and no alternative diagnosis
3. Possible Myocarditis
   a. Suggestive CMR without clinical syndrome of myocarditis, positive EKG, or positive biomarker OR
   b. Echo with wall motion abnormality and clinical syndrome of myocarditis or positive EKG OR
   c. Elevated biomarker with clinical syndrome of myocarditis or positive EKG and no alternative diagnosis.

Laboratory data: Cardiac biomarkers such as troponin-I and troponin-T are typically elevated in cases of myocarditis. Elevations in troponin have prognostic value, as Mahmood et al. showed that troponin-T values above 1.5 g/dL were associated with a fourfold increased risk of major adverse cardiovascular events [4]. Elevations in troponin are non-specific findings and more common causes such as acute coronary syndrome and demand ischemia due to sepsis, for example, must be excluded prior to making the diagnosis of ICI-associated myocarditis. Troponin-I is preferred over troponin-T due to cross-reactivity of troponin-T with skeletal muscle [22]. Often creatinine kinase (CK) and creatinine kinase-muscle/brain (CK-MB) are also elevated during myocarditis; however, given the overlap with myositis and myasthenia gravis, additional workup for these irAEs should be considered when significant elevations are observed in CK and CK-MB out of proportion to troponin elevation. Some institutions have implemented routine cardiac biomarker surveillance strategies during ICI therapy; however, it is unknown whether there is benefit to performing such surveillance due to the low incidence of myocarditis. Chuy et al. attempted this strategy in 76 patients with weekly biomarker surveillance for the first 6 weeks after starting ICI but no cases of myocarditis were observed [23]. Baseline troponin values have not been shown to be predictive of ICI myocarditis but can be helpful as a comparison if symptoms develop and there is suspicion of myocarditis after initiation of ICI [4].

Electrocardiogram: Various electrocardiogram (EKG) abnormalities have been described in patients presenting with ICI-associated myocarditis. The most concerning EKG findings that warrant immediate intervention and workup include advanced atrioventricular block and ventricular tachycardia or increased runs of non-sustained ventricular tachycardia/premature ventricular complexes. These abnormalities have been described in fulminant myocarditis and carry a high mortality [3]. Of course, other more common causes of these arrhythmias may need to be excluded. More subtle EKG changes such as prolonging PR or QRS intervals can be harbingers of myocarditis and patients with these changes should have a myocarditis workup performed. After admission for suspected myocarditis, it is common to place patients on telemetry to monitor for arrhythmias that may occur early in the disease course. Baseline EKGs are not predictive of subsequent myocarditis events [4] and similar to cardiac biomarkers, EKG surveillance strategies are of unknown benefit due to the low incidence of myocarditis [23].

Echocardiograms: Typically, with viral myocarditis, a dilated cardiomyopathy is observed. With ICI-associated myocarditis patients can present with preserved or reduced left ventricular ejection fraction [21]. Mahmood et al. described 51% of patients presenting with preserved left ventricular ejection fraction, but despite maintaining a normal left ventricular ejection fraction 38% developed major adverse cardiovascular events [4]. Supporting findings of ICI-associated myocarditis on echocardiograms include the development of a pericardial effusion and a reduction in global longitudinal strain [21]. Similar to electrocardiograms, the baseline echocardiogram before the start of ICI therapy has not been predictive of subsequent ICI-associated myocarditis [4]. In contrast to anthracycline cardiotoxicity, a depressed left ventricular ejection fraction is not necessarily a contraindication to ICI therapy.

Cardiac Magnetic Resonance Imaging: The best non-invasive diagnostic test for myocarditis is cardiac magnetic resonance imaging (CMR) because of its superior ability to characterize tissue. In the setting of viral myocarditis, CMR has shown good correlation with endomyocardial biopsy results [18]. The updated Lake Louise criteria are used for the CMR diagnosis of

myocarditis and apply a combination of myocardial edema and fibrosis [24]:

1. Main criteria (2 out of 2): If both myocardial edema and non-ischemic myocardial injury are identified, then CMR is highly suggestive of myocarditis with greater specificity. Having only one main criterion may still support the diagnosis of myocarditis in the correct clinical setting.
   a. **Myocardial edema**:
      i. Abnormal findings in T2 mapping or T2-weighted images
   b. Non-ischemic myocardial injury:
      i. Abnormal findings on T1, LGE, or ECV
2. Supportive criteria (Helpful, suggestive, not definitive):
   a. Pericarditis
      i. Evidence of pericardial effusion, or abnormal LGE/T2 or T1 findings in pericardium
   b. Left ventricular systolic dysfunction
      i. Regional or global wall motion abnormalities.

The correlation of CMR with endomyocardial biopsy in ICI-associated myocarditis is not robust. Zhang et al. found that in 103 patients with known ICI myocarditis and CMR studies, only 48% had late gadolinium enhancement. The presence of late gadolinium enhancement was found more commonly if the CMR was performed greater than 4 days after admission [11]. A limitation of this study was the lack of parametric mapping. While it has its limitations, CMR remains the best non-invasive diagnostic test for ICI-associated myocarditis and can make a definitive diagnosis of myocarditis when used in combination with the clinical presentation and/or cardiac biomarkers.

Endomyocardial biopsy: The gold standard diagnostic test for myocarditis is endomyocardial biopsy. The pathologic diagnosis is based on the Dallas Criteria which require the presence of inflammatory infiltrate and myocyte necrosis [25]. Immunohistochemical staining of the inflammatory infiltrate has shown a predominant T cell infiltration with CD8+ and CD4+ inflammatory cells, however, myeloid cells with CD68+ inflammatory cells have also been observed [3, 26]. There are reports of an antibody-mediated component with peri-capillary C4d+ staining which is seen in heart transplant antibody-mediated rejection [27]. It is recommended to obtain 4–6 biopsy samples due to the patchy nature of myocarditis and sampling error when obtaining biopsies [25]. The most common site for endomyocardial biopsy is the right ventricular septal wall. Despite obtaining 4–6 biopsy samples, ICI-associated myocarditis can have focal involvement of the myocardium, and if the right ventricular septal wall is not involved, then the biopsy will be negative. In addition, endomyocardial biopsies are performed at specialized centers with experience in this procedure and while generally safe do have a risk of major complications such as right ventricular laceration. Patients with cancer also can have thrombocytopenia which limits the ability to perform this invasive procedure.

3.3.5 Treatment

The mainstay of treatment for ICI-associated myocarditis is glucocorticoids [28]. It has been shown that early initiation of high dose glucocorticoids results in lower major adverse cardiovascular events [4, 29]. Guidelines recommend high dose steroids, at least 1–2 mg/kg/day of prednisone but many centers initiate pulse dose methylprednisolone at 500–1000 mg/day for 3 days followed by an oral steroid taper depending on the clinical response. Various tapers have been suggested, but the American Society of Clinical Oncology clinical practice guidelines recommend a taper over at least 4–6 weeks [28]. If clinical deterioration continues despite corticosteroids, then other immunomodulators have been shown to have varying success in case reports. These include mycophenolate [30], antithymocyte globulin [31], intravenous immunoglobulin [30], plasmapheresis [32], infliximab [32], alemtuzumab [33], and abatacept [34]. Given the high mortality of ICI-associated myocarditis, it is recommended to permanently discontinue ICI therapy after an episode of myocarditis [28].

3.4 Conclusion

With the increasing use of ICIs for cancer treatment, it is necessary for oncologists, general cardiologists, and cardio-oncologists to work together to promptly diagnose and treat ICI-associated myocarditis. Understanding the various benefits and limitations of available diagnostic tests and their use in combination with the clinical presentation will help guide the diagnosis and the treatment. Ongoing research will help to better standardize treatment regimens and societal guideline recommendations.

Funding
This work was supported by National Institutes of Health/National Heart, Lung, Blood Institute [T32HL076136, R01HL137562, R01HL130539, K24HL150238 to T.N.]. Dr. T. Neilan is also supported, in part, through a kind gift from A. Curtis Greer and Pamela Kohlberg.

Disclosures *TGN reports acting as a consultant for Parexel, AbbVie, H3 Biomedicine, and Intrinsic Imaging, unrelated to the current research. TGN was in a scientific advisory board for Bristol Myer Squibb related to myocarditis from immune checkpoint inhibitors.*

References

1. Postow MA, Callahan MK, Wolchok JD. Immune checkpoint blockade in cancer therapy. J Clin Oncol. 2015;33(17):1974–82.
2. Wang DY, Salem J-E, Cohen JV, Chandra S, Menzer C, Ye F, et al. Fatal toxic effects associated with immune checkpoint inhibitors: a systematic review and meta-analysis fatal toxic effects associated with immune checkpoint inhibitors fatal toxic effects associated with immune checkpoint inhibitors. JAMA Oncol. 2018;4(12):1721–8.
3. Johnson DB, Balko JM, Compton ML, Chalkias S, Gorham J, Xu Y, et al. Fulminant myocarditis with combination immune checkpoint blockade. N Engl J Med. 2016;375(18):1749–55.
4. Mahmood SS, Fradley MG, Cohen JV, Nohria A, Reynolds KL, Heinzerling LM, et al. Myocarditis in patients treated with immune checkpoint inhibitors. J Am Coll Cardiol. 2018;71(16):1755–64.
5. Moslehi JJ, Salem JE, Sosman JA, Lebrun-Vignes B, Johnson DB. Increased reporting of fatal immune checkpoint inhibitor-associated myocarditis. Lancet. 2018;391(10124):933.
6. Salem JE, Manouchehri A, Moey M, Lebrun-Vignes B, Bastarache L, Pariente A, et al. Cardiovascular toxicities associated with immune checkpoint inhibitors: an observational, retrospective, pharmacovigilance study. Lancet Oncol. 2018;19(12):1579–89.
7. Sharma P, Allison JP. The future of immune checkpoint therapy. Science (New York, NY). 2015;348(6230):56–61.
8. Schumacher TN, Schreiber RD. Neoantigens in cancer immunotherapy. Science (New York, NY). 2015;348(6230):69–74.
9. Greenwald RJ, Freeman GJ, Sharpe AH. The B7 family revisited. Annu Rev Immunol. 2005;23:515–48.
10. Linsley PS, Greene JL, Tan P, Bradshaw J, Ledbetter JA, Anasetti C, et al. Coexpression and functional cooperation of CTLA-4 and CD28 on activated T lymphocytes. J Exp Med. 1992;176(6):1595–604.
11. Zhang L, Awadalla M, Mahmood SS, Nohria A, Hassan MZO, Thuny F, et al. Cardiovascular magnetic resonance in immune checkpoint inhibitor-associated myocarditis. Eur Heart J. 2020;41(18):1733–43.
12. Awadalla M, Golden DLA, Mahmood SS, Alvi RM, Mercaldo ND, Hassan MZO, et al. Influenza vaccination and myocarditis among patients receiving immune checkpoint inhibitors. J Immunother Cancer. 2019;7(1):53.
13. Oren O, Yang EH, Molina JR, Bailey KR, Blumenthal RS, Kopecky SL. Cardiovascular health and outcomes in cancer patients receiving immune checkpoint inhibitors. Am J Cardiol. 2020;125(12):1920–6.
14. Norwood TG, Westbrook BC, Johnson DB, Litovsky SH, Terry NL, McKee SB, et al. Smoldering myocarditis following immune checkpoint blockade. J Immunother Cancer. 2017;5(1):91.
15. Matson DR, Accola MA, Rehrauer WM, Corliss RF. Fatal myocarditis following treatment with the PD-1 inhibitor nivolumab. J Forensic Sci. 2018;63(3):954–7.
16. Laubli H, Balmelli C, Bossard M, Pfister O, Glatz K, Zippelius A. Acute heart failure due to autoimmune myocarditis under pembrolizumab treatment for metastatic melanoma. J Immunother Cancer. 2015;3:11.
17. Tadokoro T, Keshino E, Makiyama A, Sasaguri T, Ohshima K, Katano H, et al. Acute lymphocytic myocarditis with anti-PD-1 antibody Nivolumab. Circ Heart Fail. 2016;9(10).
18. Caforio AL, Pankuweit S, Arbustini E, Basso C, Gimeno-Blanes J, Felix SB, et al. Current state of knowledge on aetiology, diagnosis, management, and therapy of myocarditis: a position statement of the European society of cardiology working group on myocardial and pericardial diseases. Eur Heart J. 2013;34(33):2636–48, 48a–48d.
19. Drobni ZD, Alvi RM, Taron J, Zafar A, Murphy SP, Rambarat PK, et al. Association between immune checkpoint inhibitors with cardiovascular events and atherosclerotic plaque. Circulation. 2020.
20. Neilan TG, Rothenberg ML, Amiri-Kordestani L, Sullivan RJ, Steingart RM, Gregory W, et al. Myocarditis associated with immune checkpoint inhibitors: an expert consensus on data gaps and a call to action. Oncologist. 2018;23(8):874–8.
21. Awadalla M, Mahmood SS, Groarke JD, Hassan MZO, Nohria A, Rokicki A, et al. Global longitudinal strain and cardiac events in patients with immune checkpoint inhibitor-related myocarditis. J Am Coll Cardiol. 2020;75(5):467–78.
22. Bonaca Marc P, Olenchock Benjamin A, Salem J-E, Wiviott Stephen D, Ederhy S, Cohen A, et al. Myocarditis in the setting of cancer therapeutics. Circulation. 2019;140(1):80–91.
23. Lee Chuy K, Oikonomou EK, Postow MA, Callahan MK, Chapman PB, Shoushtari AN, et al. Myocarditis surveillance in patients with advanced melanoma on combination immune checkpoint inhibitor therapy: the memorial Sloan Kettering cancer center experience. Oncologist. 2019;24(5):e196–7.
24. Ferreira VM, Schulz-Menger J, Holmvang G, Kramer CM, Carbone I, Sechtem U, et al. Cardiovascular magnetic resonance in nonischemic myocardial inflammation: expert recommendations. J Am Coll Cardiol. 2018;72(24):3158–76.
25. Aretz HT, Billingham ME, Edwards WD, Factor SM, Fallon JT, Fenoglio JJ, Jr., et al. Myocarditis. A histopathologic definition and classification. Am J Cardiovasc Pathol. 1987;1(1):3–14.
26. Ji C, Roy MD, Golas J, Vitsky A, Ram S, Kumpf SW, et al. Myocarditis in cynomolgus monkeys following treatment with immune checkpoint inhibitors. Clin Cancer Res. 2019;25(15):4735–48.
27. Balanescu DV, Donisan T, Palaskas N, Lopez-Mattei J, Kim PY, Buja LM, et al. Immunomodulatory treatment of immune checkpoint inhibitor-induced myocarditis: pathway toward precision-based therapy. Cardiovasc Pathol. 2020;47:107211.
28. Brahmer JR, Lacchetti C, Schneider BJ, Atkins MB, Brassil KJ, Caterino JM, et al. Management of immune-related adverse events in patients treated with immune checkpoint inhibitor therapy: American society of clinical oncology clinical practice guideline. J Clin Oncol. 2018;36(17):1714–68.
29. Zhang L, Zlotoff DA, Awadalla M, Mahmood SS, Nohria A, Hassan MZO, et al. Major adverse cardiovascular events and the timing and dose of corticosteroids in immune checkpoint inhibitor-associated myocarditis. Circulation. 2020;141(24):2031–4.
30. Arangalage D, Delyon J, Lermuzeaux M, Ekpe K, Ederhy S, Pages C, et al. Survival after fulminant myocarditis induced by immune-checkpoint inhibitors. Ann Intern Med. 2017;167(9):683–4.
31. Tay RY, Blackley E, McLean C, Moore M, Bergin P, Gill S, et al. Successful use of equine anti-thymocyte globulin (ATGAM) for fulminant myocarditis secondary to nivolumab therapy. Br J Cancer. 2017;117(7):921–4.
32. Frigeri M, Meyer P, Banfi C, Giraud R, Hachulla AL, Spoerl D, et al. Immune checkpoint inhibitor-associated myocarditis: a new challenge for cardiologists. Can J Cardiol. 2018;34(1):92.e1–.e3.
33. Esfahani K, Buhlaiga N, Thebault P, Lapointe R, Johnson NA, Miller WH Jr. Alemtuzumab for immune-related myocarditis due to PD-1 therapy. N Engl J Med. 2019;380(24):2375–6.
34. Salem J-E, Allenbach Y, Vozy A, Brechot N, Johnson DB, Moslehi JJ, et al. Abatacept for severe immune checkpoint inhibitor-associated myocarditis. N Engl J Med. 2019;380(24):2377–9.

4 Cardiovascular Events After Chimeric Antigen Receptor T-Cell Therapy

Lauren Balkan and Syed S. Mahmood

Key Points

- Chimeric antigen receptor (CAR) T-cells are a genetically modified autologous T-cell immunotherapy FDA approved to treat certain lymphomas and leukemias.
- Major adverse events following CAR T-cell immunotherapy include cytokine release syndrome (CRS) and neurological toxicity.
- CRS is a clinical syndrome of fever, hypotension, and hypoxia.
- Cardiovascular events may be due to poor cardiac reserve at baseline with an inability to compensate for the increased stress of cytokine release.

4.1 Introduction

Chimeric antigen receptor (CAR) T-cells are a genetically modified autologous T-cell immunotherapy and are Food and Drug Administration (FDA) approved to treat certain lymphomas and leukemias. The indications for CAR T-cells are expected to continue expanding, but presently all four FDA-approved agents (axicabtagene ciloleucel, tisagenlecleucel, brexucabtagene autoleucel, lisocabtagene maraleucel) are CD-19-directed. Cardio-oncologists should familiarize themselves with surveillance strategies for cardiovascular events following CAR T-cell therapy, given the risk for de novo arrhythmia and heart failure.

CARs are artificial proteins consisting of both antigen recognition and T-cell signaling domains [1, 2]. Manufacturing CAR T-cells can take up to several weeks. Host T-cells are obtained via leukapheresis, and are then genetically altered ex vivo to express the CAR, allowing them to attack cancer cells that express the target antigen [1, 3]. The patient undergoes lymphodepletion using cytotoxic chemotherapy, and infusion with newly created CAR T-cells.

Major adverse events following CAR T-cell immunotherapy include cytokine release syndrome (CRS) and neurological toxicity, both of which have prompted an FDA black box warning [4, 5]. CRS is a clinical syndrome of fever, hypotension, and hypoxia categorized into four grades based on severity (Table 4.1) [6]. Hemodynamic perturbance seen with CRS requires adequate cardiac reserve and is associated with marked elevations of serum cytokine levels [2]. Major adverse cardiovascular events associated with CRS include de novo arrhythmia, heart failure, and cardiac death [1, 7]. The event rate for new arrhythmias is 6.5 per 100 patients years, while that for both new onset heart failure and for cardiac death is 5.6 per 100 patients years among CD-19 targeting CAR T-cell recipients [1]. Baseline creatinine and grade >2 CRS are independently associated with cardiovascular events among CD-19 targeting CAR T-cell recipients [7]. The pathophysiology of CAR T-cell induced cardiovascular adverse events is not fully understood. One possibility is off target effects such as when CAR T-cells targeting titin resulted in cardiogenic shock and death in the two recipients [8]. In other cases, cardiovascular events are likely due to poor cardiac reserve at baseline with an inability to compensate for the increased stress of cytokine release. Both interleukin-6 (IL-6) and tumor necrosis factor-α have been implicated in myocardial dysfunction in inflammatory shock [9, 10]. Tocilizumab is an anti-IL-6-receptor antagonist that is FDA approved to manage severe CRS, and may also mitigate cardiovascular toxicity of CAR T-cells [11]. In a registry of 137 CD-19 targeting CAR

Electronic supplementary material
The online version of this chapter (https://doi.org/10.1007/978-3-030-70998-3_4) contains supplementary material, which is available to authorized users.

L. Balkan
Department of Internal Medicine, New York Presbyterian Hospital, Weill Cornell Medical Center, New York, NY, USA

S. S. Mahmood (✉)
Cardiology Division, New York Presbyterian Hospital, Weill Cornell Medical Center, New York, NY, USA
e-mail: ssm9014@med.cornell.edu

R. M. Steingart et al. (eds.), *Atlas of Imaging in Cardio-Oncology*,
https://doi.org/10.1007/978-3-030-70998-3_4

Table 4.1 American society for transplantation and cellular therapy grading system for cytokine release syndrome

	Grade 1	Grade 2	Grade 3	Grade 4
Fever Temperature ≥ 38 °C with or without constitutional symptoms	+	+	+	+
With				
Hypotension	−	+ Without need for vasopressors	+ Requiring one vasopressor without vasopressin	+ Requiring multiple vasopressors (excluding vasopressin)
And/or				
Hypoxia	−	+ Requiring nasal cannula <6L/min	+ Requiring supplemental oxygen >6L/min without positive pressure	+ Requiring positive pressure ventilation

(From Lee et al. [6]; *with permission from Elsevier*)

T-cell recipients, a shorter time from cytokine release syndrome onset to tocilizumab therapy was associated with a lower rate of cardiovascular events [1]. In particular, 95% of cardiac events were noted in patients who had a troponin elevation, and this biomarker may help identify candidates for early tocilizumab who are experiencing CRS [1]. Randomized controlled trials are needed to delineate the optimal treatment strategy for CAR T-cell-related cardiotoxicity.

4.2 Case 1

New onset atrial flutter on day three post CAR T-cell infusion in the setting of grade 3 CRS.

- De novo arrhythmias may occur in up to 12% of CAR T-cell recipients experiencing CRS grade ≥ 2 [1].
- Tocilizumab has been associated with a lower rate of major adverse cardiovascular events including atrial fibrillation, based on a registry cohort [1].

A 59-year-old man without known cardiovascular disease presented for CD-19 targeting CAR T-cell therapy for diffuse large B-cell lymphoma (DLBCL) that had been previously treated with multiple chemotherapy regiments including R-EPOCH. His baseline ECG was normal (Fig. 4.1). On day three post infusion, the patient developed grade 3 CRS, as well as new onset atrial flutter requiring rate control with beta-blockers and calcium channel blockers (Fig. 4.2). Tocilizumab was administered the same day. His transthoracic echocardiogram showed a normal left ventricular ejection fraction, and he was deemed not to require anti-coagulation based on low CHA2DS2VASc score. By day five post infusion he returned to normal sinus rhythm. On out-patient follow-up two months later he remained in normal sinus rhythm.

4.3 Case 2

Newly reduced left ventricular ejection fraction following CAR T-cell therapy resulting in cardiogenic shock.

- New onset heart failure may occur in up to 11% of CAR T-recipients experiencing CRS grade ≥ 2 [1].
- Elevated troponin may identify patients at risk for adverse cardiovascular events [1].
- Following CRS onset, the cardiovascular event risk increased 1.7-fold with each 12-hour delay to the administration of tocilizumab, based on a registry cohort [1].

A 75-year-old man with hypertension and atrial fibrillation presented with relapsed refractory DLBCL previously treated with multiple lines of therapy including R-CHOP and R-DHAX. A pretreatment echocardiogram showed a left ventricular ejection fraction of 55% (Fig. 4.3, Video 4.1). The patient underwent infusion of CD-19 targeting CAR T-cells. On day 12 post infusion he developed grade 4 CRS, and a repeat echocardiogram showed a decrease in left ventricular ejection fraction to 32% (Fig. 4.4, Video 4.2). Cardiac biomarkers revealed an elevation in B-natriuretic peptide to 1,016 pg/mL, and troponin-I to 1.59 ng/mL. The patient was treated with tocilizumab and increasing doses of pressors which were ultimately ineffective and the patient expired.

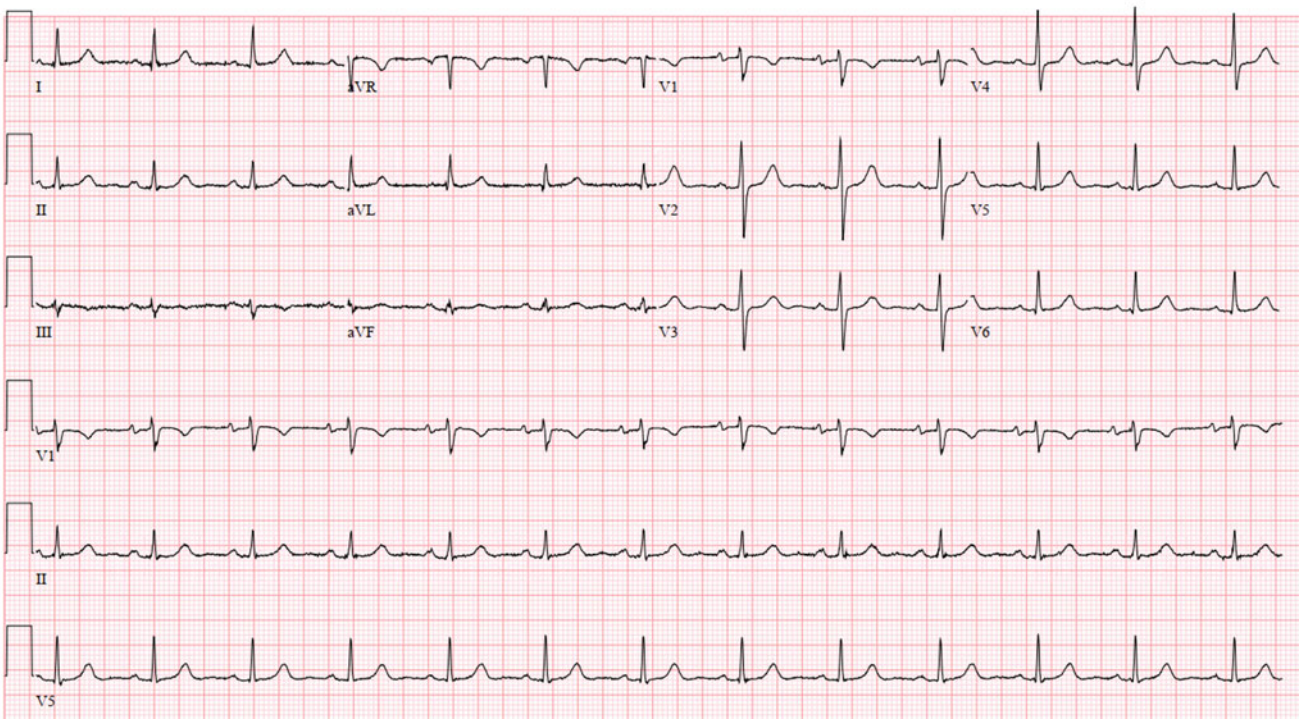

Fig. 4.1 Baseline electrocardiogram of patient showing normal sinus rhythm without evidence of atrial flutter

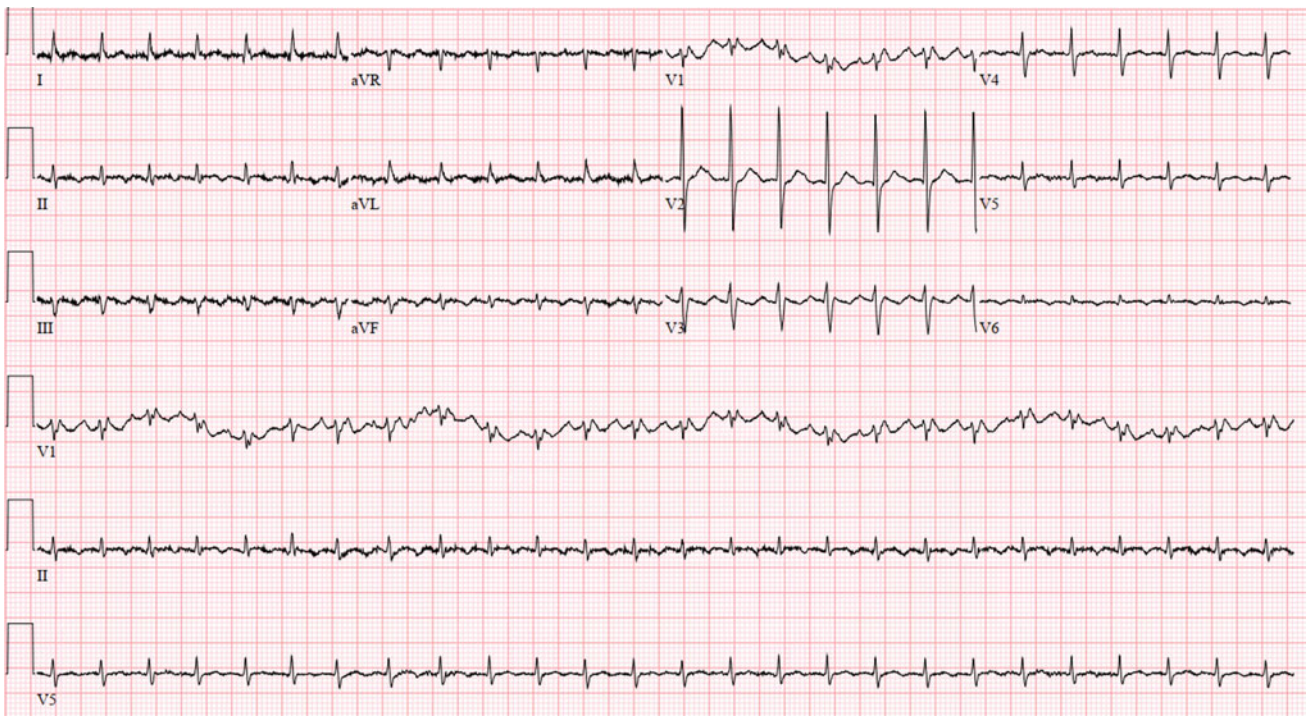

Fig. 4.2 On day 3 post CAR T-cell infusion, the patient developed new onset, symptomatic atrial flutter which resolved with tocilizumab treatment

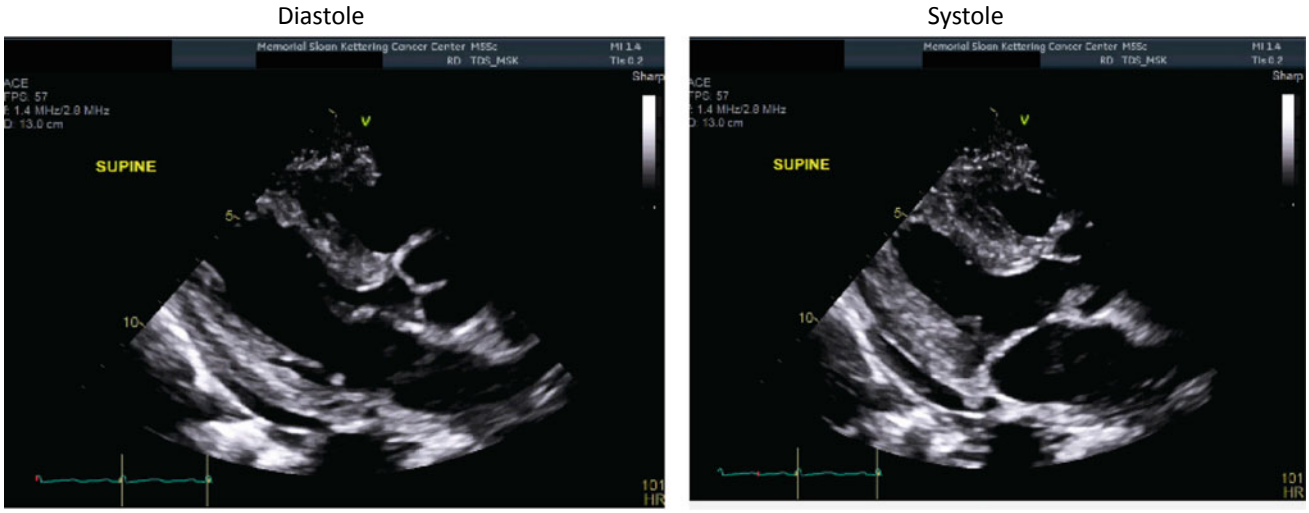

Fig. 4.3 Echocardiographic images in diastole and systole prior to CAR T-cell treatment showing normal systolic function

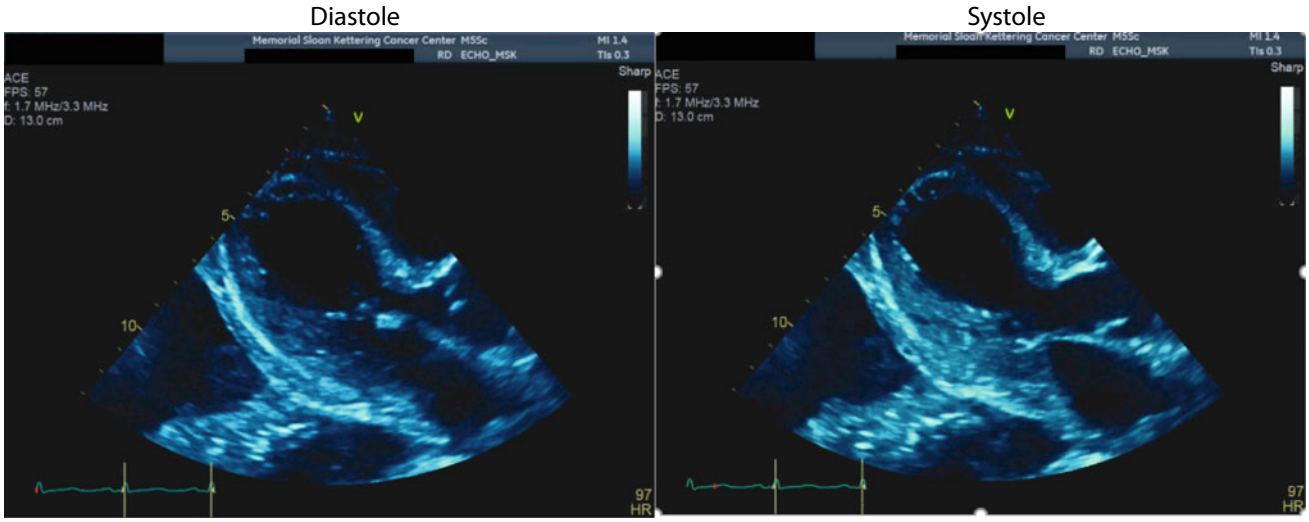

Fig. 4.4 Echocardiographic images in diastole and systole acquired while the patient experienced grade 4 CRS showing marked deterioration in systolic ventricular function compared with baseline

References

1. Alvi RM, Frigault MJ, Fradley MG, Jain MD, Mahmood SS, Awadalla M, et al. Cardiovascular events among adults treated with chimeric antigen receptor T-cells (CAR-T). J Am Coll Cardiol. 2019;74(25):3099–108. https://doi.org/10.1016/j.jacc.2019.10.038.PMID:31856966;PMCID:PMC6938409.
2. June CH, Sadelain M. Chimeric antigen receptor therapy. N Engl J Med. 2018;379:64–73.
3. Brudno JN, Kochenderfer JN. Chimeric antigen receptor T-cell therapies for lymphoma. Nat Rev Clin Oncol. 2018;15:31–46.
4. FDA. Tisagenlecleucel package label. Silver Spring, MD2018.
5. FDA. Axicabtagene package label. Silver Spring, MD2018.
6. Lee DW, Santomasso BD, Locke FL, et al. ASTCT Consensus Grading for Cytokine Release Syndrome and Neurologic Toxicity Associated with Immune Effector Cells. Biol Blood Marrow Transplant J Am Soc Blood Marrow Transplant. 2019;25:625–38.
7. Lefebvre B, Kang Y, Smith AM, Frey NV, Carver JR, Scherrer-Crosbie M. Cardiovascular effects of CAR T cell therapy: a retrospective study. JACC: Cardio Oncol. 2020;2:193–203.
8. Linette GP, Stadtmauer EA, Maus MV, et al. Cardiovascular toxicity and titin cross-reactivity of affinity-enhanced T cells in myeloma and melanoma. Blood. 2013;122:863–71.
9. Kumar A, Thota V, Dee L, Olson J, Uretz E, Parrillo JE. Tumor necrosis factor alpha and interleukin 1beta are responsible for in vitro myocardial cell depression induced by human septic shock serum. J Exp Med. 1996;183:949–58.
10. Pathan N, Hemingway CA, Alizadeh AA, et al. Role of interleukin 6 in myocardial dysfunction of meningococcal septic shock. The Lancet. 2004;363:203–9.
11. Davila ML, Riviere I, Wang X, et al. Efficacy and toxicity management of 19–28z CAR T cell therapy in B cell acute lymphoblastic leukemia. Sci Transl Med. 2014;6:224–25.

5 Introduction to Tyrosine Kinase Inhibitors: Pazopanib Cardiotoxicity

David P. Dundua, Ana G. Kedrova, Ekaterina V. Plokhova, Elena A. Zvezdkina, and Olga A. Drobiazko

Key Points

- The understanding of the role of dysregulated tyrosine kinases in cancer has produced a literal explosion in approaches to cancer treatment.
- Multikinase inhibition, although effective for cancer control, increases the likelihood of cardiovascular toxicity.
- TKIs used in cancer care have been associated with heart failure, arterial and venous vascular toxicities including myocardial ischemia and infarction, systemic and pulmonary hypertension, pulmonary embolism, peripheral vascular disease, thrombosis, QT prolongation,ventricular arrhythmias, and atrial fibrillation.

5.1 Introduction

Tyrosine kinases are mediators of critical signal transduction processes, leading to cell proliferation, differentiation, migration, metabolism, and programmed cell death. Using adenosine triphosphate, these enzymes catalyze phosphorylation of tyrosine residues in target proteins. They are primarily classified as either receptor tyrosine kinase, e.g., endothelial growth factor receptor (EGFR) or non-receptor tyrosine kinase, e.g., ABL. Tyrosine kinases are implicated in several steps of neoplastic development and progression. Normally the level of cellular tyrosine kinase phosphorylation is tightly controlled by the antagonistic effects of tyrosine kinases and tyrosine phosphatases. There are several mechanisms by which the normal homeostasis might be transformed, but the ultimate result is the constitutive activation of normally controlled pathways leading to the activation of other signaling proteins and secondary messengers which in turn initiate and perpetuate cancer development by hampering regulatory functions in cellular responses like cell division, growth, and cell death [1].

The understanding of the role of dysregulated tyrosine kinases in cancer has produced a literal explosion in approaches to cancer treatment through the development of tyrosine kinase inhibitors (TKI) in the form of monoclonal antibodies and small molecules. Ideally, these TKIs should only inhibit the dysfunctional tyrosine kinase driving the cancer. However, many TKIs are multi-kinase inhibitors by virtue of targeting the adenosine triphospate (ATP) pocket which is a commonly shared feature among TKIs. Multi-kinase inhibition, although effective for cancer control, increases the likelihood of cardiovascular toxicity [2]. With the success of these agents has come the realization that recognizing and managing cardiovascular toxicity is essential if these drugs are to realize their potential. TKIs used in cancer care have been associated with heart failure , arterial and venous vascular toxicities including myocardial ischemia and infarction, systemic and pulmonary hypertension, pulmonary embolism, peripheral vascular disease,

Electronic supplementary material
The online version of this chapter (https://doi.org/10.1007/978-3-030-70998-3_5) contains supplementary material, which is available to authorized users.

D. P. Dundua (✉) · E. V. Plokhova
Cardiology Center, Federal Scientific and Research Center, FMBA Russia, Orekhovy Bulvar, 28, 115285 Moscow, Russia
e-mail: david.doundoua@gmail.com

E. V. Plokhova
e-mail: evplokhova@gmail.com

A. G. Kedrova
Department of Oncology, Federal Scientific and Research Center, FMBA Russia, Orekhovy Bulvar, 28, 115285 Moscow, Russia
e-mail: kedrova.anna@gmail.com

E. A. Zvezdkina · O. A. Drobiazko
Department of Radiology, Federal Scientific and Research Center, FMBA Russia, Orekhovy Bulvar, 28, 115285 Moscow, Russia
e-mail: zvezdkina@yandex.ru

O. A. Drobiazko
e-mail: droa@mail.ru

R. M. Steingart et al. (eds.), *Atlas of Imaging in Cardio-Oncology*, https://doi.org/10.1007/978-3-030-70998-3_5

thrombosis, QT prolongation, ventricular arrhythmias , and atrial fibrillation [2, 3].

In this atlas, it is not possible to effectively illustrate all the reported cardiovascular effects of TKIs. The cases in this chapter and the chapters that follow illustrate the effectiveness of TKIs as anticancer agents, their adverse effects on the cardiovascular system, and the thoughtful risk/benefit compromises that are the cornerstones of best practices in cardio oncology.

Soft tissue sarcoma (STS) is an uncommon malignant disease represented in less than 1% of diagnosed malignancies in the Western world [4]. Although STS may occur anywhere in the human body it most often can be found in the extremities and chest wall. Treatment of STS includes surgical resection of the tumor with adjuvant and neoadjuvant therapy with anthracyclines, radiation, or both [5]. Long-term survival is quite stable after timely administered combination therapy, the mean metastasis-free survival being 11 years [6]. But synovial sarcoma may grow slowly and can be associated with late metastases after more than 10 years [7]. Pazopanib is an oral medication active against many kinases by virtue of its ability to inhibit ATP-mediated phosphorylation. It has exhibited inhibition of vascular endothelial growth factors (VEGFR-1, -2, and -3), platelet-derived growth factor receptors (PDGFR-α and -β), fibroblast growth factor receptors (FGFR-1 and -3), stem cell factor receptor (c-Kit), interleukin-2 receptor-inducible T-cell kinase (Itk), leukocyte-specific protein tyrosine kinase (Lck), and transmembrane glycoprotein receptor tyrosine kinase (sc-Fms). Pazopanib has been shown to be effective for the treatment of advanced renal cell carcinoma and advanced soft tissue sarcoma in patients previously treated with chemotherapy earning FDA approval for these indications [8].

A common cardiovascular side effect of the drug is the induction of hypertension [8, 9]. In patients who had systematic left ventricular ejection fraction (LVEF) assessment, myocardial dysfunction may occur in up to 11%, although congestive heart failure is very rare and is evident in about 0.5% of patients treated with this drug. When cardiotoxicity is related to pazopanib, interruption or dose reduction is usually required [8].

5.2 Case

Pazopanib: Cardiotoxicity during pazopanib treatment in a patient with a sarcoma metastatic to the mediastinum.

A 33-year-old woman was referred to the cardio-oncology service for the evaluation of right-sided heart failure. She first presented with a synovial sarcoma of the middle third of the diaphysis of the left tibia in 2006. Two courses of neoadjuvant chemotherapy with doxorubicin and cisplatin were administered, followed by amputation of the distal third of left thigh. She then received four courses of adjuvant chemotherapy with doxorubicin, ifosfamide, Mesna, and dacarbazine administered from 2006 until 2007. The anthracycline infusions were accompanied by dexrazoxane for cardiac protection because the total dose of doxorubicin well exceeded 450 mg/m^2. The patient was free of relapses, became pregnant in 2008, and delivered a healthy child in 2009. She was stable for 7 years. However, progression of disease was noted on a surveillance chest CT performed August 2016 with metastases in the left lung and tumor growth in the mediastinum. Extended lower left lobectomy with resection of pericardial segments was performed in March 2017. The tumor material was typical for synovial sarcoma. In the postoperative period, four courses of adjuvant chemotherapy were administered according to the IE-VAC regimen (includes anthracyclines).

The patient presented to the cardio-oncology service with right heart failure manifest as jugular vein distention, ankle edema, ascites, and massive left hemothorax in September 2018. She was found to have a large and metabolically active mediastinal tumor on chest CT (Fig. 5.1) and PET CT (Fig. 5.2). Compression of the right branch of main pulmonary artery (Fig. 5.3) with right ventricular and right atrial dilatation also noted on contrast CT angiography (Fig. 5.4). Chest MRI demonstrated that the whole heart was surrounded by the tumor (Fig. 5.5).

Echocardiography (not shown) revealed right ventricular (RV) and right atrial dilatation, a pulmonary artery (PA) trans stenotic gradient of 70 mmHg with LVEF of 46%. Surgical treatment and percutaneous balloon angioplasty for PA stenosis was discussed by a multidisciplinary

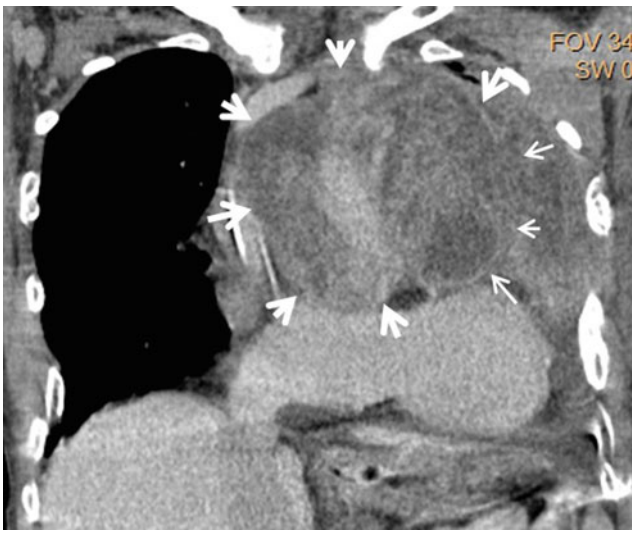

Fig. 5.1 CT pulmonary angiogram (coronal plane) shows a tumor (arrows) surrounding the heart and large vessels

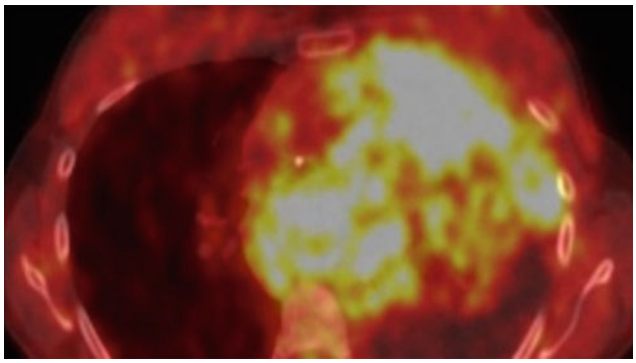

Fig. 5.2 PET-CT demonstrating a large tumor with active metabolism before treatment

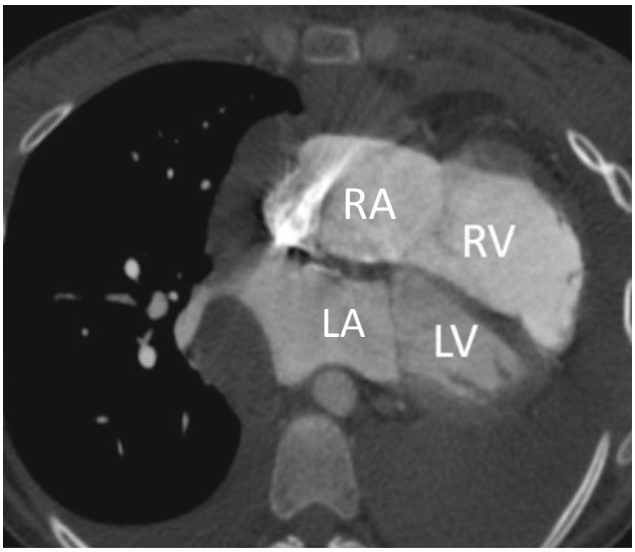

Fig. 5.4 CT contrast angiography—right ventricular (RV) dilatation. RV dimension exceeds the left ventricular (LV) dimension

team but was rejected as a therapeutic option because of the high risk and frankly unknown efficacy. Therapy with the tyrosine kinase inhibitor pazopanib was chosen.

After left thoracentesis pazopanib 800 mg once daily and spironolactone 100 mg daily were started in September 2018. Alleviation of peripheral edema and symptomatic improvement was achieved over three weeks of observation. Echocardiography in December 2018 revealed reduction of the PA gradient, the estimated PA pressure dropped to 30 mmHg and the right PA artery compression disappeared (Fig. 5.6). However as the RV size returned toward normal, the LV became dilated and globular on contrast CT (Fig. 5.7) confirmed by subsequent echocardiography where the LVEF was measured at 25%. Low dose enalapril and bisoprolol were started with gradual dose escalation. The dilated cardiomyopathy was attributed to pazopanib therapy in the setting of pretreatment with high doses of anthracyclines. Pazopanib dose interruption was deemed inappropriate since it was a very effective anti-tumor option for this patient. The drug was continued but at a reduced dose of 400 mg daily.

Further reduction of mediastinal tumor metabolism was documented on PET CT at the end of January 2019 (Fig. 5.8). LVEF by echocardiography improved up to 40%. The daily dose of pazopanib was increased back again to

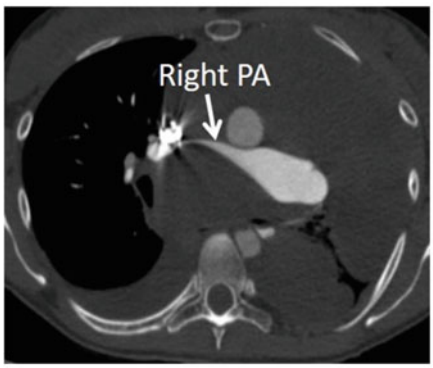

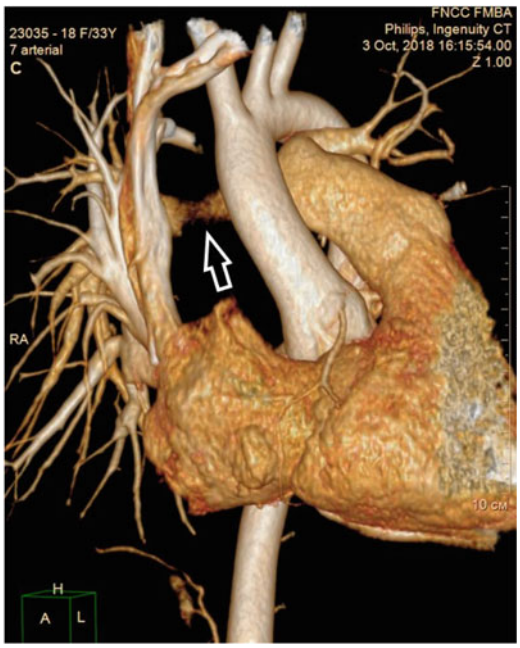

Fig. 5.3 Left panel: CT pulmonary angiogram before treatment with pazopanib: Severe right pulmonary artery (PA) stenosis. Right panel: 3D reconstruction of heart and great vessels. Severe right pulmonary artery obstruction (arrow)

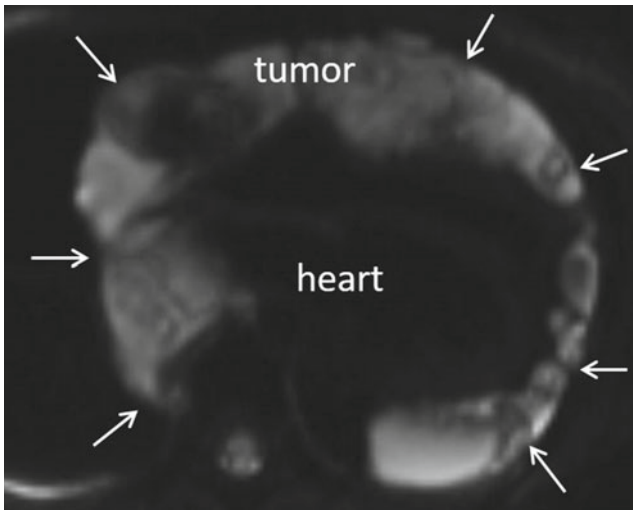

Fig. 5.5 Chest MRI (diffusion weighted imaging) of the patient demonstrating the tumor embracing the heart and great vessels

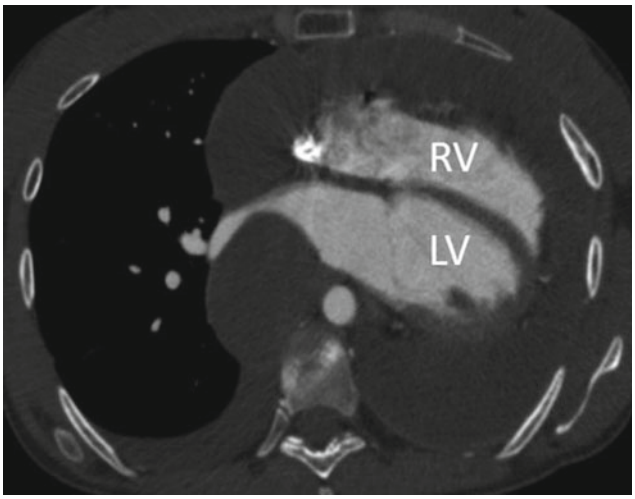

Fig. 5.7 CT contrast angiography after 8 months of pazopanib treatment demonstrating dramatic reduction in right ventricular size but the left ventricle is somewhat dilated and globular

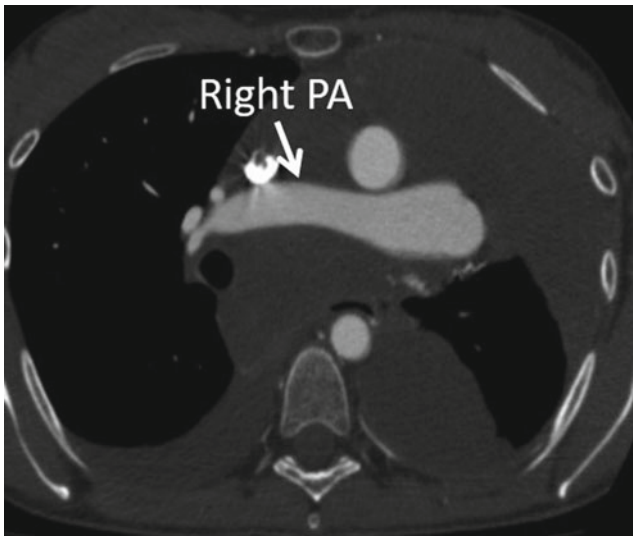

Fig. 5.6 CT pulmonary angiogram after 8 months of pazopanib treatment shows alleviation of the right pulmonary artery obstruction

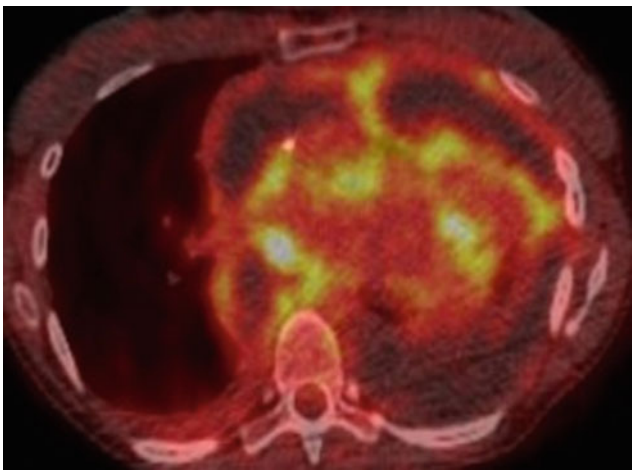

Fig. 5.8 PET-CT after eight months of pazopanib shows reduction in the size and metabolism of the sarcoma

800 mg/day without significant adverse effects. The cardiac status of the patient was stable for 10 months while on cardioprotective therapy.

Unfortunately, her condition worsened at the end of August 2019 with further spread of the disease and tumor ingrowth into the right atrium (Fig. 5.9, Video 5.1). Anticoagulation was started as pulmonary embolism prophylaxis but was complicated by an intracranial hemorrhage associated with brain metastases. She underwent emergency evacuation of an intracranial hematoma but was left with a residual focal neurologic deficit. Four weeks later in September 2019 the patient died while in palliative care.

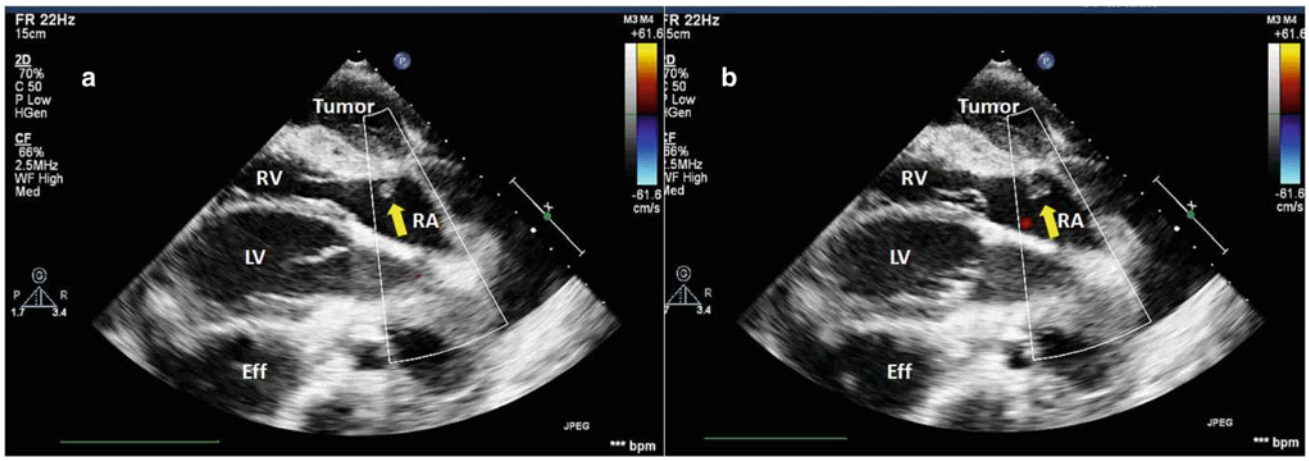

Fig. 5.9 A. Diastolic frame from echocardiogram parasternal long axis view demonstrating mass ingrowth (arrow) to the right ventricle. B. Systolic frame. The left ventricle appears mildly hypokinetic. Eff—pleural effusion, LV—left ventricle, RA—right atrium, RV—right ventricle

5.3 Conclusion

Pazopanib is an effective TKI for soft tissue sarcoma. Although hypertension is common, other cardiotoxic effects of pazopanib are rare and likely related to prior cardiotoxic treatments and abnormal ventricular function at the beginning of therapy. With an abnormal pretreatment LVEF and further reduction during pazopanib treatment, dose reduction or interruption of the TKI is indicated. In this instance, treatment with guideline directed medical therapy for left ventricular dysfunction stabilized the patient and allowed for continued anti-cancer therapy.

Reference

1. Paul MK, Mukhopadhyay AK. Tyrosine kinase—role and significance in cancer. Int J Med Sci. 2004;1(2):101–115. https://doi.org/10.7150/ijms.1.101. PMID: 15912202; PMCID: PMC1074718.
2. Cheng H, Force T. Why do kinase inhibitors cause cardiotoxicity and what can be done about it? Prog Cardiovasc Dis. 2010;53(2):114–20. https://doi.org/10.1016/j.pcad.2010.06.006. PMID: 20728698.
3. Chang HM, Moudgil R, Scarabelli T, Okwuosa TM, Yeh ETH. Cardiovascular complications of cancer therapy: best practices in diagnosis, prevention, and management: part 1. J Am Coll Cardiol. 2017;70(20):2536–51. https://doi.org/10.1016/j.jacc.2017.09.1096.
4. Siegel RL, Miller KD, Jemal A. Cancer statistics, 2020. Cancer J Clin. 2020;70(1):7. PMID: 31912902.
5. Casali P.G., Abecasis N, Bauer S., et al. Soft tissue and visceral sarcomas: ESM-EURACA clinical practice guidelines for diagnosis, treatment and follow-up. Ann Oncol. 2018;29(4):iv51–iv67. https://doi.org/10.1093/annonc/mdy096.
6. Krieg AH, Hefti F, Speth BM, et al. Synovial sarcomas usually metastasize after >5 years: a multicenter retrospective analysis with minimum follow-up of 10 years for survivors. Ann Oncol. 2011;22(458). PMID: 20716627.
7. Rothermundt C, Whelan JS, Dileo P, et al. What is the role of routine follow-up for localized limb soft tissue sarcomas? A retrospective analysis of 174 patients. Br J Cancer. 2014;110(2420). PMID: 24736584.
8. Votrient [package insert]. East Hanover, NJ: Novartis Pharmaceuticals Corporation; 2017. https://www.pharma.us.novartis.com/sites/www.pharma.us.novartis.com/files/votrient.pdf. Accessed 19 Aug 2017.
9. Pinkhas D., Ho T., Smith S. Assessment of pazopanib-related hypertension, cardiac dysfunction and identification of clinical risk factors for their development. Cardiooncology. 2017;3(5). MCID: PMC5828231. https://doi.org/10.1186/s40959-017-0024-8.

6 Tyrosine Kinase Inhibitors: Arrhythmias and Coagulopathy

Osnat Itzhaki Ben Zadok and Zaza Iakobishvili

Ibrutinib, a potent Bruton tyrosine kinase inhibitor, is an effective treatment for hematological malignancies including chronic lymphocytic leukemia, Waldenstrom's macroglobulinemia, mantle cell lymphoma, marginal zone lymphoma, and chronic graft versus host disease. However, it is associated with an increased incidence of atrial fibrillation/atrial flutter (AF) and bleeding [1, 2]. According to meta-analysis by Yun et al. [3] ibrutinib treatment was associated with a significantly higher incidence of serious AF (3.03% vs. 0.80%, RR = 3.80, 95% confidence interval [CI] = 1.56–9.29, P = 0.003), all-grade AF (8.18% vs. 0.93%, RR = 8.81, 95% CI = 2.70–28.75, P = 0.0003), and all-grade bleeding (4.85% vs. 1.55%, RR = 2.93, 95% CI = 1.14–7.52, P = 0.03) compared to control treatments.

Management of AF/flutter due to ibrutinib is challenging because of interaction with drugs used for rate control (calcium channel blockers and digoxin), rhythm control (amiodarone), and anti-coagulation [4]. Amiodarone use with ibrutinib may elevate ibrutinib plasma levels and has been associated with acute elevation of left ventricular filling pressures with resultant heart failure [5].

Case report: A 65-year-old man diagnosed with chronic lymphocytic leukemia (CLL) and treated with ibrutinib presented to the emergency department due to symptomatic atrial flutter with a rapid ventricular response (130 per minute) (Fig. 6.1). The patient previously was treated with propafenone and atenolol without anticoagulation (CHA2DS2VASC score 1). As he was unresponsive to the initial treatment with parenteral amiodarone (2 doses of 150 mg intravenous), synchronized electrical cardioversion was performed with a return to sinus rhythm. Due to profound thrombocytopenia, radiofrequency ablation of the isthmus was felt unsafe and amiodarone oral loading (1200 mg per day for 7 days) was prescribed for rhythm control. After 6 days he was admitted with new-onset mild heart failure (dyspnea, jugular vein distention) despite maintaining sinus rhythm at 65 beats per minute. Echocardiography showed new-onset elevated left ventricular filling pressure according to E/A ratio of more than 2 and characteristic S < D pattern of pulmonary vein flow (Fig. 6.2). With temporary discontinuation of amiodarone and treatment with low dose oral furosemide heart failure improved and ibrutinib was restarted. As the patient had a CHA2DS2-VASC score of 1, platelet count of 60,000/ml, and increased bleeding tendency associated with ibrutinib—a decision was made not to initiate anticoagulation.

O. I. B. Zadok
Cardiology Department, Rabin Medical Center, 39 Jabotinsky Street, 49100 Petah Tikva, Israel
e-mail: osnat.itzhaki@gmail.com

Z. Iakobishvili (✉)
Department of Community Cardiology, Tel Aviv Jaffa District, Clalit Health Services, 15 Naomi Shemer St., 5840608 Holon, Israel
e-mail: zaza.iakobishvili@gmail.com

R. M. Steingart et al. (eds.), *Atlas of Imaging in Cardio-Oncology*,
https://doi.org/10.1007/978-3-030-70998-3_6

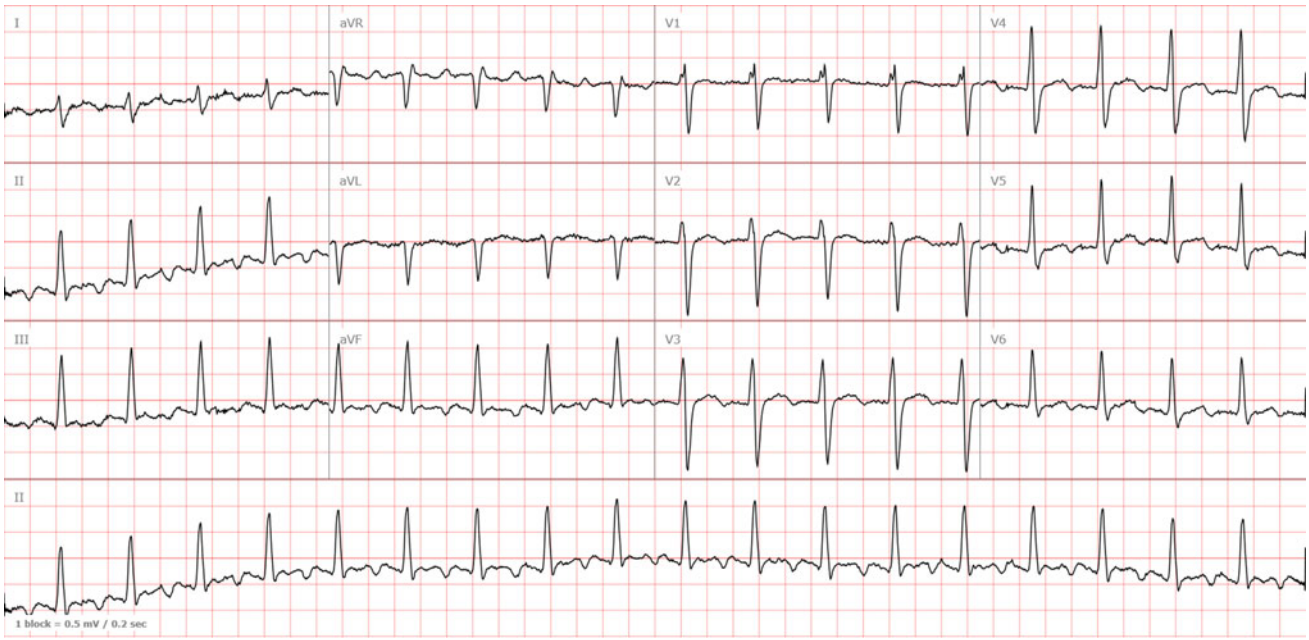

Fig. 6.1 Electrocardiogram showing atrial flutter with rapid ventricular response (130 beats/minute)

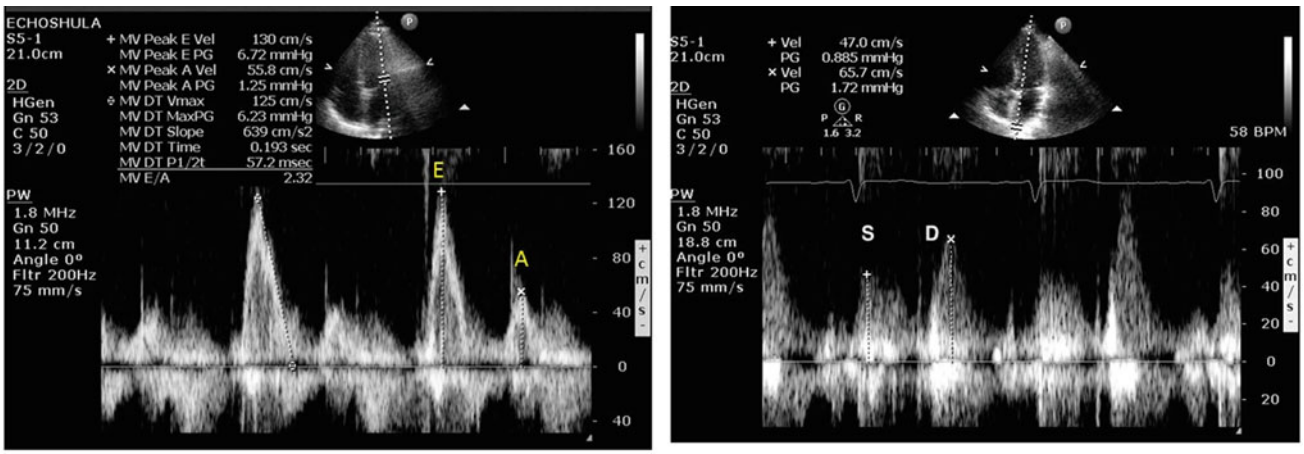

Fig. 6.2 Left panel showing mitral inflow pulse Doppler tracing demonstrating elevated LV filling pressures (E/A ratio = 2.3), which is confirmed on the right panel showing pulmonary vein pulse Doppler (S < D)

References

1. Salem JE, Manouchehri A, Bretagne M, Lebrun-Vignes B, Groarke JD, Johnson DB, et al. Cardiovascular toxicities associated with Ibrutinib. J Am Coll Cardiol. 2019;74(13):1667–78.
2. Ganatra S, Sharma A, Shah S, Chaudhry GM, Martin DT, Neilan TG, et al. Ibrutinib associated Atrial Fibrillation. JACC Clin Electrophysiol. 2018;4(12):1491–500.
3. Yun S, Vincelette ND, Acharya U, Abraham I. Risk of atrial fibrillation and bleeding diathesis associated with Ibrutinib treatment: a systematic review and pooled analysis of four randomized controlled trials. Clin Lymphoma, Myeloma Leuk [Internet]. 2017;17(1):31–7. e13. https://doi.org/10.1016/j.clml.2016.09.010.
4. Hardy-Abeloos C, Pinotti R, Gabrilove J. Ibrutinib dose modifications in the management of CLL. J Hematol Oncol. 2020;13(1):1–11.
5. Wasserstrum Y, Raanani P, Kornowski R, Iakobishvili Z. Concomitant treatment with Ibrutinib and amiodarone causing reversible heart failure syndrome. Isr Med Assoc J. 2016;18(7):433–434. PMID: 28471569.

7 Vascular Toxicity of Tyrosine Kinase Inhibitors: Peripheral Vascular and Coronary Artery Disease

Joerg Herrmann

Key Points

- Nilotinib and ponatinib stand out as tyrosine kinase inhibitors (TKIs) associated with peripheral vascular disease.
- Interference with vascular endothelial growth factor (VEGF) signaling is thought to be a common pathophysiological mechanism.
- A comprehensive cardiovascular assessment should be conducted before, during and after therapy with documentation of the peripheral pulse status and ideally the ankle-brachial index (ABI).

7.1 Introduction

Historically, most of the attention regarding cardiovascular diseases among cancer patients has been directed towards cardiac dysfunction [1, 2]. This is not to say that vascular disease has not been recognized in this patient population but incidence rates and implications had been deemed not as severe. This changed with the introduction of targeted therapies, especially those targeting the vascular endothelial growth factor (VEGF) signaling pathway, which brought the profound impact of any meddling with the vasculature to broader attention. This very topic reached another milestone with the reported outcomes for tyrosine kinase inhibitors that target Bcr-Abl (less so for agents targeting the EGF receptor, c-Met and MEK) [1, 2].

Indeed, the Bcr-Abl inhibitors, nilotinib and ponatinib stand out as *the* TKIs associated with peripheral arterial disease. In fact, the reputation of the vascular toxicity potential of Bcr-Abl inhibitors is largely founded on the initial observation of profound structural alteration of the arteries of the lower extremities in patients on nilotinib [3–5]. Subsequently, Vascular toxicity was recognized for ponatinib with even greater frequency, variety, and severity [6–10].

A major challenge in this area is the fact that these drugs are mainly given to patients with chronic myeloid leukemia (CML), who are predominantly elderly (median age at presentation 64 years) and thus at higher risk of vascular disease to begin with [11]. The presence of cardiovascular risk factors contributes to the confounding as does any unrecognized pre-existing cardiovascular disease. This being said, in a very carefully conducted study, patients on nilotinib were compared with a risk factor-matched control group, and the drug-attributable vascular risk of nilotinib clearly emerged and in a profound manner [12]. Experimental studies support The vascular toxicity potential of these drugs. In particular, studies on endothelial cells show that both drugs interfere with VEGF signaling through modulation of VEGF receptor-2 (KDR) activity. This effect is more direct for ponatinib and more indirect for nilotinib [12–14].

From a clinical perspective, it is extremely important to conduct a comprehensive cardiovascular assessment before the initiation of cancer therapy with documentation of the peripheral pulse status and ideally the ABI [15, 16]. This forms the foundation for follow-up evaluations as outlined in Table 7.1 [15, 16]. Other studies for the evaluation of the vascular status of the lower extremities as well as other vascular territories have been suggested as well [17]. These approaches may not be as cost-effective but could be meaningful in patients on ponatinib with presumed higher risk, such as those with additional cardiovascular risk factors [8]. For nilotinib, increasing ESC score categories match with increasing risk of arterial occlusive events overall, and a ESC Score of 5 or higher seems to identify very well those patients at risk for severe arterial occlusive disease [12]. For these very high-risk patients, routine screening at 3–6 months intervals seems to be very appropriate even when

J. Herrmann (✉)
Department of Cardiovascular Diseases, Mayo Clinic, Rochester, MN, USA
e-mail: herrmann.joerg@mayo.edu

R. M. Steingart et al. (eds.), *Atlas of Imaging in Cardio-Oncology*,
https://doi.org/10.1007/978-3-030-70998-3_7

Table 7.1 Recommendations for assessment of patients on Bcr-Abl TKI therapy

Symptoms	Peripheral pulse status	Risk factors	Vascular tests	F/u
None	Normal	None	None	Every 12 months
None	Reduced±	None or present	ABI	If ABI $\geq$ 0.9: 12 mo. f/u If ABI < 0.9: additional tests[a] and 6 mo. f/u
Present±	Reduced±	None or present	ABI	Vascular specialist 3–6 mo. f/u If ABI < 0.7: stop

Adapted from Breccia et al. [15], with permission from Elsevier
[a]Additional tests include exercise ABI, Duplex U/S, and lower extremity CT angiography as well as evaluation of carotid IMT and coronary CTA or stress test

asymptomatic and even though it is at present unknown what cutoffs should be used to signal a significant change so as to justify the cessation of cancer therapy. This is much easier in the setting of new-onset of symptoms and signs of ischemia and especially if severe and life-threatening clinical events such as critical limb ischemia, myocardial infarction, or stroke have occurred. Risk–benefit discussions are crucial in these patients and alternative Bcr-Abl treatment strategies under circumstances of challenging vascular risk have been discussed [5, 11].

In summary, there needs to be awareness and proper recognition and management of the vascular risk in patients undergoing certain forms of TKI therapy. At baseline, risk scores may help risk stratify but may also vastly underestimate vascular risk of patients. Accordingly, all patients should be followed carefully and vascular status should be a standard assessment not only before but also after the start of cancer therapy. Importantly, the risk of vascular disease can persist even months after discontinuation of therapy [9]. There needs to be, therefore, not only heightened but also persistent awareness for vascular disease and related risk of complications in patients on (vasotoxic) TKI therapies.

7.2 Case Report

Severe generalized atherosclerosis in a young woman after Bcr-Abl TKI therapy.

A 32-year-old white female with a history of Ph + ALL but of no other diseases, including no personal or family history of cardiovascular disease presents with bluish discoloration of the left lower extremity. In the weeks prior she developed pain in her lower extremities, even during night hours. This was unlike anything she has experienced with chronic sclerodermoid graft versus host disease after having undergone allogenic hematopoietic stem cell transplantation 1.5 years ago. Over the 6 months leading up to her transplantation, she was treated with ponatinib with an excellent morphological, cytogenetic and molecular response after failing dasatinib. Evaluation of her current presentation concluded with the diagnosis of critical limb ischemia. Computed tomography (CT) angiography showed new diffuse narrowing of the splenic artery, new proximal occlusion of the IMA and internal iliac arteries, high-grade stenoses of the external iliac arteries, occlusion of the left superficial femoral artery, and occlusion/high-grade stenoses of the tibial arteries (Fig. 7.1, left and mid panels). She underwent bilateral external iliac artery stenting, angioplasty of the left common femoral artery, and recanalization plus drug-eluting stenting of the left superficial femoral artery. Post-procedurally she developed reperfusion compartment syndrome of the left lower extremity requiring fasciotomy. On post-operative day 2, she developed acute chest pain with ST-segment elevation in the anteroseptal leads. Coronary angiography showed coronary vasospasm as well as a significant stenosis of the proximal LAD confirmed as severe atherosclerosis by IVUS (Fig. 7.1, right panels). She underwent distal left main/proximal LAD and LCX drug-eluting stenting, recovered from this episode but developed recurrent ischemia with evidence of severe in-stent restenosis requiring coronary artery bypass

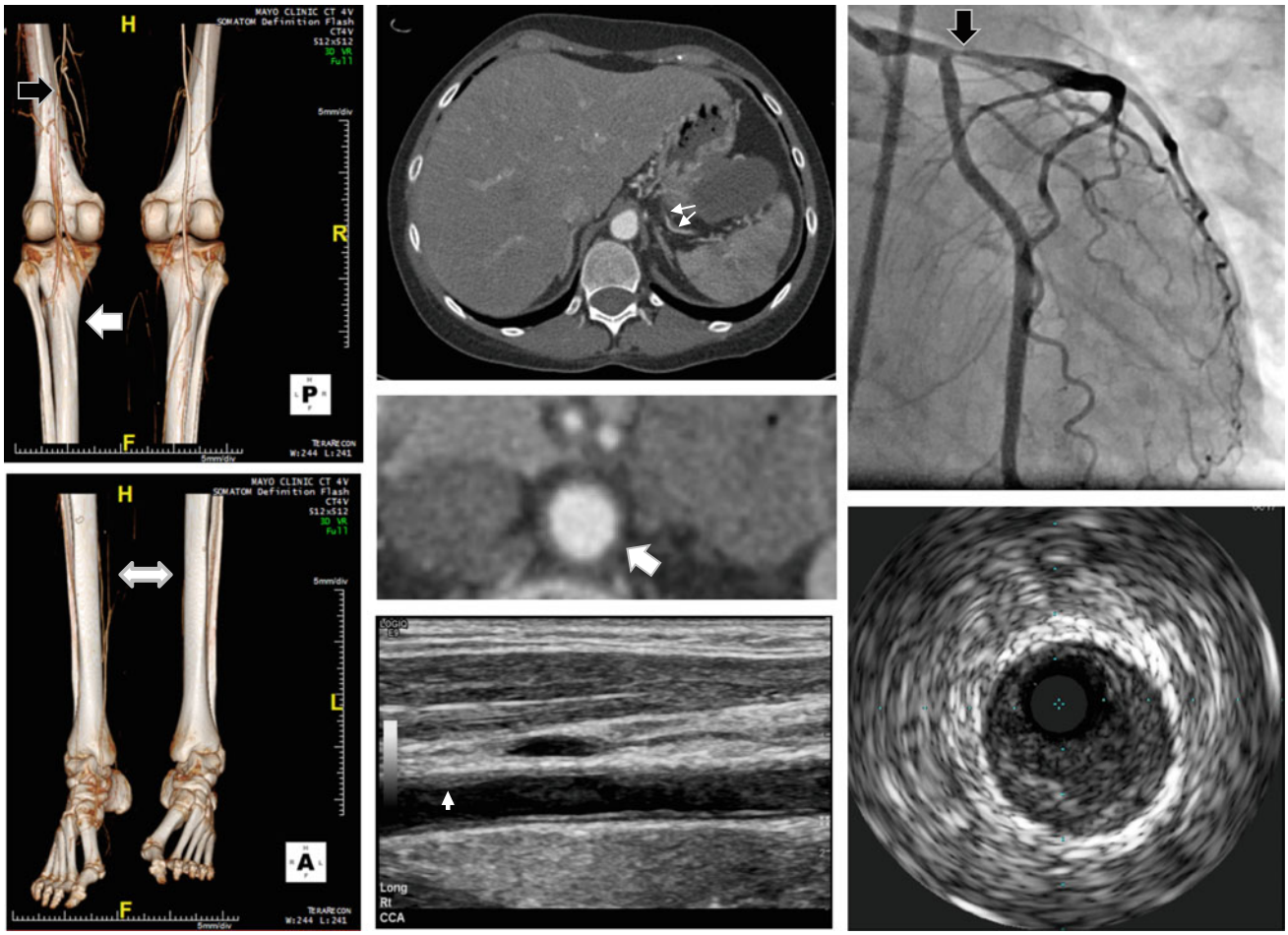

Fig. 7.1 Left upper and lower panels: Computed tomography angiography (CTA) with 3D reconstruction showing occlusion of the left superficial artery (black arrow) and poor runoff thereafter (white arrow) and poor distal circulation bilaterally (white double arrow), especially near on the left; upper middle panel: abdominal CTA showing multiple stenoses of the splenic artery (arrows) and circumferential thickening of the wall of the infrarenal aorta (arrow); lower middle panel: ultrasound of the right common carotid artery showing focal atherosclerotic plaque (arrow) and diffuse intimal thickening on the contralateral sides; right upper panel: coronary angiogram showing a high grade proximal LAD lesion (arrow), confirmed as extensive soft atherosclerotic plaque on intravascular ultrasound (right lower panel). (Reproduced with permission from Herrmann J, Bell MR, Warren RL, Lerman A, Fleming MD, Patnaik M. Complicated and Advanced Atherosclerosis in a Young Woman With Philadelphia Chromosome-Positive Acute Lymphoblastic Leukemia: Success and Challenges of BCR/ABL1-Targeted Cancer Therapy. Mayo Clin Proc. 2015 Aug;90 (8):1167–8)

surgery. Thereafter, she remained without any recurrent ischemic events; her cardiac function remained preserved.

References

1. Herrmann J. Adverse cardiac effects of cancer therapies: cardiotoxicity and arrhythmia. Nat Rev Cardiol. 2020;17(8):474–502.
2. Herrmann J. Vascular toxic effects of cancer therapies. Nat Rev Cardiol. 2020;17(8):503–22.
3. Aichberger KJ, et al. Progressive peripheral arterial occlusive disease and other vascular events during nilotinib therapy in CML. Am J Hematol. 2011;86(7):533–9.
4. Quintas-Cardama A, Kantarjian H, Cortes J. Nilotinib-associated vascular events. Clin Lymphoma Myeloma Leuk. 2012;12(5):337–40.
5. Valent P, et al. Vascular safety issues in CML patients treated with BCR/ABL1 kinase inhibitors. Blood. 2015;125(6):901–6.
6. Chai-Adisaksopha C, Lam W, Hillis C. Major arterial events in patients with chronic myeloid leukemia treated with tyrosine kinase inhibitors: a meta-analysis. Leuk Lymphoma. 2016;57 (6):1300–10.
7. Douxfils J, et al. Association between BCR-ABL tyrosine kinase inhibitors for chronic myeloid leukemia and cardiovascular events, major molecular response, and overall survival: a systematic review and meta-analysis. JAMA Oncol. 2016.
8. Moslehi JJ, Deininger M. Tyrosine kinase inhibitor-associated cardiovascular toxicity in chronic myeloid leukemia. J Clin Oncol. 2015;33(35):4210–8.
9. Nicolini FE, et al. Cardio-vascular events occurring on ponatinib in chronic phase chronic myeloid leukemia patients, preliminary analysis of a multicenter cohort. Blood. 2013;122(21):4020.

10. Herrmann J. Tyrosine kinase inhibitors and vascular toxicity: impetus for a classification system? Curr Oncol Rep. 2016;18(6):33.
11. Valent P, et al. Risk factors and mechanisms contributing to TKI-induced vascular events in patients with CML. Leuk Res. 2017;59:47–54.
12. Hadzijusufovic E, et al. Nilotinib-induced vasculopathy: identification of vascular endothelial cells as a primary target site. Leukemia. 2017;31(11):2388–97.
13. Gover-Proaktor A, et al. Bosutinib, dasatinib, imatinib, nilotinib, and ponatinib differentially affect the vascular molecular pathways and functionality of human endothelial cells. Leuk Lymphoma. 2018;1–11.
14. Gover-Proaktor A, et al. Ponatinib reduces viability, migration, and functionality of human endothelial cells. Leuk Lymphoma. 2017;58(6):1455–67.
15. Breccia M, et al. Proposal for a tailored stratification at baseline and monitoring of cardiovascular effects during follow-up in chronic phase chronic myeloid leukemia patients treated with nilotinib frontline. Crit Rev Oncol Hematol. 2016;107:190–8.
16. Breccia M, et al. Cardiovascular risk assessments in chronic myeloid leukemia allow identification of patients at high risk of cardiovascular events during treatment with nilotinib. Am J Hematol. 2015;90(5):E100–1.
17. Iliescu C, et al. SCAI expert consensus statement: evaluation, management, and special considerations of cardio-oncology patients in the cardiac catheterization laboratory (Endorsed by the Cardiological Society of India, and Sociedad Latino Americana de Cardiologia Intervencionista). Catheter Cardiovasc Interv. 2016;87(5):895–9.

8 Vascular Toxicity of Tyrosine Kinase Inhibitors: Coronary Artery Disease

Wendy Schaffer

Key points

- Dasatinib, a second-generation BCR-ABL inhibitor affects endothelial function.
- Coronary spasm should be considered as a possible mechanism of chest pain.
- Exercise testing on the drug can be a helpful diagnostic aid.
- The addition of oral nitrates controlled symptoms and normalized stress test results.

8.1 Case Report

An older man with chest pain while receiving dasatinib and ruxolitinib.

A 65-year-old man, a prior smoker, with hypertension, and unlimited exercise tolerance was diagnosed with Ph + ALL. He was admitted for expedited workup for his cancer and to initiate treatment with dasatinib and ruxolitinib. Within 3 hours of the first dose of dasatinib and ruxolitinib,

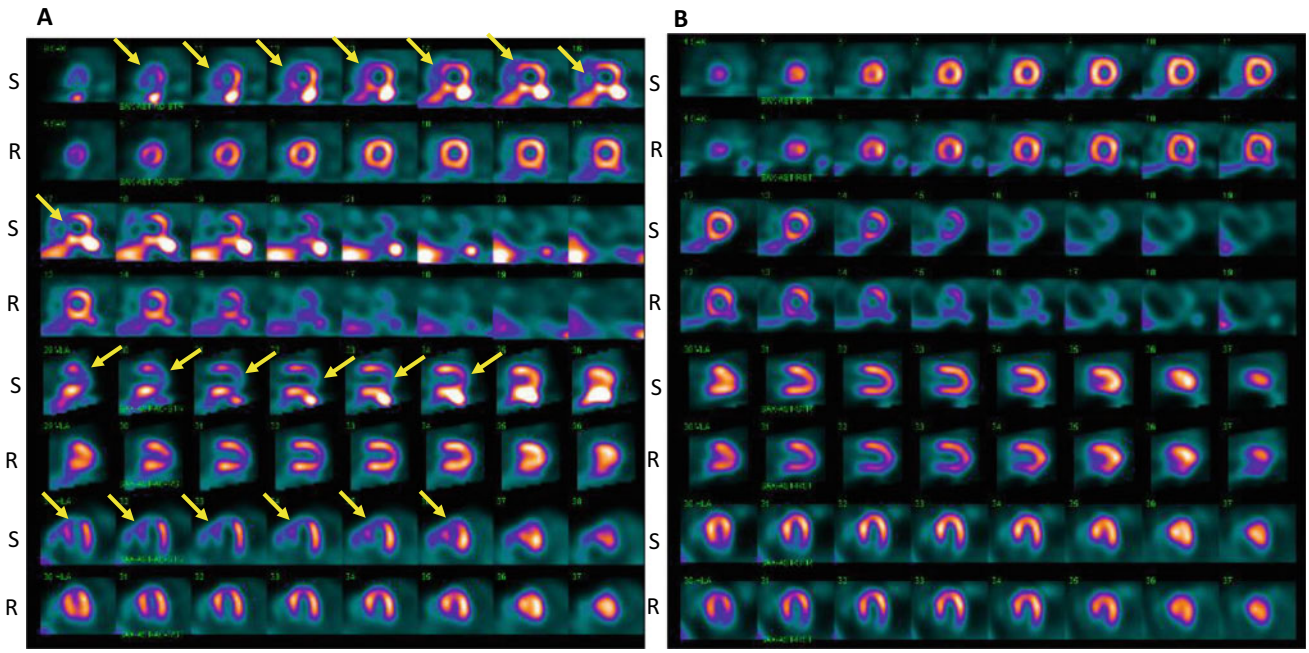

Fig. 8.1 **a** Pharmacologic stress test while patient receiving dasatinib and ruxolitinib together. On the stress images (S), there is transient ischemic dilation with severe and extensive perfusion defects (arrows) seen on all three orthogonal views. These defects resolve on rest imaging (R) consistent with a very large and severe ischemic burden. **b** Repeated pharmacologic stress test on both agents with isosorbide mononitrate added. On stress and rest imaging, ventricular size and perfusion are normal. The ischemic threat is resolved

W. Schaffer (✉)
Department of Medicine, Memorial Sloan Kettering Cancer Center, 1275 York Avenue, New York, NY 10065, USA
e-mail: Schaffew@mskcc.org

R. M. Steingart et al. (eds.), *Atlas of Imaging in Cardio-Oncology*,
https://doi.org/10.1007/978-3-030-70998-3_8

the patient reported new exertional chest pain. EKGs were unremarkable and troponins negative. The patient had an abnormal stress test while still on these medications (Fig. 8.1). Given the stress test, the medications were stopped and he underwent cardiac catheterization, which revealed no significant obstructive disease; the possibility of coronary vasospasm was raised. The oncology team stated that the patient had very few options for his high-risk disease. In this setting, prophylaxis with isosorbide mononitrate 240 mg daily was initiated. Dasatinib was restarted, then ruxolitinib was added in step-wise fashion, with the patient monitored in the hospital. He reported no further chest pain with ambulation while receiving dasatinib and isosorbide, as well as with the subsequent addition of ruxolitinib. His stress test was repeated, while on dasatinib, ruxolitinib and isosorbide mononitrate and was normal (Fig. 8.1). The patient was discharged on the medications without further complications.

8.2 Discussion

This case is a sobering reminder that despite advances in drug development and testing, cardiotoxicities in cancer therapies continue to offer clinical challenges. Neither agent in this case is thought to cause coronary vasospasm, though dasatinib, a second-generation BCR-ABL inhibitor, is the more likely culprit in that it may affect endothelial function, favoring vasoconstriction [1, 2]. Ruxolitinib, a JAK 1/2 inhibitor, may actually be cardioprotective by inducing NO synthase activity, leading to a vasodilatory state [1, 2]. What is encouraging about this case is that despite the challenges of novel oncologic agents, such as TKIs and immunotherapy, lessons learned from decades of experience with coronary ischemia from 5-FU apply (see Chap. 7). Stress testing while on cancer therapy, modification of the treatment plan with step-wise rechallenge with the two agents, and prophylaxis with nitrates were integral aspects of the cardio-oncology care that allowed the patient to continue to benefit from novel cancer therapies while avoiding potentially catastrophic cardiotoxicity.

References

1. Damrongwatanasuk R, Fradley MG. Cardiovascular complications of targeted therapies for chronic myeloid leukemia. Curr Treat Options Cardiovasc Med. 2017;19(4):24.
2. Herrmann J, Yang EH, Iliescu CA, Cilingiroglu M, Charitakis K, Hakeem A, et al. Vascular toxicities of cancer therapies: the old and the new–an evolving avenue. Circulation. 2016;133(13):1272–89.

Vascular Toxicity of Tyrosine Kinase Inhibitors: Pulmonary Hypertension

9

Anthony F. Yu

Key Points

- Chronic myelogenous leukemia (CML) is a myeloproliferative disorder associated with the Philadelphia chromosome, which expresses the fusion oncoprotein BCR-ABL1.
- Oral tyrosine kinase inhibitors (TKIs) are the mainstay of CML treatment and achieve long-term control in the majority of patients.
- In this case, we highlight severe pulmonary hypertension as an adverse effect of bosutinib in a patient with the previous history of dasatinib-induced pulmonary hypertension.
- CML patients receiving BCR-ABL TKI therapy should undergo routine clinical assessment for potential cardiovascular toxicity, and echocardiography should be performed for patients with signs or symptoms suggestive of pulmonary hypertension.

Chronic myelogenous leukemia (CML) is a myeloproliferative disorder associated with the Philadelphia chromosome t(9;22)(q34;q11), which expresses the fusion oncoprotein BCR-ABL1, a constitutively active tyrosine kinase [1]. Oral TKIs are the mainstay of CML treatment and achieve long-term control in the majority of patients. Selection of a TKI is often based upon the side effect profile of each particular agent, many of which have been associated with cardiovascular toxicities including peripheral arterial disease, myocardial infarction, stroke, and pulmonary hypertension [2].

9.1 Case Report

A 41-year-old woman was diagnosed with CML and treated in the first-line setting with dasatinib, a second-generation BCR-ABL TKI. After 2 years of treatment, she achieved a major molecular response but reported new dyspnea on exertion. A chest X-ray revealed moderate bilateral pleural effusions and an echocardiogram showed a moderate pericardial effusion with tamponade physiology and moderate pulmonary hypertension (peak tricuspid regurgitant velocity 3.8 m/s) with right ventricular enlargement. Her symptoms resolved after thoracentesis and pericardiocentesis; however, pulmonary artery (PA) pressures remained elevated 1 month later. A right heart catheterization was performed, which confirmed the diagnosis of mild precapillary pulmonary hypertension (PA 42/20 mmHg, pulmonary capillary wedge pressure (PCWP) 7 mmHg, PVR 3.3 Wood units). Dasatinib was discontinued and replaced with imatinib, and PA pressures normalized 3 months later on a follow-up echocardiogram. Due to intolerable gastrointestinal toxicity, imatinib was discontinued and replaced with bosutinib (second-generation BCR-ABL TKI). After 12 months of bosutinib, she again developed progressive and severe dyspnea (NYHA class IV). An echocardiogram revealed severe right ventricular enlargement and right ventricular systolic dysfunction (Videos 9.1 and 9.2), severe tricuspid regurgitation, and severe pulmonary hypertension (peak TR velocity 4.7 m/s) (Fig. 9.1). A right heart catheterization confirmed severe precapillary pulmonary hypertension with a PA pressure of 85/45 mmHg, PCWP of 10 mmHg, pulmonary vascular resistance of 16.6 Wood units, and cardiac index of 1.58 L/m/m^2. There was no response to 100% FiO_2 or inhaled nitric oxide. She was admitted to the cardiac care unit for management of right heart failure and severe pulmonary hypertension and treated with dobutamine and treprostinil (a prostacyclin analog). Five months after discontinuation of bosutinib, a repeat echocardiogram showed normal right ventricular size and function and normal pulmonary artery

Electronic supplementary material
The online version of this chapter (https://doi.org/10.1007/978-3-030-70998-3_9) contains supplementary material, which is available to authorized users.

A. F. Yu (✉)
Department of Medicine, Memorial Sloan Kettering Cancer Center, 1275 York Avenue, New York, NY, USA
e-mail: Yua3@mskcc.org

R. M. Steingart et al. (eds.), *Atlas of Imaging in Cardio-Oncology*, https://doi.org/10.1007/978-3-030-70998-3_9

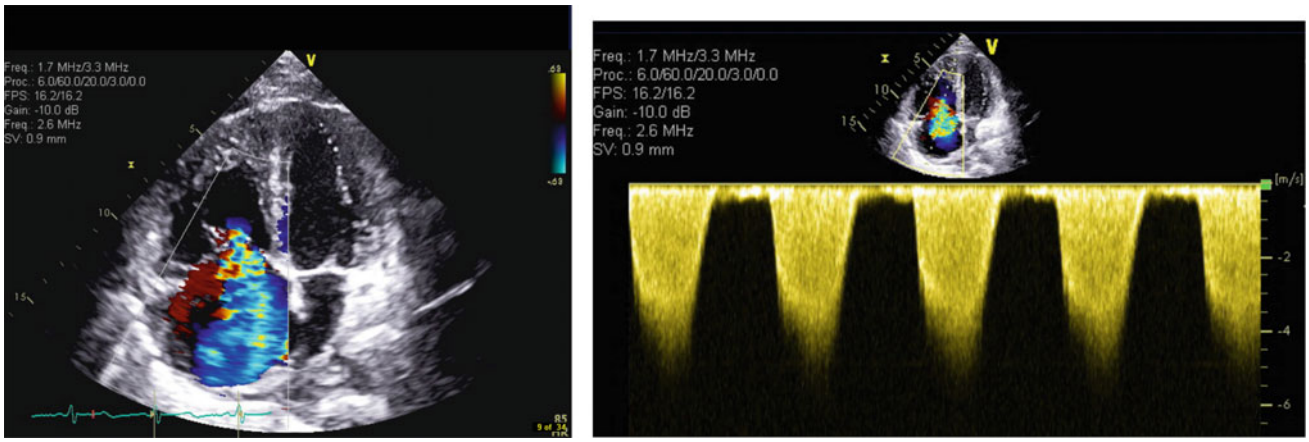

Fig. 9.1 Color (left) and continuous wave (right) Doppler of severe tricuspid regurgitation in a case of severe pulmonary hypertension attributable to BCR-ABL TKI therapy

systolic pressure. Pulmonary vasodilator therapy was gradually tapered, and 3 months later, she was clinically improved (NYHA class I) with normalization of PA pressure on a repeat right heart catheterization (PA 26/8 mmHg, PCWP 5 mmHg, PVR 2.3 Wood units).

Dasatinb, a second-generation TKI, is associated with pulmonary toxicities including pleural effusions and pulmonary hypertension [3–5]. The proposed mechanisms of dasatinib-induced pulmonary hypertenstion include Src kinase inhibition and direct endothelial damage [6]. Bosutinib, also a second-generation TKI, is associated with low rates of cardiac or pulmonary toxicities but may also inhibit Src kinase. In this case, we highlight severe pulmonary hypertension as an adverse effect of bosutinib in a patient with the previous history of dasatinib-induced pulmonary hypertension. CML patients receiving BCR-ABL TKI therapy should undergo routine clinical assessment for potential cardiovascular toxicity, and echocardiography should be performed for patients with signs or symptoms suggestive of pulmonary hypertension.

References

1. Greuber EK, Smith-Pearson P, Wang J, Pendergast AM. Role of ABL family kinases in cancer: from leukaemia to solid tumours. Nat Rev Cancer. 2013;13:559–71.
2. Moslehi JJ, Deininger M. Tyrosine kinase inhibitor-associated cardiovascular toxicity in chronic myeloid Leukemia. J Clin Oncol. 2015;33:4210–8.
3. Quintas-Cardama A, Kantarjian H, O'Brien S, Borthakur G, Bruzzi J, Munden R, Cortes J. Pleural effusion in patients with chronic myelogenous leukemia treated with dasatinib after imatinib failure. J Clin Oncol. 2007;25:3908–14.
4. Rasheed W, Flaim B, Seymour JF. Reversible severe pulmonary hypertension secondary to dasatinib in a patient with chronic myeloid leukemia. Leuk Res. 2009;33:861–4.
5. Montani D, Bergot E, Gunther S, Savale L, Bergeron A, Bourdin A, et al. Pulmonary arterial hypertension in patients treated by dasatinib. Circulation. 2012;125:2128–37.
6. Ozgur Yurttas N, Eskazan AE. Dasatinib-induced pulmonary arterial hypertension. Br J Clin Pharmacol. 2018;84:835–45.

Cardiovascular Toxicities of Proteasome Inhibitors

10

Felix Nguyen, Jose Alvarez-Cardona, and Daniel J. Lenihan

10.1 Introduction

A dramatic number of new therapies have developed over the past decade for the treatment of multiple myeloma (MM), and those treatments have resulted in substantial improvement in patient outcomes [1, 2]. There are now many classes of pharmacotherapy approved for the treatment of MM used in a host of combinations. These include immunomodulatory agents (IMiDs), dexamethasone, proteasome inhibitors (PIs), and monoclonal antibodies. PIs, including bortezomib, carfilzomib, and ixazomib, have become a mainstay of therapy for newly diagnosed MM as well as for relapsed disease. It is important to note that proteasome function is essential to maintaining homeostasis in many cell types, especially cardiomyocytes [3]. As a result of this known biological overlap, there has been concern about PIs having an important effect on the cardiovascular (CV) status of patients with MM who are undergoing active treatment. In fact, several large studies using combination therapy for MM have demonstrated an increased risk of serious CV adverse events during treatment [4–6]. The patterns of treatment for MM are constantly changing, and it is very unusual for PIs to be the only medications used, making it difficult to attribute an adverse event to one specific therapy. Furthermore, the population of patients being treated for MM has a high prevalence of coexistent CV co-morbidities [7].

Metabolically active cells are the most vulnerable to the action of PIs. These include not only clonal plasma cells but also endothelial cells and cardiomyocytes [8]. Thus, PIs have been associated with a variety of cardiotoxicities including heart failure (HF) [9], arrhythmias [10], pulmonary hypertension (PHTN) [11], and thromboembolism [12]. As a result, it is critical that multidisciplinary teams are involved in the care of these patients to improve outcomes through early diagnosis and treatment of these complications. Indeed, the utility of cardiac biomarkers and imaging modalities, such as echocardiography and cardiac magnetic resonance imaging (cMRI), has been shown to provide important diagnostic and prognostic information that can inform clinical decision-making [13]. This chapter will review the more common CV toxicities associated with PIs and present cases that highlight the role of imaging in the diagnosis and management of associated complications.

10.2 Case 1

Heart failure with preserved left ventricular ejection fraction (HFpEF).

- 73-year-old male with recently diagnosed MM who also had HFpEF
- Resistant atrial fibrillation
- Elevated cardiac biomarkers at baseline
- Management of HF throughout allowed for optimal cancer therapy

Electronic supplementary material
The online version of this chapter (https://doi.org/10.1007/978-3-030-70998-3_10) contains supplementary material, which is available to authorized users.

F. Nguyen · J. Alvarez-Cardona · D. J. Lenihan (✉)
Cardio-Oncology Center of Excellence, Washington University in St Louis, 660 South Euclid Avenue, Campus box 8086, St. Louis, MO 63110-1093, USA
e-mail: djlenihan@wustl.edu

F. Nguyen
e-mail: nguyenfd@wustl.edu

J. Alvarez-Cardona
e-mail: alvarez-cardonaj@wustl.edu

R. M. Steingart et al. (eds.), *Atlas of Imaging in Cardio-Oncology*,
https://doi.org/10.1007/978-3-030-70998-3_10

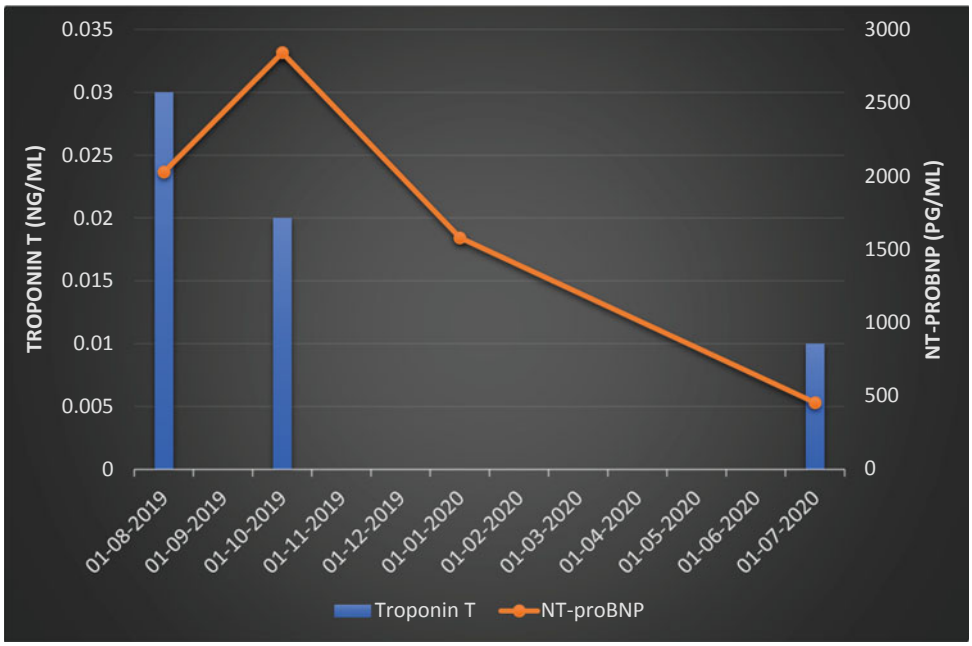

Fig. 10.1 Improvement in cardiac biomarkers over time with treatment of plasma cell dyscrasia

A 73-year-old male originally presented with persistent atrial fibrillation (AF) that was difficult to control, requiring multiple cardioversions and antiarrhythmic medications. He was found to be anemic, with bruising around his eyes, and ultimately was diagnosed with MM. His bone marrow biopsy revealed 40% plasma cells and no evidence of amyloidosis by Congo red staining. He began treatment with carfilzomib, dexamethasone, and lenalidomide. His baseline echocardiographic (echo) study showed a left ventricular ejection fraction (LVEF) of 69%. Staging of diastolic dysfunction could not be done with the most frequently used algorithm given the underlying atrial fibrillation with the absence of atrial kick. His cardiac biomarkers revealed a slightly elevated troponin T of 0.02 ng/mL (normal $\leq$ 0.01 ng/mL) and N-terminal pro-brain natriuretic peptide (NT-proBNP) of 2841 pg/mL (normal $\leq$ 300 pg/mL) (Fig. 10.1). Excess fluid attributed to HF was treated with furosemide and spironolactone and he was started on amiodarone. He was successfully cardioverted 1 month later. A repeated echo did not demonstrate any diastolic dysfunction while he was in sinus rhythm (Fig. 10.2). Several months later, the troponin values remained elevated and a subsequent cardiac MRI

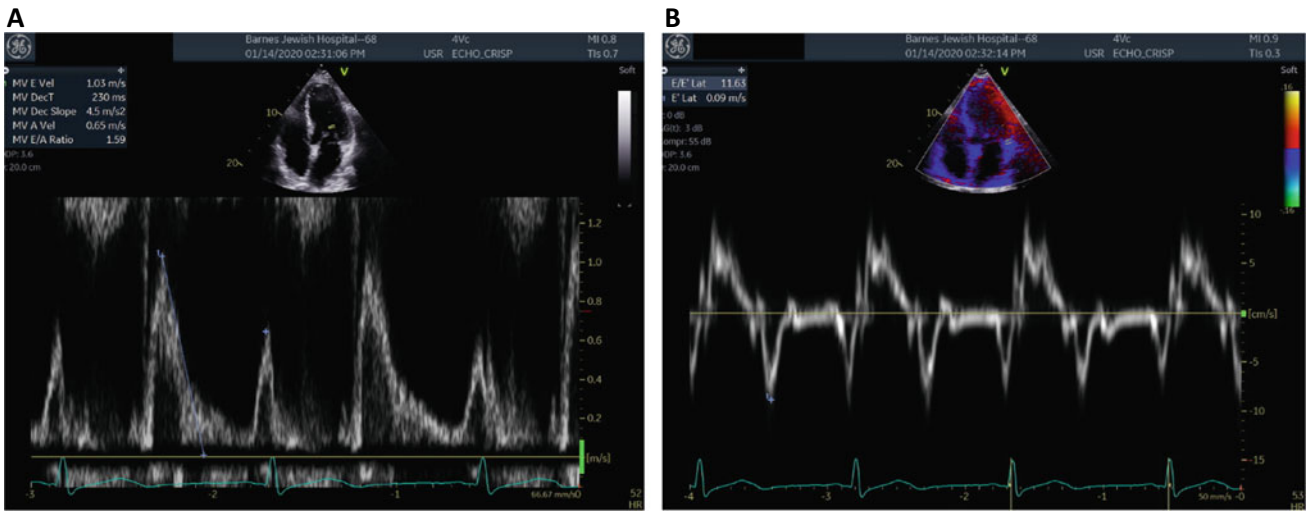

Fig. 10.2 Normal diastolic filling parameters once sinus rhythm was restored. **A** Pulsed wave Doppler of the mitral valve showing E/A ratio of 1.6 and deceleration time of 230 ms. **B** Tissue Doppler of the mitral annulus showing E' lateral of 9 cm/sec with E/E' ratio of 12

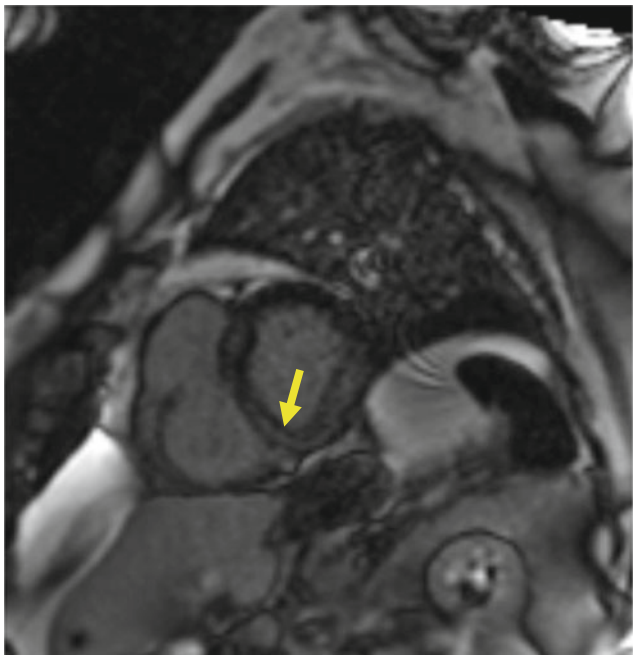

Fig. 10.3 Diffuse hyperenhancement with gadolinium contrast (arrow) consistent with cardiac amyloidosis

(cMRI) demonstrated an LVEF of 62% with overall normal function and mild basal septal hypertrophy of 1.2 cm (Video 10.1). Late gadolinium imaging was positive for patchy diffuse sub-endocardial hyper-enhancement consistent with amyloidosis (Fig. 10.3). His cardiac biomarkers 11 months later improved and were approaching normal (Fig. 10.1). His MM therapy continued throughout without interruption and he ultimately achieved remission.

10.2.1 Discussion

HF, especially HF with preserved ejection fraction (HFpEF), is a frequent manifestation of cardiac amyloidosis (CA) but it is also an important adverse effect of PI therapy, especially the irreversible proteasome inhibitor, carfilzomib. In a safety analysis of patients with MM being treated with carfilzomib (in combination therapy), 7.2% of patients were found to have new HF [9]. In another study, 23% of patients with MM treated with carfilzomib developed clinical HF, with elevations in NTproBNP and some with a reduction in LVEF [14]. The mechanism is not well understood but is possibly related to PI-induced oxidative stress within myocytes, inhibition of the proteasome, or transient endothelial dysfunction [6, 8]. Hypertension, another adverse effect of PIs, may also contribute to the development of HFpEF. Indeed, in patients undergoing combination therapy for MM, the use of biomarkers, especially NTproBNP, can help with risk stratification and monitoring for CV toxicity. A recent prospective study of patients with relapsed MM confirmed the utility of natriuretic peptides to assist in risk stratification as well as management of CV co-morbidity during treatment. Additionally, carfilzomib was associated with a much higher rate of CV events than bortezomib (a reversible inhibitor of the proteasome). A major finding of this study was that a CV adverse event was subsequently associated with worse survival [13]. It is therefore critical to monitor for CV risks and to manage these proactively to achieve the best outcome.

CA, resulting from AL amyloidosis, involves the deposition of amyloid fibrils within the extracellular matrix of the heart and can be a manifestation of MM (see chapter 18 on Cardiac Amyloidosis). Although previously believed to be found in <5% of patients with MM, CA is likely underdiagnosed [6]. Management involves addressing not only the cardiac complications of the disease, such as HF and arrhythmia [15], but also importantly eliminating the underlying amyloidogenic light chain production, for which treatments have evolved significantly over the past decade. In particular, the addition of PIs to treatment regimens for MM and AL amyloidosis has resulted in improved hematologic responses and survival [16, 17]. Current first-line regimens for MM combine a PI with an IMiD, such as lenalidomide, thalidomide, or pomalidomide, as well as dexamethasone. Bortezomib, carfilzomib, and ixazomib are the current FDA-approved PIs for this purpose. Features of cardiac involvement in AL amyloidosis can often be appreciated initially on echocardiography. Amyloid deposition within the myocardium leads to left ventricular (LV) hypertrophy and increased LV wall thickness, often >15 mm [6]. There is usually, but not always, significant diastolic dysfunction, with Doppler imaging demonstrating elevated E/e' values and short deceleration times on trans-mitral pulsed Doppler [6]. Speckle strain imaging can be both sensitive and specific showing impaired strain in the basal segments with sparing at the apex, a finding that has particularly good sensitivity and specificity [18]. In this patient, echo imaging did not show these characteristics but cMRI did indicate the likelihood of AL CA.

10.3 Case 2

Atrial thrombi in patients receiving PIs.

- 60-year-old male with AL cardiac amyloidosis
- Receiving bortezomib-based therapy
- New-onset atrial flutter
- Left atrial clot within 48 hours of atrial flutter

A 60-year-old male with AL amyloidosis initially treated with an autologous stem cell transplant and then had relapsed disease treated with cytoxan, bortezomib, and dexamethasone

(CyBorD) starting in October 2017. He presented to the hospital about 10 months later with volume overload related to HFpEF and new-onset atrial flutter (AFL). Although he was within 48 hours from the onset of arrhythmia, transesophageal echocardiography (TEE) was pursued given his increased risk of thrombosis. TEE revealed a left atrial thrombus (Fig. 10.4) in part due to his CA with a likely contribution from his combination therapy with a PI, an IMiD, and dexamethasone [7]. Cardioversion was deferred, and he was subsequently anticoagulated with apixaban. He presented again on 10/2018 for repeat TEE and possible cardioversion but was found to have persistent left atrial thrombus (Fig. 10.5). Given the persistent thrombus while receiving apixaban, he was switched to warfarin with careful prothrombin time monitoring to ensure adequate anticoagulation and was started on amiodarone 200 mg daily to assist with rate control since he was unable to tolerate b-blockade due to hypotension. Despite 100% compliance and adequate anticoagulation with therapeutic INR values over several months, repeat TEE in March 2019 revealed a persistent left atrial thrombus (Fig. 10.6). This case demonstrates that patients with CA, especially when treated for AL with PI-based therapy, have a substantial risk of persistent left atrial thrombus. Furthermore, it is unclear if one form of anticoagulation is better than another for preventing the persistent thrombus. It is our practice that these patients be *required* to undergo TEE prior to cardioversion even after adequate anticoagulation given the high likelihood for underlying intracardiac thrombus.

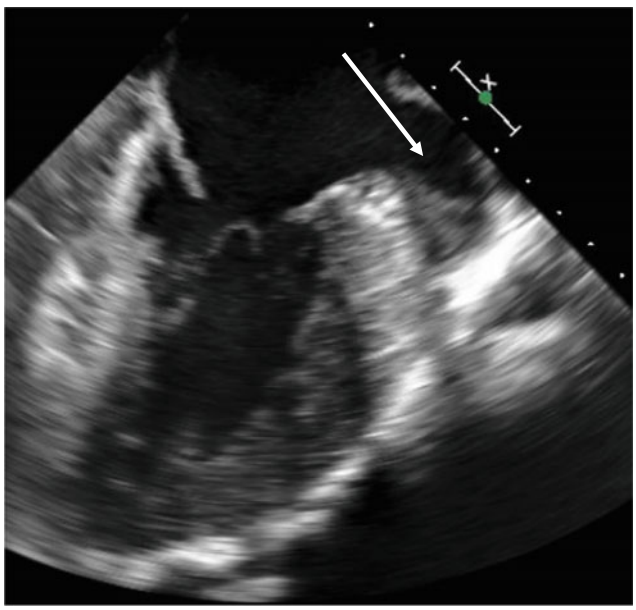

Fig. 10.4 Thrombus in a patient with cardiac amyloidosis and atrial flutter. Two-chamber view on transesophageal echocardiography demonstrating thrombus within the left atrial appendage (arrow) (August 2018)

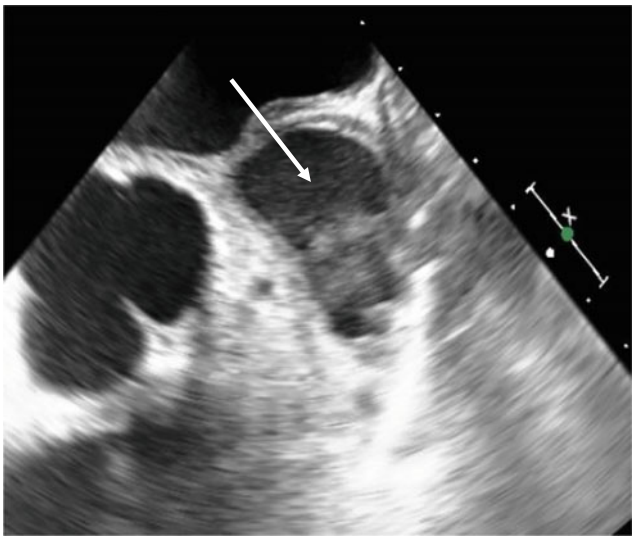

Fig. 10.5 Short-axis view at mid-esophageal level showing persistent thrombus within the appendage (arrow) (October 2018)

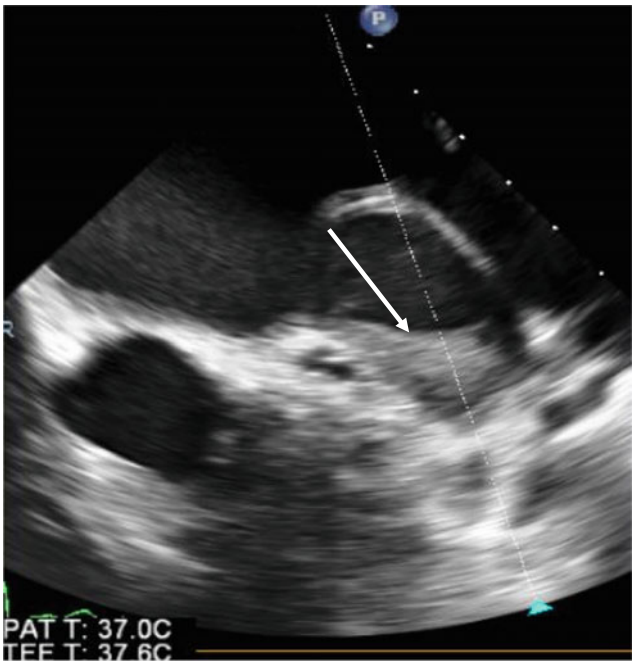

Fig. 10.6 Repeated TEE at mid-esophageal level showing continued thrombus (arrow) despite the switch from apixaban to warfarin (March 2019)

10.3.1 Discussion

Conduction abnormalities are common in CA, with atrial fibrillation (AF) or AFL and atrioventricular block often the presenting disorders. This is due largely to amyloid deposition involving the conduction system with fibrosis of the surrounding myocardium [10]. In particular, AF is associated with impaired ventricular filling, which often

leads to HFpEF . In one study, patients with AF and CA had similar success rates of cardioversion (90 vs. 94%, p = 0.47) and rates of recurrence at 1 year (48 vs. 55%, p = 0.75) as compared to those with no CA [19]. Additionally, other studies evaluating cardioversion in separate populations of ATTR and AL amyloidosis patients found similar rates of success [20, 21]. However, those with CA had much higher rates of complications following cardioversion compared to controls (14 vs. 2%, p = 0.007) [19]. These complications included bradyarrhythmias as well as ventricular tachycardia/fibrillation, all of which are typically rare following cardioversion [22]. Further complicating management in these patients involves the use of TEE prior to DC cardioversion. Patients with CA are highly susceptible to intravascular and intracardiac thrombosis, especially when receiving PIs and IMiD. Intracardiac thrombosis has been commonly identified on TEE [20], the majority of which occur in the left atrial appendage. Current guidelines from the 2014 AHA/ACC/HRS recommend at least 3 weeks of therapeutic anticoagulation prior to cardioversion ***or*** use of TEE as an alternative. A large proportion of patients (46%) had an intra-cardiac thrombus on TEE at the time of cardioversion and were either already on therapeutic anticoagulation for at least 3 weeks or were within 48 h of the onset of arrhythmia. Therefore, it has been suggested that the use of TEE with cardioversion should be imperative for patients with AF and concomitant CA, regardless of the duration of anticoagulation or time of onset from arrhythmia [19]. This would be especially true in patients undergoing therapy with PIs and IMiDs as part of the treatment of AL amyloidosis.

10.4 Case 3

Pulmonary hypertension.

- 78-year-old male, with refractory MM
- Previous AF, status post pulmonary vein isolation, and a Watchman device
- Worsened HFpEF during therapy with carfilzomib
- Developed severe pulmonary hypertension within months of starting PI therapy

A 78-year-old male, with a history of AF, was treated with one previous ablation and then a Watchman device implant (Fig. 10.7). He developed MM and due to the progression of disease over the course of many years, he was treated with multiple agents (ixazomib, elotuzumab, daratumumab, lenalidomide (an IMiD), and even bendamustine). In August 2019, he began treatment with carfilzomib and dexamethasone. Two months after starting this therapy, he presented to the hospital with worsening exertional dyspnea and was found to have new PHTN with an estimated pulmonary artery (PA) pressure of 77 mmHg on transthoracic echocardiogram (Fig. 10.8). Right heart catheterization confirmed a right atrial pressure of 12 mm Hg, right ventricular pressure of 77/16 mm Hg, an elevated PA pressure of 81/39 mmHg (mean 49 mmHg), and a pulmonary capillary wedge pressure (PCWP) of 17 mmHg. His cardiac output was 4.6 L/min with an index of 2.3 L/min/m^2. His mixed venous saturation was 50%. Carfilzomib was implicated to be the culprit for the elevated PA pressure, so it was

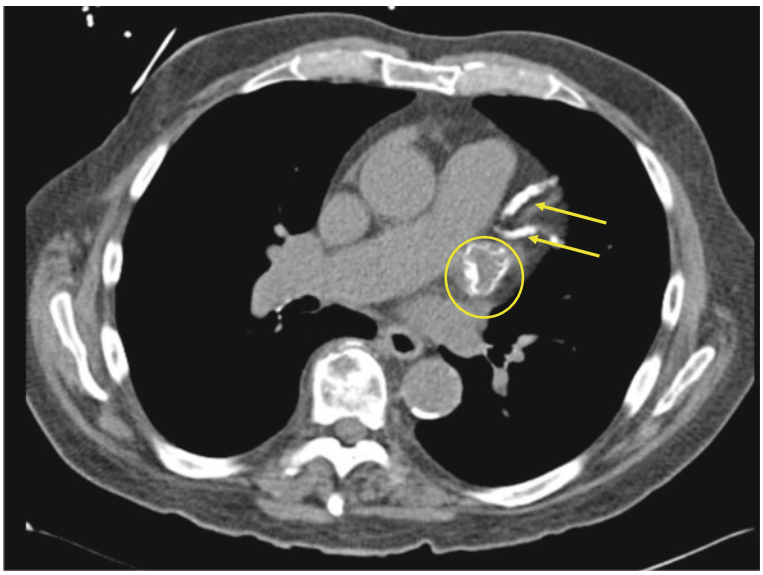

Fig. 10.7 CT scan of the chest demonstrating the Watchman device (inside a circle) lying within the left atrial appendage. The patient has a history of atrial fibrillation for which he had undergone ablation with pulmonary vein isolation and placement of a Watchman device. Diffuse coronary calcifications are also seen (arrows)

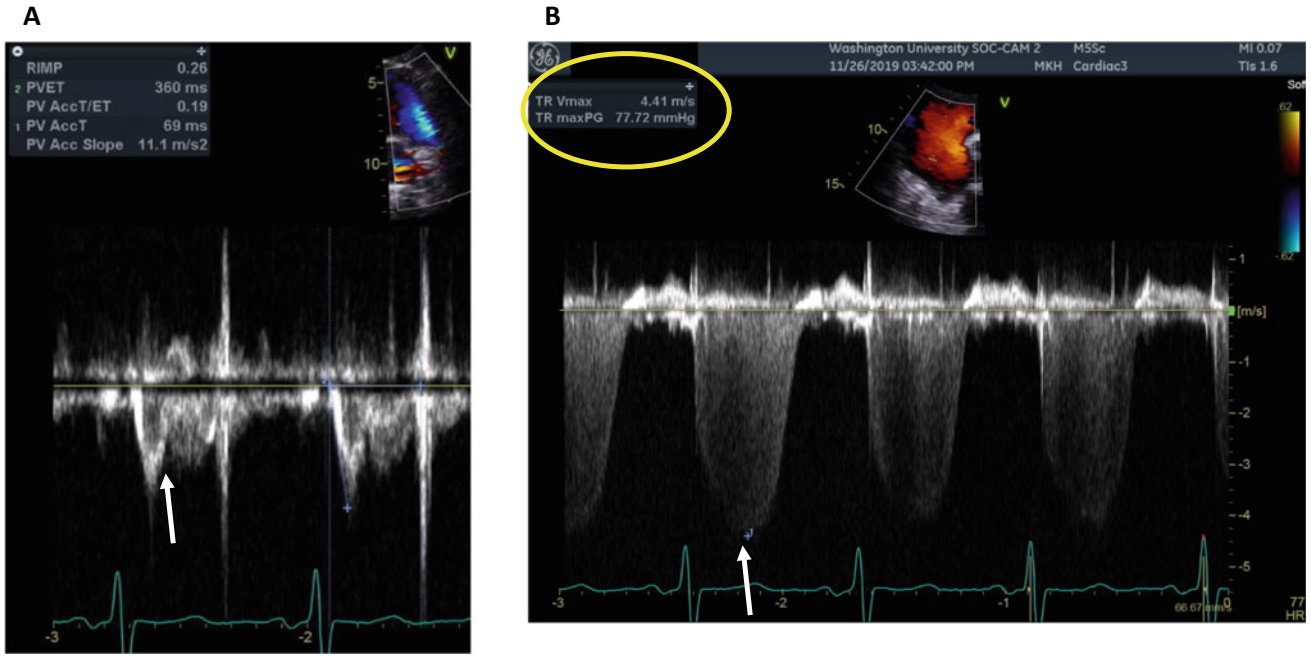

Fig. 10.8 **A** Patient with multiple myeloma and new pulmonary hypertension. Pulsed wave Doppler across the right ventricular outflow tract demonstrates mid systolic notching (arrow) of the pulmonary arterial flow with markedly shortened acceleration time 69 ms (normal > 130 ms). **B** Tricuspid regurgitant jet (arrow) with a peak velocity of 4.4 m/sec, estimating PA systolic pressure at 85 mm Hg (assuming an RA pressure of 8 mm Hg)

subsequently discontinued. A follow-up transthoracic echocardiogram 1 month later revealed a PA pressure estimate of 83 mmHg. He was enrolled in a clinical trial with tiragolumab, a novel immune checkpoint inhibitor for his MM but was found to have disease progression and elected to discontinue therapy and proceed with hospice care. This case demonstrates that CV toxicity from therapies can have a profound impact on the treatment course and ultimately patient prognosis. Although the theoretical concern of pulmonary vein stenosis from a previous ablation may have contributed to his presentation, the acuity of his decompensation following initiation of carfilzomib suggests that the PI was the primary cause for his new-onset PHTN.

10.4.1 Discussion

PHTN has been documented to be a rare complication of PIs, although available data are sparse. In an extensive analysis of myeloma patients treated with carfilzomib in the SEER (Surveillance, Epidemiology, and End Results) database, only 1% of patients developed pulmonary hypertension [11]. There was a comprehensive analysis done in patients with MM who were treated with carfilzomib, as part of the ENDEAVOR study, and there was no major elevation of PA pressure estimated on TTE throughout the study period (26.4 mmHg at baseline to 23.65 mmHg at Week 96 of follow-up) [5]. PHTN secondary to PI therapy with carfilzomib, would likely demonstrate features on echocardiography that are similar to other etiologies of PTHN and this was not seen in this trial. The pathogenesis of PHTN associated with PI therapy is unclear but may involve changes within the endothelial nitric oxide pathway [23]. As with other CV adverse events, management likely depends on the severity of PHTN and may require discontinuation of the drug in addition to other supportive treatments including diuresis. It is unknown whether PI-associated PHTN would likely improve with discontinuation of cancer therapy.

10.5 Case 4

Arterial and venous thromboembolism.

- 64-year-old female presented 6 months earlier with a fall and acute carpal tunnel syndrome
- Mild troponin elevations initially
- Developed worsening HF over the next 6 months
- Diagnosed with AL CA by biopsy
- Developed arterial and venous thrombosis
- Initiated PI-based therapy
- Despite anticoagulation, a large left atrial thrombus developed resulting in partial inflow obstruction

A 64-year-old female presented to our medical center in July 2019 after a mechanical fall during which she sustained a distal radius fracture and acute carpal tunnel syndrome. Cardiac evaluation prior to orthopedic surgery revealed abnormal troponin I (0.13 ng/mL, normal < 0.03 ng/mL) and NT-proBNP (4121 pg/mL, normal < 300 pg/mL) as well as low-QRS voltage and a pseudo-infarct pattern on 12-lead electrocardiogram. Stress myocardial perfusion imaging was unrevealing. She underwent successful surgery and was subsequently discharged. She presented again to our hospital 5 months later with progressive exertional dyspnea, weight gain, and edema. She was found to have a new first-degree AV block on ECG and diastolic dysfunction on TTE. An endomyocardial biopsy confirmed a diagnosis of AL amyloidosis. Her hospitalization was complicated by acute limb ischemia involving her right popliteal artery requiring thrombo-embolectomy. She also had an acute ischemic stroke requiring aspiration thrombectomy. She was started on anticoagulation with apixaban and her plasma cell dyscrasia was treated with CyBorD. She was admitted again for upper gastrointestinal bleeding requiring esophagogastroduodenoscopy. Repeated transthoracic echocardiography showed a reduced ejection fraction of 32%, grade 3 diastolic dysfunction, and a new left atrial thrombus despite ongoing anticoagulation (Video 10.2) (see chapter 16 on Masses Involving the Heart and Vasculature).

This patient's hospital course was complicated by mixed cardiogenic and septic shock requiring vasopressors that could not halt her progressive decline and ultimate death. Even though there were telltale signs of potential cardiac involvement from CA present in July 2019, the definitive diagnosis leading to treatment was not made until 6 months later (Fig. 10.9). Early identification of disease and earlier treatment perhaps at the time when the abnormal biomarkers and ECG were noted would very likely have improved the outcome for this patient. It is also clear that she was highly thrombogenic and suffered multiple vascular complications, even prior to starting treatment for her amyloidosis.

10.5.1 Discussion

Patients with MM and AL amyloidosis are at elevated risk of thrombosis due to both disease- and treatment-related factors. In particular, intracardiac thrombosis is common and can be demonstrated by echocardiography (TEE more sensitive than TTE) in patients with AL amyloid associated with multiple myeloma [12, 20]. A variety of risk factors identifiable on echo have been shown to reflect an increased thrombosis risk. Those with more extensive cardiac amyloidosis, as described by higher grades of diastolic dysfunction were found to be at higher risk [20]. Higher E/A

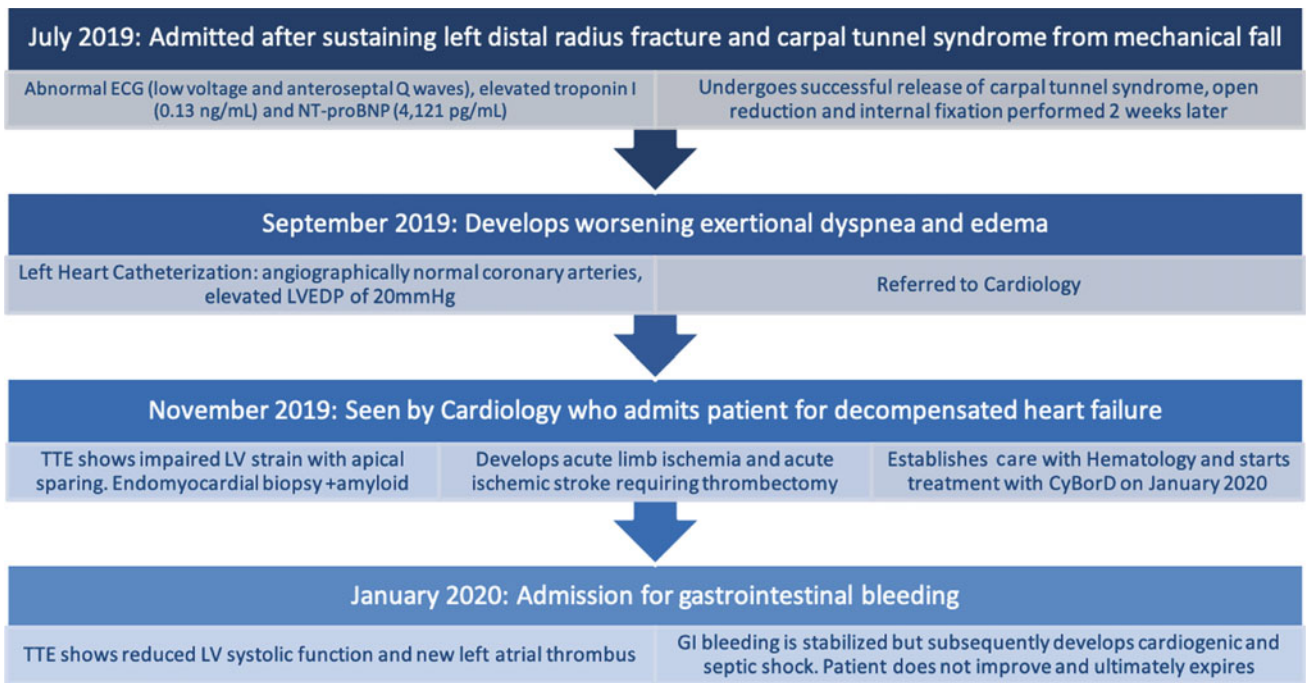

Fig. 10.9 Timeline from initial presentation to final admission. Initial evidence of amyloidosis with cardiac involvement is present during July 2019 admission. The diagnosis is not made until an admission in November 2019 at which time the patient is started on anticoagulation. Treatment for the plasma cell dyscrasia is initiated on January 2020, about 6 months after the initial presentation

and E/e' ratios and shorter mitral deceleration times were also associated with thrombosis risk. To further complicate matters, there is substantial additional risk conferred when combining the use of PIs with IMiDs, such as thalidomide or lenalidomide which are typical medications used in first-line regimens for multiple myeloma [5, 24–26]. In the ASPIRE study, patients treated with lenalidomide and dexamethasone combined with carfilzomib had higher rates of venous thromboembolism as compared to those treated with lenalidomide and dexamethasone alone (10 vs. 6.2%) [25]. Anticoagulation is the mainstay for the management of thrombosis in these patients. However, there have been data showing thrombosis may continue to persist despite anticoagulation. In a study evaluating intra-cardiac thrombosis using cMRI in patients who have CA, a high prevalence of thrombi was found, particularly in those with AF (13.1%) [27]. All patients with AF in the study were reportedly on long-term anticoagulation (46% on warfarin, 54% on a direct oral anticoagulant) at the time of imaging. Such findings suggest that when thromboses occur in these patients, they may be particularly resistant to conventional therapy. Indeed, prophylactic anticoagulation has been proposed as a strategy to prevent or decrease clot burden. Guidelines from ASCO recommend that in patients with MM receiving thalidomide- or lenalidomide-based (IMiD) regimens, the use of either aspirin or low molecular weight heparin is warranted in lower-risk patients and low molecular weight heparin in higher-risk patients [28].

References

1. Rajkumar SV. Multiple myeloma: 2020 update on diagnosis, risk-stratification and management. Am J Hematol. 2020;95:548–67.
2. Kumar SK, Dispenzieri A, Lacy MQ, Gertz MA, Buadi FK, Pandey S, et al. Continued improvement in survival in multiple myeloma: changes in early mortality and outcomes in older patients. Leukemia. 2014;28:1122–8.
3. Willis MS, Patterson C. Proteotoxicity and cardiac dysfunction—Alzheimer's disease of the heart? N Engl J Med. 2013;368:455–64.
4. Stewart AK, Rajkumar SV, Dimopoulos MA, et al. Carfilzomib, lenalidomide, and dexamethasone for relapsed multiple myeloma. N Engl J Med. 2015;372:142–52.
5. Chari A, Stewart AK, Russell SD, et al. Analysis of carfilzomib cardiovascular safety profile across relapsed and/or refractory multiple myeloma clinical trials. Blood Adv. 2018;2:1633–44.
6. Waxman AJ, Clasen S, Hwang WT, et al. Carfilzomib-associated cardiovascular adverse events: a systematic review and meta-analysis. JAMA Oncol. 2018;4:e174519.
7. Li W, Cornell RF, Lenihan D, et al. Cardiovascular complications of novel multiple myeloma treatments. Circulation. 2016;133:908–12.
8. Gavazzoni M, Lombardi CM, Vizzardi E, et al. Irreversible proteasome inhibition with carfilzomib as first line therapy in patients with newly diagnosed multiple myeloma: Early in vivo cardiovascular effects. Eur J Pharmacol. 2018;838:85–90.
9. Siegel D, Martin T, Nooka A, et al. Integrated safety profile of single-agent carfilzomib: experience from 526 patients enrolled in 4 phase II clinical studies. Haematologica. 2013;98:1753–61.
10. Ridolfi RL, Bulkley BH, Hutchins GM. The conduction system in cardiac amyloidosis: clinical and pathologic features of 23 patients. Am J Med. 1977;62:677–86.
11. Fakhri B, Fiala MA, Shah N, Vij R, Wildes TM. Measuring cardiopulmonary complications of carfilzomib treatment and associated risk factors using the SEER-Medicare database. Cancer. 2020;126:808–13.
12. DaLi F, D EW, K OJ et al. Intracardiac thrombosis and embolism in patients with cardiac amyloidosis. Circulation. 2007;116:2420–26.
13. Cornell RF, Ky B, Weiss BM, et al. Prospective study of cardiac events during proteasome inhibitor therapy for relapsed multiple myeloma. J Clin Oncol. 2019;37:1946–55.
14. Danhof S, Schreder M, Rasche L, Strifler S, Einsele H, Knop S. 'Real-life' experience of preapproval carfilzomib-based therapy in myeloma—analysis of cardiac toxicity and predisposing factors. Eur J Haematol. 2016;97:25–32.
15. Falk RH, Alexander KM, Liao R, Dorbala S. AL (light-chain) cardiac amyloidosis: a review of diagnosis and therapy. J Am Coll Cardiol. 2016;68:1323–41.
16. Giancaterino S, Urey MA, Darden D, Hsu JC. Management of arrhythmias in cardiac amyloidosis. JACC Clin Electrophysiol. 2020;6:351–61.
17. Kastritis E, Leleu X, Arnulf B, et al. A randomized phase III trial of melphalan and dexamethasone (MDex) versus bortezomib, melphalan and dexamethasone (BMDex) for untreated patients with AL amyloidosis. Blood. 2016;128:646–746.
18. Gertz MA, Dispenzieri A. Systemic amyloidosis recognition, prognosis, and therapy: a systematic review. JAMA. 2020;324:79–89.
19. Phelan D, Collier P, Thavendiranathan P, et al. Relative apical sparing of longitudinal strain using two-dimensional speckle-tracking echocardiography is both sensitive and specific for the diagnosis of cardiac amyloidosis. Heart. 2012;98:1442–8.
20. El-Am EA, Dispenzieri A, Melduni RM, et al. Direct current cardioversion of atrial arrhythmias in adults with cardiac amyloidosis. J Am Coll Cardiol. 2019;73:589–97.
21. Loungani RS, Rehorn MR, Geurink KR, et al. Outcomes following cardioversion for patients with cardiac amyloidosis and atrial fibrillation or atrial flutter. Am Heart J. 2020;222:26–9.
22. Donnellan E, Wazni OM, Hanna M, et al. Atrial fibrillation in transthyretin cardiac amyloidosis: predictors, prevalence, and efficacy of rhythm control strategies. JACC Clin Electrophysiol. 2020;6:1118–27.
23. Grönberg T, Nuotio I, Nikkinen M, et al. Arrhythmic complications after electrical cardioversion of acute atrial fibrillation: the FinCV study. Europace. 2013;15:1432–5.
24. DaLi F, S SI, Matthew M et al. Intracardiac thrombosis and anticoagulation therapy in cardiac amyloidosis. Circulation. 2009;119:2490–7.
25. Chari A, Hajje D. Case series discussion of cardiac and vascular events following carfilzomib treatment: possible mechanism, screening, and monitoring. BMC Cancer. 2014;14:915.
26. Sonneveld P, Asselbergs E, Zweegman S, et al. Phase 2 study of carfilzomib, thalidomide, and dexamethasone as induction/consolidation therapy for newly diagnosed multiple myeloma. Blood. 2015;125:449–56.
27. Wang M, Martin T, Bensinger W, et al. Phase 2 dose-expansion study (PX-171-006) of carfilzomib, lenalidomide, and low-dose dexamethasone in relapsed or progressive multiple myeloma. Blood. 2013;122:3122–8.

28. Stewart AK, Rajkumar SV, Dimopoulos MA, et al. Carfilzomib, lenalidomide, and dexamethasone for relapsed multiple myeloma. New Engl J Med. 2014;372:142–52.
29. Fradley MG, Groarke JD, Laubach J, et al. Recurrent cardiotoxicity potentiated by the interaction of proteasome inhibitor and immunomodulatory therapy for the treatment of multiple myeloma. Br J Haematol. 2018;180:271–5.
30. Martinez-Naharro A, Gonzalez-Lopez E, Corovic A, et al. High prevalence of intracardiac thrombi in cardiac amyloidosis. J Am Coll Cardiol. 2019;73:1733–4.
31. Key NS, Khorana AA, Kuderer NM, et al. Venous thromboembolism prophylaxis and treatment in patients with cancer: ASCO clinical practice guideline update. J Clin Oncol. 2019;38:496–520.

11 Cardiac Complications of 5-Fluorouracil (5FU) and Capecitabine Therapy

Wendy Schaffer

Key Points

- The complex pathophysiology of 5-FU results in a broad spectrum of cardiac toxicity including chest pain/angina, ischemia, non-STEMI and STEMI, silent ischemia, brady and tachyarrhythmias, QT prolongation, heart failure, and stress cardiomyopathy.
- Management includes avoiding/discontinuing 5-FU, dose reduction, bolus 5 FU therapy, anti-anginals, inpatient cardiac monitoring during therapy, and aggressive treatment of cardiac risk factors and established cardiac disease.

11.1 Introduction

Synthesized in 1957 by Heidelberger et al. [1], 5-fluorouracil (5-FU) is a pyrimidine analog that disrupts DNA synthesis [1]. 5-FU-based chemotherapy is the standard of care for adjuvant treatment of stage II and II colorectal cancer (high-risk node-negative and node-positive disease) with a 20–30% reduction in mortality [2]. It is a front-line agent for potentially curable, as well as metastatic, pancreatic cancer, metastatic esophageal and gastric cancer, early-stage breast cancer with residual disease after anthracycline-based therapy, metastatic breast, and head and neck cancers [3–9]. It is humbling to realize it took almost 20 years to recognize 5-FU associated cardiac toxicity, when a 48-year-old man presented with chest pain and EKG changes during 5-FU infusion [10]. Despite the wide-spread use of 5-FU for more than 50 years, the pathophysiology of 5-FU cardiotoxicity is still not fully understood. 5-FU induced coronary vasospasm has been reproduced in vitro and in vivo models, but 5-FU has also been shown to promote cardiac hypertrophy, myocardial necrosis, apoptosis of myocardial and endothelial cells, and thrombus formation [11–16]. The complex pathophysiology of 5-FU results in a broad spectrum of cardiac toxicity including chest pain/angina, ischemia, non-STEMI and STEMI, silent ischemia noted on EKG or ambulatory monitoring, brady and tachyarrhythmias, QT prolongation, heart failure, and a stress cardiomyopathy [1, 17–21]. Management strategies include avoiding/discontinuing 5-FU-based therapies, dose reduction, bolus rather than continuous infusion, anti-anginal therapy, and cardiac monitoring, as well as guideline-directed aggressive treatment of underlying cardiac risk factors and established cardiac disease. Each patient's treatment plan, when confronted with 5-FU cardiotoxicity or concern for 5-FU cardiotoxicity, is best formulated with a careful risk–benefit assessment of the oncologic options and outcomes with the patient's oncology team. The following cases explore some of the clinical presentations of 5-FU cardiotoxicity as well as management strategies that may prove helpful in practice.

11.2 Case 1

Dyspnea in a young woman without cardiac risk factors [22].

- A 38-year-old woman with no cardiac risk factors or cardiac disease with recurrent breast cancer was started on capecitabine.
- She reported dyspnea with mild exertion and an inability to tolerate her usual high-intensity workouts.
- A stress echocardiogram was performed while still on the capecitabine, during which she manifested shortness of breath, was able to tolerate only 5 min 18 s, 7 METs. The EKG demonstrated very mild ST elevation.

Electronic supplementary material
The online version of this chapter (https://doi.org/10.1007/978-3-030-70998-3_11) contains supplementary material, which is available to authorized users.

W. Schaffer (✉)
Department of Medicine, Memorial Sloan Kettering Cancer Center, 1275 York Avenue, New York, NY 10065, USA
e-mail: Schaffew@mskcc.org

R. M. Steingart et al. (eds.), *Atlas of Imaging in Cardio-Oncology*,
https://doi.org/10.1007/978-3-030-70998-3_11

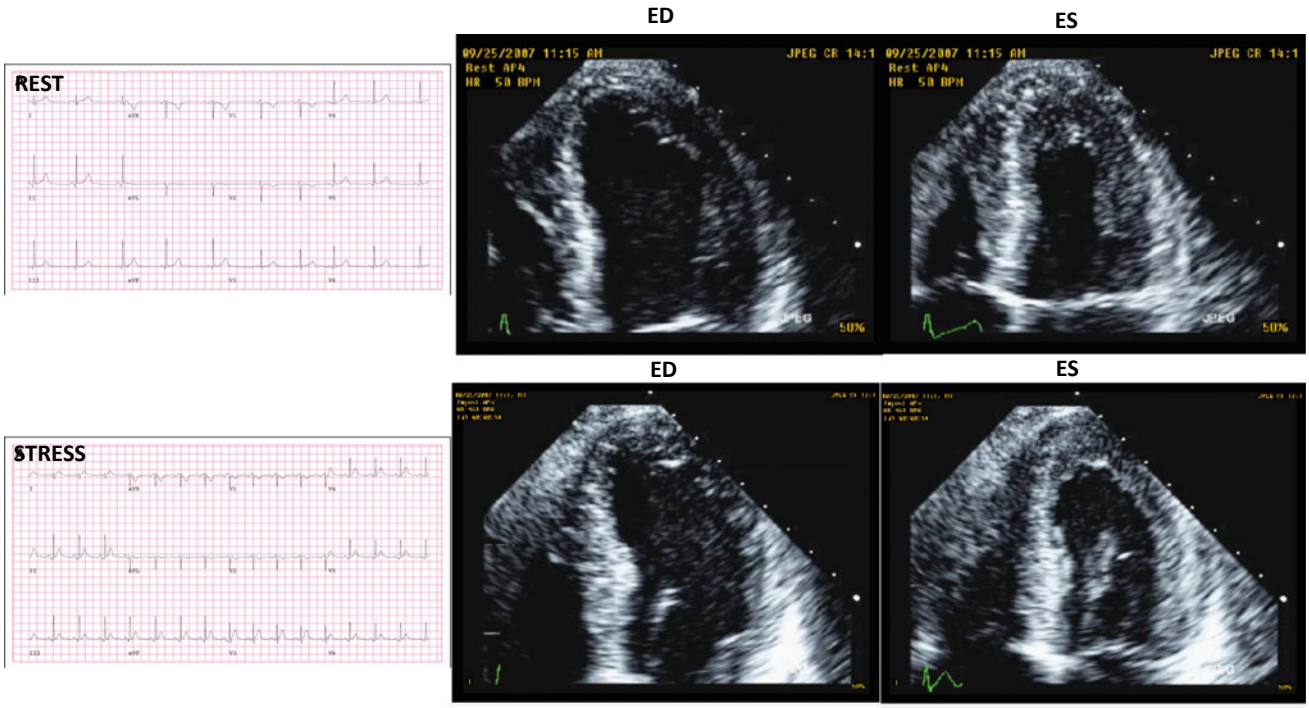

Fig. 11.1 End diastolic (ED) and end systolic (ES) frames from echocardiographic apical four-chamber rest and stress studies showing apical wall motion abnormality with a decline in LV EF with exercise. Accompanying EKG was normal at rest and showed mild ST segment elevation with exercise

Post-exercise imaging demonstrated a decline in EF with apical hypokinesis (Fig. 11.1, Video 11.1).

- She was observed in the hospital following the abnormal stress test with negative troponins, and a normal CT coronary angiogram.
- Capecitabine was discontinued and the patient underwent a normal stress echo 10 days later and was able to exercise to 15.1 METs without dyspnea.

11.2.1 Discussion

This patient did not experience any long-term sequelae from exposure to 5-FU. Her oncology team listened closely to her complaints of dyspnea while on capecitabine, referred her to the cardio-oncology service and appropriate testing was performed. Stress testing while on 5-FU (whether while on the oral pro-drug capecitabine or on the 5-FU infusion pump) can be helpful to assess for ischemia. A CT coronary angiogram was appropriate to rule out underlying obstructive coronary artery disease in a patient without a high pre-test probability for a disease where formal coronary angiography could be more useful in consideration of a revascularization strategy. The follow-up normal stress test after stopping capecitabine was helpful to confirm the etiology of her symptoms and the initially ischemic stress test. This patient's high-risk stress test precluded further exposure to 5-FU, given the myriad of other options available to treat advanced breast cancer with comparable oncologic outcomes. A thoughtful discussion with the cardio-oncologist, the oncologist, and the patient in cases such as this is essential to explore the necessity of 5-FU-based treatment in the setting of the observed cardiac risk.

11.3 Case 2

Cardiac arrest in a young man without cardiac risk factors.

- A 28-year-old man with metastatic ileal adenocarcinoma with no cardiac disease or risk factors for the disease was started on FOLFOX, tolerating six cycles without cardiac complications.
- Two days after completion of the seventh cycle, he had a documented ventricular tachycardia arrest while swimming at a YMCA. He was treated with CPR and AED shocks by bystanders. A technically challenging EKG acquired by the Emergency Medical Services staff on resuscitation was notable for inferolateral ST elevation and hyperacute appearing T waves, as demonstrated in Fig. 11.2.

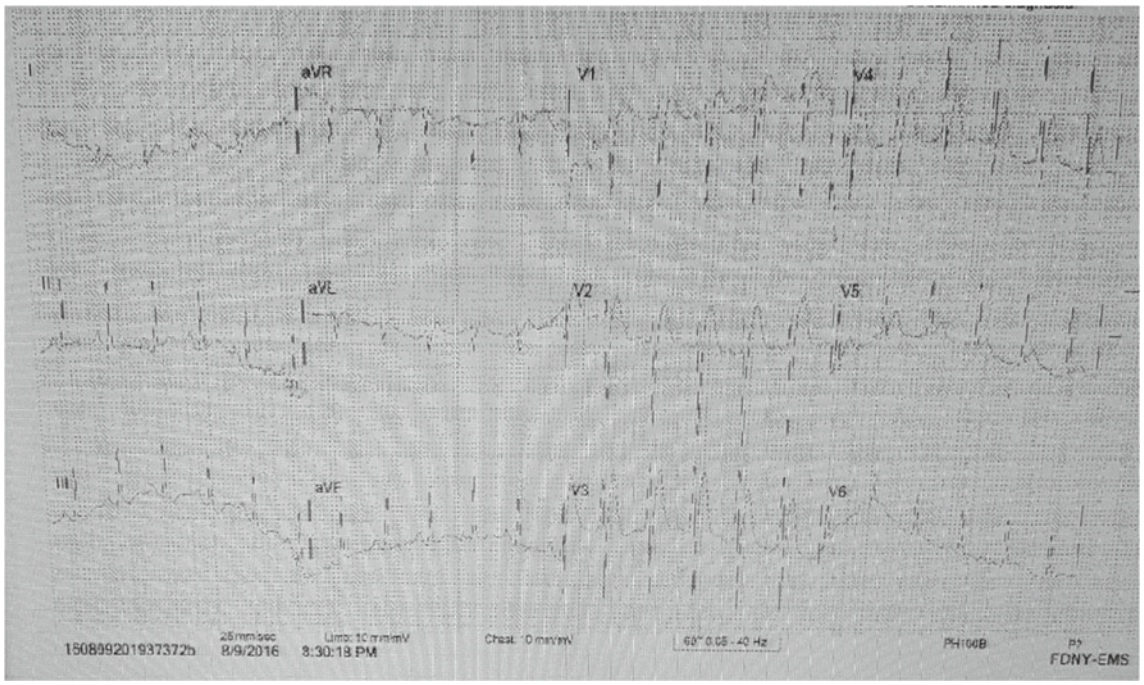

Fig. 11.2 12 lead EKG acquired in the field after resuscitation by Emergency Medical Services. In this technically challenging tracing, ST segment elevation is seen and the T waves are peaked and prominent

- Post-resuscitation testing included echocardiogram, cardiac catheterization, cardiac MRI, EP study, and stress echocardiogram, all of which were entirely normal.
- Patient stated that the only difference between the final cycle of 5FU and prior cycles is that he resumed high-level exercise sooner than usual. In retrospect, he admitted to mild chest pain after each dose of 5-FU.
- Per recommendations of his cardio-oncologist, an ICD was not implanted.
- Discussions with the patient, oncologist, and cardio-oncologist determined that the benefit of further challenges with 5-FU-based treatment was outweighed by the risk and no further 5-FU-based treatment was administered. He had no further cardiac events.

11.3.1 Discussion

The cited incidence of a cardiac event with 5-FU spans a wide range in the literature, due to variation in the definition of and methods for identifying a cardiac event, the selected patient population and underlying cardiac risk factors, and the dose and delivery of 5-FU. In one systematic review of studies each with over 400 patients, the incidence of a cardiac event was 1.2–4.3%, with treatment-related mortality of 0–0.5% [23]. Though the comparatively low treatment-related mortality is reassuring, a small, prospective study with ambulatory EKG monitoring demonstrated that a little over 50% of patients without established coronary artery disease have significant EKG changes (ST depression or ST elevation), notably without evidence of myocardial damage by serial biomarkers, while on the 5-FU infusion pump [24]. The incidence of arrhythmias, especially life-threatening arrhythmias, is unknown but certainly low, especially in patients without underlying cardiac risk factors. That said, once a life-threatening event has occurred, it is incumbent on the cardio-oncology and oncology teams to examine all other oncologic options before considering re-challenge. Though the decision not to re-challenge a patient who had a cardiac arrest seems straightforward, it is worth examining the pros and cons closely. The patient, extraordinarily young with very advanced cancer, tolerated several cycles of 5-FU without incident, though in retrospect he reported chest pain with each cycle. On discussion with the oncologist, cardio-oncologist, and patient, the oncologist felt the patient had other treatment options that could be explored. Sadly, the patient's disease progressed too quickly to allow the question to be readdressed. Whether continued 5-FU-based therapy could have been tolerated with aggressive management strategies and whether this would have altered the eventual outcome is unknown.

11.4 Case 3A

ST segment elevation myocardial infarction (STEMI) in an older man with suspected underlying coronary artery disease and ongoing angina.

- A 60-year-old man, a prior smoker, with hypertension, hyperlipidemia, and locally advanced rectal cancer was started on neoadjuvant 5-FU-based chemotherapy (FOLFOX). Marked coronary calcification was noted on CT scanning performed for cancer staging (Fig. 11.3).
- He alerted the oncology team prior to initiation of 5-FU-based therapy that he had angina. He provided records of a recent cardiac evaluation, including a normal echocardiogram and pharmacologic nuclear stress test with normal perfusion. His cardiologist had started him on appropriate guideline-directed medical therapy (GDMT) for his risk factors with the plan to perform a cardiac catheterization if his symptoms persisted.
- The patient reported his typical anginal symptoms to the oncology team with the first cycle of FOLFOX with 5-FU IV bolus and 48H infusion pump.
- The oncologist dose reduced the 5-FU for the second cycle and the patient reported improvement in his anginal symptoms.
- With the third cycle, the patient had severe chest pain while at home on the 5-FU infusion pump. He presented to an emergency room. The infusion was discontinued. EKG demonstrated anterior ST elevation with reciprocal ST depression. Troponins were markedly elevated.
- Emergent cardiac catheterization revealed two-vessel coronary disease. The patient received drug-eluting stents to the LAD and RCA and was placed on dual anti-platelet therapy (DAPT).
- Six weeks later, the patient was rechallenged with 5-FU with IV bolus alone (FLOX), in a monitored inpatient setting, without complications.
- Subsequent cycles were given in the outpatient setting, with bolus 5-FU alone (FLOX), without further cardiac complications.
- The patient underwent successful surgical resection on uninterrupted aspirin. Clopidogrel was held.

11.4.1 Case 3B

Angina in an older man with cardiac risk factors who had tolerated 5-FU therapy for several years.

- A 60-year-old man, a prior smoker, was diagnosed with metastatic colon cancer in 2014 and had been maintained on 5-FU-based chemotherapy continuously since diagnosis.

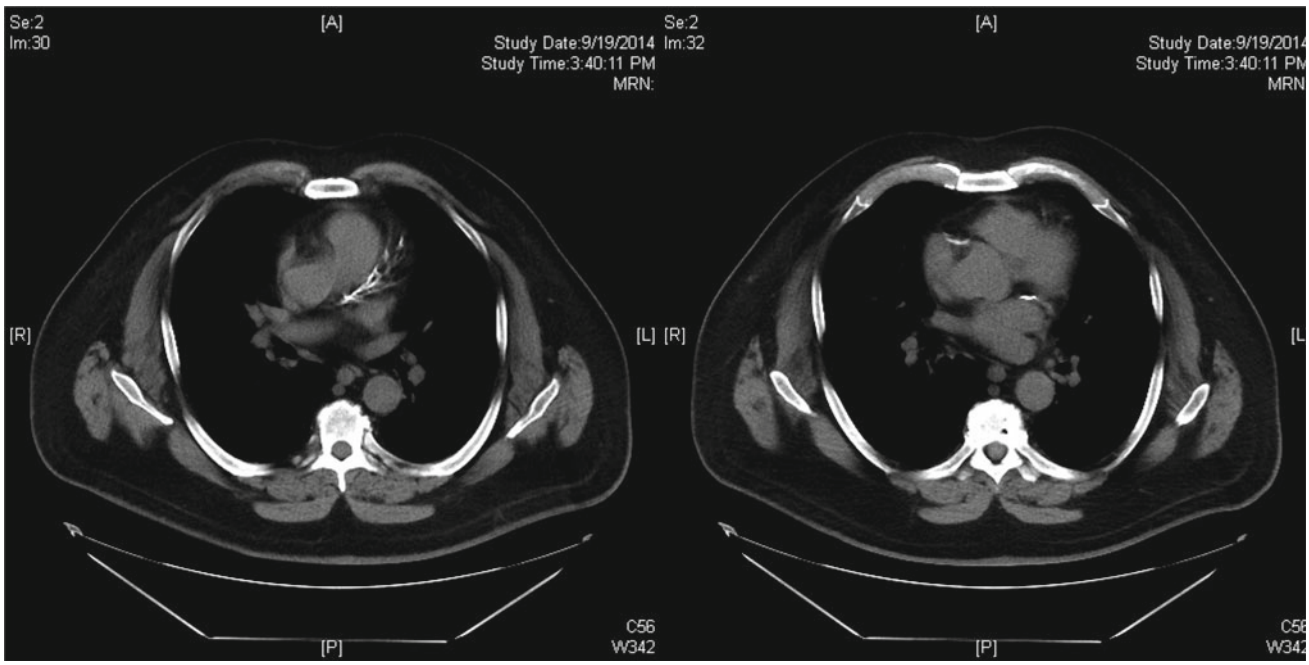

Fig. 11.3 Extensive coronary calcium seen on the patient's staging CT of chest/abdomen/pelvis

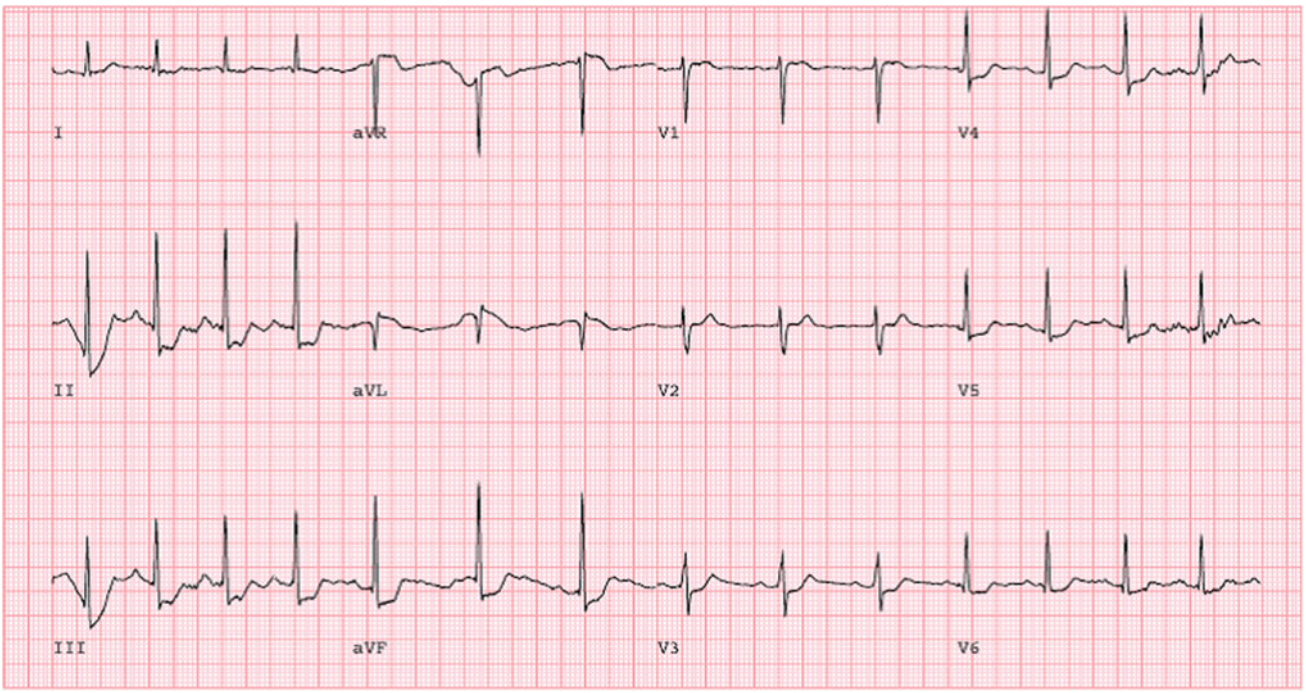

Fig. 11.4 Stress test done during a 5 FU infusion that shows marked ST segment depression despite treatment with diltiazem in a patient who developed angina after having tolerated 5-FU for several years

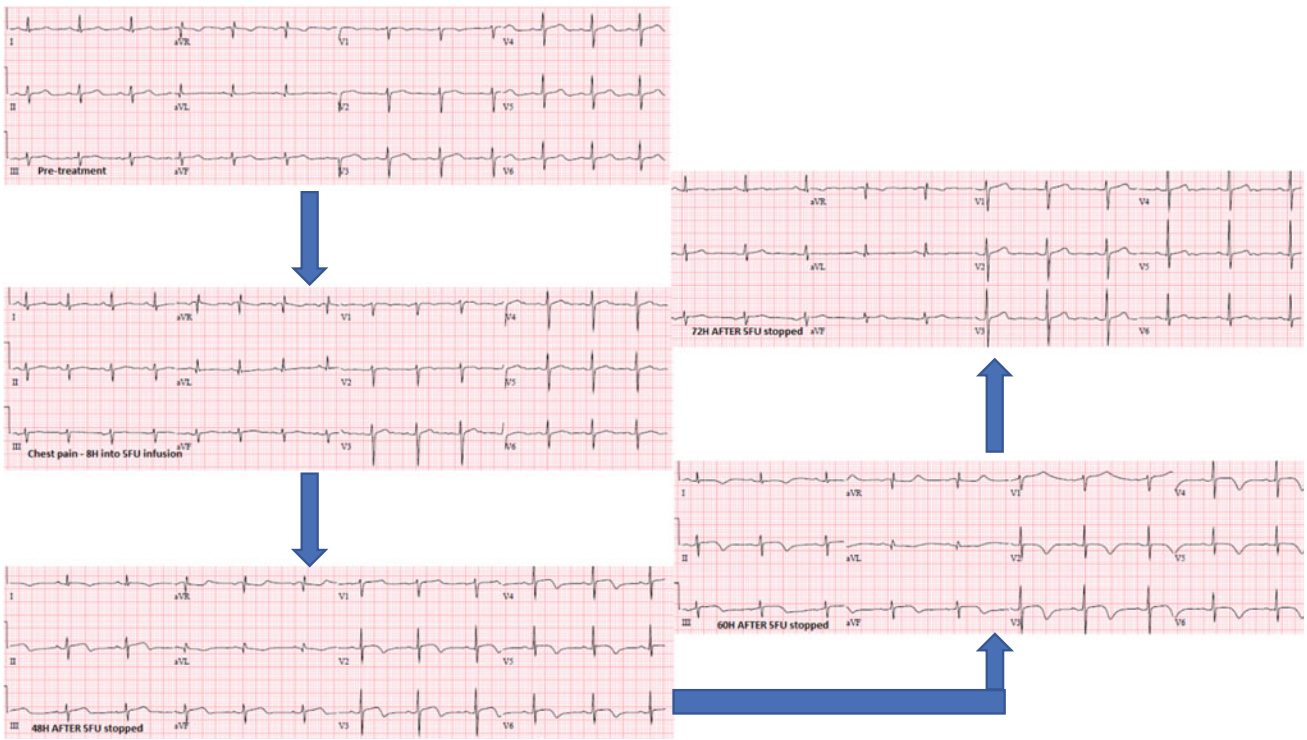

Fig. 11.5 The time evolution of the EKG abnormalities during 5 FU re-challenge

- In 2018, he reported to his oncologist chest pressure when walking up hills that he had noticed over the last several months.
- His resting echocardiogram and EKG were entirely normal.
- Given the significant benefit, he was deriving from 5-FU, the cardio-oncologist and oncologist agreed with the patient's consent to try to continue 5-FU treatment.
- He was started on diltiazem with improvement in his symptoms.
- A stress echo was performed on diltiazem and with the 5FU infusion pump.
- The patient experienced mild angina at 5 min with low heart rate and at that relatively low heart rate EKG demonstrated horizontal ST depression (Fig. 11.4). Post-exercise echo demonstrated apical, anteroseptal akinesis with a decline in LV EF.
- The 5-FU infusion was discontinued.
- An urgent cardiac catheterization was performed, demonstrating 95% ostial left main disease. He received a drug-eluting stent to the left main and was started on DAPT, in addition to GDMT.
- One month after PCI, he was rechallenged with 5-FU bolus only (FLOX) in a monitored setting without cardiac complications.
- He was continued on outpatient 5-FU bolus therapy with stable disease for several more years without cardiac complications.

11.4.2 Discussion

In case 3A, though the patient did not have known coronary artery disease by echocardiography, EKG, or nuclear stress test, review of the patient's CT scan performed for the evaluation of the extent of his oncologic disease revealed extensive coronary calcification. The same was the case for the patient in case 3B, though the patient was on no GDMT when first presenting with chest pain. Cancer patients often have chest CT or PET/CT that can be reviewed for coronary atherosclerosis. Though these scans cannot provide information on the degree of obstruction, nor does a scan without coronary calcification entirely rule out coronary disease, the finding of extensive coronary calcification should be addressed with risk factor modification and further work-up prior to initiating 5-FU-based therapy. The cardiologist for the patient in case 3A had planned a cardiac catheterization if the patient's anginal symptoms did not respond to medical therapy. The oncologist appropriately dose reduced the patient's 5-FU when the patient reported chest pain. In retrospect, coordinated care by the cardiologist and the oncologist might have pre-empted the events following the third cycle. For patients with ongoing anginal symptoms or a large ischemic burden despite GDMT, referral to a cardio-oncologist is imperative prior to initiating 5-FU-based therapies and to ensure appropriate cardiac care during cancer treatment. For these high-risk patients, it is reasonable to consider inpatient monitoring for the first dose of 5-FU.

Not surprisingly, the published data defining the incidence of cardiac events on 5-FU in patients with known ischemic heart disease is small (well less than 5% of the data sets), with a wide range of reported incidence (5–15%), dependent on factors such as patient inclusion criteria, the definition of cardiac event, and dose and mode of delivery of 5-FU [20, 23, 25]. In consenting a patient for 5-FU-based therapy, it is reasonable to cite a 5% or higher risk of significant cardiac events for patients with known coronary disease. It is important to put this risk in perspective with the known benefit of 5-FU with respect to the patient's cancer, as well as to emphasize that any chest pain or shortness of breath with 5-FU or its oral prodrug, capecitabine, may represent a potentially life-threatening event and must be reported to healthcare providers immediately.

In case 3B, GDMT for coronary artery disease, as recommended independently of the patient's cancer status, was imperative to allow for continued 5-FU based chemotherapy. Revascularization in the setting of accelerating anginal symptoms and a high-risk stress test allowed the patient to continue successfully with 5-FU based therapy for several more years. Data are not available to guide the decision as to when to start or resume 5-FU-based therapy after cardiac revascularization, and thus the decision is based on a consensus opinion in consultation with the patient, the oncologist, the interventional cardiologist or cardiothoracic surgeon, and the cardio-oncologist involved in the patient's care. The patients in both case 3A and case 3B were admitted for cardiac monitoring when resuming 5-FU-based therapy, a reasonable practice that allows for timely intervention should anginal symptoms/signs recur with re-challenge, though no specific data quantify the benefit.

In case 3A and case 3B, after revascularization, and in discussion with the oncologist and the cardio-oncologist, each patient's chemotherapy was changed from FOLFOX to FLOX. With respect to 5-FU, FOLFOX includes a bolus and a 48H infusion, whereas FLOX includes a bolus alone. The overall dose, administration schedule, and non-cardiac side effect profiles are different. Continuous infusion 5-FU may carry a higher risk of cardiac events than bolus alone [23, 26–28]. The incidence of events with capecitabine appears similar to 5-FU continuous infusion over 5 days [23, 26, 27, 29]. One frequently cited study of patients, mostly with colorectal or head and neck cancers, found an incidence of cardiac toxicity, defined as symptoms and/or EKG changes, of 2.3% with bolus 5-FU alone compared to 6.7% when 5-FU was delivered by prolonged infusion (with similar

cardiac toxicity with oral capecitabine) [26]. Though head-to-head comparisons of FOLFOX versus FLOX are not available, for example, in the adjuvant treatment of stage 2/3 colorectal cancer, significant data from the Mosaic and NSABP trials support the use of FOLFOX over FLOX [30]. It is imperative that the cardio-oncologist and the oncologist discuss how changes in dose/delivery of 5-FU therapy may affect the oncologic outcome. As with case 3A and case 3B, it is reasonable to ask the oncologist to consider bolus 5-FU alone when the risk of cardiac toxicity with prolonged infusion of 5-FU is prohibitively high.

11.5 Case 4

A young woman without cardiac risk factors with stress cardiomyopathy.

- A 45-year-old woman with metastatic colon cancer was started on 5-FU based therapy with FOLFOX (bolus + 48H infusion pump).
- At pump disconnect, she reported that she had experienced stuttering chest pain and dyspnea for the prior 12H.
- EKG demonstrated <1 mm ST elevation. She was transferred for emergent cardiac catheterization given on-going symptoms and EKG findings.
- Angiogram revealed normal coronary arteries and severe global hypokinesis, LV EF 20%. She required hemodynamic support with an intra-aortic balloon pump and pressors. Troponin was borderline elevated.
- Over the next few days, she was stabilized and hemodynamic support was discontinued.
- EKGs evolved with pronounced ST-T wave abnormalities.
- She was discharged on low-dose carvedilol.
- Outpatient echocardiogram 2 weeks later demonstrated normal LV systolic function. The patient had no symptoms or signs of heart failure.
- Given the patient's young age and lack of other comparable treatment options, the oncologist, cardio-oncologist, and patient agreed to attempt re-challenge in a highly monitored setting with prophylaxis (nitrates, calcium-channel blockers and continued carvedilol).
- One month after the initial event, the patient was admitted to a cardiac care unit for re-challenge on low dose carvedilol, nitrates, and calcium channel blockers. She was treated with a reduced dose 5-FU, bolus with a proposed 48H infusion.
- At 36H, the patient reported chest pain and the 5-FU infusion pump was discontinued. EKGs demonstrated similar evolution, initially < 1 mm ST elevation evolving over the next several days with marked ST-T wave abnormalities (Fig. 11.5). Echocardiogram demonstrated moderate-severe global hypokinesis, LV EF 34%. Troponins were normal throughout. The patient remained hemodynamically stable.
- The EF normalized within days and the patient was discharged on low dose carvedilol. Other agents were discontinued due to asymptomatic low blood pressure.
- The patient was not rechallenged.

11.5.1 Discussion

Data suggest cardiac events occur most frequently during the first .5-FU cycle, incidence twice to eight times higher than with later cycles [25, 28, 31–34]. Median onset is reported within 72H of initiating 5-FU [31, 33, 34]. The effect of oral capecitabine is similar to a continuous low-dose infusion of 5-FU [23]. Though the incidence of cardiac events with capecitabine is higher during the first cycle, 5.2% vs 1.3% in later cycles, the onset of cardiac toxicity is even less predictable, as might be expected with delivery via an oral pro-drug [32].

Dose reduction and prophylaxis with anti-anginal therapy (usually nitrates and/or calcium channel blockers) as attempted in case 4, as well as bolus rather than continuous infusion, may be helpful, as suggested in published algorithms [26, 34–36]. Given the complex pathophysiology of 5-FU cardiotoxicity, these measures are not always sufficient to prevent events, as demonstrated in case 4. Careful inpatient monitoring allowed re-challenge in a controlled setting with timely discontinuation of the 5-FU infusion pump and appropriate cardiac care.

In the acute setting, treatment of 5-FU cardiotoxicity includes nitrates and/or calcium channel blockers to address possible vasospasm, as well as GDMT for ACS/STEMI if underlying coronary artery disease cannot be definitively ruled out. As in case 4, emergent cardiac catheterization is recommended in the presence of significant ST-segment elevation, depression, new LBBB or hemodynamic instability. Stress cardiomyopathy is a less common but reported cardiac toxicity of 5-FU therapy [37]. Case 4 is prototypical with severe decline in LV function, minimal EKG changes initially with the evolution of deep T wave inversions over hours to days, and borderline elevated troponin, as well as recovery of LV systolic function over a short period without significant pharmacologic intervention. Case 4 also demonstrates recurrent events with re-challenge with 5-FU, as can be seen with stress cardiomyopathy in other settings. Given the risk to the patient in this circumstance despite all efforts to rechallenge safely, discontinuation of 5-FU-based therapy was the only option.

References

1. Heidelberger C, Chaudhuri NK, Danneberg P, et al. Fluorinated pyrimidines, a new class of tumour-inhibitory compounds. Nature. 1957;179(4561):663–6.
2. Benson AB, Venook AP, Al-Hawary MM, et al. NCCN guidelines insights: colon cancer, version 2.2018. J Natl Compr Canc Netw. 2018;16(4):359–369.
3. Khorana AA, Mangu PB, Berlin J, et al. Potentially Curable Pancreatic Cancer: American society of clinical oncology clinical practice guideline update. J Clin Oncol. 2017;35(20):2324–8.
4. Sohal DP, Mangu PB, Khorana AA, et al. Metastatic pancreatic cancer: American society of clinical oncology clinical practice guideline. J Clin Oncol. 2016;34(23):2784–96.
5. Oshaughnessy JA, Blum J, Moiseyenko V, et al. Randomized, open-label, phase II trial of oral capecitabine (Xeloda) vs. a reference arm of intravenous CMF (cyclophosphamide, methotrexate and 5-fluorouracil) as first-line therapy for advanced/metastatic breast cancer. Ann Oncol. 2001;12(9):1247–1254.
6. Fumoleau P, Largillier R, Clippe C, et al. Multicentre, phase II study evaluating capecitabine monotherapy in patients with anthracycline- and taxane-pretreated metastatic breast cancer. Eur J Cancer. 2004;40(4):536–42.
7. Masuda N, Lee SJ, Ohtani S, et al. Adjuvant Capecitabine for breast cancer after preoperative chemotherapy. N Engl J Med. 2017;376(22):2147–59.
8. Colevas AD, Yom SS, Pfister DG, et al. NCCN Guidelines insights: head and neck cancers, version 1.2018. J Natl Compr Canc Netw. 2018;16(5):479–490.
9. Enzinger PC, Burtness BA, Niedzwiecki D, et al. CALGB 80403 (Alliance)/E1206: A randomized phase ii study of three chemotherapy regimens plus cetuximab in metastatic esophageal and gastroesophageal junction cancers. J Clin Oncol. 2016;34 (23):2736–42.
10. Roth A, Kolaric K, Popovic S. Letter: cardiotoxicity of 5-fluorouracil (NSC-19893). Cancer chemotherapy reports Part 1. 1975;59(6):1051–1052.
11. Tsibiribi P, Bui-Xuan C, Bui-Xuan B, et al. Cardiac lesions induced by 5-fluorouracil in the rabbit. Hum Exp Toxicol. 2006;25 (6):305–9.
12. Cwikiel M, Zhang B, Eskilsson J, Wieslander JB, Albertsson M. The influence of 5-fluorouracil on the endothelium in small arteries. An electron microscopic study in rabbits. Scanning Microscopy. 1995;9(2):561–576.
13. Cwikiel M, Eskilsson J, Wieslander JB, Stjernquist U, Albertsson M. The appearance of endothelium in small arteries after treatment with 5-fluorouracil. An electron microscopic study of late effects in rabbits. Scanning Microscopy. 1996;10(3):805–818; discussion 819.
14. Cwikiel M, Eskilsson J, Albertsson M, Stavenow L. The influence of 5-fluorouracil and methotrexate on vascular endothelium. An experimental study using endothelial cells in the culture. Ann Oncol. 1996;7(7):731–737.
15. Luwaert RJ, Descamps O, Majois F, Chaudron JM, Beauduin M. Coronary artery spasm induced by 5-fluorouracil. Eur Heart J. 1991;12(3):468–70.
16. Sudhoff T, Enderle MD, Pahlke M, et al. 5-Fluorouracil induces arterial vasocontractions. Ann Oncol. 2004;15(4):661–4.
17. Stewart T, Pavlakis N, Ward M. Cardiotoxicity with 5-fluorouracil and capecitabine: more than just vasospastic angina. Intern Med J. 2010;40(4):303–7.
18. Talapatra K, Rajesh I, Rajesh B, Selvamani B, Subhashini J. Transient asymptomatic bradycardia in patients on infusional 5-fluorouracil. J Cancer Res Ther. 2007;3(3):169–71.
19. Wacker A, Lersch C, Scherpinski U, Reindl L, Seyfarth M. High incidence of angina pectoris in patients treated with 5-fluorouracil. A planned surveillance study with 102 patients. Oncology. 2003;65(2):108–112.
20. Labianca R, Beretta G, Clerici M, Fraschini P, Luporini G. Cardiac toxicity of 5-fluorouracil: a study on 1083 patients. Tumori. 1982;68(6):505–10.
21. Schober C, Papageorgiou E, Harstrick A, et al. Cardiotoxicity of 5-fluorouracil in combination with folinic acid in patients with gastrointestinal cancer. Cancer. 1993;72(7):2242–7.
22. Goldsmith YB, Roistacher N, Baum MS. Capecitabine-induced coronary vasospasm. J Clin Oncol Off J Am Soc Clin Oncol. 2008;26(22):3802–4.
23. Polk A, Vaage-Nilsen M, Vistisen K, Nielsen DL. Cardiotoxicity in cancer patients treated with 5-fluorouracil or capecitabine: a systematic review of incidence, manifestations and predisposing factors. Cancer Treat Rev. 2013;39(8):974–84.
24. Rezkalla S, Kloner RA, Ensley J, et al. Continuous ambulatory ECG monitoring during fluorouracil therapy: a prospective study. J Clin Oncol Off J Am Soc Clin Oncol. 1989;7(4):509–14.
25. Meyer CC, Calis KA, Burke LB, Walawander CA, Grasela TH. Symptomatic cardiotoxicity associated with 5-fluorouracil. Pharmacotherapy. 1997;17(4):729–36.
26. Kosmas C, Kallistratos MS, Kopterides P, et al. Cardiotoxicity of fluoropyrimidines in different schedules of administration: a prospective study. J Cancer Res Clin Oncol. 2008;134(1):75–82.
27. Tsavaris N, Kosmas C, Vadiaka M, et al. 5-fluorouracil cardiotoxicity is a rare, dose and schedule-dependent adverse event: a prospective study. J BUON Off J Balkan Union Onco. 2005;10 (2):205–11.
28. Kelly C, Bhuva N, Harrison M, Buckley A, Saunders M. Use of raltitrexed as an alternative to 5-fluorouracil and capecitabine in cancer patients with cardiac history. Eur J Cancer. 2013;49 (10):2303–10.
29. Van Cutsem E, Hoff PM, Blum JL, Abt M, Osterwalder B. Incidence of cardiotoxicity with the oral fluoropyrimidine capecitabine is typical of that reported with 5-fluorouracil. Ann Oncol. 2002;13(3):484–5.
30. Sharif S, O'Connell MJ, Yothers G, Lopa S, Wolmark N. FOLFOX and FLOX regimens for the adjuvant treatment of resected stage II and III colon cancer. Cancer Invest. 2008;26 (9):956–63.
31. Meydan N, Kundak I, Yavuzsen T, et al. Cardiotoxicity of de Gramont's regimen: incidence, clinical characteristics and long-term follow-up. Jpn J Clin Oncol. 2005;35(5):265–70.
32. Ng M, Cunningham D, Norman AR. The frequency and pattern of cardiotoxicity observed with capecitabine used in conjunction with oxaliplatin in patients treated for advanced colorectal cancer (CRC). Eur J Cancer. 2005;41(11):1542–6.

33. Akhtar SS, Salim KP, Bano ZA. Symptomatic cardiotoxicity with high-dose 5-fluorouracil infusion: a prospective study. Oncology. 1993;50(6):441–4.
34. Jensen SA, Sorensen JB. Risk factors and prevention of cardiotoxicity induced by 5-fluorouracil or capecitabine. Cancer Chemother Pharmacol. 2006;58(4):487–93.
35. Cianci G, Morelli MF, Cannita K, et al. Prophylactic options in patients with 5-fluorouracil-associated cardiotoxicity. Br J Cancer. 2003;88(10):1507–9.
36. Clasen SC, Ky B, O'Quinn R, Giantonio B, Teitelbaum U, Carver JR. Fluoropyrimidine-induced cardiac toxicity: challenging the current paradigm. J Gastrointest Oncol. 2017;8(6):970–9.
37. Grunwald MR, Howie L, Diaz LA Jr. Takotsubo cardiomyopathy and Fluorouracil: case report and review of the literature. J Clin Oncol. 2012;30(2):e11-14.

Cisplatin and Carboplatin

12

Lili Zhang and Michelle N. Johnson

Key Points

- Platinum-based agents are the backbone of therapeutic regimens in many cancer types.
- Cisplatin-based regimens have been associated with thromboembolic complications, affecting both venous and arterial systems.
- The pathogenesis may include hypomagnesemia, vascular damage, alterations in platelet aggregation, increased von Willebrand factor, and damage to endothelial cells.
- The incidence of venous thromboembolism with cisplatin was 1.92% and for arterial thromboembolism 0.67%, as reported in systemic review and meta-analysis studies.
- Cisplatin is associated with a long term increased risk of coronary artery disease.
- Carboplatin is more water-soluble and induces fewer adverse reactions than cisplatin.

12.1 Introduction

Platinum-based agents belong to alkylating antineoplastic agents. They are the backbone of most chemotherapeutic regimens in many cancer types, including testicular cancer, ovarian cancer, cervical cancer, breast cancer, lung cancer, bladder cancer, and head and neck cancer [1]. Platinum-based drugs, including the globally approved cisplatin, carboplatin, and oxaliplatin, are neutral platinum (II) complexes that when combined with water molecules bind with DNA. The platinum DNA adducts can impede cellular processes and lead to cellular apoptosis. Cisplatin is the first-generation platinum-based drug. Carboplatin is a derivative of cisplatin with a similar mechanism of action but different toxicity.

12.2 Cisplatin

Cisplatin has dose-limiting side-effects, such as nephrotoxicity, ototoxicity, hepatotoxicity, and gastrointestinal dysfunction. Besides these toxicities, many survivors may experience acute or chronic cardiovascular complications that can impair their quality of life [2]. Cisplatin-based regimens have been associated with a wide range of thromboembolic complications, affecting both venous and arterial systems [3, 4]. The pathogenesis may include hypomagnesemia, vascular damage, alterations in platelet aggregation, increased von Willebrand factor, and damage to endothelial cells via increased formation of procoagulant endothelial microparticles [5, 6]. A large retrospective analysis of 932 patients treated with cisplatin-based chemotherapy for any type of malignancy at Memorial Sloan-Kettering Cancer Center revealed that 18% of patients experienced venous or arterial thromboembolic events (TEE) during treatment or within 4 weeks of the last dose. TEE included deep vein thrombosis (DVT) alone in 49.7%, pulmonary embolus (PE) alone in 25.4%, DVT plus PE in 13.6%, arterial TEE alone in 8.3%, or DVT plus arterial TEE in 3.0%. The arterial TEE primarily consisted of myocardial infarction (10.5%) and cerebrovascular accident/transient ischemic attack (57.9%). Most patients experienced TEE within 100 days of initiation of treatment [7]. In a prospective study of 108 patients with stage III to IV non-small cell lung cancer treated with cisplatin and gemcitabine, 19 (17.6%) of 108 patients experienced a TEE

Electronic supplementary material
The online version of this chapter (https://doi.org/10.1007/978-3-030-70998-3_12) contains supplementary material, which is available to authorized users.

L. Zhang
Cardio-Oncology Program, Division of Cardiology, Department of Medicine, Montefiore Medical Center, Albert Einstein College of Medicine, 111 E 210th Street, Bronx, NY 10467, USA
e-mail: lilizhan@montefiore.org

M. N. Johnson (✉)
Department of Medicine, Memorial Sloan Kettering Cancer Center, 1275 York Avenue, New York, NY 10065, USA
e-mail: Johnsom1@mskcc.org

R. M. Steingart et al. (eds.), *Atlas of Imaging in Cardio-Oncology*,
https://doi.org/10.1007/978-3-030-70998-3_12

and 4 of those 19 patients died as a result of the event [8]. However, the overall reported incidence of venous and arterial TEE appears lower in randomized controlled trials. In a systemic review and meta-analysis of 8,216 patients from 38 randomized controlled trials, the incidence of venous TEE was 1.92% (95% CI, 1.07 to 2.76%) and of arterial TEE was 0.67% (95% CI, 0.40 to 0.95%) in patients treated with cisplatin-based chemotherapy. The relative risk of venous TEE for cisplatin-based versus non-cisplatin-based chemotherapy was 1.67 (95% CI, 1.25 to 2.23; P = 0.01) and of arterial TEE was 1.36 (95% CI = 0.86 to 2.17; P = 0.19) [9, 10].

Long-term, the use of cisplatin is associated with an increased risk of coronary artery disease (CAD) even many years after completion of the therapy. In 1,463 long-term survivors of unilateral testicular cancer, 8.0% of patients experienced atherosclerotic disease and 5.6% were diagnosed with CAD during a median follow-up time of 19 years. Treatment with cisplatin, bleomycin, and etoposide alone had a 5.7-fold higher risk for CAD compared with surgery only and a 3.1-fold higher risk for myocardial infarction compared with control [11]. Studies have reported a 1.4- to 7-fold higher CAD risk among cisplatin-treated testicular cancer survivors than in either the general population or in testicular cancer survivors managed with surgery alone [11–15]. Endothelial dysfunction associated with cisplatin-based chemotherapy represents a possible pathogenic pathway [16, 17]. In addition, platinum concentrations 20–30 years after platinum administration were significantly higher than those of controls, that is, the retention of platinum in the plasma was found up to 20 years after treatment [18].

Cisplatin infrequently causes heart failure (HF) and cardiomyopathy attributed to differing pathological effects, including myocardial ischemia, increased oxidative stress, and apoptosis [19]. Additionally, platinum-containing chemotherapy requires administration of a high intravenous fluid volume. Rather than the direct toxicity of these drugs, exacerbation of pre-existing myocardial impairment is often the cause of HF. In a longitudinal cohort of 37 patients, echocardiograms were obtained at 10 months and 6.9 years after starting cisplatin-based chemotherapy. Diastolic cardiac parameters became significantly impaired compared with healthy age-matched males and one patient developed LVEF <50% [20]. In another study, after 3 months of starting with cisplatin-based chemotherapy for testicular cancer, acute reduction of left ventricular (LV) end-diastolic volume, LV stroke volume, and diastolic function (the ratio of early diastole and atrial filling velocities across the mitral valve) by cardiac magnetic resonance imaging was reported [21]. It has been demonstrated that elevations in troponin and N- terminal pro-brain natriuretic peptide occurred occasionally during cisplatin administration in non-small cell lung cancer patients [22].

Cisplatin is also associated with arrhythmias, such as bradycardia, conduction disturbances, atrial fibrillation, supraventricular tachycardia, and ventricular tachycardia/fibrillation [2, 23–25]. Other cardiac complications of cisplatin include autonomic cardiovascular dysfunction, both hypertension and hypotension, Raynaud's phenomenon, angina, myocarditis, and pericarditis [19].

12.3 Carboplatin

Carboplatin is a second-generation platinum-containing anti-cancer drug. It is more water-soluble and induces fewer adverse reactions than cisplatin. The cardiotoxicities of carboplatin are uncommon. It is thought that carboplatin-induced oxidative stress with subsequent tissue injury and reactive oxygen species may lead to cardiotoxicities [26].

Cardiac toxic effects of carboplatin have been occasionally reported in clinical trials and case reports. For example, in a phase II trial of 27 patients with recurrent squamous cell carcinoma of the head and neck treated with the paclitaxel–carboplatin combination, one patient had severe cardiotoxicity 12 hours after the completion of the first chemotherapy infusion, which required hospitalization for 5 days. Treatment of this patient was subsequently interrupted [27]. Yano et al. reported a case of vasospastic angina following the administration of carboplatin and etoposide in a patient with small cell lung carcinoma. This patient developed acute chest pain, ST elevation on the electrocardiogram, and subsequent cardiopulmonary arrest [28]. Similarly, a case of unstable angina in a patient with advanced melanoma was reported. The patient had a history of coronary artery disease and first experienced angina with a cisplatin-containing regimen. Two years later, the patient again developed acute chest pressure approximately 20 min into his cycle 2 infusion of carboplatin [29]. Another patient experienced heart failure after completing six cycles of carboplatin and gemcitabine for metastatic urothelial cancer [30]. In a group of 31 female patients with ovarian cancer receiving treatment with paclitaxel and carboplatin, at the 3–4 month autonomic nervous system assessment, 19% of the patients had systolic orthostatic hypotension and the same percentage had diastolic orthostatic hypotension. Parasympathetic heart innervation was significantly reduced during follow-up compared with age- and gender-matched healthy controls but sympathetic skin response was not affected [31]. In addition, atrial flutter has been reported in patients who underwent carboplatin administration [32].

The following cases are examples of cardiovascular complications due to platinum agents.

12.4 Case 1

Acute coronary syndrome with cisplatin demonstrating:

- Thrombogenicity of cisplatin in coronary arteries.
- Potential need for anticoagulation in the setting of active chemotherapy.
- Carboplatin is better tolerated than cisplatin.

A 24-year-old male with stage IIIA non-seminomatous germ cell tumor s/p three cycles of etoposide *and* cisplatin, 3 days later, he developed chills, low-grade fever, and chest discomfort. He presented to the emergency room where he developed retrosternal pressure radiating to the right arm, associated with nausea and severe vomiting. An ECG was performed (Fig. 12.1).

The EKG showed diffuse ST elevation. Troponin was elevated at 2.3 ng/ml, given the diffuse nature of ST elevations, his age, and absence of cardiac risk factors, he was admitted with myopericarditis. Echocardiography was performed (Fig. 12.2, Video 12.1) which revealed extensive wall motion abnormalities with akinesis of the inferior apical wall, distal anterior wall, distal interventricular septum and apex. *There was evidence of an atypical thrombus at the apex*. He was then immediately taken for cardiac catheterization (Fig. 12.3).

Catheterization showed total occlusion of the proximal to mid LAD with thrombus. The thrombus was aspirated three times with approximately 80 mL of clot being removed. He then received a drug-eluting stent to the LAD. Only intimal thickening was described at the site of the thrombus. He was referred for a CT scan (Fig. 12.4).

CAT scan showed a filling defect at the left ventricular apex. Given the presence of LV thrombus, he received triple therapy with aspirin and plavix and was bridged with enoxaparin to warfarin until he had a therapeutic INR. He was also treated with atorvastatin, metoprolol, and lisinopril. He was switched from warfarin to enoxaparin and ultimately to a direct oral anticoagulat for a total of 3 months of therapy. Repeat echocardiogram showed no evidence of a focal thrombus.

He was then admitted for telemetry monitoring for cycle 4 of etoposide and carboplatin therapy. He tolerated these agents without further cardiac event.

12.5 Case 2. Splenic Infarct and Hepatic Artery Thrombosis

Arterial thrombosis with cisplatin.

A 48-year-old man with clinical stage IIA non-seminoma testis germ cell tumor had elevated tumor markers, bilateral disease on CT scan, and bilateral enlarged lymph nodes. He underwent left orchiectomy and retroperitoneal lymph node dissection. Pathology confirmed non-seminoma testis germ cell tumor. Postoperatively, HCG remained elevated prompting recommendation for adjuvant chemotherapy. He was prescribed etoposide and cisplatin (EP).

One week after starting treatment with EP, he presented with complaints of bloating and abdominal pain, which had been getting progressively worse over the past few days. He described severe discomfort radiating up to his ribs and down back toward the flank. He was referred for CT imaging of the abdomen (Fig. 12.5).

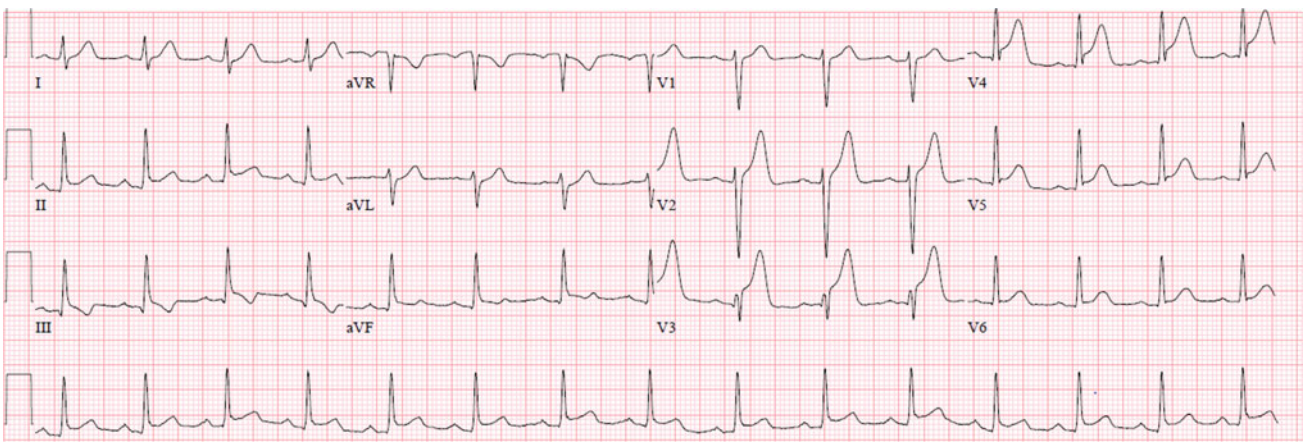

Fig. 12.1 ECG on presentation with diffuse ST segment elevation

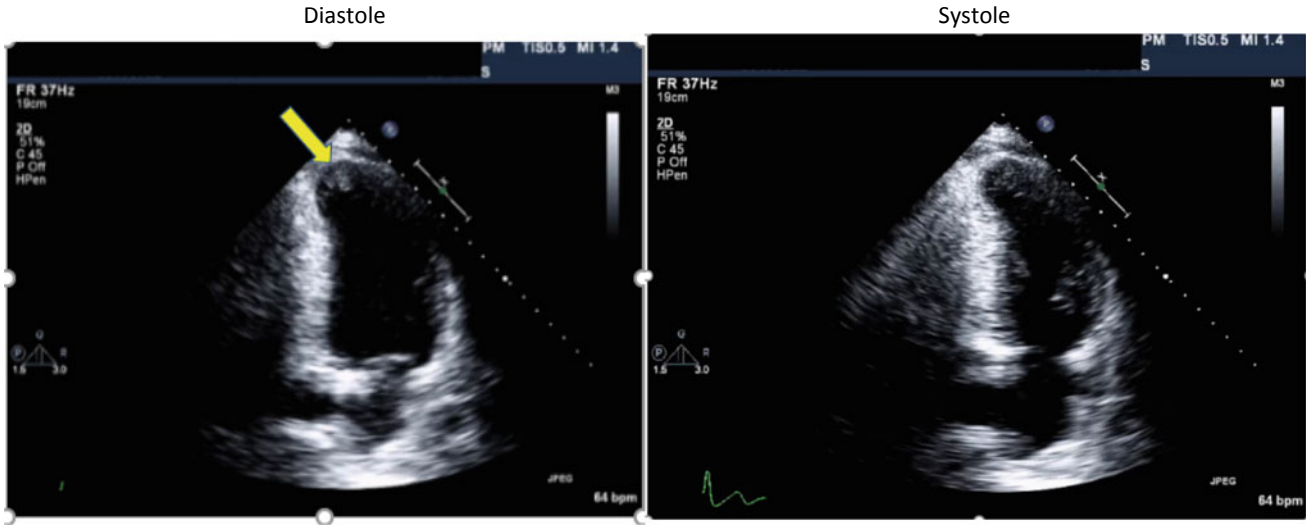

Fig. 12.2 Echocardiogram with apical mass (arrow) and regional wall motion abnormality

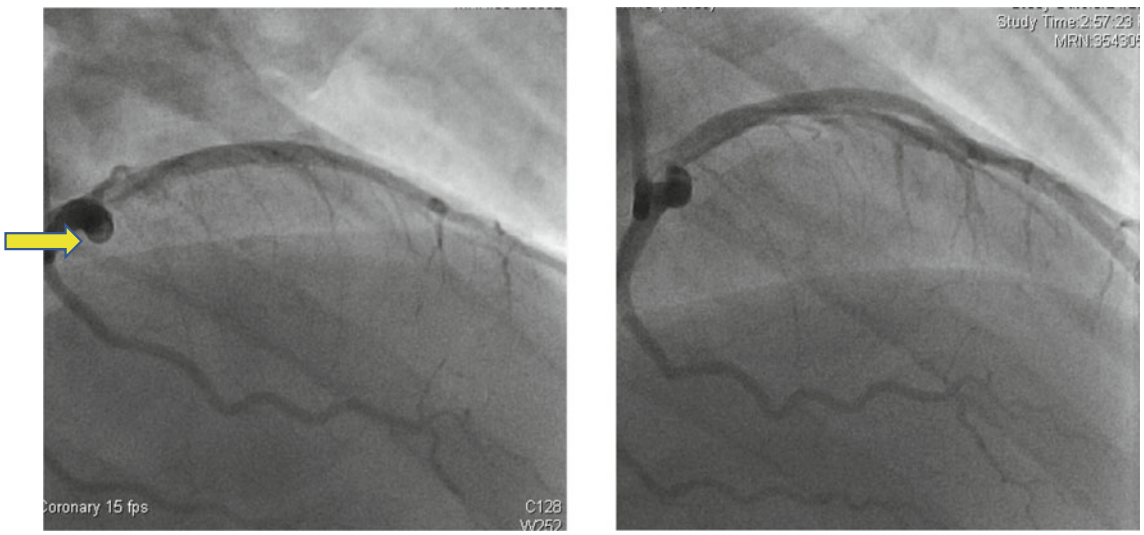

Fig. 12.3 Left coronary system showing thrombotic occlusion of left anterior descending artery (arrow)

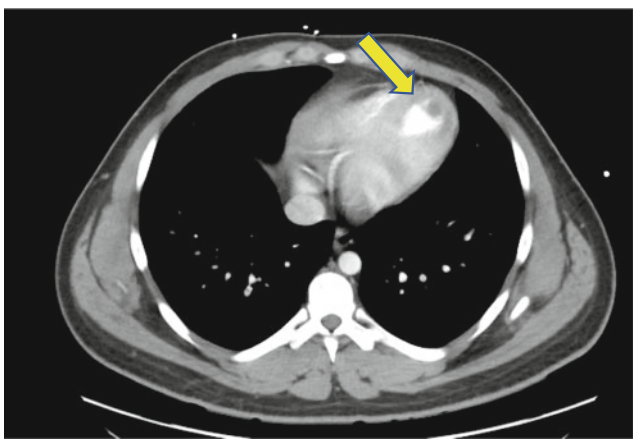

Fig. 12.4 CAT scan showing left ventricular thrombus (arrow)

CT showed a wedge-shaped defect in the spleen consistent with acute infarct. There was also stenosis at the origin of the celiac axis with post-stenotic dilatation, and also noted was a new thrombus in this celiac axis with thrombosis of the proximal hepatic artery. He was admitted to the hospital where the hematology service recommended anticoagulation and the vascular surgery service agreed with treating conservatively without surgery. He was started on intravenous heparin and transitioned to enoxaparin.

Given the potential risk of developing life-threatening arterial thrombosis with the second cycle of EP, the patient was switched to carboplatin and etoposide. It was felt that the risk of another potential catastrophic arterial thrombosis was higher than the risk of relapse due to the use of carboplatin substituting for cisplatin.

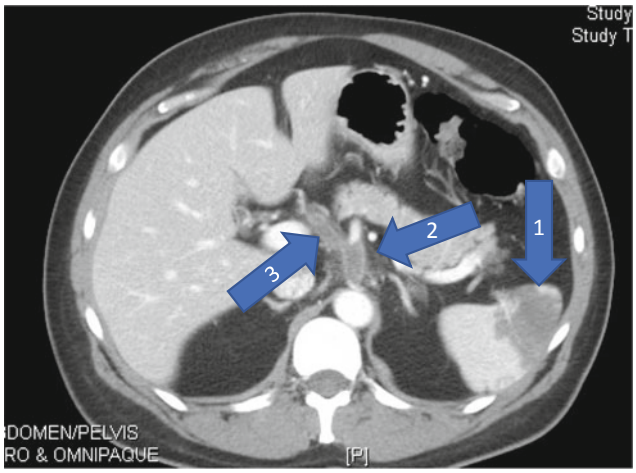

Fig. 12.5. 1. New splenic infarct. 2. Celiac axis thrombosis likely caused by proximal stenosis and dissection at the bifurcation of the celiac trunk. 3. Thrombosis of the proximal hepatic artery

12.6 Case 3: Femoral Arterial Thrombosis

Arterial thrombosis managed conservatively. A 34-year-old man with a history of stage I seminoma presented with right testicular mass and underwent orchiectomy and radiation therapy. There was evidence of lymph node involvement and possible disease of the left apex of the lung. Oncology consult recommended EP for a total of four cycles. He tolerated chemotherapy well without any requirement for hospitalizations.

However, a few days after completing chemotherapy, he presented to urgent care with right lower extremity pain. While he was having blood drawn, he had a witnessed syncopal episode with facial twitching and hand drifting to the left. He had no prior history of seizures. He underwent imaging of the head, which was unremarkable, and was diagnosed with vasovagal syncope.

Two days later, he underwent a restaging CT scan (Fig. 12.6). CT showed a new small non-occlusive thrombus in the right common femoral artery. In retrospect, he noted that over the prior week, he had worsening right lower extremity pain initially while walking but subsequently had been experiencing rest pain. He was found to have slightly cold toes and weak dorsalis pedis pulse. He was started on enoxaparin. Vascular surgery was consulted. Symptoms and clinical findings seemed out of proportion to CT results prompting recommendations for CT angiogram. CT angiogram revealed previously noted non-occlusive thrombus of the right common femoral artery, occlusion of the peroneal artery with the reconstitution of flow distally as well as occlusion of the posterior tibial artery. He was managed conservatively with enoxaparin.

12.7 Case 4: Arterial Thrombus Requiring an Invasive Procedure

The patient is a 43-year-old male with a recent diagnosis of non-seminoma embryonal cell carcinoma of the left testicle status post-left radical orchiectomy. CT revealed pulmonary nodules consistent with metastatic disease. He began chemotherapy with EP × 4.

Following cycle 2 (day 7), he developed acute R foot pain and bluish discoloration in the setting of 1 to 2 days of right lower extremity pain. On examination, there was no palpable pedal or dorsalis pedal, or popliteal pulses on the right but the femoral pulse was palpable. He underwent emergent CTA (Fig. 12.7).

CTA revealed a right occlusive thrombus involving the entire length of the profunda femoris artery and in the

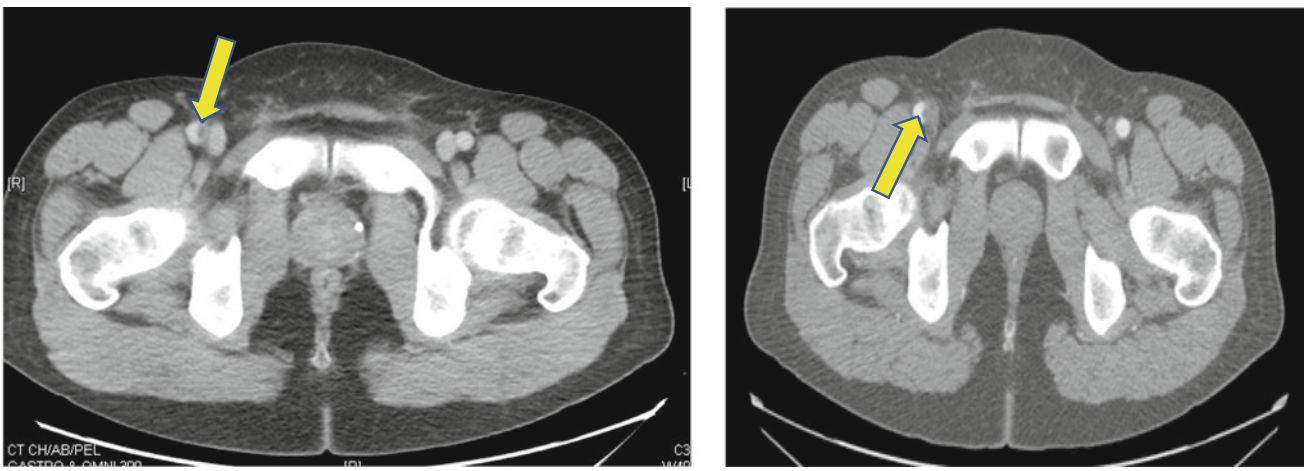

Fig. 12.6 CAT scan with non-occlusive thrombus in right femoral artery

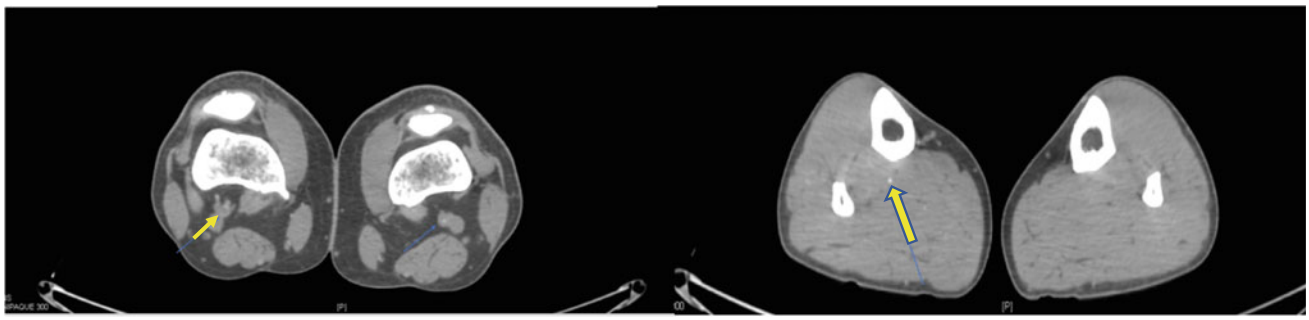

Fig. 12.7 CT angiogram still frames with non-occlusive thrombus within the right common femoral artery with occlusion of both the right peroneal and posterior tibial arteries with the reconstitution of flow distally

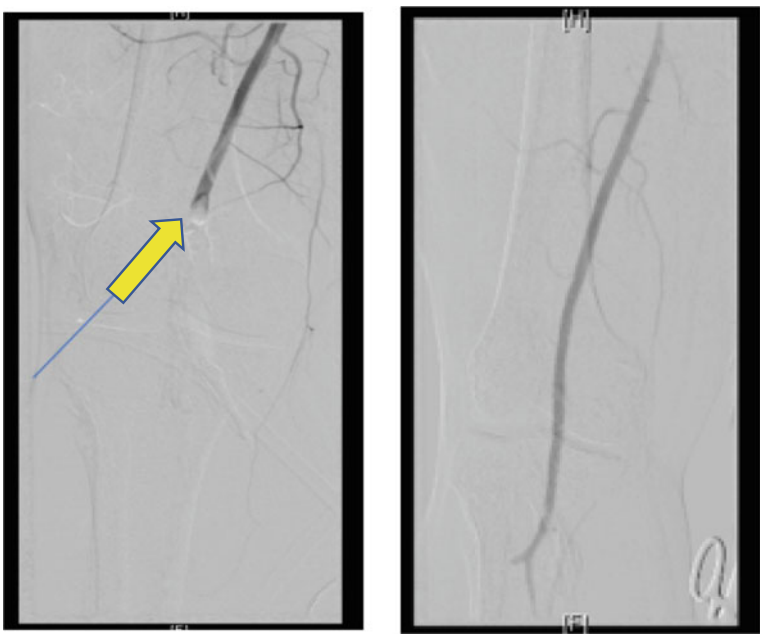

Fig. 12.8 Left panel: Arrow shows the meniscus off the embolus in the right popliteal artery. Right panel: Post-embolectomy with right popliteal artery flow restored

tibioperoneal trunk. He underwent RLE embolectomies and received enoxaparin injections. He was switched to carboplatin for the remaining two cycles and completed treatment without further event (Fig. 12.8).

References

1. Ho GY, Woodward N, Coward JI. Cisplatin versus carboplatin: comparative review of therapeutic management in solid malignancies. Crit Rev Oncol Hematol. 2016;102:37–46.
2. Dugbartey GJ, Peppone LJ, de Graaf IA. An integrative view of cisplatin-induced renal and cardiac toxicities: molecular mechanisms, current treatment challenges and potential protective measures. Toxicology. 2016;371:58–66.
3. Herrmann J, Yang EH, Iliescu CA, et al. Vascular toxicities of cancer therapies: the old and the new–an evolving avenue. Circulation. 2016;133:1272–89.
4. Doll DC, List AF, Greco FA, Hainsworth JD, Hande KR, Johnson DH. Acute vascular ischemic events after cisplatin-based combination chemotherapy for germ-cell tumors of the testis. Ann Intern Med. 1986;105:48–51.
5. Lechner D, Kollars M, Gleiss A, Kyrle PA, Weltermann A. Chemotherapy-induced thrombin generation via procoagulant endothelial microparticles is independent of tissue factor activity. J Thromb Haemost. 2007;5:2445–52.
6. Togna GI, Togna AR, Franconi M, Caprino L. Cisplatin triggers platelet activation. Thromb Res. 2000;99:503–9.
7. Moore RA, Adel N, Riedel E, et al. High incidence of thromboembolic events in patients treated with cisplatin-based chemotherapy: a large retrospective analysis. J Clin Oncol Off J Am Soc Clin Oncol. 2011;29:3466–73.
8. Numico G, Garrone O, Dongiovanni V, et al. Prospective evaluation of major vascular events in patients with nonsmall cell lung carcinoma treated with cisplatin and gemcitabine. Cancer. 2005;103:994–9.
9. Proverbs-Singh T, Chiu SK, Liu Z, et al. Arterial thromboembolism in cancer patients treated with cisplatin: a systematic review and meta-analysis. J Natl Cancer Inst. 2012;104:1837–40.
10. Seng S, Liu Z, Chiu SK, et al. Risk of venous thromboembolism in patients with cancer treated with Cisplatin: a systematic review and meta-analysis. J Clin Oncol. 2012;30:4416–26.

11. Haugnes HS, Wethal T, Aass N, et al. Cardiovascular risk factors and morbidity in long-term survivors of testicular cancer: a 20-year follow-up study. J Clin Oncol. 2010;28:4649–57.
12. Kero AE, Järvelä LS, Arola M, et al. Cardiovascular morbidity in long-term survivors of early-onset cancer: a population-based study. Int J Cancer. 2014;134:664–73.
13. van den Belt-Dusebout AW, Nuver J, de Wit R, et al. Long-term risk of cardiovascular disease in 5-year survivors of testicular cancer. J Clin Oncol. 2006;24:467–75.
14. Meinardi MT, Gietema JA, van der Graaf WT, et al. Cardiovascular morbidity in long-term survivors of metastatic testicular cancer. J Clin Oncol. 2000;18:1725–32.
15. Huddart RA, Norman A, Shahidi M, et al. Cardiovascular disease as a long-term complication of treatment for testicular cancer. J Clin Oncol. 2003;21:1513–23.
16. Nuver J, Smit AJ, Sleijfer DT, et al. Microalbuminuria, decreased fibrinolysis, and inflammation as early signs of atherosclerosis in long-term survivors of disseminated testicular cancer. Eur J Cancer. 2004;40:701–6.
17. Yu M, Han J, Cui P, et al. Cisplatin up-regulates ICAM-1 expression in endothelial cell via a NF-kappaB dependent pathway. Cancer Sci. 2008;99:391–7.
18. Gietema JA, Meinardi MT, Messerschmidt J, et al. Circulating plasma platinum more than 10 years after cisplatin treatment for testicular cancer. Lancet. 2000;355:1075–6.
19. el El-Awady SE, Moustafa YM, Abo-Elmatty DM, Radwan A. Cisplatin-induced cardiotoxicity: mechanisms and cardioprotective strategies. Eur J Pharmacol. 2011;650:335–41.
20. Altena R, Hummel YM, Nuver J, et al. Longitudinal changes in cardiac function after cisplatin-based chemotherapy for testicular cancer. Ann Oncol. 2011;22:2286–93.
21. van Schinkel LD, Willemse PM, van der Meer RW, et al. Chemotherapy for testicular cancer induces acute alterations in diastolic heart function. Br J Cancer. 2013;109:891–6.
22. Demkow U, Biatas-Chromiec B, Stelmaszczyk-Emmel A, et al. The cardiac markers and oxidative stress parameters in advanced non-small cell lung cancer patients receiving cisplatin-based chemotherapy. EJIFCC. 2011;22:6–15.
23. Raja W, Mir MH, Dar I, Banday MA, Ahmad I. Cisplatin induced paroxysmal supraventricular tachycardia. Indian J Med Paediatr Oncol. 2013;34:330–2.
24. Dolci A, Dominici R, Cardinale D, Sandri MT, Panteghini M. Biochemical markers for prediction of chemotherapy-induced cardiotoxicity: systematic review of the literature and recommendations for use. Am J Clin Pathol. 2008;130:688–95.
25. Ozcan I, Cirit A, Kiykim A. Recurrent complete atrioventricular block during cisplatin infusion: a case report. J Clin Exp Cardiol. 2011;02.
26. Cheng CF, Juan SH, Chen JJ, et al. Pravastatin attenuates carboplatin-induced cardiotoxicity via inhibition of oxidative stress associated apoptosis. Apoptosis. 2008;13:883–94.
27. Pivot X, Cals L, Cupissol D, et al. Phase II trial of a paclitaxel-carboplatin combination in recurrent squamous cell carcinoma of the head and neck. Oncology. 2001;60:66–71.
28. Yano S, Shimada K. Vasospastic angina after chemotherapy by with carboplatin and etoposide in a patient with lung cancer. Jpn Circ J. 1996;60:185–8.
29. Khan S, Chen CL, Brady MS, et al. Unstable angina associated with cisplatin and carboplatin in a patient with advanced melanoma. J Clin Oncol. 2012;30:e163-4.
30. Tiong FL, Cornillet L, Houede N. Cardiac failure caused by the association of carboplatin and gemcitabine chemotherapy in a patient with metastatic urothelial cancer: a case report. J Clin Case Rep. 2015;5:670.
31. Dermitzakis EV, Kimiskidis VK, Lazaridis G, et al. The impact of paclitaxel and carboplatin chemotherapy on the autonomous nervous system of patients with ovarian cancer. BMC Neurol. 2016;16:190.
32. Zakaria S, Lu KY, Nussenblatt V, Browner I. Atrial flutter associated with carboplatin administration. Ann Pharmacother. 2011;45:e59.

13 Cardiac Risk Assessment Prior to Hematopoietic Stem Cell Transplantation: Cases and Management Strategies

Wendy Schaffer

Key Points

- Cardiac risk assessment is a standard component of the pre-hematopoietic stem cell transplantation (HCT) screening, which considers performance status, left ventricular ejection fraction (LVEF), pulmonary function tests, and existing cardiovascular (CV) comorbidities.
- Carefully formulated management strategies based on the CV assessment can help mitigate the cardiac risk associated with physiologic stressors during the peri-HCT period.
- In patients with high risk or unstable coronary artery disease (CAD), the decision to revascularize prior to HCT should be made by a cardio-oncologist in collaboration with the transplant oncologist and the interventional cardiologist, weighing the risk of delaying transplant with the benefit of revascularization.
- With meticulous multidisciplinary care from the transplant team and the cardio-oncology service, carefully selected patients with LV systolic dysfunction can proceed with HCT without prohibitively increased risk.
- Patients with arrhythmias during HCT have increased length of transplant hospitalization, increased transplant-related mortality, and decreased overall survival at 1 year.

13.1 Introduction

Hematopoietic stem cell transplantation (HCT) represents an extended period of physiologic stress that is especially challenging for patients with cardiac co-morbidities. Peripheral blood stem cell grafts and improved supportive care have made HCT accessible to older adults who are more likely to have concurrent cardiac disease [1, 2]. Cardiac risk assessment is a standard component of the pre-HCT screening, which takes into account performance status, left ventricular ejection fraction (LVEF), pulmonary function tests, and existing cardiovascular comorbidities. The HCT-comorbidity index currently used by transplant teams to predict non-relapse mortality with increased risk associated with valvular heart disease (3 points), arrhythmias (1 point), or cardiac dysfunction (1 point, defined as coronary artery disease requiring medical treatment or revascularization, myocardial infarction, congestive heart failure or EF $\leq$ 50%) [3]. Non-relapse mortality (NRM) at 2 years with a score of 1–2 is 21% and increases to 41% with a score above 2 [4]. However, how accurately it applies to contemporary HCT is uncertain, as this comorbidity index scoring system was developed more than 15 years ago. Routine stress testing does not add significant prognostic information [5–7]. Once cardiovascular assessment has been completed, carefully formulated management strategies can help mitigate the cardiac risk associated with physiologic stressors during the peri-HCT period such as thrombocytopenia, anemia, tachycardia, hypotension, fluid challenges, and electrolyte imbalance [1]. Though transfusion requirements vary greatly depending on underlying cancer, prior treatments, and HCT conditioning, one study of patients with non-Hodgkin's lymphoma or multiple myeloma demonstrates the degree of physiologic stress of HCT, with median of 21 days to platelets above 50K and median transfusion of 5 platelet units (range 1–74) and 3 red blood cell units (range 0–30) [1]. As many as 10–20% of patients undergoing HSCT are transferred to the intensive care unit with mortality rates >50% [1, 4, 8]. Drug interactions limit options for cardiac care, further complicated by renal dysfunction in 20% of patients and hepatic dysfunction in 30% [9]. Optimal cardiac care during HCT includes meticulous volume management and electrolyte repletion and frequent adjustments of guideline-directed medical therapy of cardiac risk factors

W. Schaffer (✉)
Department of Medicine, Memorial Sloan Kettering Cancer Center, 1275 York Avenue, New York, NY 10065, USA
e-mail: Schaffew@mskcc.org

R. M. Steingart et al. (eds.), *Atlas of Imaging in Cardio-Oncology*,
https://doi.org/10.1007/978-3-030-70998-3_13

and established cardiac disease, as dictated by hemodynamics and engraftment status. The following cases demonstrate some of the challenges of assessing and managing cardiac risk in the setting of HCT.

13.2 Coronary Artery Disease and HCT

13.2.1 Case 1A

An older man with cardiac risk factors, pan-cytopenic due to transfusion-dependent myelodysplastic syndrome planned for allogeneic HCT reports chest pain when severely anemic.

- A 65-year-old man, a prior smoker, with hypertension and elevated cholesterol, pan-cytopenic and transfusion-dependent (platelets and red blood cells) myelodysplastic syndrome (MDS) reported recent onset exertional chest pain when hemoglobin (Hb) level in the 7 g/dL range, as compared to Hb in the 9 g/dL range.
- EKG with non-specific ST abnormality, borderline elevated troponin, and normal LV function on echocardiogram.
- Given pancytopenia and plan for HCT, aggressive medical therapy for presumed coronary artery disease (CAD) with beta-blocker and statin was initiated to manage symptoms and proceed with HCT. Aspirin was held given severe thrombocytopenia.
- Patient then presented prior to HCT with neutropenic fever with Hb around 9 g/dL, EKG (Fig. 13.1) with ST depression and troponin now markedly elevated.
- With platelet support, a cardiac catheterization demonstrated severe multi-vessel disease.
- Discussion ensued with the oncologist, transplant oncologist, interventional cardiologist, and cardio-thoracic surgeon, with a consensus that coronary artery bypass grafting (CABG) would be preferred over multi-vessel percutaneous coronary intervention (PCI) due to anatomy and urgent need to proceed with HCT, despite risks related to thrombocytopenia and neutropenia.
- Patient underwent uncomplicated CABG with platelet support, followed 3 months later by allogeneic HCT, also without cardiac complications

13.2.2 Case 1B

An older man with multiple myeloma and no known cardiac risk factors has an ST elevation myocardial infarction (STEMI) prior to autologous HCT.

- A 56-year-old man with no known cardiac risk factors and multiple myeloma was planned for admission for autologous HCT, having already successfully completed stem cell collection.

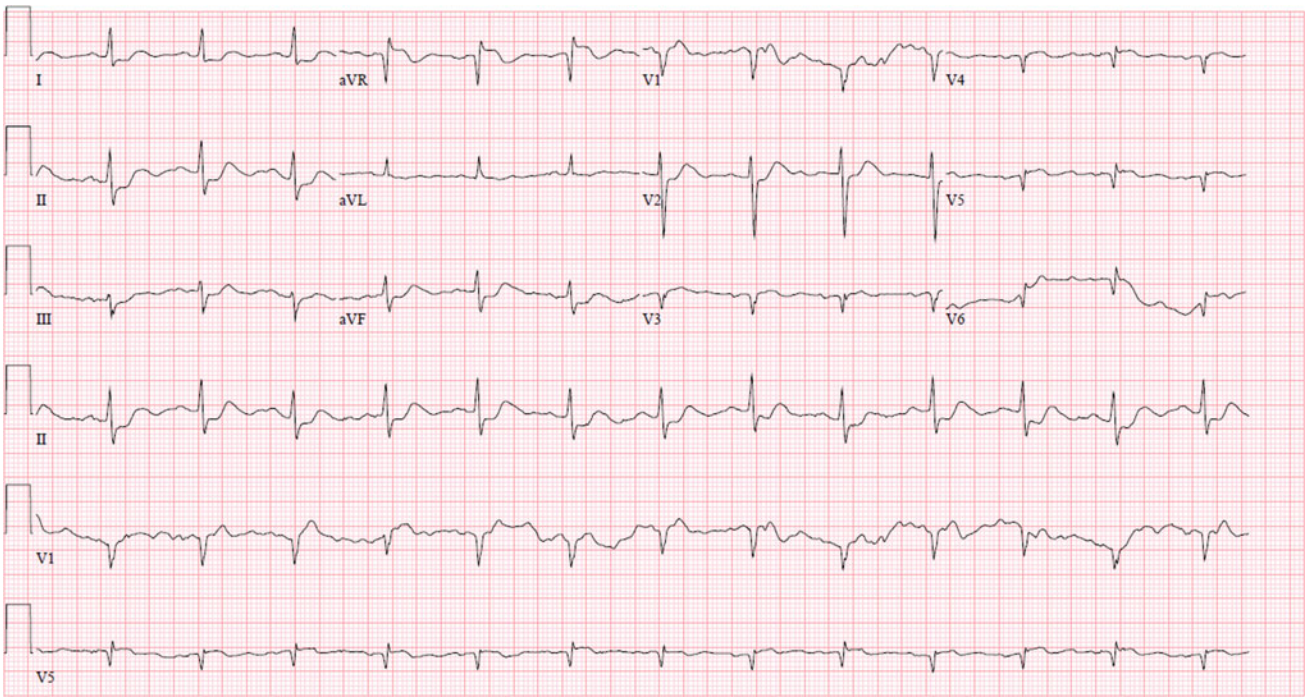

Fig. 13.1 EKG with ST depression suggestive of ischemia in a 65-year-old man with MDS and neutropenic fever being considered for allogeneic HCT. Cardiac catheterization performed with platelet support demonstrated severe multi-vessel disease

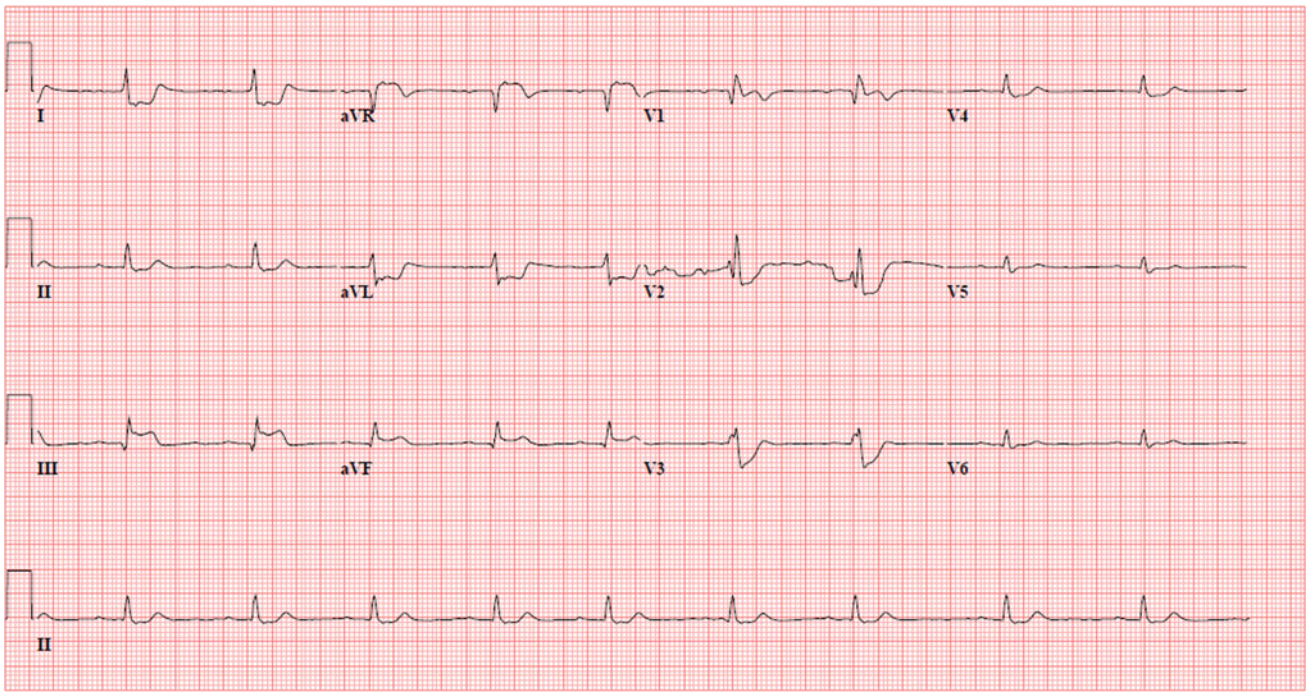

Fig. 13.2 EKG consistent with inferior STEMI in a 56-year-old man with multiple myeloma 1 week prior to planned admission for autologous HCT. A drug-eluting stent was placed on the right coronary artery. Transplant was postponed and other therapies for multiple myeloma were successfully pursued

- One week prior to admission, he presented to an outside hospital with an EKG (Fig. 13.2) consistent with an inferior STEMI and received a drug-eluting stent (DES) to the right coronary artery (RCA). No other obstructive disease was identified. LVEF was borderline decreased with inferior wall hypokinesis.
- HCT was postponed and he continued on guideline-directed medical therapy (GDMT) including dual antiplatelet therapy (DAPT) for his CAD.
- His multiple myeloma remained relatively quiescent for over a year, at which time other treatment options were pursued, as either superior or comparable to autologous HCT from an oncologic perspective.
- The patient continues on GDMT for his CAD including DAPT without cardiac complications.

13.2.3 Discussion

There are little published data on patients with CAD undergoing HCT, a case report from 1994, and a retrospective study of about 70 patients with established CAD [10, 11]. In the retrospective study, slightly more than half of the patients underwent autologous transplant, almost all peripheral stem cell grafts, with more than 85% receiving myeloablative conditioning predominantly for lymphoma, leukemia, and multiple myeloma [10]. Though it is reassuring that ICU admission, transplant-related mortality, and overall survival at 1 year were similar to a matched group without coronary artery disease, the cases included in this study were carefully selected through the transplant screening process [10]. Sections 13.2.1 and 13.2.2 demonstrate the challenges of caring for patients with higher risk CAD peri-transplant. In Sect. 13.2.1, given the patient's severe thrombocytopenia, anemia, and neutropenia, an initial effort was made to determine if GDMT of his CAD with a higher Hb transfusion cutoff would alleviate the patient's symptoms. When the patient presented with pneumonia, hemodynamically stable, with a Hb of 9 g/dL and had an ischemic EKG and elevated troponin, it became clear that the patient's CAD was too severe to manage through transplant and that the risks of cardiac catheterization in this thrombocytopenic, anemic, neutropenic patient were unavoidable if he was to proceed to transplant. As well, discussions with his oncologist and transplant oncologist revealed that he had no other available treatment options besides allogeneic HCT, which could be curative. When catheterization demonstrated extensive multi-vessel disease, the interventionalist, in discussion with the cardio-thoracic surgeon, felt the risk of trying to keep the patient on DAPT for an extended period of time while dependent on platelet transfusions outweighed the upfront risk of infection and bleeding with CABG given the patient's thrombocytopenia and neutropenia. The

oncologist felt that from the oncologic standpoint, the patient would have time to recover from the CABG prior to proceeding with HCT without compromising the oncologic outcome. For transplant, the patient's aspirin was discontinued when platelets were less than 50K, resumed when platelets above 50K, statin was held due to medication interactions, and Hb was kept above 7 g/dl. The patient had no cardiac complications and post-transplant reported that overall he felt better than he had in years. In Sect. 13.2.2, the patient had undergone stem cell collection and was planned for autologous HCT. He postponed admission until after his daughter's wedding and had an inferior STEMI at the wedding. He presented post-event with a new-generation DES to the RCA, EF borderline, no symptoms of heart failure. In discussions with his multiple myeloma oncologist, his disease was under control and transplant could be delayed. A decision was made to monitor his multiple myeloma carefully and continued GDMT for his CAD. As compared to the patient in Sect. 13.2.1, autologous HCT in patients with multiple myeloma can be life-prolonging but is not curative. As is often the case with multiple myeloma, the patient in Sect. 13.2.2 had and continues, several years after his STEMI, to have multiple treatment options that are comparable to HCT. The STEMI and placement of a DES were the initial reasons that HCT was postponed, but eventually the consensus was that there were other treatment options that the patient and oncologist as a team preferred to pursue.

If there is clinical concern that a patient has a high risk or unstable CAD, evaluation prior to HCT is warranted, including stress testing and/or cardiac catheterization. The decision to revascularize prior to HCT should be made by a cardio-oncologist in collaboration with the transplant oncologist and the interventional cardiologist, weighing the risk of delaying transplant with the benefit of revascularization. The method of revascularization, PCI with new generation drug-eluting stent(s) vs CABG, should be decided in the context of the patient's cancer and the expected minimum required duration of DAPT. Though DAPT is often recommended for up to 1 year from stent placement, it is not uncommon to use cutoffs of 3 months or even shorter when a patient has a narrow window of opportunity for HCT, especially when HCT is potentially a curative procedure for a life-threatening cancer [12]. It is common to discontinue aspirin when platelets drop below 50K for other indications (for example, after CABG), but platelets less than 20K may be a more appropriate cutoff if the patient has a recent DES [13]. Further informing the discussion of aspirin use with severe thrombocytopenia are two studies that confirm aspirin continues to have a significant benefit in cancer patients with an acute coronary syndrome (ACS), even in the setting of severe thrombocytopenia [14, 15]. Aspirin should be restarted when the patient has engrafted with platelets above the chosen cutoff. Statins are often discontinued for HCT due to drug interactions, and restarted post-transplant admission, but there is no definite contraindication. Rosuvastatin at a reduced dose, as well as pravastatin, is often well tolerated.

13.3 Pulmonary Hypertension and HCT

13.3.1 Case 2A

A young woman with familial myelodysplastic syndrome decompensates with syncope and severe pulmonary hypertension during conditioning for allogeneic HCT.

- A 20-year-old woman with myelodysplastic syndrome and no cardiac history was admitted for allogeneic HCT. Her conditioning began with the infusion of antithymoctye globulin (ATG) to reduce the risk of GVHD. This was complicated by disseminated intravascular coagulation requiring large volume transfusions.
- An echo was performed due to lightheadedness while doing physical therapy and then syncope in the setting of nausea.
- Echo (Fig. 13.3) demonstrated severe RV enlargement and hypokinesis, a flattened septum consistent with RV pressure/volume overload, and a hyperdynamic and

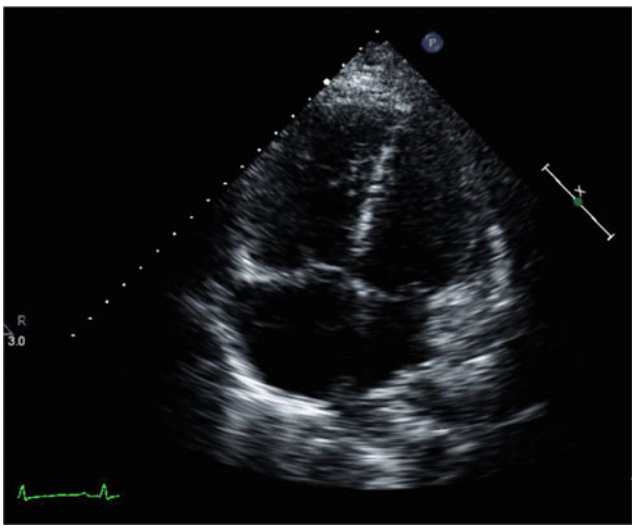

Fig. 13.3 Echo image (apical four-chamber view) demonstrating a severely enlarged RV with a flattened septum consistent with RV pressure/volume overload in a 20-year-old woman with MDS who was admitted for allogeneic HCT. She had received antithymoctye globulin (ATG) to reduce the risk of GVHD, complicated by disseminated intravascular coagulation and severe pulmonary hypertension. Transplant was delayed to address the elevated pulmonary pressures and allow the right heart to recover

underfilled LV. Pulmonary pressure on the echo was indeterminate.

- PE protocol CT demonstrated no pulmonary embolus. An emergent right heart catheterization (RHC) was performed with severely elevated pulmonary pressures.
- The patient was treated with inhaled nitric oxide, vasopressin, milrinone, and diuresis and discharged on tadalafil, ambrisentan, and furosemide.
- HCT was postponed until echo evidence of normal RV size and function as well as clinical improvement in her exercise capacity.
- Prior to her re-admission for allogeneic HCT, there was discussion as to whether a repeated RHC was indicated. The pulmonary hypertension center where the patient was managed deemed this unnecessary given her right heart function had normalized on repeat echo with normal pulmonary artery (PA) pressure.
- During her transplant admission, she received ATG with pre-medications without complications. When severe mucositis limited PO intake, tadalafil was changed to IV sildenafil. With meticulous management of the patient's fluid status, she did well, with no significant cardiac complications.
- Over the subsequent 2 years, furosemide and ambrisentan were titrated off, tadalafil dose was reduced. RHC was essentially normal and the patient continues to do well on low dose tadalafil.

13.3.2 Case 2B

A woman with multiple prior cancers and treatment-related myelodysplastic syndrome decompensates with micafungin-induced hemolytic shock during conditioning for HCT, with severe right heart dysfunction and pulmonary embolus.

- A 42-year-old woman with a prior history of breast cancer treated with lumpectomy and chemotherapy, as well as sarcoma treated with resection and chemotherapy, lifetime dose of doxorubicin 400 mg/m^2, was admitted for allogeneic HCT in the setting of therapy-related MDS.
- Prior to HCT, she developed multi-organ failure attributed to a micafungin-induced hemolytic reaction, with pressor-dependent shock, acute renal failure, and disseminated intravascular coagulation (DIC).
- EKG demonstrated a new right bundle branch block (RBBB). Troponins were markedly elevated. LV function on echo was hyperdynamic with a flattened septum suggesting right ventricular (RV) pressure/volume overload and dilated and hypokinetic RV (Fig. 13.4).

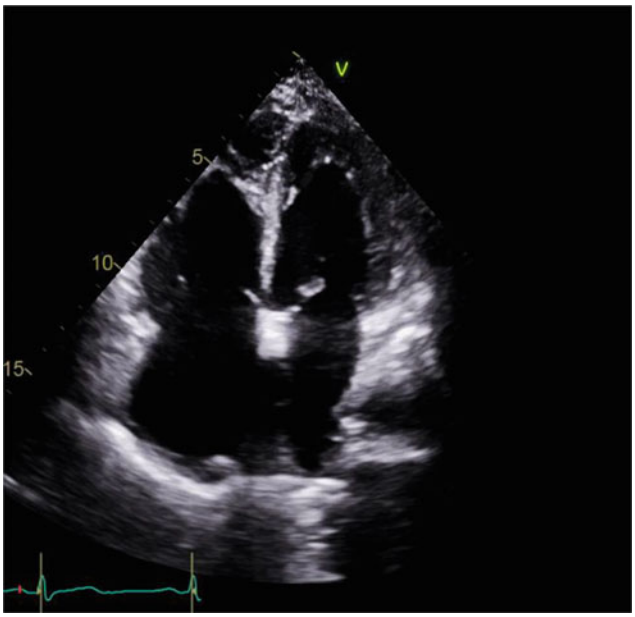

Fig. 13.4 EKG with a new right bundle branch block (RBBB) in a 42-year-old woman with myelodysplastic syndrome admitted for allogeneic HCT who developed pulmonary hypertension and right heart failure in the setting of a micafungin-induced hemolytic reaction, with pressor-dependent shock, and pulmonary embolism (PE). Transplant was delayed to allow for right heart function to recover

- CT demonstrated subsegmental pulmonary embolism (PE). Anticoagulation was initiated when platelets were recovered. Hemodynamics and RV function recovered with supportive care in the ICU.
- HCT was postponed until echo demonstrated normal RV size and function, as well as clinical improvement in her exercise capacity.
- During her transplant admission, anti-fungals were adjusted and administered without complications. LMWH was dose adjusted based on the severity of thrombocytopenia.
- With meticulous management of fluid status and electrolytes, the patient did well with no significant cardiac complications.

13.3.3 Discussion

There are no large scale clinical trials addressing the management of pre-existing pulmonary hypertension in the setting of HCT. Acutely decompensated right heart failure/severe pulmonary hypertension requires intensive care unit support and when possible the expertise of a dedicated pulmonary hypertension center. When identified pre-HCT, it is imperative that pulmonary hypertension and right heart dysfunction be addressed prior to proceeding. In Sect. 13.3.1,

the patient developed acute, severe pulmonary vasoconstriction as part of her reaction to ATG. In Sect. 13.3.2, the patient's RV dysfunction seemed out of proportion to the CT findings of a subsegmental PE, raising the possibility that some degree of underlying RV dysfunction may have contributed. Regardless, in both cases, HCT was aborted and the transplant team was able to formulate an oncologic plan that allowed the right heart time to recover from the acute physiologic insult. There is no algorithm as to the appropriate recovery time before proceeding to HCT. In Sect. 13.3.1, the patient's transplant was postponed approximately 6 months, while in Sect. 13.3.2, the transplant proceeded after 2 months. In both cases, the patient, family, and transplant team had extended discussions with the cardio-oncology team concerning risks and benefits of delaying HCT and management in the peri-transplant setting. Re-admission for HCT included meticulous fluid management, and repletion of electrolytes. In Sect. 13.3.1, an algorithm was established for the management of the patient's pulmonary hypertension medications in the setting of medication interactions, as well as an inability to take PO medications due to severe mucositis, and in Sect. 13.3.2, a similarly outlined plan was in place for the management of anti-coagulation in the setting of severe thrombocytopenia and then engraftment during HCT. Clearly, these are high-risk transplants but with careful cardiovascular care, the risk may not be prohibitive.

13.4 Reduced LV Systolic Function and HCT

13.4.1 Case 3A

A middle-aged man with a moderate-to-severe ischemic cardiomyopathy undergoes autologous HCT, followed by allogeneic HCT for multiple myeloma.

- A 53-year-old man with a family history of early coronary disease and multiple myeloma reported exertional dyspnea.
- EKG suggested anterior infarct (Fig. 13.5). Echo demonstrated a moderately reduced LVEF of 35% with akinesis of the apical septum and moderate hypokinesis of the other segments.
- Catheterization demonstrated a totally occluded left anterior descending artery (LAD) and severe RCA disease with collaterals from the RCA and left circumflex (LCx) to the LAD territory.
- The patient underwent CABG complicated by symptomatic orthostatic hypotension treated with midodrine.
- LVEF remained unchanged (35–40% on multiple echos).
- Patient was without heart failure symptoms but continued with orthostatic hypotension, intolerant to angiotensin-converting enzyme inhibitors (ACEI), and beta-blockers for his ischemic cardiomyopathy.

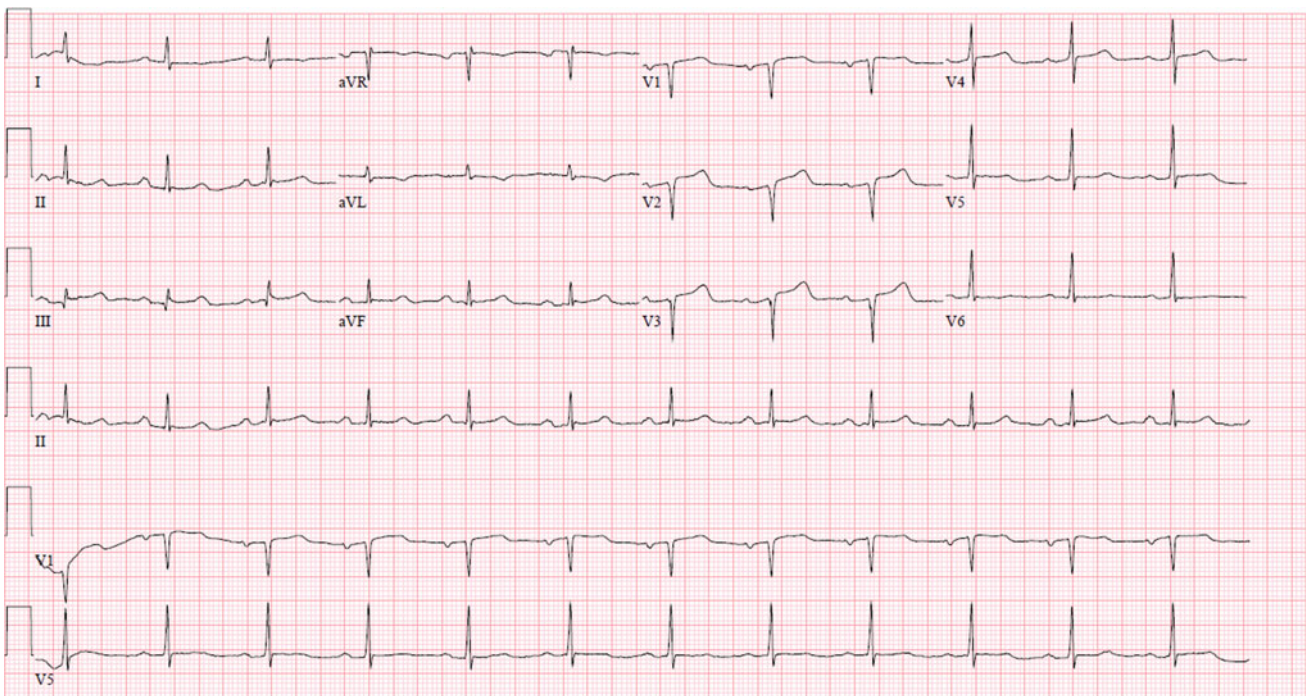

Fig. 13.5 EKG with evidence of an anterior infarct in a 53-year-old man with multiple myeloma, newly diagnosed moderate ischemic cardiomyopathy who subsequently underwent CABG prior to autologous HCT, followed 2 years later by allogeneic HCT

- Four months post-CAGB, the patient tolerated autologous HCT complicated only by orthostatic hypotension requiring careful fluid management and continued midodrine.
- Two years later, with EF essentially unchanged and no intervening heart failure exacerbations, the patient underwent reduced-intensity allogeneic HCT, again only complicated by orthostatic hypotension.
- More than a decade after the first HCT, the patient continues in remission from his multiple myeloma.

13.4.2 Case 3B

A middle-aged woman with relapsed peripheral T-cell lymphoma/leukemic transformation is found to have a severe bi-ventricular failure on screening echo for allogeneic HCT.

- A 49-year-old woman with hypertension and peripheral T-cell lymphoma, initially treated with CHOP (cyclophosphamide, doxorubicin 300 mg/m^2, vincristine, and prednisone), was noted to have a leukemic transformation to acute lymphoblastic leukemia. With few other options, the patient is treated with mitoxantrone (80 mg/m^2).
- Echo prior to mitoxatrone was entirely normal.
- Four months later, screening echocardiogram for allogeneic HCT demonstrated severe biventricular failure with LVEF 26%, moderately elevated PA pressure, and moderate mitral regurgitation (MR) (Fig. 13.6).
- Patient was treated with carvedilol 6.25 mg twice daily and lisinopril 5 mg daily, doses limited by hypotension, and diuretics.
- She was subsequently admitted several times for heart failure and infections, delaying transplant for 6 months.
- Echo immediately prior to transplant admission demonstrated mild improvement in LV and RV function (LV EF 41%, mild RV dysfunction), borderline elevated PA pressure, severe diastolic dysfunction, and moderate MR.
- Reduced-intensity allogeneic HCT was complicated by renal dysfunction and episodes of volume overload managed with diuretics.
- The patient subsequently did well from the cardiac standpoint but succumbed to relapsed disease 2 years after transplant.

13.4.3 Discussion

Historically, patients with an EF <50% were ineligible for HCT [16]. The challenges of HCT in this population are multiple, fluid loading, acute kidney injury, hypoalbuminemia, hypotension, and hypertension. Even mild systolic dysfunction is the cause for concern, and moderate-to-severe LV dysfunction, as seen in Sect. 13.4.1, is often considered too difficult to manage in the setting of HCT. Many patients receive anthracyclines preceding transplant, as was the case with the patient in Sect. 13.4.2, where the additional anthracycline exposure to control the patient's disease with mitoxatrone was unavoidable [17]. That said, a number of studies now demonstrate that carefully selected patients with impaired LV systolic function can proceed with HCT without prohibitively increased risk compared to patients with normal systolic function [18–20]. As was the case with both patients presented, there are more cardiac complications with allogeneic HCT in patients with

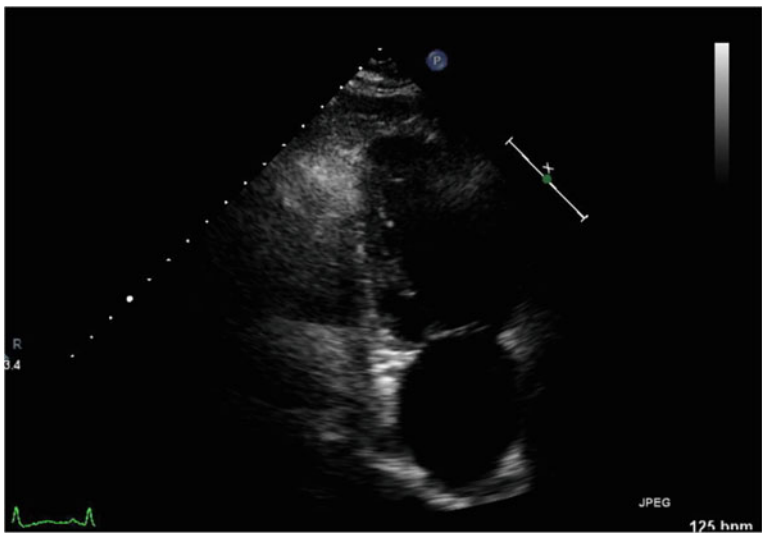

Fig. 13.6 Echo image with new LV dysfunction secondary to anthracyclines in a 49-year-old woman with acute lymphoblastic leukemia planned for allogeneic HCT. Transplant was delayed and GDMT was initiated

LV EF $\leq$ 45% who also have at least one cardiac risk factor (prior smoking, hypertension, hyperlipidemia, CAD, arrhythmia, or prior CHF), but 100-day non-relapse mortality (NRM) is not increased compared to patients with preserved LV function [18]. Both patients in Sects. 13.4.1 and 13.4.2 had few alternative options, and both patients were willing to accept the upfront risk associated with HCT for the possibility of significant benefit. Not surprisingly, the most common cardiac complications are heart failure and atrial arrhythmias [18, 19]. The patient in Sect. 13.4.1 did not have heart failure complications with transplant despite the significantly reduced LVEF. The patient in Sect. 13.4.2 had multiple heart failure admissions both before and after transplant, which were comanaged by the transplant and cardio-oncology teams. In the published literature, patients with reduced LV systolic function most frequently receive reduced-intensity conditioning, as did the patients in Sects. 13.4.1 and 13.4.2 [18, 19]. Whether this deference to patients' reduced cardiac function is necessary is not clear but should be considered on a patient-by-patient basis by the cardio-oncologist and the transplant oncologist when assessing patients with reduced LV function for HCT. There are no formal guidelines as to the management of patients with LV dysfunction during the transplant admission. As with Sects. 13.4.1 and 13.4.2, inpatient cardio-oncology consultation, co-management with the transplant team, aggressive efforts to maintain euvolemia in the setting of IV hydration and transfusions and a baseline brain natriuretic peptide (BNP) on admission have been helpful. On discharge from the transplant admission, meticulous outpatient cardiac care in cooperation with the transplant team continues to be imperative to manage post-transplant cardiac complications, including orthostatic hypotension, fluid overload, hypertension, and heart failure. A re-evaluation of LV systolic function within a few weeks of discharge or as clinically indicated may be helpful to establish a new baseline from which to titrate or initiate cardiac medications.

13.5 Atrial Fibrillation and HCT

13.5.1 Case 4

An older man with poorly controlled atrial fibrillation is considered for allogeneic HCT for relapsed CLL.

- A 66-year-old man with hypertension, diabetes, and atrial fibrillation on full anti-coagulation had a screening EKG allogeneic HCT for relapsed CLL that demonstrated atrial fibrillation with poorly control ventricular rate and no ischemic changes (Fig. 13.7).
- Patient had been diagnosed with atrial fibrillation 4 years prior, DC cardioversion in the past, most recently chronic

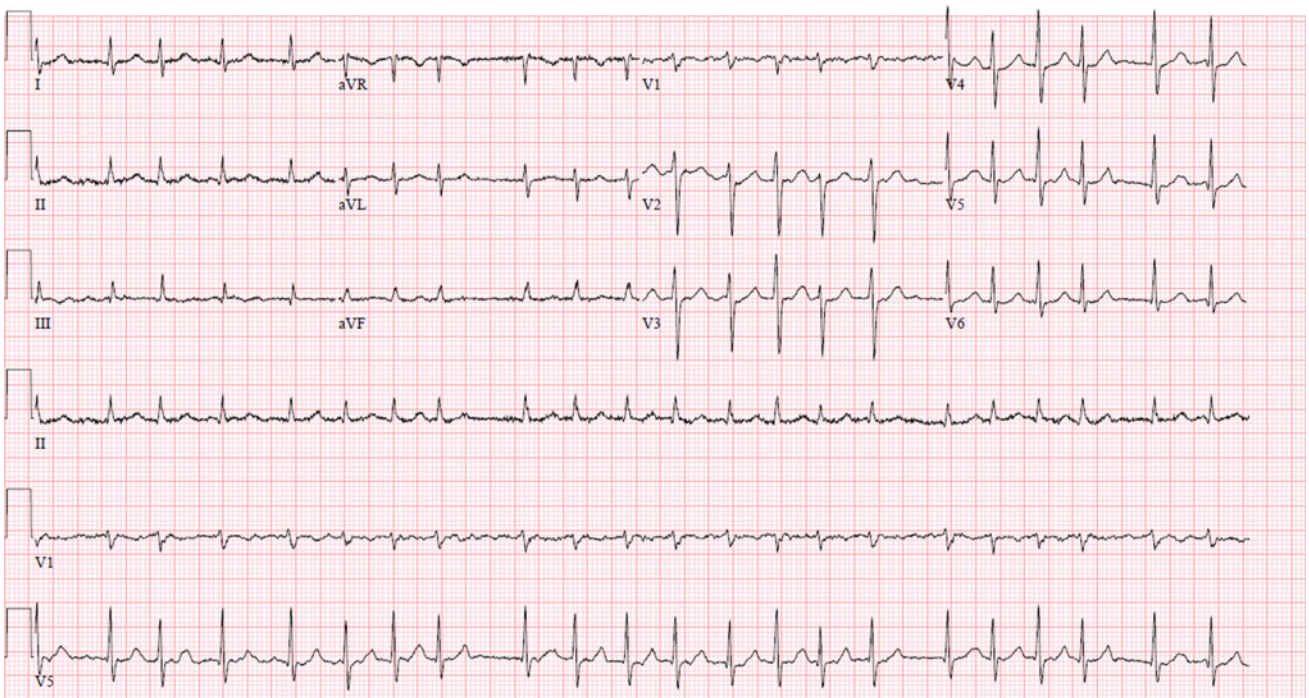

Fig. 13.7 EKG with atrial fibrillation with poorly control ventricular rate and no ischemic changes in a 66-year-old man planned for allogeneic HCT for relapsed CLL. Transplant was delayed to allow for improved heart rate control with beta-blockers and amiodarone

persistent atrial fibrillation on metoprolol succinate 100 mg daily and full anti-coagulation.
- Pre-transplant demonstrated normal LV/RV systolic function, severe left atrial enlargement, no significant valve disease. Holter confirmed paroxysmal atrial fibrillation with sustained rates to 140 s.
- Patient reported mild dyspnea with usual activities, exam demonstrated bibasilar rales, and bilateral edema.
- Patient's beta-blocker was uptitrated as blood pressure allowed, several days of diuretics were prescribed, and amiodarone was initiated with improvement in rate control and periods of normal sinus rhythm (NSR).
- Patient underwent allogeneic HCT on metoprolol and amiodarone, complicated by episodes of rapid ventricular rate requiring titration of A-V nodal blockers, discharged on metoprolol and amiodarone.
- Amiodarone was continued for 2 years after HCT, then discontinued with concerns for pulmonary toxicity.

13.5.2 Discussion

A number of studies suggest atrial arrhythmias during HCT are associated with poorer outcomes [21–23]. Patients with arrhythmias during HCT have increased length of transplant hospitalization, increased transplant-related mortality and decreased overall survival at one year [21–23]. Patients with underlying atrial arrhythmias, like the patient in Sect. 13.5.1, are at increased risk [21]. Arrhythmias occur more commonly with allogeneic HCT, compared to autologous [21, 22]. Myeloablative conditioning does not appear to be more arrhythmogenic than nonmyeloablative conditioning [21, 22]. As presented in Sect. 13.5.1, rate control before transplant, continuing anti-arrhythmics with consideration of renal/hepatic dysfunction, electrolyte abnormalities, tolerance for PO medications, drug interactions, and aggressive management of arrhythmias during HCT is recommended. There are no data on rhythm vs rate control. Underlying stressors, such as infection, should be addressed, with efforts to avoid severe anemia, fluid overload, and severe electrolyte imbalance [22, 24]. The usual risk calculators for risk of thromboembolic event vs the risk of bleeding do not appropriately address the unique circumstances of HCT [25]. Instead, recommendations derived from anticoagulation for venous thrombosis in the setting of severe thrombocytopenia are more appropriate, with reasonable safety and efficacy: Anticoagulation with full-dose LMWH until platelets less than 50K, half dose for platelets 25–50, and then no anticoagulation for platelets less than 25 until engraftment and platelets stable above 25K [26]. In general, direct oral anticoagulants (DOACs) are not recommended in the HCT setting for atrial fibrillation due to thrombocytopenia. This algorithm has successfully adhered to the patient in Sect. 13.5.1 during the transplant admission and in the immediate post-transplant setting without bleeding or thromboembolic complications.

13.6 Summary

HCT poses a unique challenge for patients with underlying cardiac comorbidities and places all patients at risk for cardiac complications. As demonstrated in the cases reviewed here, a thoughtful collaboration between the cardio-oncologist and the transplant team is imperative to improving patient outcomes during this period of intense physiologic stress.

References

1. Mileshkin LR, Seymour JF, Wolf MM, et al. Cardiovascular toxicity is increased, but manageable, during high-dose chemotherapy and autologous peripheral blood stem cell transplantation for patients aged 60 years and older. Leuk Lymphoma. 2005;46 (11):1575–9.
2. Sirohi B, Powles R, Treleaven J, et al. The role of autologous transplantation in patients with multiple myeloma aged 65 years and over. Bone Marrow Transplant. 2000;25(5):533–9.
3. Sorror ML, Maris MB, Storb R, et al. Hematopoietic cell transplantation (HCT)-specific comorbidity index: a new tool for risk assessment before allogeneic HCT. Blood. 2005;106(8):2912–9.
4. Afessa B, Azoulay E. Critical care of the hematopoietic stem cell transplant recipient. Crit Care Clin. 2010;26(1):133–50.
5. Bolwell BJ. Are predictive factors clinically useful in bone marrow transplantation? Bone Marrow Transplant. 2003;32(9):853–61.
6. Hertenstein B, Stefanic M, Schmeiser T, et al. Cardiac toxicity of bone marrow transplantation: predictive value of cardiologic evaluation before transplant. J Clin Oncol. 1994;12(5):998–1004.
7. Jain B, Floreani AA, Anderson JR, et al. Cardiopulmonary function and autologous bone marrow transplantation: results and predictive value for respiratory failure and mortality. The University of Nebraska Medical Center Bone Marrow Transplantation Pulmonary Study Group. Bone Marrow Transplant. 1996;17 (4):561–568.
8. Bayraktar UD, Shpall EJ, Liu P, et al. Hematopoietic cell transplantation-specific comorbidity index predicts inpatient mortality and survival in patients who received allogeneic transplantation admitted to the intensive care unit. J Clin Oncol Off J Am Soc Clin Oncol. 2013;31(33):4207–14.
9. Gooley TA, Chien JW, Pergam SA, et al. Reduced mortality after allogeneic hematopoietic-cell transplantation. N Engl J Med. 2010;363(22):2091–101.
10. Stillwell EE, Wessler JD, Rebolledo BJ, et al. Retrospective outcome data for hematopoietic stem cell transplantation in patients with concurrent coronary artery disease. Biol Blood Marrow Transplant J Am Soc Blood Marrow Transplant. 2010.
11. Schechter D, Drakos P, Nagler A. Underlying coronary artery disease and successful bone marrow transplantation: a case report. Bone Marrow Transplant. 1994;13(5):665–6.
12. Grines CL, Bonow RO, Casey DE, et al. Prevention of premature discontinuation of dual antiplatelet therapy in patients with

coronary artery stents: a science advisory from the American Heart Association, American College of Cardiology, Society for Cardiovascular Angiography and Interventions, American College of Surgeons, and American Dental Association, with representation from the American College of Physicians. J Am Coll Cardiol. 2007;49(6):734–9.
13. Deloughery TG. Between Scylla and Charybdis: antithrombotic therapy in hematopoietic progenitor cell transplant patients. Bone Marrow Transplant. 2012;47(10):1269–73.
14. Sarkiss MG, Yusuf SW, Warneke CL, et al. Impact of aspirin therapy in cancer patients with thrombocytopenia and acute coronary syndromes. Cancer. 2007;109(3):621–7.
15. Feher A, Kampaktsis PN, Parameswaran R, Stein EM, Steingart R, Gupta D. Aspirin is associated with improved survival in severely thrombocytopenic cancer patients with acute myocardial infarction. Oncologist. 2017;22(2):213–21.
16. Bearman SI, Petersen FB, Schor RA, et al. Radionuclide ejection fractions in the evaluation of patients being considered for bone marrow transplantation: risk for cardiac toxicity. Bone Marrow Transplant. 1990;5(3):173–7.
17. Itoh M, Iwai K, Kotone-Miyahara Y, et al. Successful allogeneic bone marrow transplantation for acute myelogenous leukemia after drug-induced cardiomyopathy. Tohoku J Exp Med. 2004;204 (1):85–91.
18. Qazilbash MH, Amjad AI, Qureshi S, et al. Outcome of allogeneic hematopoietic stem cell transplantation in patients with low left ventricular ejection fraction. Biol Blood Marrow Transplant J Am Soc Blood Marrow Transplant. 2009;15(10):1265–70.
19. Hurley P, Konety S, Cao Q, Weisdorf D, Blaes A. Hematopoietic stem cell transplantation in patients with systolic dysfunction: can it be done? Biol Blood Marrow Transplant J Am Soc Blood Marrow Transplant. 2015;21(2):300–4.
20. Tang WH, Thomas S, Kalaycio M, et al. Clinical outcomes of patients with impaired left ventricular ejection fraction undergoing autologous bone marrow transplantation: can we safely transplant patients with impaired ejection fraction? Bone Marrow Transplant. 2004;34(7):603–7.
21. Tonorezos ES, Stillwell EE, Calloway JJ, et al. Arrhythmias in the setting of hematopoietic cell transplants. Bone Marrow Transplant. 2015;50(9):1212–6.
22. Hidalgo JD, Krone R, Rich MW, et al. Supraventricular tachyarrhythmias after hematopoietic stem cell transplantation: incidence, risk factors and outcomes. Bone Marrow Transplant. 2004;34(7):615–9.
23. Feliz V, Saiyad S, Ramarao SM, Khan H, Leonelli F, Guglin M. Melphalan-induced supraventricular tachycardia: incidence and risk factors. Clin Cardiol. 2011;34(6):356–9.
24. Fatema K, Gertz MA, Barnes ME, et al. Acute weight gain and diastolic dysfunction as a potent risk complex for post stem cell transplant atrial fibrillation. Am J Hematol. 2009;84(8):499–503.
25. Lane DA, Lip GY. Use of the CHA(2)DS(2)-VASc and HAS-BLED scores to aid decision making for thromboprophylaxis in nonvalvular atrial fibrillation. Circulation. 2012;126(7):860–5.
26. Mantha S, Miao Y, Wills J, Parameswaran R, Soff GA. Enoxaparin dose reduction for thrombocytopenia in patients with cancer: a quality assessment study. J Thromb Thrombolysis. 2017;43 (4):514–8.

The Role of Myocardial Perfusion Imaging in Cardiac Clearance of Cancer Patients

14

Josef J. Fox and Howard Weinstein

14.1 Introduction

Many effective forms of treatment are currently available for cancer patients including surgery, systemic therapy (e.g. chemotherapy, immunotherapy), bone marrow and stem cell transplants, and radiation therapy. Each of these therapeutic categories confers substantial benefit and some degree of cardiovascular risk. Careful attention is warranted especially in patients with known heart disease.

The goals of pre-cancer therapy cardiac evaluation include risk assessment and mitigation, and communication with oncologists, surgeons, patients, and family. The evaluation must take a holistic approach if it is to rightfully balance risk, benefit, costs, and individual preferences.

When considering the paradigm of the pre-treatment patient, particularly a patient before surgery, the level of acceptable risk can be highly subjective. Many patients prefer to undergo an intervention with high initial risk with a chance for cure or palliation rather than suffering an inexorable downhill course without treatment. The pre-treatment cardiology consultant must anticipate the patient's needs as treatment options and risk tolerance change.

ACC/AHA guidelines [1] offer a readily applied approach to the preoperative evaluation of general surgical patients. This approach can also prove useful for the other categories of therapeutic cancer interventions. Although prior guidelines separated patients and operations into three categories – (1) High risk; emergent major operations, particularly in the elderly, prolonged procedures with large fluid shifts, and blood loss; (2) Intermediate risk, head and neck, intraperitoneal and intrathoracic, orthopedic and prostate surgery; and (3) Low risk, endoscopic, superficial, and breast – current guidelines recognize only low risk (<1% morbidity) and elevated risk categories. These new guidelines employ the clinical risk factors from the Revised Cardiac Risk Index, including ischemic heart disease; compensated or prior heart failure; cerebrovascular disease; diabetes mellitus, and renal insufficiency. If further risk stratification is indicated, stress testing may be performed [2].

The following cases illustrate the process of pre-therapy risk assessment for a variety of cancer therapies and patient presentations, ranging from relatively straightforward low risk to complex higher-risk scenarios.

14.2 Case 1

Key Points

- The need for immediate versus delayed cancer surgery dictates available options.
  - Surgery for lung, colon, and head/neck cancers often cannot be delayed.
    To stabilize the cancer, neoadjuvant drug therapy or radiation therapy is sometimes employed.
    Recovery from cardiac interventions must be prompt.
  - Prostate and renal tumors, generally, do not require urgent or emergent therapies.
    Cardiac interventions can play out longer intervals if necessary.

A 56-year-old active man with newly diagnosed Gleason 3 + 4 = 7 prostate cancer underwent evaluation for radical prostatectomy. Cardiac risk factors included mild obesity, controlled hypertension, and hypercholesterolemia. He underwent a successful right hip replacement 4 years prior

Electronic supplementary material
The online version of this chapter (https://doi.org/10.1007/978-3-030-70998-3_14) contains supplementary material, which is available to authorized users.

J. J. Fox (✉) · H. Weinstein
Department of Medicine, Memorial Sloan Kettering Cancer Center, 1275 York Avenue, New York, NY 10065, USA
e-mail: foxj@mskcc.org

H. Weinstein
e-mail: weinsteh@mskcc.org

R. M. Steingart et al. (eds.), *Atlas of Imaging in Cardio-Oncology*,
https://doi.org/10.1007/978-3-030-70998-3_14

to the current presentation without complication. He had a strong family history of early coronary artery disease (CAD); his father required open heart surgery (four-vessel coronary artery bypass grafting) in his 50s and died at age 60 due to a stroke.

On initial evaluation by his urologist, he admitted to mild anginal symptoms for several months. He was referred to cardiology and underwent a preoperative exercise nuclear Technetium-99m sestamibi myocardial perfusion imaging (MPI) scan. Although the patient had reasonable exercise tolerance, the study was consistent with significant stress-induced ischemia.

The patient exercised according to the Bruce protocol for 06:29 min, achieving a work level of 7.0 METS and 78% of the maximal, age-predicted heart rate. The resting blood pressure of 136/97 mmHg rose to a maximum blood pressure of 183/95 mmHg. The exercise test was stopped due to marked ST depressions, accompanied by mild anginal pain and dyspnea at peak stress (Fig. 14.1a).

The perfusion scan showed:

- Multiple reversible defects consistent with stress-induced ischemia.
- Transient ischemic dilatation of left ventricle suggestive of multivessel disease.
- Normal left ventricular ejection fraction (LVEF) of 65% (Fig. 14.1b).

The patient was referred for cardiac catheterization where he was found to have a severe three-vessel disease, including LM disease (Fig. 14.1c, Video 14.1). Because of the limitations imposed by angina, and the severity of the CAD where revascularization clearly offers a better long-term prognosis than medical therapy, he was referred for 5vCABG. After his bypass, he was discharged on metoprolol, statins, and aspirin.

Now fully recovered from his CABG procedure, exercising daily without symptoms, he is awaiting prostatectomy, which is scheduled to take place approximately 4 months after his diagnosis of prostate cancer.

14.3 Case 2

The risk/benefit of a procedure is often weighed differently by the patient and the members of the medical team including surgeons, oncologists, and cardiologists. Risk categories of the thresholds are of course arbitrary, but the following discussion is put forward as a potentially useful frame of reference for practitioners of the art of cardio-oncology.

Key Points

(1) For patients whose medical conditions have been optimized, a curative or palliative cancer surgical procedure that carries a $\ll$10% estimated risk of morbidity or mortality is generally acceptable to the patient and the rest of the cardio-oncology team.
(2) When the surgical risk estimates are higher, for example, 11–20%, alternative medical, radiation, or surgical approaches to cancer therapy are aggressively sought, but in the practice of cardio-oncology such risk is not deemed "prohibitive" under the proper circumstances.
(3) When the risks of treatment exceed even these lofty thresholds, goals of care should be reexamined.

A 58-year-old male former smoker with non-insulin-dependent diabetes, peripheral vascular disease, CAD is status post two drug-eluting stents to the right coronary artery (RCA) in 2011. He received a Xience stent to the RCA in 2013 for recurrent angina and 90% stenosis of the proximal RCA but distal to the prior stent. He had no recurrence of angina since 2013. An echocardiogram in 2017 was normal. He works full time in construction doing manual labor without cardiac symptoms but does have intermittent claudication. He takes ASA and clopidogrel.

In July 2019, a lung lesion was discovered on a routine chest X-ray. A PET/CT scan demonstrated a 2.5 cm FDG-avid left upper lobe spiculated lung mass. Biopsy by interventional radiology yielded adenocarcinoma, and he was scheduled for a lobectomy. A preoperative nuclear stress test was ordered by his thoracic surgeon.

The patient underwent sestamibi rest/stress myocardial perfusion imaging (MPI) with combined regadenoson and low-level treadmill exercise. Stress ECG showed ST depressions in the inferolateral leads suggestive of ischemia. Perfusion images (Fig. 14.2 and Video 14.2) showed a medium-sized area of moderate ischemia in the inferior/posterior wall; probable additional small area of ischemia in the distal anterior wall, EF >60%.

The patient was considered at intermediate perioperative cardiovascular risk and medical management was recommended, as he was not limited by angina and left ventricular function and myocardial perfusion did not suggest that his long-term prognosis or functional status would be improved more by coronary revascularization than medical therapy. Furthermore, coronary revascularization would have delayed needed cancer surgery. If the cardiovascular status of the cancer patient is stable, as is generally practiced for non-cardiac surgery, decisions regarding coronary revascularization should be dictated by the long-term consequences of revascularization rather than its impact on cancer

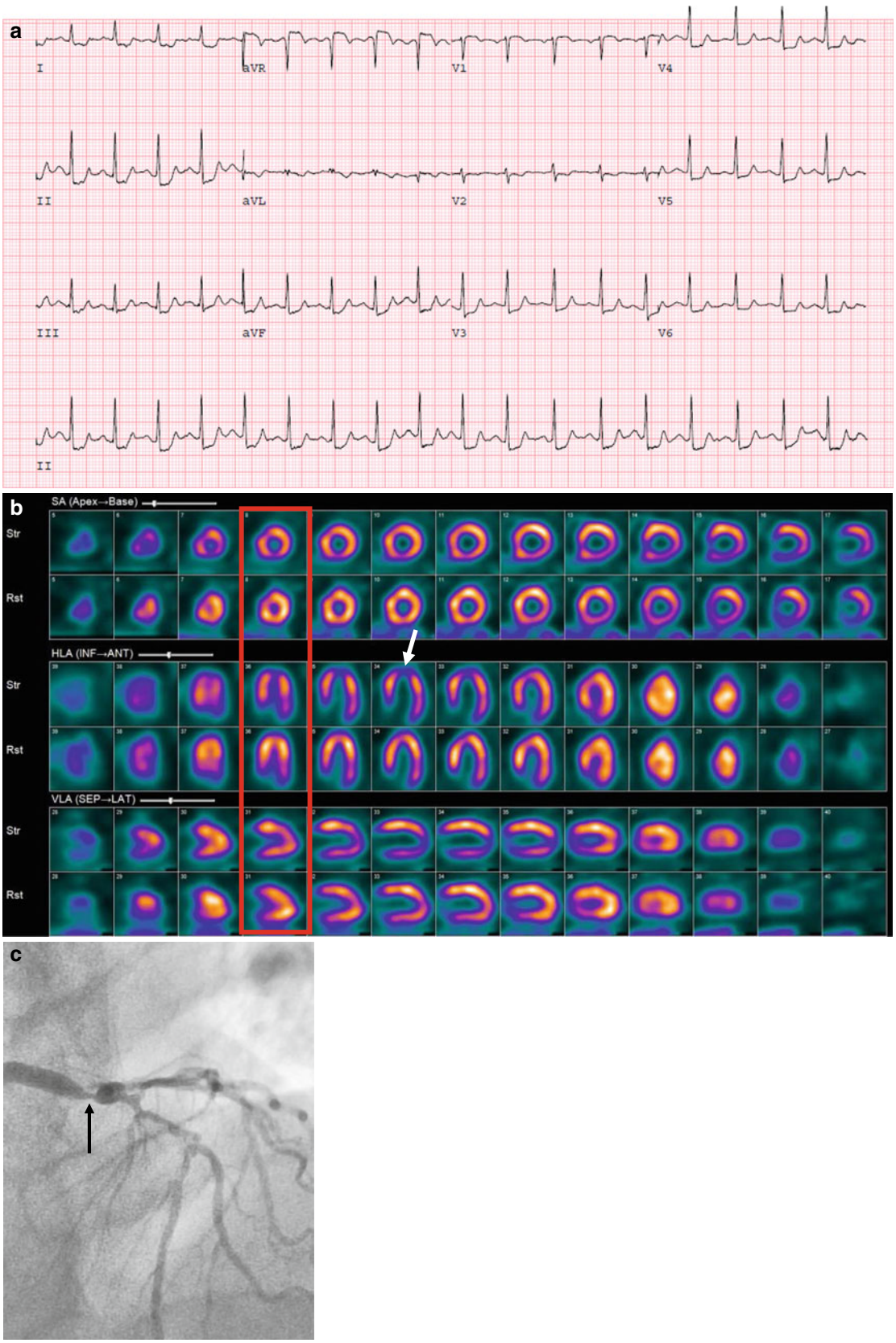

Fig. 14.1 **a** Treadmill ECG at near-peak stress showing horizontal ST segment depression, approximately 2 mm, in leads II, III, avF, v3–v6. ECG changes were accompanied by mild angina which resolved spontaneously in early recovery. **b** Tc-99m Sestamibi stress (Str) and rest (Rst) SPECT arranged in short axis (SA), horizontal long axis (HA) and vertical long axis (VLA) slices. Multiple reversible perfusion defects are present, most severe at the apex (white arrow), consistent with stress-induced ischemia. A high-risk feature of the scan is reversible chamber dilatation (TID) of left ventricle (well-seen within the red box) suggestive of multivessel disease. **c** Left main (arrow) and triple vessel disease was confirmed on subsequent coronary angiogram

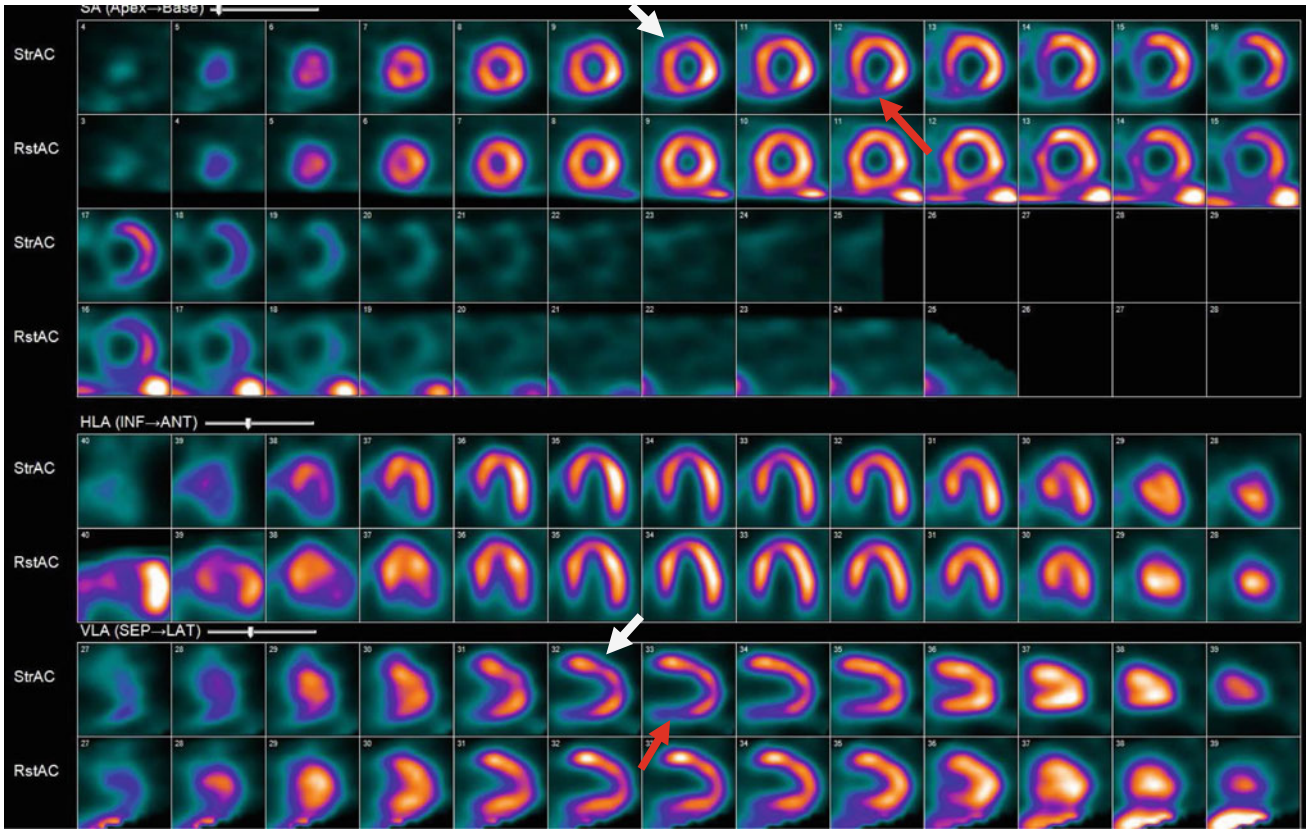

Fig. 14.2 Tc-99m-Sestamibi stress (StrAC) and rest (RstAC) attenuation corrected images show a medium-sized area of moderate ischemia in the inferior/posterior wall (red arrows), and probable small area of mild ischemia in the distal anterior wall (white arrows). No reversible chamber dilatation is identified, and left ventricular systolic function is globally normal (gated images not shown). The study findings confer an intermediate risk for perioperative cardiac events, and in conjunction with clinical context, revascularization is not warranted

operation risk [1]. He underwent left upper lobectomy and regional lymphadenectomy and tolerated the procedure well. Post-operative ECGs did show T-wave inversions in inferior leads that resolved on subsequent ECG 8 hours later. Troponin levels were negative.

14.4 Case 3

The risk of a procedure may be altered by the cancer–host interaction. The thrombogenicity of tumors, the duration and complexity of tumor resection and restorative surgical components, and the potential for interventions to release cardiotoxic agents are unique to cancer surgery. Performance status is often compromised by cancer, as weight loss, anemia, and hypoproteinemia impair metabolic status, and chemotherapy and radiation promote deconditioning and effort intolerance. Moreover, prior or current chemotherapy may have a direct cardiotoxic effect, resulting in an increased risk profile.

A 54-year-old male former smoker underwent percutaneous coronary intervention (PCI) in 2004 and received a Cypher stent for a total occlusion of the RCA, with a residual 50% long mid-LAD lesion. In 2014, he had acute chest tightness. Coronary angiogram showed three-vessel CAD, and he received three drug-eluting stents (DES) to circumflex and LAD, as well as two additional stents to mid and distal RCA. In August 2019, he had a CVA requiring tPA, with minimal residual deficits. He had sub-optimally controlled diabetes (HgbA1c 8.2%) and was mildly hypertensive.

In March 2020, he was diagnosed with COVID-19 infection and was admitted to an outside hospital. No cardiac complications were reported. After 3 weeks, he was discharged to receive a 2-week course of apixaban. He returned to work as a construction site supervisor where he experienced fatigue, but no anginal symptoms. Subsequently, he developed rectal bleeding and, in June 2020, was diagnosed with rectal cancer (T3bN+).

The cardiology service was consulted to assess the risk of fluoropyrimidine-based neoadjuvant therapy with capecitabine (pro-drug of 5FU) prior to surgery. An ischemic evaluation was recommended, given his past history and the established potential for cardiotoxicity with capecitabine. Resting ECG and echocardiogram were essentially normal.

N-13 Ammonia PET myocardial perfusion study (Fig. 14.3a–c and Video 14.3) showed a large area of moderate-severe reversibility in the inferolateral and lateral wall. Anterior wall perfusion was normal. Myocardial flow reserve (MFR) was measured and was abnormal in the RCA territory 1.39 (nl > 2.0).

Although he had no chest pain, he was very limited by severe exertional fatigue. He underwent coronary angiography, which showed multivessel CAD. Notably, a mid-RCA 70% in-stent restenosis was the culprit lesion responsible for the extensive reversible perfusion defect on PET imaging, that lesion was dilated and a new stent was placed.

Medical therapy for CAD included metoprolol, ramipril, atorvastatin, and dual-antiplatelet therapy. Cancer therapy with simultaneous radiation and capecitabine was started. After a month of therapy, rectal symptoms were improved and rectal bleeding was resolved. However, he reported new-onset atypical chest pain/epigastric pain and capecitabine was held briefly. His symptoms were resolved and he was restarted on capecitabine, which he tolerated well without evidence of cardiotoxicity. His fatigue is gradually improving and he is scheduled for surgery in early 2021.

Key Points

- Extra vigilance for the potential cardiotoxicity of fluoropyrimidine-based therapy is required in the presence of known CAD (see Chap. 11 on Cardiac Complications of 5-Fluorouracil (5FU) and Capecitabine Therapy) [3, 4].
- Depending on the perceived need for 5FU-based therapy, aggressive medical therapy with or without revascularization is not uncommonly administered to allow the use of these therapies in the face of CAD with careful cardiac monitoring (sometimes inpatient) during 5FU therapy. Admittedly, these practices are largely based on clinical experience and expert opinion rather than hard scientific evidence.

14.5 Case 4

A 59-year-old man with hypertension, obesity and metastatic renal cell carcinoma who had a left nephrectomy and was then maintained on a therapeutic protocol with lenvatinib and everolimus.

During an oncology visit in May 2020, he reported several weeks of dyspnea on exertion (DOE) associated with chest pressure. Cardiology evaluation recommended holding lenvatinib/everolimus, and he was referred for a nuclear stress test. During the pharmacologic stress test, he developed severe chest pressure after regadenoson and isotope injection. He was given aminophylline without relief, however, his pain improved after multiple doses of sublingual nitroglycerin. The ECG during stress was notable for ST depression in inferior and anterior leads (Fig. 14.4a). Troponin was detectable at 0.48 ng/ml. After stabilization, he was able to undergo the post-stress imaging portion of the study within 2 hours of the isotope injection. The study showed a moderate-sized area of ischemia in the lateral/inferolateral wall with normal global systolic function (Fig. 14.4b and Video 14.4).

Pt was then sent for a left heart catheterization which showed severe 70% distal left main stenosis and 90% ostial LCx stenosis with non-obstructive disease elsewhere.

After discussion between the cardiology and oncology teams, the patient underwent uncomplicated CABG ×2 (LIMA-LAD and SVG-LCx) and was discharged 5 days later. Lenvatinib, a VEGF antagonist was discontinued as a potential contributor to his accelerated anginal syndrome.

A follow-up CT scan 1 month later showed an enlarging descending colon mass with new hepatic lesions and increasing lymphadenopathy. Cardiology was again consulted for risk assessment prior to colonoscopy and possible colectomy. The patient denied angina, DOE, or other cardiac symptoms since undergoing CABG.

In August 2020, he underwent laparotomy and left colectomy without cardiac complication despite requiring packed red blood cell transfusion for blood loss. He is now maintained on Nivolumab (PD-1 inhibitor).

Key Points

- Hypertension is a class effect of VEGF signaling pathway inhibitors. Vascular toxicity is a complication of many of these agents (see Chaps. 5–9).
- Non-cardiac surgery following uncomplicated CABG surgery can be performed with the expectation of low cardiac risk. Further cardiac testing is generally not required [1].

14.6 Case 5

Many cancer patients in need of surgery have already undergone external beam radiation therapy (XRT). Antecedent XRT to the chest may result in accelerated coronary atherosclerosis (see Chap. 23) [5].

A 67-year-old man, a former smoker with COPD, with a history of laryngeal cancer who had been treated with chemotherapy and radiation in 2015. In November 2019, the patient presented with dysphagia; biopsy of a distal esophageal stricture revealed a squamous cell carcinoma. He was treated with chemo/radiotherapy (Carboplatin/Taxol + 50.0 Gr in 28 fractions) with good response that completed

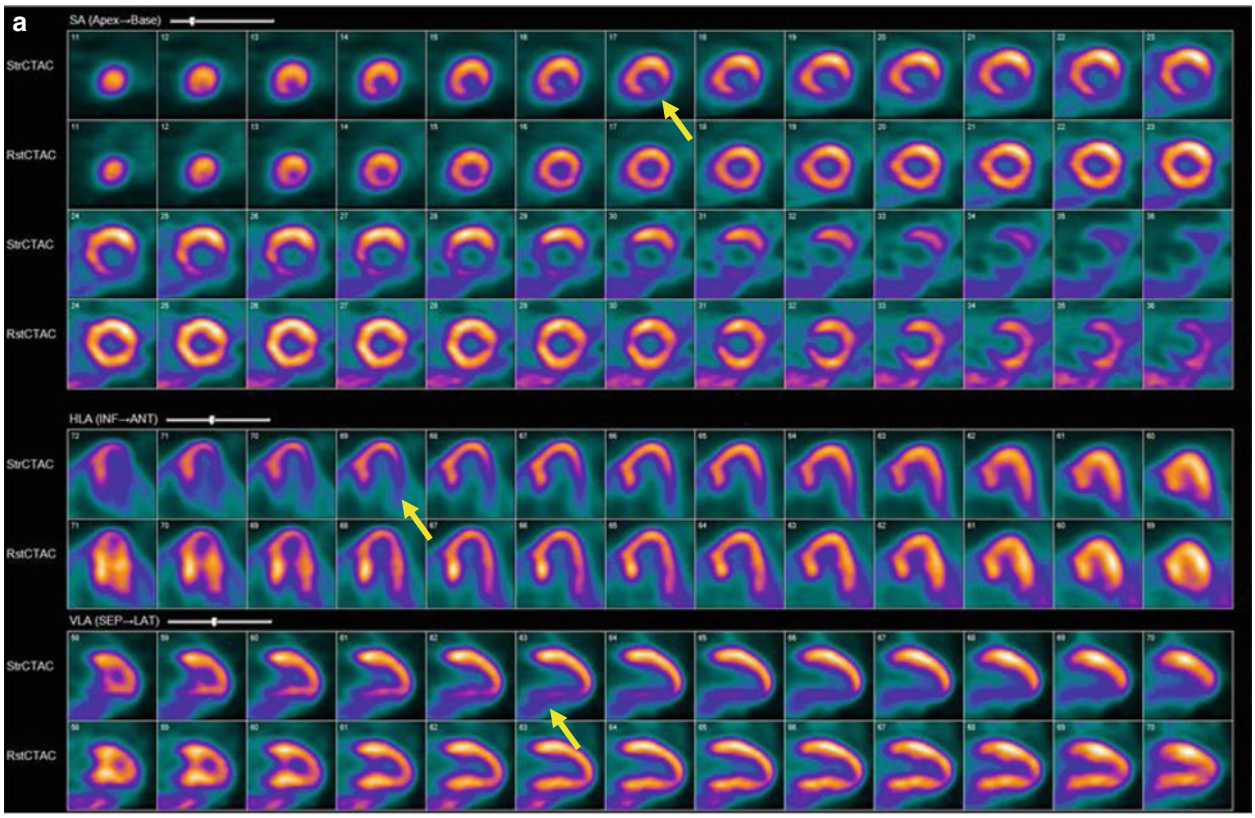

Fig. 14.3 **a** N-13 Ammonia PET myocardial perfusion images at stress (StrCTAC) and rest (RstCTAC) arranged in short axis (SA), horizontal long axis (HA) and vertical long axis (VLA) slices show a large area of moderate-severe reversibility in the inferior and inferolateral walls. Arrows point to the reversible perfusion defects in representative slices in the three orthogonal planes. Anterior wall perfusion is normal. Minimal reversible chamber dilatation is identified at stress. **b** Stress (top), rest (middle), and reversibility (bottom) polar maps displayed in the standard 17 segment model confirming extensive stress-induced ischemia predominantly involving the inferior and inferolateral walls. **c** Myocardial blood flow (MBF) and flow reserve (MFR) module in the 4DM Corridor software (Michigan, USA). MBF and MFR are derived from the dynamic PET images. Time-activity curves at stress and rest are shown at top. Polar maps on left side of the image show stress (top) and rest (middle) blood flow in ml/min/g and MFR (bottom) for each of the 17 standard segments. The table at bottom of the image shows abnormal MFR (reserve) of 1.39 in RCA territory (normal >2.0) with normal blood flow in LAD and LCX. MFR = Stress MBF/Rest MBF

in mid-2020. In August 2020, he underwent repeated endoscopy revealing recurrent invasive carcinoma.

An FDG-PET/CT was performed in September 2020, which did not show evidence of metastatic disease. However, extensive coronary artery calcium was incidentally noted on the CT component of the study (Fig. 14.5a, Video 14.5). The tumor board consensus was that surgery was preferable to brachytherapy.

On preoperative evaluation, he reported exercise tolerance restricted by fatigue and dyspnea (1 flight of stairs). He denied classic angina but described symptoms consistent with GERD. A nuclear stress test was ordered given his age, smoking history, prior chemotherapy, chest radiation, as well as evidence of extensive coronary artery calcium.

Myocardial perfusion study at rest and pharmacologic stress showed no evidence for stress-induced ischemia or prior infarct. Left ventricular chamber size and systolic function were normal (LVEF > 70%) (Fig. 14.5b). Esophageal surgery was uneventful.

Key Points

- Incidental calcium may be detected on cross-sectional imaging studies obtained for cancer staging, particularly the non-contrast CT component.
- Although coronary calcium increases the risk for cardiac events [6], the presence of calcium does not necessarily imply functional stenosis. This can be assessed non-invasively by MPI.

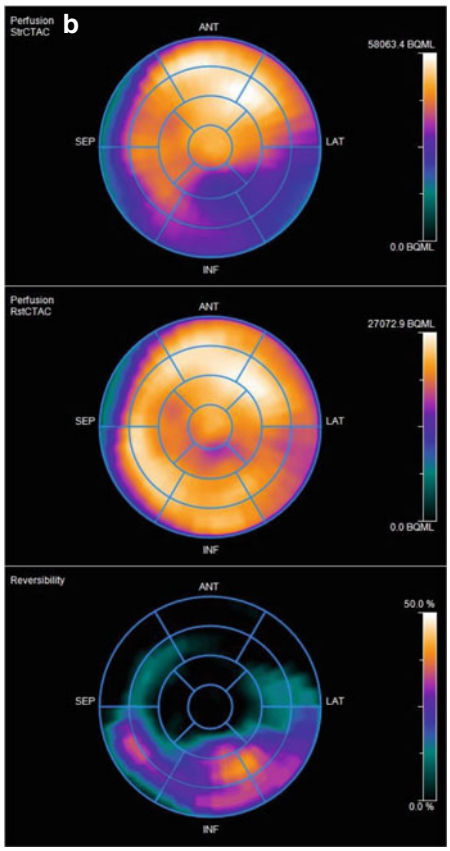

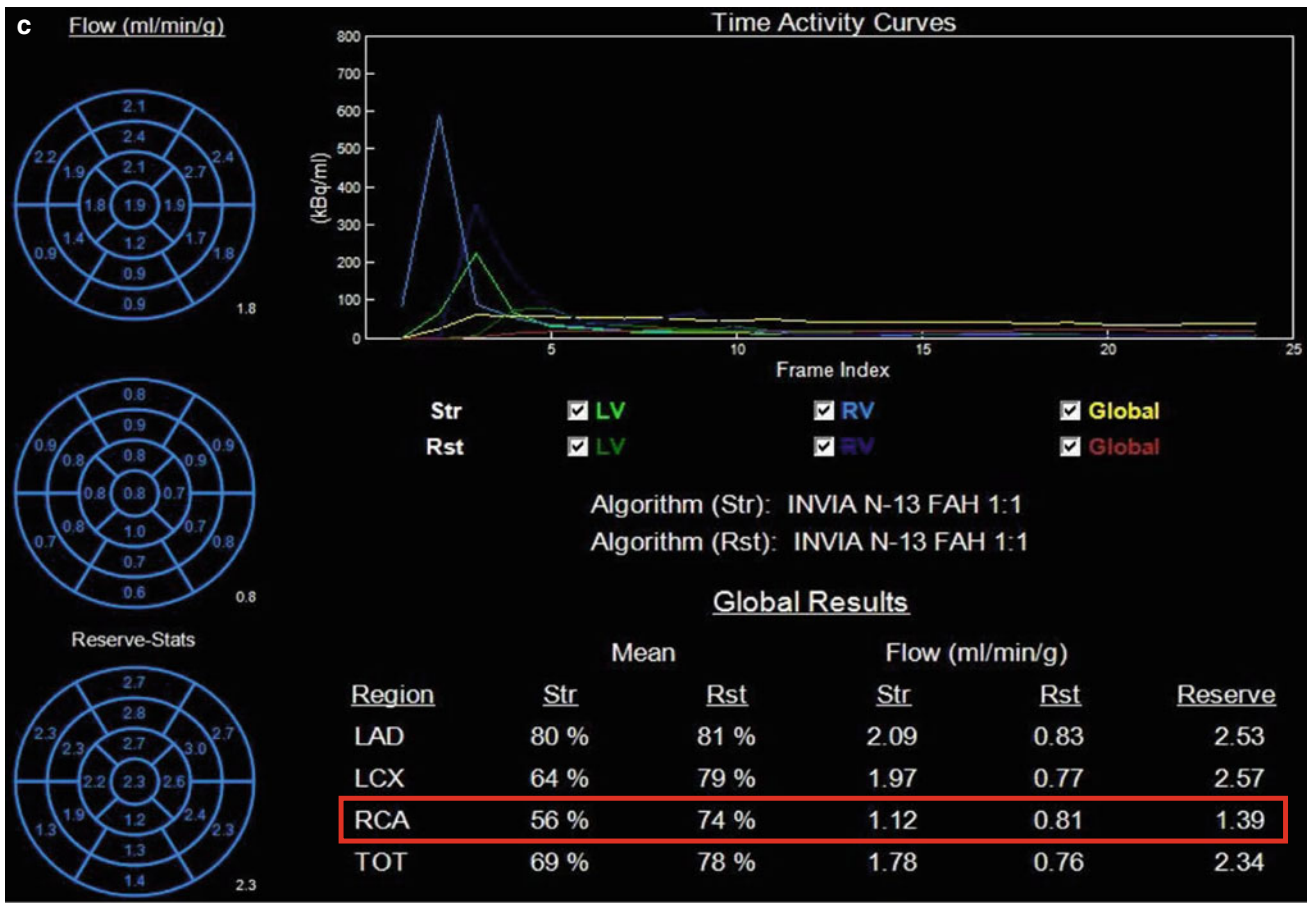

Fig. 14.3 (continued)

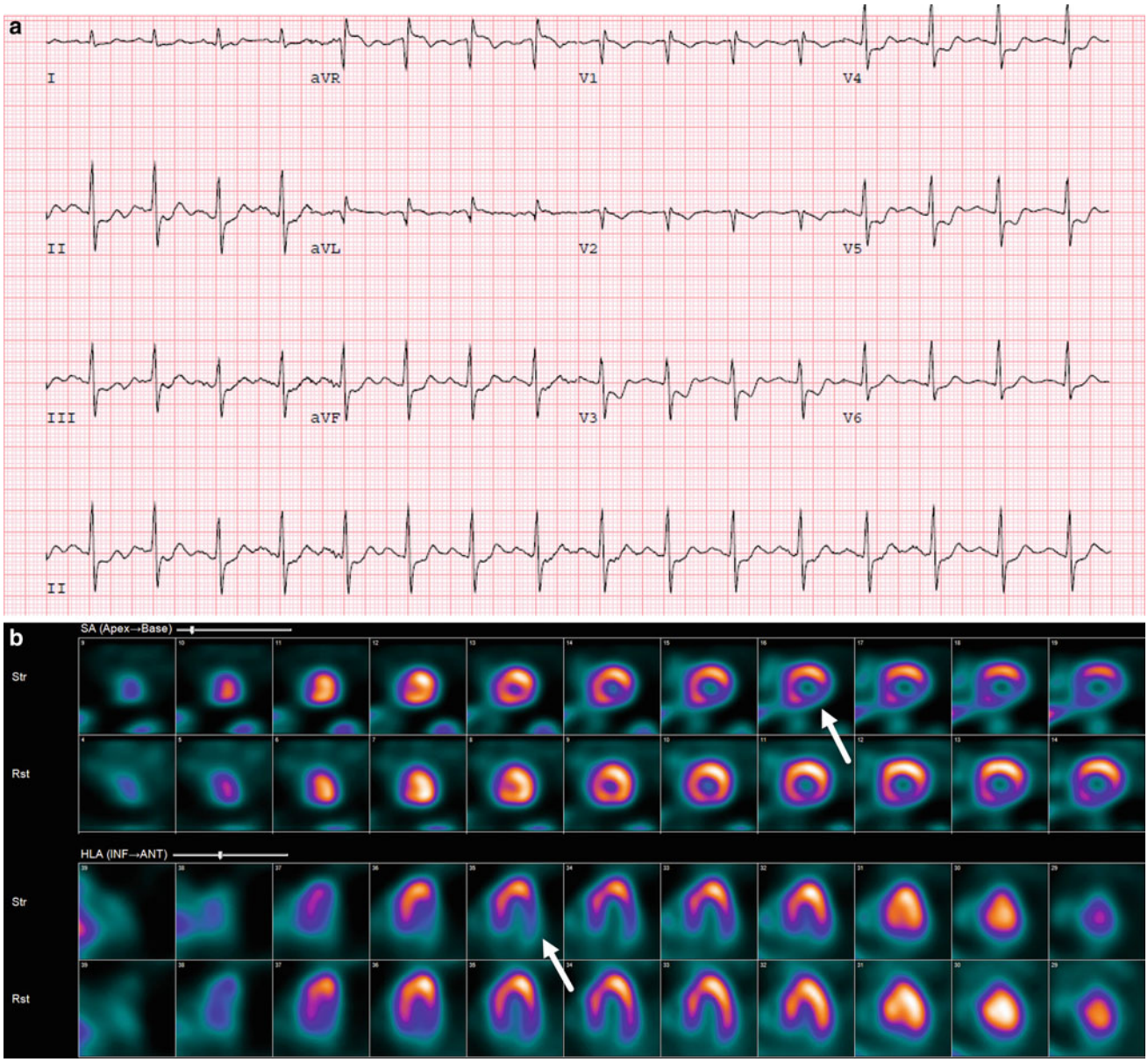

Fig. 14.4 **a** Pharmacologic stress ECG notable for down-sloping ST depression (~2.5 mm) in anterior and inferior leads at 8 min post regadenoson injection, consistent with coronary steal phenomenon and ischemia. ECG changes were accompanied by severe chest pain which began at 6–7 min post injection. Chest pain abated after IV administration of aminophylline 100 mg and multiple doses of sublingual nitroglycerin. Patient remained normotensive to hypertensive throughout the stress procedure, with a maximum heart rate of 113 bpm. Regadenoson is a selective A2A adenosine receptor agonist delivered intravenously as a unit bolus of 0.4 mg. The maximum hyperemia usually occurs 2–3 min post injection, however, side effects may last for up to 20 min in the absence of aminophylline reversal. **b** Tc-99m-Sestamibi stress (Str) and rest (Rst) SPECT images displayed in short axis (SA) and horizontal long axis (HLA) slices show a medium-sized area of moderate to severe ischemia in the lateral/inferolateral wall (white arrows)

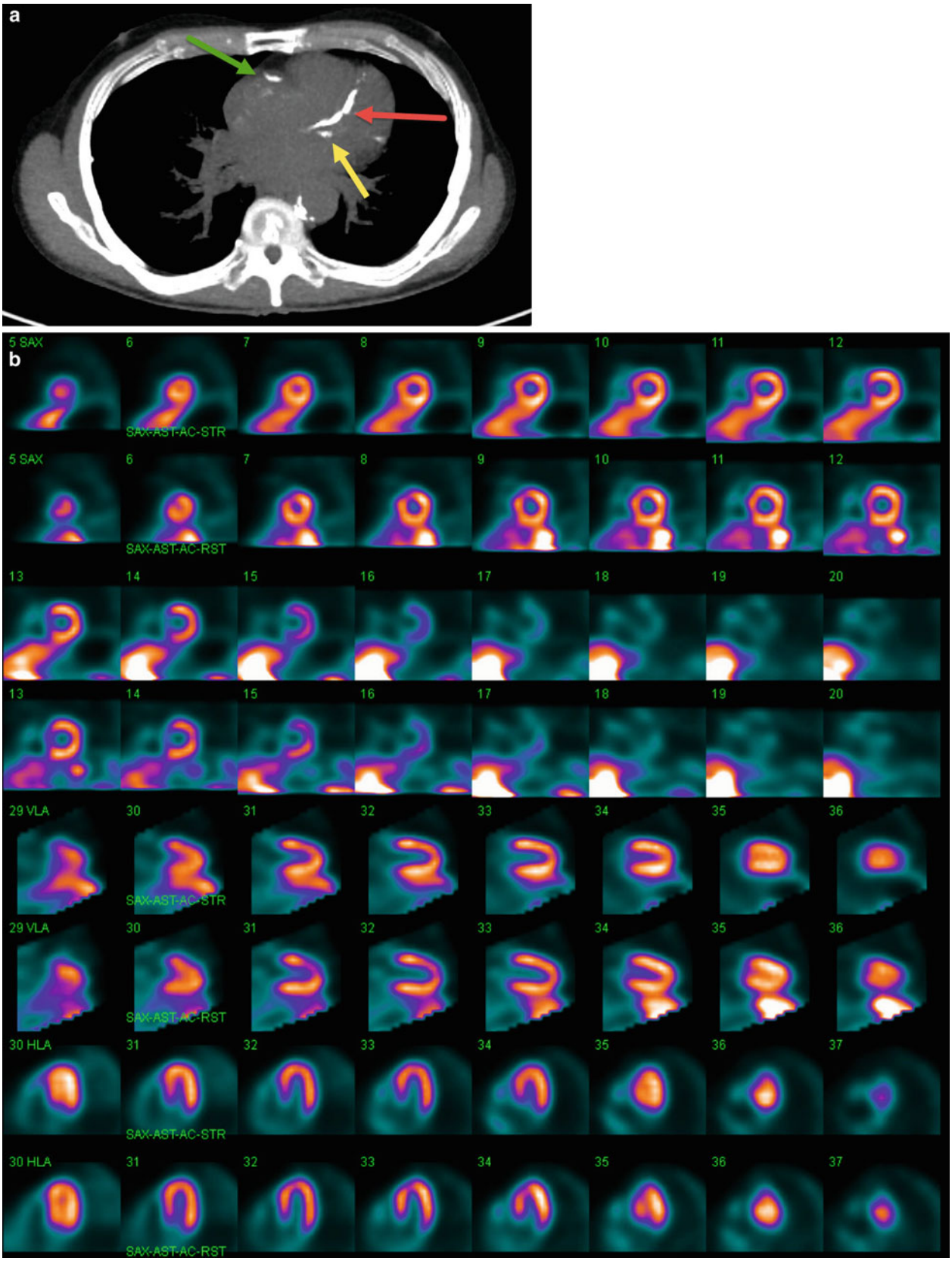

Fig. 14.5 **a** CT of the chest obtained for oncologic staging as part of an FDG PET/CT study incidentally demonstrates extensive coronary artery calcium in the LAD (red arrow), LCx (yellow arrow) and RCA (green arrow) arteries. The CT images are compressed for better depiction of disease extent. **b** Sestamibi MPI at rest and pharmacologic stress shows no evidence for stress-induced ischemia or prior infarct. Left ventricular systolic function was normal on gated images (not shown)

14.7 Case 6

The issue of how long the prognostic accuracy of a stress MPI remains valid has not been established for the purpose of preoperative risk stratification. That is, for how many months or years after a normal stress MPI can we assume a low operative risk? For general patient referrals, an attempt was made to determine the "warranty period" of a normal scan in a study involving more than 7,000 patients [7, 8]. In patients without previous CAD, risk (events per unit time) from the time of imaging was uniform for a mean of 2 years while for patients with known CAD the risk increased over time. The duration of the predictive power of a normal scan was affected by multiple clinical factors. For example, diabetic women had an annual event rate >3 times that of non-diabetic women and their risks accelerated over time.

A 69-year-old woman smoker with a history of monoclonal immunoglobulin deposition disease, status post high-dose melphalan and autologous stem cell transplant in 2002; ESRD status post-renal transplantation 2005 with chronic renal insufficiency (Cr 1.4, eGFR 40 ml/min); was treated for lung cancer with left VATS and left upper lobe wedge resection in 2010. The patient also had hypertension, hyperlipidemia, and extensive vascular disease. Her father had early-onset CAD.

Years later, in 2019, she was being followed for a slowly enlarging right lower lobe solid lung nodule, which on biopsy was found to be adenocarcinoma of the lung. Cardiology was consulted for preoperative risk assessment prior to planned resection.

She reported no chest pain with ambulation; however, her exercise tolerance was limited by claudication. No history of TIA, stroke, arrhythmia, syncope, or heart failure. Her medications included cyclosporine, CellCept, and prednisone for her kidney transplant. She was also receiving lisinopril, aspirin 81 mg, clopidogrel 75 mg, atorvastatin, ezetimibe, and amlodipine.

Her known vascular disease includes aneurysmal dilation of 4.5 cm of the descending thoracic aorta, mild-moderate carotid artery stenosis, and extensive lower extremity vascular disease requiring multiple interventional procedures. On CT scan, coronary artery calcifications were incidentally noted. A remote nuclear stress test with sestamibi SPECT in 2012 was normal.

In November 2019, she was referred for an N-13 ammonia PET MPI study with regadenoson stress. Her stress test revealed a large area of severe ischemia in the septum and apex, likely representing mid to distal LAD disease, single-vessel, with normal LV function (Fig. 14.6a, b; Video 14.6A-C). Myocardial flow reserve was 1.7 in the ischemic territory and normal elsewhere (>2.0).

In view of her significant vascular disease, extensive coronary calcium, and impaired renal function, coronary angiography was considered a high-risk procedure. This was discussed with the patient and she declined coronary angiogram in favor of medical management. Given the abnormal MPI, surgical resection of her lung lesion was considered at moderately high risk for perioperative cardiac complications. The patient opted instead for radiation therapy.

Key Points

- Coronary calcium discovered incidentally during CT scanning of the chest should be noted in the radiology report.
- Chronic kidney disease is a known risk factor for atherosclerotic progression. Thus it is not surprising that under these circumstances, MPI would show significant myocardial ischemia 7 years after a reportedly normal perfusion scan.
- The "warranty period" of a normal perfusion study will vary according to the clinical circumstance of the cancer patient.

14.8 Case 7

Stem cell transplants are generally considered high-risk procedures akin to high-risk surgical procedures [9]. The risk is elevated by the presence of left ventricular systolic dysfunction (LVSD) and CAD.

A 62-year-old man former smoker with CAD and three stents placed in 2008, HTN, DM Type 2, LVSD (baseline EF 40–45%), AFIB s/p cardioversion and ablation (maintained on apixaban) was diagnosed with primary CNS lymphoma in 2018. After chemotherapy, the cardiology service was consulted for cardiac risk assessment prior to autologous stem cell transplant (ASTCT). Sestamibi MPI with pharmacologic stress was ordered which showed (Fig. 14.7a):

(1) Medium-sized scar involving the inferior and inferolateral walls with mild to moderate peri-infarct ischemia. (2) Dilated left ventricular chamber size. Subtle transient ischemic dilatation. (3) Mildly decreased LVEF of 45%.

In conjunction with his past history, the patient was deemed at high risk for transplant, and intensive medical

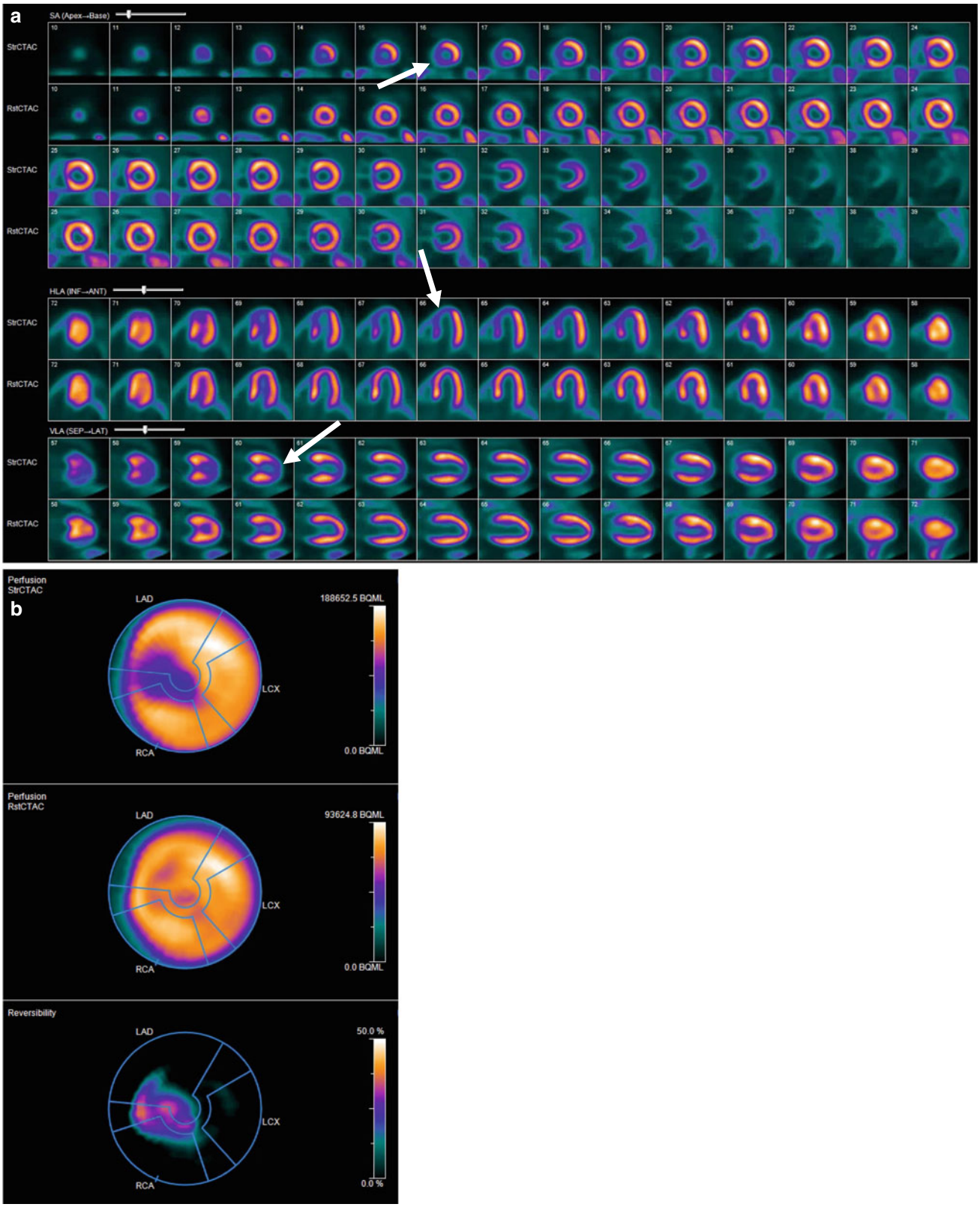

Fig. 14.6 **a** N-13 Ammonia PET myocardial perfusion images at stress (StrCTAC) and rest (RstCTAC) arranged in short axis (SA), horizontal long axis (HA), and vertical long axis (VLA) slices show a large area of severe ischemia in the septum and apex (white arrows). **b** Stress (top), rest (middle), and reversibility (bottom) polar maps displayed in the standard 17 segment model confirm a dense reversible perfusion defect in the mid to distal septum and apex, consistent with ischemia

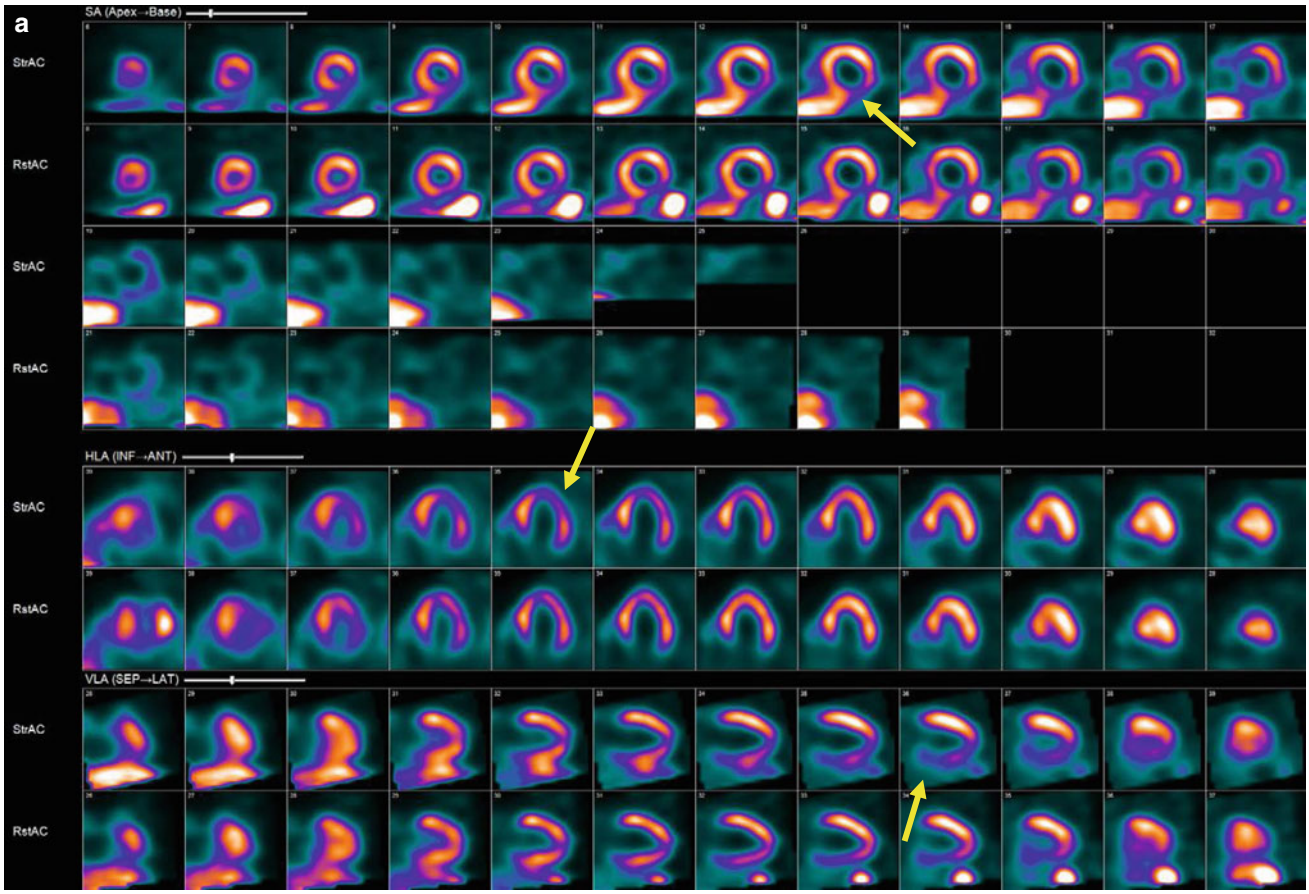
a
SA (Apex→Base)
StrAC
RstAC
StrAC
RstAC
HLA (INF→ANT)
StrAC
RstAC
VLA (SEP→LAT)
StrAC
RstAC

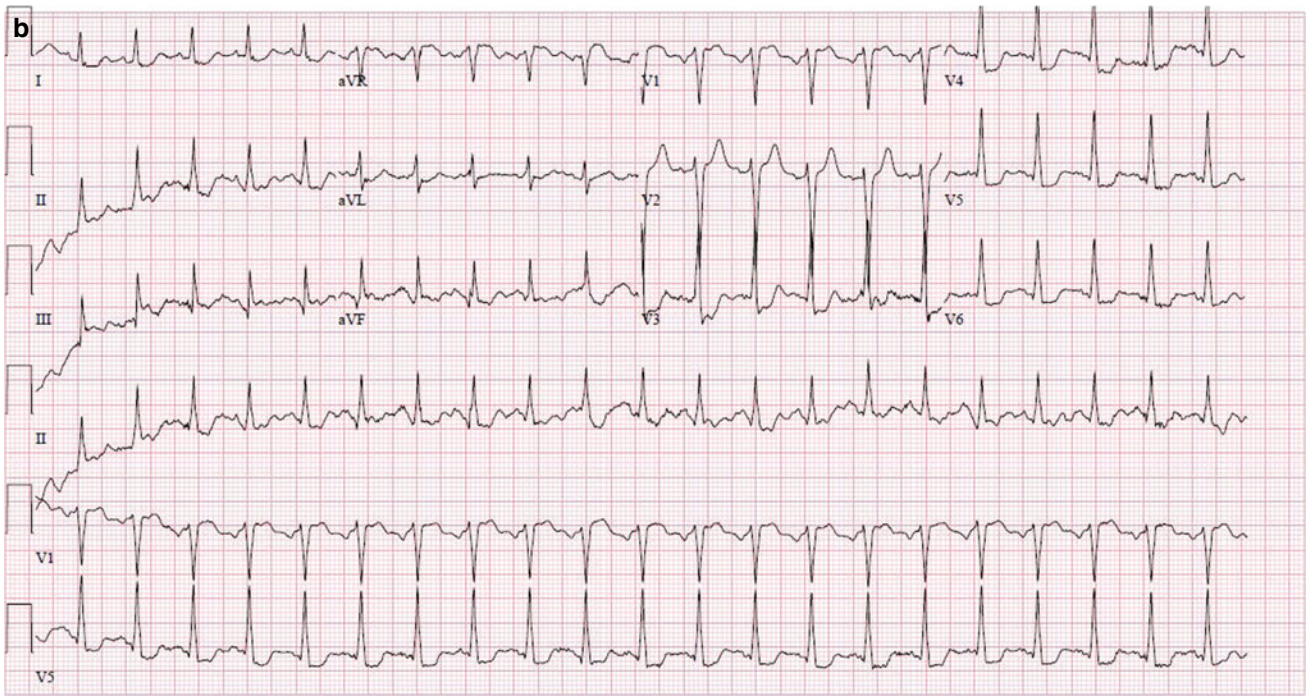
b
I
aVR
V1
V4
II
aVL
V2
V5
III
aVF
V3
V6
II
V1
V5

◀ **Fig. 14.7** **a** Sestamibi MPI with pharmacologic stress shows a medium sized partially reversible defect involving the inferior and inferolateral walls suggestive of infarct with peri-infarct ischemia (arrows). Left ventricular chamber size is mildly dilated and there is subtle transient ischemic dilatation. Mildly decreased LVEF of 45% on gated images (not shown). Due to the urgency of the patient's oncologic status, the decision was made to forego further coronary investigation, and to proceed with autologous stem cell transplant (ASTCT). **b** Resting ECG obtained 10 days after transplant procedure shows sinus tachycardia with ventricular rate of 129 bpm and marked ST abnormality, possible anterolateral subendocardial injury. Troponin level at this time peaked at 3.5 ng/mL. The patient was treated with guideline-directed medical therapy and recovered. **c** Three months later, the patient underwent an N-13 ammonia PET MPI study. The provided images show a large territory of moderate to severe ischemia involving the inferior and lateral walls, extending into apex and inferoseptum (Arrows). Mild transient ischemic dilatation of the left ventricle is again noted. Compared to the prior SPECT study (14.7a), the PET study suggests a larger territory of at-risk myocardium. **d** Dynamic PET data yield an abnormal MFR of 1.68 in the ischemic territory (red circle)

management was advised. The patient was presented at the Adult Bone Marrow Transplant Conference and the consensus was to proceed with ASTCT if the patient and family accepted the risk. They did consent and the patient underwent the transplant procedure in October 2018. The procedure was complicated by NSTEMI with flash pulmonary edema, new ST depressions on ECG (Fig. 14.7b) and positive troponin level (peak 3.5 ng/mL). He responded well to diuresis and guideline-directed medical therapy.

In December 2018, the patient returned for follow-up where he denied any objective cardiac symptoms but admitted to fatigue. He was mildly hypotensive (BP 94/63, HR 73). ECG: NSR 69, ST-T abnormality in the anterolateral leads. A repeated echocardiogram showed a drop in LVEF to 40% with new wall motion abnormalities, and therefore a repeated nuclear study was ordered.

The patient underwent an N-13 ammonia PET MPI study, which was abnormal (Fig. 14.7c):

1. Large territory of moderate to severe ischemia involving the inferior and lateral walls, extending into apex and inferoseptum (MFR 1.68 in the ischemic territory) (Fig. 14.7d).
2. Mild transient ischemic dilatation of the left ventricle.
3. Decreased left ventricular systolic function with LVEF of 40% (Video 14.7).

Compared to the sestamibi MPI study obtained 3 months prior, the PET study suggested a larger territory of at-risk myocardium.

His cardiologist consulting with the oncology team, referred the patient for cardiac catheterization and revascularization. In January 2019, the patient had staged PCI to the circumflex and LAD with drug-eluting SYNERGY stents. The right coronary artery showed a chronic total occlusion with collaterals and was treated medically.

Key Points

- PET MPI demonstrated a much larger ischemic perfusion defect than a SPECT MPI a few months prior. Although this was possibly due to the greater accuracy of PET imaging [10, 11], rapid progression of CAD was also a possibility. Cancer and its therapies are notorious for their ability to accelerate the process of atherothrombosis. The practice of cardio-oncology requires particular vigilance for changing clinical signs and symptoms. More frequent follow-up testing compared with the practice of cardiology in the general population is likely indicated to sort through the sometimes vague and nonspecific clinical clues presented by cancer patients during and after cancer treatment. (See the discussion in Case 6 above about the "warranty" of a normal MPI).
- The value of exercise treadmill or bicycle testing without imaging is highly limited in the cancer patient because a reasonable level of exercise is often not possible.
- In patients who are referred for pharmacologic MPI, assessment with PET when available is preferable to SPECT.

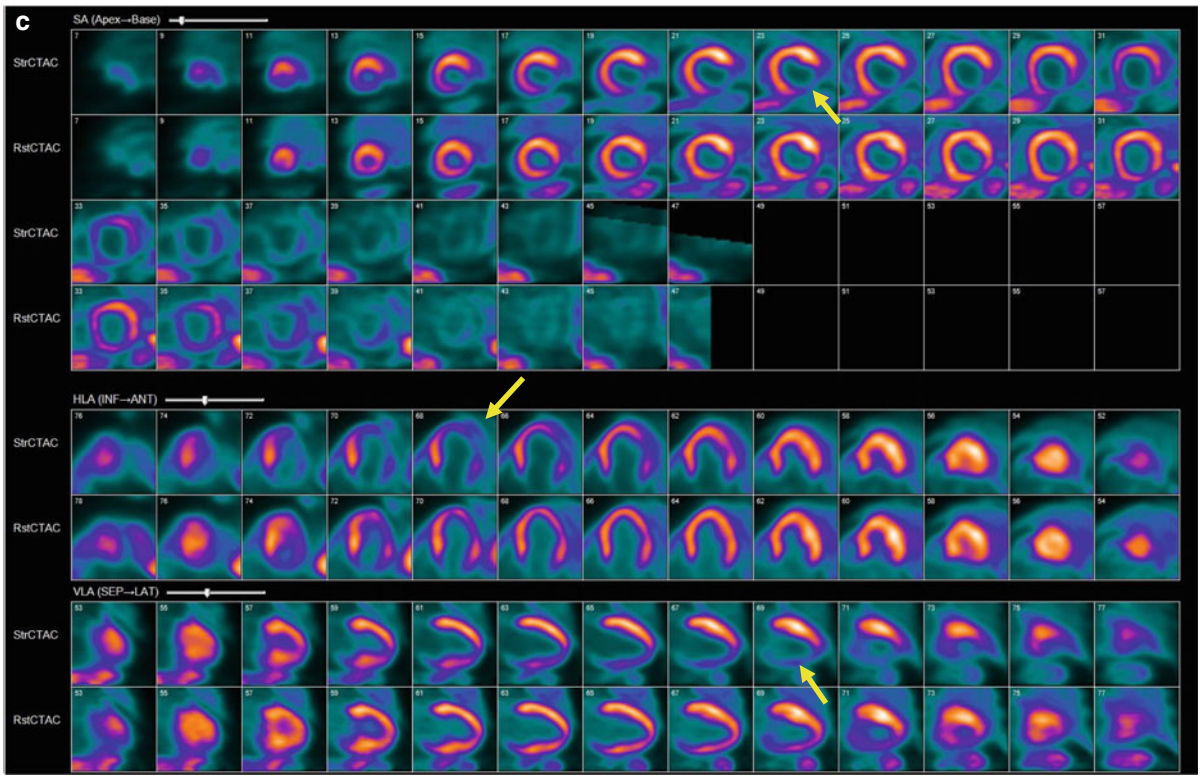

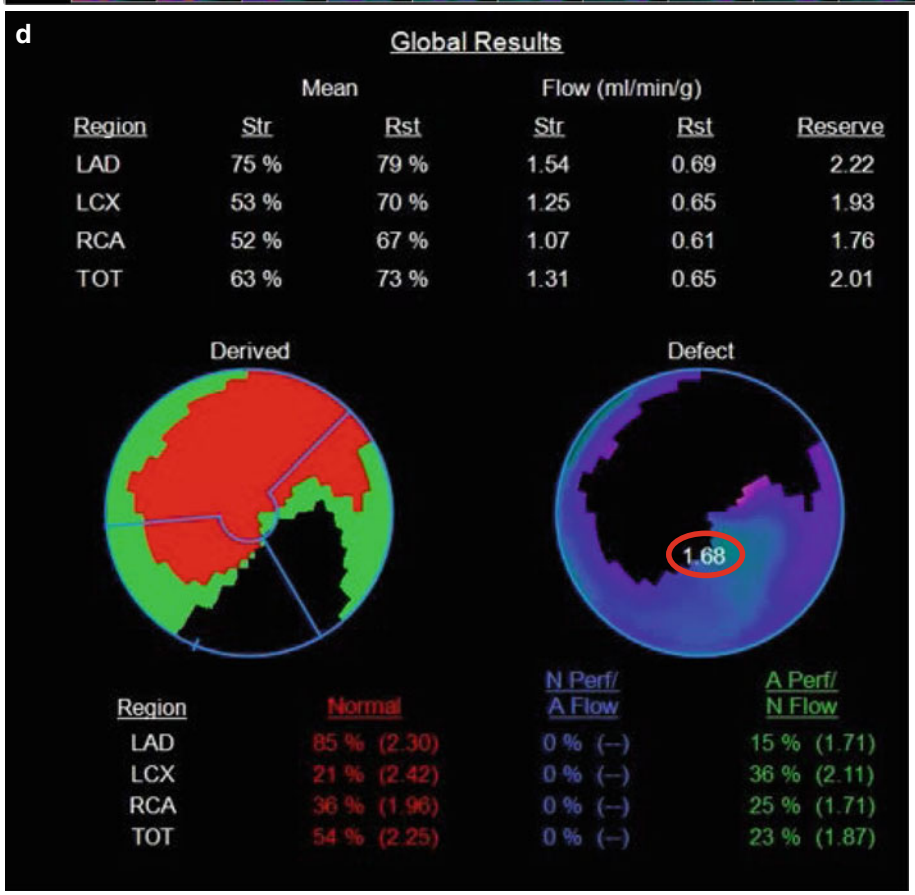

Fig. 14.7 (continued)

References

1. Fleisher LA, et al. 2014 ACC/AHA guideline on perioperative cardiovascular evaluation and management of patients undergoing noncardiac surgery: executive summary: a report of the American college of cardiology/American heart association task force on practice guidelines. Circulation. 2014;130(24):2215–45.
2. Weinstein H, Steingart R. Myocardial perfusion imaging for preoperative risk stratification. J Nucl Med. 2011;52(5):750–60.
3. Layoun ME, et al. Fluoropyrimidine-induced cardiotoxicity: manifestations, mechanisms, and management. Curr Oncol Rep. 2016;18(6):35.
4. Herrmann J, et al. Vascular toxicities of cancer therapies: the old and the new–an evolving avenue. Circulation. 2016;133(13): 1272–89.
5. Kim L, et al. Contemporary understandings of cardiovascular disease after cancer radiotherapy: a focus on ischemic heart disease. Curr Cardiol Rep. 2020;22(11):151.
6. Blaha MJ, et al. Comparing risk scores in the prediction of coronary and cardiovascular deaths: coronary artery calcium consortium. JACC Cardiovasc Imaging. 2020.
7. Hachamovitch R, et al. Determinants of risk and its temporal variation in patients with normal stress myocardial perfusion scans: what is the warranty period of a normal scan? J Am Coll Cardiol. 2003;41(8):1329–40.
8. Small GR, Ruddy TD. Are there any guarantees with the warranty period for normal stress SPECT myocardial perfusion imaging? J Nucl Cardiol. 2020;27(2):542–6.
9. Oliveira GH, et al. Cardiovascular risk assessment and management of patients undergoing hematopoietic cell transplantation. Bone Marrow Transplant. 2020.
10. Schindler TH, et al. Appropriate use criteria for PET myocardial perfusion imaging. J Nucl Med. 2020;61(8):1221–65.
11. Murthy VL, et al. Clinical quantification of myocardial blood flow using PET: joint position paper of the SNMMI cardiovascular council and the ASNC. J Nucl Med. 2018;59(2):273–93.

Perioperative Management of the Cancer Patient

15

Howard Weinstein

Key Points

- Perioperative myocardial ischemia peaks early postoperatively and can manifest as infarction, heart failure, arrhythmias and myocardial injury, all of which carry an adverse prognosis.
- Aggressive medical therapy is preferred, but when necessary coronary revascularization is best accomplished after recovery from cancer surgery.
- Management of perioperative atrial fibrillation and anticoagulation is central to the practice of cardio-oncology.
- Perioperative device management demands a unified cardiology, anesthesia, and surgical service approach.

15.1 Coronary Artery Disease and Myocardial Ischemia/Infarction

15.1.1 Case 1. Perioperative Myocardial Infarction

Assessing perioperative risk in cancer patients presents special challenges. In addition to sharing common morbidities with the general population, cancer patients incur additional risks related to their malignancies and to their cancer therapies. These unique features carry over into the postoperative period as well and decision-making in the perioperative period can be complex. This chapter will illustrate some of the key issues in treating perioperative cancer patient.

A 68-year-old man with hypertension and hyperlipidemia was diagnosed with advanced rectal adenocarcinoma. He received FOLFOX and capecitabine along with radiation therapy. His preoperative EKG is shown in Fig. 15.1. He was free of chest pain and was walking 2 miles daily prior to surgery and underwent a robotic partial colectomy and diverting loop ileostomy. During his 8-h intraoperative course, he developed hypertension treated with esmolol, followed by hypotension treated with phenylephrine. ST depression was observed intraoperatively. In the recovery room, new anterolateral ST depression and T-wave inversions were seen (Fig. 15.2), but the patient denied chest pain or shortness of breath. The physical exam was unremarkable. Initial troponin was negative. A bedside echocardiogram showed severe inferolateral and apical hypokinesis (Fig. 15.3, Video 15.1). Acute postoperative myocardial infarction (MI) was diagnosed by the EKG and echo findings. After conferring with the surgical team, the patient received aspirin and metoprolol and was transferred to a tertiary center for urgent cardiac catheterization. He was found to have three-vessel coronary artery disease (CAD) including stenosis of the proximal left anterior descending (LAD) and first diagonal and total occlusion of the distal right coronary artery (RCA) with left-to-right collaterals. Troponin peaked at 73 ng/dl. His course was complicated by systolic dysfunction requiring intra-aortic balloon pump support, atrial fibrillation with rapid ventricular response requiring amiodarone, and a suspected left ventricular thrombus treated with intravenous heparin. He developed hemoperitoneum on heparin. Cardiac MRI ultimately showed no evidence of left ventricular thrombus and he was transferred back to the cancer center to recuperate from bowel surgery. He then underwent uncomplicated coronary bypass surgery 5 weeks after his perioperative myocardial infarction. He underwent a second low anterior resection for dehiscence 9 months after the first procedure and tolerated this procedure well, with minimal detected

Electronic supplementary material
The online version of this chapter (https://doi.org/10.1007/978-3-030-70998-3_15) contains supplementary material, which is available to authorized users.

H. Weinstein (✉)
Department of Medicine, Memorial Sloan Kettering Cancer Center, 1275 York Avenue, New York, NY 10065, USA
e-mail: weinsteh@mskcc.org

R. M. Steingart et al. (eds.), *Atlas of Imaging in Cardio-Oncology*,
https://doi.org/10.1007/978-3-030-70998-3_15

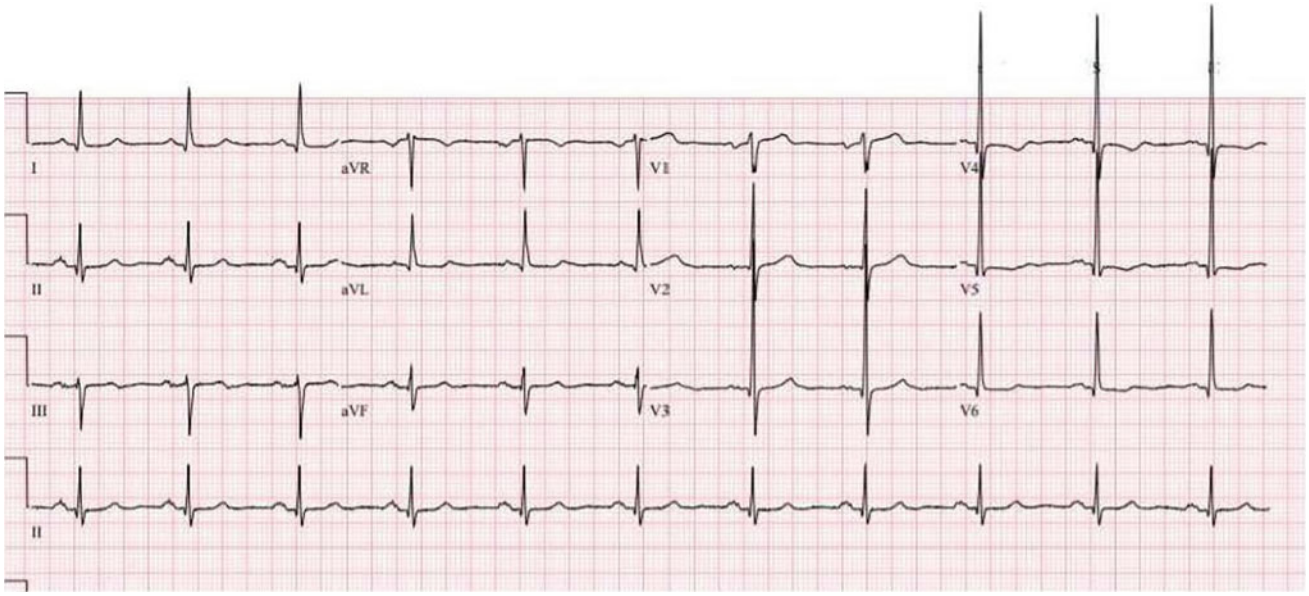

Fig. 15.1 Preoperative EKG. QRS voltages suggest left ventricular hypertrophy. Nonspecific ST and T-wave changes are noted in the anterolateral leads

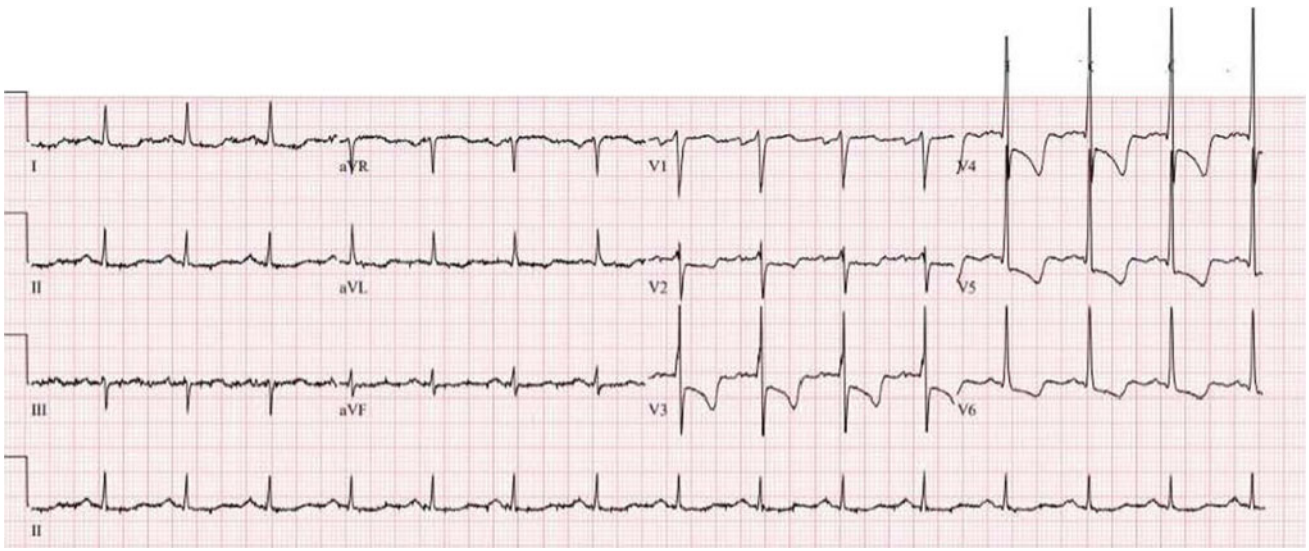

Fig. 15.2 Early postoperative EKG. Marked ST depression is now evident across the precordial leads and T-wave inversion has replaced nonspecific T-wave changes

troponin. His left ventricular function improved to near-normal levels with a residual apical wall motion abnormality and no physical limitations.

This case illustrates the intraoperative onset of severe ischemia during a prolonged oncologic procedure in a patient with no prior history of chest pain or exercise intolerance, and the decision-making that followed. The patient underwent early cardiac catheterization to define the coronary anatomy. Weighing the risk of perioperative bleeding, he was then given the opportunity to recover from his cancer surgery prior to undergoing coronary revascularization. After coronary revascularization, left ventricular function improved and he was able to tolerate further necessary colon surgery.

Perioperative myocardial ischemia peaks in the early postoperative period, in its most severe form resulting in acute MI [1, 2]. Intraoperative ischemia is less common and is infrequently associated with postoperative events.

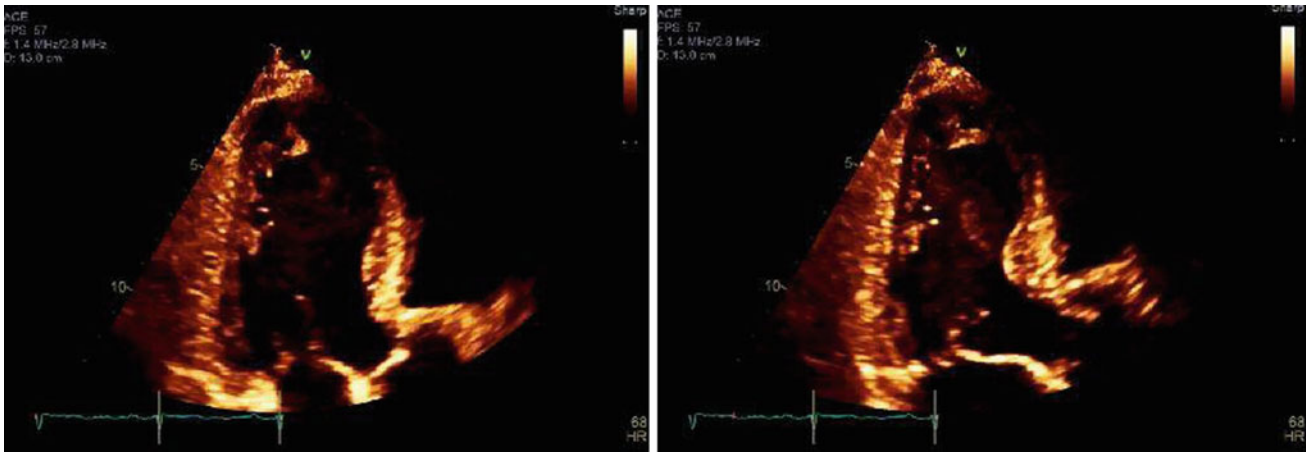

Fig. 15.3 Echocardiographic diastolic (left) and systolic (right) frames showing regional wall motion abnormalities in the lateral wall and apex

Perioperative MI typically is preceded by ST depression, evolving into a non-ST elevation acute coronary syndrome (ACS) within 24–48 h of surgery, incurring a similar mortality rate to non-surgical MI (10–15% in-hospital). Acute ischemia results from either supply/demand mismatch (Type 2 MI, more prevalent with severe underlying coronary stenoses and peaking relatively early after surgery) or from plaque rupture (Type 1 MI, typically involving mid-grade coronary lesions and developing throughout the perioperative period) [2, 3].

Other ischemic precipitants such as atrial fibrillation with rapid ventricular response, hypotension, and bleeding may occur later. Management imperatives include normalization of blood pressure, rhythm or ventricular rate control, control of bleeding and stabilized Hgb, infection control, and cardioprotective therapies such as beta-blockers. Patients with Type 2 MI typically receive additional guideline-directed therapy including antiplatelet agents, unfractionated or low-molecular weight heparin and statins, if feasible in the early postoperative period. However, the value of therapies with a bleeding risk requires a careful risk/benefit analysis. Cardiac catheterization should be expedited if ischemia recurs or cannot be controlled medically, or results in hemodynamic instability, heart failure, or malignant arrhythmias. Many stabilized patients prefer to recover from cancer surgery before undertaking invasive procedures (as in Case 1). If angiography is not undertaken to investigate an ischemic insult, noninvasive testing to exclude high-risk CAD should be considered prior to discharge or soon thereafter. The choice of approach to the intermediate and longer term management of CAD is determined case by case, after a careful evaluation of expected cancer therapies, cancer prognosis, functional status, and patient preference.

15.1.2 Case 2. Other Consequences of Perioperative Myocardial Ischemia.

A 68-year-old man with an apical lung tumor underwent a right thoracotomy and chest wall resection and reconstruction, with intrapleural pneumolysis. The history was significant for hypertension, high cholesterol, and stenting of the LAD 7 years earlier for jaw pain, with a subsequent angiogram 3 years prior to surgery (prompted by an abnormal stress test) that showed moderate disease of the circumflex, diffuse disease of the OM and LAD with a patent stent, and severe disease of a non-dominant RCA. The patient was treated medically and, prior to his thoracotomy, had low normal LV function with inferior and septal hypokinesis. His preoperative EKG is shown in Fig. 15.4.

The procedure was extensive, requiring alpha agonists, volume repletion, and blood transfusion. He had ST depression perioperatively but was asymptomatic. He developed respiratory failure on day 4 and a pulmonary embolism was suspected by CT. He was diuresed for coexisting pulmonary edema. He developed transient atrial fibrillation with rapid ventricular response. Echocardiography showed normal LV function but moderate RV dysfunction and pulmonary hypertension. He then developed a sigmoid perforation and underwent a sigmoid resection and colostomy. Concurrent bronchoscopy showed mucous plugging with clots. Two days later, he became hypoxemic and bradycardic, progressing to asystole. He was resuscitated but had further episodes of bradycardia and multiple episodes of non-sustained ventricular tachycardia. Transient ST elevation and PR depression were noted in some limb leads (Fig. 15.5). Troponin peaked at 22 ng/dl. Repeat echo showed severe RV dysfunction. The patient

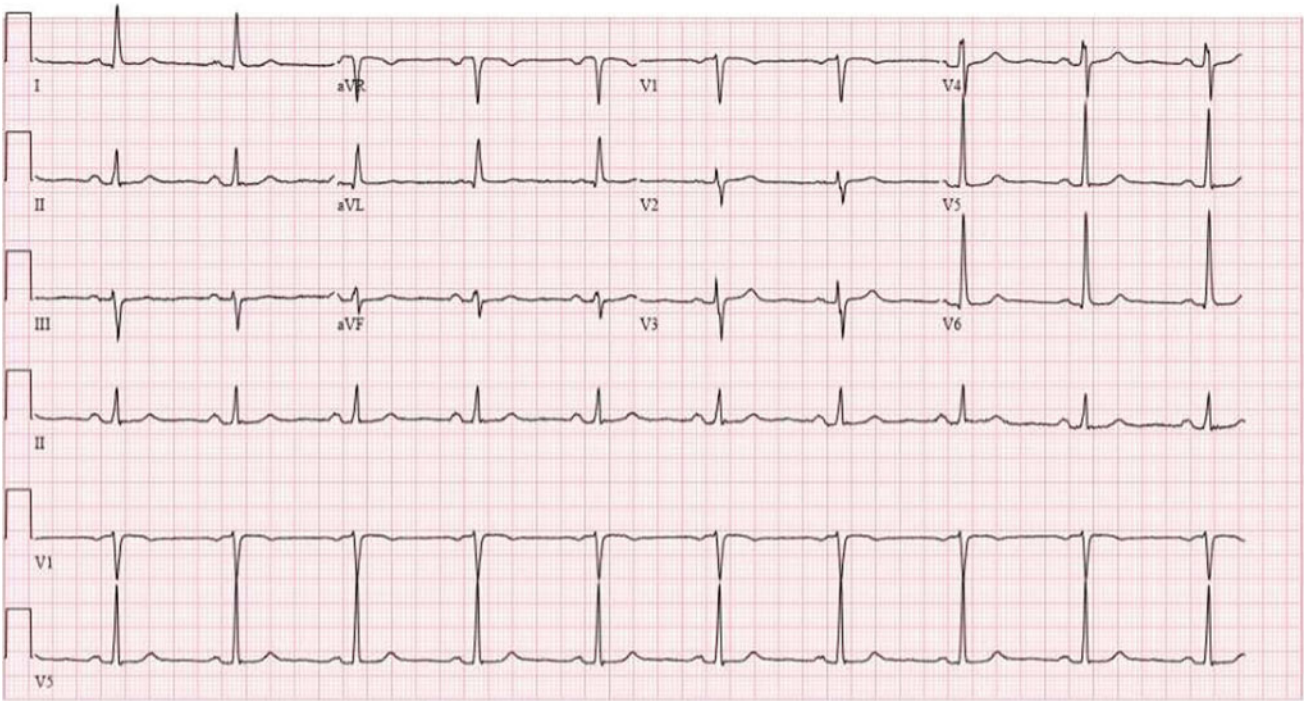

Fig. 15.4 Essentially normal preoperative EKG without ST changes

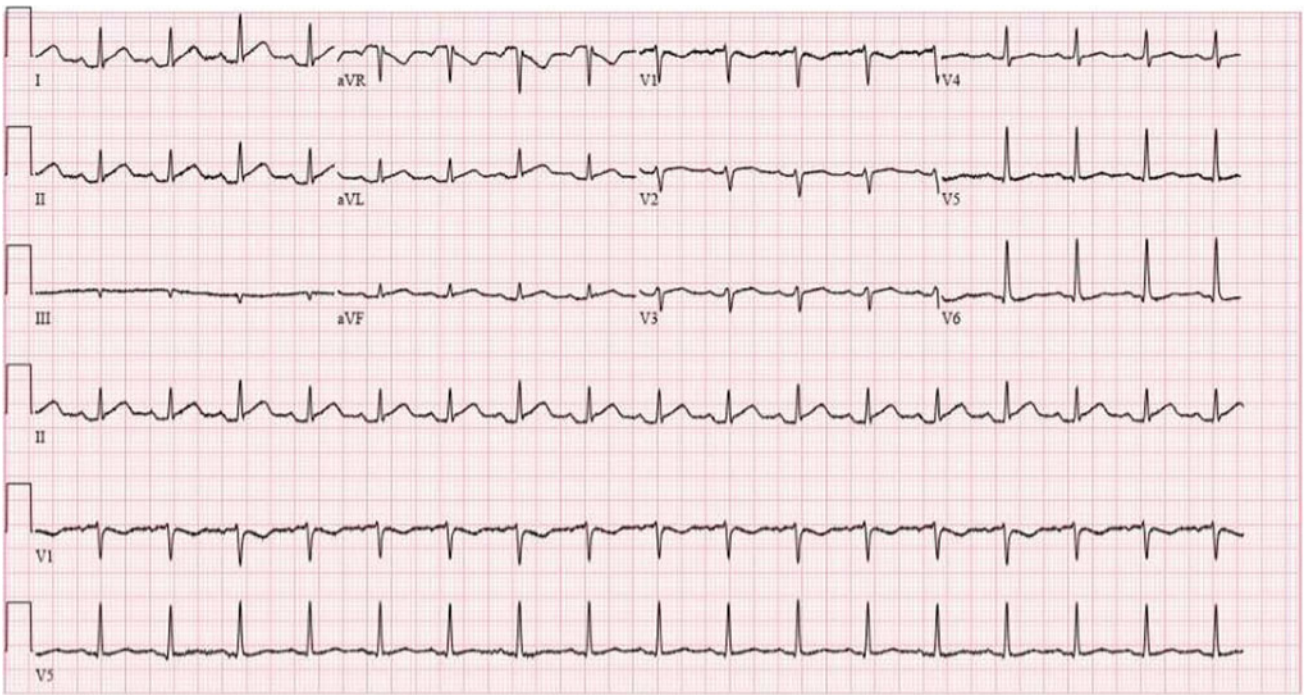

Fig. 15.5 Postoperative EKG. ST elevation of 1.5 mm is now appreciated in leads 1, II, and aVL. PR depression is seen in these leads, described in pericarditis. Focal ST elevation and PR depression are commonly seen in cancer and cancer surgery-related pericarditis, contrasted with the diffuse changes seen with viral or idiopathic pericarditis

was transferred to a tertiary heart center where cardiac catheterization showed severe stenosis of the mid-circumflex with collaterals, and nonobstructive CAD in the remaining vessels. He received stents to the mid and distal circumflex. He continued to have episodes of bradycardia, his RV dysfunction persisted and, after a prolonged course with refractory ARDS and septic shock the patient expired.

This case illustrates several aspects of perioperative cancer care. Acute myocardial ischemia may have manifested initially as atrial fibrillation and, later, as malignant arrhythmias. ST elevation was not associated with chest pain and the extensive thoracic surgery, ARDS and perioperative pulmonary embolism were confounding factors in the diagnosis of ischemia that ultimately led to the patient's demise despite coronary revascularization.

Although ST-elevation MI is relatively uncommon after surgery, its occurrence in the perioperative cancer patient requires critical decision-making. This dramatic event (which can occur throughout the perioperative period) can be difficult to differentiate from acute pericarditis, particularly in thoracic surgery patients where the pericardium is often breached during surgery and a localized current of injury may be seen. In such patients, troponin levels may be detected by the time the index EKG is acquired. Patients with STEMI after cancer surgery occasionally present with chest pain but, more typically, have no or vague symptoms. They may appear diaphoretic, dyspneic, tachycardic, or with overt heart failure or shock. Electrical instability may be present. Where symptoms and EKG findings are subtle or nonspecific, recognition of acute STEMI is challenging, and a bedside echocardiogram may help to confirm or exclude this diagnosis. Immediate direct angioplasty is indicated; thrombolysis is contraindicated in the perioperative patient. A judgment must be solicited urgently from the surgical team about the risk of bleeding on antithrombotic and antiplatelet therapy before proceeding with coronary angiography. Not uncommonly, treatment is limited to intensive medical management until the patient's bleeding risk is deemed acceptable for coronary interventions.

15.2 Perioperative Chest Pain

Perioperative chest pain is often difficult to diagnose, as symptoms may be vague or absent [3]. In cancer patients, assessing perioperative chest pain is particularly challenging. Symptoms may be referred from an abdominal, breast, or thoracic source. Pleuro-pericardial pain is common and can divert attention from an ischemic cause. Nonspecific EKG changes complicate the diagnosis of ischemia and biomarkers may be elevated due to pulmonary embolism, myopericarditis, intraoperative cardiac manipulations, and heart failure. When biomarkers are negative or minimally elevated and the chest pain is deemed potentially ischemic, bedside echocardiography followed by noninvasive testing should be considered, preferably with pharmacologic perfusion imaging.

15.3 Perioperative Myocardial Injury (PMI) After Noncardiac Surgery

The section on management of perioperative ischemia would not be complete without a discussion about perioperative myocardial injury after noncardiac surgery. This entity has been recently characterized in the general perioperative population [3] and its recognition and management raise important questions in the cancer population as well [4].

The need to diagnose PMI is particularly acute in the perioperative cancer patient, given the correlation between cancer and cardiac risk factors [5]. Detection of PMI by EKG is unreliable [4]. Hence in a study of 2018 consecutive patients deemed at high perioperative risk (by virtue of age or the presence of vascular disease) who underwent noncardiac surgery, evidence for PMI was sought by measuring high sensitivity troponin and by ischemic symptoms, new EKG changes or imaging abnormalities suggesting infarct) [3]. PMI defined by high sensitivity troponin release (16% of patients) was accompanied by typical chest pain in only 6%, and by any ischemic symptoms in 18%. Mortality was markedly higher after PMI (8.9 vs. 1.5% without PMI at 30 days, independent of the presence of the other diagnostic criteria). Fourteen percent of PMI events were deemed primarily extracardiac in cause (mostly from sepsis/infection), and this group had a striking 30-day mortality of 32%. Patient management was largely conservative in this subgroup of patients with PMI, with cardiac catheterization recommended in only 10% of patients, in keeping with the expected pathophysiology of supply–demand mismatch from hypotension, anemia, and tachycardia (versus plaque rupture) in this group [6]. Findings were consistent with prior studies, allowing for differences in study populations [7]. The authors of this study advocated continued monitoring of high sensitivity troponin to identify this high-risk group with PMI but acknowledged that randomized trials were needed to test the effectiveness of such surveillance on clinical and economic outcomes.

In the POISE trial that evaluated the protective effect of perioperative metoprolol, 5% had an MI in the first 30 days [8]. A subsequent cohort study of perioperative MI assessed the characteristics and short-term outcome of perioperative MI (defined by autopsy findings or elevated troponin and either ischemic symptoms, pathologic Q-waves, ischemic changes on EKG, coronary artery intervention, or cardiac imaging evidence of MI) [4]. Most MIs occurred within 48 h of surgery; two-thirds did not have cardiac symptoms. Thirty-day mortality was 11.6%, versus 2.2% in those without an MI, unaffected by the presence of symptoms.

These authors also advocated routine postoperative troponin monitoring to detect PMI.

Should biomarker surveillance now be recommended in perioperative cancer patients at high clinical risk for PMI? As an editorialist argues [9], there is no specific protocol for treating PMI, few patients in the study underwent testing for CAD and only 29% had a change in their medical management [4]. As there are limited data as to the treatment of PMI, it remains open whether routine perioperative troponin testing improves outcomes or "opens a Pandora's box of additional testing and treatment."

15.4 Case 3. Atrial Fibrillation

An 87-year-old female with hypertension was evaluated preoperatively for an extensive maxillectomy. She reported an episode of severe chest pain 30 years earlier that was not investigated until several years later, when an echocardiogram was reported to show a prior MI. She had no further chest pain and was active, without symptoms. She had a history of paroxysmal atrial fibrillation with the last documented episode occurring 3 years earlier. She had no history of stroke or TIA. She was not fully anticoagulated but was treated with clopidogrel (having had hives and bronchospasm on aspirin). She had a long history of asthma dating to her youth that was quiescent for many years but recurred at menopause. However, she tolerated low-dose beta-blockers. She was hypertensive in the clinic. A preoperative pharmacologic perfusion study to assess for CAD showed no evidence of ischemia or infarct and an outside echocardiogram showed normal biventricular function with moderate TR, mild MR, mild diastolic dysfunction, and mild bi-atrial dilatation.

She underwent a left maxillectomy, modified radical neck dissection, tracheostomy, and palate/orbital floor resection with an anesthesia time of 11 h and received phenylephrine and extensive amounts of fluid, albumin, and packed cells. She had postoperative hypotension and bradycardia and was markedly anemic, requiring further transfusion. Anterior T-wave inversion developed (Fig. 15.6) but troponins were negative. Overnight, she desaturated, and a chest X-ray showed bibasilar opacities indicating either atelectasis or pneumonia (Fig. 15.7). On postoperative day 2, she developed an irregular narrow complex tachycardia (Fig. 15.8) associated with chest tightness and palpitations and was diagnosed with atrial fibrillation with rapid ventricular response. Her beta-blocker dose was increased, and she spontaneously reverted to sinus rhythm. She then developed a brief run of Mobitz type II second-degree AV block in conjunction with nausea and vomiting, deemed vagally mediated. Her beta-blocker was withheld and subsequently resumed at a lower dose. Because of her high stroke risk from atrial fibrillation (CHADS-Vasc 5), she was started on apixaban 2.5 mg b.i.d. and clopidogrel was discontinued.

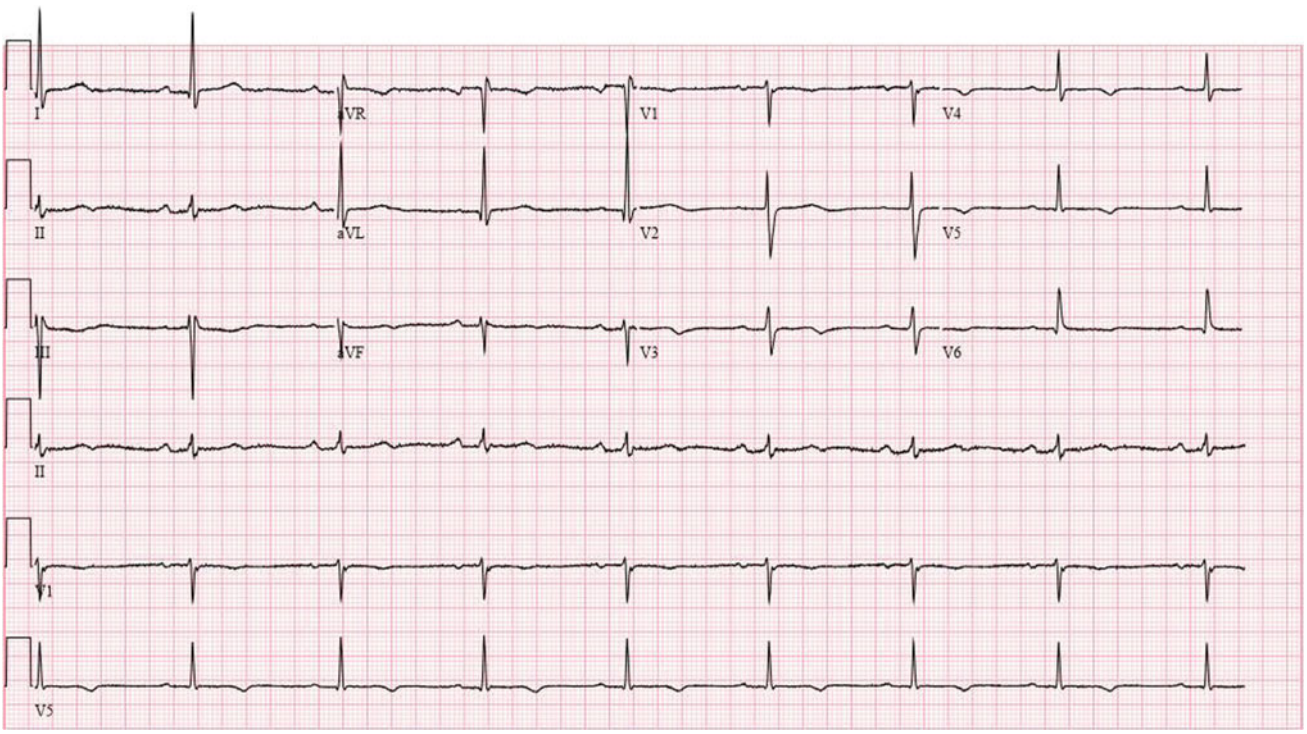

Fig. 15.6 Early postoperative EKG. Anterior T-wave inversion is evident, potentially representing ischemia

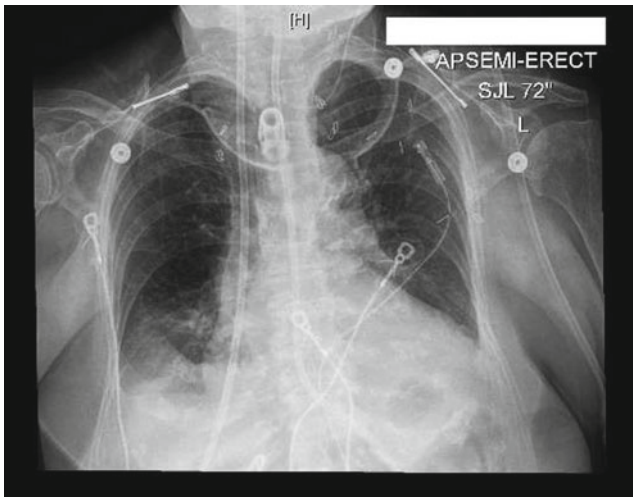

Fig. 15.7 Postoperative chest X-ray. Bibasilar opacities are evident, indicating atelectasis and/or pneumonia

She was gently diuresed. She was discharged 2 weeks after surgery and was asymptomatic when reevaluated 1 month later, tolerating her apixaban and low-dose beta-blockers.

This case introduces some key concepts pertaining to perioperative atrial fibrillation in the cancer patient. This elderly patient had a high a priori risk of perioperative atrial fibrillation from her advanced age and history of this arrhythmia. Additional substrates for atrial fibrillation then developed intraoperatively and in the early postoperative period, including prolonged surgery, extensive fluid and blood administration, severe anemia, hypotension, possible myocardial ischemia, hypoxemia, and intrathoracic disease. Conduction system disease (common in the elderly) complicated the use of AV nodal blockers, and, with her history of asthma, dosing of her beta-blocker required careful consideration. The occurrence of perioperative atrial fibrillation prompted a re-evaluation of her anticoagulation strategy and the initiation of adjusted dose oral anticoagulation.

Atrial fibrillation is the most common sustained arrhythmia (2% of the general population, 10% by age 80) [10]. The multiple common substrates between atrial fibrillation and cancer [10] and the increasing occurrence of cancer in the elderly [11] link these two diagnoses. Studies in cancer surgery report high rates of perioperative atrial fibrillation, particularly after lung surgery; the most frequent form of cancer-related atrial fibrillation occurs postoperatively [11], principally after lung cancer surgery, where rates as high as 60% have been reported. As such, management of atrial fibrillation is a significant burden of care in postoperative cancer patients. Pathophysiologic factors leading to perioperative atrial fibrillation have been reviewed [11]. Modifiable factors include duration of surgery, surgical complications, postoperative blood transfusion, and the use of colon conduits during esophagectomy. As in the non-surgical setting, the response to anticoagulation may be unpredictable in cancer patients [12] and vitamin K antagonists, when used for DVT, incur a sixfold risk of bleeding in cancer (versus

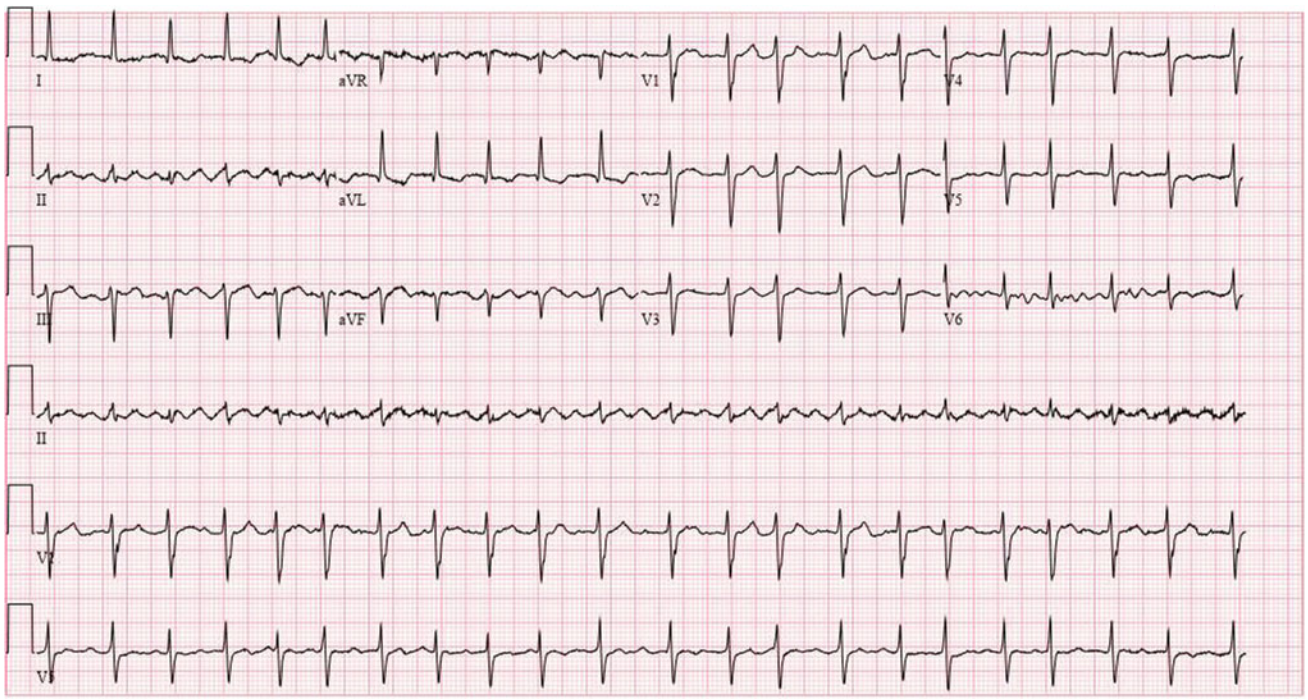

Fig. 15.8 Postoperative EKG showing atrial fibrillation/flutter, with rapid ventricular response

non-cancer patients) [13]. A recent study in 24,000 patients calls into question the accuracy of the CHADS-2 scale in predicting stroke risk in new-onset cancer-associated atrial fibrillation (occurring after the cancer diagnosis) [14], thus complicating decision-making. In our practice, we favor a strategy of ventricular rate control and risk-based anticoagulation in stable patients over rhythm management with either electrical or chemical cardioversion. This approach recognizes the persistent substrate for recurrent atrial fibrillation in the perioperative patient, the high likelihood of spontaneous reversion to sinus rhythm within 2 weeks of surgery [15, 16] and the desire to avoid further procedures in the postoperative period. Some data suggest that prophylactic amiodarone at 30 mg IV immediately after surgery followed by 60 mg b.i.d. for 5 days reduces the risk of atrial fibrillation after lung surgery [17]. A possible algorithm for the management of atrial fibrillation in the cancer patient is provided in reference [11]. As in postoperative atrial fibrillation in the general population, risk assessment for stroke versus bleeding is predicated on an expectation of either persistent or recurrent atrial fibrillation after recovery from surgery. In a study of 77 consecutive patients with perioperative atrial fibrillation after cancer surgery followed with event monitors, 31% developed recurrent atrial fibrillation, asymptomatic in 92% of these patients; the recurrence of atrial fibrillation was associated with hypertension and elevated creatinine [18]. If atrial fibrillation persists for more than a day or two postoperatively, it is reasonable to consider treating patients with a low bleeding risk and anything other than a negligible stroke risk with anticoagulation, particularly in the presence of hypertension or renal insufficiency. Frequently, patients undergo prolonged periods of outpatient monitoring to document the presence or absence of recurrent atrial fibrillation. Caution is advised as a recent meta-analysis showed that perioperative atrial fibrillation, although transient and self-limiting, still incurs an elevated risk of subsequent stroke, particularly after noncardiac surgery [19].

Although cancer is not currently included in the CHADS-Vasc scale, malignancy represents a hypercoagulable state in many patients, and clinicians may weigh this in their treatment of atrial fibrillation.

15.5 Perioperative Anticoagulation

The decision-making for perioperative anticoagulation or antiplatelet agents after cancer surgery (regardless of the indication) must take into account future cancer therapies. Hence, the bleeding risk of both the malignancy itself and of subsequent chemotherapy with expected thrombocytopenia must be considered. Direct oral anticoagulants should be deferred for at least 2 weeks after genitourinary or gastrointestinal cancer surgery to avoid anastomotic bleeding from a local anticoagulant effect [20]. Oncologists favor low-molecular weight heparin for anticoagulation in actively treated cancer patients, over warfarin and even direct oral anticoagulants, for its added stability in the face of fluctuating platelet counts and bleeding risk. Patients are then transitioned to direct-acting oral anticoagulants for prolonged anticoagulation courses.

15.6 Case 4. Perioperative Cardiac Device Management

An 83-year-old man with hypertension, diabetes, and paroxysmal atrial fibrillation was evaluated prior to resection of a cutaneous melanoma on his abdomen. He had an acute myocardial infarction in 1993, presenting with 2 days of indigestion, and underwent bypass surgery. His indigestion resolved after his bypass and he remained free of chest pain until 3 years prior to cancer surgery, when he presented with dyspnea and worsening pedal edema. In hospital, he had sustained ventricular tachycardia and was cardioverted. A biventricular pacemaker-ICD was implanted to manage both his malignant arrhythmia and his coexisting left ventricular dysfunction. Cardiac catheterization showed severe underlying CAD and 95% stenosis of a saphenous vein graft to a large first diagonal. He received a drug-eluting stent to this graft. One year prior to cancer surgery, he underwent a transcutaneous aortic valve replacement (TAVR) for moderate to severe aortic stenosis. Based on recommendations made in the preoperative cardiology consultation, his biventricular ICD, evident on both a preoperative chest X-ray (Fig. 15.9) and EKG (Fig. 15.10) was managed perioperatively with the placement of a dedicated magnet over the device to deactivate

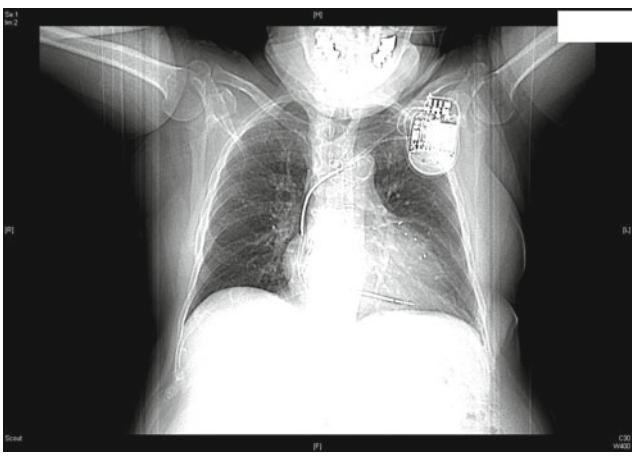

Fig. 15.9 Preoperative chest X-ray. Note the ICD pulse generator in the left upper quadrant of the chest and the thick coils from the device coursing into the right ventricle. Midline sternotomy wires are evident from prior bypass surgery

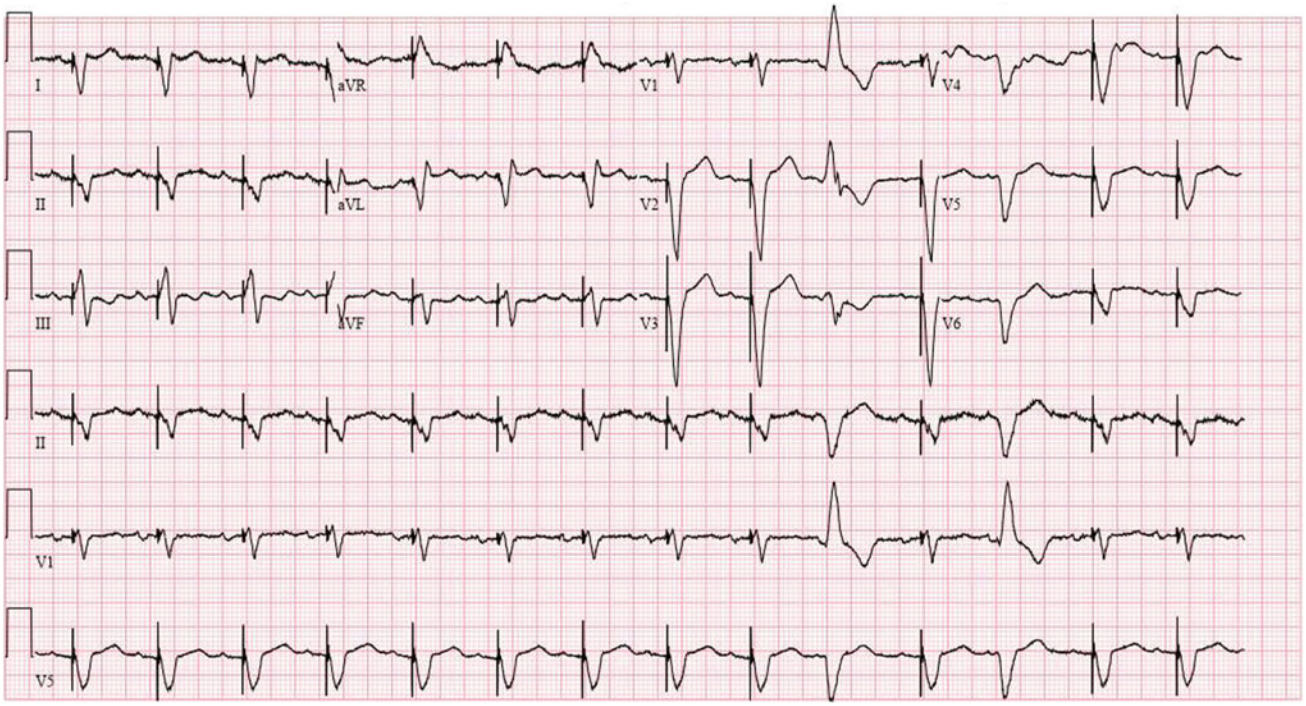

Fig. 15.10 Preoperative EKG. Native P-waves are tracked by the device and biventricular pacing spikes are evident after each P wave. Premature ventricular complexes are noted (absence of pacing spikes and change in QRS morphology)

anti-tachycardia therapies during the procedure. The patient was not pacemaker dependent; reprogramming of pacing capabilities was not required.

This case illustrates the key findings of a biventricular ICD on EKG and chest X-ray. The strategy employed intraoperatively, including magnet placement over the device and the preferential use of bipolar electrocautery, prevented the delivery of spurious shocks by the ICD in response to electrocautery in the nearby surgical field, potentially interpreted by the device as ventricular fibrillation.

A team approach to managing implantable cardiac devices is essential in the periprocedural period [21]. This begins with a careful preoperative evaluation of the indication, current status, and perioperative management requirements of the device. Recommendations for perioperative device management are detailed in a preoperative cardiology consultation and communicated separately to the surgical service and a dedicated cardiology and anesthesiology team, so that intraoperative and postoperative device therapies may be implemented.

15.7 Case 5. Perioperative Heart Failure

A 77-year-old woman was evaluated preoperatively for a radical neck dissection. Her extensive history included hypertension, diabetes, hyperlipidemia, peripheral vascular disease, paroxysmal atrial fibrillation, and a long history of mitral regurgitation and heart failure. Some 20 years prior to cancer surgery, she underwent the insertion of a mechanical mitral prosthesis, complicated by post-pericardiotomy syndrome requiring pericardiocentesis. She had chronic heart failure and was now limited by both exertional dyspnea and by hip and knee replacements. She was free of chest pain for several years, and recent perfusion imaging had shown no evidence of CAD. She was treated with warfarin for both paroxysmal atrial fibrillation and for her prosthetic mitral prosthesis. She required midodrine for chronic hypotension. A preoperative echocardiogram showed mild global left ventricular dysfunction and a normally functioning mitral prosthesis. Her preoperative EKG is shown in Fig. 15.11. She was deemed at elevated, but not prohibitive, risk for this strongly indicated procedure. Her warfarin was bridged with low molecular weight heparin around the time of surgery.

On the first postoperative day from the extensive neck dissection, she required re-operation for bleeding. A junctional tachycardia with mild ST changes was noted (Fig. 15.12) followed by atrial fibrillation (Fig. 15.13). Another operation was needed for a tracheostomy, and minimally elevated troponin levels were now detected. She then developed runs of ventricular tachycardia (VT) (Fig. 15.14) and was started on IV amiodarone, with persistent ventricular ectopy but no further runs of VT. She was treated with diuretics and nitrates for suspected heart failure.

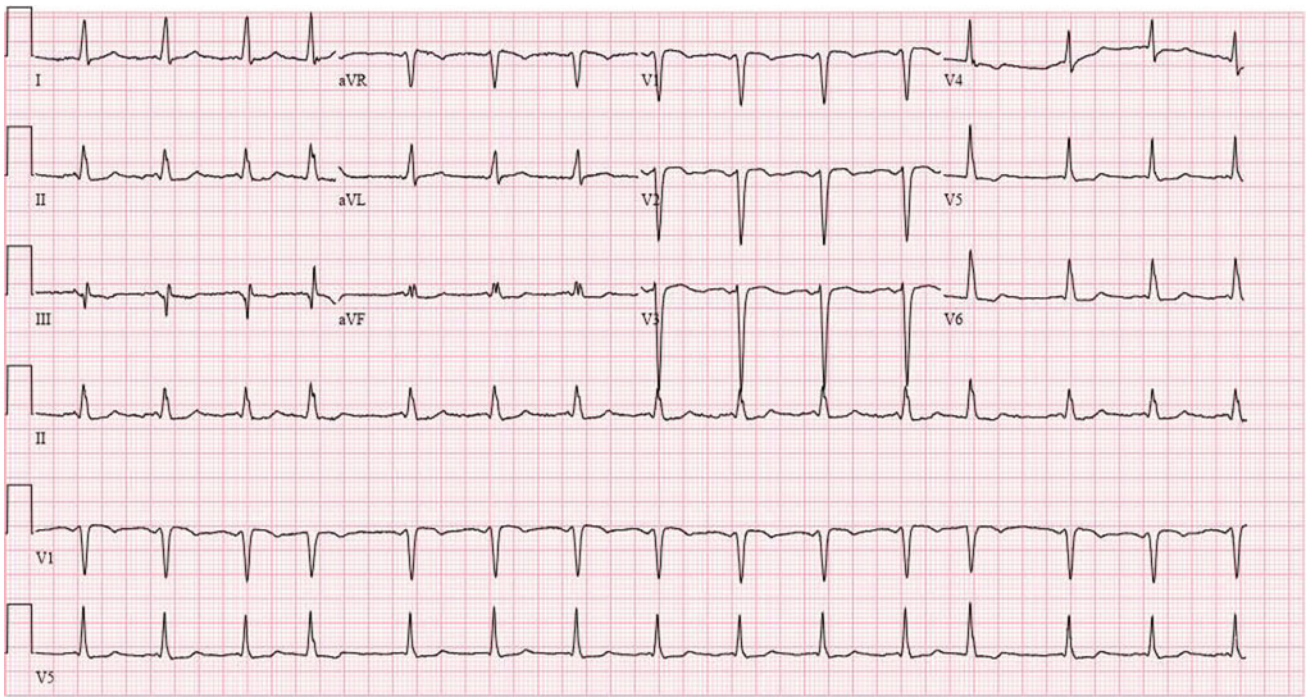

Fig. 15.11 Preoperative EKG. QRS duration is prolonged and a nonspecific ST and T wave pattern is seen

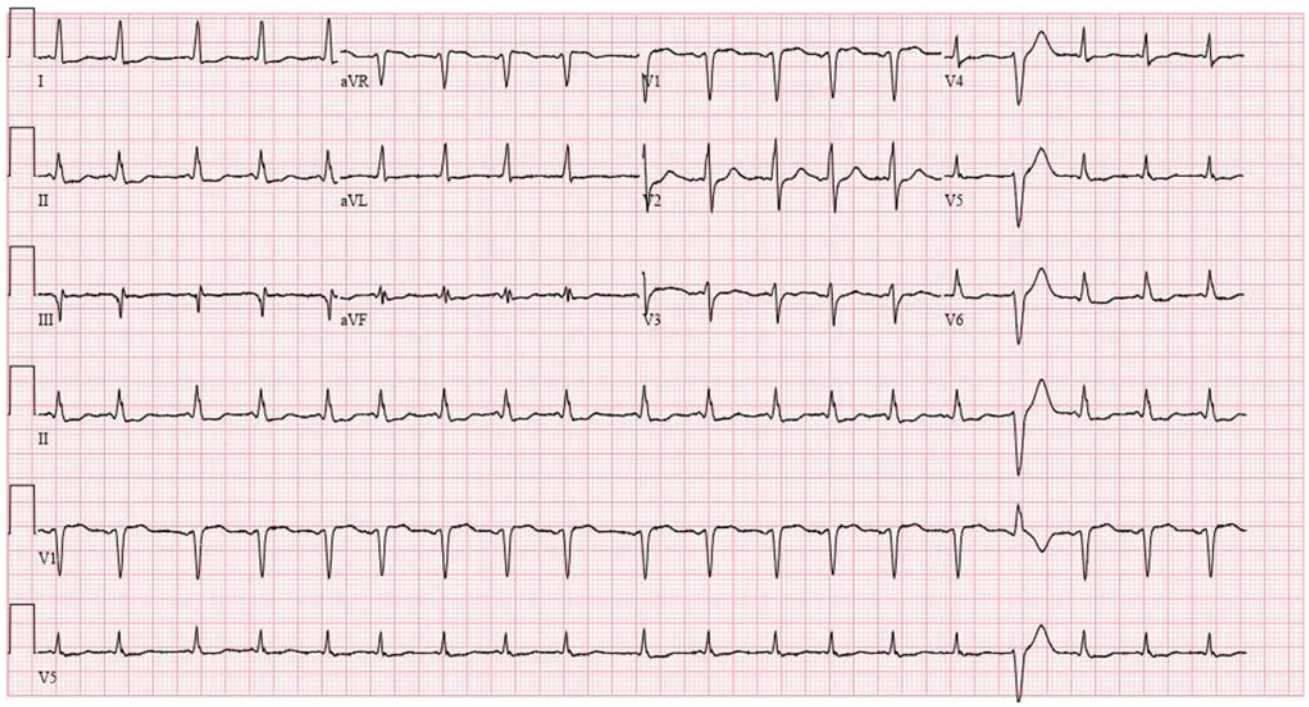

Fig. 15.12 Early postoperative EKG. P-waves are less evident. A junctional tachycardia is suspected

A postoperative echo continued to show left ventricular dysfunction (Fig. 15.15, Video 15.2). She developed bacteremia from multiple organisms, aspiration pneumonia, hematuria (remaining on heparin), and postoperative hypertension (treated with hydralazine). Her course was complicated by more overt congestive heart failure with a brain natriuretic peptide (BNP) exceeding 1100 pg/ml and congestion on chest X-ray requiring mechanical ventilation

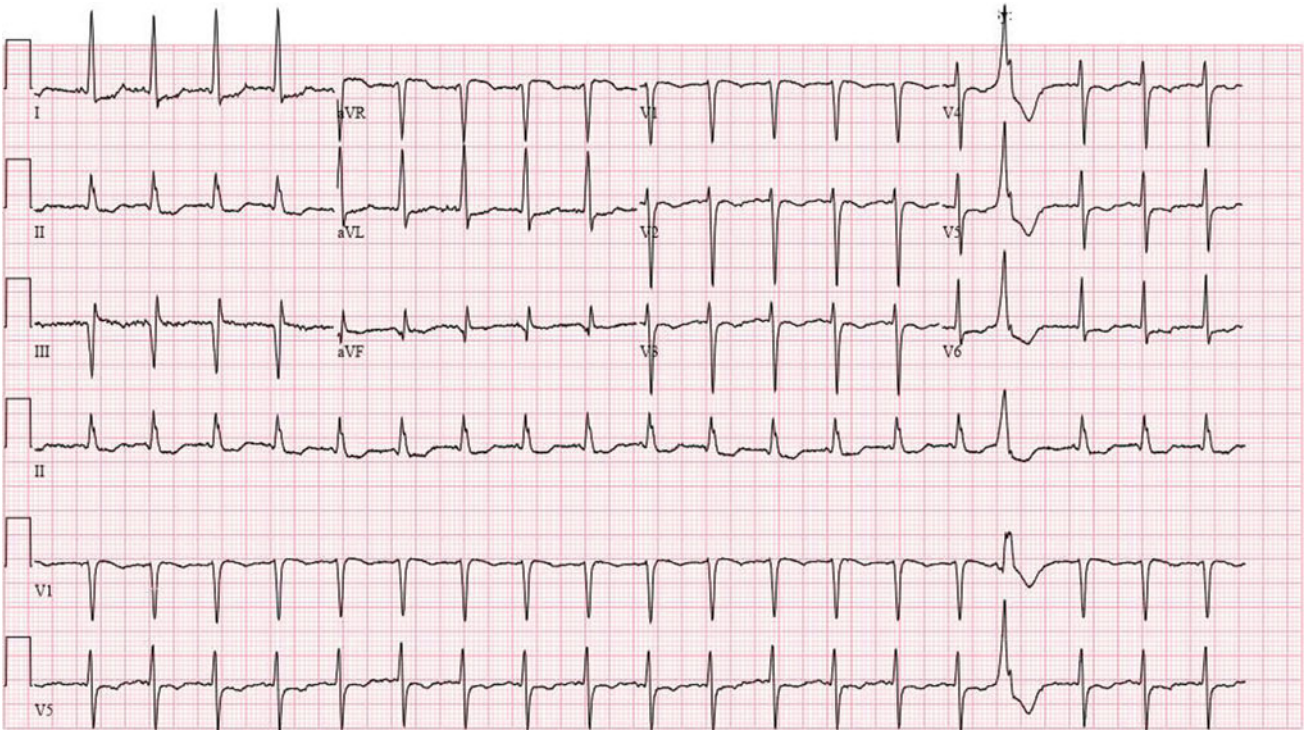

Fig. 15.13 Postoperative EKG. Atrial fibrillation is likely and ST depression is now more evident

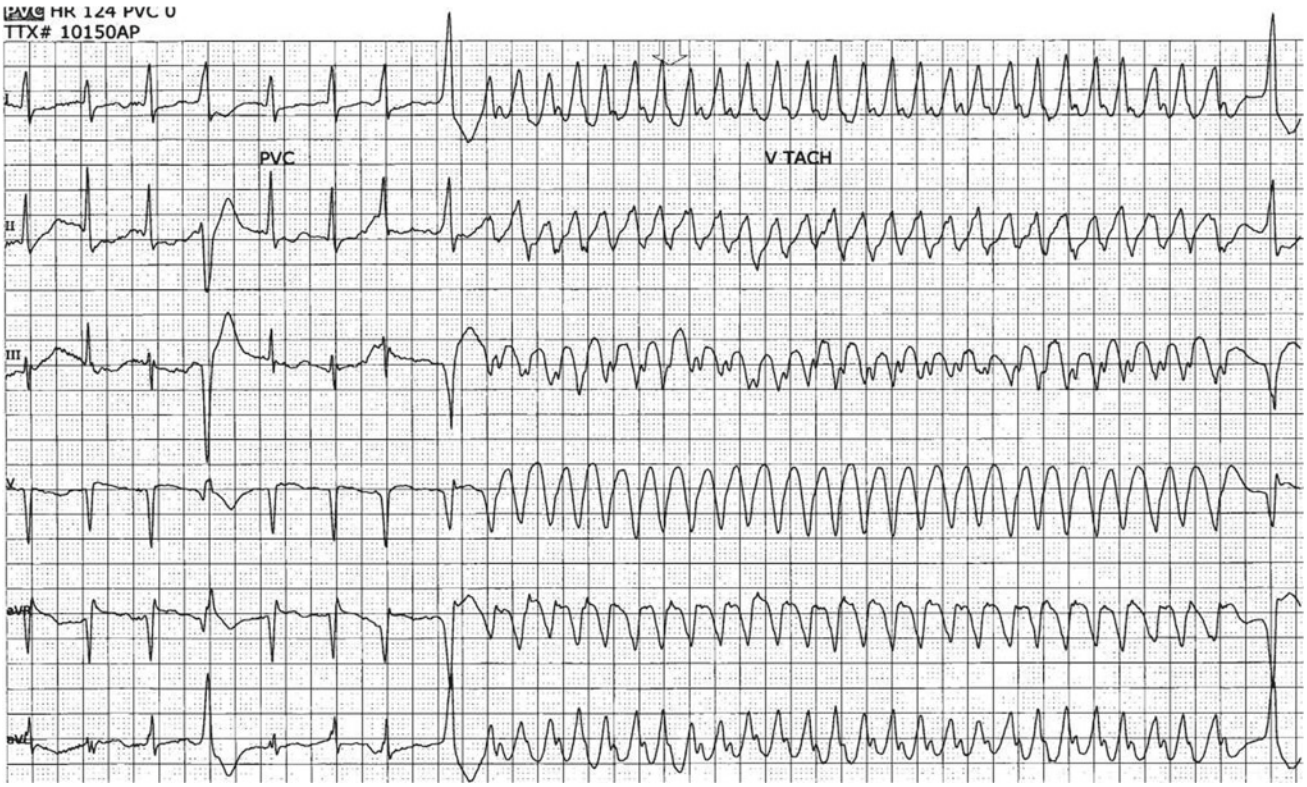

Fig. 15.14 Rhythm strips. An ectopic complex appears to initiate a run of wide complex (ventricular) tachycardia

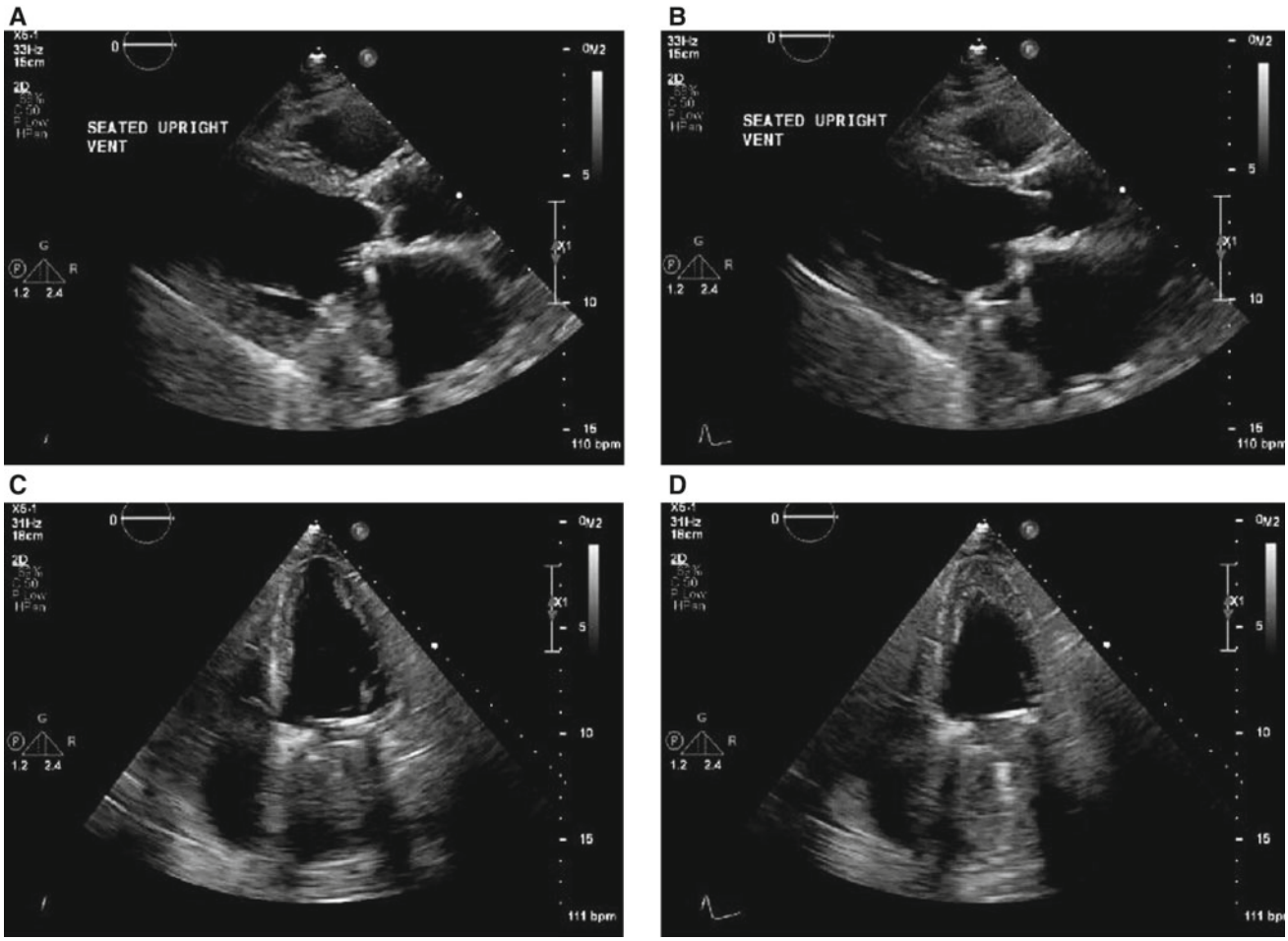

Fig. 15.15 Diastolic (**A**, **C**) and systolic (**B**, **D**) frames from parasternal long axis (top) and apical four-chamber (bottom) echocardiographic studies. There is moderate global hypokinesis of the left ventricle. Shadowing from the mitral valve prosthesis is seen

and further diuretics (Fig. 15.16). Warfarin was resumed. The patient was discharged home in atrial flutter with a controlled ventricular response.

This case illustrates the perioperative management of heart failure further complicating an extensive postoperative course in a patient with underlying left ventricular dysfunction and a prosthetic mitral valve. Heart failure developed in the context of both atrial and ventricular arrhythmias, possible ischemia or perioperative myocardial injury (an entity described separately in this chapter), sepsis, perioperative bleeding, and pneumonia. The diagnosis of heart failure in the presence of coexisting radiologic evidence of pneumonia was supported by the marked elevation in BNP. An attempt was made to maintain full anticoagulation throughout the perioperative period, because of the perceived high stroke risk from both atrial fibrillation and from her mechanical mitral prosthesis in the thrombogenic mitral position.

Although heart failure adversely affects most surgical outcomes [22], there are limited data on the management of heart failure in perioperative patients. Best practices should incorporate current heart failure guidelines set forth by the American College of Cardiology [23]; reviews of heart failure occurring in the perioperative period provide further insight [24–26]. Recognition of heart failure in the perioperative cancer patient may be challenging because, as is the case for perioperative ischemia, symptoms are often absent or vague. Signs such as tachypnea, tachycardia, hypoxemia, and pulmonary rales are nonspecific and there is an overlap of the key diagnostic features of heart failure with pneumonia and pulmonary embolism. The use of biomarkers such as BNP is limited by elevated values with other diagnoses. Preoperative BNP failed to predict perioperative heart failure in gastrointestinal cancer patients [27]. Simple clinical predictors may be more accurate. In head and neck cancer surgery patients, major cardiac events (especially heart failure) were predicted best by intravenous fluid and packed cell administration on the day of surgery [28], with heart failure occurring in 11% of patients who received >4L of fluids. It is important to recognize that venodilators

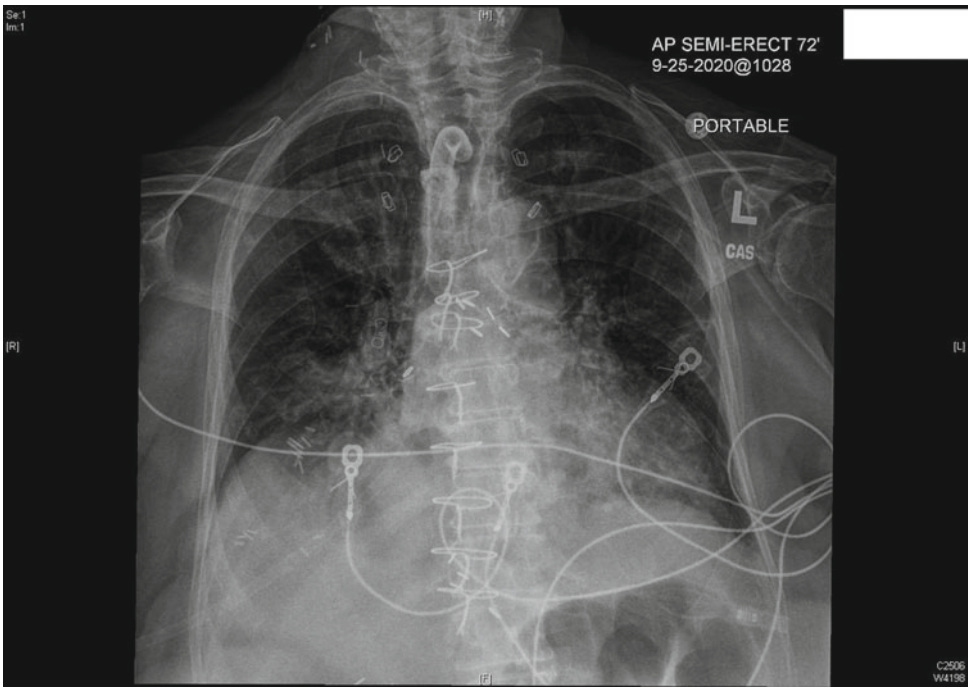

Fig. 15.16 Postoperative portable chest X-ray. Bilateral focal consolidations, pulmonary edema, and small bilateral pleural effusions are evident. Midline sternotomy wires are present from prior mitral valve replacement

continue to play a role in treating perioperative heart failure, and that standard heart failure therapies typically possess venodilating properties [29].

Perioperative diastolic heart failure is not uncommon and should be included in the differential when heart failure is suspected, particularly when its precipitants (anemia, hypoxemia, infection, tachycardia, non-sinus rhythms, extreme volume changes, myocardial ischemia, hypertension, and high sympathetic stimulation) are present [30].

References

1. Landesberg G. The pathophysiology of perioperative myocardial infarction: facts and perspectives. J Cardiothorac Vasc Anesth. 2003;17(1):90–100.
2. Landesberg G, Beattie WS, Mosseri M, Jaffe AS, Alpert JS. Perioperative myocardial infarction. Circulation. 2009;119 (22):2936–44.
3. Puelacher C, Lurati Buse G, Seeberger D, Sazgary L, Marbot S, Lampart A, et al. Perioperative myocardial injury after noncardiac surgery: incidence, mortality, and characterization. Circulation. 2018;137(12):1221–32.
4. Devereaux PJ, Xavier D, Pogue J, Guyatt G, Sigamani A, Garutti I, et al. Characteristics and short-term prognosis of perioperative myocardial infarction in patients undergoing noncardiac surgery: a cohort study. Ann Intern Med. 2011;154(8):523–8.
5. Janssen-Heijnen ML, Szerencsi K, van de Schans SA, Maas HA, Widdershoven JW, Coebergh JW. Cancer patients with cardiovascular disease have survival rates comparable to cancer patients within the age-cohort of 10 years older without cardiovascular morbidity. Crit Rev Oncol Hematol. 2010;76(3):196–207.
6. Roffi M, Patrono C, Collet JP, Mueller C, Valgimigli M, Andreotti F, et al. 2015 ESC guidelines for the management of acute coronary syndromes in patients presenting without persistent ST-segment elevation: task force for the management of acute coronary syndromes in patients presenting without persistent ST-segment elevation of the European Society of Cardiology (ESC). Eur Heart J. 2016;37(3):267–315.
7. Ekeloef S, Alamili M, Devereaux PJ, Gogenur I. Troponin elevations after non-cardiac, non-vascular surgery are predictive of major adverse cardiac events and mortality: a systematic review and meta-analysis. Br J Anaesth. 2016;117(5):559–68.
8. Devereaux PJ, Goldman L, Yusuf S, Gilbert K, Leslie K, Guyatt GH. Surveillance and prevention of major perioperative ischemic cardiac events in patients undergoing noncardiac surgery: a review. CMAJ. 2005;173(7):779–88.
9. Mandawat A, Newby LK. High-sensitivity troponin in noncardiac surgery: pandora's box or opportunity for precision perioperative care? Circulation. 2018;137(12):1233–5.
10. Camm AJ, Kirchhof P, Lip GY, Schotten U, Savelieva I, Ernst S, et al. Guidelines for the management of atrial fibrillation: the task force for the management of atrial fibrillation of the European Society of Cardiology (ESC). Europace. 2010;12(10):1360–420.
11. Farmakis D, Parissis J, Filippatos G. Insights into onco-cardiology: atrial fibrillation in cancer. J Am Coll Cardiol. 2014;63(10):945–53.
12. Lee AY. Deep vein thrombosis and cancer: survival, recurrence, and anticoagulant choices. Dis Mon. 2005;51(2–3):150–7.
13. Connolly SJ, Ezekowitz MD, Yusuf S, Eikelboom J, Oldgren J, Parekh A, et al. Dabigatran versus warfarin in patients with atrial fibrillation. N Engl J Med. 2009;361(12):1139–51.
14. Hu YF, Liu CJ, Chang PM, Tsao HM, Lin YJ, Chang SL, et al. Incident thromboembolism and heart failure associated with new-onset atrial fibrillation in cancer patients. Int J Cardiol. 2013;165(2):355–7.
15. Rostagno C, La Meir M, Gelsomino S, Ghilli L, Rossi A, Carone E, et al. Atrial fibrillation after cardiac surgery: incidence, risk factors, and economic burden. J Cardiothorac Vasc Anesth. 2010;24(6):952–8.
16. Walsh SR, Tang T, Gaunt ME, Schneider HJ. New arrhythmias after non-cardiothoracic surgery. BMJ. 2006;333(7571):715.

17. Riber LP, Christensen TD, Jensen HK, Hoejsgaard A, Pilegaard HK. Amiodarone significantly decreases atrial fibrillation in patients undergoing surgery for lung cancer. Ann Thorac Surg. 2012;94(2):339–44; discussion 45–6.
18. Higuchi S, Kabeya Y, Matsushita K, Arai N, Tachibana K, Tanaka R, et al. Perioperative atrial fibrillation in noncardiac surgeries for malignancies and one-year recurrence. Can J Cardiol. 2019;35(11):1449–56.
19. Lin MH, Kamel H, Singer DE, Wu YL, Lee M, Ovbiagele B. Perioperative/postoperative atrial fibrillation and risk of subsequent stroke and/or mortality. Stroke. 2019;50(6):1364–71.
20. Radaelli F, Fuccio L, Paggi S, Bono CD, Dumonceau JM, Dentali F. What gastroenterologists should know about direct oral anticoagulants. Dig Liver Dis. 2020;52(10):1115–25.
21. Crossley GH, Poole JE, Rozner MA, Asirvatham SJ, Cheng A, Chung MK, et al. The Heart Rhythm Society (HRS)/American Society of Anesthesiologists (ASA) expert consensus statement on the perioperative management of patients with implantable defibrillators, pacemakers and arrhythmia monitors: facilities and patient management this document was developed as a joint project with the American Society of Anesthesiologists (ASA), and in collaboration with the American Heart Association (AHA), and the Society of Thoracic Surgeons (STS). Heart Rhythm. 2011;8(7):1114–54.
22. Turrentine FE, Sohn MW, Jones RS. Congestive heart failure and noncardiac operations: risk of serious morbidity, readmission, reoperation, and mortality. J Am Coll Surg. 2016;222(6):1220–9.
23. Yancy CW, Jessup M, Bozkurt B, Butler J, Casey DE Jr, Colvin MM, et al. 2017 ACC/AHA/HFSA focused update of the 2013 ACCF/AHA guideline for the management of heart failure: a report of the American college of cardiology/American heart association task force on clinical practice guidelines and the heart failure society of America. Circulation. 2017;136(6):e137–61.
24. Henes J, Rosenberger P. Systolic heart failure: diagnosis and therapy. Curr Opin Anaesthesiol. 2016;29(1):55–60.
25. Smit-Fun V, Buhre WF. The patient with chronic heart failure undergoing surgery. Curr Opin Anaesthesiol. 2016;29(3):391–6.
26. Soussi S, Chatti K, Mebazaa A. Management of perioperative heart failure. Curr Opin Anaesthesiol. 2014;27(2):140–5.
27. Ishiguro T, Gyouda Y, Yoshizawa A, Arakawa K. BNP measurement for perioperative management. Masui. 2009;58(5):604–8.
28. Haapio E, Kinnunen I, Airaksinen JK, Irjala H, Kiviniemi T. Excessive intravenous fluid therapy in head and neck cancer surgery. Head Neck. 2017;39(1):37–41.
29. Valchanov KP, Arrowsmith JE. The role of venodilators in the perioperative management of heart failure. Eur J Anaesthesiol. 2012;29(3):121–8.
30. Ryu T, Song SY. Perioperative management of left ventricular diastolic dysfunction and heart failure: an anesthesiologist's perspective. Korean J Anesthesiol. 2017;70(1):3–12.

Masses Involving the Heart and Vasculature

16

Anna Plitt, Jonathan W. Weinsaft, and Angel T. Chan

Key Points

- Sarcoma, melanoma, lymphoma, lung and breast cancers most commonly metastasize to the heart.
- Thrombi can occur as isolated masses (i.e., bland thrombus), or be superimposed complications of cardiac metastases (i.e., tumor-thrombus).
- Some neoplasms can be treated via targeted anti-cancer therapies.
- Thrombus can often be resolved with anticoagulation.
- Cardiac magnetic resonance imaging (CMR) can identify cardiac masses based on tissue characteristics.

16.1 Introduction

Nearly 17 million people in the U.S. are living with cancer [1]—survivorship has markedly improved in the past decades, highlighting the importance of effective strategies to surveil cancer complications in this population. Cancer patients are at risk for developing cardiac masses, including primary or metastatic neoplasm as well as thrombus. Primary cardiac neoplasms are rare, whereas autopsy studies of patients with advanced (stage IV) systemic cancer have identified cardiac metastases in up to 20% of patients [2–6]. Tumors that most commonly metastasize to the heart include sarcoma, melanoma, lymphoma, lung and breast cancers [4, 7]. For example, in a consecutive series of 18,751 subjects undergoing autopsy, lung (39%) and breast (10%) cancers , and lymphoma (10%) were the leading primary neoplasms responsible for cardiac involvement [8]. However, cardiac metastases can occur with cancers not typically associated with cardiac involvement, as evidenced by recent cross-sectional studies by our group for which tumors such as thyroid, central nervous system, and hepatic malignancies had metastasized to the heart [2, 5].

Cardiac metastases may be clinically silent, or result in symptoms such as dyspnea, chest pain, or palpitations [9]. Neoplasm location can impact clinical presentation: metastases with intramyocardial invasion may result in ischemia or infarction with elevated cardiac biomarkers (e.g., troponin): ECG manifestations can range from non-specific repolarization changes to localized ST segment elevation (due to coronary invasion) [10]. Cardiac conduction system involvement can result in ventricular or atrial arrhythmias as well as heart block [11]. Metastases with prominent cardiac chamber involvement can produce symptoms due to mass effect, including hemodynamic compromise due to impaired cardiac filling, contractile or valve dysfunction, pulmonary embolism in cases of right-sided tumor involvement, and cerebrovascular or peripheral embolic events in cases of left-sided tumor involvement [12].

Systemic neoplasms can metastasize to the heart via four mechanisms: (1) direct extension, (2) retrograde extension (lymphatic spread), (3) hematogenous spread, or (4) transvenous extension (via the inferior vena cava or pulmonary veins). Direct extension to the heart or pericardium is associated with lung carcinomas and primary mediastinal tumors such as thymoma. Retrograde extension via lymphatics is a common pathway for carcinomas that frequently spread to the pulmonary hilar or mediastinal lymph nodes. Hematogenous spread is the typical route by which melanoma, sarcomas, leukemia, and renal cell

Electronic supplementary material
The online version of this chapter (https://doi.org/10.1007/978-3-030-70998-3_16) contains supplementary terial, which is available to authorized users.

A. Plitt · A. T. Chan (✉)
Department of Medicine, Memorial Sloan Kettering Cancer Center, 1275 York Avenue, New York, NY 10065, USA
e-mail: Chana5@mskcc.org

A. Plitt
e-mail: plitta@mskcc.org

J. W. Weinsaft
Department of Medicine, Weill Cornell Medicine, Cardiology Service, 525 East 68th Street, New York, NY 10021, USA

R. M. Steingart et al. (eds.), *Atlas of Imaging in Cardio-Oncology*,
https://doi.org/10.1007/978-3-030-70998-3_16

carcinoma metastasize to the heart. Transvenous extension can occur via inferior vena cava spread to the right side of the heart (commonly associated with renal cell cancer), or the pulmonary veins to the left side of the heart (i.e., with primary or metastatic lung tumors). Thrombi can occur as isolated masses (i.e., bland thrombus), or be superimposed complications of cardiac metastases (i.e., tumor-thrombus). Thrombogenesis can occur in cancer patients due to upregulation of systemic hematologic coagulation pathways, stasis, or foreign hardware such as indwelling central venous catheters commonly placed in advanced cancer patients [13].

Accurate identification of cardiac neoplasms and thrombi is of critical importance to guide therapeutic decision-making and prognostic risk stratification: some neoplasms can be treated via targeted anti-cancer therapies, whereas thrombus can often be resolved with prompt, effective anticoagulation. However, cardiac masses can be challenging to identify on conventional imaging such as echocardiography as neoplasm and thrombus can appear similar to one another. Furthermore, cases of mural thrombus or intramyocardial neoplasm can be challenging to distinguish from surrounding myocardium. Whereas both types of cardiac masses can have similar morphology, neoplasm requires vascular supply for tumorigenesis whereas thrombus is intrinsically avascular. Cardiac magnetic resonance imaging (CMR) can identify cardiac masses based on tissue characteristics. Using the technique of late gadolinium enhancement (LGE), cardiac MRI differentiates neoplasm from thrombus based on presence or absence of vascularity as manifested by contrast enhancement [2, 5, 14–17]. In prior research by our group, the magnitude of contrast enhancement of cardiac masses has been shown to correlate with metabolic activity as established by FDG-PET, and incremental utility of LGE-CMR has been demonstrated for detection of thrombi or neoplasms with extensive tumor necrosis [3].

Cardiac masses impact morbidity, mortality, and therapeutic decisions for cancer patients. In a retrospective analysis of 330 cancer patients with cardiac masses (n = 190) and matched controls (n = 140), LGE-CMR detected cardiac neoplasms in 66% and thrombi in 34% of cases [18]. In these patients with cardiac masses, embolic events occurred in 20% with a median time of 1.3 months from MRI identification of the mass to the embolic event. Cumulative embolic events were threefold higher in patients with cardiac masses versus controls (20% vs. 7%, $p = 0.001$). As expected, embolic event type varied based on cardiac mass location: right-sided intracavitary lesions were associated with a threefold increase in pulmonary embolism (20% vs. 6%, $p = 0.02$) whereas left-sided lesions were associated with increased cerebrovascular events (18% vs. 7%, $p = 0.13$). In addition, cardiac masses identified as having an intracavitary location on MRI (25% vs. 7%, $p < 0.001$) or as being highly mobile (38% vs. 12%, $p = 0.001$) were associated with increased embolic event rates.

Prior studies by our group have also shown that differentiation between cardiac neoplasm and thrombus on cardiac MRI also provides utility with mortality risk prediction. Mortality risk was similar between patients with cardiac thrombi and control patients matched for cancer type and stage (hazard ratio [HR] = 0.82 [CI 0.35–1.89], $p = 0.64$) [2]. In contrast, cardiac metastasis was associated with more advanced disease and significantly higher mortality. Patients with cardiac metastasis showed increased mortality compared to patients with cardiac thrombi (HR 3.06 [CI = 1.84 – 5.1], $p < 0.001$) as well as matched controls (HR 2.08 [CI = 1.42 – 3.04], $p < 0.001$) during a median follow-up of 9.4 months [IQR 3.6–23.2] [2, 12]. Mortality differed in relation to tissue characteristics of cardiac metastasis. Patients with diffusely enhancing cardiac metastasis had near equivalent mortality to matched controls ($p = 0.55$), whereas prognosis was worse among patients with heterogeneously enhancing cardiac metastasis ($p < 0.001$)—including increased 6-month (46% vs. 23%) and 1-year (65% vs. 37%) mortality in respective case–control comparisons (both $p < 0.01$) [12]. In addition, the presence of a heterogeneously enhancing cardiac metastasis conferred higher risk for mortality (HR 2.37 [CI 1.49–3.77], $p < 0.001$) than the number of lesions (HR 1.62 [CI 1.27–2.07], $p < 0.001$) or lesion size (1.08 per 5 cm [CI 0.51–2.27], $p = 0.85$) suggesting increased vascularity and tumor hypoxia/necrosis are associated with aggressive tumors [12].

16.2 Cases 1.1 and 1.2: Cardiac MRI for Differentiating Right Atrial Tumor from Thrombus

Differentiating cardiac mass subtypes such as neoplasm versus thrombus is important for therapeutic decision-making.

- Cardiac MRI offers assessment of cardiac structure, morphology, location, and tissue characterization of cardiac masses.
- Cardiac MRI with long TI late gadolinium enhancement imaging enables neoplasm to be differentiated from thrombus based on the presence or absence of contrast enhancement: cardiac neoplasm enhances (due to vascular supply) whereas cardiac thrombus does not (due to avascularity).

16.2.1 Case 1.1

A 68-year-old woman with metastatic melanoma was referred to cardiology clinic for further evaluation of a cardiac mass. Oncologic history was notable for melanoma of right upper back and axillary lymph nodes diagnosed 4 years prior. The patient underwent complete resection and entered surveillance monitoring. She subsequently developed gastrointestinal bleeding and anemia and was noted to have recurrence of melanoma (gastric, lung, lymphatic metastases). Gastric lesions were cauterized and the patient began therapy with ipilimumab, cyclophosphamide, vincristine and dacarbazine, and a trial drug (ABT888 and bendamustine). Because of disease progression the trial drug was stopped and the patient had surveillance with cardiac MRI which showed normal bi-ventricular function as well as cardiac masses with heterogeneous contrast enhancement—consistent with neoplasm (Fig. 16.1, panel A; Video 16.1; panel A done without contrast shows the motion of the tumor). The patient was started on a clinical trial with immunotherapy but had progression of disease with brain metastasis and expired 4 months later.

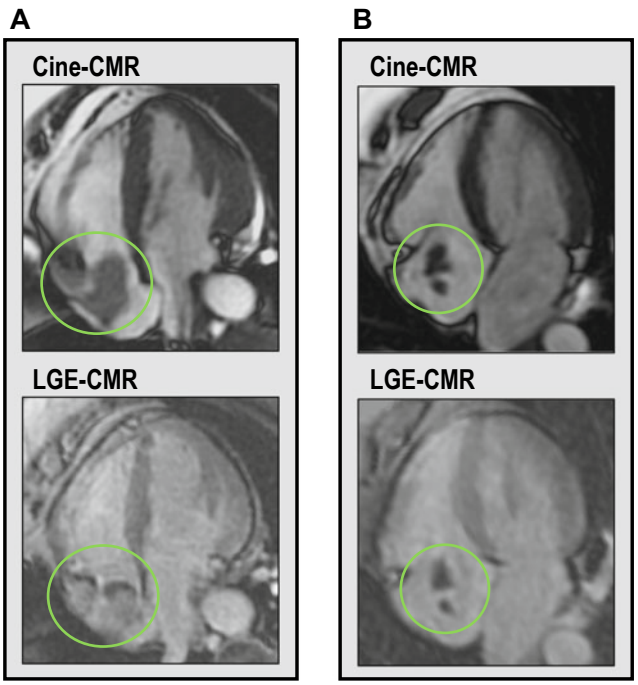

Fig. 16.1 Right atrial masses on cardiac MRI: **a** Still frames from cine-CMR showing tumor appearing as bilobed right atrial mass (top panel) with long inversion time (TI) on late gadolinium enhancement CMR (TI 600 ms) in bottom panel compared with thrombus **b** that has a similar appearance to tumor on upper panel cine-CMR but clearly showing no late gadolinium enhancement on lower panel. The mediport catheter tip associated with this thrombus was not seen on these MRI slices.

16.2.2 Case 1.2

A 43-year-old woman with stage IV adenocarcinoma of the breast with metastases to soft tissue, bone and liver treated with doxorubicin, pembrolizumab, and radiation therapy. The patient had a mediport placed 6 months earlier for chemotherapy administration. Echocardiogram showed normal cardiac function but there was a sessile echodensity attached to the lateral right atrial wall (1.6 × 1.0 cm). Cardiac MRI was ordered for tissue characterization of the cardiac mass and showed a mobile, ovoid-shaped lesion in the right atrium (2.0 × 0.8 cm) at the postero-lateral wall (Fig. 16.1b upper panel, Video 16.1 panel B). Some MRI slices (not shown) showed that the mass was near the mediport catheter tip. The mass demonstrated absence of contrast enhancement on cardiac MRI (Fig. 16.1b lower panel), consistent with thrombus. The patient was started on anticoagulation and a follow-up echocardiogram after 3 months of anticoagulation showed a reduction in size of the thrombus. Typically once a mass is recognized on echocardiography and characterized by MRI imaging, follow-up with echocardiography alone is sufficient.

16.3 Case 2. Neoplasm Invading Through Pulmonary Vein to Left Atrium

Systemic neoplasms can invade the heart via four mechanisms: (1) direct extension, (2) retrograde extension (lymphatic spread), (3) hematogenous spread, and (4) transvenous extension (via the inferior vena cava or pulmonary veins).

A 52-year-old woman with oncologic history notable for cervical cancer diagnosed 1.5 years prior to presentation. She underwent treatment with chemo/radiation therapy, and debulking total hysterectomy/bilateral salpingo-oophorectomy. She was found to have metastatic disease to the lungs 3 months prior to presentation and was subsequently started on a protocol consisting of durvalumab and tremelimumab, immunotherapy against PD-L1 and CTLA-4. She subsequently developed a recurrent right pleural effusion requiring pleur-x catheter drainage. Follow-up chest CT demonstrated a new right middle lobe mass infiltrating the right superior pulmonary vein and the left atrium, prompting urgent care evaluation. On presentation, physical exam was notable for decreased right-sided breath sounds. ECG demonstrated sinus rhythm without marked change in depolarization or repolarization pattern. She was admitted to the telemetry unit and cardiac MRI showed a mass (2.2 × 1.1 cm) in the right superior pulmonary vein and left atrium that demonstrated contrast enhancement, consistent with metastasis (Fig. 16.2, Video 16.2). Given the new malignant pleural effusion the chemotherapy regimen was adjusted to bevacizumab/carboplatin/taxol.

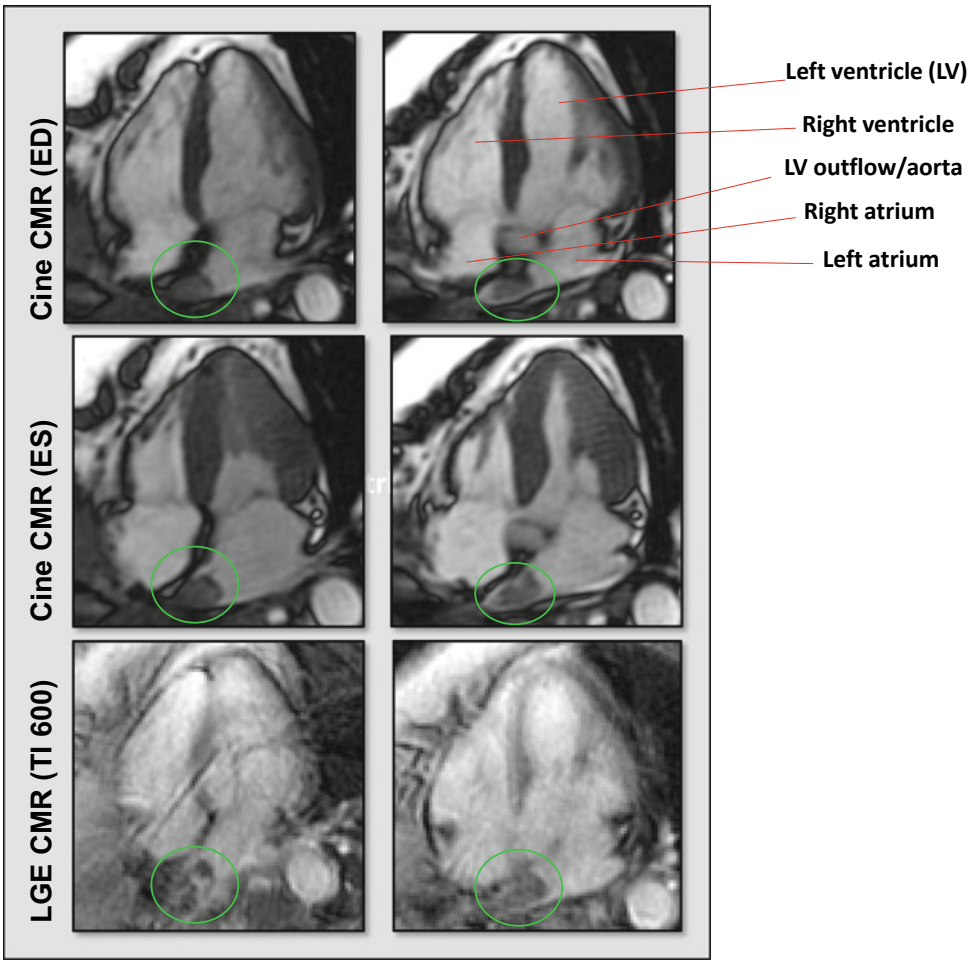

Fig. 16.2 Metastatic cervical cancer invading from pulmonary vein to the left atrium in four-chamber view (left) and five-chamber view (right). Still frame from cine-CMR showing cardiac mass (circled) in end diastolic (ED) and end systolic (ES) frames. Long TI LGE-CMR (TI 600 ms) showed heterogenous contrast enhancement pattern within the mass consistent with metastasis

16.4 Case 3. Primary Cardiac Neoplasm Progressing from Diffusely Enhancing to Mixed to Predominantly Avascular Neoplastic Mass

A 51-year-old male with no prior cardiac history presented with chest pain for 4 weeks. An echocardiogram showed a cardiac mass involving the superior pulmonary vein. The patient underwent an endoscopic robotic resection of the left atrial mass involving the superior pulmonary vein and the left atrial appendage with replacement of the mitral valve. Pathology demonstrated the mass to be a cardiac intimal sarcoma. Six months after initial surgery, cardiac MRI showed a small region of diffuse late gadolinium enhancement in mid-anterior left ventricular wall (Fig. 16.3, Video 16.3) suspicious for cancer recurrence. Subsequent cardiac MRI exams demonstrated progressive lesion growth; surgical resection and percutaneous ablation options were not deemed feasible. The sarcoma was found to have an MDM2 mutation and an MDM2 inhibitor was started without therapeutic response as evidenced by progressive lesion growth on serial MRI. Approximately 2.5 years after initial resection, perfusion MRI demonstrated increasing vessel tortuosity within the mass concerning for coronary fistula and/or aneurysm. Subsequent MRI exams demonstrated progressive lesion growth; post-contrast tissue characterization demonstrated progressive avascularity within central aspects of the mass (previously enhancing) consistent with new onset tumor necrosis. The patient was started on pazopanib and gemcitabine therapy. Approximately, 4 years after initial diagnosis, an MDM2 inhibitor was resumed, but the patient continued to have progression of disease prompting radiation and immunotherapy. One month after radiation therapy, he was admitted to an outside hospital for chest pain and anterior ST elevation myocardial infarction. Cardiac catheterization confirmed tumor compression of the LAD with sparing of RCA and LCx. There was a large aneurysm involving mid to distal LAD and a 95% stenosis of the mid to distal first diagonal branch. The patient had gastrointestinal (GI) bleeding and was not started on anticoagulation. A follow-up cardiac MRI showed moderately decreased LV and RV functions due to tumor adherence to pericardium.

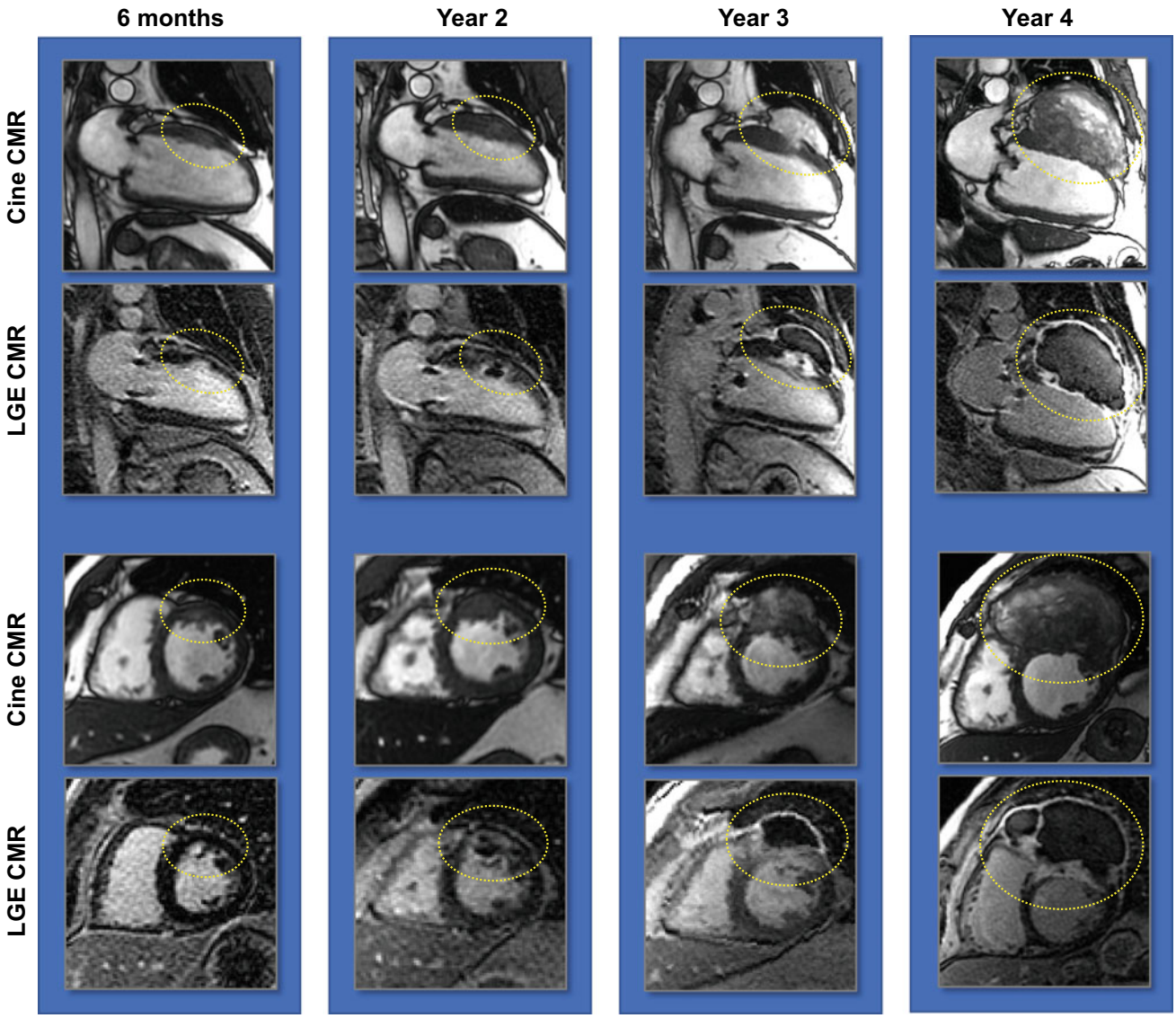

Fig. 16.3 Long-axis (top two panels) and short-axis (bottom two panels) frames from serial cardiac MRIs. Six months after resection of primary cardiac sarcoma from left atrium, with recurrence in the mid-anterior left ventricular wall showing increased T2 signal intensity on cine-CMR suggestive of increased edema (top) and a small subendocardial and mid-endocardial hyperenhancement (bottom) and both the long- and short-axis views. In year 2, left ventricular wall thickness increased at the mid-anterior region on frame from cine-CMR and heterogeneously enhanced on LGE-CMR. In year 3, the mid-anterior left ventricular wall mass further increased in size on cine-CMR. The lesion showed hyperenhancement in mid-anterior LV wall and increased peripheral hyperenhancement with central necrosis of the lesion. In year 4, the lesion further progressed as a very large primarily necrotic mass with peripheral rim of enhancement

16.5 Cases 4.1–4.3: MR/PET Comparison

Cardiac MRI and PET are the two most commonly used imaging modalities to detect and characterize cardiac neoplasms—^{18}FDG PET detects tumor metabolic activity whereas cardiac MRI detects tumor vascularity.

- Comparison between cardiac MRI and ^{18}FDG whole body PET showed a direct correlation between the degree of tumor vascularity and metabolic activity.
- Tumors with diffusely enhancing lesions on cardiac MRI showed high ^{18}FDG avidity on whole body PET whereas tumors with minimal contrast enhancement or thrombus lack FDG avidity.

16.5.1 Case 4.1

An 83-year-old man with non-Hodgkin's lymphoma diagnosed 9 years ago as a right paratracheal mass, biopsy

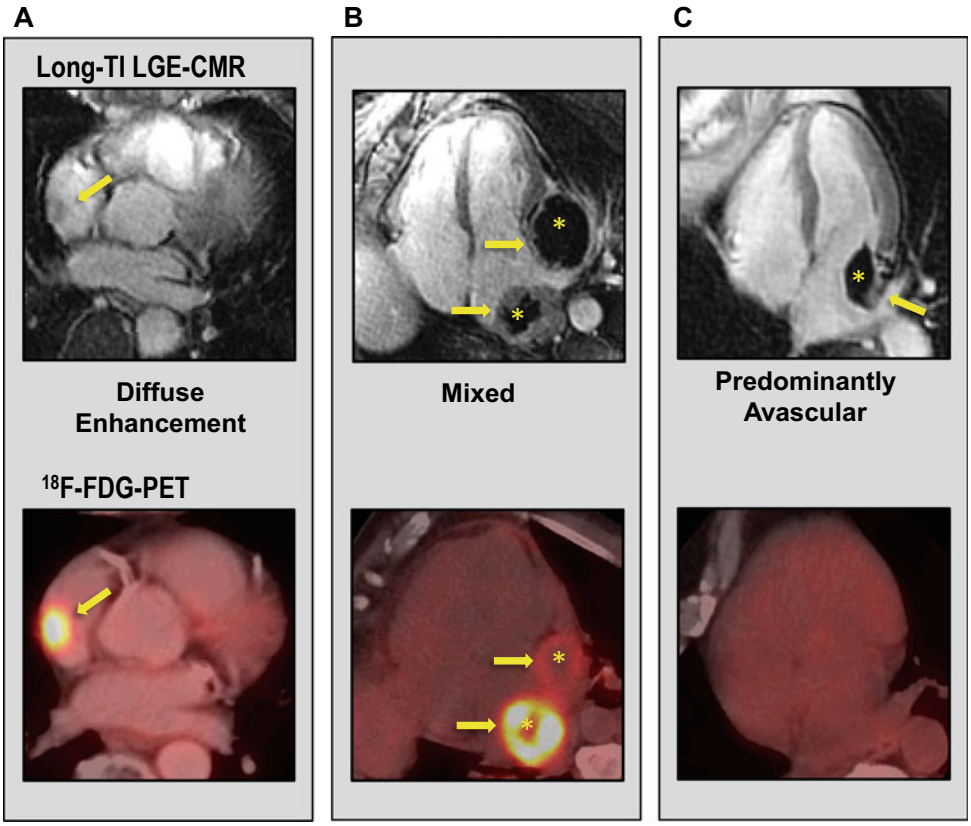

Fig. 16.4 Correlation between contrast cardiac MRI (top) and ^{18}F-FDG-PET (bottom): **a** diffusely enhancing right atrial neoplasm on cardiac MRI in a patient with non-Hodgkin's lymphoma and corresponding highly FDG avid mass on ^{18}F-FDG-PET (bottom). **b** Heterogeneously enhancing masses in left atrium and the pericardial space near left atrial-ventricular groove (MRI top) in a patient with metastatic non-small cell lung cancer and ^{18}F-FDG-PET (bottom) showing differential FDG avidity. **c** Predominantly avascular mass in left atrium near left atrial appendage on cardiac MRI (top) and non-FDG avid mass on PET (bottom) in a patient with angiosarcoma

confirmed as follicular lymphoma. He had received radiation to the right paratracheal region and mediastinum. He had multiple recurrences and received treatment with rituximab. A ^{18}F-FDG-PET for disease monitoring demonstrated increased splenic avidity as well as a new FDG avid mass either abutting or within the lateral wall of right atrium with SUV of ~13 (Fig. 16.4a). A follow-up cardiac MRI demonstrated a diffusely enhancing ovid neoplasm in the superior-posterior aspect of the right atrium (1.5 cm × 0.8 cm) at the orifice of the superior vena cava, corresponding to the FDG avid mass noted on PET (Fig. 16.4a). He received radiation therapy (24 Gy) to the right atrial mass followed by rituximab, gemcitabine, cyclophosphamide, vincristine, and dexamethasone (R-GCVP). A follow-up ^{18}F-FDG-PET showed complete remission. Unfortunately, the patient had additional recurrences with poor tolerance to treatments and thus treatment was discontinued. The patient expired 20 months later.

16.5.2 Case 4.2

A 78-year-old man with a history of poorly differentiated stage IV non-small cell lung cancer presented to cardiology clinic for further evaluation of an abnormal ECG. Oncologic history was notable for a newly identified large mediastinal mass and bilateral pulmonary nodules diagnosed during a hospital admission 3 weeks prior, at which time he had presented to the emergency room with atrial fibrillation and was found to have a loculated pericardial effusion and tamponade requiring pericardiocentesis. CT imaging revealed a mediastinal mass that was biopsied and interpreted as poorly differentiated non-small cell lung cancer. Treatment was initiated with carboplatin and pemetrexed. In clinic, exam was notable for 1 + pitting edema. Repeat echocardiogram revealed an echo dense mass adjacent to the left atrium and thus cardiac PET and MRI were pursued. MRI revealed a large, irregularly contoured mediastinal mass abutting the posterior and superior aspects of the left atrium and extending within the pericardium adjacent to the left ventricular basal mid-anterior and lateral walls with peripheral enhancement. PET demonstrated minimal FDG avidity in these regions (Fig. 16.4b). Due to rapid progression of the disease resulting in compression of the right main pulmonary artery, a repeat biopsy was done showing a poorly differentiated sarcomatoid pleomorphic malignant neoplasm and radiation therapy was started. The patient expired 4 months following the initial diagnosis.

16.5.3 Case 4.3

A 66-year-old man with HTN was diagnosed with metastatic angiosarcoma while undergoing workup for low back pain. Six months later in preparation for systemic chemotherapy, he underwent chest CT which demonstrated a pulmonary embolism, as well as a suspected left atrial mass. Cardiac MRI (for further characterization of the cardiac lesion) demonstrated a mass extending from the left atrial appendage to the lateral aspect of the left atrial chamber; post-contrast tissue characterization demonstrated prominent central hypoenhancement with minimal peripheral hyperenhancement consistent with poorly vascularized neoplasm. Follow-up cardiac MRI showed an increase in the size of the left atrial mass which continued to demonstrate minimal peripheral enhancement; FDG-PET imaging was indeterminant (Fig. 16.4c). Given its enhancement on MRI, the lesion was deemed consistent with metastatic intracardiac neoplasm. The patient's disease progressed despite multiple chemotherapy regimens and he expired 1.5 years after diagnosis.

16.6 Case 5. Mobile Metastasis at Aortic Valve Causing Discordance Between Cardiac MRI Contrast Enhancement and FDG Avidity on PET

Cardiac MRI showed better detection of highly mobile cardiac neoplasm.

A 52-year-old man underwent excision of a spindle cell sarcoma of the gastric and esophageal mucosa. On routine follow-up (10 months after initial diagnosis), he was noted to have a cardiac murmur which prompted an echocardiogram that showed a mass on the aortic valve. He underwent cardiac surgery with resection of the mass on the aortic valve confirmed as spindle cell sarcoma. Metastatic disease within 1 year of initial diagnosis suggested a highly aggressive tumor but the role of adjuvant therapy has not been well established in such cases. Ongoing frequent surveillance was pursued. On follow-up (at 24 months) a new adrenal nodule and small osseous sclerotic lesions were detected and the lesions were treated with radiation therapy and gemcytabine/docetaxel were begun. Cardiac MRI demonstrated an irregularly contoured mobile mass in the aortic root, which was partially adherent to the left coronary aortic valve cusp. Post-contrast tissue characterization of the mass demonstrated enhancement, consistent with neoplasm (Fig. 16.5). Video images show marked mobility of the mass associated with the aortic valve (Video 16.4). Treatment with doxorubicin and olaratumab was started, after which the patient developed a hemorrhagic stroke. He then underwent repeated surgical resection of the aortic valve mass. Pathology again revealed spindle cell carcinoma, prompting treatment with doxorubicin, ifosfamide, and mesna (AIM). Over the course of the following year, metastatic disease progressed despite multiple regimens of chemotherapy and radiation therapy. He expired approximately 3 years following the initial diagnosis.

16.7 Case 6. Highly Mobile Right Ventricular Neoplasm Causing Pulmonary Embolism

A 62-year-old man with myxofibrosarcoma presented with acute shortness of breath. Oncologic history was notable for initial diagnosis of right axillary myxofibrosarcoma 3 months prior to presentation. He underwent resection with negative margins but post-operatively was diagnosed with pulmonary emboli and was started on anticoagulation. Further workup revealed a right-sided pulmonary embolism as well as a right ventricular mass with severe right ventricular dilation and impaired systolic function. Surgical intervention was not deemed feasible, he was started on anticoagulation and transferred to our institution for further management of metastatic disease. His treatment regimen consisted of doxorubicin, ifosfamide, and mesna (AIM). Cardiac MRI demonstrated a large RV mass with RV hypokinesis (Fig. 16.6, Video 16.5). The patient subsequently developed high-grade myelodysplastic syndrome and was transferred to hospice care.

16.8 Case 7. Intra-Myocardial Mass with STEMI Presentation

A 59-year-old man with history of hypertension, diabetes mellitus, and metastatic hepatocellular carcinoma (HCC) who initially presented to urgent care with chief complaints of odynophagia, dysphagia, and shortness of breath. Oncologic history was notable for diagnosis of HCC 9 years prior to presentation with subsequent liver transplant 3 years after the initial diagnosis. He remained in remission for 5 years but subsequently developed metastases throughout the axial and appendicular skeleton. On cardiac MRI, the left ventricular inferior wall demonstrated asymmetric thickening with associated diffuse hyperenhancement (Fig. 16.7); decreased FDG uptake was present in this region on ^{18}F-FDG whole body PET. Cine CMR showed focal thickening of the inferior wall but preserved systolic function in a small cavity (Video 16.6). The patient underwent targeted radiation treatment and initiated treatment with a tyrosine kinase inhibitor (regorafenib). On admission, the patient was hemodynamically stable but uncomfortable appearing, and his cardiac exam revealed a grade IV/VI systolic murmur at the left upper sternal border. He was

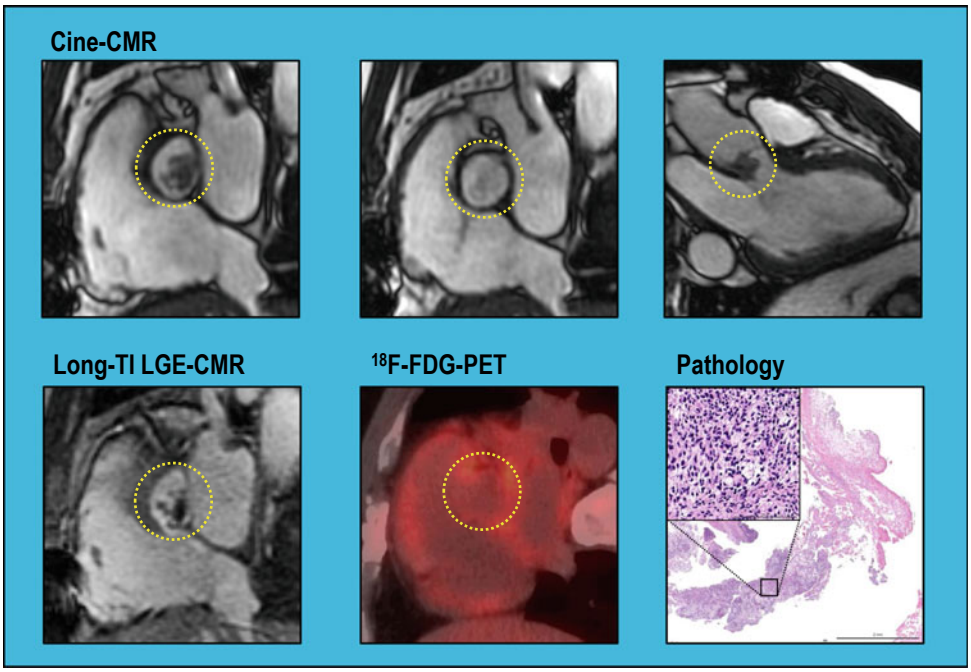

Fig. 16.5 Frames from cine-CMR, upper left at end diastole (ED), upper middle at end systole (ES) showing mobile mass on the ventricular side of the aortic valve with the valvular location best seen in the upper right image. Lower left image shows the mass to have heterogenous contrast uptake pattern consistent with a metastasis. The mass showed no FDG uptake on PET in the lower middle panel. Surgical pathology of aortic valve shown on the lower right panel confirmed spindle cell carcinoma

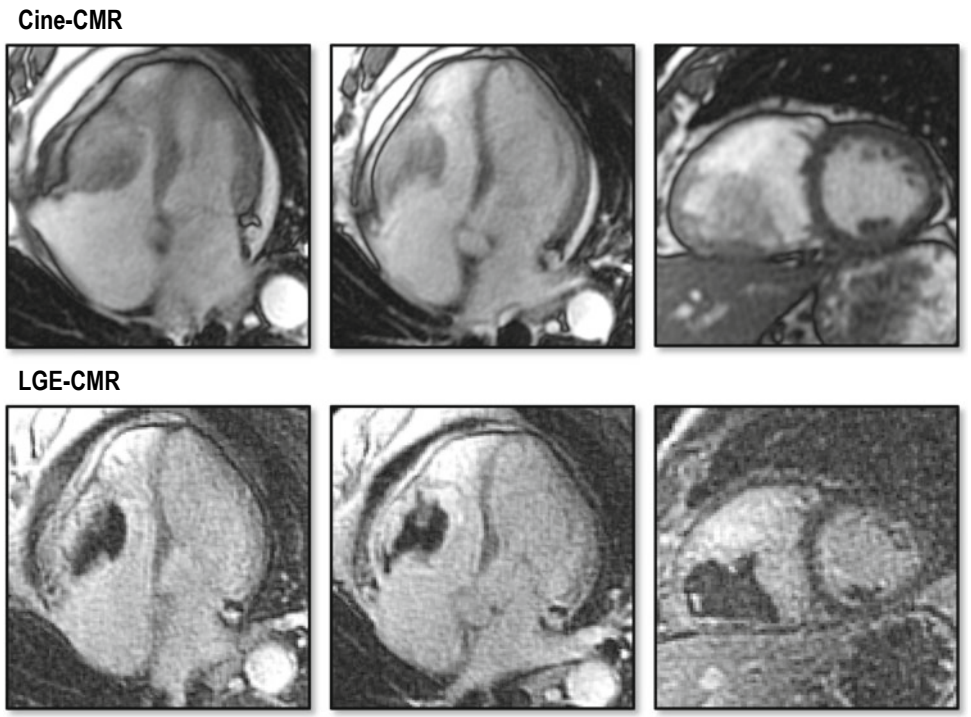

Fig. 16.6 Large right ventricular neoplasm with heterogenous contrast uptake on long TI LGE-CMR (TI 600 ms) consistent with metastasis in a patient with metastatic right axillary myxofibrosarcoma. Frames from cine-CMR (top), LGE-CMR (bottom). Four-chamber view (left), five-chamber view (middle), and mid chamber short-axis view (right)

started on empiric treatment for presumed esophagitis; however, the hospital course was complicated by progressive shortness of breath and lethargy. ECG showed inferior ST elevations (Fig. 16.8a). Troponin was elevated at 0.4 ng/mL (normal cutoff value <0.06 ng/ml). Repeated ECG showed resolution of the ST elevations and patient remained chest pain free. CT angiography revealed a large mass invading the inferior and inferoseptal left ventricular walls and encasing the right coronary artery (Fig. 16.8b). He was treated with beta blockers and pain control was achieved. He was continued on immunosuppressive therapy and ultimately discharged to home hospice.

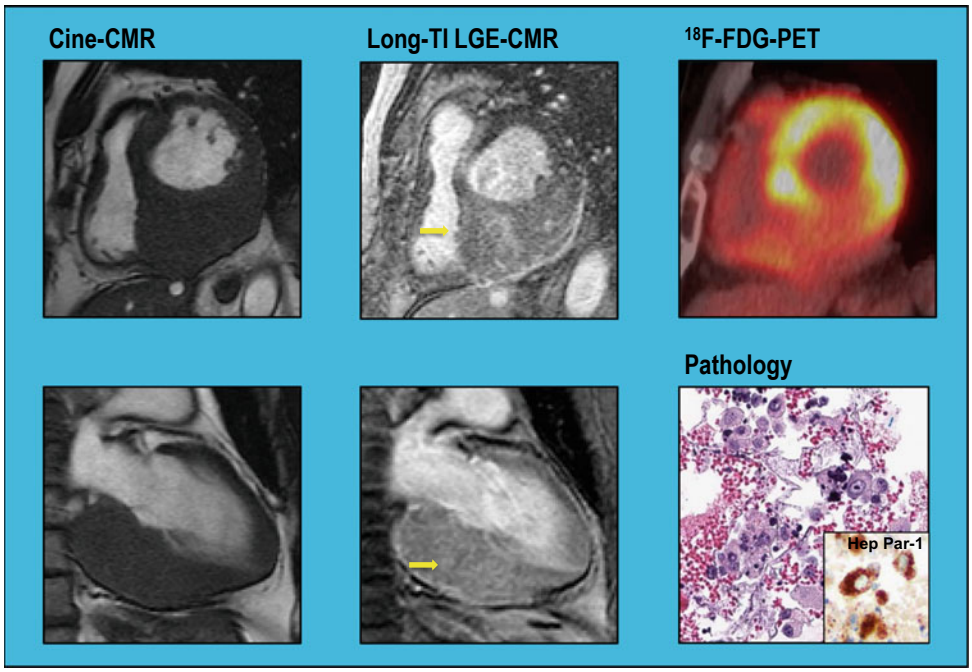

Fig. 16.7 Hepatocellular carcinoma metastasized to inferior wall of left ventricle with asymmetrical thickening of left ventricular wall shown in still frame cine-CMR short-axis image, top and long-axis image, bottom. This region showed diffuse enhancement on LGE-CMR in the middle panels (arrows). There was no FDG uptake in the mass as shown in the upper right panel. Pathology of lymph node biopsy in lower right image showed cells which were positive for Hep par-1 staining consistent with hepatocellular carcinoma

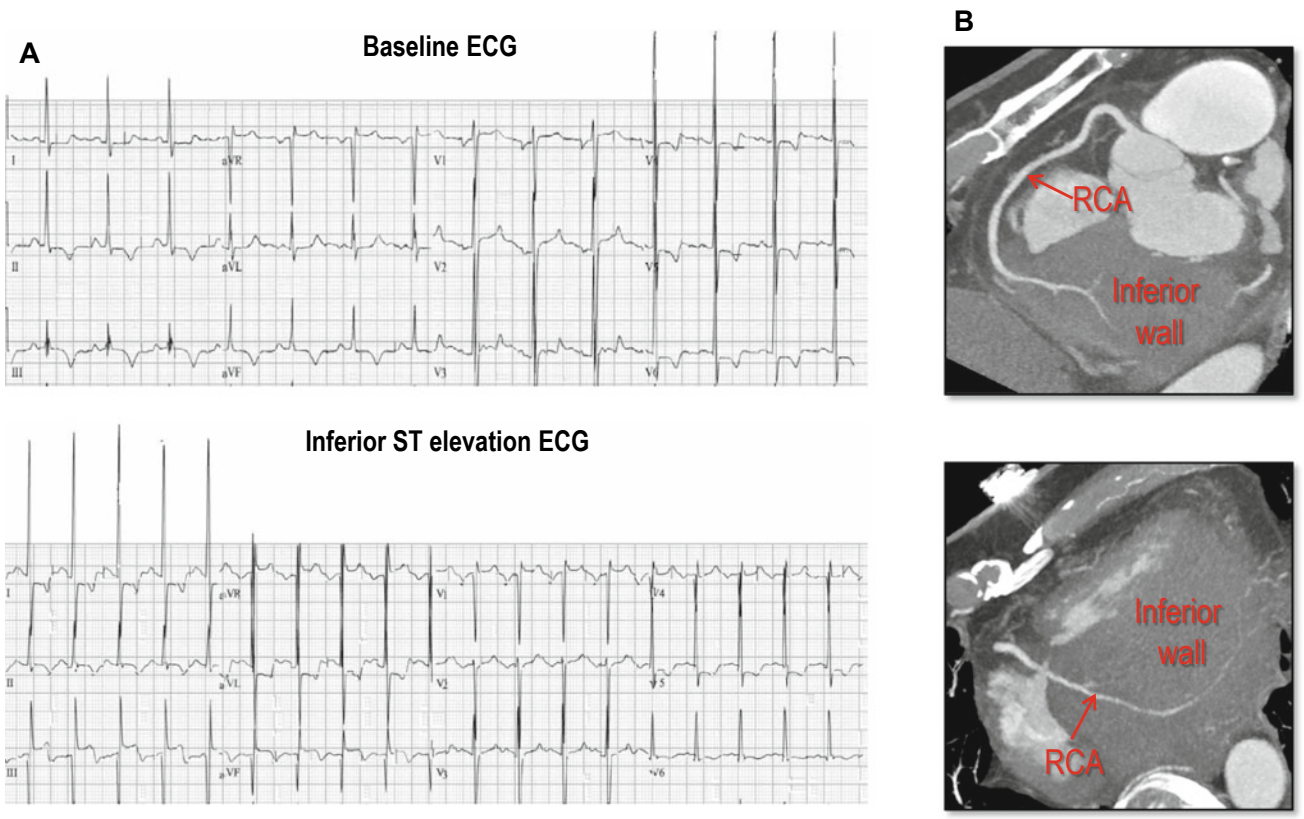

Fig. 16.8 **a** Baseline EKG with prominent voltage and diffuse t-wave inversions. Bottom panel: EKG with inferior ST elevation. **b** CT coronary angiogram showing the tumor encasing the right coronary artery (RCA)

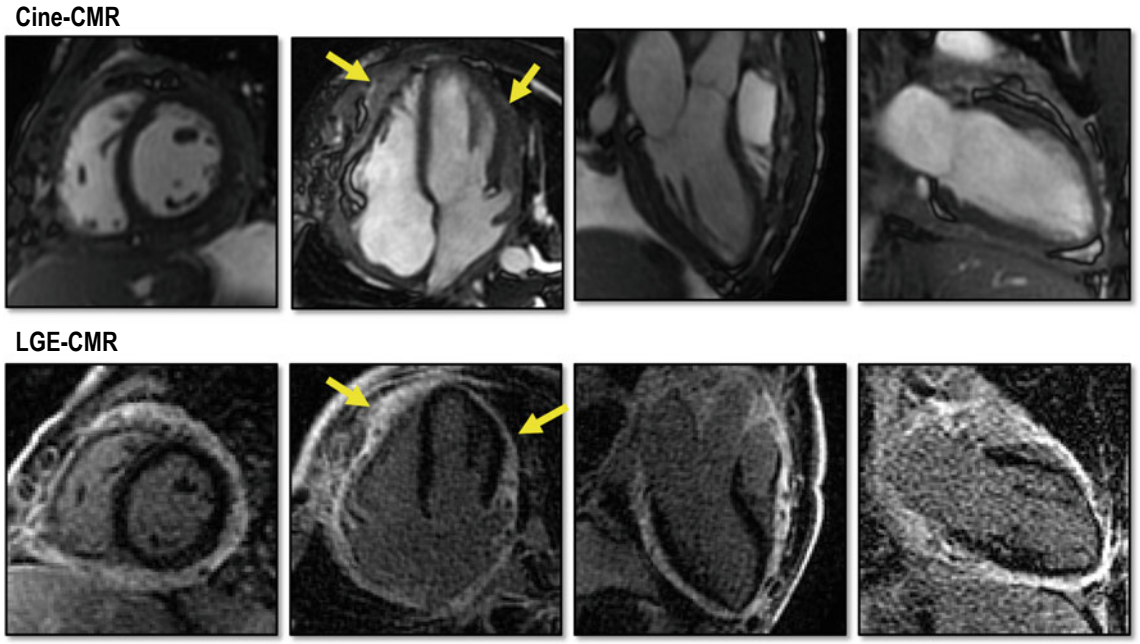

Fig. 16.9 Cardiac MRI in short-axis and long-axis views showing metastatic angiosarcoma presenting as thickened pericardium adherent to the left and right ventricles (arrows) on still images of cine-CMR studies and diffuse contrast uptake in the region of the pericardium (arrows) on LGE-CMR consistent with tumor invasion

16.9 Case 8. Pericardial Neoplasm Causing Constriction

A 22-year-old man with cardiac angiosarcoma metastatic to lungs presented to urgent care with the chief complaint of chest pain and shortness of breath. Oncologic history was notable for diagnosis of cardiac angiosarcoma 4 months prior to presentation confirmed by biopsy. Due to recurrent pericarditis with pericardial effusions, the patient had undergone a pericardial window operation and was treated with doxorubicin and ifosfamide. Cardiac MRI demonstrated circumferential thickening and diffuse late gadolinium enhancement of the pericardium extending to the superior and the inferior vena cavae consistent with metastatic neoplasm (Fig. 16.9). Physical exam was notable for lower extremity edema and mild abdominal distention. Labs were notable for mild troponin elevation (peak 0.89 ng/mL). ECG demonstrated sinus tachycardia with right axis deviation. Chest X-ray showed bibasilar consolidations with increased pleural effusions. The patient was treated with antibiotics; a pericardial catheter was placed which yielded serosanguinous drainage. Repeated cardiac MRI demonstrated a thickened pericardium with decreased bi-ventricular function (LVEF 50% RVEF 39%), with imaging features (prominent septal bounce) concerning for constrictive physiology (Video 16.7). On hospital, on day 6, patient developed hypoxemic respiratory failure and expired.

References

1. Caspar T, El Ghannudi S, Ohana M, Labani A, Lawson A, Ohlmann P, Morel O, De Mathelin M, Roy C, Gangi A, Germain P. Magnetic resonance evaluation of cardiac thrombi and masses by T1 and T2 mapping: an observational study. Int J Cardiovasc Imaging. 2017;33:551–9.
2. Chan AT, Plodkowski AJ, Pun SC, Lakhman Y, Halpenny DF, Kim J, Goldburg SR, Matasar MJ, Moskowitz CS, Gupta D, Steingart R, Weinsaft JW. Prognostic utility of differential tissue characterization of cardiac neoplasm and thrombus via late gadolinium enhancement cardiovascular magnetic resonance among patients with advanced systemic cancer. J Cardiovasc Magn Reson. 2017;19:76.
3. Chan AT, Fox J, Perez Johnston R, Kim J, Brouwer LR, Grizzard J, Kim RJ, Matasar M, Shia J, Moskowitz CS, Steingart R, Weinsaft JW. Late gadolinium enhancement cardiac magnetic resonance tissue characterization for cancer-associated cardiac masses: metabolic and prognostic manifestations in relation to whole-body positron emission tomography. J Am Heart Assoc. 2019;8:e011709.
4. Lam KY, Dickens P, Chan AC. Tumors of the heart. A 20-year experience with a review of 12,485 consecutive autopsies. Archives of pathology & laboratory medicine. 1993;117:1027–31.
5. Pun SC, Plodkowski A, Matasar MJ, Lakhman Y, Halpenny DF, Gupta D, Moskowitz C, Kim J, Steingart R, Weinsaft JW. Pattern and prognostic implications of cardiac metastases among patients with advanced systemic cancer assessed with cardiac magnetic resonance imaging. J Am Heart Assoc. 2016;5.
6. Verso M, Agnelli G. Venous thromboembolism associated with long-term use of central venous catheters in cancer patients. J Clin Oncol Off J Am Soc Clin Oncol. 2003;21:3665–75.
7. Klatt EC, Heitz DR. Cardiac metastases. Cancer. 1990;65:1456–9.

8. Bussani R, De-Giorgio F, Abbate A, Silvestri F. Cardiac metastases. J Clin Pathol. 2007;60:27–34.
9. Yusuf SW, Bathina JD, Qureshi S, Kaynak HE, Banchs J, Trent JC, Ravi V, Daher IN, Swafford J. Cardiac tumors in a tertiary care cancer hospital: clinical features, echocardiographic findings, treatment and outcomes. Heart Int. 2012;7:e4.
10. Wilson SR, Leonard JP, Geyer JT, Osborne JR, Weinsaft JW. A Worrisome interventricular septum. J Am Coll Cardiol. 2011;58:e43.
11. Subramanyam P, Mahmood SS, Dinsfriend W, Pastore RD, Martin P, Chan AT, Weinsaft JW, Cheung JW. Infiltrative lymphoma-associated bradycardia and cardiac conduction abnormalities. JACC CardioOncol. 2020;2:135.
12. Chan AT, Dinsfriend W, Kim J, et al. Risk stratification of cardiac metastases using late gadolinium enhancement cardiovascular magnetic resonance: prognostic impact of hypo-enhancement evidenced tumor avascularity. Journal of Cardiovascular Magnetic Resonance 2021;23:42.
13. Plodkowski AJ, Chan A, Gupta D, Lakhman Y, Kukar N, Kim J, Perez-Johnston R, Ginsberg MS, Steingart RM, Weinsaft JW. Diagnostic utility and clinical implication of late gadolinium enhancement cardiac magnetic resonance for detection of catheter associated right atrial thrombus. Clin Imaging. 2020;62:17–22.
14. Fussen S, De Boeck BWL, Zellweger MJ, Bremerich J, Goetschalckx K, Zuber M, Buser PT. Cardiovascular magnetic resonance imaging for diagnosis and clinical management of suspected cardiac masses and tumours. Eur Heart J. 2011;32:1551–60.
15. Pazos-Lopez P, Pozo E, Siqueira ME, Garcia-Lunar I, Cham M, Jacobi A, Macaluso F, Fuster V, Narula J, Sanz J. Value of CMR for the differential diagnosis of cardiac masses. JACC Cardiovasc Imaging. 2014;7:896–905.
16. Gomes AS, Lois JF, Child JS, Brown K, Batra P. Cardiac tumors and thrombus: evaluation with MR imaging. Am J Roentgenol. 1987;149:895–9.
17. Mousavi N, Cheezum Michael K, Aghayev A, Padera R, Vita T, Steigner M, Hulten E, Bittencourt S, Dorbala S, Di Carli MF, Kwong Y, Dunne R, Blankstein R. Assessment of cardiac masses by cardiac magnetic resonance imaging: histological correlation and clinical outcomes. J Am Heart Assoc. 2019;8:e007829.
18. Chan AT, Dinsfield W, Steingart R, Weinsaft JW. Prognostic utility of differential contrast-enhancement patterns on late gadolinium enhancement cardiac MRI (LGE-CMR) in patients with cancer-associated cardiac masses. European Society of Cardiology Congress 2020; Amsterdam, Netherland.

Carcinoid Heart Disease

17

Darwin F. Yeung, Sushil Allen Luis, and Heidi M. Connolly

17.1 Introduction

Neuroendocrine tumors are rare neoplasms that predominantly originate from the gastrointestinal tract. They secrete vasoactive substances that produce the constellation of flushing, diarrhea, and bronchospasm known as carcinoid syndrome. These substances cause plaque-like deposits to form on endocardial surfaces resulting in predominantly right-sided valve abnormalities that represent the hallmark feature of carcinoid heart disease. Echocardiography is the imaging modality of choice to assess the degree of cardiac involvement. Advances in diagnostic imaging, medical therapies, and interventional techniques have contributed to a decline in incidence of carcinoid heart disease and improved outcomes.

17.2 Epidemiology

Carcinoid heart disease was first described in the 1950s [1]. Since then, the incidence of neuroendocrine tumors has increased from ~1 per 100,000 in 1973 to ~7 per 100,000 in 2012 [2]. Among patients with neuroendocrine tumors, approximately 20% exhibit features of carcinoid syndrome [3]. Of these patients, 50–70% demonstrate echocardiographic evidence of carcinoid heart disease, although the prevalence may be closer to 20% in recent years due to more timely medical treatment [4, 5].

17.3 Pathophysiology

Neuroendocrine tumors can originate in any part of the body but most commonly occur in the gastrointestinal and respiratory tracts [6]. The tumors themselves grow slowly but secrete up to 40 different vasoactive products including 5-hydroxytryptamine (5-HT, serotonin) and tachykinins. Tumors that release these vasoactive substances often occur in the midgut (distal duodenum to proximal colon) and infrequently in the foregut (distal esophagus to proximal duodenum and lungs) and hindgut (distal colon) [7].

Carcinoid heart disease results in part from the plaque-like deposition of these substances onto the endocardial surfaces of valves, subvalvular apparatus, and cardiac chambers, as well as onto the intimal layer of great vessels [6]. Patients with more significant cardiac disease have higher levels of tachykinins and serotonin metabolites [4]. The histopathological abnormalities are similar to those caused by anorectic drugs and ergot derivatives, which act on serotonin receptors [8, 9].

17.4 Clinical Manifestations

Neuroendocrine tumors are generally slow-growing and thus rarely produce symptoms related to mass effects. Instead, clinical manifestations of the disease primarily result from the vasoactive substances that they produce. While patients with non-functioning tumors might be asymptomatic, those with functioning tumors demonstrate the characteristic symptoms of carcinoid syndrome including flushing, diarrhea, and bronchospasm [10].

In addition, patients with right-sided heart valve abnormalities may develop symptoms of right heart failure

Electronic supplementary material
The online version of this chapter (https://doi.org/10.1007/978-3-030-70998-3_17) contains supplementary material, which is available to authorized users.

D. F. Yeung (✉)
Department of Medicine, Division of Cardiology, University of British Columbia, Vancouver, British Columbia, Canada
e-mail: darwin.yeung@ubc.ca

S. A. Luis · H. M. Connolly
Department of Cardiovascular Medicine, Mayo Clinic, Rochester, Minnesota, United States
e-mail: luis.s@mayo.edu

H. M. Connolly
e-mail: connolly.heidi@mayo.edu

R. M. Steingart et al. (eds.), *Atlas of Imaging in Cardio-Oncology*, https://doi.org/10.1007/978-3-030-70998-3_17

including fatigue, dyspnea, and edema. Physical examination may reveal ascites, edema, pleural effusion, a parasternal lift due to right ventricular (RV) enlargement, a systolic murmur of tricuspid regurgitation (TR) along the left lower sternal border that augments with inspiration, and an elevated jugular venous pressure with a prominent V wave due to severe TR [11].

17.5 Diagnosis

17.5.1 Biomarkers of Neuroendocrine Tumors and Carcinoid Heart Disease

5-hydroxyindoleacetic acid (5-HIAA) is a by-product of serotonin metabolism. A 24-h urinary 5-HIAA has a 70% sensitivity and a 90% specificity for the diagnosis of well-differentiated neuroendocrine tumors, with a > 90% specificity for midgut tumors, which are more likely to secrete serotonin [7]. Serum 5-HIAA can be used as a convenient alternative [7, 11]. Increased 5-HIAA levels are associated with progression of carcinoid heart disease and increased mortality [12].

Chromogranin A (CgA) is a glycoprotein that is secreted by most neuroendocrine tumors and therefore serves as a general biomarker of both functioning and non-functioning tumors [7]. CgA has been shown to have a 100% sensitivity but only 30% specificity in predicting carcinoid heart disease [11]. In contrast, it demonstrates a relatively high specificity in identifying metastatic disease [7]. It is therefore mainly used in follow-up to assess recurrence or progression of disease.

Among patients with known neuroendocrine tumors, N-terminal pro-brain natriuretic peptide (NT-proBNP) represents the most effective biomarker to detect the presence of carcinoid heart disease [11]. Its high negative predictive value makes it effective in ruling out cardiac involvement [5].

17.5.2 Multimodality Imaging for the Assessment of Carcinoid Heart Disease

Two-dimensional transthoracic echocardiography with Doppler is the imaging modality of choice for the evaluation of patients with suspected or known carcinoid heart disease (Table 17.1).

Other echocardiographic techniques can refine the assessment. Administration of agitated saline facilitates the detection of a right-to-left inter-atrial shunt. Transesophageal echocardiography offers better visualization of the atrial septum and valves. Three-dimensional echocardiography provides en face views of valves that can help with surgical planning [13]. Myocardial deformation (strain) analysis identifies subclinical cardiac chamber impairment.

Ancillary imaging modalities such as cardiac computed tomography (CT) and magnetic resonance imaging (MRI) provide high-resolution images of cardiac structures that may have been challenging to define on echocardiography.

17.5.2.1 Valvular Heart Disease

The hallmark feature of carcinoid heart disease is the development of thickened, retracted, and fixed valve leaflets resulting in regurgitation, stenosis, or both. The tricuspid valve is involved in over 90%, the pulmonary valve in ~70% of cases, and the mitral and aortic valves < 30% of the time [13]. TR is the most common valve lesion. The degree of regurgitation and stenosis can be estimated in qualitative, semi-quantitative, and quantitative terms using various Doppler techniques [14, 15].

Table 17.1 Echocardiographic assessment of carcinoid heart disease

- Valve abnormalities
  - Valves are thickened, retracted, and fixed resulting in regurgitation, stenosis, or both
  - Right-sided valves (tricuspid > pulmonic) are predominantly involved
  - Left-sided valves (mitral > aortic) are sometimes involved but usually in the setting of an inter-atrial shunt, or high tumor burden
  - Following operative intervention, prosthetic valve function is assessed
- Cardiac chamber remodeling and dysfunction
  - Right-sided chamber enlargement usually develops along with eventual systolic and diastolic dysfunction in response to progressive right-sided valve disease
  - Left-sided chamber abnormalities can occur with left-sided valve disease
- Inter-atrial shunt such as a patent foramen ovale or atrial septal defect
  - Right-to-left shunting can predispose patients to hypoxemia or left-sided valve disease
  - Atrial septum should be assessed by color Doppler and agitated saline in all patients
- Pericardial disease
  - Pericardial effusions are often small and infrequently hemodynamically significant
  - Constrictive pericarditis occurs rarely, most often after cardiac surgical intervention
- Metastatic carcinoid tumors that infiltrate the myocardium are uncommon

Right-sided valves are more commonly affected than left-sided valves as vasoactive substances are thought to be metabolized in the lungs. Left-sided valve disease has been associated with an inter-atrial shunt and high tumor burden. Bronchopulmonary carcinoid tumors do not cause left-sided valve disease in the absence of liver metastases or a patent foramen ovale [16].

17.5.2.2 Cardiac Chamber Remodeling and Dysfunction

The ventricles dilate in response to chronic volume overload from significant regurgitation and hypertrophy in response to chronic pressure overload from significant downstream stenosis. In either case, ventricular dysfunction eventually develops. Similarly, atrial dilatation occurs due to downstream valve stenosis or regurgitation, or ventricular impairment.

Right-sided chamber enlargement and dysfunction often occur in patients with carcinoid heart disease due to progressive right-sided valve disease. Similar left-sided chamber abnormalities can occur in the presence of significant left-sided valve disease.

Impairment in RV function and valvular dysfunction can eventually lead to right-sided heart failure. In the future, identification of subclinical chamber impairment by strain imaging may play a more prominent role in risk-stratifying patients to determine the optimal timing of intervention [17].

Several echocardiographic scoring systems have been developed, which grade the severity of carcinoid heart disease based on right-sided valve leaflet mobility and thickness, valvular regurgitation or stenosis, and ventricular size and function [18]. These scoring systems correlate with NT-pro-BNP and serum 5-HIAA, and can be used to follow disease progression.

17.5.2.3 Atrial Level Shunt

The presence of an inter-atrial shunt such as a patent foramen ovale (PFO) or an atrial septal defect has important implications in carcinoid heart disease. In the setting of elevated right atrial (RA) pressure due to right-sided heart disease, significant right-to-left shunting can result in cyanosis and hypoxemia which can occur at rest or with activity and contribute to symptoms [19]. Furthermore, a right-to-left shunt increases the likelihood of left-sided valve disease as vasoactive substances enter the left side of the heart without being metabolized by the lungs [20]. The atrial septum should therefore be carefully interrogated by color Doppler and agitated saline in all patients with carcinoid tumors.

17.5.2.4 Pericardial Disease

Metastatic lesions within the pericardium are rare [21]. In contrast, pericardial effusions were found in 14% of patients with carcinoid heart disease in one cohort [22]. These effusions are generally small and rarely hemodynamically significant although large effusions requiring intervention have been reported [21, 22]. Constrictive pericarditis is similarly uncommon [23].

17.5.2.5 Metastatic Carcinoid Tumor Infiltration of the Myocardium

Myocardial metastases were found in approximately 4% of patients in one series [22]. In rare instances, the tumor may represent the only manifestation of carcinoid heart disease [24]. These tumors can generally be visualized by echocardiography if they are at least 1.0 cm in size; smaller lesions are more likely to be visualized by cardiac CT or MRI.

17.6 Management

The management of patients with carcinoid heart disease involves a multi-pronged approach that combines medical treatment with surgical intervention to reduce morbidity and mortality. This is accomplished by reducing tumor burden, lowering vasoactive substance levels, managing valvular heart disease, and treating symptoms caused by vasoactive substances or heart failure.

17.6.1 Medical Management

Somatostatin analogs such as octreotide represent the cornerstone of treatment for carcinoid syndrome. These medications reduce symptoms, lower vasoactive substance levels, and delay disease progression [25]. They may also be responsible for the decline in incidence of carcinoid heart disease among patients with neuroendocrine tumors and carcinoid syndrome [5].

Second-line therapies for refractory symptoms include: interferon alpha [26], the mTOR inhibitor everolimus [27], the serotonin synthesis inhibitor telotristat [28], and peptide receptor radionuclide therapy such as 177-Lutetium dotatate or 90-Yttrium edotreotide [29].

Medications to treat right-sided heart failure are limited to diuretics, which may provide temporary relief of edema but may also reduce cardiac output and worsen fatigue without altering the course of carcinoid heart disease.

17.6.2 Surgical Management

Surgical resection of the primary tumor can be considered depending on its size, location, pathologic grade, metastatic spread, patient comorbidities, and effect on adjacent structures [30].

In patients with metastatic disease to the liver, further reduction in tumor burden can be achieved by hepatic

resection or transcatheter arterial embolization [31]. Reducing the tumor burden in the liver can delay disease progression and may improve survival but does not cause regression of carcinoid heart disease.

Although severe carcinoid heart disease previously represented a contraindication to hepatic resection, valve replacement has been found to reduce the complications of excessive bleeding caused by elevated right-sided pressure and is now recommended prior to the procedure [32].

Surgical valve replacement remains the only treatment with mortality benefit for symptomatic carcinoid heart disease. Surgery is generally indicated when valve lesions become severe and symptomatic. When all four valves are severely diseased, quadruple valve replacement can be performed [33].

Bioprosthetic valves are generally preferred over mechanical valves for right-sided valves since they have a lower risk of thrombosis and generally do not require indefinite anticoagulation. Therapies that lower vasoactive substance levels should be optimized prior to operation to reduce disease recurrence.

Closure of an inter-atrial shunt should be performed at the time of cardiac surgery in the absence of contraindications to prevent left-sided valve disease [20]. Rarely, percutaneous closure of an inter-atrial shunt is performed for symptomatic desaturation in a patient with valve disease that does not yet meet indications for operative intervention.

Anesthetic agents and surgical manipulation can stimulate the release of vasoactive substances and precipitate a life-threatening carcinoid crisis characterized by hypotension, arrhythmias, and bronchospasm. Adequate perioperative control of carcinoid syndrome including treatment with octreotide infusion is recommended [34]. The perioperative management is best facilitated by a multidisciplinary care team.

17.7 Outcomes

The prognosis of carcinoid heart disease has been improving over time [35]. The median survival of patients with established carcinoid heart disease has increased from 1.5 years in the early 1980s to 4.4 years by the late 1990s.

Valve intervention before the presence of advanced cardiac symptoms has demonstrated increasingly favorable outcomes. This may have contributed to this improvement in survival [35–37]. Short-term mortality post-cardiac surgery decreased from 29% in the mid-1980s to 5% in the mid-2000s [36]. Perioperative mortality is associated with older age, worse functional class, cytotoxic chemotherapy, tobacco use, and chronic kidney disease [36, 37].

Prosthetic valve thrombosis is an increasingly recognized postoperative complication that has been found to occur even in bioprosthetic valves implanted in the tricuspid position [37]. Consensus guidelines therefore recommend anticoagulation for 3 to 6 months following valve replacement and surveillance echocardiography after stopping anticoagulation [11].

17.8 Case 1

Case summary. This is a classic case of carcinoid heart disease.

- A baseline cardiac assessment including echocardiography is recommended in all patients with carcinoid tumors who have symptoms or signs of cardiac disease, elevated NT-proBNP, or in those being referred for hepatic resection. The hallmark features of carcinoid heart disease include thickened, retracted, and fixed right-sided valves with corresponding right-sided chamber enlargement.
- Medications that lower vasoactive substance levels could theoretically delay the progression of carcinoid heart disease but have not been demonstrated to cause regression of established disease. Valve replacement is the only effective treatment for severe valve disease. To avoid perioperative and prosthetic valve risks, cardiac surgery is generally deferred until the onset of heart failure or RV systolic dysfunction.
- Careful inspection of the atrial septum must be performed by color Doppler and agitated saline during the baseline echocardiogram. In this case, a PFO was not detected on the transthoracic study but found intra-operatively. A PFO should be closed at the time of surgery to reduce the risk of developing left-sided valve disease.

A 52-year-old man presented with abdominal pain, nausea, and vomiting. An exploratory laparotomy revealed small bowel tumors that were resected and found to be of neuroendocrine origin. Postoperatively, elevated 5-HIAA levels along with symptoms of carcinoid syndrome suggested the presence of residual disease although there was no metastatic spread to the liver or lungs. A somatostatin analog was initiated. Echocardiogram showed thickened right-sided valves, moderate TR, severe pulmonary regurgitation (PR), right-sided chamber enlargement, and preserved RV systolic function. He remained asymptomatic from a cardiac perspective until 12 years later when he developed worsening dyspnea, edema, and ascites. Repeated echocardiography showed an increase in TR compared to baseline (Fig. 17.1, Videos 17.1–17.7). Given the onset of heart failure, he

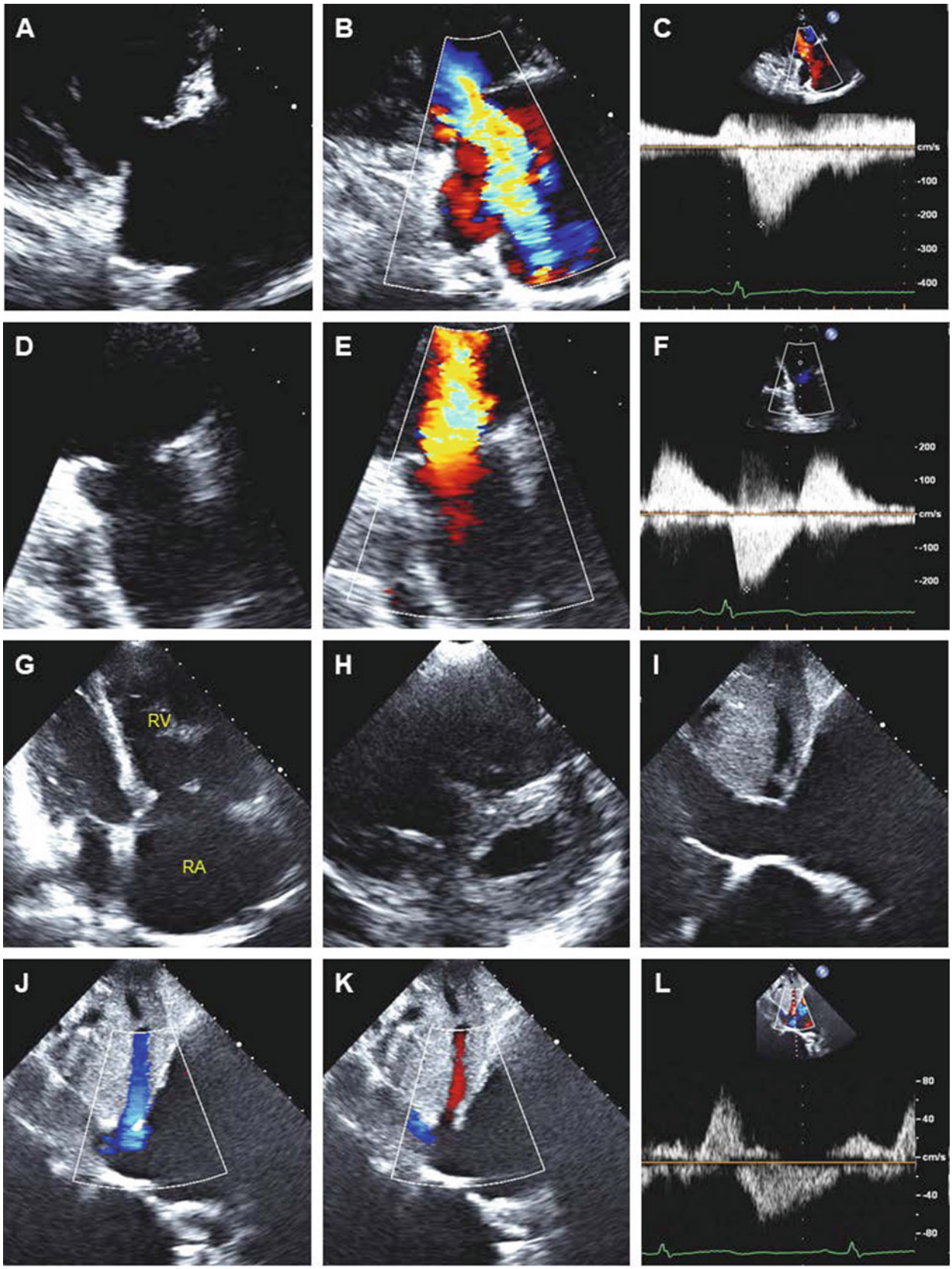
A
B
C
cm/s
-100
-200
-300
-400
D
E
F
200
100
cm/s
-100
-200
G
RV
RA
H
I
J
K
L
80
40
cm/s
-40
-80

◀ **Fig. 17.1** Classic echocardiographic-Doppler findings of carcinoid heart disease. The tricuspid valve is thickened, retracted, and fixed with a wide coaptation gap (**A**) resulting in severe TR suggested by color Doppler (**B**) and by the dense, triangular-shaped continuous wave (CW) Doppler profile during systole (**C**). The pulmonary valve has a similar morphology with cusp thickening (**D**) with severe PR evidenced by color Doppler (**E**) and by the CW profile during diastole (**F**). Chronic volume overload from severe TR and PR causes severe RA and RV enlargement in this para-apical two-dimensional image (**G**) and septal flattening during diastole noted on short-axis imaging (**H**). The dilated inferior vena cava with minimal collapse on inspiration suggests elevated RA pressure (**I**). Color Doppler of the hepatic vein shows normal forward flow (in blue) during diastole (**J**) and abnormal flow reversal (in red) during systole (**K**), which is also captured by pulsed wave (PW) Doppler (**L**), indicating severe TR

underwent tricuspid and pulmonary valve replacement. A PFO was found intra-operatively and surgically closed. The patient survived another 4 years with no significant cardiac issues.

17.9 Case 2

Case summary. This is a case of a patient with neuroendocrine ovarian tumors who developed carcinoid heart disease of all four valves requiring quadruple valve replacement.

- Patients with ovarian neuroendocrine tumors without hepatic metastasis often develop carcinoid heart disease since vasoactive products released from the ovaries bypass the liver and avoid being metabolized. Resection of tumors confined to the ovaries could be curative and halt progression of carcinoid heart disease.
- Carcinoid heart disease predominantly affects the right-sided heart valves but can similarly involve the left-sided heart valves, particularly in the presence of an inter-atrial shunt or extensive tumor burden. Nevertheless, significant left-sided valve disease can still occur without these conditions, as in this case.
- Carcinoid heart disease represents a rare circumstance in which all four valves are severely diseased. Quadruple valve replacement is occasionally performed with reasonable outcomes.

A 68-year-old woman presented with abdominal pain, diarrhea, and flushing. She eventually underwent a small bowel resection and total abdominal hysterectomy with bilateral salpingo-oophorectomy for well-differentiated neuroendocrine tumors within the small bowel and ovaries. There was regional spread but no hepatic or pulmonary metastases. She was post-operatively treated with a somatostatin analog. Three months later, she developed rapidly progressive dyspnea, orthopnea, and edema requiring hospitalization. Echocardiography revealed thickening and restriction of all four valves with moderate TR, severe PR, moderate–severe mitral regurgitation (MR), and moderate–severe aortic regurgitation (AR) (Fig. 17.2, Videos 17.8–17.15). All cardiac chambers were enlarged with low normal biventricular systolic function. No inter-atrial shunt was identified. Given the presence of significant valve disease causing decompensated heart failure, she underwent a quadruple valve replacement. The gross appearance of the valves and the histopathologic findings were consistent with carcinoid heart disease (Fig. 17.3). She was discharged in stable condition within 10 days and survived another 2 years after surgery.

17.9.1 Case 3

Case summary. This is a complex case of a patient with carcinoid heart disease who experienced hypoxemia related to significant right-to-left inter-atrial shunting, symptomatic severe right-sided valve disease, and bioprosthetic valve obstruction due to possible thrombus.

- Dyspnea, cyanosis, and hypoxemia represent an uncommon presentation of carcinoid heart disease related to right-to-left shunting through a PFO. Patients describe a pattern of dyspnea that worsens from a supine to standing position known as orthodeoxia-platypnea, which is thought to be a result of mechanical deformation of the atrial septum or right atrium.
- Transcatheter valve-in-valve replacement was not available at the time but now represents a potential option to manage bioprosthetic valve dysfunction in contemporary practice.
- Prosthetic valve obstruction related to thrombus is an increasingly recognized complication following valve replacement in patients with carcinoid heart disease. In addition to indefinite antiplatelet therapy, warfarin anticoagulation is now recommended for 3 to 6 months following valve replacement with a bioprosthetic valve. Periodic reassessment of prosthetic valve function is advised after stopping anticoagulation. Re-initiation of warfarin is suggested if prosthesis function deteriorates as a result of suspected thrombosis [13].

64-year-old man was referred for cardiac evaluation after presenting with exertional dyspnea. His medical history was significant for a small bowel carcinoid tumor with metastases to his liver for which he underwent small bowel resection 9 years earlier. Within weeks of his current presentation, he developed marked dyspnea that worsened

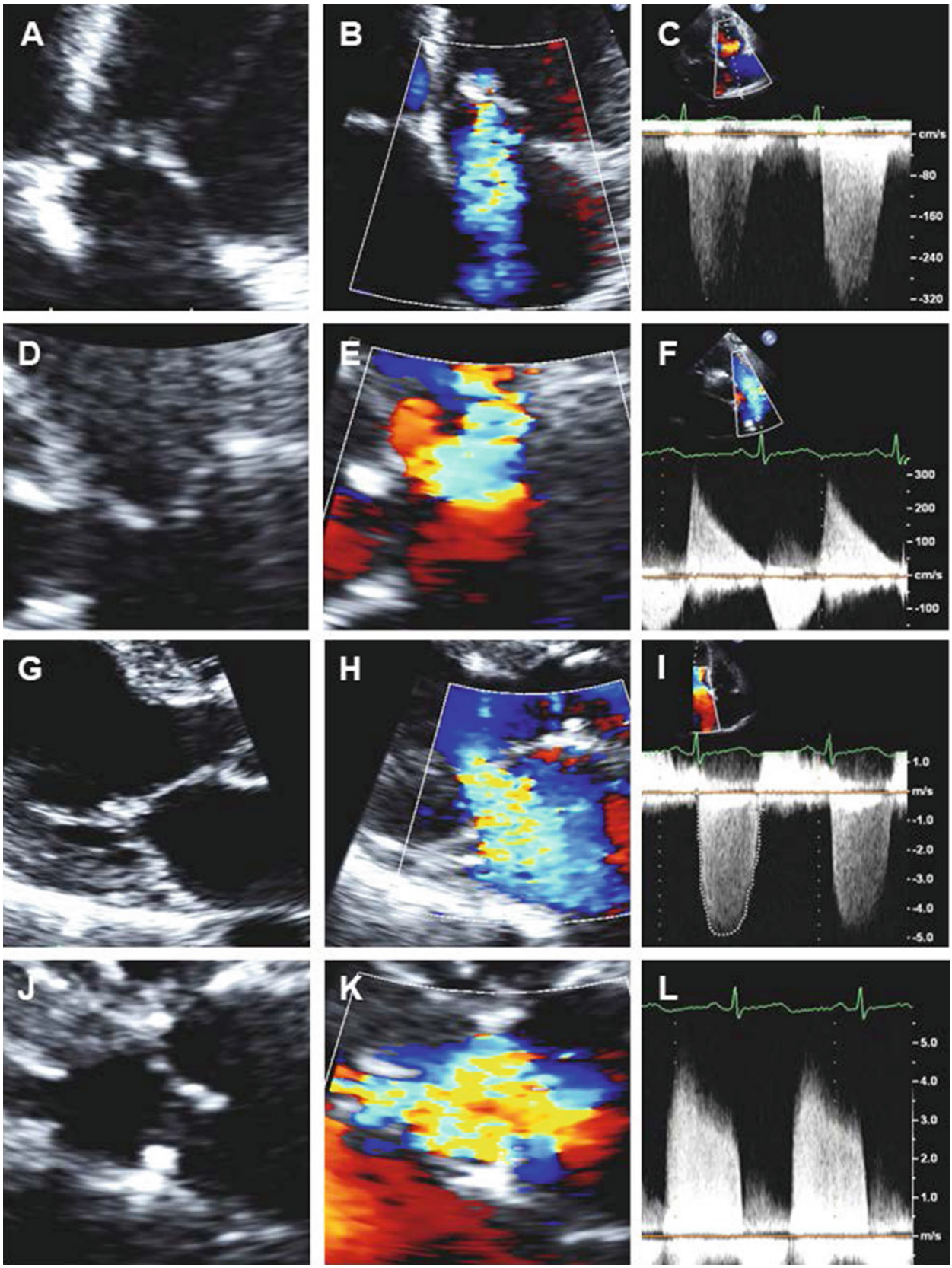
A
B
C
cm/s
-80
-160
-240
-320
D
E
F
300
200
100
cm/s
-100
G
H
I
1.0
m/s
-1.0
-2.0
-3.0
-4.0
-5.0
J
K
L
5.0
4.0
3.0
2.0
1.0
m/s

◀ **Fig. 17.2** Carcinoid heart disease involving all four valves. There is diffuse valve thickening and retraction. The septal leaflet of the tricuspid valve is relatively more restricted (**A**) resulting in suboptimal coaptation and moderate TR as shown by color Doppler (**B**) and by the holosystolic, parabolic CW profile of moderate density (**C**). The pulmonary valve is fixed with a coaptation gap (**D**) leading to severe PR detected by color Doppler (**E**) and by the dense triangular-shaped diastolic CW profile (**F**). The posterior leaflet of the mitral valve is tethered causing anterior leaflet override (**G**) and at least moderate posteriorly directed MR suggested by color Doppler (**H**) and by the holosystolic, parabolic CW profile of moderate density (**I**). There is similar restriction of the aortic valve cusps resulting in malcoaptation (**J**) and moderate–severe AR evidenced by the wide regurgitant jet on color Doppler (**K**) and by the dense diastolic CW profile (**L**)

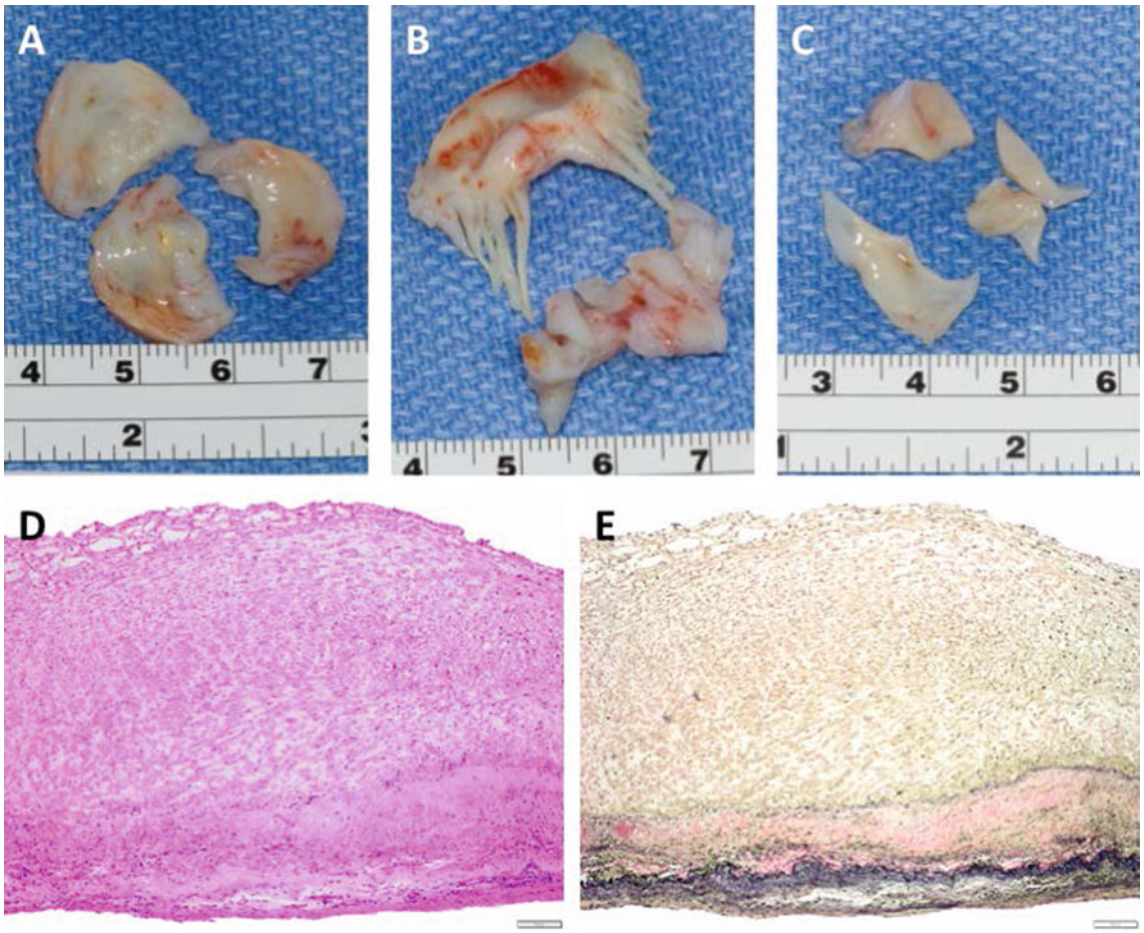

Fig. 17.3 Pathologic findings of carcinoid heart disease. Surgically resected aortic (**A**), mitral (**B**), and pulmonary (**C**) valves show glistening, white leaflets with diffuse, irregular thickening. Photomicrographs of the resected pulmonary valve with hematoxylin and eosin (**D**) and Verhoeff–van Gieson (**E**) stains show proliferative lesions with a loose myxoid extracellular matrix, more dense lesions with collagen deposition, and focal inflammatory infiltrates with focal disruption

from a supine to standing position. Physical examination revealed cyanosis with oxygen saturation in the low 80 s and a systolic murmur along the left sternal border that augmented with inspiration. Echocardiography showed thickened, retracted, and fixed right-sided valves, severe TR and moderate–severe PR, right-sided chamber enlargement with preserved RV systolic function, and a PFO with continuous right-to-left shunting (Fig. 17.4, Videos 17.16–17.19). Invasive hemodynamic assessment revealed a normal RA pressure suggesting that his symptoms were primarily due to inter-atrial shunting rather than valve disease. To avoid surgical risk, he underwent percutaneous PFO closure and received maintenance somatostatin analog treatment thereafter. A small residual shunt remained but there was significant symptom reduction, resolution of cyanosis, and normalization of oxygen saturation. He remained well for a year before experiencing another decline in exercise tolerance. Repeat echocardiogram showed an increase in PR and a reduction in RV systolic function (Fig. 17.5, Videos 17.20–17.25). He underwent cardiac surgery to replace his right-sided valves, remove the PFO closure device, and surgically close the

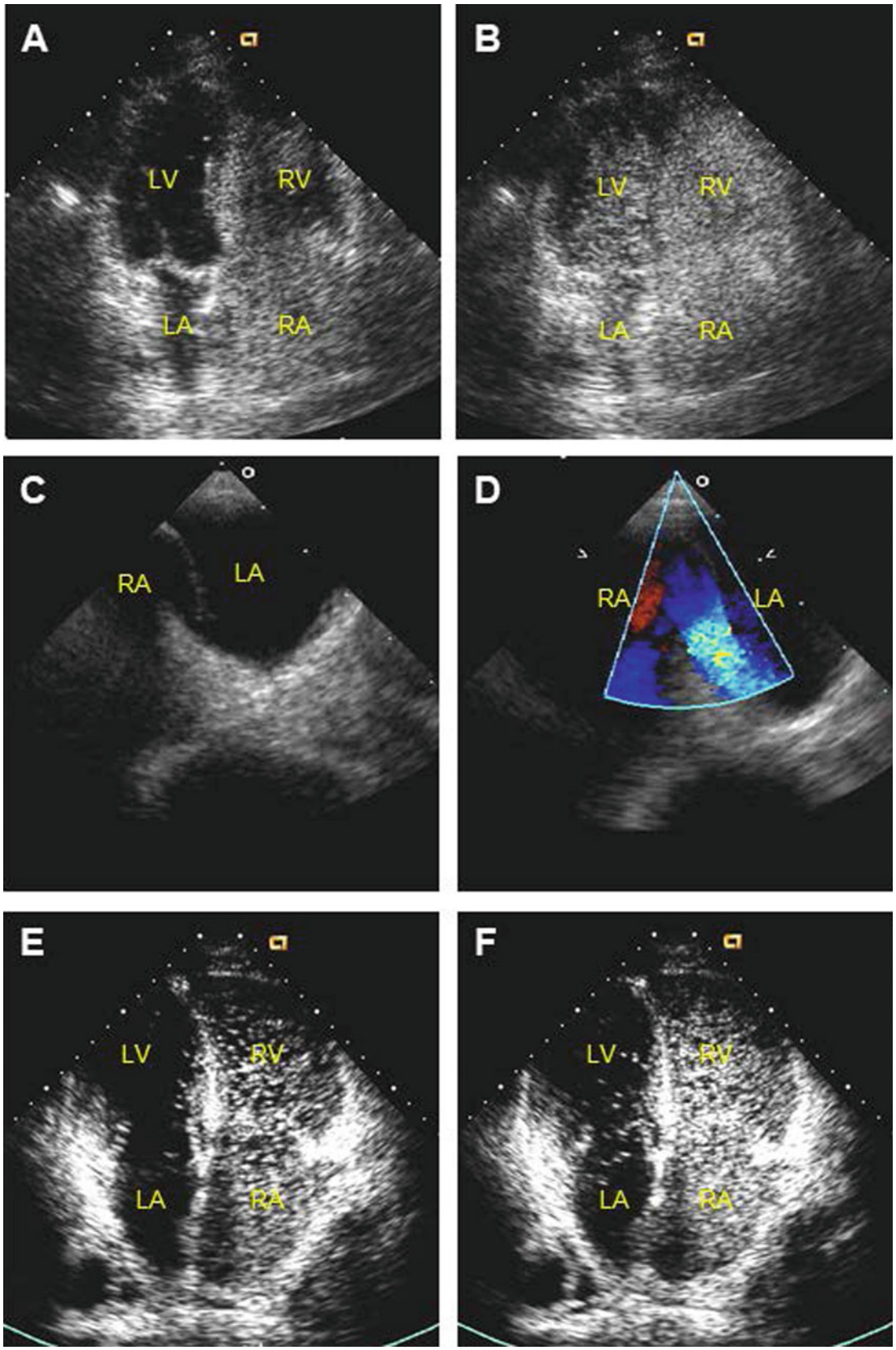

Fig. 17.4 PFO with right-to-left shunt. Baseline transthoracic echocardiogram with agitated saline shows entry of bubbles into the RA and RV (**A**) followed immediately by near opacification of the left atrium and ventricle (**B**) suggesting the presence of a large right-to-left shunt. Transesophageal echocardiography confirms the presence of a PFO (**C**) with continuous right-to-left shunting (**D**). Follow-up echocardiogram with agitated saline after percutaneous PFO closure shows entry of bubbles in the right-sided chambers (**E**) followed by a relatively small number of bubbles in the left side of the heart within three cardiac cycles (**F**) consistent with a small residual shunt across the atrial septum

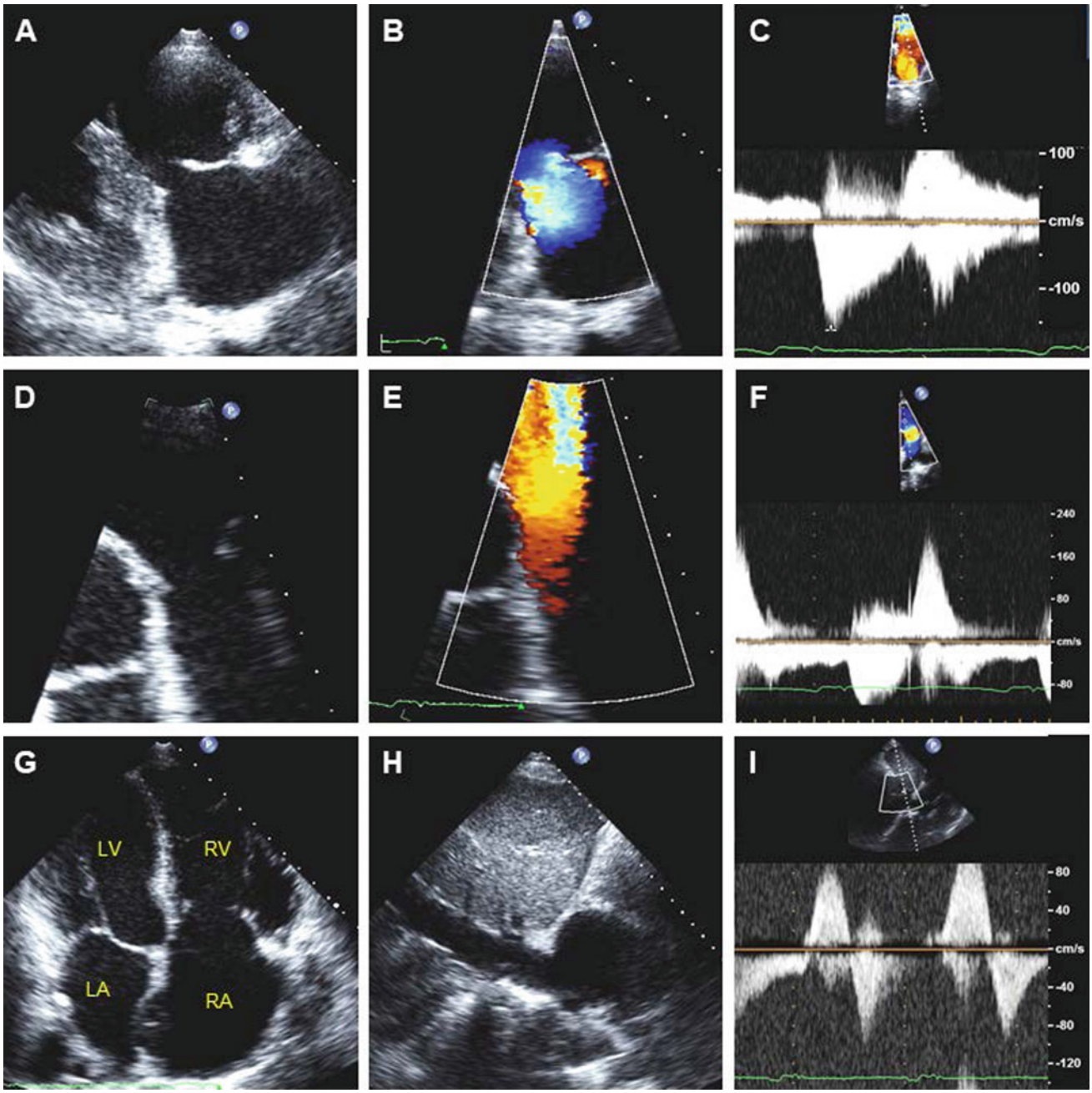

Fig. 17.5 Classic findings of carcinoid heart disease. There is thickening, retraction, and immobility of the tricuspid (**A**) and pulmonary (**D**) valves. The coaptation gaps are so wide that the resultant jets of severe TR (**B**) and PR (**E**) appear laminar by color Doppler. Dense, triangular-shaped CW Doppler profiles across the tricuspid valve during systole (**C**) and across the pulmonary valve during diastole (**F**) are consistent with severe regurgitation. There is RA and RV enlargement (**G**) due to chronic volume overload as well as inferior vena cava dilatation due to RA pressure elevation (**H**). PW Doppler at the hepatic vein shows characteristic systolic flow reversal of severe TR (**I**)

PFO. His exercise capacity improved significantly until a year later when he developed worsening dyspnea. A moderate severely elevated mean gradient of 35 mmHg was found across the pulmonary valve bioprosthesis, which was attributed to pannus and thrombus (Fig. 17.6, Videos 17.26–17.30). After excluding large thrombus burden on the valve by intracardiac echocardiography, he underwent percutaneous balloon valvuloplasty and was thereafter maintained on anticoagulation. The mean gradient across the valve decreased to 18 mmHg and his symptoms improved. He survived two more years with no further cardiac issues.

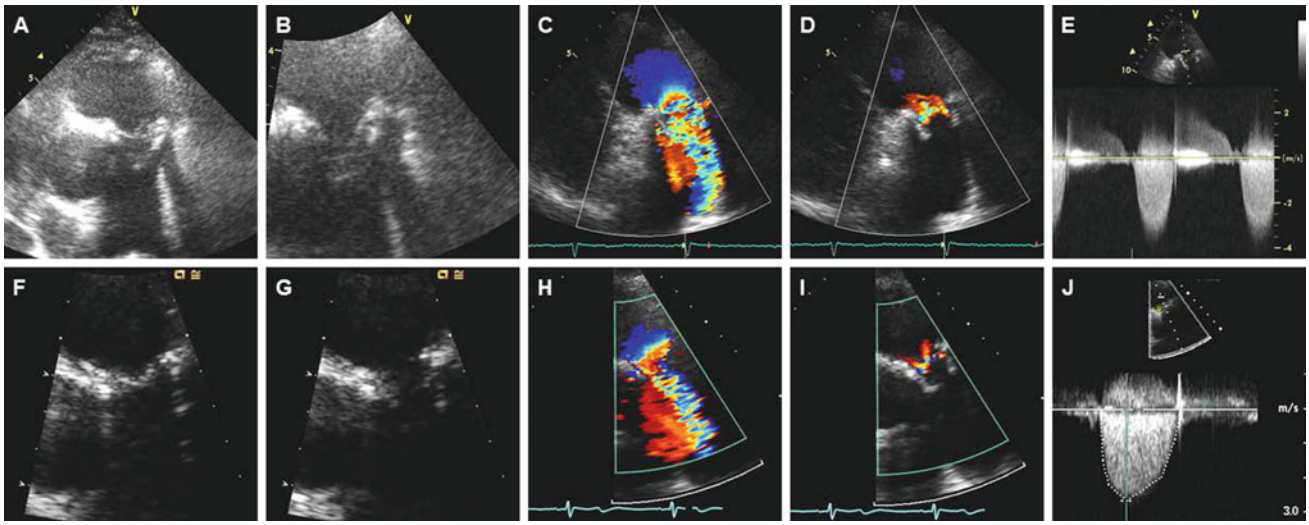

Fig. 17.6 Pulmonary valve bioprosthesis obstruction. The leaflets of the pulmonary valve bioprosthesis appear thickened with a possible echodensity representing pannus or thrombus on the ventricular aspect of the anterior leaflet seen during diastole (**A**). During systole, the leaflets appear restricted while in the open position (**B**). Color Doppler shows prominent flow acceleration across the bioprosthesis during systole suggesting significant obstruction (**C**). There is only mild prosthetic regurgitation during diastole by color Doppler (**D**) and CW Doppler (**E**). CW Doppler shows a mean gradient of 35 mmHg consistent with moderate–severe stenosis (**E**). After anticoagulation and valvuloplasty, the previously seen echodensity is no longer visualized (**F**), the leaflets appear slightly less restricted (**G**), the flow acceleration is less prominent (**H**), the degree of prosthetic regurgitation is unchanged (**I**), and the mean gradient has decreased to 18 mmHg (**J**) suggesting less obstruction

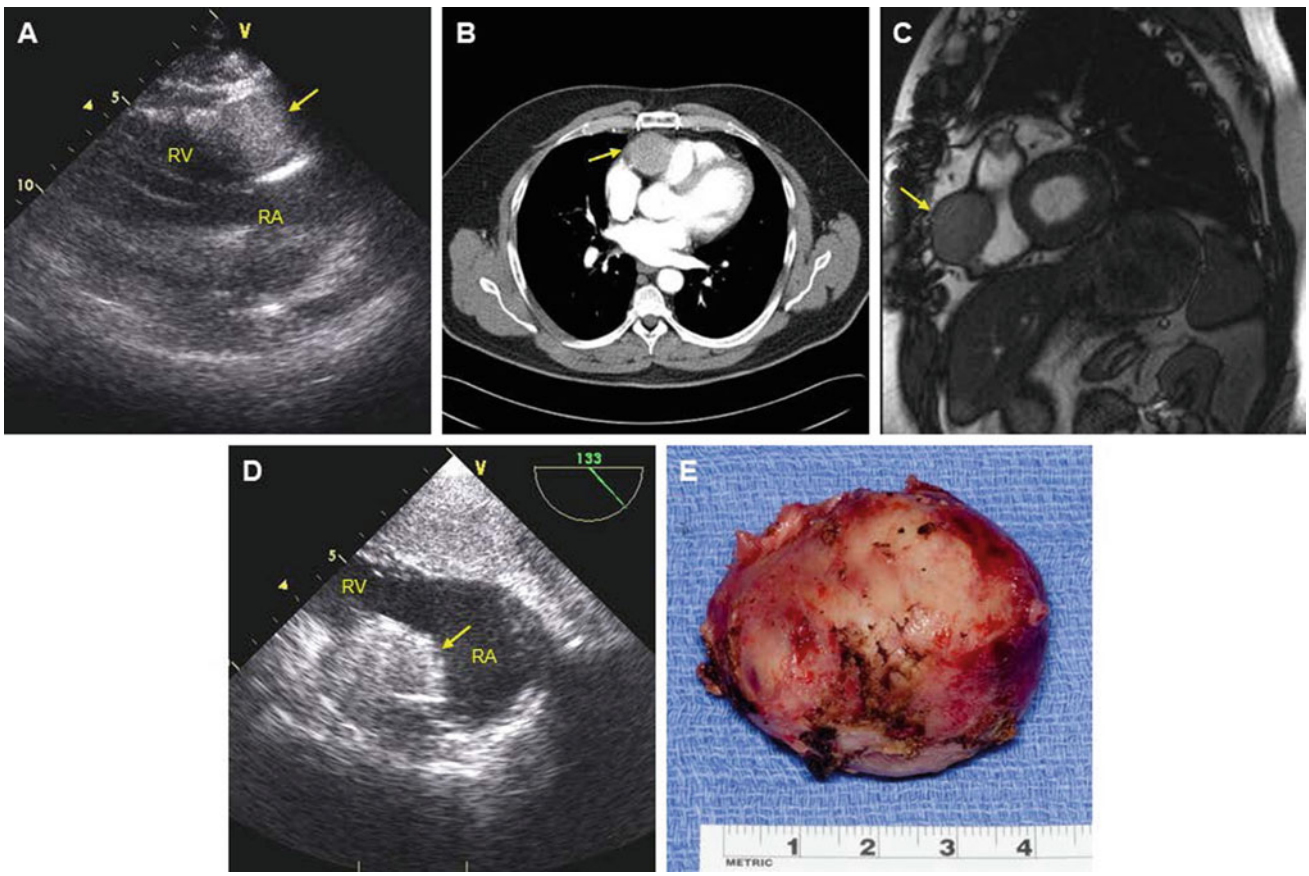

Fig. 17.7 Metastatic carcinoid tumor infiltrating the RV anterior free wall is visualized by transthoracic echocardiography (RV inflow view) (**A**), cardiac CT (**B**), cardiac MRI (**C**), transesophageal echocardiography (transgastric view) (**D**), and after surgical excision (E**E**)

17.9.2 Case 4

Case summary. This is a rare case of a patient with a metastatic carcinoid tumor infiltrating the RV wall with no valve involvement.

55-year-old man with a history of metastatic carcinoid disease presented with constant chest tightness and dyspnea. Cardiac imaging revealed a large circular homogeneous mass originating from the base of the RV anterior free wall with no valve involvement (Fig. 17.7, videos 17.31–17.34). He underwent cardiac surgery to excise the mass, which revealed a 3.5 × 4.5 cm tumor in the RV free wall surrounded by a thin layer of muscle and fat. Pathology confirmed metastatic carcinoid tumor. He survived another 9 years with no further cardiac issues.

References

1. Zoghbi WA, Adams D, Bonow RO, et al. Recommendations for noninvasive evaluation of native valvular regurgitation: a report from the american society of echocardiography developed in collaboration with the society for cardiovascular magnetic resonance. J Am Soc Echocardiogr. 2017;30:303–71.
2. Baumgartner H, Hung J, Bermejo J, et al. Echocardiographic assessment of valve stenosis: EAE/ASE recommendations for clinical practice. J Am Soc Echocardiogr. 2009;22:1–23.
3. De Jesus T, Luis SA, Ryu JH, et al. Carcinoid heart disease in patients with bronchopulmonary carcinoid. J Thorac Oncol. 2018;13:1602–5.
4. Haugaa KH, Bergestuen DS, Sahakyan LG, et al. Evaluation of right ventricular dysfunction by myocardial strain echocardiography in patients with intestinal carcinoid disease. J Am Soc Echocardiogr. 2011;24:644–50.
5. Dobson R, Cuthbertson DJ, Jones J, et al. Determination of the optimal echocardiographic scoring system to quantify carcinoid heart disease. Neuroendocrinology. 2014;99:85–93.
6. Chowdhury MA, Taleb M, Kakroo MA, Tinkel J. Carcinoid heart disease with right to left shunt across a patent foramen ovale: a case report and review of literature. Echocardiography. 2015;32:165–9.
7. Mansencal N, Touhami I, Mitry E, Rougier P, Dubourg O. Patent foramen ovale in carcinoid heart disease. Int J Cardiol. 2010;142:e29-31.
8. Łepska L, Pisiak S, Dudziak M. A case of carcinoid pericardial metastases and massive effusion. Kardiol Pol. 2013;71:881.
9. Pellikka PA, Tajik AJ, Khandheria BK, et al. Carcinoid heart disease: clinical and echocardiographic spectrum in 74 patients. Circulation. 1993;87:1188–96.
10. Johnston SD, Johnston PW, O'Rourke D. Carcinoid constrictive pericarditis. Heart. 1999;82:641–3.
11. Pandya UH, Pellikka PA, Enriquez-Sarano M, Edwards WD, Schaff HV, Connolly HM. Metastatic carcinoid tumor to the heart: echocardiographic-pathologic study of 11 patients. J Am Coll Cardiol. 2002;40:1328–32.
12. Caplin ME, Pavel M, Ćwikła JB, et al. Lanreotide in metastatic enteropancreatic neuroendocrine tumors. N Engl J Med. 2014;371:224–33.
13. Pavel ME, Baum U, Hahn EG, Schuppan D, Lohmann T. Efficacy and tolerability of pegylated IFN-alpha in patients with neuroendocrine gastroenteropancreatic carcinomas. J Interferon Cytokine Res. 2006;26:8–13.
14. Yao JC, Shah MH, Ito T, et al. Everolimus for advanced pancreatic neuroendocrine tumors. N Engl J Med. 2011;364:514–23.
15. Kulke MH, Hörsch D, Caplin M, et al. 37LBA Telotristat etiprate is effective in treating patients with carcinoid syndrome that is not adequately controlled by somatostatin analog therapy (the Phase 3 TELESTAR clinical trial)(abstr). Eur J Cancer. 2015;51:S728.
16. Strosberg J, El-Haddad G, Wolin E, et al. Phase 3 trial of 177Lu-Dotatate for midgut neuroendocrine tumors. N Engl J Med. 2017;376:125–35.
17. Kunz PL, Reidy-Lagunes D, Anthony LB, et al. Consensus guidelines for the management and treatment of neuroendocrine tumors. Pancreas. 2013;42:557–77.
18. Bernheim AM, Connolly HM, Rubin J, et al. Role of hepatic resection for patients with carcinoid heart disease. Mayo Clin Proc. 2008;83:143–50.
19. Lillegard JB, Fisher JE, Mckenzie TJ, et al. Hepatic resection for the carcinoid syndrome in patients with severe carcinoid heart disease: does valve replacement permit safe hepatic resection? J Am Coll Surg. 2011;213:130–8.
20. Arghami A, Connolly HM, Abel MD, Schaff HV. Quadruple valve replacement in patients with carcinoid heart disease. J Thorac Cardiovasc Surg. 2010;140:1432–4.
21. Castillo JG, Silvay G, Solís J. Current concepts in diagnosis and perioperative management of carcinoid heart disease. Semin Cardiothorac Vasc Anesth. 2013;17:212–23.
22. Møller JE, Pellikka PA, Bernheim AM, Schaff HV, Rubin J, Connolly HM. Prognosis of carcinoid heart disease: analysis of 200 cases over two decades. Circulation. 2005;112:3320–7.
23. Nguyen A, Schaff HV, Abel MD, et al. Improving outcome of valve replacement for carcinoid heart disease. J Thorac Cardiovasc Surg. 2019;158(99–107):e2.
24. Connolly HM, Schaff HV, Abel MD, et al. Early and late outcomes of surgical treatment in carcinoid heart disease. J Am Coll Cardiol. 2015;66:2189–96.
25. Caplin ME, Pavel M, Ćwikła JB, et al. Lanreotide in metastatic enteropancreatic neuroendocrine tumors. N Engl J Med. 2014;371:224–33.
26. Pavel ME, Baum U, Hahn EG, Schuppan D, Lohmann T. Efficacy and tolerability of pegylated IFN-alpha in patients with neuroendocrinegastroenteropancreatic carcinomas. J Interferon Cytokine Res. 2006;26:8–13.
27. Yao JC, Shah MH, Ito T, et al. Everolimus for advanced pancreatic neuroendocrine tumors. N Engl J Med. 2011;364:514–23.
28. Kulke MH, Hörsch D, Caplin M, et al. 37LBA Telotristat etiprate is effective in treating patients with carcinoid syndrome that is not adequately controlled bysomatostatin analog therapy (the Phase 3 TELESTAR clinical trial)(abstr). Eur J Cancer. 2015;51:S728.
29. Strosberg J, El-Haddad G, Wolin E, et al. Phase 3 Trial of 177Lu-Dotatate for Midgut Neuroendocrine Tumors. N Engl J Med. 2017;376:125–135.
30. Kunz PL, Reidy-Lagunes D, Anthony LB et al. Consensus guidelines for the management and treatment of neuroendocrine tumors. Pancreas. 2013;42:557–77.
31. Bernheim AM, Connolly HM, Rubin J, et al. Role of hepatic resection for patients with carcinoid heart disease. Mayo Clin Proc. 2008;83:143–50.
32. Lillegard JB, Fisher JE, Mckenzie TJ, et al. Hepatic resection for the carcinoid syndrome in patients with severe carcinoid heart disease: does valvereplacement permit safe hepatic resection? J Am Coll Surg. 2011;213:130–8.
33. Arghami A, Connolly HM, Abel MD, Schaff HV. Quadruple valve replacement in patients with carcinoid heart disease. J Thorac Cardiovasc Surg.2010;140:1432–4.

34. Castillo JG, Silvay G, Solís J. Current concepts in diagnosis and perioperative management of carcinoid heart disease. Semin Cardiothorac Vasc Anesth.2013;17:212–23.
35. Møller JE, Pellikka PA, Bernheim AM, Schaff HV, Rubin J, Connolly HM. Prognosis of carcinoid heart disease: analysis of 200 cases over two decades.Circulation. 2005;112:3320–7
36. Nguyen A, Schaff HV, Abel MD, et al. Improving outcome of valve replacement for carcinoid heart disease. J Thorac Cardiovasc Surg. 2019;158:99–107.e2.
37. Connolly HM, Schaff HV, Abel MD, et al. Early and Late Outcomes of Surgical Treatment in Carcinoid Heart Disease. J Am Coll Cardiol. 2015;66:2189–2196.

Cardiac Amyloidosis

18

Katherine Lee Chuy, Saurabh Malhotra, and Jennifer E. Liu

18.1 Introduction

Amyloidosis, from the Latin word *amylum* meaning starch, refers to nonspecific conditions in which proteins misfold and form starch-like insoluble fibrils with subsequent extracellular tissue deposition. There are over 30 amyloidogenic proteins identified that cause various diseases depending on the precursor protein that misfolds [1, 2]. The two most common systemic forms are light chain (AL) and transthyretin (ATTR) amyloidosis which are named according to its precursor protein. Although both types of amyloidosis share similar ultrastructure features and frequently involve the heart, each has its unique pathophysiology, clinical presentation, organ involvement, treatment strategies, and prognosis (Table 18.1). Cardiac involvement is the leading cause of morbidity and mortality. Early diagnosis is a key determinant of prognosis but often elusive and delayed due to the multisystemic presentations that are mistaken for more commonly occurring conditions. Education and awareness of both patients and physicians are essential as many patients have severe cardiac dysfunction at diagnosis due to advanced amyloid deposition and die within 6–12 months of presentation. Development of new treatment holds promise to transform outcome. In this chapter, cases are presented with accompanying imaging studies to illustrate the spectrum of clinical presentation, diagnosis, and management of cardiac amyloidosis and highlight the challenges encountered in clinical practice.

Electronic supplementary material
The online version of this chapter (https://doi.org/10.1007/978-3-030-70998-3_18) contains supplementary material, which is available to authorized users.

K. Lee Chuy · S. Malhotra
Cook County Health, John H. Stroger Jr. Hospital of Cook County, 1901 W. Harrison Street, Suite 3620, Chicago, IL 60612, USA
e-mail: katherine.leechuy@gmail.com

S. Malhotra
e-mail: saurabh.malhotra@cookcountyhhs.org

J. E. Liu (✉)
Department of Medicine, Memorial Sloan Kettering Cancer Center, New York, NY, USA
e-mail: liuj1234@mskcc.org

R. M. Steingart et al. (eds.), *Atlas of Imaging in Cardio-Oncology*,
https://doi.org/10.1007/978-3-030-70998-3_18

18.2 Pathophysiology

18.2.1 AL Amyloidosis

AL amyloidosis is a plasma cell dyscrasia where the amyloidogenic precursor protein comes from monoclonal immunoglobulin light chains produced in excess by clonal plasma cells in the bone marrow or by other B cell dyscrasias. Although the misfolded light chains form amyloid fibrils which can deposit in essentially any organ, the heart is involved in more than 50% of cases. Other sites involved include the kidneys, liver, GI tract, tongue, and peripheral or autonomic nervous system. Multiorgan involvement is common. The incidence of amyloidosis has remained stable with an estimated 4000-4500 cases annually in the United States but the prevalence has increased over the past decade with at least 12,000 adults in the US living with AL amyloidosis due to earlier detection and improved survival [3]. Amyloid deposits lead to organ dysfunction by disruption of the tissue architecture or direct cellular toxicity from amyloid fibrils.

18.2.2 TTR Amyloidosis

In TTR amyloidosis, the amyloid protein is transthyretin which is produced in the liver. TTR normally transfers thyroxine and retinol in the blood. It circulates predominantly as a tetramer but destabilizes into monomers which are prone to misfold and aggregate into amyloid fibrils in the disease state. There are two subtypes of TTR amyloidosis: wild-type TTR and variant TTR. In wild-type TTR, also known as senile systemic amyloidosis, the transthyretin protein is structurally normal but gradually deposits due to the aging process

Table 18.1 Summary of amyloid subtype classification

Amyloid subtype	Acquired or hereditary	Precursor protein	Usual decade at onset	Organs involved	Treatment	Prognosis
AL	Acquired	Monoclonal light chains	50+	Any tissue except for the brain; heart involved in >50% cases	Chemotherapy targeting the plasma cells	Poor in the setting of advanced heart disease; median survival 11 months
Familial TTR	Hereditary	Mutant TTR	20–70+ ; depending on the specific mutation	Peripheral and autonomic neuropathy; heart	Agents targeting hepatic synthesis of TTR, stabilize the tetramer or degrade the fibrils; liver transplantation	Average survival of 7–12 years after diagnosis
Senile	Acquired	Wild-type TTR	70+	Heart, carpal tunnel	Same as familiar TTR except for liver transplant	Average survival of 4 years after diagnosis

AL light chain; *TTR* transthyretin

primarily in the heart and occasionally in the soft tissues of the wrist causing carpal tunnel syndrome. Wild-type TTR is underdiagnosed and increasingly recognized as a cause of heart failure with preserved ejection fraction (HFpEF). Hereditary TTR is caused by more than 100 delineated mutations in the TTR gene, leading to structurally abnormal or variant transthyretin. The mutations are inherited in an autosomal dominant fashion and manifest with varying geographic distribution and phenotypic expression. In the US, the most commonly encountered mutation is the V122I (substitution of valine for isoleucine at position 122), which is present in 3–3.5% of individuals of African descent and significantly associated with heart failure [4].

18.3 Clinical Manifestation

Cardiac amyloidosis, regardless of the subtype, presents as an infiltrative cardiomyopathy with restrictive physiology due to the amyloid deposition in the myocardium. Heart failure is often the first manifestation with predominant right-sided symptoms. Patients can have angina with normal coronaries due to amyloid infiltration of intramyocardial and micro-vessels. Syncope can often be exertional due to a low and fixed cardiac output, which may be an ominous sign associated with poor prognosis. Patients will often develop orthostatic hypotension related to autonomic dysfunction. Conduction abnormalities causing bradyarrhythmia, particularly heart block, are common, which may also potentially cause syncope or presyncope. Atrial fibrillation (AF) as well as ventricular arrhythmia and sudden cardiac death are common in patients with advanced disease. In addition to the cardiac manifestation, other systemic illnesses are common in patients with AL amyloidosis due to multiorgan involvement. Multiorgan involvement is rare in patients with wild-type TTR with the exception of carpal tunnel syndrome. Neuropathy and cardiac involvement are common in mutant TTR depending on the nature of the mutation.

18.4 Diagnosis and Management

Cardiac amyloidosis is often first suspected on echocardiography in a patient being evaluated for heart failure symptoms. Distinctive echocardiographic features include nondilated ventricles with concentric left ventricular (LV) thickening, often labeled incorrectly as “hypertrophy” as the pathological process is infiltrative and not myocyte hypertrophy. The low-voltage ECG, reported to be present in 47% of patients with AL amyloidosis and biopsy-proven cardiac involvement, is likely due to the amyloid fibrils insulating the myocytes from transmitting the voltage to the ECG. Low voltage on ECG is less common in the TTR subtypes. A disconnection between “LV hypertrophy (LVH)” on echo and normal/low voltage on ECG is a strong clue to the diagnosis in the right clinical context. Right ventricular wall thickening, thickened valves, and atrial septal thickening are also commonly seen on echo. The amyloid deposition increases echogenicity of the myocardium giving rise to a “granular or sparkling” appearance. The LVEF is usually preserved until late in the disease process. Patients can have a spectrum of diastolic dysfunction from Grade I diastolic dysfunction with normal filling pressures initially to restrictive physiology with progression

of myocardial infiltration. Global longitudinal strain (GLS) is often reduced, out of proportion to EF, with a characteristic apical sparing pattern where longitudinal strain is worse at the base and mid/ventricular regions compared to the apex. GLS can play a significant role in the diagnosis by differentiating cardiac amyloidosis from other causes of thickened myocardial walls [5].

Cardiac magnetic resonance imaging (MRI) can provide incremental value in the diagnostic evaluation when amyloid is suspected [6]. In addition to showing detailed information on cardiac structure and function, it can provide myocardial tissue characterization and help differentiate amyloidosis from other causes of thickened myocardium. Due to the interstitial expansion and fibrosis from amyloid deposition, late gadolinium enhancement (LGE) is commonly observed as well as abnormal myocardial extracellular volume quantification and myocardial nulling time. The pattern of LGE can be variable from diffuse to patchy, subendocardial to transmural, not specific enough to make the diagnosis for amyloidosis. Though it provides diagnostic utility, a negative MRI study does not exclude the presence of amyloid. When wall thickening and LGE are present in MRI, these findings must always be integrated with other clinical features in the evaluation with consideration of other forms of cardiomyopathy that may share similar phenotype, such as hypertrophic cardiomyopathy [7].

Echocardiography or MRI imaging cannot distinguish AL from TTR cardiac amyloidosis. Biopsy evidence of amyloid deposits with accurate fibril typing is essential for proper diagnosis and treatment. Amyloid fibrils bind Congo red stain, yielding the pathognomonic apple-green birefringence under polarized light microscopy which remains the gold standard for identifying amyloid deposits. After Congo red confirms the amyloid deposits, it is essential to use mass spectroscopy for typing the amyloid as AL versus TTR.

Technetium pyrophosphate (^{99m}Tc-PYP) scanning is an isotope-based technique commonly used for bone scanning which can detect TTR as a diffuse pattern of uptake in the heart of patients with transthyretin cardiac amyloid. This method has excellent diagnostic accuracy in the right clinical context. If cardiac amyloidosis is suspected based on clinical findings and suggestive echo/ECG, and screening for AL amyloidosis with serum and urine immunofixation and serum-free light chain assay is negative, the specificity and positive predictive value for cardiac TTR amyloidosis with grade 2 or 3 cardiac uptake (cardiac uptake equal to or greater than rib uptake) on the PYP scan have been reported to be 100%, allowing one to make an expedited diagnosis without the need for tissue biopsy [8]. The need to make an expedited diagnosis has become increasingly relevant given the emergence of effective treatment.

18.5 Management

Therapy for cardiac amyloidosis is twofold: supportive care for cardiac-related symptoms and treatment of the underlying disease targeting the amyloid precursor protein. Diuretics are the mainstay for heart failure therapy. Midodrine or fludrocortisone is used to treat orthostatic hypotension. Beta blockers are safe to use but may not be well tolerated in this population. While amiodarone has also been shown to be safe to use, it has not shown any survival benefit. AF is often poorly tolerated given the underlying cardiac impairment, requiring electrical cardioversion and/or amiodarone for rhythm control. Anticoagulation is strongly indicated in the setting of AF regardless of the CHADS Vasc score given the high risk of intracardiac thrombi associated with cardiac amyloidosis [9]. Calcium channel blockers can bind to the amyloid fibrils and may have significant negative ionotropic and bradycardic effect leading to heart failure and hemodynamic instability. Digoxin can also bind to the amyloid fibrils and should be avoided due to increased risk of digoxin toxicity. Permanent pacemaker (PPM) implantation is common for symptomatic bradycardia. The benefit of automatic implantable cardioverter defibrillators (AICDs) for primary prevention in patients is unproved and whether appropriate AICD therapy translates into overall survival benefit remains unclear [10]. At the current time, the indications for PPMs and AICDs in patients with cardiac amyloidosis are based on the general clinical guidelines.

The major aim in the treatment of AL amyloidosis is to target the plasma cells that are generating the abnormal precursor protein. First line therapy is high-dose melphalan therapy followed by stem cell transplant. However, given the potential high transplant-related mortality, its usage is limited to a selected group of patients with adequate cardiac, pulmonary, and renal function. Other agents such as proteasome inhibitors and immunomodulating agents have also been shown to be effective in controlling the light chain levels. There are also direct amyloid targeting antibodies under investigation. A host of therapies and therapeutic drug classes has emerged for the treatment of TTR amyloid targeting different stages in the amyloidogenic TTR production. Agents in development or approved for clinical use include silencers to suppress TTR synthesis in the liver, stabilizers to bind to the TTR tetramer and inhibit its dissociation into monomers, and degraders to remove or resorb the deposited amyloid fibrils. Tafamidis, a transthyretin kinetic stabilizer, was recently granted FDA fast track status after positive results of the Phase 3 trial showing a decrease in overall mortality and 30-month hospitalization in patients with TTR cardiomyopathy treated with tafamidis compared to placebo [11]. Liver transplantation can be considered in

young patients with TTR amyloidosis with primary neuropathic phenotype. In addition, a recent study showed that cardiac transplant outcome was similar in carefully selected patients with cardiac amyloidosis compared with patients who underwent transplantation for other heart failure causes [12].

18.6 Prognosis

Prognosis is determined by the extent of cardiac involvement. Circulating amyloidogenic light chain level is also a major determinant of prognosis in AL amyloidosis. TTR is a more indolent disease and generally has a better prognosis than AL amyloidosis. Serum cardiac biomarkers troponin and NT-proBNP are sensitive markers of cardiac involvement and strongly prognostic in AL amyloidosis. A well-validated prognostic staging system based on biomarkers was developed by the Mayo Clinic for use in patients with newly diagnosed AL amyloidosis. The utility of this staging system was later improved with the addition of light chain levels [13]. Global longitudinal strain is also an independent robust predictor of survival that provides incremental prognostic value to the Mayo Staging system [14]. Prognosis for AL amyloidosis has markedly improved over the years due to advances in chemotherapeutic options that control light chains though outcome for patients with advanced cardiac disease at diagnosis has remained poor with survival often less than 1 year. Improved survival is associated with cardiac response to treatment defined by reduction in NT-proBNP which is more likely to occur in patients who achieved complete hematologic response [15].

18.7 Case 1

Key points:

- Diagnosis of cardiac AL amyloidosis is often delayed due to its relative rarity and confusing multisystemic presentation.
  - One-third of patients are diagnosed more than 1 year after onset of symptoms and after visits to multiple specialists.
- Mismatch of "LVH" on echo and low/normal voltage on ECG should be a major clue for cardiac amyloidosis in the right clinical context.
- Tissue diagnosis of amyloid deposition with amyloid subtyping is mandatory. Abdominal fat pad is commonly attempted to minimize biopsy-associated risk with reported sensitivities as high as 84% in AL amyloidosis. If negative, proceeding to biopsy the clinically involved organ may be necessary.

A 54-year-old woman with a history of carpal tunnel syndrome developed cough and dyspnea on exertion (DOE). Extensive workup for cough included referrals to allergy, GI, and ENT with no definite etiology found and no improvement on treatment for allergies or esophageal reflux. Her symptoms continued to progress over the next 12 months with DOE after one block and dizziness with exertion. She then experienced two episodes of exertional syncope and was admitted to the hospital. An EKG done showed first-degree AV block with low voltages (Fig. 18.1). Physical exam was notable for orthostatic hypotension and congestive heart failure. 2D transthoracic echocardiogram (TTE) revealed concentric LVH (Figs. 18.2, 18.3 and 18.4, Videos 18.1 and 18.2) with preserved EF. Cardiac catheterization showed no evidence of obstructive CAD. Labs were notable for elevated BNP 923 and nondetectable troponin. Upon consultation with a heart failure specialist, a cardiac MRI was performed which showed delayed gadolinium enhancement suggestive of cardiac amyloidosis (Fig. 18.5). Subsequent hematologic workup including serum and urine electrophoresis and immunofixation, and serum-free light chain assay revealed lambda light chain plasma cell dyscrasia. Fat pad biopsy, however, was negative. Finally, she underwent endomyocardial biopsy, which was positive for amyloid deposition with AL subtype on mass spectroscopy. The diagnosis of AL amyloidosis with cardiac and nervous system involvement was finally made 12–16 months after onset of symptoms.

18.8 Case 2

Key Points:

- Defining the cause of LV wall thickening can be very challenging given the overlap in the clinical phenotype among the different etiologies.
- When non-invasive findings are inconsistent in supporting a diagnosis, additional testing should be performed to confirm, including tissue biopsy. In the case below, the absence of high voltage on ECG, which is unusual given the significant LV hypertrophy on echo and MRI, should raise suspicion for alternative diagnosis other than hypertrophic cardiomyopathy.
- It is essential to consider mimics of hypertrophic cardiomyopathy such as cardiac amyloidosis or Fabry disease before committing patients to major treatment decisions.

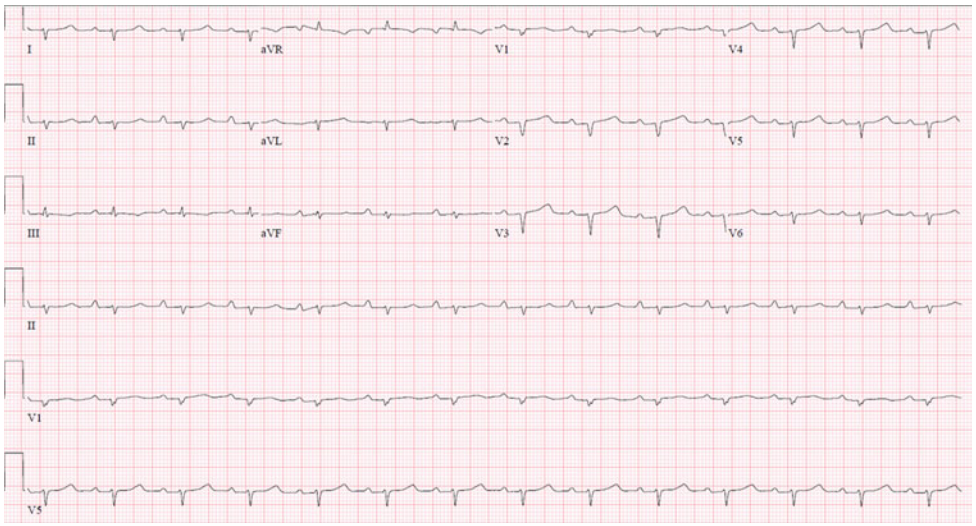

Fig. 18.1 ECG shows normal sinus rhythm with first-degree AV block; poor R wave progression, and low voltage

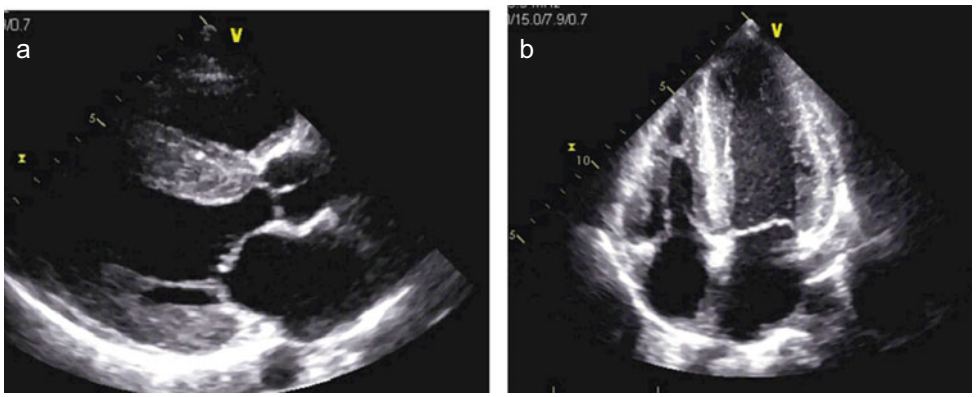

Fig. 18.2 **a** Parasternal long-axis view. Interventricular septum thickness measured 1.8 cm. Calculated LV mass = 164 gm/m2 consistent with concentric "left ventricular hypertrophy." **b** Apical four-chamber view. Left atrium is dilated (LA volume = 38 ml/m2). Thickening of right ventricular wall

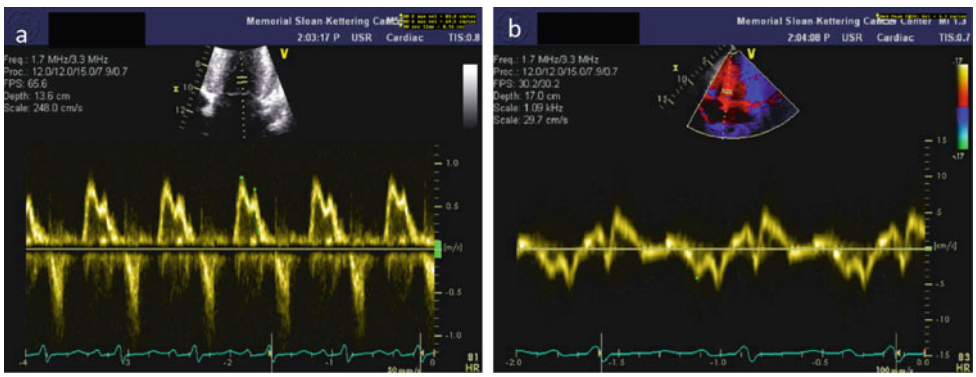

Fig. 18.3 **a** Pulsed wave Doppler of the mitral inflow: mitral E/A ratio = 1.2, deceleration time 160 ms. **b** Tissue Doppler of the mitral annulus 4.1 cm/sec. E/E' = 20 consistent with high LV filling pressure

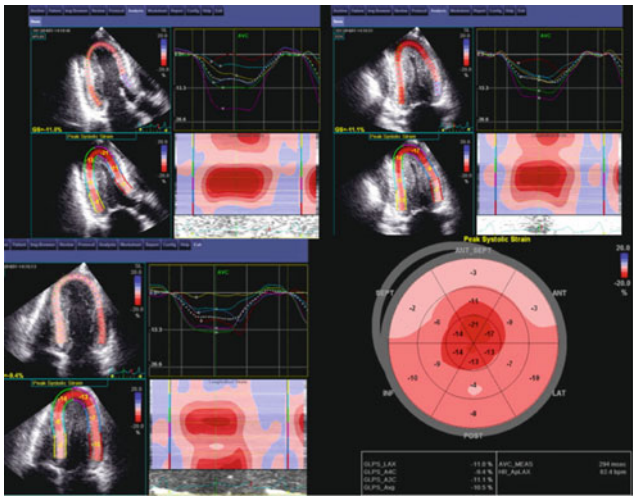

Fig. 18.4 Global longitudinal strain of −10.5% with the bull's eye showing apical sparing pattern

- Systolic anterior motion of the mitral valve is a non-specific finding that can be seen commonly in other conditions besides hypertrophic cardiomyopathy.

A 53-year-old man presented with three episodes of syncope while playing basketball. He had no past medical history and was feeling well until 3 months prior when he started noticing dyspnea on exertion. He saw his primary care physician. An ECG done showed nonspecific T wave abnormality consistent with possible ischemia (Fig. 18.6). He went to see a cardiologist and underwent cardiac evaluation including a cardiac catheterization showing nonobstructive coronary artery disease; TTE (Figs. 18.7 and 18.8, Videos 18.3 and 18.4) showing asymmetric septal hypertrophy (ASH), normal ejection fraction (EF), no systolic anterior motion (SAM), abnormal diastolic function, and mildly reduced global longitudinal strain (Figs. 18.9 and 18.10); cardiac MRI showing ASH and LGE in midmyocardial distribution affecting most of the septum and the apical tip of the ventricle consistent with interstitial fibrosis in a pattern suggestive of hypertrophic cardiomyopathy (Fig. 18.11). His labs were notable for troponin I of 0.03 ng/mL and BNP of 169 pg/ml. The patient then underwent upright bicycle stress echo which showed SAM with a peak outflow tract gradient of 44 mm Hg at peak exercise (Figs. 18.12 and 18.13, Video 18.5). Given these findings, he was diagnosed with hypertrophic obstructive cardiomyopathy and underwent myomectomy (Fig. 18.14, Video 18.6). Unfortunately, the pathology of the resected myocardium showed AL amyloid deposition. Follow-up hematological workup confirmed the diagnosis of lambda light chain plasma cell dyscrasia.

18.9 Case 3

Key points:

- TTR amyloid cardiomyopathy may go undiagnosed for years as it mimics hypertrophic heart disease often

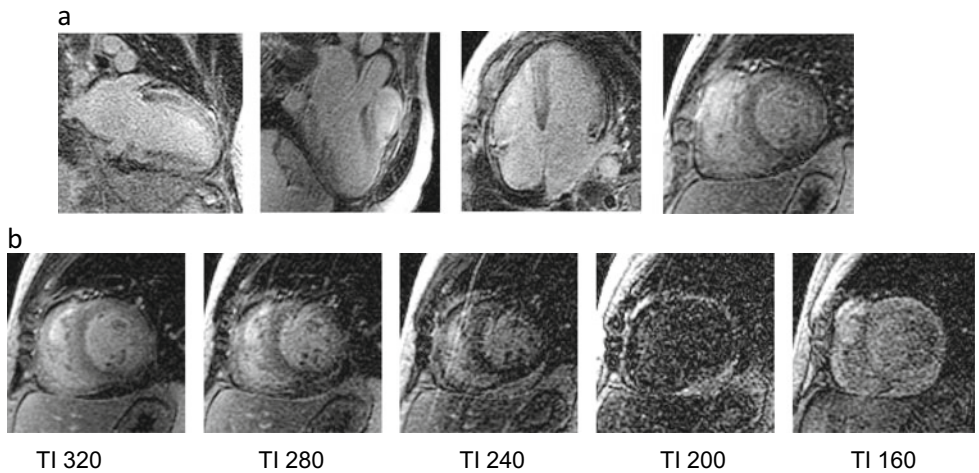

Fig. 18.5 **a** Cardiac MRI showing diffuse late gadolinium enhancement involving all the LV wall. **b** Myocardium nulling at a much lower inversion time (200 ms) where both myocardium and blood pool are nulling

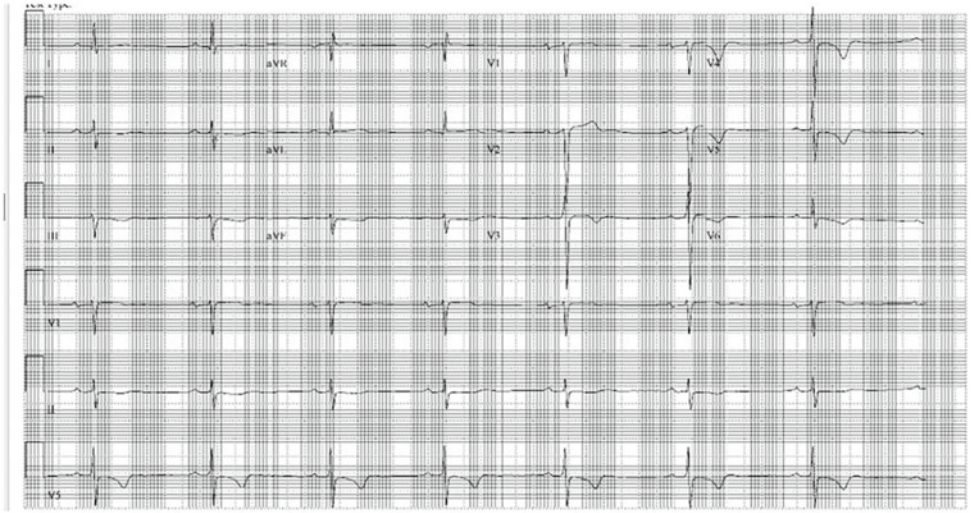

Fig. 18.6 ECG showing sinus rhythm with repolarization abnormality consistent with anterolateral ischemia

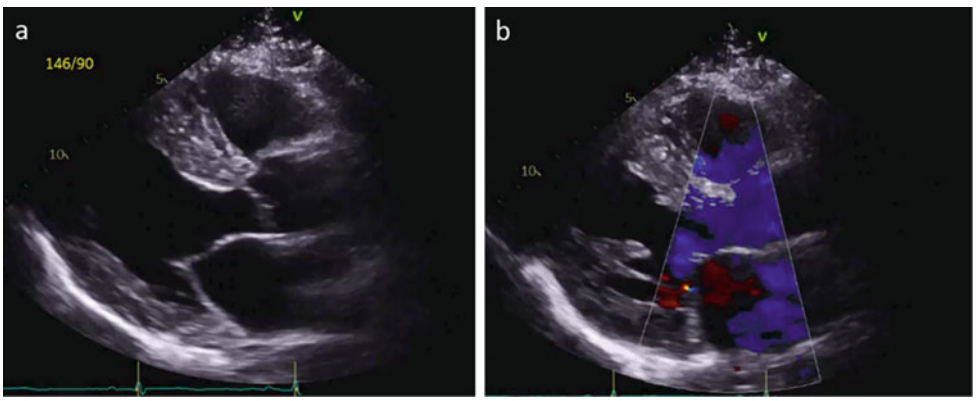

Fig. 18.7 **a** Parasternal long-axis view showing asymmetric septal hypertrophy with IVS = 1.6 cm; LVIDd 5.0 cm; PW 1.2 cm; LV mass 139 gm/2. No evidence of systolic anterior motion of the mitral valve. **b** Color Doppler shows no evidence of turbulent flow across the outflow trace and no mitral regurgitation. IVS = interventricular septal thickness; LVIDd = left ventricular internal dimension in diastole; PW = posterior wall

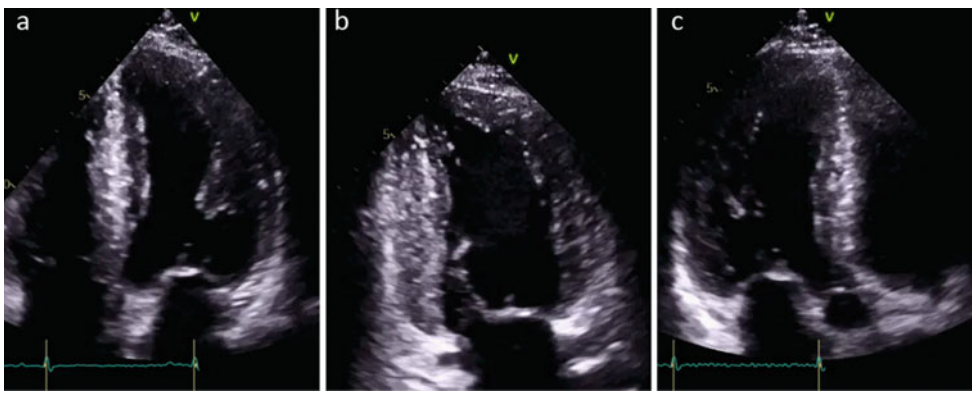

Fig. 18.8 **a** Apical four-chamber view. **b** Apical two-chamber view. **c** Apical three-chamber view. LV EF = 65%; left atrial volume = 41 ml/m2 consistent with mildly dilated left atrium. No systolic motion noted. LVEF = left ventricular ejection fraction. See Video 18.4

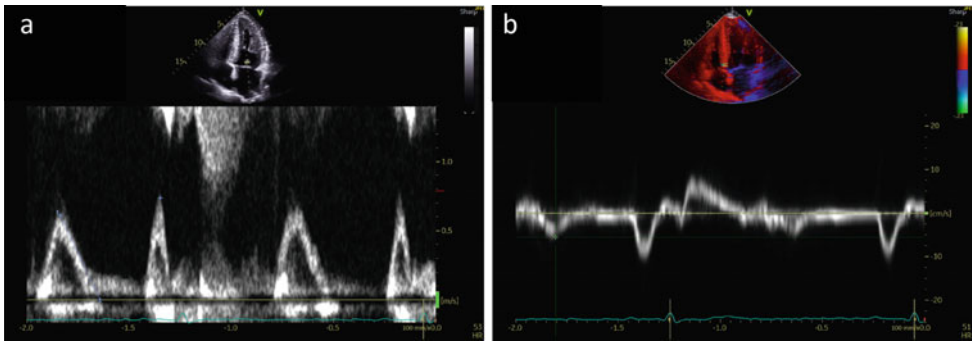

Fig. 18.9 **a** Pulsed wave Doppler of the mitral valve. Mitral E/A ratio 0.83. **b** Tissue Doppler E' = 6 cm/sec mitral E/e' 8.5; lateral E/e' = 6.8. Abnormal relaxation with normal LV filling pressure

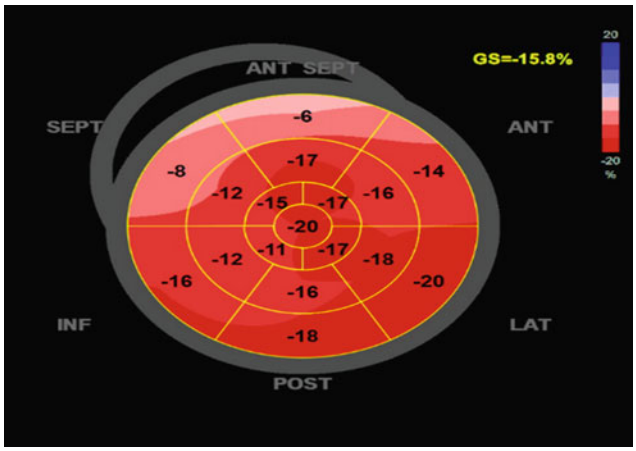

Fig. 18.10 Longitudinal strain bull's eye plot showing a nonspecific pattern. Global strain value of −15.8 which is mildly reduced

attributed to other more prevalent pathologies such as hypertension, diabetes, and obesity.

- Although HFpEF is considered the classic phenotype associated with TTR-related amyloidosis, a substantial portion of patients will present with HF with reduced ejection fraction (HFrEF) at the time of diagnosis if advanced disease is present [16].
- The diagnosis of TTR cardiac amyloidosis can be made non-invasively with nuclear imaging in the absence of a plasma cell or B cell dyscrasia, i.e., no monoclonal gammopathy and normal serum-free light chain ratio.
- Further classification of TTR cardiac amyloidosis as wild type or variant is important as management includes education, counseling, and genetic testing of family members in cases of variant or hereditary disease.

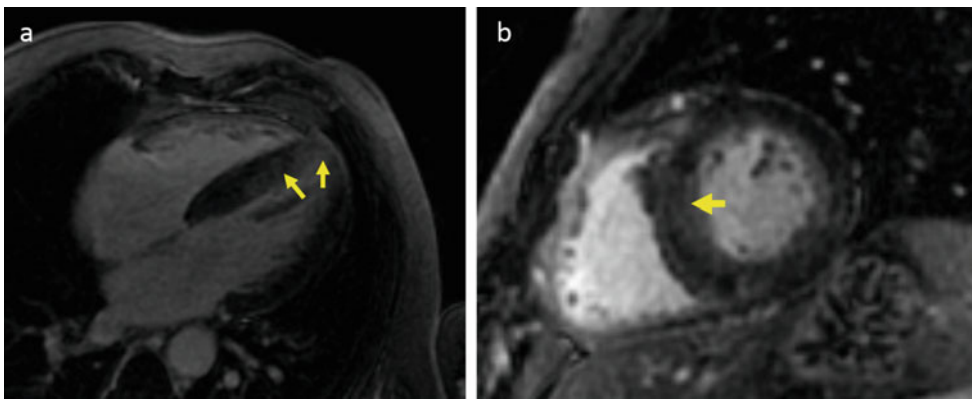

Fig. 18.11 Cardiac MRI showing asymmetric septal hypertrophy with late gadolinium in midmyocardial distribution affecting the septum and the apical tip. **a** Four-chamber view of the left ventricle. **b** short axis of the left ventricle

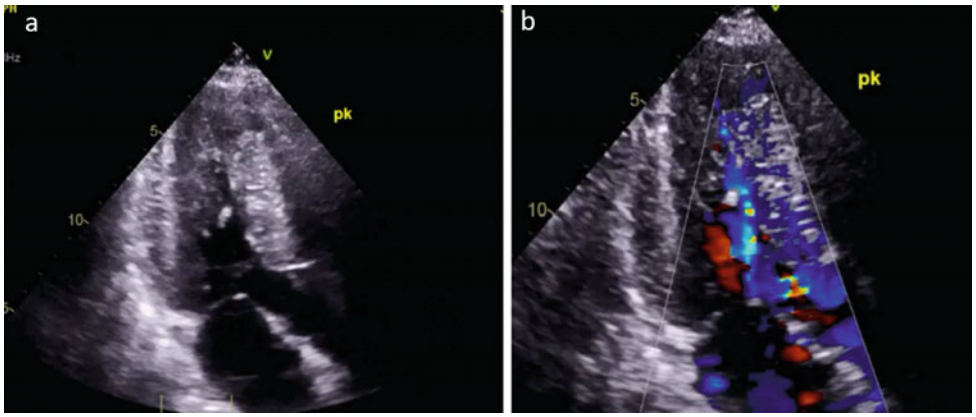

Fig. 18.12 Bicycle stress echocardiogram. A. Apical three chamber view showing the presence of systolic anterior motion at peak exercise. B. Color Doppler shows evidence of turbulent flow across the LV outflow tract

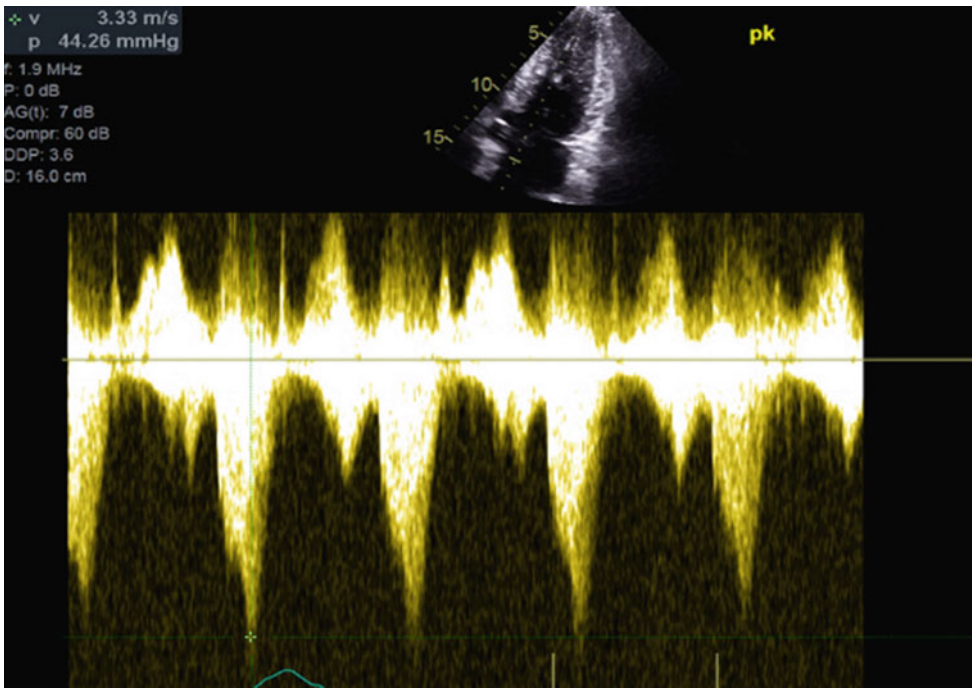

Fig. 18.13 Doppler of left ventricular outflow tract showing a peak instantaneous gradient of 44 mm Hg

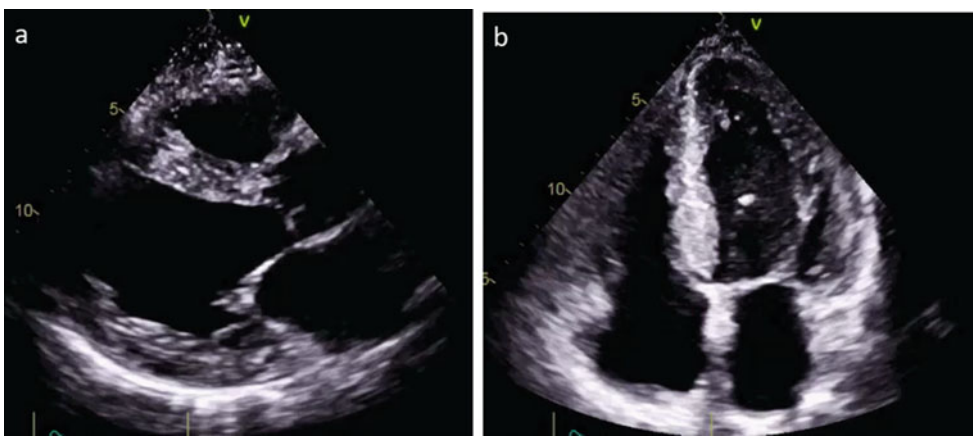

Fig. 18.14 See video 6. Post-myomectomy **a** Parasternal long-axis view. **b** Apical four-chamber view. Pathology of the resected myocardium: AL amyloid deposition

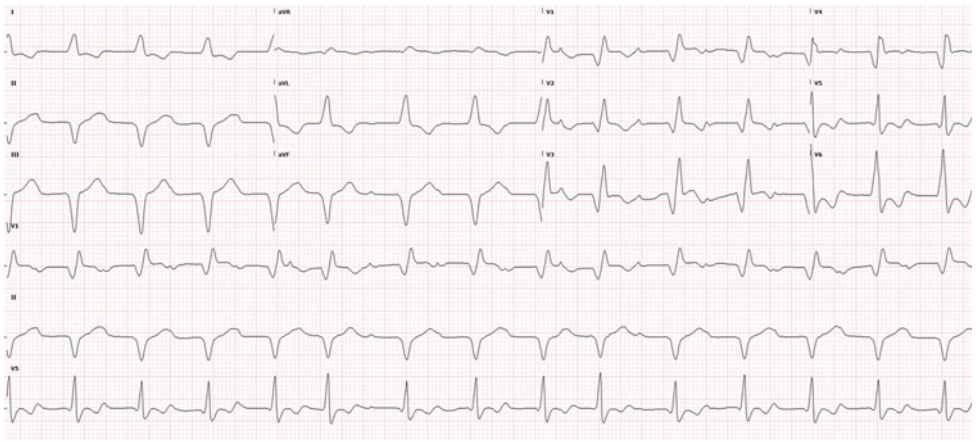

Fig. 18.15 ECG showing sinus rhythm with first-degree AV block, occasional premature supraventricular complexes, right bundle branch block

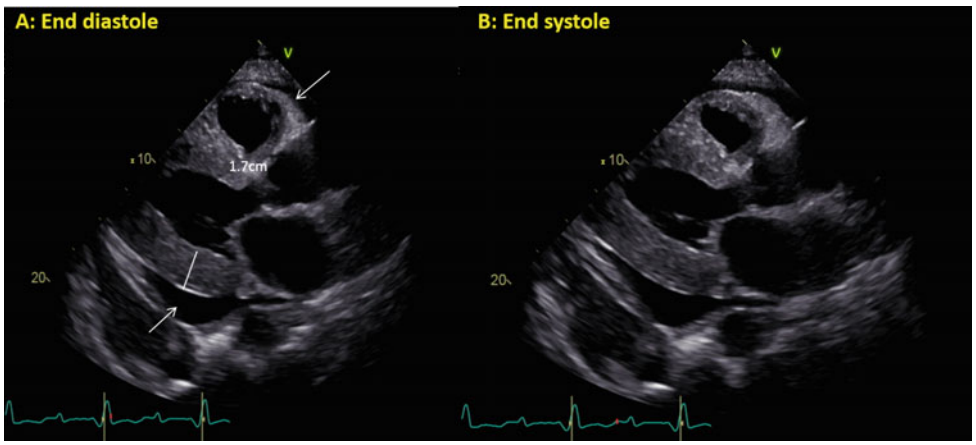

Fig. 18.16 2D transthoracic echocardiogram. Parasternal long-axis view at **a** end diastole and **b** end systole showing severe concentric left ventricular hypertrophy, increased ventricular mass, and a free-flowing circumferential small-to-moderate-sized pericardial effusion (arrows). Interventricular septal thickness 1.7 cm, posterior wall thickness 1.8 cm. Left ventricular ejection fraction 15–20%

- Anticoagulation is indicated for patients with cardiac amyloidosis and AF due to increased thromboembolic risk regardless of CHADSVasc score.

A 76-year-old Haitian man with hypertension and heart failure with reduced ejection fraction, and a history of several hospitalizations for heart failure for the past 6 years, presented with decompensated heart failure. Prior workup ruled out hemodynamically significant coronary artery disease. He had chronically elevated levels of cardiac troponins and natriuretic peptides. ECG showed normal sinus rhythm with first-degree AV block and right bundle branch block (Fig. 18.15). Echocardiogram showed severe concentric left ventricular (LV) hypertrophy and increased ventricular mass with diffuse hypokinesis and an ejection fraction of 15–20%, elevated LV filling pressures, right ventricular dilation and hypertrophy, and a small-to-moderate pericardial effusion. Strain echocardiogram showed decreased global longitudinal strain of −1.6% with a relative apical sparing pattern (Figs. 18.16 and 18.17, Video 18.7). Given suspicion for cardiac amyloidosis, cardiac magnetic resonance was performed which showed biventricular hypertrophy and dysfunction, elevated native T1 relaxation time, and diffuse delayed gadolinium enhancement involving both atria, ventricles, and the interatrial septum—findings consistent with cardiac amyloidosis (Fig. 18.18). Serum and urine electrophoresis and light chains showed no monoclonal gammopathy and normal free light chain levels and ratio. Technetium-99 m pyrophosphate (PYP) scintigraphy showed marked radiotracer uptake in the myocardium strongly suggestive of transthyretin (TTR) cardiac amyloidosis, with a semiquantitative or visual grade of 3 and a

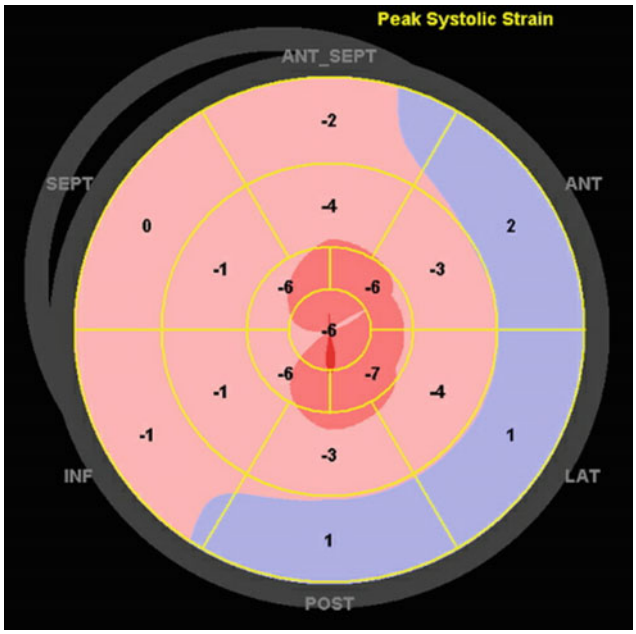

Fig. 18.17 Strain echocardiogram showing decreased global longitudinal strain (-1.6%) with a relative apical sparing pattern

heart-to-contralateral lung (H/CL) ratio of 1.6 at 1 h after radiotracer injection (Fig. 18.19). Genetic testing revealed the presence of the V142I mutation. He was diagnosed with hereditary TTR cardiac amyloidosis years after initial heart failure hospitalization.

The patient's disease course was notable for new-onset AF requiring anticoagulation, autonomic neuropathy with orthostatic hypotension requiring discontinuation of guideline-directed medical treatment (GDMT) for heart failure, and gastroparesis requiring prokinetics. He was started on doxycycline, tauroursodeoxycholic acid (TUDCA), and tafamidis. Genetic testing was offered to his brother who tested negative for any pathologic mutations.

18.10 Case 4

Key points:

- Multiple combinations of forms of monoclonal gammopathy (such as monoclonal gammopathy of undetermined significance, smoldering or asymptomatic multiple

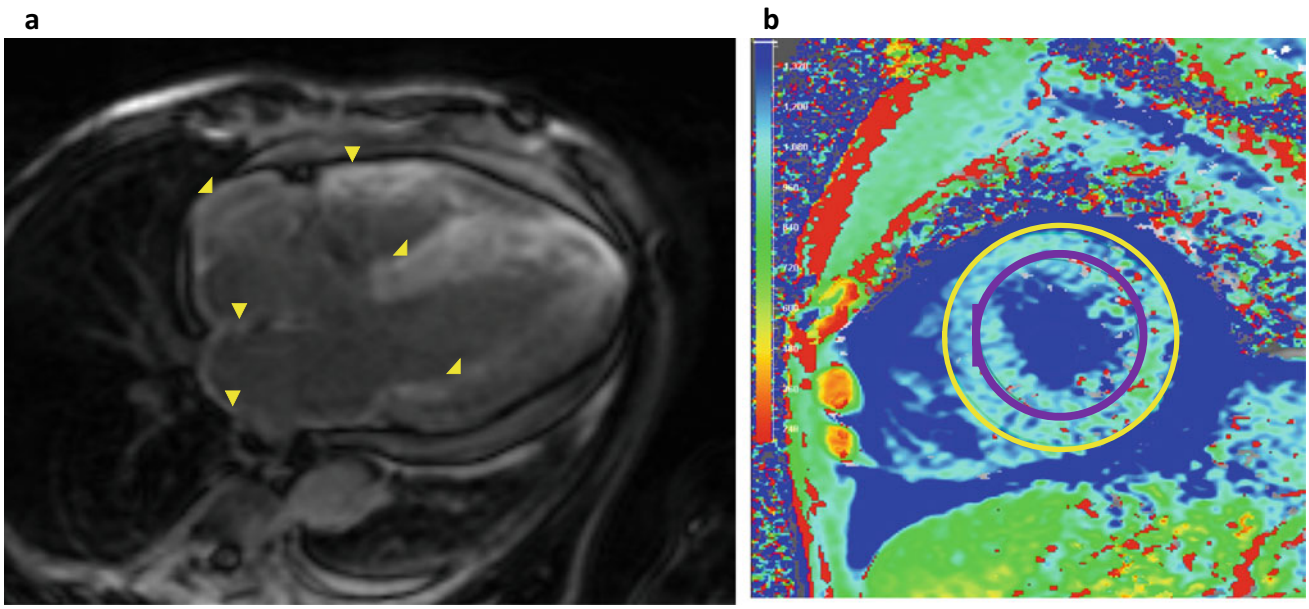

Fig. 18.18 Cardiac magnetic resonance. **a** Four-chamber view showing diffuse biatrial, biventricular, and interatrial septum late gadolinium enhancement on phase-sensitive inversion recovery sequence (arrowheads indicate myocardial enhancement which appears brighter when compared to blood). **b** Precontrast modified Look-Locker imaging (MOLLI) sequence acquired in short-axis orientation at mid-left ventricular cavity. Image depicts elevated native myocardial T1 at 1141 ms, which is abnormally elevated and is seen in patients with amyloidosis. Images acquired on Canon Vantage Titan/Zen Edition 1.5 T MR system

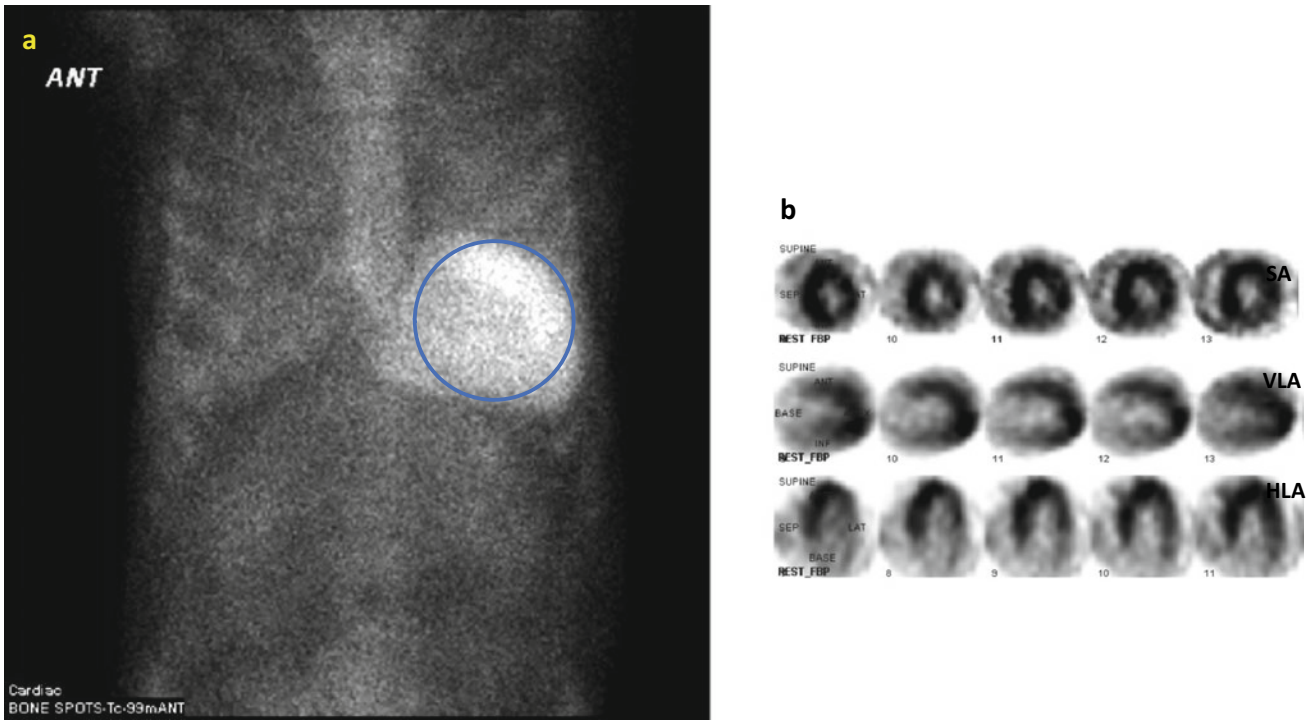

Fig. 18.19 **a** Technetium-99 m pyrophosphate (Tc-99 m PYP) scintigraphy at 1 h after radiotracer injection showing myocardial PYP uptake, with a semiquantitative or visual grade of 3 and heart-to-contralateral lung (H/CL) ratio of 1.6. **b** SPECT confirms myocardial radiotracer uptake. *SA*, short axis; *VLA*, vertical long axis; *HLA*, horizontal long axis

myeloma, and multiple myeloma) and cardiac amyloidosis can exist within a patient [17]. Proper identification of cardiac amyloidosis subtype, whether AL versus ATTR, is important due to prognostic and treatment implications.
  - Differentiation of AL from ATTR is critical due to the rapidly progressive course in AL.
  - A misdiagnosis of AL can lead to unnecessary chemotherapy or light chain-suppressive therapy with associated treatment-related adverse effects, and potentially missing a hereditary disease.
- Biopsy is necessary in patients with cardiac amyloidosis and monoclonal gammopathy for accurate diagnosis.
  - In cases of negative or equivocal results from less invasive organ biopsies (e.g., abdominal fat pad, rectal, bone marrow), biopsy of an involved organ such as the heart to optimize sensitivity should be pursued.
- Patient's decisions should be respected in cases of biopsy deferral or refusal. In these cases, the value of close follow-up and clues from overall clinical picture including disease course should not be discounted.

An 81-year-old African American female with a history of heart failure with preserved EF, persistent AF, stable stage 3 chronic kidney disease, diabetes mellitus, and mild cognitive impairment was referred to cardiology clinic for recurrent heart failure hospitalizations over the past year. Blood pressure was in the low-normal range (100–110/50–60 mmHg) and she remained in rate-controlled AF off any AV nodal blockers. ECG showed rate-controlled AF with low-voltage QRS complexes (Fig. 18.20). Echocardiogram with strain imaging showed moderate concentric left ventricular hypertrophy and mild diffuse hypokinesis with an ejection fraction of 40–45%, biatrial dilation, RV dilation and dysfunction, severe tricuspid regurgitation, and decreased GLS of −12% with a relative apical sparing pattern (Fig. 18.21). Cardiac magnetic resonance showed diffuse biventricular and biatrial late gadolinium enhancement, highly suggestive of cardiac amyloidosis (Fig. 18.22). Technetium-99 m pyrophosphate (PYP) scintigraphy was strongly suggestive of transthyretin (TTR) cardiac amyloidosis, with a semiquantitative or visual grade of 3 and H/CL ratio of 1.4 at 1 h after radiotracer injection (Fig. 18.23). Hematological testing demonstrated an IgA-kappa monoclonal gammopathy (serum IgA 644 mg/dL, serum kappa FLC 26.1 mg/L) with an elevated serum-free light chain (FLC) ratio of 4.18 (normal 0.26–1.65). A bone marrow biopsy was subsequently performed, which showed 20% plasma cells without any amyloid deposition. However, the diagnosis of light chain amyloidosis (AL) could still not be

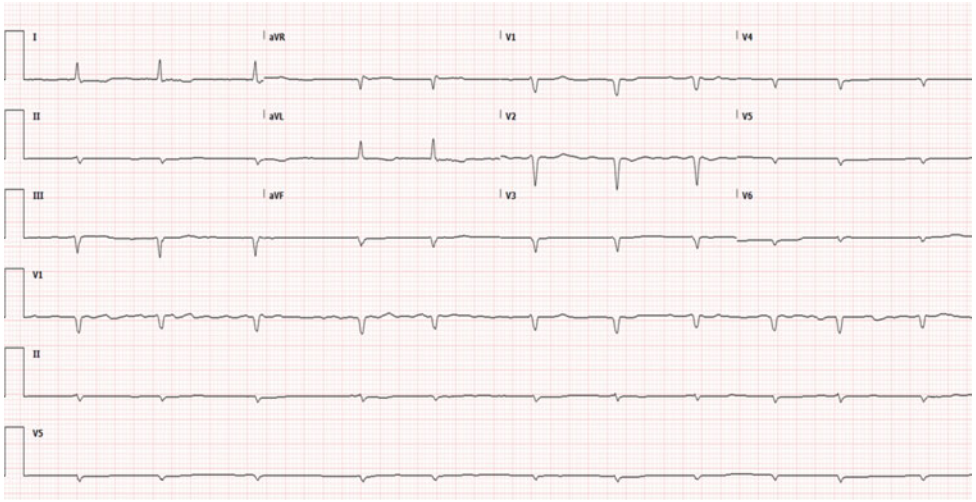

Fig. 18.20 ECG, rate-controlled atrial fibrillation with low-voltage QRS complexes

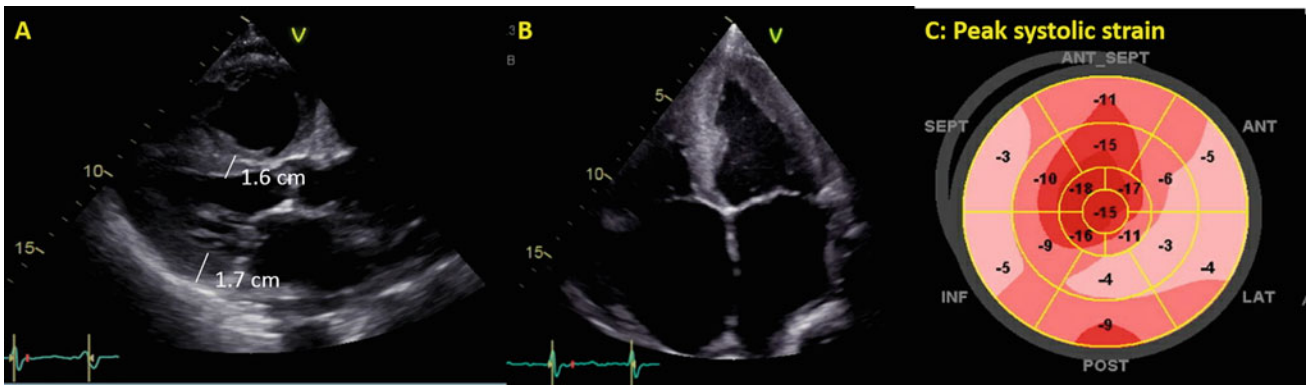

Fig. 18.21: 2D transthoracic echocardiogram **a** parasternal long axis and **b** apical four-chamber views in end diastole showing concentric moderate left ventricular hypertrophy, right ventricular dilation, and biatrial dilation. **c** Strain echocardiogram showing decreased left ventricular global longitudinal strain (−12.0%) with a relative apical sparing pattern

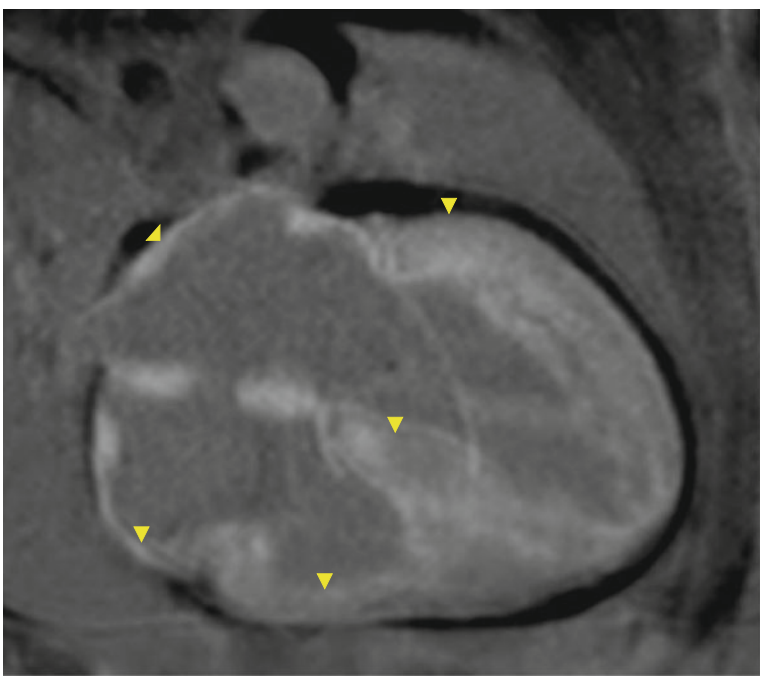

Fig. 18.22 Cardiac magnetic resonance four-chamber view, showing diffuse biatrial and biventricular myocardial late gadolinium enhancement on phase-sensitive inversion recovery sequence (arrowheads indicate myocardial enhancement which appears brighter when compared to blood). Image acquired on Canon Vantage Titan/Zen Edition 1.5 T MR system

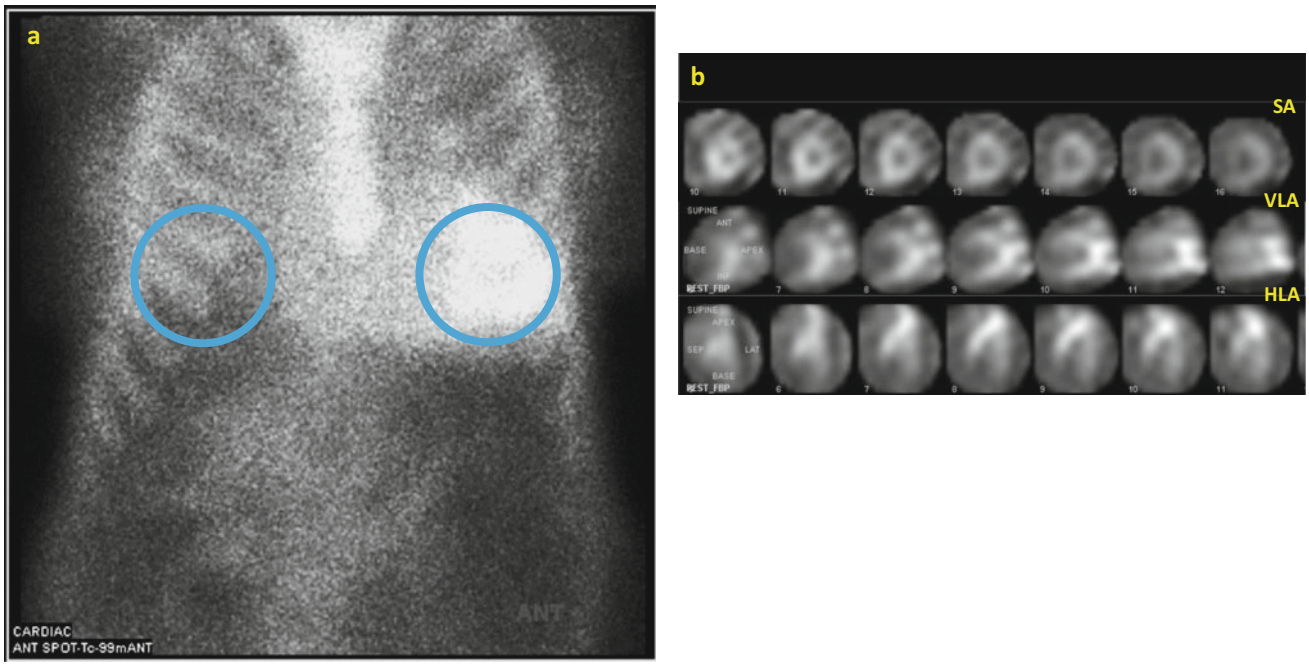

Fig. 18.23 **a** Technetium-99 m pyrophosphate (Tc-99 m PYP) scintigraphy 1 h after radiotracer injection showing marked radiotracer uptake with a semiquantitative grade of 3 and a heart-to-contralateral lung (H/CL) ratio of 1.4. **b** SPECT images confirm myocardial PYP uptake. *SA*, short axis; *VLA*, vertical long axis; *HLA*, horizontal long axis

definitively excluded without biopsy of an involved organ—in this case an endomyocardial biopsy (EMB). After discussion with the patient, family, and primary hematologist regarding procedural risks of EMB and treatment-related adverse effects of chemotherapy in the likelihood of diagnosis of AL, EMB was deferred. From the hematological standpoint, she was diagnosed as smoldering or asymptomatic multiple myeloma.

Follow-up showed stable levels of serum FLC, unexpected in the course of untreated AL. Genetic testing revealed the presence of the V122Ile variant allele. She required de-escalation of medications for heart failure due to hypotension, and intensification of diuretic regimen. The patient was ultimately diagnosed as hereditary TTR cardiac amyloidosis with concomitant smoldering multiple myeloma. She was started on doxycycline, tauroursodeoxycholic acid (TUDCA), and tafamidis for disease-specific TTR cardiac amyloidosis therapy.

18.11 Case 5

Key points:

- Pseudosevere aortic stenosis can be seen in patient with TTR amyloidosis due to decreased stroke volume, particularly in those with reduced EF [18].
- Recognition of TTR amyloidosis prior to aortic valve replacement is crucial for appropriate management.
- Cardiac CT angiography with aortic valve calcium scoring is valuable in assessing severity of aortic stenosis in patients with conflicting parameters on echocardiogram.
- Accumulation of immunoglobulin-free light chains in the absence of a hematologic disorder can be seen in patients with chronic kidney disease.

An 82-year-old man was evaluated for a history of recurrent heart failure hospitalizations, paroxysmal atrial fibrillation with resting bradycardia, and stable stage 3 non-proteinuric chronic kidney disease. Vital signs showed blood pressures in the low-normal range and heart rate of 54 beats per minute. ECG showed sinus rhythm with first-degree AV block and low-voltage QRS complexes in limb lead (Fig. 18.24). Echocardiogram showed moderate left ventricular hypertrophy with severe diffuse hypokinesis, ejection fraction of 25–30%, and decreased global longitudinal strain of −8.3% with a relative apical sparing pattern (Fig. 18.25, Video 18.8). He also had mildly thickened aortic valve leaflets with reduced leaflet separation and low-flow low-gradient severe aortic stenosis with a peak velocity of 2.4 m/s, peak gradient of 23 mmHg, dimensionless index of 0.22, aortic valve area (continuity equation) of 0.7 cm^2, and indexed valve area of 0.35 cm^2/m^2 (Fig. 18.26, Video 18.9). Cardiac computed tomography

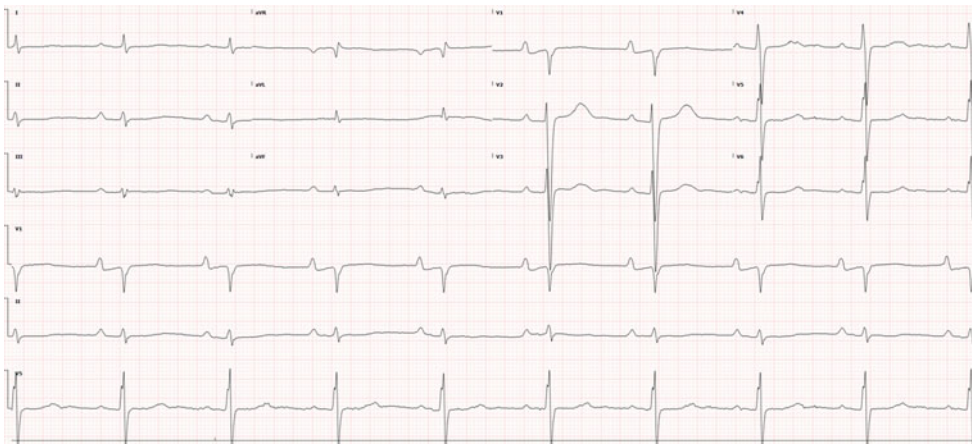

Fig. 18.24 ECG showing sinus rhythm, first-degree AV block, and low-voltage limb lead QRS complexes

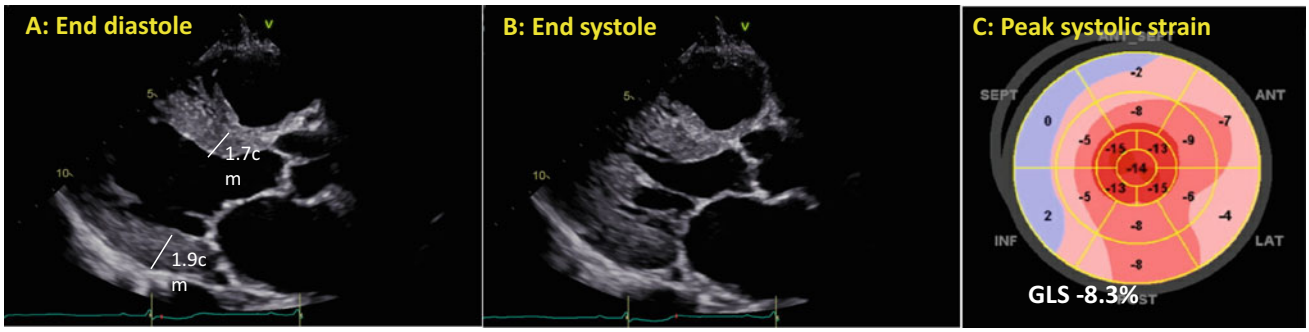

Fig. 18.25: 2D transthoracic echocardiogram with strain. Parasternal long-axis view at **a** end diastole and **b** end systole showing severe concentric left ventricular hypertrophy and increased ventricular mass. Interventricular septal thickness 1.7 cm, posterior wall thickness 1.9 cm. Left ventricular ejection fraction 25–30%. C) Speckle tracking strain imaging showing decreased global longitudinal strain (-8.3%) with a relative apical sparing pattern

(CT) for assessment of aortic stenosis severity showed aortic valve calcium score of 1645 Agatston units (cutoff for severe AS in men: 2065 Agatston units) and aortic valve area (by planimetry) of 1.54 cm^2, consistent with mild-to-moderate aortic stenosis (Fig. 18.27). Evaluation of cardiac amyloidosis was pursued. Hematologic evaluation showed no monoclonal gammopathy and nonspecific elevations of serum-free light chains with a normal kappa/lambda ratio. Technetium-99 m pyrophosphate (PYP) scintigraphy showed a semiquantitative or a visual grade of 3 and H/CL of 1.6, which were confirmative for transthyretin (TTR) cardiac amyloidosis (Fig. 18.28). Genetic testing was negative for any pathologic mutations. This diagnosis of wild-type TTR cardiac amyloidosis was made almost 2 years after initial heart failure hospitalization. His disease course was characterized by intolerance to standard heart failure therapies and discontinuation of beta blocker and ACE inhibitor. He was started on doxycycline, tauroursodeoxycholic acid (TUDCA), and tafamidis.

18.12 Case 6

Key points:

- Cardiac ischemia can occur despite normal coronaries due to amyloid infiltration of the intramyocardial or micro-vessels, perhaps accounting for this patient's EKG changes.
- Complete hematologic response and changes in NT-proBNP with treatment are strongly correlated with better survival.
- Patients who achieved hematologic response are more likely to have cardiac response [15].

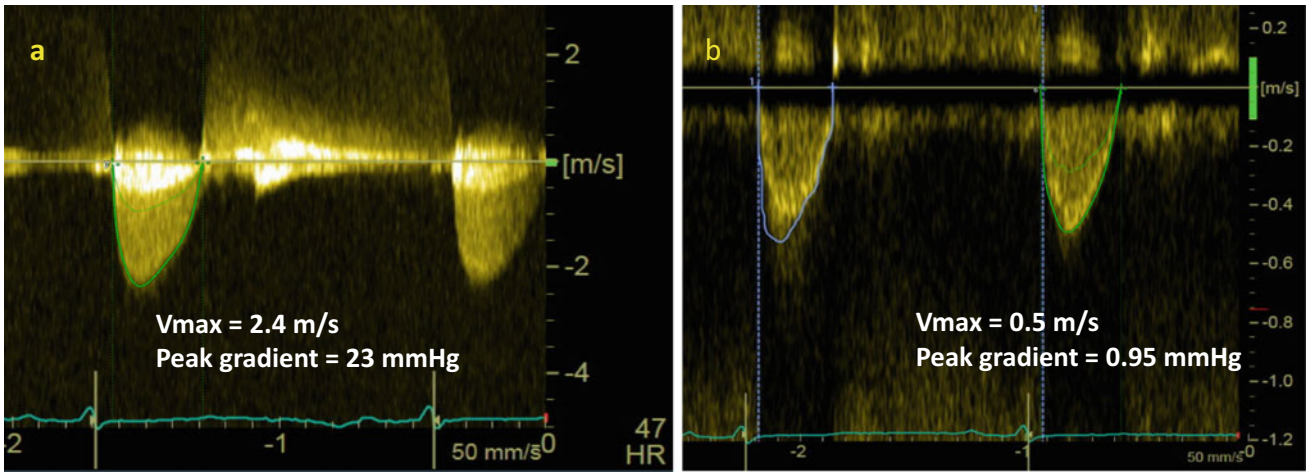

Fig. 18.26 **a** Continuous wave Doppler through aortic valve and **b** pulse wave Doppler through the left ventricular outflow tract showing a peak velocity of 2.4 m/s, peak gradient of 23 mmHg through the aortic valve. Dimensionless index is 0.22. The aortic valve area calculated by continuity equation is 0.7 cm^2 (indexed to body surface area 0.35 cm^2/m^2). Measurements consistent with low-flow low-gradient severe aortic stenosis. *Vmax*, maximum velocity

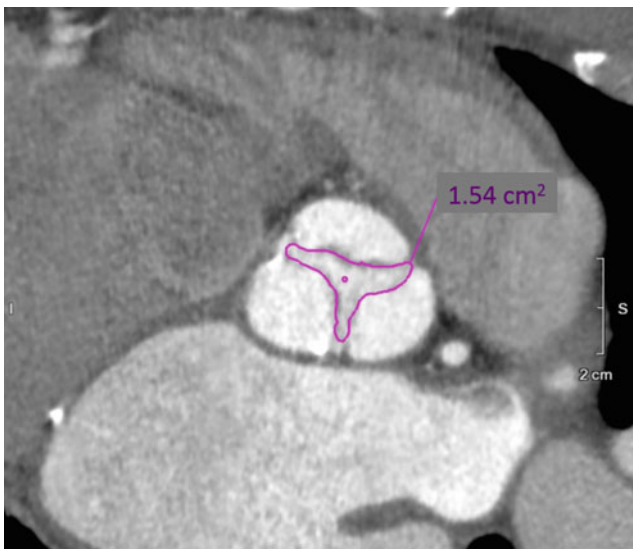

Fig. 18.27 Cardiac computed tomography angiography at the level of the aortic valve in systole showing a planimetered aortic valve area of 1.54 cm^2. The corresponding aortic valve calcium score was 1645 Agatston units

This is a 58-year-old woman with history of AL amyloidosis with neurologic, renal, and cardiac involvement. One and a half years prior to her diagnosis, she started to experience pain in her shoulders, lower neck, and legs as well as paresthesia in the hands and feet, and dyspnea on exertion. She was referred for a rheumatologic workup which showed elevated ESR and was presumed to have polymyalgia rheumatica. She was started on prednisone with some relief. She then developed congestive heart failure and was admitted to the hospital. Her ECG showed ST and T wave changes suggestive of anterolateral ischemia (Fig. 18.29). 2D echocardiogram revealed concentric LV hypertrophy with LVEF of 33% and GLS of 6.1% (Fig. 18.30, Video 18.10). Her serum cardiac biomarkers were elevated (troponin I = 0.79 ng/ml; NT-proBNP 3312 pg/ml). She underwent cardiac catheterization which showed normal coronary arteries though LV filling pressure was elevated with a LV end diastolic pressure of 25 mm Hg. She was started on Lasix with symptomatic improvement. For the management of her AL amyloidosis, bortezomib and dexamethasone were started followed by high-dose melphalan therapy with stem cell transplant. She responded well and achieved hematologic complete remission. She remained in complete remission 2 years post treatment with significant improvement in functional capacity to NYHA Class I. Follow-up echo showed improvement in LVEF to 50% and GLS to −14.1% (Fig. 18.31, Video 18.11). The NT-proBNP was significantly lower at 513 pg/ml.

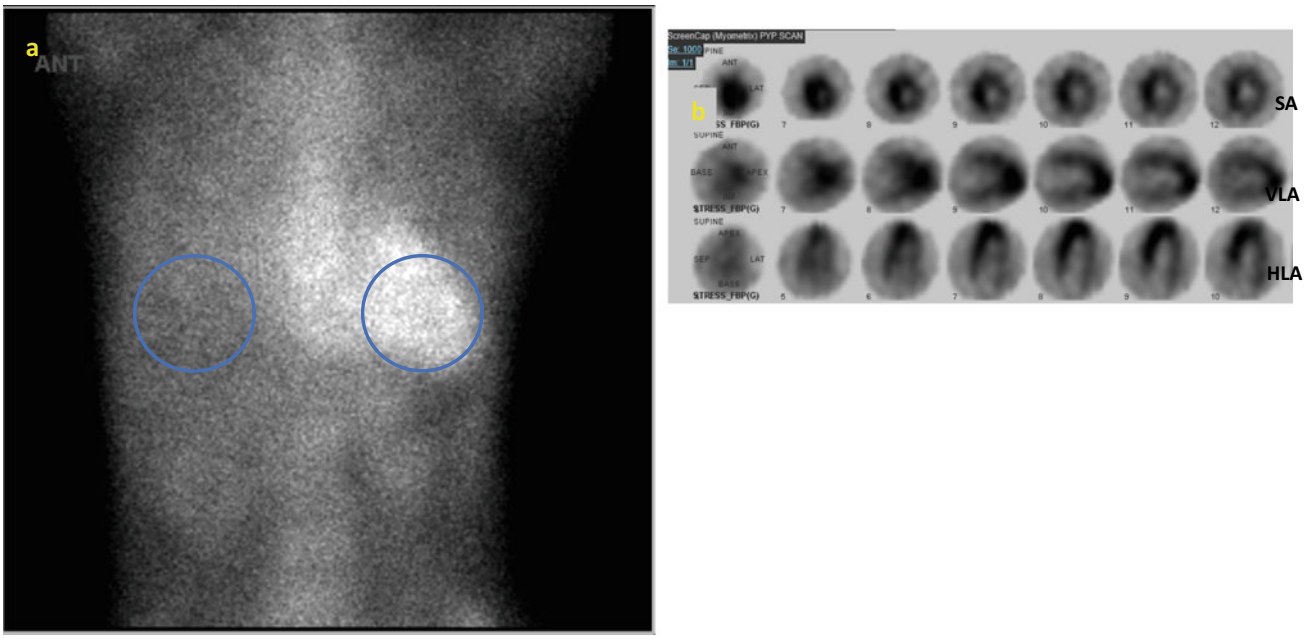

Fig. 18.28 **a** Technetium-99 m pyrophosphate (PYP) scintigraphy 1 h after radiotracer injection showing myocardial PYP uptake with a semiquantitative or visual grade of 3 and heart-to-contralateral lung (H/CL) ratio of 1.6. **b** PYP SPECT confirming myocardial radiotracer uptake. *SA*, short axis; *VLA*, vertical long axis; *HLA*, horizontal long axis

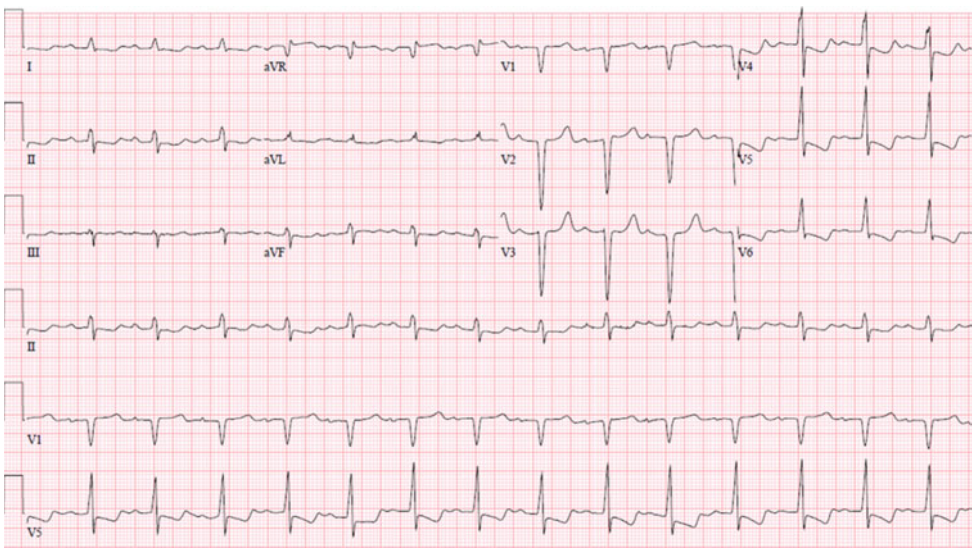

Fig. 18.29 ECG shows sinus rhythm with poor R wave progression; ST and T wave abnormality consistent with anterolateral ischemia

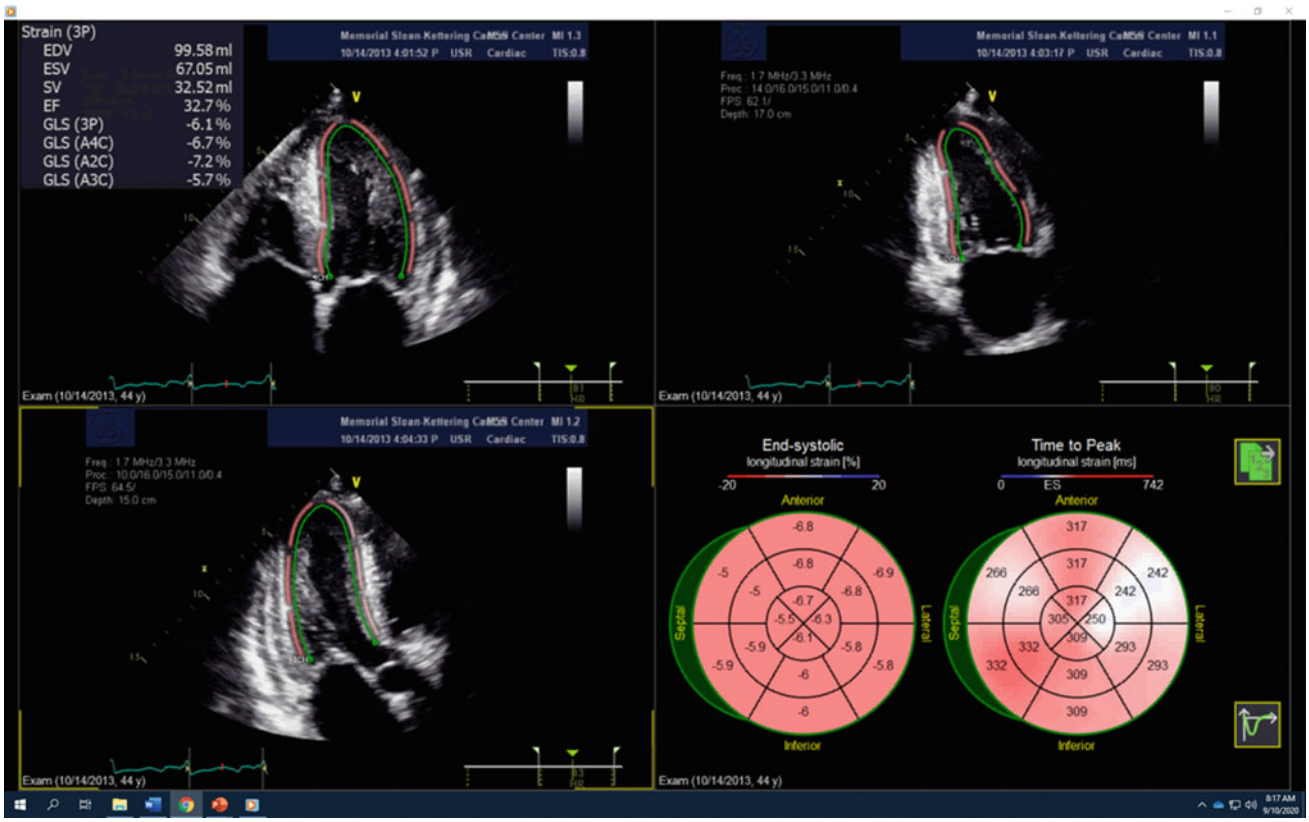

Fig. 18.30 Echo at the time of CHF presentation shows LVEF of 33% with a GLS of −6.1%

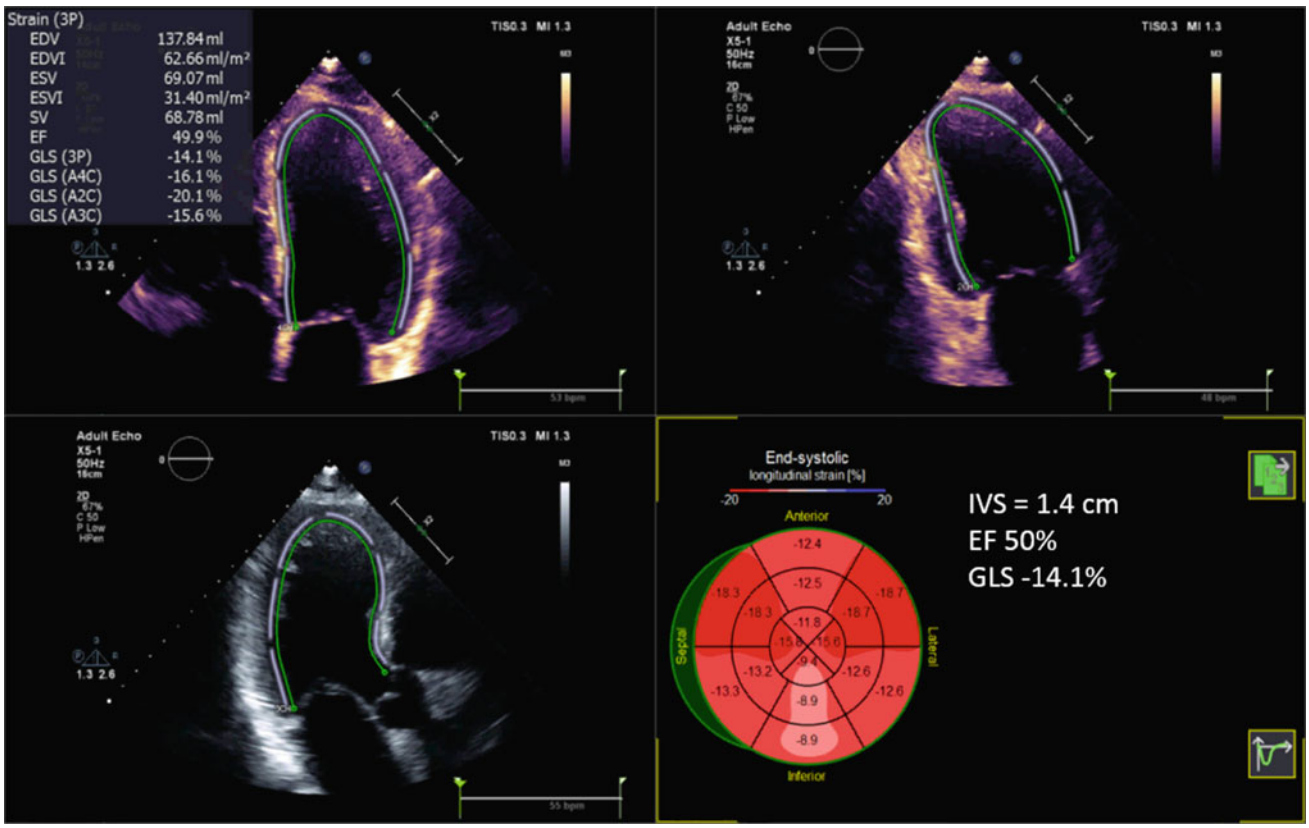

Fig. 18.31 Echo after control of light chains showing an increase in LVEF to 50% and GLS to −14.1%

References

1. Kholova I, Niessen HW. Amyloid in the cardiovascular system: a review. J Clin Pathol. 2005;58:125–33.
2. Sipe JD, Benson MD, Buxbaum JN, et al. Nomenclature 2014: amyloid fibril proteins and clinical classification of the amyloidosis. Amyloid. 2014;21:221–4.
3. Quock TP, Yan T, Chang E, Guthrie S, Broder MS. Epidemiology of AL amyloidosis: a real-world study using US claims data. Blood Adv. 2018;2:1046–53.
4. Damrauer SM, Chaudhary K, Cho JH, et al. Association of the V122I hereditary transthyretin amyloidosis genetic variant with heart failure among individuals of African or Hispanic/Latino ancestry. JAMA. 2019;322:2191–202.
5. Phelan D, Collier P, Thavendiranathan P, et al. Relative apical sparing of longitudinal strain using two-dimensional speckle-tracking echocardiography is both sensitive and specific for the diagnosis of cardiac amyloidosis. Heart. 2012;98:1442–8.
6. Syed IS, Glockner JF, Feng D, et al. Role of cardiac magnetic resonance imaging in the detection of cardiac amyloidosis. JACC Cardiovasc Imaging. 2010;3:155–64.
7. Philippakis AA, Falk RH. Cardiac amyloidosis mimicking hypertrophic cardiomyopathy with obstruction: treatment with disopyramide. Circulation. 2012;125:1821–4.
8. Gillmore JD, Maurer MS, Falk RH, et al. Nonbiopsy diagnosis of cardiac transthyretin amyloidosis. Circulation. 2016;133:2404–12.
9. El-Am EA, Dispenzieri A, Melduni RM, et al. Direct current cardioversion of atrial arrhythmias in adults with cardiac amyloidosis. J Am Coll Cardiol. 2019;73:589–97.
10. Lin G, Dispenzieri A, Kyle R, Grogan M, Brady PA. Implantable cardioverter defibrillators in patients with cardiac amyloidosis. J Cardiovasc Electrophysiol. 2013;24:793–8.
11. Maurer MS, Schwartz JH, Gundapaneni B, et al. Tafamidis treatment for patients with transthyretin amyloid cardiomyopathy. N Engl J Med. 2018;379:1007–16.
12. Barrett CD, Alexander KM, Zhao H, et al. Outcomes in patients with cardiac amyloidosis undergoing heart transplantation. JACC Heart Fail. 2020;8:461–8.
13. Kumar S, Dispenzieri A, Lacy MQ, et al. Revised prognostic staging system for light chain amyloidosis incorporating cardiac biomarkers and serum free light chain measurements. J Clin Oncol. 2012;30:989–95.
14. Pun SC, Landau HJ, Riedel ER, et al. Prognostic and added value of two-dimensional global longitudinal strain for prediction of survival in patients with light chain amyloidosis undergoing autologous hematopoietic cell transplantation. J Am Soc Echocardiogr. 2018;31:64–70.
15. Palladini G, Dispenzieri A, Gertz MA, et al. New criteria for response to treatment in immunoglobulin light chain amyloidosis based on free light chain measurement and cardiac biomarkers: impact on survival outcomes. J Clin Oncol. 2012;30:4541–9.
16. Asif T, Araujo T, Singh V, Malhotra S. High prevalence of heart failure with reduced ejection fraction in patients with transthyretin cardiac amyloidosis. J Nucl Cardiol. 2020;27:1044–6.
17. Lee Chuy K, Gomez J, Malhotra S. Coexistent transthyretin amyloid cardiomyopathy and monoclonal gammopathy: diagnostic challenges and prognostic implications. J Nucl Cardiol. 2020.
18. Sperry BW, Jones BM, Vranian MN, Hanna M, Jaber WA. Recognizing transthyretin cardiac amyloidosis in patients with aortic stenosis: impact on prognosis. JACC Cardiovasc Imaging. 2016;9:904–6.

Stress-Induced Cardiomyopathy

19

Richard M. Steingart

Key Points

- Takotsubo syndrome is conveniently defined by the Mayo clinic criteria [1].
- Takotsubo syndrome prognosis is worse in patients with cancer than without cancer.
- Deep T-wave inversions are characteristic.
- Apical ballooning with left ventricular dysfunction out of proportion to troponin elevation is also characteristic.
- Ventricular function typically improves over days to weeks.
- Coronary artery disease should be excluded in every case.
- Non-ischemic cardiomyopathy should be considered in every case.

19.1 Introduction

The diagnosis and management of ventricular dysfunction is central to the practice of cardio-oncology. There is a high prevalence of hypertensive, ischemic, and valvular heart diseases in cancer patients. Superimposed on this disease background, cancer patients are exposed to cardiotoxic medical treatments, major surgeries, infections, profound emotional stressors, disorders of clotting and bleeding, autoimmune assaults, hormonal disruptions, and paraneoplastic syndromes all of which can contribute to ventricular dysfunction. Physician-scientists and clinicians strive to compartmentalize ventricular dysfunction into distinct categories as an aid in the understanding of the disease. But the practice of cardio-oncology does not often afford such a luxury in that most clinical presentations involving ventricular dysfunction have multifactorial determinants. That said, exploring the entity of stress cardiomyopathy provides a good conceptual framework for the examination of acute ventricular dysfunction in cancer patients.

Stress-induced cardiomyopathy or the Takotsubo syndrome as defined by the Mayo clinic criteria [1]:

1. Transient akinesis or dyskinesis of the left ventricular apical and mid-ventricular segments with regional wall motion abnormalities extending beyond a single epicardial vascular distribution.
2. Absence of obstructive coronary artery disease (CAD) or angiographic evidence of acute plaque rupture.
3. New electrocardiographic abnormalities (ST-segment elevation or T-wave inversion).
4. Absence of
   a. Recent significant head trauma.
   b. Intracranial bleeding.
   c. Pheochromocytoma.
   d. Obstructive epicardial CAD.
   e. Myocarditis.
   f. Hypertrophic cardiomyopathy.

Stress cardiomyopathy is a common occurrence among cancer patients, but as will be illustrated by the cases presented in this chapter, the pathophysiology of left ventricular dysfunction in cancer patients is far from clear-cut. Joy et al. describe an analysis of the National Inpatient Survey (NIS) taken between 2007 and 2013. The NIS is a stratified sample of 20% of United States hospitals. The hospital mortality for Takotsubo syndrome patients with cancer was 13.8% compared with 2.9% in those without cancer [2]. Risks for mortality included solid cancer, stroke, and heart failure. In a report of the International Takotsubo Registry, malignancy was present in 16.6% of patients with the syndrome, and not surprisingly, cancer patients with Takotsubo syndrome had a highly adverse long-term prognosis

Electronic supplementary material
The online version of this chapter (https://doi.org/10.1007/978-3-030-70998-3_19) contains supplementary material, which is available to authorized users.

R. M. Steingart (✉)
Department of Medicine, Memorial Sloan Kettering Cancer Center, 1275 York Avenue, New York, NY 10065, USA
e-mail: steingar@mskcc.org

R. M. Steingart et al. (eds.), *Atlas of Imaging in Cardio-Oncology*,
https://doi.org/10.1007/978-3-030-70998-3_19

compared to Takotsubo patients without malignancy in whom the prognosis is generally favorable. In cancer patients, physical factors were common triggers, whereas emotional stressors were common Takotsubo precipitants in those without cancer [3].

The pathophysiology of the Takotsubo syndrome is controversial [4]. Angelini argues that the entity results from coronary spasm and the only reliable test for Takotsubo syndrome is to reproduce coronary spasm and left ventricular dysfunction with intracoronary acetylcholine infusion, which is rarely if ever employed in clinical practice [4]. Further, the heightened spasticity that can be provoked by acetylcholine testing around the time of Takotsubo presentation appears to be a transient phenomenon that disappears between 1 and 10 days after the onset of the syndrome [4]. Angelini acknowledges that the excess catecholamine myocyte toxicity theory currently holds sway over coronary spasticity as the mechanism behind the Takotsubo syndrome. Microvascular dysfunction may also play a role. These mechanisms can be activated by various stressors, which include emotional or psychological stress, infection, surgery, medications, and exacerbation of chronic diseases. Certain cancer drugs have been implicated in triggering this Takotsubo cardiomyopathy (e.g., 5FU) [5]. A genetic predisposition for Takotsubo syndrome has also been postulated given the preponderance of familial cases [4].

Hypotension, tachycardia, anemia, prothrombic states, cytokine excess, surgical stresses, emotional stress, electrolyte disturbances, large and small vessel coronary disease, altered vessel reactivity, catecholamine excess, drug toxicities, preexisting myocardial scarring, and/or valvular disease commonly coexist in cancer patients. These circumstances are vastly different from the Takotsubo syndrome originally described in emotionally stressed middle-aged women who were presumed to have otherwise "normal" hearts [6]. This complexity in the cancer patient is what makes the cases from our Memorial Sloan Kettering experience in this Atlas so interesting and important.

19.2 Case 1. Rapid Resolution of Takotsubo Left Ventricular Dysfunction in the Setting of Metastatic Cancer and Sepsis

A 35-year-old woman with HIV, metastatic pancreatic cancer presenting with sepsis, shock treated with vasopressors underwent echocardiography which demonstrated the classic features of the Takotsubo syndrome (Fig. 19.1, Video 19.1). Just 2 weeks later after treatment of sepsis, extubation, and discontinuation of vasopressors, the echocardiogram was normal. (Fig. 19.1, Video 19.1) This rapid resolution of left ventricular dysfunction is characteristic of the classically described Takotsubo syndrome. This patient received low-dose diuretics, beta-blockers, and ace inhibitors with dosing limited by low blood pressure. There is some evidence that ACE inhibitors or angiotensin receptor blockers may potentiate ventricular recovery and prevent recurrence [7]. Interestingly, there is no compelling evidence that beta-blockers are helpful in this regard. In the unusual circumstance where Takotsubo syndrome is associated with outflow tract obstruction and hypotension due to hyperdynamic motion at the base of the heart, beta-blockers can be useful in select cases by relieving the outflow obstruction [7].

19.3 Case 2. Takotsubo Left Ventricular Dysfunction Late After Adriamycin Therapy for Breast Cancer with Atypical Features and a Prolonged Course to Recovery

A 55-year-old woman underwent neoadjuvant doxorubicin-based chemotherapy for breast cancer in 2007, ejection fraction (EF) by MUGA was 62% at the start of therapy. Shortly thereafter she was admitted to a local hospital with pneumonia and tachycardia EF 55%. After recovery from this episode, she underwent bilateral mastectomy and radiation therapy. She was admitted again some six months later with RUQ pain, nausea, and vomiting. Cardiology consulted, echocardiogram reported as normal with EF 55%. A day or two after that echocardiogram, EF by MUGA scan was 20%. Transferred to MSKCC where repeat EF by echo was 20%. Cardiac monitoring showed sinus rhythm with runs of SVT. CT pulmonary angiogram negative for pulmonary embolism but splenic and kidney infarcts were present. She was started on anticoagulation, low-dose ace inhibitor, and carvedilol. Nuclear stress test was negative for ischemia, with a dilated ventricle consistent with cardiomyopathy. Carvedilol and lisinopril up titrated to full dosing. Over the course of 1.5–2 years, the EF rose into the normal range confirmed by echocardiographic and MUGA studies. The course of her disease is shown in Fig. 19.2 and Video 19.2.

In the echocardiogram acquired at the time of the patient's presentation with acute shortness of breath, there is a suggestion of mild apical ballooning with relatively preserved motion at the base of the heart but the images are not classic for the "apical ballooning" syndrome. Speaking in favor of a Takotsubo-like syndrome, there was evidence that ventricular function was normal the day before the abnormal study was done, and myocardial infarction was ruled out. Speaking against a Takotsubo like syndrome was the slow recovery of ventricular function over more than a year. Classically, Takotstubo recovery is rapid as shown in Video 19.1. One can speculate that the etiology of the ventricular

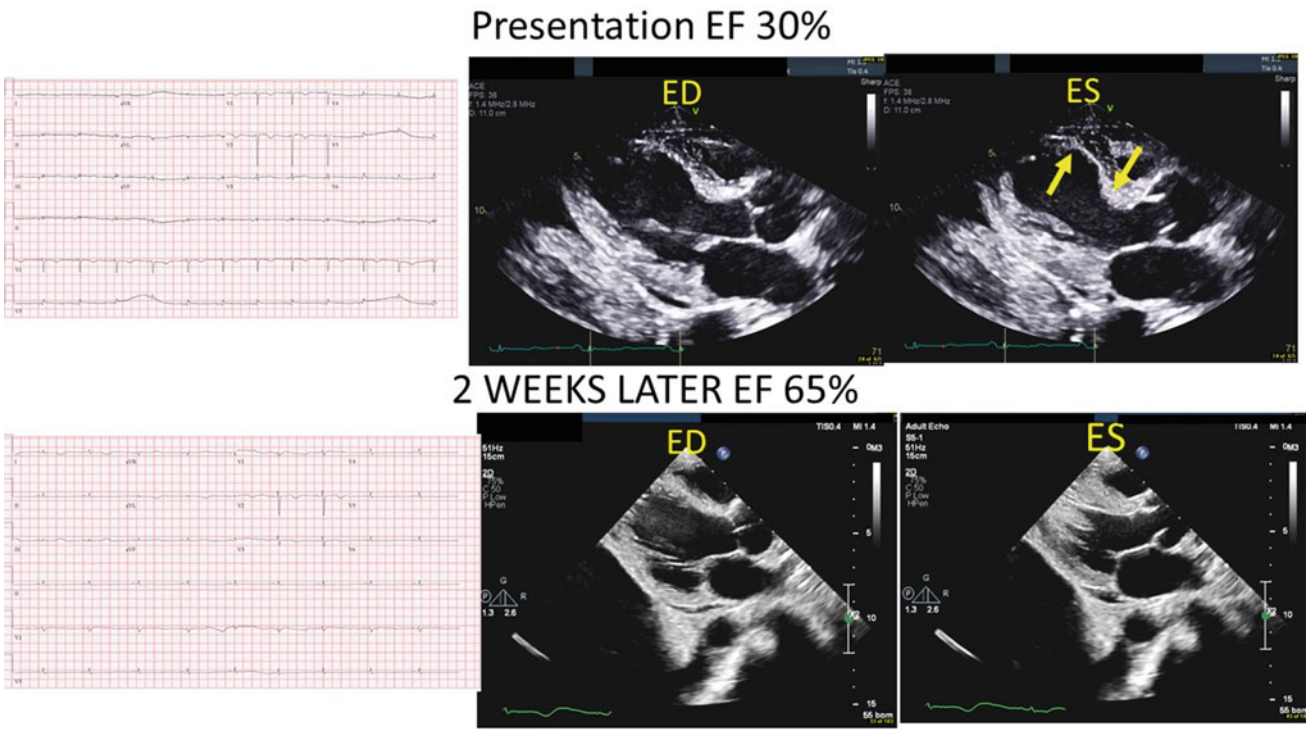

Fig. 19.1 Top panel, End diastolic (ED) and end systolic (ES) frames from echocardiogram recorded while patient on pressor support in the ICU, intubated. Up facing arrow in ES frame illustrates characteristic apical ballooning. Down facing arrow shows a neck at the base of the ventricle caused by hyperdynamic wall motion in this zone. Ejection fraction (EF) 30%. In some patients, this hyperdynamic motion at the base of the heart is associated with hemodynamically significant outflow tract obstruction. Bottom panel, Two weeks later after treatment of sepsis, discontinuation of vasopressors with the patient extubated, wall motion is normal and the EF has risen to 65%. The patient had started treatment with low dose ACE inhibitors and beta blockers

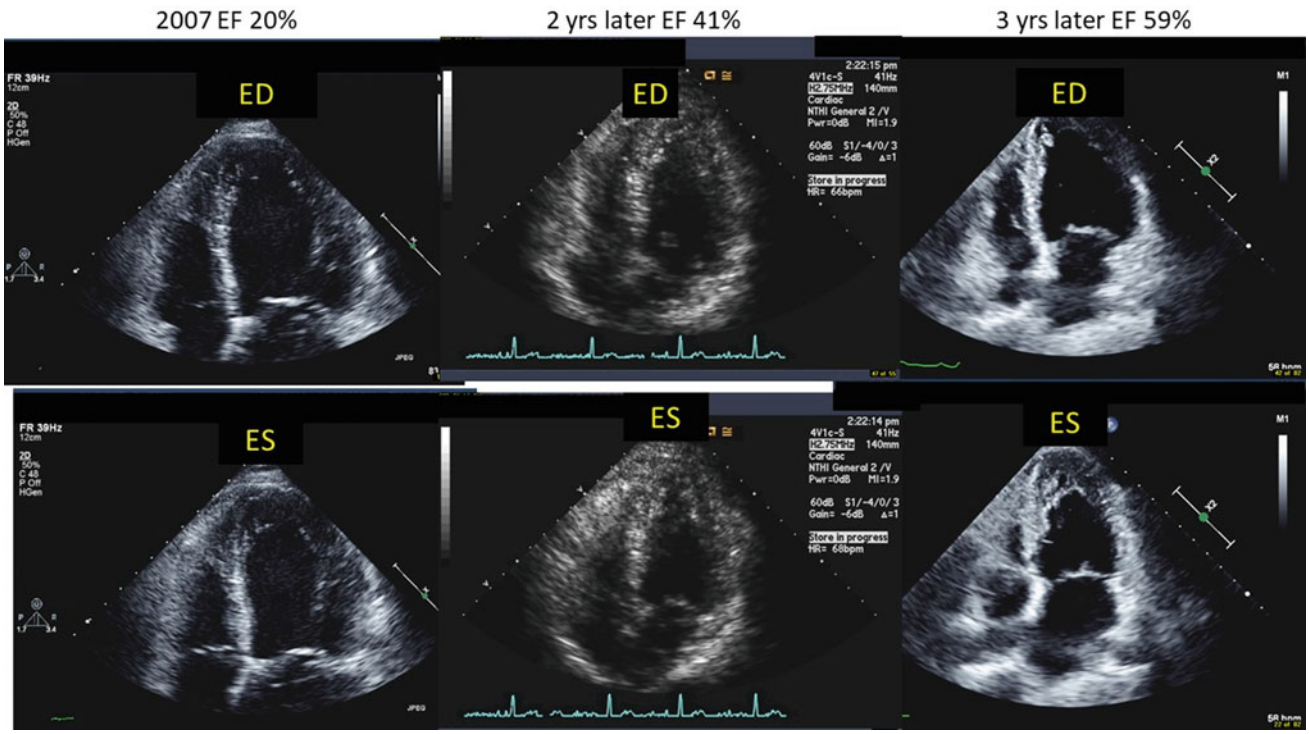

Fig. 19.2 ED and ES images at presentation with heart failure, and then at approximately one and two years after the index event which was consistent with the Takotsubo syndrome

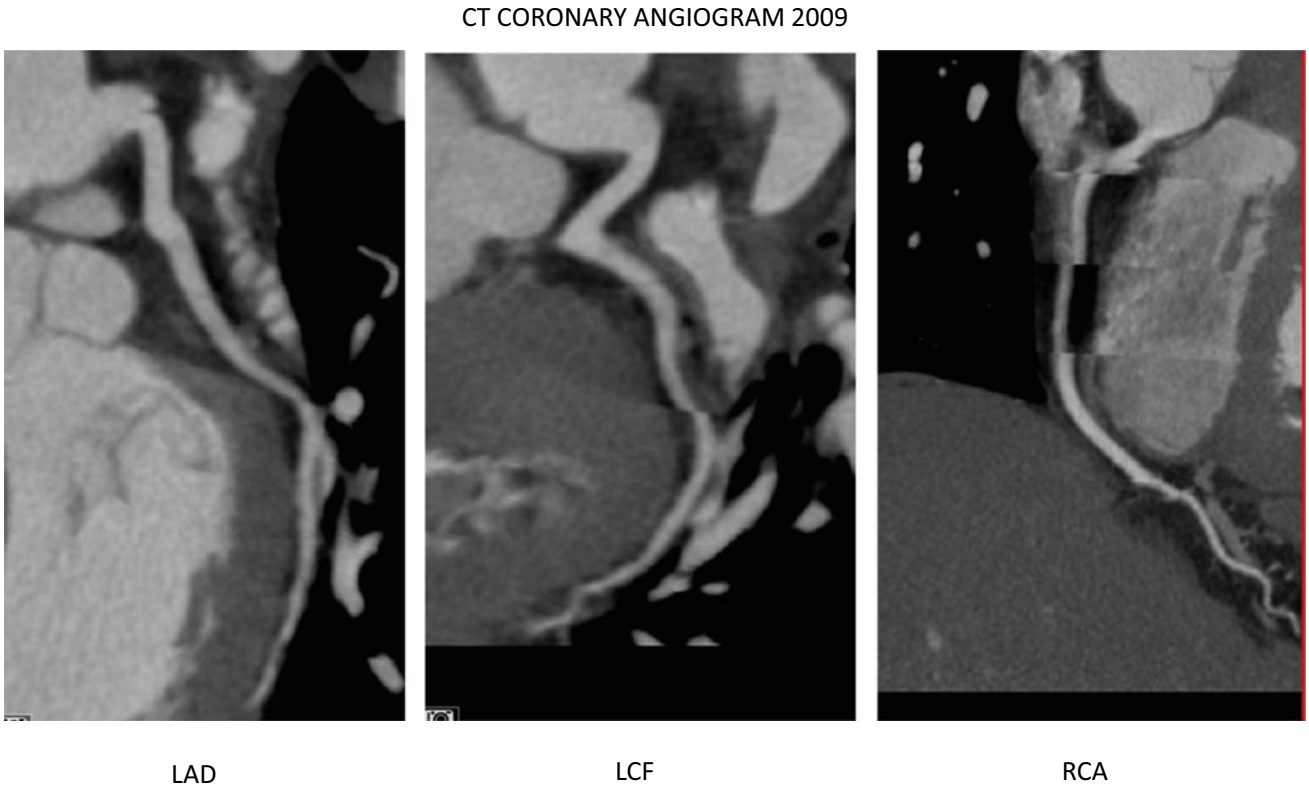

Fig. 19.3 CT coronary angiogram revealing no significant obstructive coronary artery disease. The possibility of coronary artery disease should be entertained in every cancer patient that presents with ventricular dysfunction

dysfunction observed in this patient was multifactorial with elements of prior Adriamycin exposure, infection, and "stress" all playing a role.

To ensure that obstructive CAD was not contributing to left ventricular dysfunction, the patient underwent CT coronary angiography which revealed normal coronary arteries (Fig. 19.3).

As part of her continued follow up on guideline-directed medical therapy, a cardiac MRI was performed years later demonstrating an EF of 49% at the lower limit of normal with qualitative mild diffuse hypokinesis. There was no evidence for scarring by gadolinium scanning. MRI during the acute phase of the Takotsubo syndrome can show myocardial edema in a pattern not consistent with an acute coronary syndrome which can be helpful when CAD is in the differential. Cardiac MRI is probably the gold standard for EF determination, particularly if echocardiographic images are substandard and MRI can be helpful in searching for cardiac thrombi. Myocardial properties demonstrated by MRI can also aid in the differential diagnosis of myocardial inflammation or infiltration when used in the proper clinical context (Video 19.3) [7].

The patient remains asymptomatic with excellent exercise tolerance to the current day maintained on ACE inhibitors, beta-blockers, and aspirin. Ventricular function remains within the normal range by continued echocardiographic surveillance.

19.4 Case 3. Takotsubo Leading to Alterations in Chemotherapeutic Regimen. Cancer Control is Associated with Improvement in Ventricular Function

An 81-year-old woman with B cell lymphoma, past history of hypertension, hyperlipidemia, and interstitial lung disease presents with progressive dyspnea, weight loss with aggressive lung lesions. Echocardiogram EF is 40%. EKG evolving T-wave changes and prolonged QT interval. Torsades has been described uncommonly during the acute

phase of Takotsubo syndrome. Chest X-ray demonstrates masses and infiltrates consistent with extensive tumor involvement in the lungs (Fig. 19.4).

She was treated with RCDOP (rituximab, cyclophosphamide, pegylated liposomal doxorubicin, vincristine, and prednisone) × 2 cycles with clinical improvement. RCDOP was chosen over RCHOP (rituximab, cyclophosphamide, doxorubicin, vincristine, and prednisone) to avoid doxorubicin in the face of cardiomyopathy. Aside from one dose of intravenous furosemide, no cardiovascular medications were administered. With this treatment, her breathlessness improved and repeat imaging 2 to 3 weeks later showed improvement in the EKG T-wave abnormalities and dramatic improvement in cardiac function on echo (EF = 64%) and pulmonary disease on chest X-ray. The chemotherapy regimen was changed to RCHOP (Fig. 19.5, Video 19.4).

19.5 Case 4. Takotsubo Syndrome with Apical Thrombus

An 80-year-old man has laryngeal cancer and stage IVB diffuse large cell lymphoma involving the GI tract. After the fourth cycle of R-CHOP, he is hospitalized with watery diarrhea, abdominal cramping, and hypotension. Empirically treated with antibiotics but cultures negative. Admission EKG showed low voltage, serial EKGs showed Q waves and ST elevation. Troponin is minimally elevated. Echocardiogram with Takotsubo pattern, apical thrombus, and EF 35%, confirmed by MRI (Fig. 19.6, Video 19.5).

Full-dose anticoagulation was started. The patient's blood pressure was too low to tolerate guideline-directed medical therapy. Essentially after rest, rehydration, and anticoagulation, the apical thrombus resolved and echocardiographic

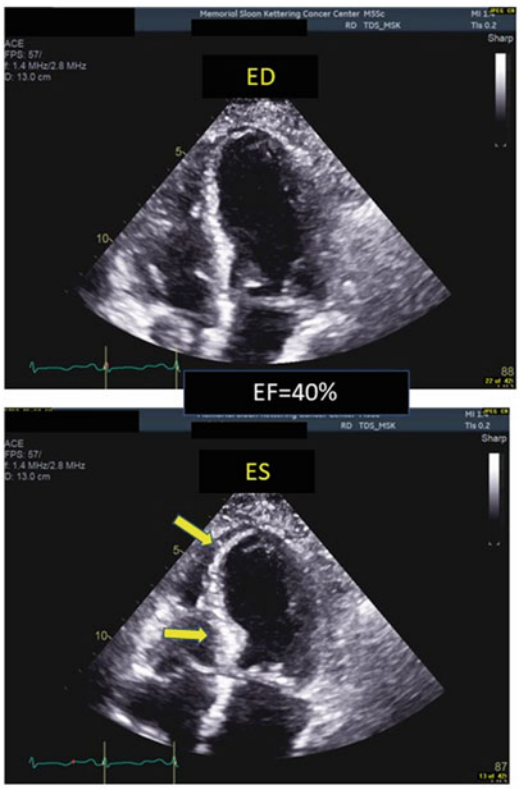

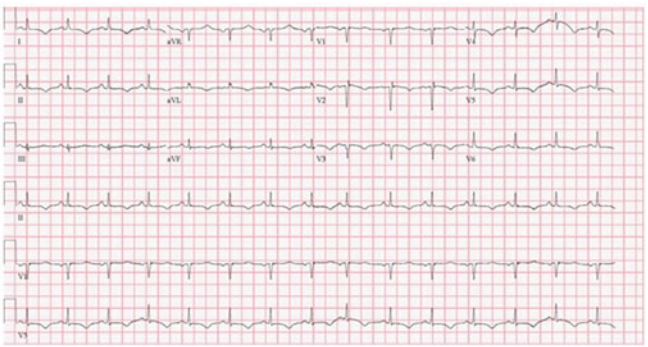

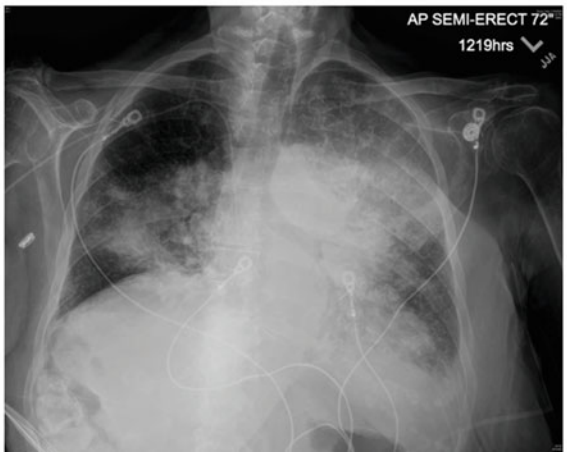

Fig. 19.4 Still frame ED and ES images from echocardiogram on presentation. EF 40%. Arrows demonstrate apical ballooning and a neck at the base from relatively preserved motion, both characteristic of Takotsubo syndrome. The EKG on presentation shows T inversion and prolonged QTc and the chest x-ray demonstrates masses and infiltrates consistent with extensive tumor involvement in the lungs with airway obstruction. The elevated right hemidiaphragm is a chronic finding

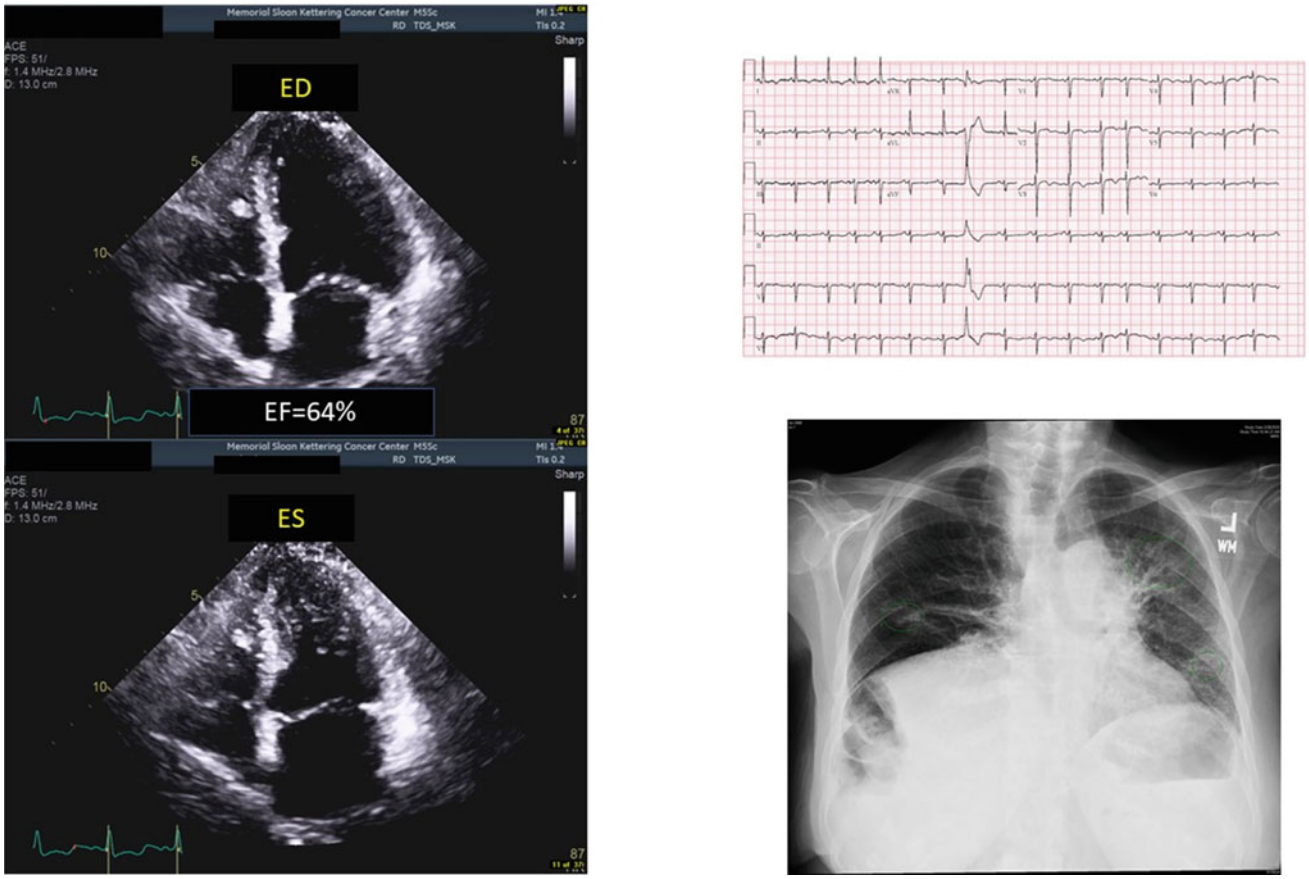

Fig. 19.5 Still frame ED and ES images from the echocardiogram after treatment with RCDOP which resulted in marked improvement in the patient's respiratory distress. EF = 64%. Chest X-ray shows significant improvement in the pulmonary masses/infiltrates, and the EKG shows improvement in the T-wave abnormalities

wall motion normalized over a period of weeks, EF 65%. In a registry of Takotsubo syndrome, apical thrombi were rare. Only an elevated troponin was predictive of its presence. All patients were treated with anticoagulation with resolution [8].

19.6 Case 5. Acute Coronary Syndrome Versus Takotsubo Syndrome in a Cancer Patient

A 69-year-old man with hypertension, obesity was noted to be diaphoretic, hypoxic, and hypotensive on day two post 10-hour anterior–posterior resection for recurrent colorectal cancer. Presenting EKG revealed marked ST-segment depression in lateral leads, troponin 1.5. Echocardiogram with EF 31% interpreted as diffuse hypokinesis with relative sparing of the base, differential diagnosis Takotsubo versus acute coronary syndrome (Fig. 19.7). Marked ST-segment depression on the EKG is not characteristic of Takotsubo, but ventricular dysfunction out of proportion to the troponin rise is (Video 19.6).

Cardiac catheterization showed proximal multivessel CAD that was treated with multivessel coronary stenting. One month after stenting, the echocardiographic EF was 43% (not shown), and 6 months later, the EF was 58% with a small residual regional wall motion abnormality in the apical aspect of the septum (Video 19.6). This delayed recovery of ventricular function is consistent with acute coronary syndrome rather than Takotsubo syndrome where recovery is often seen in days following the event. The workup of the Takotsubo syndrome must always exclude the presence of CAD. The extent of testing required to accomplish this of course depends on the nature of the clinical presentation.

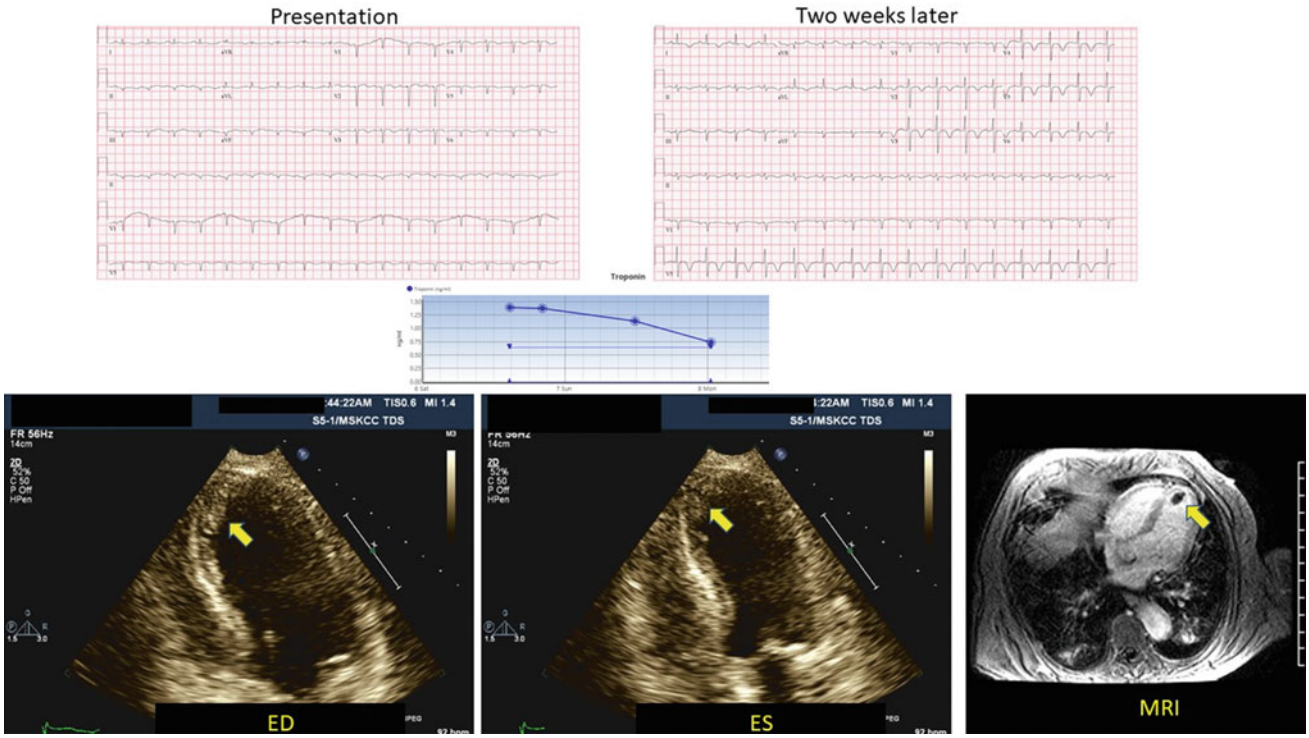

Fig. 19.6 Admission EKG showed low voltage, and minimal ST elevation. Over days, EKG evolved to show deep T-wave inversions. Troponin I was minimally elevated and down trending. ED and ES images from the echocardiogram soon after admission EF 35%. The arrows point to a likely mass adherent to the septal aspect of the apex; the apex balloons with systole. MRI confirms the presence of the mass (arrow) with tissue characteristics of thrombus. Further tissue characterization showed no scarring to the ballooning apex effectively excluding coronary disease as the mechanism behind these findings

19.7 Case 6. Unexplained EKG Changes Prior to Melanoma Surgery

A 68-year-old woman with no past cardiovascular history was referred for resection of melanoma from under a toenail. While waiting for surgery, her son was struck by a car and hospitalized in a coma with traumatic brain injury. He was reported as missing for more than a week and the family was unaware of his whereabouts. The patient went to see her Internist with complaints of extreme anxiety and insomnia. EKG showed mild nonspecific ST-segment changes and an echocardiogram was reported to be normal. Comparison EKGs were not available. She was treated with anxiolytics and then referred to our cardiology clinic weeks later for pre-melanoma surgery assessment because of the abnormal EKG. She had no chest pain or SOB, only anxiety and insomnia (Fig. 19.8).

The EKG on presentation for presurgical testing revealed T-wave abnormalities and minimal ST-segment depression. Two days later during preoperative cardiology consultation, the EKG had evolved to show deep T-wave inversions (Fig. 19.8). A resting echocardiogram at that time showed possible apical hypokinesis, not definitive so a stress echo was performed. That more conclusively demonstrated a small region of apical dyskinesis (Video 19.7). No other abnormalities were noted. The coronary calcium score was 0. A presumed diagnosis of Takotsubo cardiomyopathy was made and the melanoma surgery was delayed for about a month to allow for recovery from the probable stress related insult. Treatment was begun with low-dose ACE inhibitors. PET scanning revealed increased uptake only in the involved toe. That is, there was no evidence for metastatic disease.

In that interval waiting for surgery, the COVID-19 pandemic was accelerating in NYC and her toe surgery was delayed by a total of 2.5 months. She experienced cough and fever in that interval but tested negative for COVID. Her husband developed severe COVID-related pneumonia and the patient did not undergo follow-up COVID testing. Following recovery from the cough, her exercise tolerance remained excellent. Her follow-up EKG did not show the expected resolution of the ST-T changes so a cardiac MRI was ordered (Fig. 19.9, Video 19.8). The cardiac MRI revealed apical thickening and otherwise normal wall motion. There was no late gadolinium enhancement. The working diagnosis was reconsidered from Takotsubo cardiomyopathy to a variant of apical hypertrophic cardiomyopathy previously undetected. The EKG changes first noted

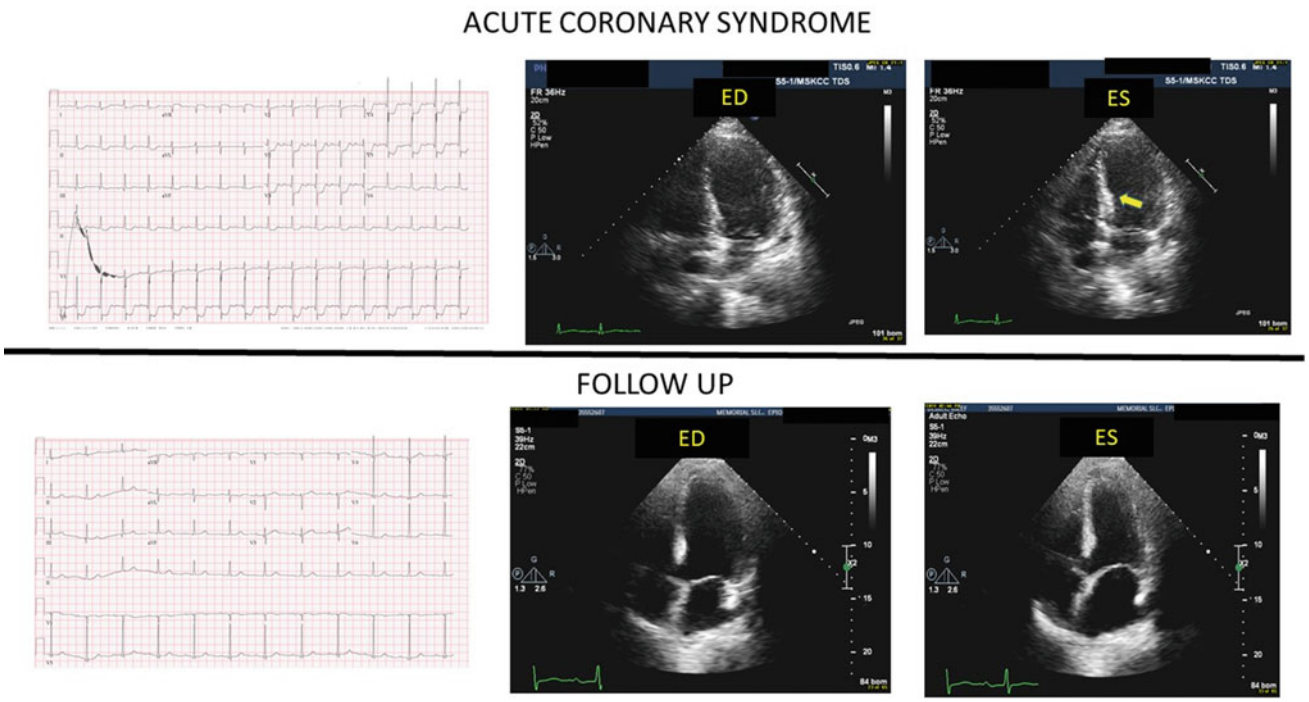

Fig. 19.7 Top panel EKG and echocardiogram two days after major cancer surgery when patient was found to be diaphoretic and hypotensive. EKG shows marked ST segment depression, resting echocardiogram shows large apical regional wall motion abnormality with better motion at the base producing a waist as indicated by the arrow. EF 31%. Bottom panel, EKG 3 months later showing resolution of ST depression but some loss of R wave in the precordial leads. Resting echocardiogram at that time reveals recovery of the EF to 65% with perhaps a small residual regional wall motion abnormality in the apical septum

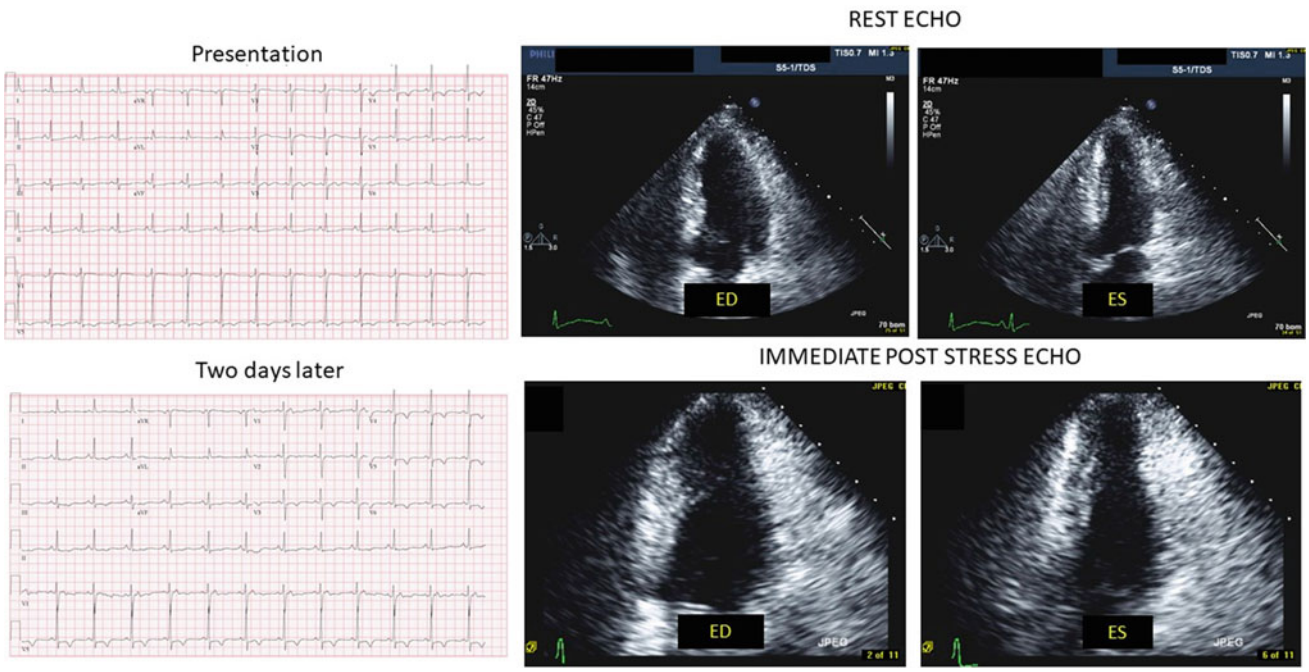

Fig. 19.8 EKG done during presurgical visit showing T-wave abnormality. EKG two days later during preoperative cardiology consultation shows marked T-wave inversions. Classic EKG changes of Takotsubo can evolve over days after the precipitating event. Rest echocardiogram suggests the possibility of an apical wall motion abnormality, seen to be more obvious in the ES image immediately post stress

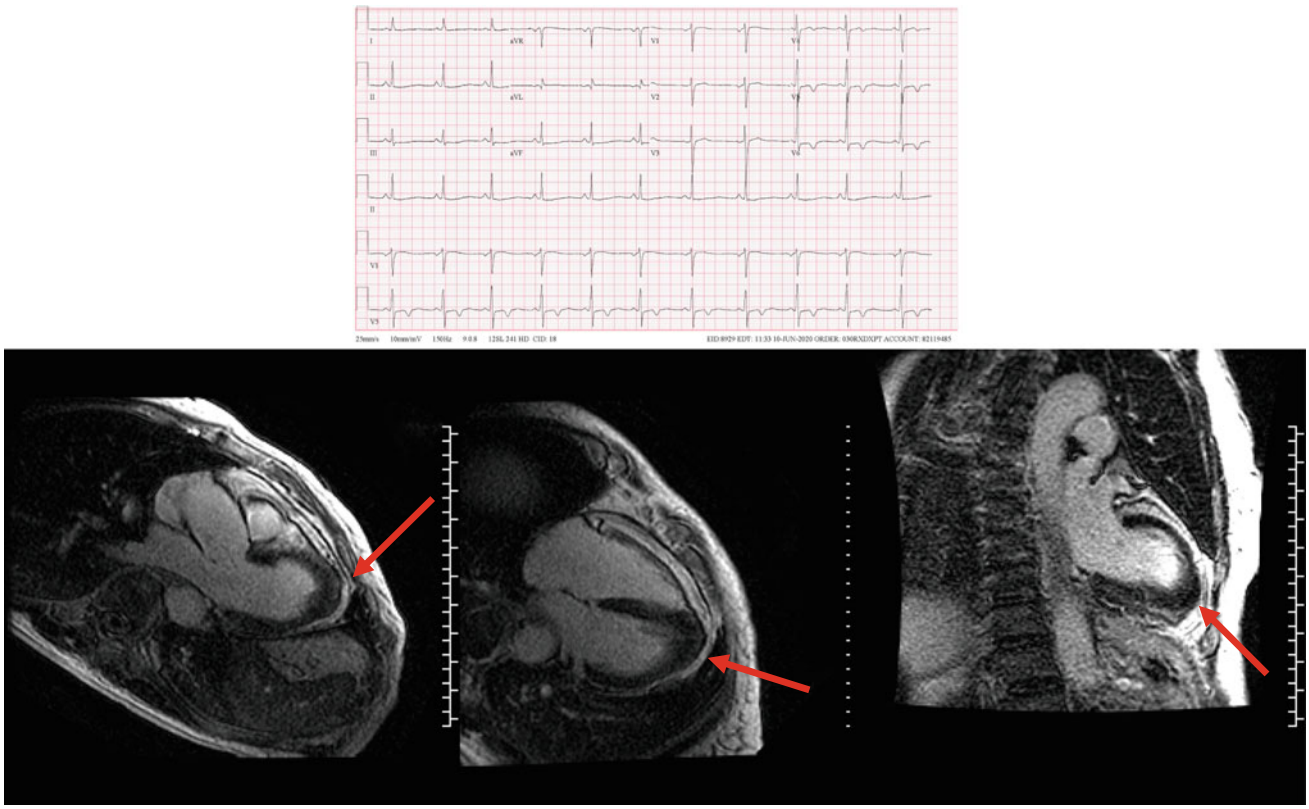

Fig. 19.9 Some three months after presentation EKG changes persist and MRI late gadolinium images demonstrating increased apical wall thickness and no hyperenhancement that would suggest scarring. Arrows point to apical thickening

around the time of her emotionally traumatic life events could have been related to the stress, and or the underlying cardiomyopathy. The persistence of the EKG changes is better explained by the hypertrophic cardiomyopathy. She underwent surgical removal of the toe melanoma without incident. Cardiology follow-up with serial imaging is planned.

19.8 Case 7. Recurrent Stress-Related Ventricular Dysfunction

A 61–year-old woman with metastatic ovarian cancer with paraneoplastic syndrome polymyositis being treated with taxol and intermittent steroids presents with acute respiratory failure in the setting of pneumonia and septic shock. EKG showed sinus tachycardia and echocardiogram showed hyperdynamic left ventricular function (Fig. 19.10, Video 19.9). She received treatment for infection and after a 10-day hospital course was discharged to a rehabilitation facility. One day after discharge, she was re-hospitalized with hypotension and was intubated for worsening dyspnea in the setting of recurrent aspiration pneumonia. She briefly required pressor support. EKG showed sinus tachycardia with T-wave inversion and, on echocardiogram, the EF had fallen to 27% with relative sparing of the basal segments. Troponin I was mildly elevated and trended down (Fig. 19.10, Video 19.9).

Upon improvement of respiratory status and increase in blood pressure, ACE inhibitors, and beta-blockers were slowly uptitrated. Repeat testing showed an increase in EF to 35% and undetectable troponin. On continued medical therapy 1 year later, the echocardiogram was essentially normal with an EF of 58%. Cardiac medications were discontinued and the patient was considered NYHA clinical class I. Ongoing chemotherapy included carboplatin, paclitaxel, and liposomal doxorubicin. She then developed nausea and vomiting due to bowel obstruction. She underwent extensive bowel resection with a diverting loop colostomy. Three days post operation, she developed an SVT responsive to IV beta-blockers. Echocardiogram showed diffuse LV dysfunction, motion perhaps preserved at the base with an EF of 25%. Troponin rose to over 2.0 and EKG again showed T-wave inversion. The patient was discharged home on low-dose carvedilol and lisinopril (Fig. 19.10, Video 19.9).

In the general population, the recurrence rate for the Takotsubo syndrome has been reported at 4%, [9] but in our experience in cancer patients, multiple bouts of reversible left ventricular dysfunction are not uncommonly seen

depending on the course of cancer and its treatments. Again, this case is somewhat atypical because of the slow recovery of ventricular function following the initial bout of left ventricular dysfunction.

19.9 Case 8. Takotsubo Syndrome, Pulmonary Embolism, Coronavirus Infection

A 57-year-old woman former smoker, obese, hypertensive with metastatic lung adenocarcinoma to the brain, spine, and pleura was treated with osimertinib. Course complicated by cardiac arrest due to a hemothorax, then a second cardiac arrest precipitated by a pulmonary embolism. Complications include acute renal failure, bilateral deep vein thrombosis, and cerebral infarction. Inferior vena cava filter placed and she received multiple transfusions. After resuscitation from cardiac arrest, echocardiogram and EKG were done consistent with Takotsubo syndrome, both markedly different from a baseline study done 1 month earlier (Fig. 19.11, Video 19.10).

Over the course of a week, left ventricular function recovered. However, 1 week after that, she developed recurrent respiratory failure from a massive PE, source upper extremity, and subclavian deep vein thrombosis. The pulmonary embolism was treated with thrombolytic therapy. EKG showed sinus tachycardia and right bundle branch block. Echocardiogram showed an enlarged right ventricle but preserved left ventricular function. (Fig. 19.11, Video 19.10) Current treatment includes osimertinib, full dose anticoagulation, lisinopril, and hydrochlorothiazide. This patient's course illustrates how variable an individual's cardiac response can be to various stressors.

19.10 Case 9. Takotsubo and Incidental Coronary Artery Disease?

A 76-year-old woman with hypertension was receiving neoadjuvant chemotherapy with gemcitabine and cisplatin prior to planned surgery for muscle-invasive bladder cancer. Before she could have the surgery, she was admitted to the hospital with very severe pelvic pain and a urinary tract infection. MRI done for the extent of disease evaluation showed no metastases but did reveal a subacute cerebellar infarct. Echocardiogram to search for the source of the infarction showed left ventricular dysfunction, an EF of 41%, and wall motion abnormalities consistent with the Takotsubo syndrome. A ventricular thrombus was not visualized. A cardiac MRI may have been better suited for the discovery of ventricular thrombi in this case. The EKG

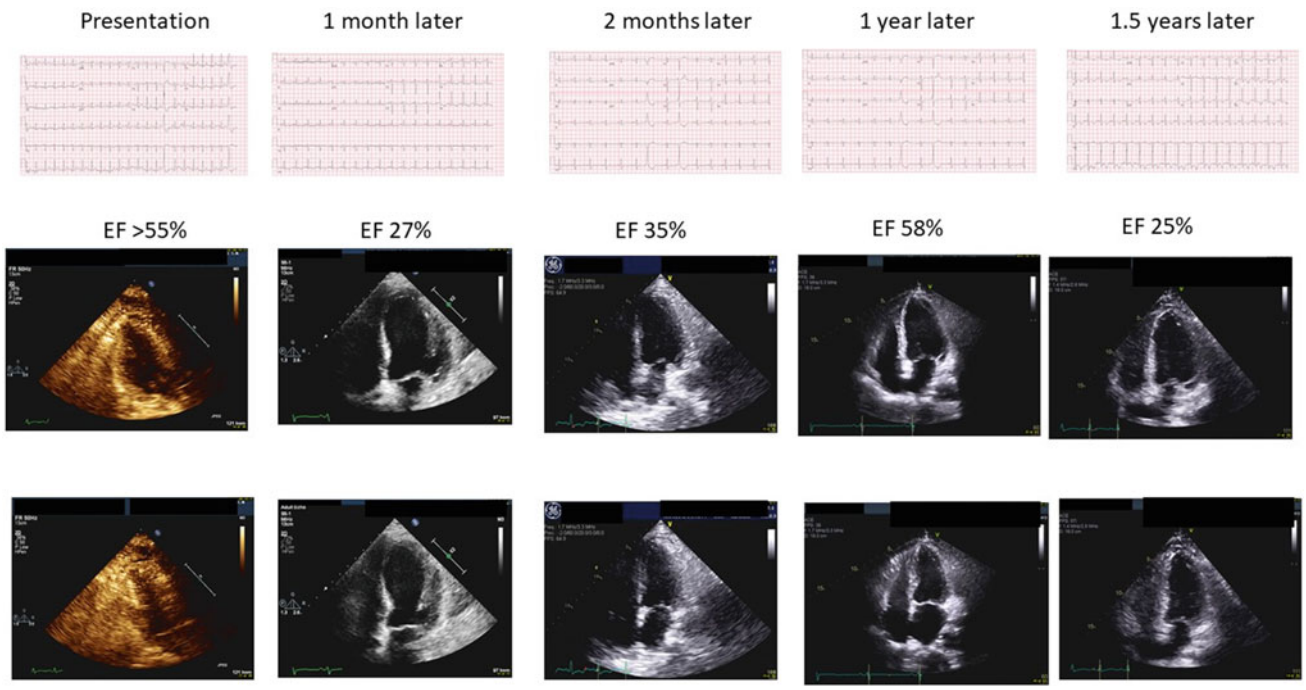

Fig. 19.10 Serial EKGs and echocardiograms showing sinus tachycardia and normal ventricular function at presentation then dynamic EKG changes accompanying left ventricular dysfunction, followed by slow recovery of ventricular function toward baseline (1 to 2 months and 1 year later), then recurrent ventricular dysfunction (1.5 years later) in a woman with ovarian cancer being treated with chemotherapy and surgery for cancer and its many complications

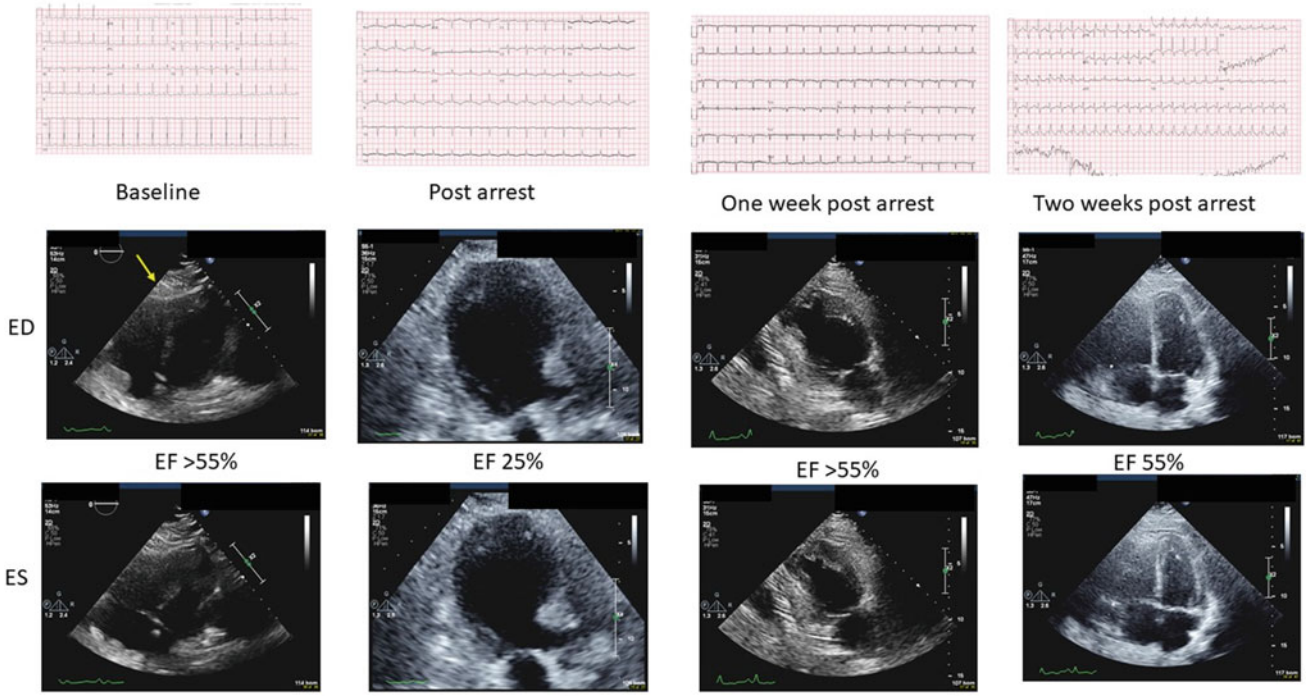

Fig. 19.11 Serial EKGs and end diastolic (ED) and end systolic (ES) frames from echocardiograms done during four timepoints. These are technically limited studies due to extreme clinical circumstances at the time of echo acquisition. First panel to the left shows EKG and echocardiogram at time of initial presentation. EKG is essentially normal. Echocardiogram at ED shows flattening of the septum and a suggestion of right ventricular enlargement. The yellow arrow points to a pericardial mass, presumed to be lung adenocarcinoma. The end systolic image indicates that left ventricular systolic function is normal, right ventricular function not well seen. After cardiac arrests, EKG shows T-wave inversion. Left ventricle is dilated and globular with reduced ejection fraction, motion relatively preserved at the base giving a Takotsubo like appearance. Then there is near normalization of the EKG and left ventricular function, just one week after the cardiac arrest. Two weeks post arrest the EKG shows sinus tachycardia with RBBB in the face of a massive pulmonary embolus. Of interest, the echocardiogram shows preservation of left ventricular systolic function and a dilated, perhaps hypokinetic right ventricle, better seen in Video 19.10

showed evolving deep T-wave inversions. Troponins were minimally elevated. The ventricular dysfunction observed on echocardiogram was out of proportion to the degree of troponin elevation as is common in the Takotsubo syndrome (Fig. 19.12, Video 19.11).

Throughout, the patient had no cardiovascular symptoms. CT coronary angiogram showed a 50–70% proximal LAD stenosis and pharmacologic nuclear perfusion stress test revealed a large fixed apical defect with minimal reversibility. The relative contributions of stress cardiomyopathy versus obstructive coronary artery disease to the presentation were debated and a decision was made to treat the patient medically with beta-blockers, ASA, and statins. Repeat echocardiogram 2 weeks after admission showed an improvement of the EF to 51% with only a small residual apical regional wall motion abnormality.

The planned surgery was postponed for 1.5 months at which time she underwent a total cystectomy, lymph node dissection, and ileal conduit. There were no cardiovascular complications. At follow-up 6 months later, the patient was NYHA clinical class I with a normal echocardiogram, EF 64%. Carvedilol was discontinued and her blood pressure was controlled with amlodipine. Taken together, the presentation suggests that coronary disease was not a significant factor in the presentation, and the severe fixed apical defect on perfusion imaging represented a marked blood flow reduction to the ballooning myocardial segment rather than scarring, a conclusion supported by the minimal troponin elevation. One and one half years later, she succumbed to metastatic bladder cancer with no further cardiovascular or cerebrovascular events.

19.11 Conclusions

Ventricular dysfunction in the cancer patient is common, with contributions from the Takotsubo syndrome, ischemic heart disease, sepsis, immune insults, drug toxicity, and

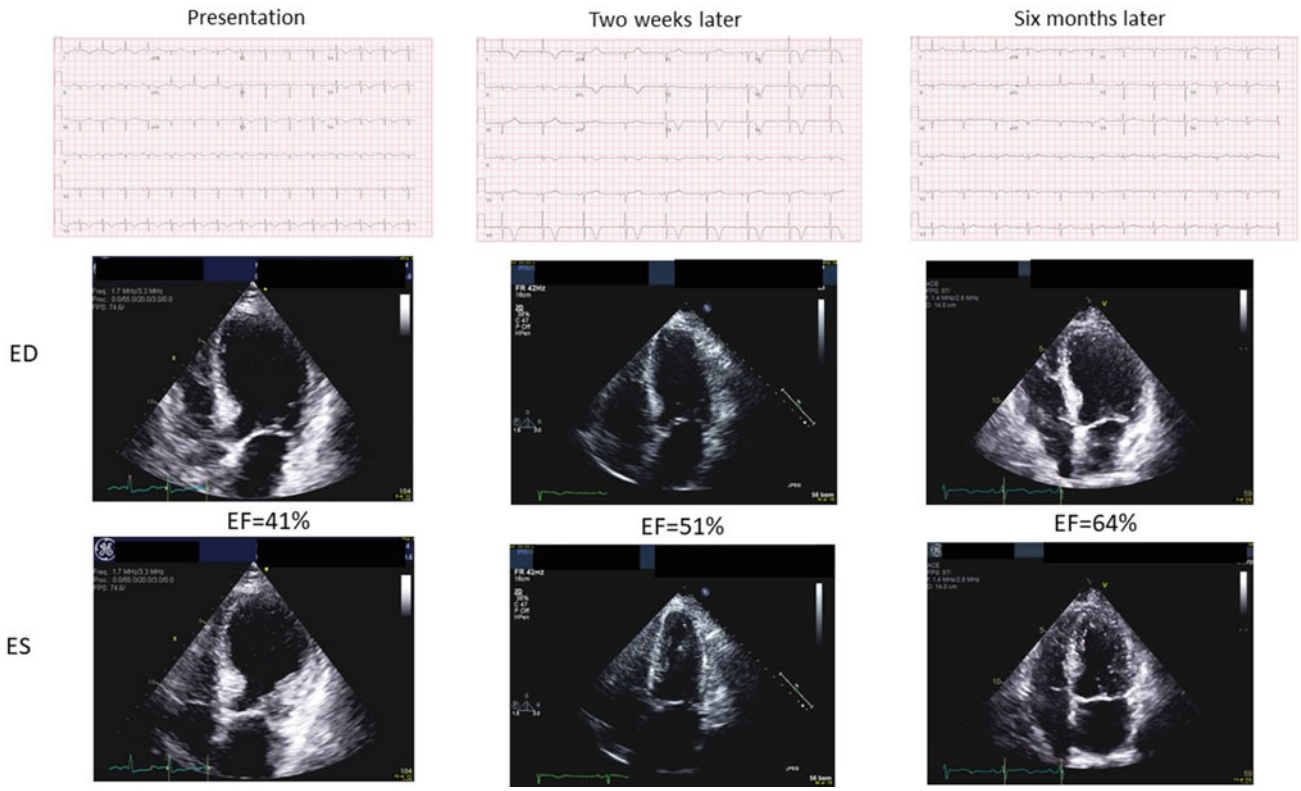

Fig. 19.12 Serial EKGs, end diastolic (ED) and end systolic (ES) echo frames in a woman with bladder cancer who underwent echocardiography to evaluate for possible source of a subacute cerebral infarct discovered during workup for metastatic disease. On the initial image, the echocardiogram shows reduced EF, and characteristic apical ballooning but no left ventricular thrombus. Repeat study some two week later shows improvement in the EF toward normal and perhaps a small residual apical regional wall motion abnormality. Seven months after the initial study the EF and regional wall motion are normal. Note the progression of deep T-wave abnormalities on the EKG even as the echocardiogram was improving. Last EKG has reverted to normal

more. Nowhere in the practice of cardiology is the thoughtful application of high-quality imaging more important. Serial imaging is of particular value.

References

1. Bybee KA, Kara T, Prasad A, et al. Systematic review: transient left ventricular apical ballooning: a syndrome that mimics ST-segment elevation myocardial infarction. Ann Intern Med. 2004;141 (11):858–65.
2. Joy PS, Guddati AK, Shapira J. Outcomes of Takotsubo cardiomyopathy in hospitalized cancer Patients. J Cancer Res Clin Oncol. 2018;144:1539–45.
3. Victoria L. Cammann VL, Sarcon A, Ding KJ, et al. Clinical features and outcomes of patients with malignancy and Takotsubo syndrome: observations from the international Takotsubo registry. J Am Heart Assoc. 2019;8:e010881. https://doi.org/10.1161/JAHA.118.010881.
4. Angelini P, Uribe C. Is transient Takotsubo syndrome associated with cancer? Why, and with what implications for oncocardiology? J Am Heart Assoc. 2019;8:e013201. https://doi.org/10.1161/JAHA.119.013201.
5. Desai A, Noor A, Joshi, Kim AS. Takotsubo cardiomyopathy in cancer patients. Cardio-Oncol. 2019;5:7. https://doi.org/10.1186/s40959-019-0042-9.
6. Dote K, Sato H, Tateishi H, Uchida T, Ishihara M. Myocardial stunning due to simultaneous multivessel coronary spasms: a review of 5 cases. J Cardiol. 1991;21:203–14. [PMID: 1841907]
7. Ghadri JR, Wittstein IS, Prasad A, et al. International expert consensus document on Takotsubo syndrome (Part II): diagnostic workup, outcome, and management. Eur Heart J. 2018;39 (22):2047–62. https://doi.org/10.1093/eurheartj/ehy077.
8. Santoro F, Stiermaier T, Tarantino N, et al. Left ventricular thrombi in Takotsubo syndrome: incidence, predictors, and management: results from the GEIST (German Italian stress cardiomyopathy) registry. J Am Heart Assoc. 2017;6(12):e006990. https://doi.org/10.1161/JAHA.117.006990. PMID: 29203578; PMCID: PMC5779019.
9. El-Battrawy I, Santoro F, Stiermaier et al. Takotsubo syndrome: results from the GEIST registry. J Am Heart Assoc. 2019;8(9): e010753. https://doi.org/10.1161/JAHA.118.010753. PMID: 31046506; PMCID: PMC6512083.

Arterial Thrombosis and Marantic Endocarditis

20

Carol L. Chen

20.1 Introduction

In 1865, Armand Trousseau was the first to systemically describe the connection between thrombosis and cancer through autopsy studies [1]. The risk of venous thromboembolism (VTE) in cancer is far better described in comparison to arterial thrombosis in cancer patients. However, with increased cancer survival and novel vascular targeted cancer therapies, arterial thromboembolic events (ATE) have been increasingly reported. Using a SEER-Medicare dataset of over 270,000 newly diagnosed cancer patients, Navi et al. observed an ATE incidence of 4.7% within the first 6 months after cancer diagnosis. ATE marked those with worse prognosis with a three-fold increase in mortality and a high risk for the recurrent thromboembolic event (37%) at 6 months. Patients with metastatic disease had a ten-fold increase in the likelihood of developing ATE within the first month of cancer diagnosis [2]. ATE may precede a malignancy diagnosis and has been observed to be the first sign of cancer. Various solid tumor types, more commonly mucinous adenocarcinoma, as well as leukemias, such as acute promyelocytic leukemia are associated with increased ATE risk. An individual's ATE risk is a combination of personal risk factors, cancer characteristics, and vascular toxicity of therapy (Fig. 20.1).

Trousseau noted that thromboses often occurred in limbs distant from the site of visceral tumors and wondered about the connection between cancer and this phenomenon. He hypothesized that cancer and other diseases caused changes in the behavior and composition of blood, an "*excess of fibrin, and an increase of white globules*" resulting in a hypercoagulable state [1]. Over the past 150 years, much has been elucidated about why cancer patients are prone to thrombosis. Tumor cells promote clot formation through many pathways. Platelets are stimulated to aggregate by circulating tumor cells. Macrophages are activated by malignant cells to release tumor necrosis factor (TNF), interleukin-1(IL1), and interleukin-6 (IL6) which promote the coagulation cascade. Damaged endothelial cells attract platelet deposition and activate tissue factor. Tissue factor is a potent activator of the coagulation cascade. Tumor cells themselves contain procoagulants such as cysteine proteases and tissue factor which also directly activate coagulation factors [3]. Disseminated intravascular coagulation (DIC) is frequently seen in cancer patients, especially in acute promyelocytic leukemia (APML) as well as end-stage cancer. It is marked by diffuse systemic microvascular and large-vessel thrombosis which then leads to consumption of coagulation factors and hemorrhage. Individual risk factors which result in endothelial cell dysfunction such as atherosclerotic disease and diabetes are also important to consider in overall arterial thrombosis risk.

The addition of cancer therapies which have vascular activity into this milieu further exacerbates the hypercoagulable state. Cisplatin causes acute vascular toxicity resulting in vasospasm and thromboembolic events, both venous and arterial [4]. Endothelial cell dysfunction due to cisplatin toxicity also results in acceleration of atherosclerosis leading to increased risk of myocardial infarction in subsequent decades [5]. Many targeted cancer therapies affect angiogenesis by disrupting various vascular signaling pathways. Vascular endothelial growth factor (VEGF) is involved in multiple pathways which contribute to the homeostasis of endothelial cell function and platelet activation. ATE, including myocardial infarctions and ischemic strokes, has been well described with VEGF inhibitors. Disruption of VEGF signaling also promotes plaque vulnerability, thus accelerating underlying atherosclerosis. Patients with high atherosclerotic risk should be screened and medically

Electronic supplementary material
The online version of this chapter (https://doi.org/10.1007/978-3-030-70998-3_20) contains supplementary material, which is available to authorized users.

C. L. Chen (✉)
Department of Medicine, Memorial Sloan Kettering Cancer Center, 1275 York Avenue, New York, NY 10065, USA
e-mail: chenc@mskcc.org

R. M. Steingart et al. (eds.), *Atlas of Imaging in Cardio-Oncology*,
https://doi.org/10.1007/978-3-030-70998-3_20

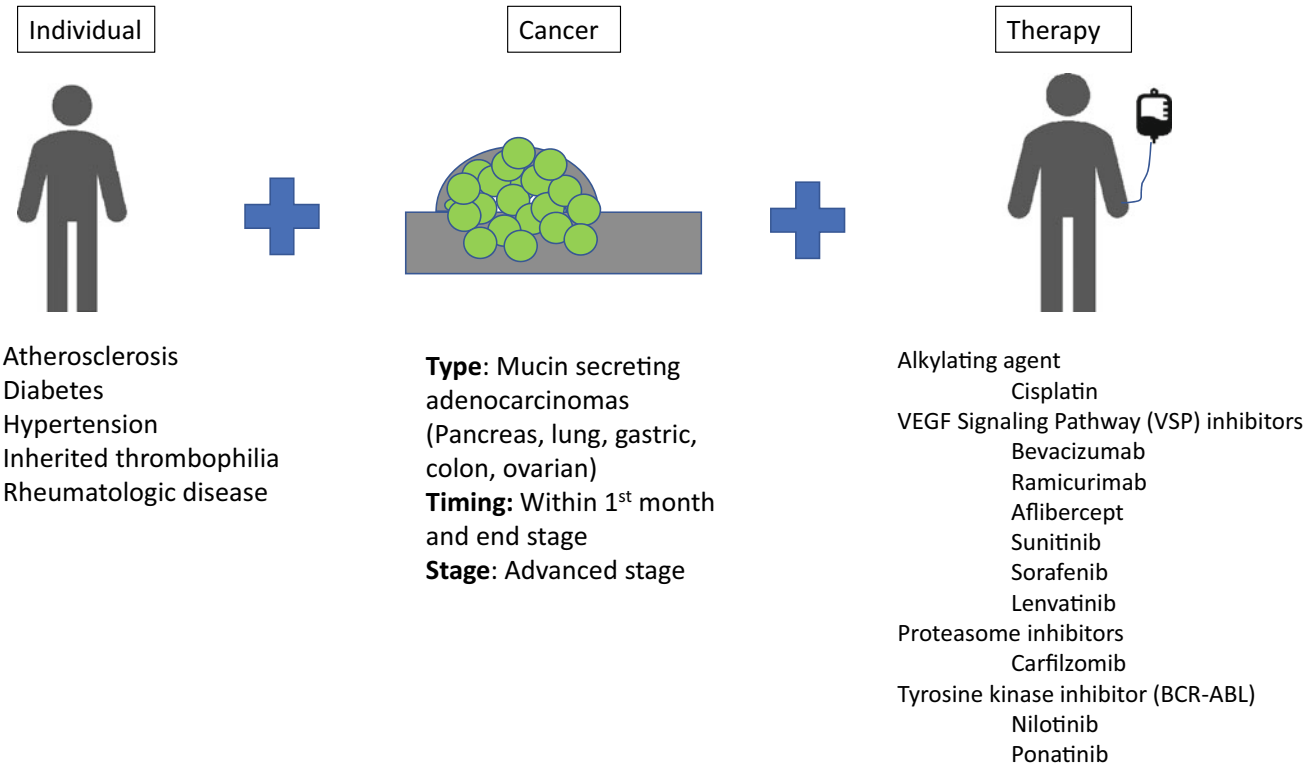

Fig. 20.1 A cancer patient's overall arterial thromboembolic risk is due to complex combination of individual risk factors, cancer characteristics, and toxicity of therapy

optimized prior to starting therapy. Even within a class of drug therapy, there are different risks of ATE. Within the tyrosine kinase inhibitor class for the treatment of chronic myelogenous leukemia (CML), only newer generation drugs, nilotinib, and ponatinib, have been strongly associated with profound peripheral arterial disease, but not earlier drugs. In many cases, CML is now a chronic disease. The result is that many patients will be on therapy for more than a decade. Patients with underlying peripheral arterial disease have markedly increased risk, so screening and surveillance with ankle-brachial index are highly recommended [6]. As the list continues to grow, clinicians must stay knowledgeable about the possible ATE risk with new therapies.

Nonbacterial thrombotic endocarditis (NBTE) is another mechanism of ATE frequently seen in cancer patients. Unlike infectious endocarditis vegetations, almost 50% of NBTE are associated with systemic arterial emboli [7]. An autopsy study suggests an incidence of NBTE of 4% in end-stage cancer patients [8] while an echo study demonstrated that 19% of patients with disseminated adenocarcinoma had NBTE [9]. NBTE reflects the underlying hypercoagulable state. Vegetations consist of platelet, fibrin, and inflammatory cells superficially attached to valve leaflets, most commonly aortic and mitral, at points of turbulence. Although NBTE vegetations do not generally cause the destruction of valve leaflets, fibrosis and scarring can result in significant valve dysfunction. Treatment of underlying disease, as well as anticoagulation with heparin or low molecular weight heparin, is recommended to mitigate high thromboembolism risk. Vitamin K antagonist therapy has resulted in recurrent thromboembolism in cancer patients and is not used for NBTE treatment [10]. Surgery, usually valve sparing, is reserved for select patients who have a good prognosis and high risk of systemic embolization.

Recognition of ATE risk and manifestations has become vital for clinicians as older patients with increased atherosclerotic risk are being treated and more vascular toxic therapies are developed. Unlike VTE prophylaxis in cancer patients, the benefit of antiplatelet and anticoagulation prophylaxis for ATE during cancer treatment has not been proven. The spectrum of patient presentations ranges from asymptomatic to critically ill with neurologic defects, ischemic limbs, and myocardial infarction. Rapid recognition and diagnosis are critical for best outcomes, and appropriate treatment with anticoagulation may decrease the risk of recurrent events.

20.2 Case 1: Bevacizumab Therapy Causes Spontaneous Aortic Thrombus

- ATE may be asymptomatic and incidentally diagnosed on imaging.
- Prompt anticoagulation may be important to decrease the risk of further ATE.

A 56-year-old man with metastatic colon cancer with progressive disease began systemic bevacizumab in addition to 5 fluoruracil-based therapy. Three months later, repeat scans were performed to investigate disease response. Hepatic metastases were unchanged, however, a new contrast defect was noted in the aortic arch just distal to the subclavian artery origin (Fig. 20.2a–c). The patient had no stigmata of peripheral arterial embolism. Bevacizumab, a monoclonal antibody against VEGF molecular, has a high incidence of ATE [11]. Treatment was halted, and patient was admitted for expedited work-up. A transesophageal echocardiogram (TEE) was performed and demonstrated a large pedunculated echogenic mass attached to the aortic lumen with moderate mobility (Fig. 20.3, Video 20.1). There was no intracardiac thrombus. There was no underlying atherosclerosis of the aorta noted on CT or TEE. Anticoagulation with heparin infusion was started immediately. Cardiothoracic surgery was consulted regarding management. Since the patient was asymptomatic with no findings of distal embolism and surgical resection would entail high risk of embolization and delay further cancer treatment, the medical team and patient decided to proceed with anticoagulation. There are several case reports of aortic thrombus with bevacizumab which reported successful treatment with anticoagulation. Patient was transitioned from low molecular weight heparin to oral anticoagulation and resumed chemotherapy with 5-fluorouracil alone shortly after discharge from the hospital. A CT scan was repeated 1 month later and demonstrated a smaller mass (Fig. 20.2d–f). The contrast defect completely resolved after 3 months of anticoagulation therapy. The patient developed progression of disease and was re-challenged with bevacizumab while continuing anticoagulation therapy. The patient did not develop any other thrombotic complications but died of progressive disease the following year.

20.3 Case 2: Newly Diagnosed Stage IV Pancreatic Cancer Presenting with ATE and VTE

- ATE risk is highest the first month after diagnosis, especially in advanced stage cancer.
- Although DIC is not a common event in cancer patients, it is associated with shortened survival, especially if underlying cancer cannot be treated.

A 78-year-old man who presented with severe weight loss and loss of functional status was diagnosed with metastatic pancreatic cancer and started palliative gemcitabine therapy. Five days later he presented to the emergency room with dyspnea on exertion. He was found to be hypoxic and required high flow oxygen. It was also noted on admission that his right lower extremity was mildly swollen with bluish

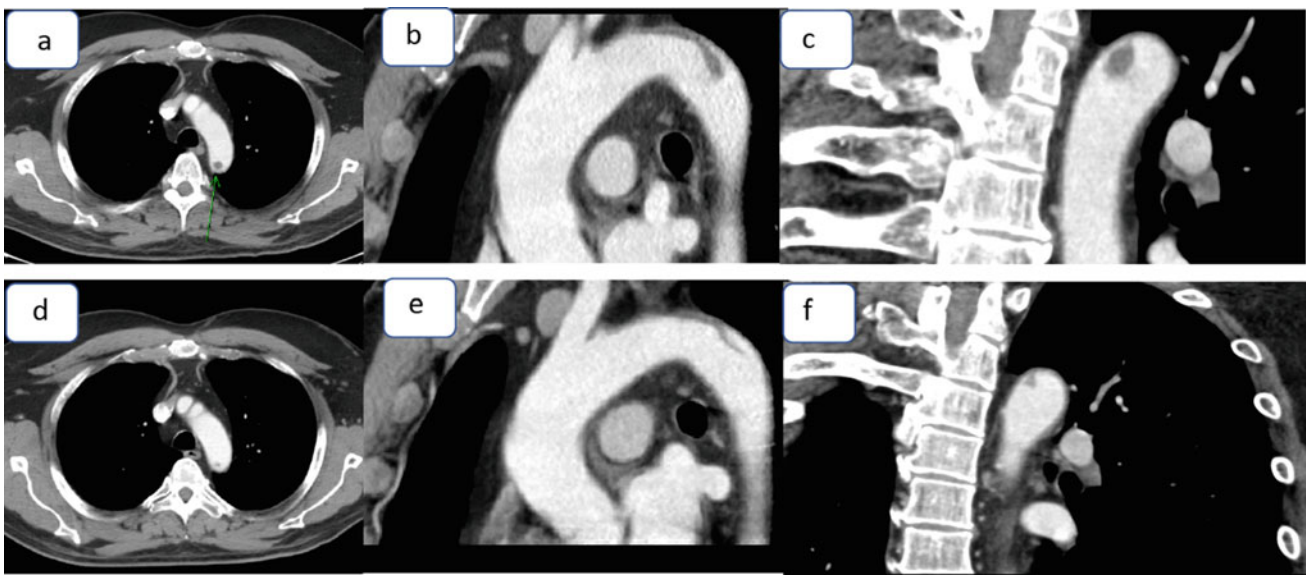

Fig. 20.2 Aortic thrombus. Contrast defect with attachment in the lumen aortic arch extending distally. **a–c** Initial images. **d–f** After 1 month of anticoagulation therapy, contrast defect is smaller. After 3 months of anticoagulation therapy the contrast defect was no longer seen

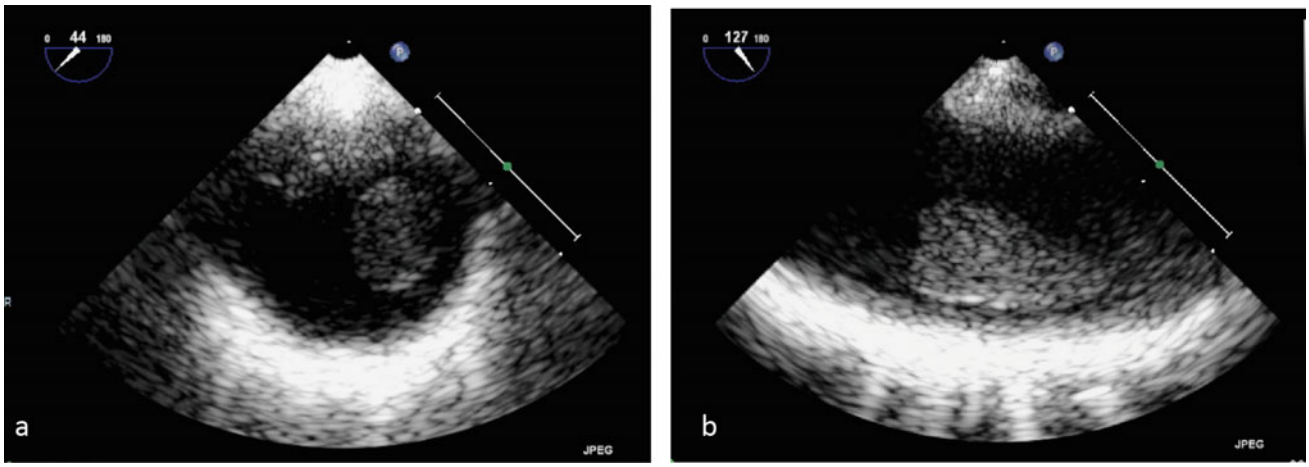

Fig. 20.3 Transesophageal echocardiogram demonstrates large mobile echodensity (see Video 20.1). **a** short axis, **b** long axis

discoloration of forefoot and toes with decreased sensation in his foot and a faint dorsalis pedis pulse in comparison to the left. CT angiogram of chest, abdomen, pelvis, and lower extremities (Figs. 20.4 and 20.5) was performed and revealed bilateral segmental pulmonary emboli, splenic infarct, arterial thromboses of the right femoral and peroneal artery, and thrombosis of the right iliac vein. Doppler studies also showed right calf, popliteal and femoral vein thrombosis. He also had developed new unexpected thrombocytopenia with a decline in platelet count from 177 k/mcL to 78 k/mcL since receiving his first dose of gemcitabine. This degree of thrombocytopenia was unexpected with gemcitabine therapy, and he was evaluated for DIC. The abnormalities of coagulation which can be seen in DIC are prolonged PT, PTT, increased fibrin split products, decreased fibrinogen, and thrombocytopenia. His labs showed mildly prolonged PT 18.3 s (normal 9.3–13.5 s), mildly decreased fibrinogen of 147 mg/dl (normal 190-387 mg/dl), and other DIC labs were within normal limits. An inferior vena cava filter was placed, and he was treated with therapeutic heparin infusion in the intensive care unit for several days. His lower extremity exam improved, however, he continued to require high levels of oxygen support. Five days later, his platelet count dropped to 37 k/mcL, and he was switched temporarily to fondaparinux while heparin-induced thrombocytopenia (HIT) was ruled out. When HIT antibodies were found to be negative, anticoagulation was discontinued due to high likelihood that his thrombocytopenia was due to progressive DIC with a high bleeding risk. He was unable to receive further systemic chemotherapy and transitioned to home hospice, expiring three weeks later.

20.4 Case 3: End-Stage Cancer with Massive Systemic Thromboses, ATE, VTE, and NBTE

- Most common and devastating arterial thrombotic events are cerebrovascular infarcts.
- Patients with cancer and CVA should undergo workup for NBTE.
- If recurrent CVA, have a high suspicion for NBTE.

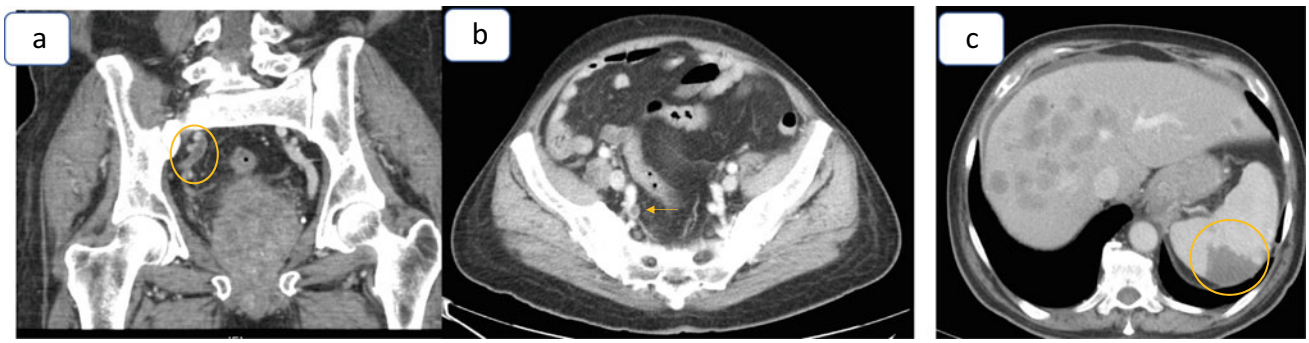

Fig. 20.4 **a–b** Right internal iliac vein thrombus seen as a filling defect. **c** Wedge-shaped splenic infarct

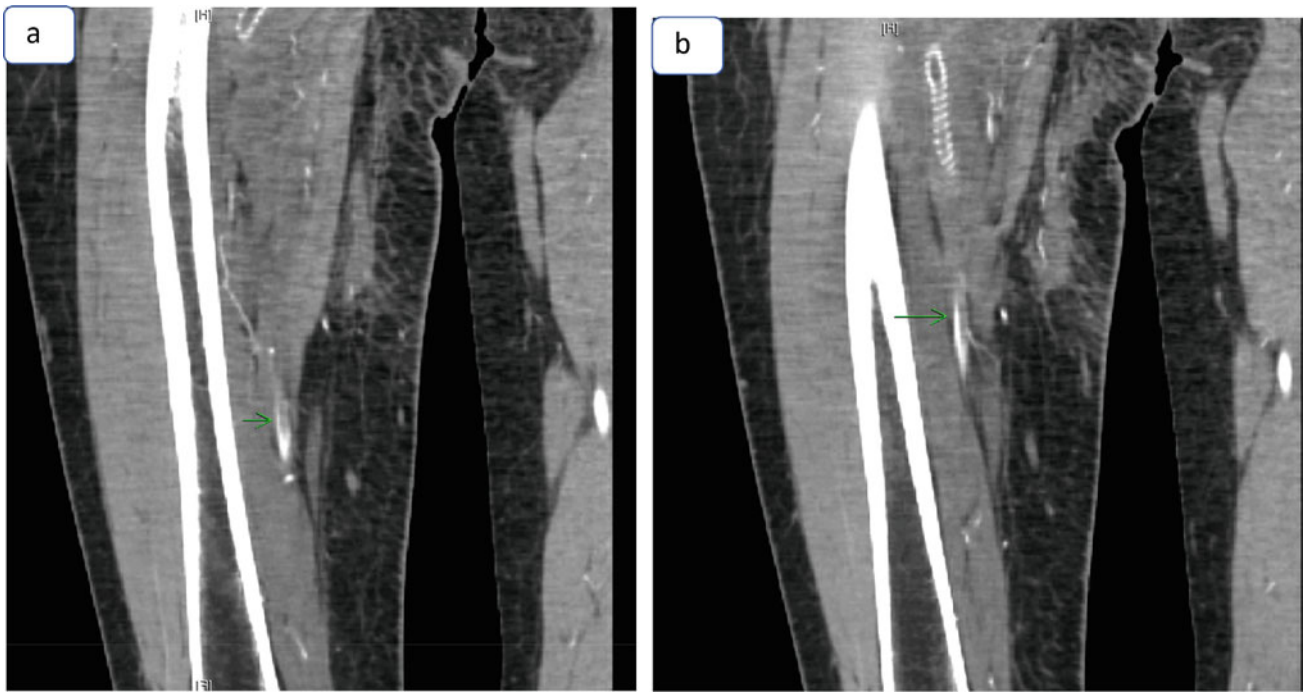

Fig. 20.5 **a–b** Contrast defect in right femoral artery consistent with partial thrombosis

A 68-year-old man with metastatic prostate cancer with extensive involvement of bone, lymph nodes, and lung presented to the emergency room with new visual field defects and right upper extremity numbness concerning for ischemic stroke. On examination, he had right-hand dysmetria, right homonymous hemianopsia, and right optic ataxia. Magnetic resonance imaging of the brain showed bihemispheric anterior and posterior strokes which were suggestive of central embolic phenomenon (Fig. 20.6). Continuous telemetry monitoring did not demonstrate atrial fibrillation, and there was no evidence for shunt by echocardiogram. His TEE demonstrated mitral valve vegetation (Fig. 20.7, Video 20.2) and no other source of embolism. An infectious workup was negative. He was treated for ischemic infarct and NBTE with low molecular weight heparin at therapeutic levels. A few weeks later, he was readmitted with new left-sided visual field defect. Repeat head scan demonstrated new bioccipital hemorrhages with small adjacent bleed in the left parietal lobe consistent with hemorrhagic conversion of prior infarcts. Anticoagulation was discontinued. He then suddenly became aphasic with right arm weakness. Emergent CT and angiogram were performed demonstrating occlusive middle cerebral artery thrombus with new areas of acute loss of gray-white in the left frontal and parietal lobes. He was not a candidate for thrombolytic therapy with his known brain hemorrhage. NBTE is frequently associated with recurrent thromboembolism in cancer patients. Recurrent thromboembolic events despite treatment with anticoagulation often herald imminent death. Hospice support was elected by patient and his family, and he died several days later.

20.5 Case 4: Newly Diagnosed Early-Stage Pancreatic Cancer with NBTE and Hereditary Thrombophilia

- Inherited thrombophilia should also be worked up when NBTE is diagnosed in the cancer patient.
- NBTE can resolve when treated with heparin and underlying disease is under control.

A 59-year-old patient with prior history of CAD s/p remote CABG, peripheral vascular disease, hypertension and diabetes, chronic pancreatitis presented with a newly diagnosed isolated pancreatic lesion consistent with malignancy. He underwent TTE prior to pancreatectomy due to history of decreased systolic function. On transthoracic echocardiogram images, mitral valve prolapse was noted with unusual shaggy thickening of mitral valve leaflets suspicious for vegetations. (Fig. 20.8, Video 20.3) A follow-up transesophageal echo was performed which showed vegetations along the coapting atrial surfaces of both mitral leaflet tips ("kissing lesions") with resultant mild mitral regurgitation (Fig. 20.9, Video 20.4). An infectious etiology was not suspected since the patient was afebrile and without leukocytosis, and multiple blood cultures were negative. He was treated for NBTE with low molecular weight heparin until he

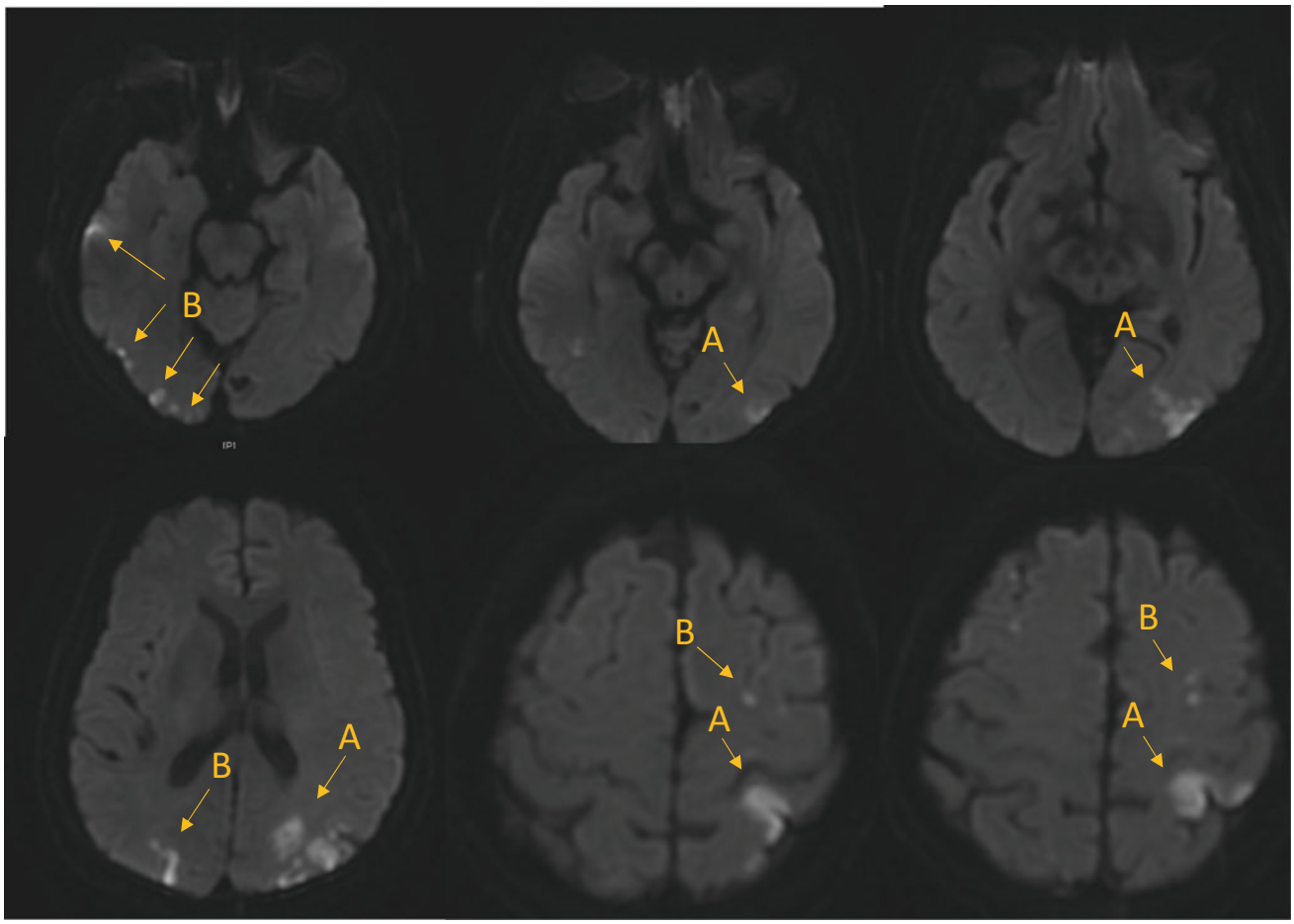

Fig. 20.6 MRI diffusion-weighted imaging. Multiple areas of restricted diffusion within left parieto-occipital junction (A arrows) and additional smaller lesions within bilateral cerebral hemispheres (B arrows)

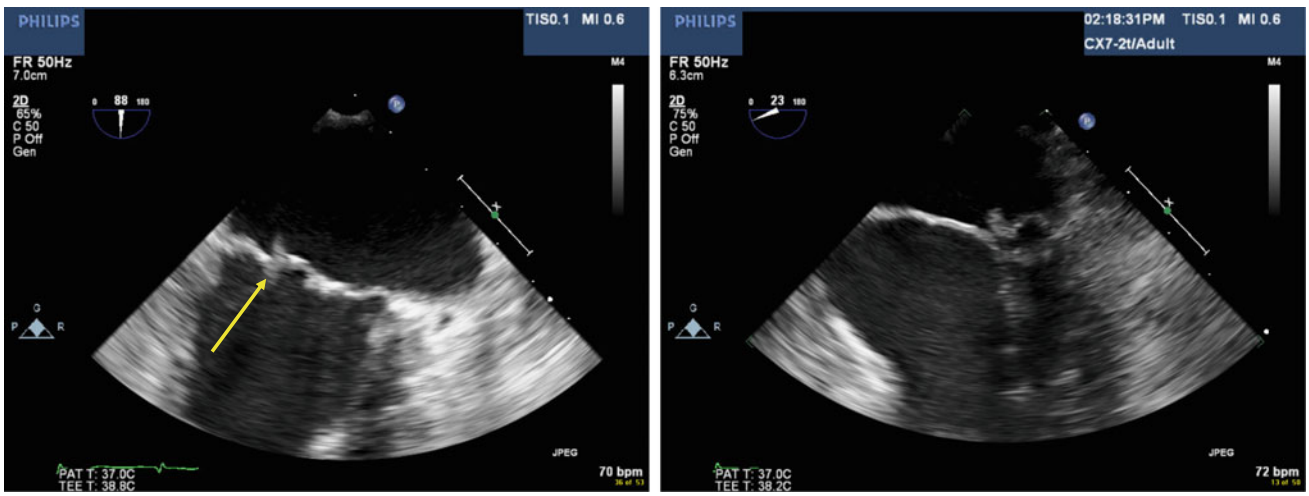

Fig. 20.7 Mobile echo density on the atrial aspect of the anterior mitral leaflet at the closure line (arrow). See Video 20.2

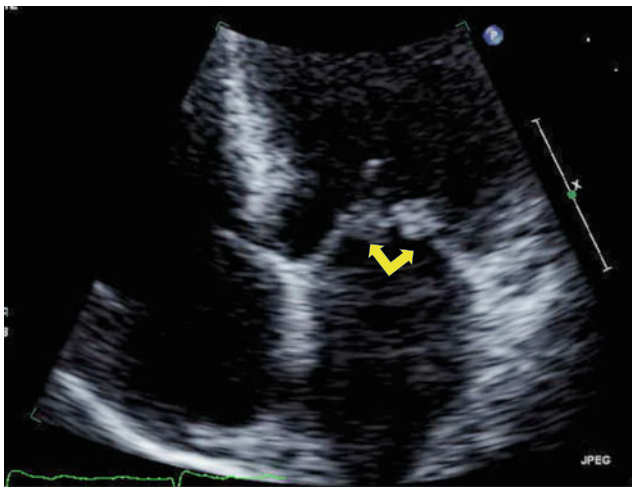

Fig. 20.8 Transthoracic echocardiogram shows thickening of mitral leaflet tips (arrows)

underwent total pancreatectomy. On his baseline labs, he was also noted to have prolonged PTT of 47.5 s (normal 25–38.5 s). He was diagnosed with antiphospholipid syndrome when lupus anticoagulant and anticardiolipin antibodies were markedly elevated. In a subpopulation of cancer patients, previously undiagnosed inherited thrombophilia or rheumatologic disease may also play a role in arterial thrombosis. Surgical pathology showed diffuse intraductal papillary mucinous neoplasm (IPMN) with microinvasive colloid carcinoma, T1N0. No further cancer therapy was indicated. After surgery, he was maintained on therapeutic low molecular weight heparin for NBTE as per American College of Chest Physician guidelines [10]. Warfarin treatment of thrombosis in cancer patients has not been shown to decrease recurrent thrombotic risk and is not recommended [10]. A follow-up echo 3 months after surgery showed marked resolution of NBTE (Fig. 20.10, Video 20.5). Since NBTE had resolved and he had no residual cancer,

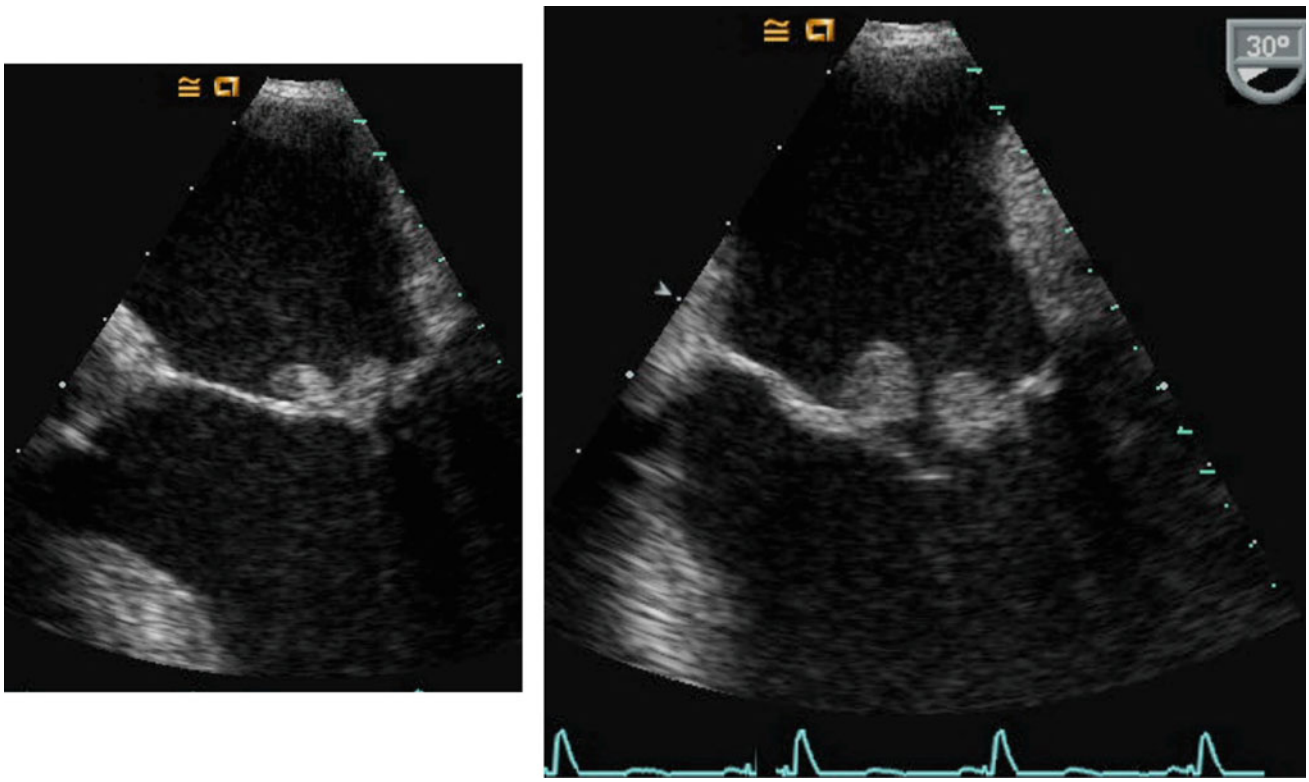

Fig. 20.9 TEE shows classic NBTE "kissing lesions." Large mobile echo densities are attached to the atrial aspect of the mitral leaflets at the closure line (see Video 20.4)

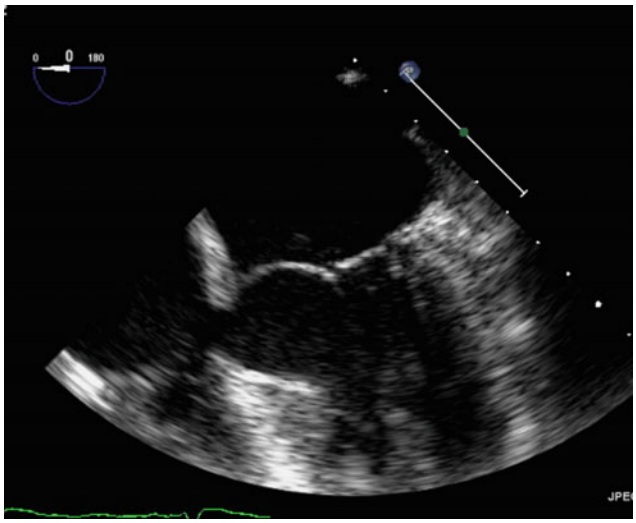

Fig. 20.10 Repeat TEE demonstrates resolution of NBTE (see Video 20.5)

anticoagulation was switched to vitamin K antagonist as treatment for antiphospholipid syndrome. A patient's underlying risk factors should continue to be treated during and after cancer therapy is completed.

The occurrence of ATE almost always interrupts cancer treatment and negatively affects outcomes. It remains unknown if any prophylactic regimen will decrease risk and whether there is a subgroup whose risk is too high to be treated with vascular targeting therapies. Attention needs to be paid to personal risk factors, such as atherosclerosis and other diseases of endothelial cell dysfunction.

References

1. Metharom P, Falasca M, Berndt MC. The History of Armand Trousseau and Cancer-Associated Thrombosis. Cancers (Basel) 2019;11.
2. Navi BB, Reiner AS, Kamel H, et al. Risk of arterial thromboembolism in patients with cancer. J Am Coll Cardiol. 2017;70:926–38.
3. Bick RL. Cancer-associated thrombosis. N Engl J Med. 2003;349:109–11.
4. Moore RA, Adel N, Riedel E, et al. High incidence of thromboembolic events in patients treated with cisplatin-based chemotherapy: a large retrospective analysis. J Clin Oncol. 2011;29:3466–73.
5. Meinardi MT, Gietema JA, van der Graaf WT, et al. Cardiovascular morbidity in long-term survivors of metastatic testicular cancer. J Clin Oncol. 2000;18:1725–32.
6. Aghel N, Delgado DH, Lipton JH. Cardiovascular toxicities of BCR-ABL tyrosine kinase inhibitors in chronic myeloid leukemia: preventive strategies and cardiovascular surveillance. Vasc Health Risk Manag. 2017;13:293–303.
7. Lopez JA, Fishbein MC, Siegel RJ. Echocardiographic features of nonbacterial thrombotic endocarditis. Am J Cardiol. 1987;59:478–80.
8. Chomette G, Auriol M, Baubion D, de Frejacques C. [Non-bacterial thrombotic endocarditis. Autopsy study, clinico-pathological correlations (author's transl)]. Ann Med Interne (Paris) 1980;131:443–7.
9. Edoute Y, Haim N, Rinkevich D, Brenner B, Reisner SA. Cardiac valvular vegetations in cancer patients: a prospective echocardiographic study of 200 patients. Am J Med. 1997;102:252–8.
10. Whitlock RP, Sun JC, Fremes SE, Rubens FD, Teoh KH. Antithrombotic and thrombolytic therapy for valvular disease: antithrombotic therapy and prevention of thrombosis, 9th ed: American college of chest physicians evidence-based clinical practice guidelines. Chest. 2012;141:e576S-600S.
11. Scappaticci FA, Skillings JR, Holden SN, et al. Arterial thromboembolic events in patients with metastatic carcinoma treated with chemotherapy and bevacizumab. J Natl Cancer Inst. 2007;99:1232–9.

Pericardial Effusion, Tamponade, and Constrictive Pericarditis

21

Bénédicte Lefebvre, Yu Kang, and Marielle Scherrer-Crosbie

21.1 Introduction

The normal pericardium is a bilayer fibroelastic sac: the outer fibrous and the inner serous pericardium. The latter is itself divided into two components; a visceral layer adjacent to the epicardium and a more external parietal layer. In between, a small amount of fluid (up to 25 mL) acts as a natural lubricant [1]. When excessive fluid accumulates in this pericardial space or when the pericardium becomes thickened and stiffened, one of three pericardial compressive syndromes may occur; cardiac tamponade, constrictive pericarditis and effusive–constrictive pericarditis. Pericarditis may be the first clinical manifestation of a non-diagnosed cancer. Twelve percent of patients with no known malignancy presenting with acute pericarditis with or without pericardial effusion will subsequently be diagnosed with cancer within 5 years. The presence of pericardial effusion is associated with a higher overall hazard ratio for the diagnosis of cancer than having pericarditis only (HR 3.59 vs HR 2.04) [2].

Pericardial syndrome in oncology patients may be secondary to cancer, malignancy complications, or side effects of cancer therapy. Echocardiography, a portable, low-cost, and non-irradiating technique is often performed as first line. Other modalities such as computer tomography (CT) and cardiac magnetic resonance imaging (CMR) may also be used in the diagnosis and evaluation of pericardial syndrome.

21.2 Etiologies of Pericardial Syndrome

21.2.1 Pericarditis and Pericardial Effusions

Among patients with known cancer, the most common etiology of pericardial disease is malignant involvement, which is identified in up to 60% of effusions [3]. In the remainder, idiopathic pericarditis is most common, while prior radiation therapy is thought to be contributory in 10–20%. Chemotherapy can also increase the risk of pericardial effusion, as well as the risk of opportunistic viral or bacterial infections.

In autopsy studies, malignant extension or involvement of the pericardium was detected in 1–20% of cancer cases [3, 4]. Neoplastic diseases invading the pericardium directly or via metastatic spreading through the lymphatics or bloodstream are much more frequent than the rare occurrence of primary pericardial tumors such as fibrosarcoma, mesothelioma, and angiosarcoma. The most common neoplastic diseases involving the pericardium are advanced lung cancer, breast cancer, melanoma, leukemia, and lymphoma [5].

The mechanisms triggering pericardial effusions are not limited to cancer itself. Chemotherapy-related acute pericarditis and pericardial effusions are occasionally observed, with an incidence up to 1–2% following exposure to traditional chemotherapy agents such as fludarabine, cytarabine, doxorubicin, docetaxel, and cyclophosphamide [6]. Interleukin-2 (IL-2) treatment used for renal cell carcinoma and melanoma may lead to capillary leak syndrome and it is estimated that between 2.5 and 5% of patients undergoing that treatment will present with pericarditis or myocarditis [7]. Lately, it has been recognized that tyrosine kinase

Electronic supplementary material
The online version of this chapter (https://doi.org/10.1007/978-3-030-70998-3_21) contains supplementary material, which is available to authorized users.

B. Lefebvre (✉) · Y. Kang
Hospital of the University of Pennsylvania, 3400 Civic Center Boulevard, Philadelphia, PA 19104, USA
e-mail: Benedicte.lefebvre@pennmedicine.upenn.edu

Y. Kang
e-mail: Yu.kang@pennmedicine.upenn.edu

M. Scherrer-Crosbie
Director of the Echocardiography Laboratory, Hospital of the University of Pennsylvania, 11–131 South Tower, PCAM, 3400 Civic Center Boulevard, Philadelphia, PA 19104, USA
e-mail: Marielle.scherrer-crosbie@pennmedicine.upenn.edu

R. M. Steingart et al. (eds.), *Atlas of Imaging in Cardio-Oncology*,
https://doi.org/10.1007/978-3-030-70998-3_21

inhibitors (such as dasatinib or imatinib) [8] and immune checkpoint inhibitors (ICI) [9, 10] may cause acute pericarditis, pericardial effusion and cardiac tamponade. Recently, a large systemic evaluation of the cases from the WHO global database has shown that ICI-associated pericardial diseases were more prevalent in men (60%) and that mortality was as high as 21% [11]. Radiotherapy to the chest is also well known to be related to acute pericarditis and pericardial effusion [12].

In the oncology patient, an infectious etiology of pericardial effusion is less common. However, patients who are immunocompromised due to treatment of an underlying malignancy may develop infectious or autoimmune pericardial effusions, and the infectious effusion, especially fungal, is associated with high mortality [13]. Moderate to large pericardial effusion or tamponade can develop post stem cell transplant with a reported incidence of 0.8–3.1% in the literature [14, 15]. The pathogenetic mechanism underlying the development of this complication is thought to be due to inflammation secondary to graft versus host disease (GVHD) though the occurrence of the pericardial effusion may not necessarily concur with active manifestations of GVHD. In one study, pericardial effusion was not noted in patients undergoing autologous stem cell transplantation [14, 15].

21.2.2 Constrictive Pericarditis

Constrictive pericarditis (CP) is a condition where a usually thickened pericardium is non-compliant and compresses the heart, leading to elevated and equalized intra-cardiac and intrapericardial diastolic pressures. In oncology patients, it may be secondary to a fibrotic pericardium following radiation treatment, typically seen >20 years post-treatment. Radiation adjacent to the heart is widely used for mediastinal lymphoma, esophageal, breast, and lung cancer. Pericardial disease following radiation is seen in 4–20% of patients but can be seen in up to 50% in particular cancers and treatments [16, 17]. Although no safe dose is recommended, the risk of pericardial disease post-radiation increases with a higher mean heart dose. A mean heart dose of equal to or greater than 30 Gy and/or daily fraction dose of more than 2 Gy/day are considered high-risk for the develeopment of radiation-induced cardiac complications [17, 18]. Nowadays, with the use of new radiation techniques such as prone-position radiation for breast cancer patients, deep-inspiration, appropriate shielding, breath-hold radiation for lung cancer patients, the increasing use of proton therapy radiation as opposed to photon therapy, and reduction in target volumes and radiation dose as imaging techniques are improving, CP is rapidly diminishing in frequency. It has been estimated that using these techniques may decrease the incidence of pericarditis from 20 to 2.5% [17]. Constrictive pericarditis may also be related to the presence of pericardial effusion in the delayed acute phase of pericarditis especially when echogenic fibrinous and frond-like coating strands are present [19].

21.2.3 Effusive–Constrictive Pericarditis

Effusive–constrictive pericarditis (ECP) is a rare entity, may be difficult to identify, and thus, is underdiagnosed. Radiation and malignancy-related complications are the two most-prevalent risk factors for the development of ECP [20, 21].

21.3 Pathophysiology of Cardiac Tamponade, Constrictive Pericarditis, and Effusive–Constrictive Pericarditis

Cardiac tamponade is the decompensated phase that occurs after sudden and/or excessive effusion accumulation leading to inappropriate filling of the cardiac chambers and increased intrapericardial pressure. During inspiration, the intrathoracic pressure decreases and is transmitted to the right side of the heart, leading to an increase in venous return to the right heart. Usually, the normal pericardium can stretch to accommodate physiologic changes in cardiac volume. However, in both cardiac tamponade and constrictive pericarditis, the cardiac volume is constrained by the intrapericardial fluid (tamponade) or by the inelastic and non-compliant pericardium (CP). As a result, there is exaggerated interventricular interaction with accentuated respiratory changes in right and left heart filling. As the filling occurs in the right ventricle, the interventricular septum shifts and there is an abrupt bounce toward the left to accommodate the increased right-sided volume. This concept is termed “interventricular dependence.” Although both entities exhibit similar hemodynamic changes, there are important pathophysiological differences between them. In cardiac tamponade, the primary abnormality is compression of cardiac chambers due to an increase in the intrapericardial pressure. Whereas in CP, the thickened, fibrotic pericardium prevents the normal inspiratory decrease in intrathoracic pressure to be transmitted to the cardiac chambers. During inspiration, as the pulmonary veins are outside of the pericardium, there is a decrease in the pulmonary venous pressure, but not in the left ventricular pressure as the non-compliant pericardium does not transmit the negative intrathoracic pressure. This leads to a decrease in the transpulmonary gradient (mean pulmonary artery pressure–left atrial pressure) and a reduction in the filling pressure of the left ventricle.

Effusive–constrictive pericarditis shares similar pathophysiological features with constrictive pericarditis though signs of tamponade can also be present.

21.4 Imaging in Cardiac Tamponade, Constrictive Pericarditis, and Effusive–Constrictive Pericarditis

21.4.1 Echocardiography

Echocardiography plays a major role in the identification of pericardial effusion, evaluation of the hemodynamic significance when cardiac tamponade is suspected, guidance of the appropriate timing of pericardiocentesis, and identification of constrictive pericarditis. A structured approach when performing an echocardiogram in pericardial disease includes two-dimensional, M-mode and Doppler echocardiography to assess: (1) quantity of pericardial effusion; (2) cardiac chambers collapse; (3) motion of the interventricular septum during respiration; (4) respiratory variation of flow patterns in atrioventricular valves and ventricular outflow tracts; (5) inferior vena cava dimension and collapsibility and hepatic vein flow pattern. Additionally, mitral septal and lateral tissue Doppler e' velocities are helpful if constriction or effusive–constrictive pericarditis is suspected [22, 23]. Of note, loculated effusions are more common when scarring has supervened, in which only selected chambers are compressed. As a result, the typical physical, hemodynamic and echocardiographic signs of cardiac tamponade may be absent [19].

Patients suffering from CP without any underlying cardiomyopathy typically have a normal septal mitral e' amplitude (>8 cm/s). This can be used to differentiate patients with other cardiomyopathies such as restrictive etiology (medial mitral e' < 8 cm/s) [24]. "Annulus reversus" can also be seen and refers to the unusual phenomenon where the lateral tissue doppler e' is lower than the mitral septal tissue doppler e'. This is thought to be secondary to the lateral wall being tethered to the thick, fibrotic and non-compliant pericardium [25]. Further, the left ventricular filling pressure cannot be estimated with the mitral E/e' ratio as septal e' is usually preserved or accentuated despite increased LV filling pressure. In fact, an inverse relationship between E/e and pulmonary capillary wedge pressure has been shown in patients with CP. This phenomenon, termed "annulus paradoxus," is thought to occur based on the fact that the more severe constriction with a higher LV filling pressure, the more accentuated the longitudinal motion of the medial mitral annulus is to compensate for the limited lateral expansion of the heart [26].

It is important to note that the absence of visualization of a calcified and echo-bright pericardium does not exclude the diagnosis of CP. Assessment of the pericardium thickness by transthoracic echocardiography is not accurate or sensitive due to the lower resolution. However, studies have shown a close correlation between the pericardial measurement done with transesophageal echocardiography (TEE) and computed tomography ($r \geq 0.95$, SE $\leq$ 0.06 mm, $p < 0.0001$). On TEE, the mean normal pericardial thickness was noted to be 1.2 ± 0.8 mm ($\pm$SD) and was not exceeding 2.5 mm (95% sensitive and 86% specific if pericardium was ≥ 3 mm) [27]. See Table 21.1 for a summary of the different echocardiographic characteristics of cardiac tamponade and constrictive pericarditis compared to normal individuals.

Effusive–constrictive physiology is more easily diagnosed with invasive techniques aiming at measuring intracardiac or intrapericardial pressures during pericardiocentesis, however, a careful echocardiographic examination can help ascertain the diagnosis. Clues include failure of normalization of respiratory variation inflow across the mitral or tricuspid valves, continuous large plethoric IVC, or abnormal respirophasic interventricular septum shift immediately after pericardial drainage. Certain echocardiographic characteristics found pre-pericardiocentesis may be predictive of the development of ECP. Loculated and/or fibrinous effusion, abnormal respiratory interventricular septum bounce, end-diastolic reversal flow into the hepatic veins in expiration, and respiratory variation of the mitral inflow velocity were all more marked and frequent in patients who would develop ECP post-pericardiocentesis. Mitral valve tissue Doppler e' was also higher in the ECP group [28].

21.4.2 Computed Tomography and Cardiac Magnetic Resonance

Computed tomography (CT) can be useful in evaluating pericardial thickening and visualizing calcification of the pericardium. However, it is important to note that CT may overestimate the amount of pericardial effusion especially when images acquired are not gated (if acquiring in systole vs diastole). CT can also detect extracardiac lesions, such as pleural effusion, enlargement of lymph nodes, and mediastinal tumors. The attenuation value of the pericardial fluid on CT can help differentiate the type of pericardial effusion: typically, an attenuation value >60 Hounsfield units supports the presence of blood; an attenuation value between 20 and 60 Hounsfield units supports the presence of an exudate, and an attenuation value <10 Hounsfield units supports the presence of a transudate [29].

Cardiac magnetic resonance imaging (CMR) offers advantages over CT or echocardiography. Not only can it provide a comprehensive evaluation of the ventricles and their functions, characterization of masses, and infiltrative

Table 21.1 Summary of the Echocardiographic Characteristics of Cardiac Tamponade and Constrictive Pericarditis [23, 24]

Characteristics	Normal heart	Cardiac tamponade	Constrictive pericarditis
Pericardium	Thin pericardium with no or physiologic pericardial effusion	Small to large effusion, swing of the heart within the effusion	May see thickening, calcification, and/or pericardial effusion Best seen on TEE
Atrial Size	Normal	Depends on the underlying heart disease	Biatrial enlargement
Collapse of cardiac chambers	None	Diastolic collapse of any cardiac chamber, usually right-sided	None
Interventricular septum motion with inspiration	No brisk movement unless bundle branch block or post-pericardiotomy	Ventricular septal "bounce" toward LV during inspiration (opposite during expiration)	Ventricular septal "bounce" toward LV during inspiration (opposite during expiration)
M-mode findings mid-LV	Normal motion	"Bounce" of the interventricular septum and decreased LV size during inspiration	Same as tamponade and flattening of the posterior LV wall in late diastole
Respiration variation of mitral and tricuspid inflow E-wave	Mitral variation in expiration of < 25% and tricuspid variation in inspiration of < 40%	Decreased mitral inflow, variation of > 25% in inspiration and increased tricuspid variation in inspiration of > 40% (opposite in expiration)	Decreased mitral inflow variation of > 25% in inspiration and increased tricuspid variation in inspiration of > 40% (opposite in expiration)
Mitral septal and lateral tissue doppler e' (cm/s)	Mitral medial e' > 7 cm/s and lateral e' > 10 cm/s	Usually normal	Mitral medial e' > 8 cm/s **Annulus reversus**: mitral lateral e' < mitral septal e'
LV filling pressure	Mitral E/e' is a good surrogate to estimate filling pressure		Cannot use mitral E/e' as e' is usually normal and preserved despite elevated pressure (**Annulus paradoxus**)
IVC	Should be < 2.1 cm with inspiratory collapse > 50%	Plethoric dilated IVC	Same as tamponade
Hepatic veins patterns with expiration	Forward flow during expiration	End-diastolic reversal flow into hepatic vein during expiration	Same as tamponade
Strain	Normal		Global longitudinal strain normal, decreased circumferential strain

Summary of the different echocardiographic characteristics of cardiac tamponade and constrictive pericarditis compared to normal individuals.
IVC: Inferior vena cava, LV: Left ventricle, TEE: Transesophageal echocardiogram

processes, it is also very useful in evaluating the presence of myocardial inflammation (increased signal in T2-weighted short tau inversion recovery sequence (STIR)), pericardial thickening or pericardial fibrosis. Different techniques are offered to diagnose constrictive pericarditis in addition to visual inspection of the pericardium. CMR allows precise measurement of the pericardial thickness. Following contrast administration, the presence of late gadolinium enhancement in the pericardium is a sign of fibrosis. The acquisition of real-time free-breathing cine images allows visualization of the interventricular septal bounce during inspiration. Myocardial tagging (saturation of the myocardium in a grid-like fashion) demonstrates adhesions between the fibrotic pericardium and the myocardium.

21.5 Treatment Options

Treatment for acute pericarditis in patients with cancer follows the same medical regimen as with non-cancer patients and consists first of high-dose non-steroidal anti-inflammatory drugs (NSAIDs) and colchicine (see guidelines, Adler et al. [22]). For cardiac tamponade, treatment requires immediate removal of pericardial effusion. This is usually performed with pericardiocentesis first or with the surgical pericardial window when effusion re-accumulates. Loculation of pericardial fluid may result in an inability to aspirate pericardial contents either for diagnosis or relief of tamponade [19]. It is important to treat the underlying etiology (chemotherapy and radiation as needed).

With constrictive pericarditis, treatment options are limited and may involve surgical pericardiectomy with incomplete efficacy and poor outcomes [30]. Studies have described poor survival following pericardiectomy in patients suffering from radiation-induced CP with a 5-year survival reaching only 11% compared to 80% in idiopathic cases [31].

Treatment of pericardial diseases is dependent on the etiology and usually involves treating the underlying cause; this will be explained in greater detail in the clinical cases below.

21.6 Case 1

Case summary: A 56-year-old male with chronic myelogenous leukemia, who presented with recurrent fibrinous pericardial tamponade and developed constrictive pericarditis later.

- Signs or symptoms suspicious for cardiac tamponade imply the need for urgent pericardiocentesis, which usually significantly relieves the symptoms of tamponade.
- Pericardial effusion containing echogenic fibrinous and frond-like coating strands is associated with the development of constrictive pericarditis [19].

A 56-year-old male originally diagnosed with chronic myelogenous leukemia with P210 BCR-ABL rearrangement 5 years ago, was treated with imatinib (tyrosine kinase inhibitor). Two years after, he reported progressive back pain and weakness of lower extremities. MRI and cerebrospinal fluid cytology confirmed intracranial B-cell neoplasia and he was treated with intrathecal chemotherapy, R-Hyper CVAD (rituximab, cyclophosphamide, vincristine, doxorubicin, dexamethasone, methotrexate, and cytarabine) and switched from imatinib to dasatinib. Six months afterward, he presented to the emergency department with 3 days of worsening cough and dyspnea and was diagnosed with multifocal enterovirus pneumonia with pericardial effusion. Transthoracic echocardiogram revealed a large pericardial effusion with findings suggestive of cardiac tamponade (Videos 21.1 and 21.2, Figs. 21.1 and 21.2).

The patient underwent pericardiocentesis with the removal of 350 mL of bloody exudative fluid and his symptoms were relieved significantly. He was treated with methylprednisone, however had recurrent pericardial effusion treated with two other pericardiocenteses after 2 and 8 months, respectively, and repeated cytologic and flow cytometry examination of the pericardial fluid were negative. The etiology of the pericardial effusion remained unclear, with differential diagnosis including viral infection, recurrence of disease, or dasatinib-induced effusion (present in approximately 1% of patients treated with dasatinib). He discontinued dasatinib permanently given recurrent tamponade. High-dose aspirin and colchicine were not ideal given his thrombocytopenia and acute kidney injury. After the fourth episode of pericardial tamponade, the patient underwent a surgical pericardial window. Cardiac catheterization showed severely elevated intrapericardial pressures which were successfully reduced from 29 to 3 mmHg after removal of 750 mL of bloody fluid, and patient's systolic pressure increased from 100 to 140 mmHg.

After 6 months, the patient remained asymptomatic. However, a follow-up echocardiogram revealed evidence of constrictive physiology with respiratory interventricular septal shift and diastolic interventricular septal "bounce" without tissue Doppler septal to lateral velocity paradox. CT showed widely thickened pericardium (Videos 21.3, 21.4 and 21.5, Figs. 21.3, 21.4, 21.5 and 21.6).

21.7 Case 2

Case Summary: A 69-year-old woman with acute myeloid leukemia, who presented with cardiac tamponade in the context of severe serositis due to graft versus host disease (GVHD). With the treatment of GVHD, the patient recovered well without recurrence of pericardial effusion.

- Rarely, pericardial effusion and tamponade can develop as a consequence of graft versus host disease after allogeneic stem cell transplant.

This 69-year-old woman was diagnosed with AML 3 years prior to presentation and was originally induced with daunorubicin (total 60 mg/m^2) and cytarabine (100 mg/m^2) ("3 + 7" induction regimen) with residual AML. Therefore, she underwent high-dose cytarabine (1500 mg/m^2) with

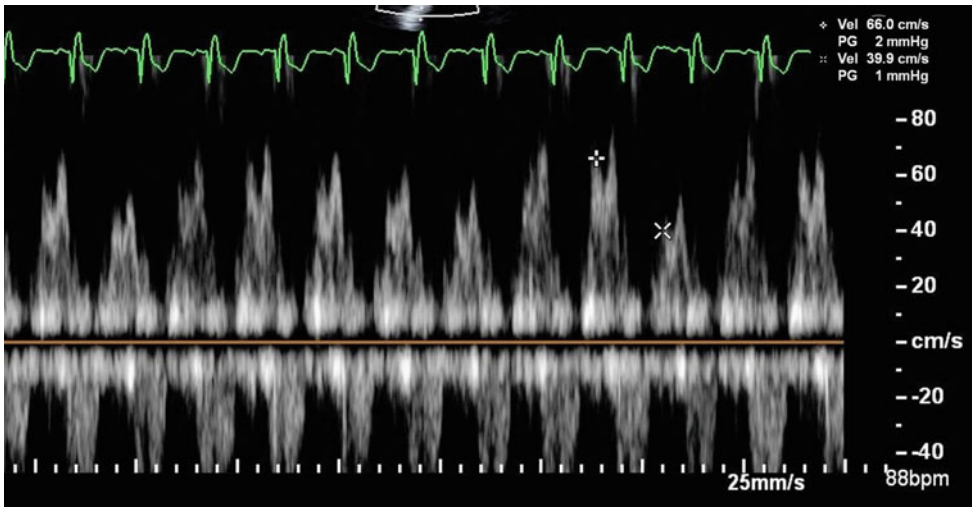

Fig. 21.1 Inspiratory reduction in mitral peak E-wave velocity greater than 25%. A positive respiratory variation of the tricuspid valve inflow is characterized by an increase by more than 40% of the E-wave velocity during inspiration. A positive respiratory variation of the mitral valve inflow E-wave velocity is a decrease of more than 25% of E velocity during inspiration. The opposite would be seen during expiration. To measure the respiratory variation, the following formula is used: Respiration Variation of Mitral or Tricuspid Valve Inflow $= \frac{E\ Expiration - E\ Inspiration}{E\ Expiration}$. Unfortunately, the respirator was not used in this patient. Here, despite no respirator, we can imagine the end-expiration and end-inspiration values (shown by the "+"). In this patient, the respiration variation of mitral inflow = (66−40)/66 = 39%

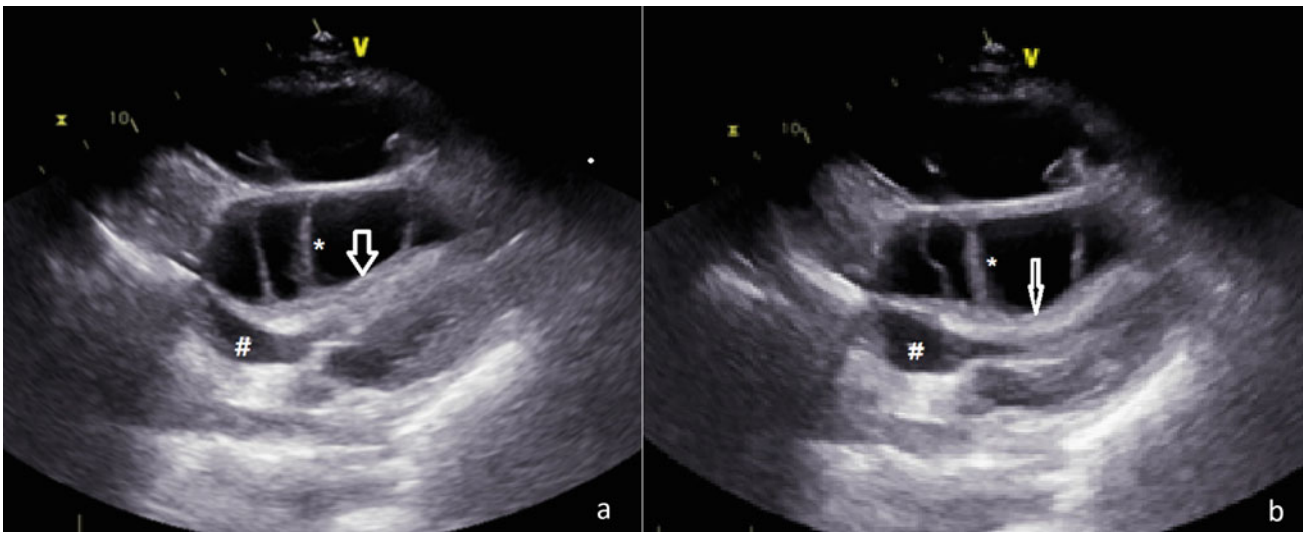

Fig. 21.2 A and B are subcostal views and still figures from video 1. A is taken at end-systole and B at end-diastole and show the collapse of the right ventricle (arrow). *: fibrinous strands; #: right atrium

complete remission. Prior to bone marrow transplantation, conditioning treatment was given (fludarabine and busulfan).

Following an allogeneic bone marrow transplant, the patient developed GVHD with cutaneous symptoms. A few months later, serositis with bilateral pleural effusion started despite treatment with tacrolimus and methotrexate. She presented to the emergency department due to respiratory distress. Transthoracic echocardiogram demonstrated large pericardial effusion and tamponade (Videos 27.6 and 21.7, Figs. 21.7, 21.8 and 21.9). She underwent urgent pericardiocentesis with bilateral chest tube insertion. Due to rapid reaccumulation of fluid with pre-tamponade physiology, the patient was sent for a surgical pericardial window with excellent results. She was started on rituximab (a chimeric monoclonal antibody targeting B cells lymphocytes, acting as an immunomodulator), high-dose prednisone with slow tapper, and ruxolitinib (a JAK inhibitor) to treat GVHD. Patient recovered well afterward without recurrent pericardial effusion.

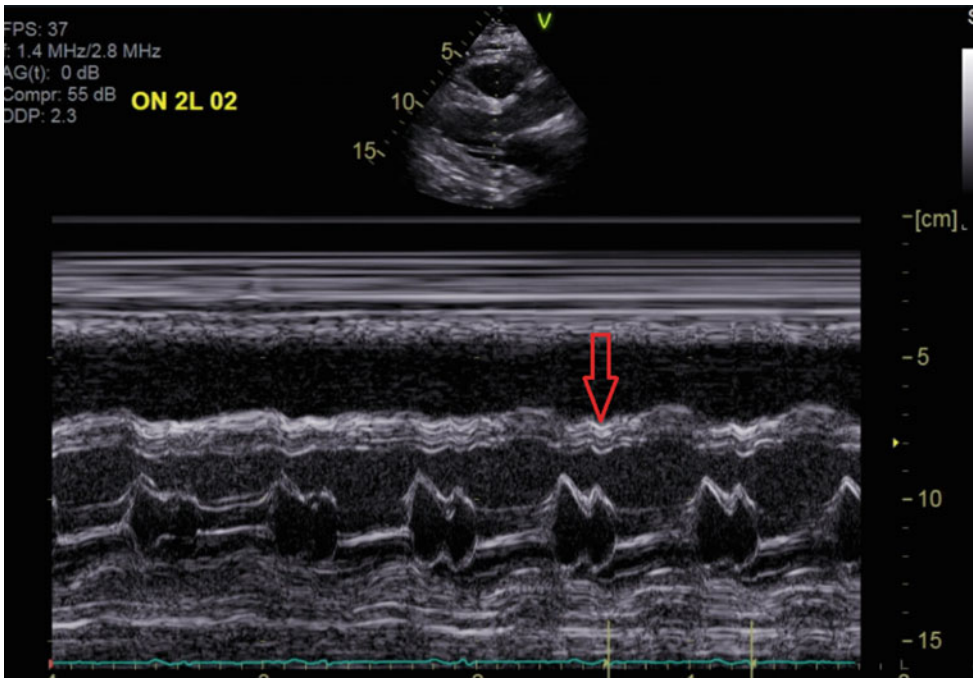

Fig. 21.3 Diastolic interventricular septal "bounce" demonstrated by M-mode echocardiography (shown by arrow). During inspiration, an increase in venous return to the right heart occurs due to the reduction of intrathoracic pressure. However, with the constraint of pericardial fluid, the decrease in the pulmonary venous pressure leads to a reduction in the filling pressure of the left ventricle, Therefore, the interventricular septum shifts and there is an abrupt bounce toward the left to accommodate the increased right-sided volume

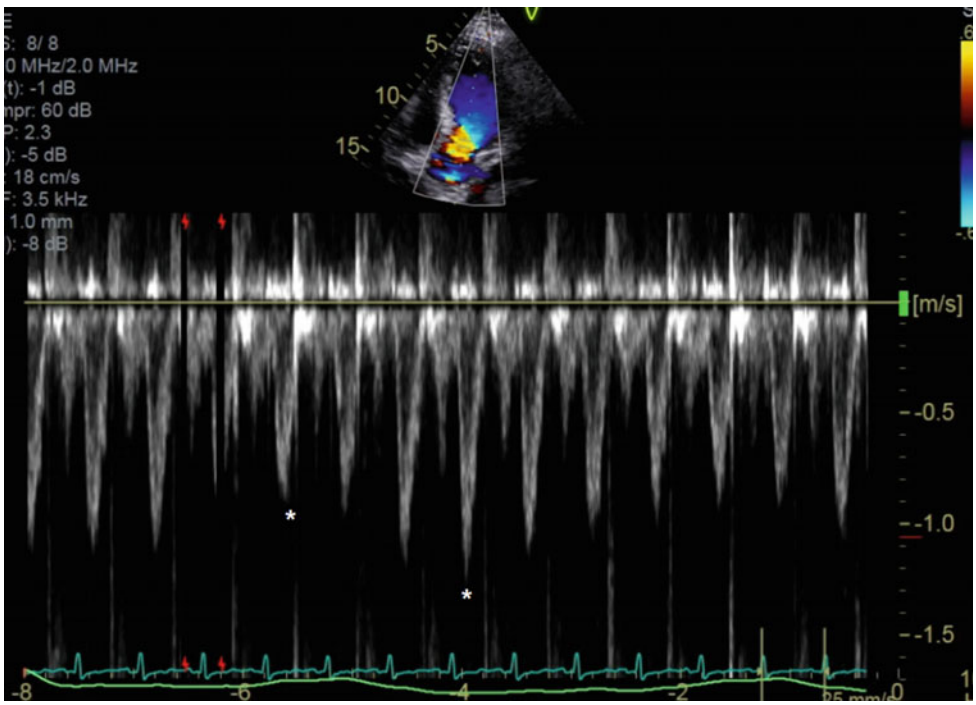

Fig. 21.4 Reduction in flow greater than 25% in the left ventricular outflow tract during inspiration. The respiration variation of left ventricular outflow tract = (130 −88)/ 130 = 32%

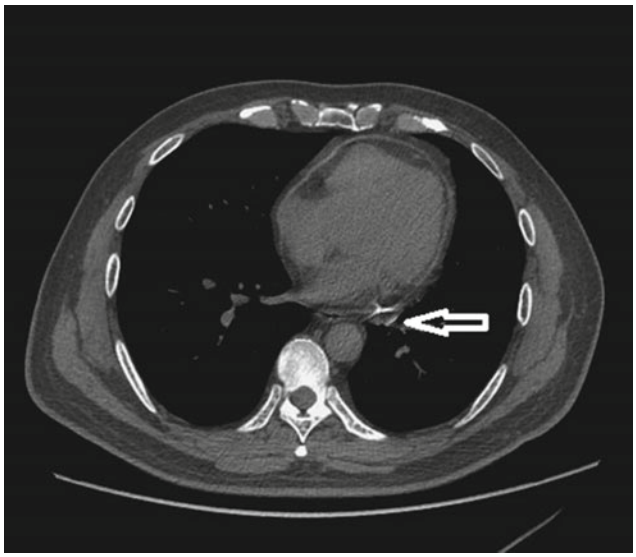

Fig. 21.5 CT showed widely thickened pericardium with mild calcification (indicated by arrow)

21.8 Case 3

Case Summary: 45-year-old male treated more than 30 years ago with mantle field radiation for Hodgkin's lymphoma, with constrictive pericarditis.

- Radiation-induced constrictive pericarditis usually occurs several decades after treatment.
- Symptoms can be insidious and progressive, and the diagnosis may be hard to make at first if not sought after. Here the patient presented with progressive and worsening dyspnea over 5 years.
- As radiation may also cause accelerated coronary artery disease, an ischemic workup may be warranted.
- Among childhood survivors of Hodgkin's lymphoma treated with mediastinal radiation, the incidence of CP was found to be 7% [32].

A 45-year-old man was diagnosed with Hodgkin's lymphoma at age 12 and treated with ABVD (adriamycin, bleomycin, vinblastine, and dacarbazine, total dose adriamycin 100 mg/m^2) and mantle field radiation ($\sim$4000 cGy) with complete remission. Following remission, the patient did not have any follow-up for the next 25 years. After multiple visits complaining of dyspnea, he was diagnosed with hypertension and started on chlorthalidone 25 mg daily. Dyspnea was thought to be secondary to uncontrolled hypertension, deconditioning, and obesity (BMI 38 mg/m^2). After worsening of symptoms despite blood pressure control, the patient was referred to a cardiologist. An echocardiogram was done and showed features of constrictive pericarditis (Videos 21.8, 21.9 and 21.10, Figs. 21.10, 21.11, 21.12, 21.13, 21.14, 21.15 and 21.16). The treatment plan is limited: optimization of blood pressure and filling pressure and ultimately, referral to a high-volume center for pericardiectomy with varied results and often incomplete resolution of symptoms.

21.9 Case 4

Case Summary: a 71-year-old lady with recurrent metastatic breast cancer previously treated with anthracycline and radiation presenting with cardiac tamponade. Despite undergoing pericardiocentesis, the patient remained very

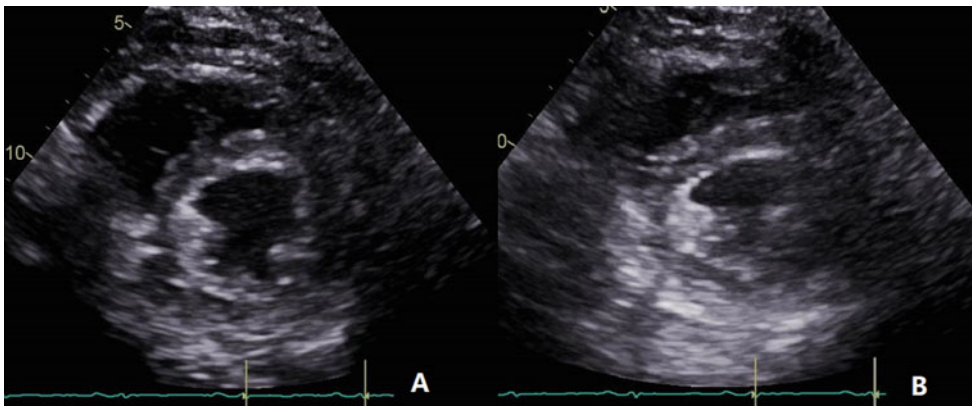

Fig. 21.6 Still figures from Video 21.4. **a** and **b** are parasternal short-axis views of the left ventricle. **a** shows the interventricular septum during expiration at end-diastole and **b** shows the interventricular septum during inspiration at end-diastole (see Video 21.4)

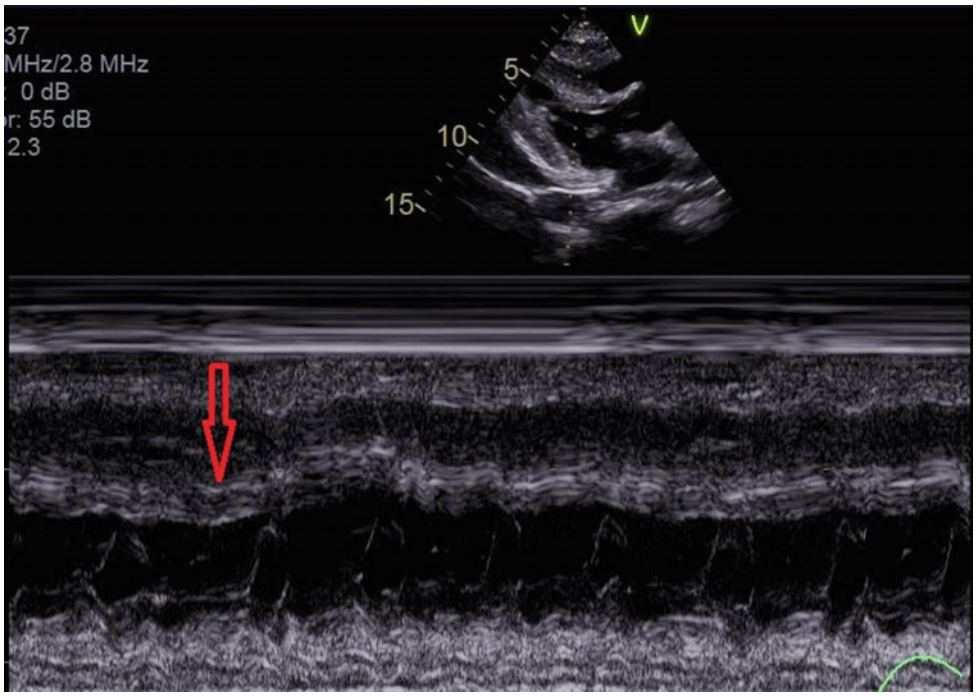

Fig. 21.7 M-mode demonstrating interventricular septum bulging into the left ventricle during inspiration (shown by arrow)

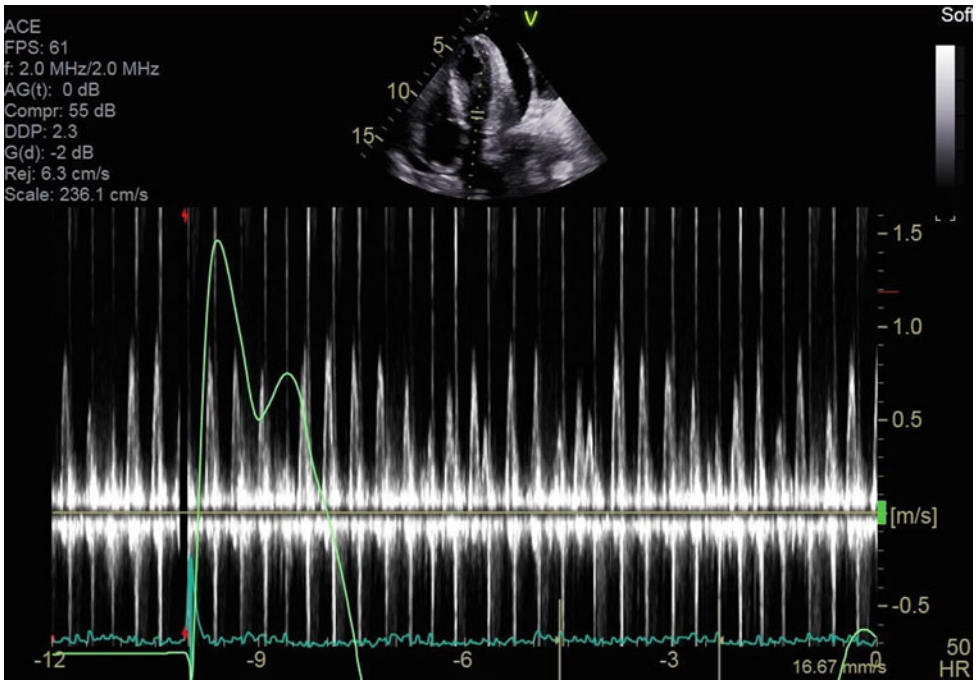

Fig. 21.8 Inspiratory reduction in mitral peak E-wave velocity greater than 25% (as explained before, the inspiratory reduction in mitral peak E-wave velocity = (114 - 50)/114 = 56%)

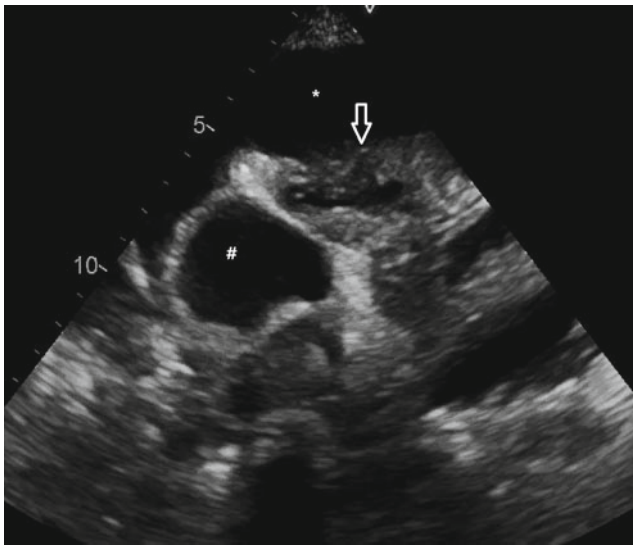

Fig. 21.9 Still image from video 6 showing the large pericardial effusion (shown by *), and the collapse of the right ventricle depicted by the arrow. The right atrium is shown by the # sign

dyspneic and was later diagnosed with effusive–constrictive pericarditis.

- Although rare, it is important to recognize effusive–constrictive physiology as an explanation for worsening or stable dyspnea and tachycardia in patients post-pericardiocentesis.

We present a case of a 71-year-old female, originally diagnosed 25 years prior with right-sided breast cancer treated at that time with radical mastectomy, anthracycline for six cycles, radiation (unclear total dose and mean heart dose), and tamoxifen. Fifteen years later, she presented with nodes positive, ER-positive, left breast cancer treated with mastectomy, Taxotere for six cycles, radiation (unclear total dose and mean heart dose), and tamoxifen then anastrozole (non-steroidal aromatase inhibitor). A few years afterward, she was diagnosed with metastatic breast carcinoma to pelvic bones, mediastinal nodes, liver. and pleura. She was treated with capecitabine with the progression of disease. She presented to the emergency department with 2 weeks of worsening dyspnea and was found to be in tamponade physiology and atrial fibrillation with rapid ventricular rate. Her vital signs in the ED are as follows: BP 110/62 mmHg and pulsus paradoxus of 6 mmHg (likely underestimated due to atrial fibrillation), HR 130–160 bpm in atrial fibrillation, afebrile (91.9 °F/36.6 °C), respiratory rate 21/min and saturation 94% on room air. She underwent a pericardiocentesis with progressive dyspnea and hypotension. Videos 21.11, 21.12, 21.13, 21.14, 21.15, 21.16 and 21.17 and Figs. 21.17, 21.18 and 21.19 show the extent and the hemodynamic consequences of the pericardial effusion.

Following the pericardiocentesis, despite removing 300 cc of sero-sanguinous fluid, spontaneous conversion into normal sinus rhythm, the patient remained very dyspneic and tachycardic. Another echocardiogram was performed within 1 h of the procedure and showed interventricular septal bounce and mitral annulus reversus (higher medial than lateral e' values), signs of constriction (Videos 21.18, 21.19, 21.20 and 21.21, Figs. 21.20, 21.21, 21.22 and 21.23). Although the cytology of the pericardial fluid was inconclusive for malignancy, the tamponade was

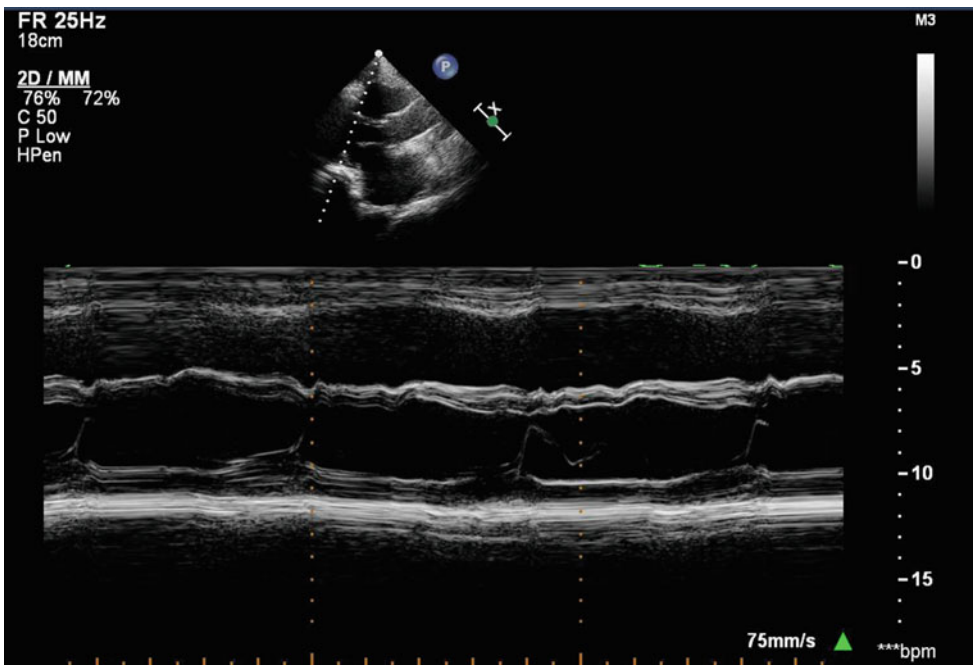

Fig. 21.10 M-mode through the mid-left ventricle in parasternal long axis showing flattening of the posterior LV wall in late diastole (shown by *) as a sign of the fixed cardiac volume

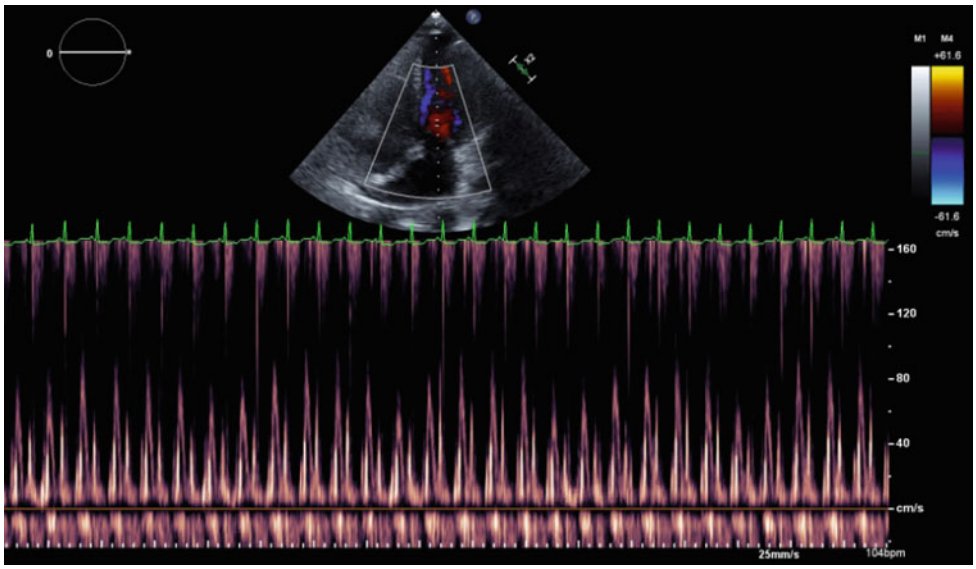

Fig. 21.11 Respiratory variation of the mitral valve inflow E-wave velocity. For precise measurement, the sweep speed should be increased and unfortunately, the respirator was not used. A positive respiratory variation of the mitral valve inflow E-wave velocity is decreased by 25–40% of E velocity during inspiration. Here, despite no respirator, we can imagine the end-expiration and end-inspiration values (shown by the *). The calculation would be as follows: $Respirationvariation\ ofmitralvalveinflow = \frac{90\ cm/s - 60\ cm/s}{90\ cm/s} = 33\%$

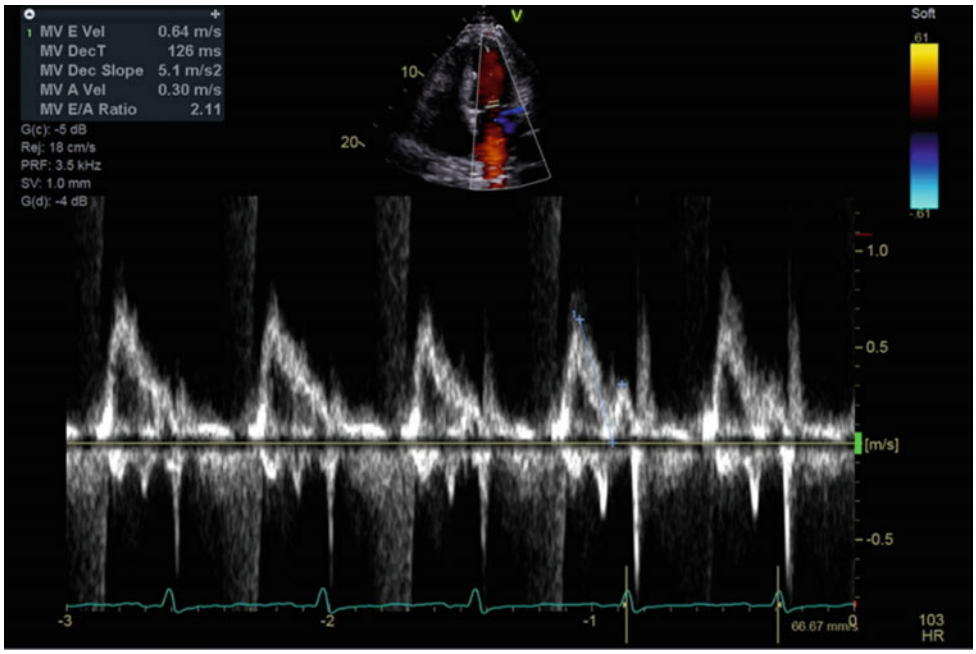

Fig. 21.12 The mitral valve E/A is 2.1 with a short deceleration time which may be a sign of restrictive cardiomyopathy as a consequence of previous radiation or grade 3 diastolic dysfunction

likely secondary to the progressive metastatic breast cancer, and the effusive–constrictive physiology a consequence of her previous radiation therapies especially to the left breast more than 10 years prior to the current presentation. Unfortunately, the patient suffered from a pathologic fracture of the left femoral neck, underwent extensive surgery, and deteriorated during recovery. She passed away in comfort care from metastatic breast cancer. Videos 21.22, 21.23 and 21.24 and Fig. 21.24 depict the findings from ECP on cardiac magnetic resonance and were taken from another patient (lung cancer with radiation 15 years ago) and status-post pericardial window who presented with effusive–constrictive physiology.

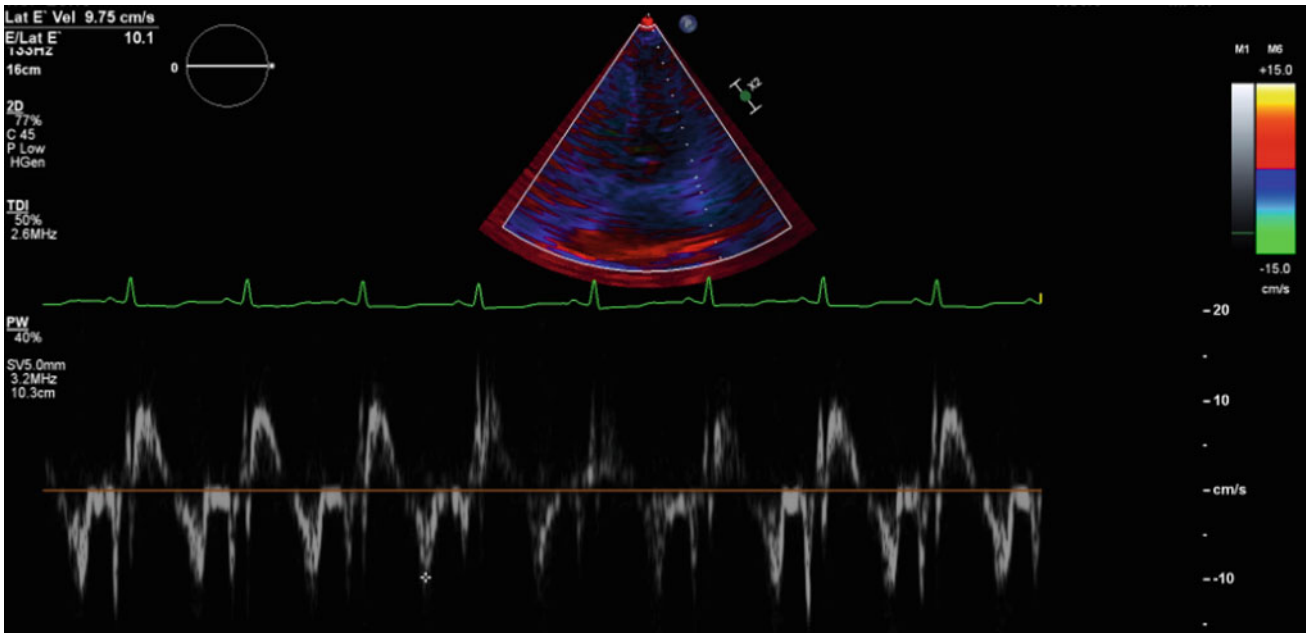

Fig. 21.13 The mitral lateral (9.75 cm/s) and medial (13.5 cm/s) e' demonstrate the "annulus reversus" (higher medial than lateral e' value) which is a sign of constriction

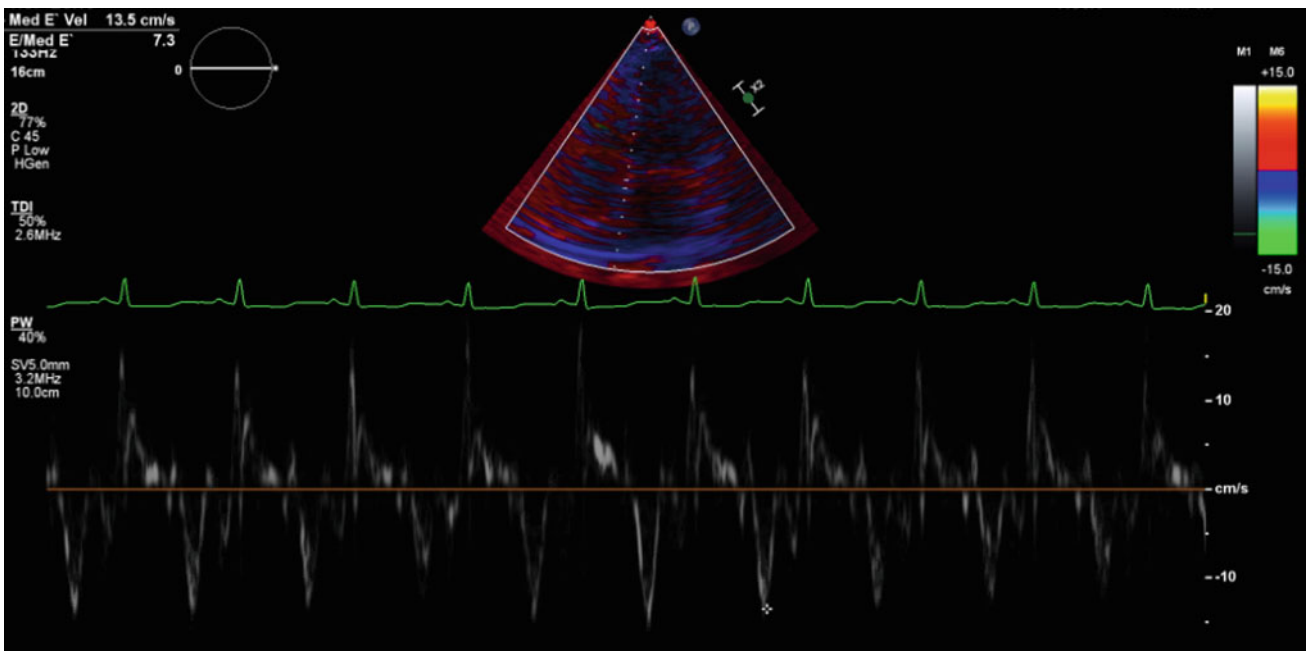

Fig. 21.14 The mitral lateral (9.75 cm/s) and medial (13.5 cm/s) e' demonstrate the "annulus reversus" (higher medial than lateral e' value) which is a sign of constriction

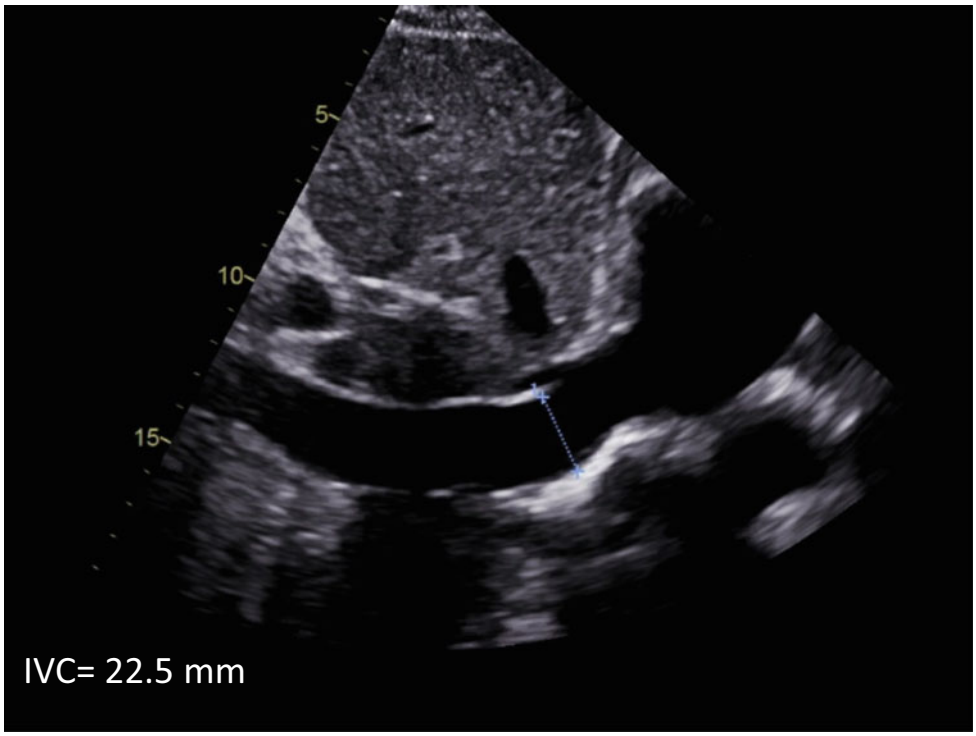

Fig. 21.15 Dilated inferior vena cava (22.5 mm) which was not collapsing during inspiration (not shown)

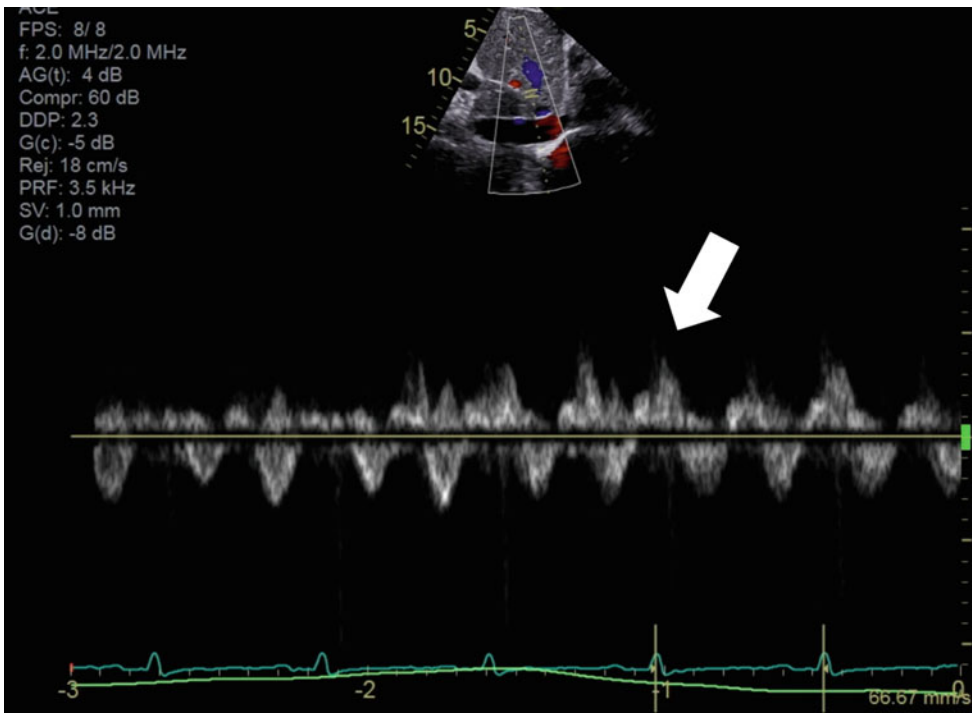

Fig. 21.16 Pulse Doppler of the hepatic veins showing variation and reversal of the flow during late diastole at expiration (arrow). Hepatic venous flow abnormalities (blunting or frank reversal of diastolic flow with expiration and systolic venous flow predominance) have high positive and negative predictive values for cardiac tamponade and CP. This finding was first described in a study of 13 patients with CP showing a 100% specificity and a 68% sensitivity [33]. The popular mnemonic "RICE" is often taught to cardiology fellows in order to remember this important hepatic finding (**R**estriction **I**nspiration, **C**onstriction **E**xpiration)

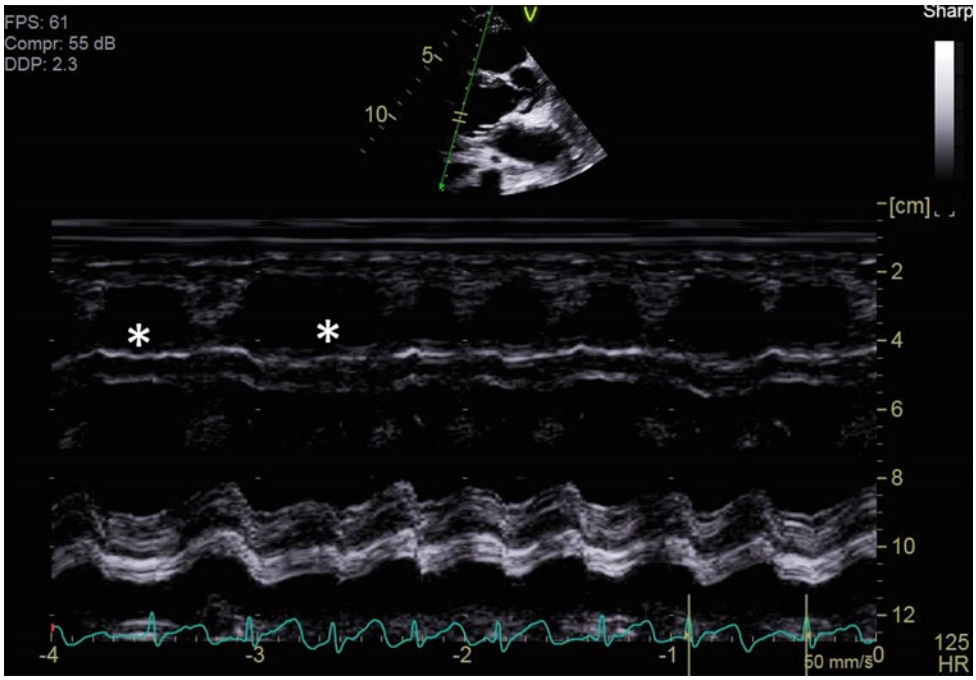

Fig. 21.17 M-mode through the mid-left ventricle in parasternal long axis showing flattening of the posterior LV wall in late diastole (see *)

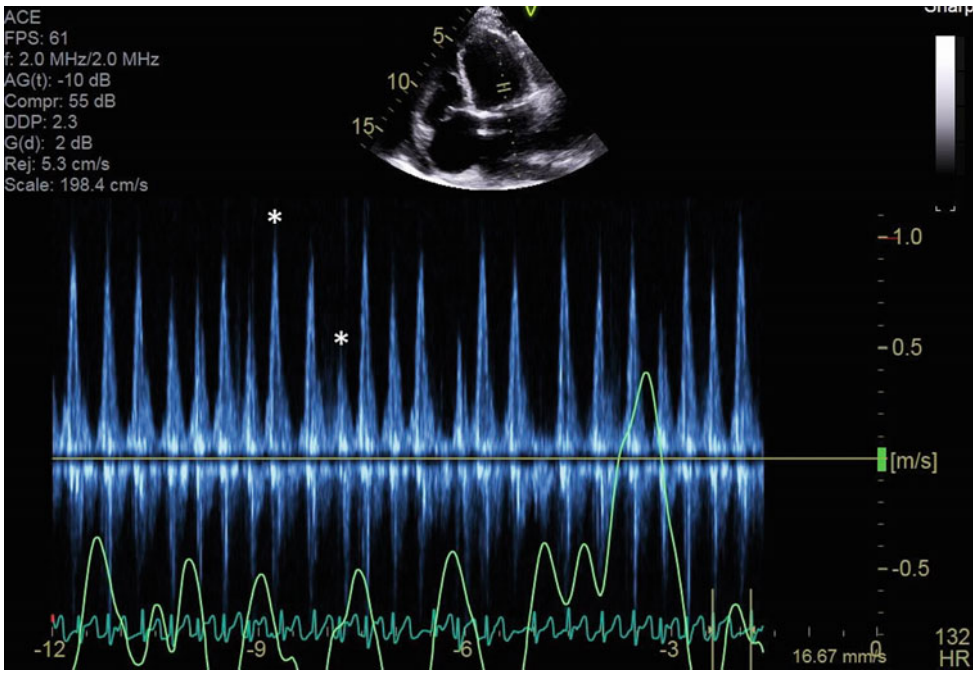

Fig. 21.18 Respiratory variation of the mitral valve inflow E-wave velocity. For precise measurement, the sweep speed should be increased. The patient was very dyspneic and the baseline of the respirator is chaotic. There is a positive respiratory variation of the mitral valve inflow E with a decreased up to 50% of E velocity during inspiration (see *). To measure the respiratory variation, the formula used is: the E velocity at the first beat post-expiration (ascending slope)—the E velocity at the first beat post-inspiration (descending slope) divided by E velocity the post-expiration

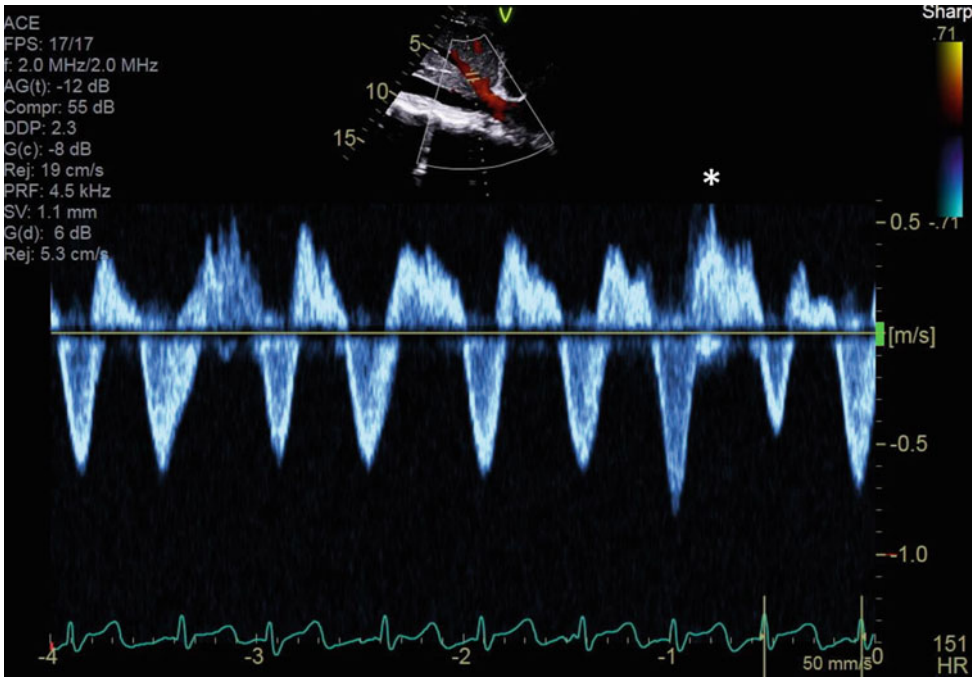

Fig. 21.19 Although there is no respirator during the pulse doppler of the hepatic veins, there is variation and reversal of the flow during late diastole (see *)

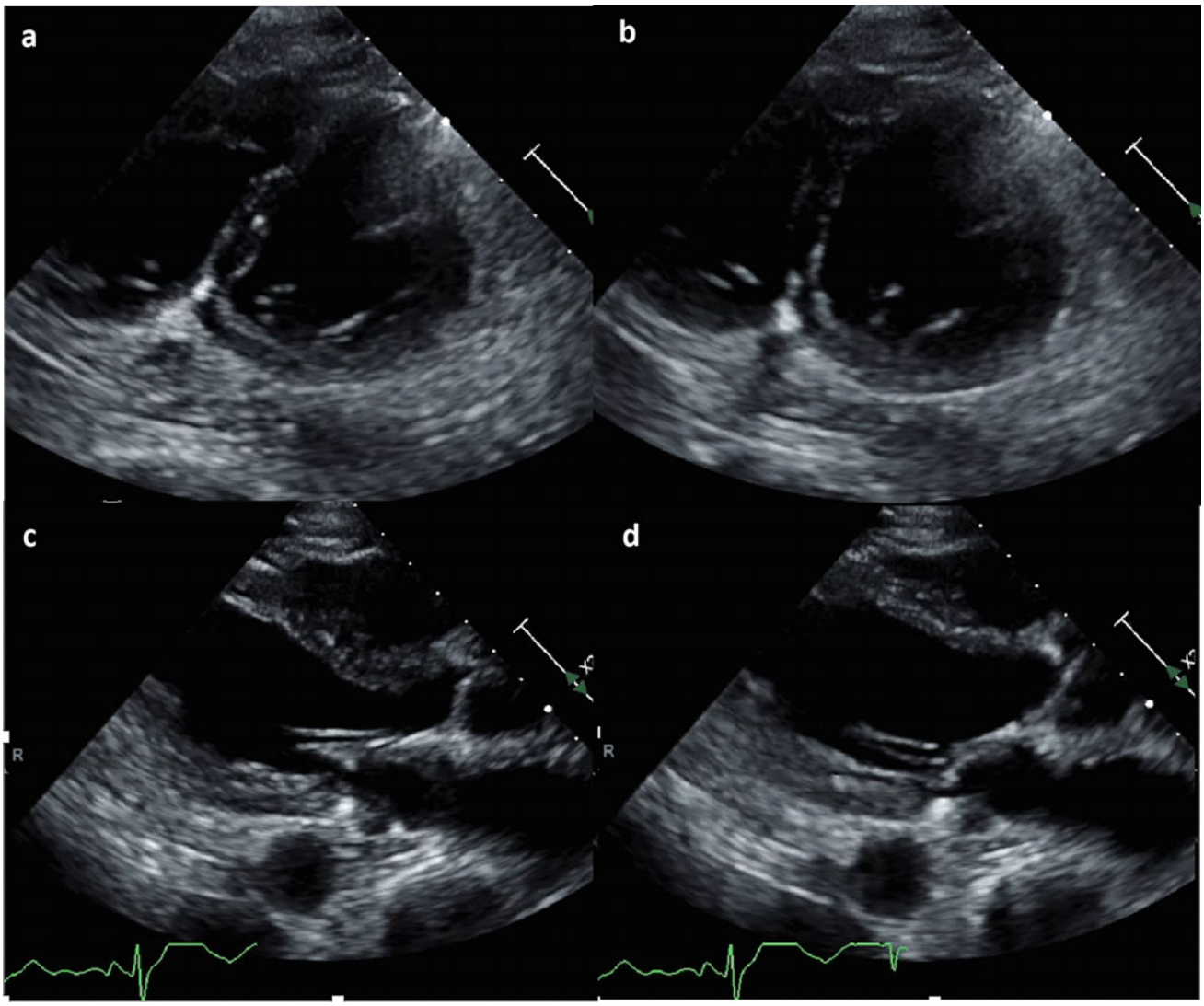

Fig. 21.20 This figure demonstrates the interventricular septum bounce during inspiration. **a** and **b** are parasternal short axis and figure **a** demonstrates a flat interventricular septum during inspiration whereas figure **b** depicts the normal movement of the interventricular septum during expiration. **c** and **d** are parasternal long axis showing the interventricular septum bounce (into the left ventricle) during inspiration in figure **c** and the normal interventricular septum movement during expiration in figure **d**. See Videos 18 and 19 of the interventricular septum bounce

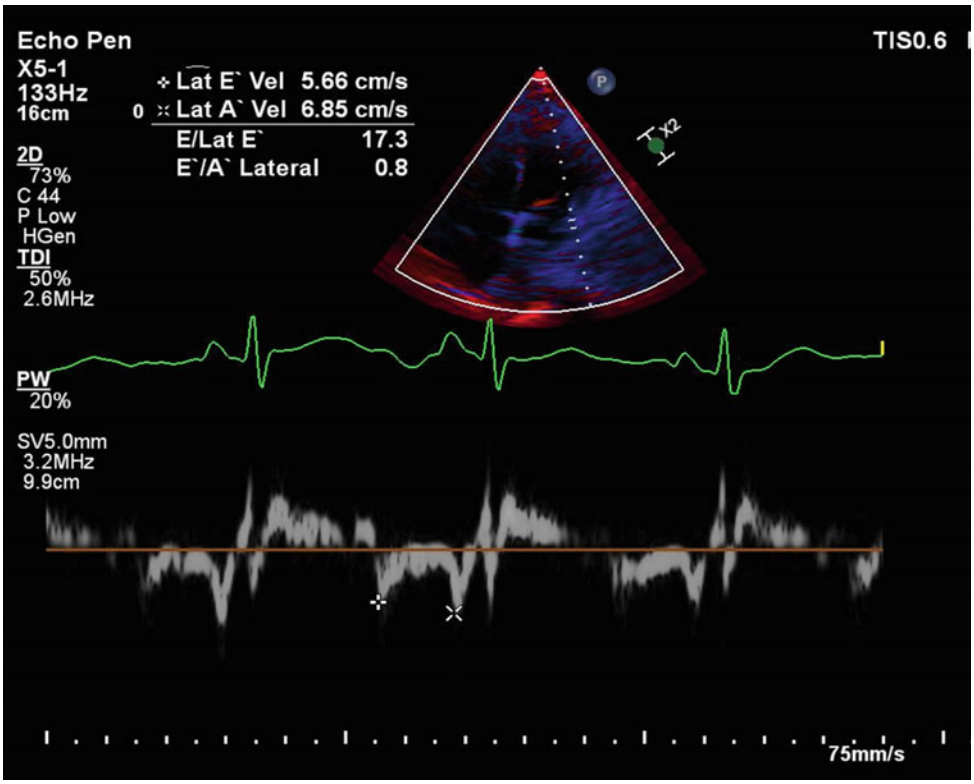

Fig. 21.21 The mitral lateral (6 cm/s) and medial (8 cm/s) e' demonstrate the annulus reversus (higher medial than lateral e' value) which is a sign of constriction

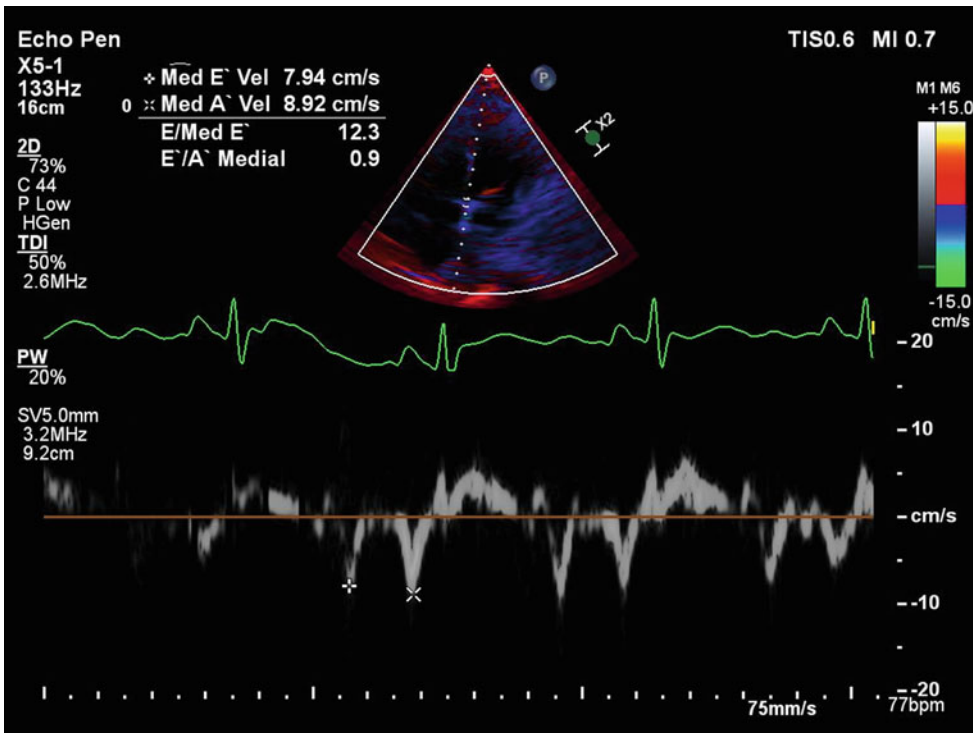

Fig. 21.22 The mitral lateral (6 cm/s) and medial (8 cm/s) e' demonstrate the annulus reversus (higher medial than lateral e' value) which is a sign of constriction

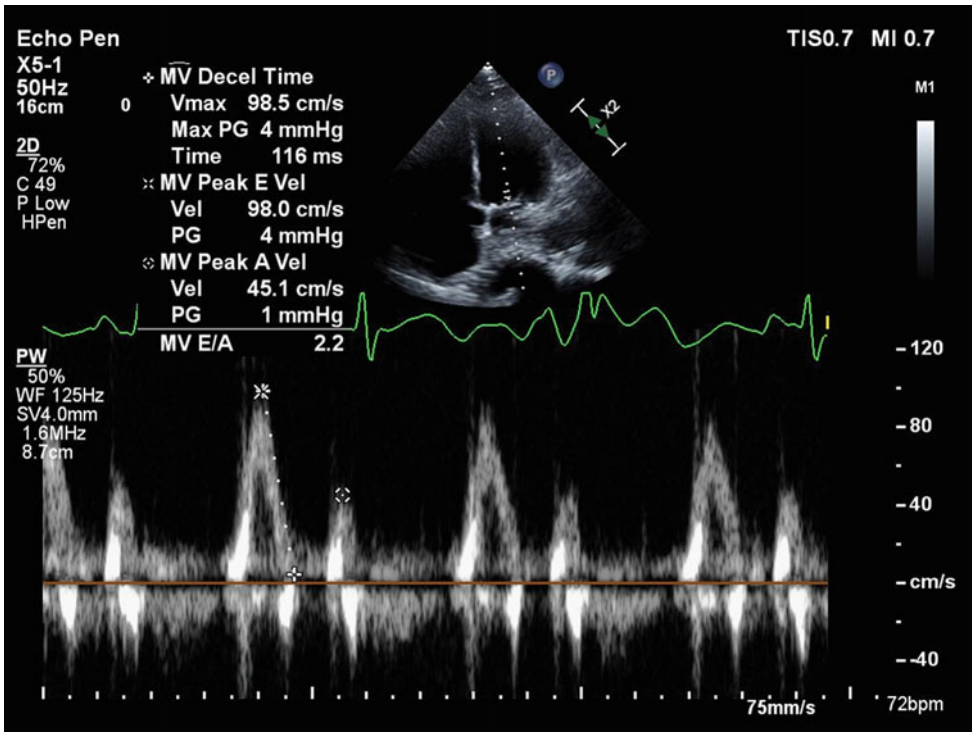

Fig. 21.23 The mitral valve E/A is 2.2 with short deceleration time which may be a sign of a restrictive cardiomyopathy as a consequence of previous radiation or grade 3 diastolic dysfunction. However, given the respirophasic interventricular septum bounce, the normal mitral valve e' and the annulus reversus, the findings are more consistent with a presentation of constriction (however there may be a mixed presentation with some features of restriction)

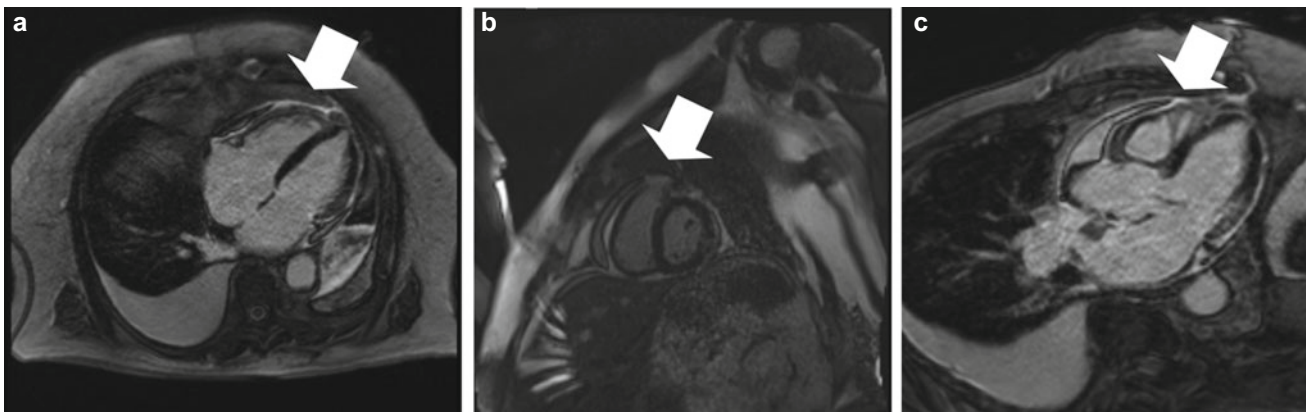

Fig. 21.24 **a–c** are delayed enhancement sequences showing late gadolinium enhancement uptake at the right ventricle (see arrows). There is a small pericardial effusion and a moderate right-sided pleural effusion

References

1. Moncada R, Baker M, Salina M, Demos T, Churchill R, Love L, et al. Diagnostic role of computed tomography in pericardial heart disease: congenital defects, thickening, neoplasms, and effusions. Am Heart J. 1982;103(2):263–82.
2. Søgaard KK, Sørensen HT, Smeeth L, Bhaskaran K. Acute pericarditis and cancer risk: a matched cohort study using linked UK primary and secondary care data. J Am Heart Assoc. 2018;7 (16):e009428.
3. Maisch B, Ristic A, Pankuweit S. Evaluation and management of pericardial effusion in patients with neoplastic disease. Prog Cardiovasc Dis. 2010;53(2):157–63.
4. Klatt EC, Heitz DR. Cardiac metastases. Cancer. 1990;65 (6):1456–9.
5. Imazio M, Colopi M, De Ferrari GM. Pericardial diseases in patients with cancer: contemporary prevalence, management and outcomes. Heart Br Card Soc. 2020;106(8):569–74.
6. Chang H-M, Okwuosa TM, Scarabelli T, Moudgil R, Yeh ETH. Cardiovascular complications of cancer therapy: best practices in diagnosis, prevention, and management: part 2. J Am Coll Cardiol. 2017;70(20):2552–65.
7. Ala CK, Klein AL, Moslehi JJ. cancer treatment-associated pericardial disease: epidemiology, clinical presentation, diagnosis, and management. Curr Cardiol Rep. 2019;21(12):156.
8. Kelly K, Swords R, Mahalingam D, Padmanabhan S, Giles FJ. Serosal inflammation (pleural and pericardial effusions) related to tyrosine kinase inhibitors. Target Oncol. 2009;4(2):99–105.
9. Escudier M, Cautela J, Malissen N, Ancedy Y, Orabona M, Pinto J, et al. Clinical features, management, and outcomes of immune checkpoint inhibitor-related cardiotoxicity. Circulation. 2017;136(21):2085–7.
10. Hu J-R, Florido R, Lipson EJ, Naidoo J, Ardehali R, Tocchetti CG, et al. Cardiovascular toxicities associated with immune checkpoint inhibitors. Cardiovasc Res. 2019;115(5):854–68.
11. Salem J-E, Manouchehri A, Moey M, Lebrun-Vignes B, Bastarache L, Pariente A, et al. Cardiovascular toxicities associated with immune checkpoint inhibitors: an observational, retrospective, pharmacovigilance study. Lancet Oncol. 2018;19(12):1579–89.
12. Ning MS, Tang L, Gomez DR, Xu T, Luo Y, Huo J, et al. Incidence and predictors of pericardial effusion after chemoradiation therapy for locally advanced non-small cell lung cancer. Int J Radiat Oncol Biol Phys. 2017;99(1):70–9.
13. Liu J, Mouhayar E, Tarrand JJ, Kontoyiannis DP. Fulminant Cryptococcus neoformans infection with fatal pericardial tamponade in a patient with chronic myelomonocytic leukaemia who was treated with ruxolitinib: Case report and review of fungal pericarditis. Mycoses. 2018;61(4):245–55.
14. Liu Y-C, Chien S-H, Fan N-W, Hu M-H, Gau J-P, Liu C-J, et al. Risk factors for pericardial effusion in adult patients receiving allogeneic haematopoietic stem cell transplantation. Br J Haematol. 2015;169(5):737–45.
15. Norkin M, Ratanatharathorn V, Ayash L, Abidi MH, Al-Kadhimi Z, Lum LG, et al. Large pericardial effusion as a complication in adults undergoing SCT. Bone Marrow Transplant. 2011;46(10):1353–6.
16. Szpakowski N, Desai MY. Radiation-Associated Pericardial Disease. Curr Cardiol Rep. 2019;21(9):97.
17. Lancellotti P, Nkomo VT, Badano LP, Bergler-Klein J, Bergler J, Bogaert J, et al. Expert consensus for multi-modality imaging evaluation of cardiovascular complications of radiotherapy in adults: a report from the European Association of Cardiovascular Imaging and the American Society of Echocardiography. J Am Soc Echocardiogr Off Publ Am Soc Echocardiogr. 2013;26 (9):1013–32.
18. Armenian SH, Lacchetti C, Barac A, Carver J, Constine LS, Denduluri N, et al. Prevention and monitoring of cardiac dysfunction in survivors of adult cancers: American society of clinical oncology clinical practice guideline. J Clin Oncol. 2017;35 (8):893–911.
19. Kim S-H, Song J-M, Jung I-H, Kim M-J, Kang D-H, Song J-K. Initial echocardiographic characteristics of pericardial effusion determine the pericardial complications. Int J Cardiol. 2009;136 (2):151–5.
20. Sagristà-Sauleda J, Angel Ferrer J, Sánchez A, Permanyer-Miralda G, Soler-Soler J. Effusive–constrictive pericarditis. N Engl J Med. 2004;7.
21. Ntsekhe M, Wiysonge CS, Commerford PJ, Mayosi BM. The prevalence and outcome of effusive constrictive pericarditis : a systematic review of the literature. Cardiovasc J Afr. 2012;23 (5):281–5.
22. Adler Y, Charron P, Imazio M, Badano L, Barón-Esquivias G, Bogaert J, et al. 2015 ESC Guidelines for the diagnosis and management of pericardial diseases. Eur Heart J. 2015;36(42):2921–64.
23. Klein AL, Abbara S, Agler DA, Appleton CP, Asher CR, Hoit B, et al. American society of echocardiography clinical recommendations for multimodality cardiovascular imaging of patients with pericardial disease. J Am Soc Echocardiogr. 2013;26(9):965-1012.e15.
24. Nagueh SF, Smiseth OA, Appleton CP, Byrd BF, Dokainish H, Edvardsen T, et al. Recommendations for the evaluation of left ventricular diastolic function by echocardiography: an update from the American society of echocardiography and the European association of cardiovascular imaging. J Am Soc Echocardiogr. 2016;29(4):277–314.
25. Reuss CS, Wilansky SM, Lester SJ, Lusk JL, Grill DE, Oh JK, et al. Using mitral 'annulus reversus' to diagnose constrictive pericarditis. Eur J Echocardiogr. 2009;10(3):372–5.
26. Ha Jong-Won, Oh Jae K., Ling Lieng H., Nishimura Rick A., Seward James B., Tajik A. Jamil. Annulus paradoxus. Circulation. 2001;104(9):976–8.
27. Ling LH, Oh JK, Tei C, Click RL, Breen JF, Seward JB, et al. Pericardial thickness measured with transesophageal echocardiography: feasibility and potential clinical usefulness. J Am Coll Cardiol. 1997;29(6):1317–23.
28. Kim KH, Miranda WR, Sinak LJ, Syed FF, Melduni RM, Espinosa RE, et al. Effusive-constrictive pericarditis after pericardiocentesis. JACC Cardiovasc Imaging. 2018;11(4):534–41.
29. Xu B, Kwon DH, Klein AL. Imaging of the pericardium: a multimodality cardiovascular imaging update. Cardiol Clin. 2017;35(4):491–503.
30. Murashita T, Schaff HV, Daly RC, Oh JK, Dearani JA, Stulak JM, et al. experience with pericardiectomy for constrictive pericarditis over eight decades. Ann Thorac Surg. 2017;104(3):742–50.
31. George TJ, Arnaoutakis GJ, Beaty CA, Kilic A, Baumgartner WA, Conte JV. Contemporary etiologies, risk factors, and outcomes after pericardiectomy. Ann Thorac Surg. 2012;94(2):445–51.
32. Greenwood RD, Rosenthal A, Cassady R, Jaffe N, Nadas AS. Constrictive pericarditis in childhood due to mediastinal irradiation. Circulation. 1974;50(5):1033–9.
33. von Bibra H, Schober K, Jenni R, Busch R, Sebening H, Blömer H. Diagnosis of constrictive pericarditis by pulsed doppler echocardiography of the hepatic vein. Am J Cardiol. 1989;63 (7):483–8.

Introduction to the Cardiac Implications of Radiotherapy

22

Lior Z. Braunstein and Oren Cahlon

Since shortly after Wilhelm Roentgen's discovery of the X-ray in 1895 [1], ionizing radiation has been used to treat a variety of benign and malignant conditions alike. Early applications of X-rays were limited to superficial cutaneous lesions due to the underperformance of poorly penetrating low-energy beams at significant tissue depth. The discovery of naturally occurring isotopes [2] and the later development of the linear accelerator [3] allowed for more energetic penetrating photons to treat deeply seated lesions such as the visceral or brain tumors that today are routinely ablated in non-invasive fashion. With the development of high-energy beams, however, emerged a concurrent need to protect critical deep structures that might now be at risk of radiation injury.

Although contemporary radiotherapy is largely delivered using high-energy photons (i.e., X-rays and gamma rays), the physical properties of particle-based beams are routinely exploited for their dosimetric advantages. To illustrate, X-rays deposit energy along a beam path that gradually dissipates while traversing the patient, typically yielding an "exit dose" beyond the target tumor that exposes distal tissues. Protons, conversely, by virtue of having mass and charge, maximally interact with tissue at an energetically predetermined depth (the "Bragg peak"), fully depositing energy at a given depth and sparing the tissues beyond (Fig. 22.1). This fundamental property of proton-based techniques is often exploited to limit normal-tissue toxicity, as in the treatment of pediatric central nervous system malignancies where the ability to spare adjacent developing brain structures preserves cognitive function [4, 5]. Aside from photons and protons, other particle beams including electrons, neutrons, and carbon ions, among other investigational approaches, are also in use.

The central challenge of radiotherapy, as alluded to above, is striking a balance between sufficient tumor dose and adequate sparing of adjacent non-target tissues. This principle is perhaps best illustrated by the history of breast and thoracic radiation. Prior to the advent of effective systemic therapies for breast cancer, disease control was exceedingly poor and adjuvant (i.e. post-operative) radiotherapy was broadly employed following mastectomy. These early efforts typically treated the regional lymph node basins comprehensively (including the internal mammary nodes) yet lacked three-dimensional thoracic imaging or techniques that might allow for cardiac avoidance, as is standard today. Consequently, long-term follow-up of these early patients demonstrated an excess of deaths among those receiving post-mastectomy radiation, suggesting that radiotherapy was partly contributing to a reduction in survival [6]. Focused analyses from that era have variably identified the causes of excess mortality among those receiving radiation as acute myocardial infarction [7] or "cardiovascular disease" more generally, prompting modifications to field design and a reconsideration of the appropriate risk–benefit considerations [8].

Cardiotoxic sequelae were similarly observed, if more dramatically, among patients with Hodgkin lymphoma who relied extensively on nodal irradiation prior to the advent of contemporary systemic regimens [9]. Often young at the time of radiation, these patients sustained elevated cardiac doses from wholesale treatment of the mediastinal lymph nodes and were broadly reported to exhibit an increased risk of valvular disease, atherosclerosis, and cardiomyopathies [10–13].

As evidence for the cardiac implications of radiotherapy mounted, a seminal study conducted by Darby et al. yielded what has now become a landmark finding [14]. In a population-based case–control study among 2168 women who underwent breast cancer radiotherapy, rates of major coronary events appeared to increase linearly with mean

L. Z. Braunstein (✉) · O. Cahlon
Department of Radiation Oncology, Memorial Sloan Kettering Cancer Center, 1275 York Avenue, Box 22, New York, NY 10065, USA
e-mail: BRAUNSTL@mskcc.org

O. Cahlon
e-mail: cahlono@mskcc.org

R. M. Steingart et al. (eds.), *Atlas of Imaging in Cardio-Oncology*,
https://doi.org/10.1007/978-3-030-70998-3_22

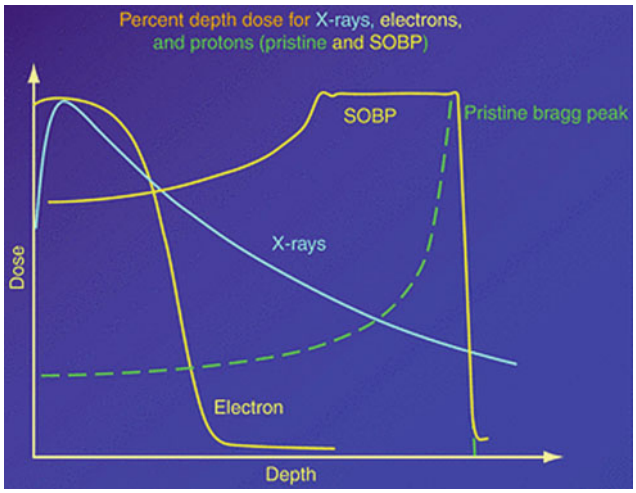

Fig. 22.1 Percent depth dose for X-Rays, electrons, and protons (Pristine peak and spread-out Bragg peak—SOBP). (From Hasson et al. [23]; with permission from Springer Nature.)

heart dose by 7.4% per gray (95% CI 2.9 to 14.5). Whereas mean heart doses in this outdated cohort ranged significantly higher than currently allowable limits, the report was particularly notable for demonstrating that there is no lower bound below which radiation ceases to influence cardiac risk. Mindful of these findings, contemporary practice has significantly mitigated heart dose and concomitant cardiovascular risk as discussed below.

To revisit the utility of adjuvant breast radiation since the early days when cardiac avoidance was not practicable, a series of landmark trials recently evaluated the benefits of comprehensive adjuvant radiation for breast cancer in the context of contemporary planning techniques and a nuanced appreciation for cardiac risk. The MA.20 [15] and EORTC 22922 [16] trials randomized patients to receive regional nodal irradiation following lumpectomy or mastectomy and, in contrast to the historical findings above, both trials observed a 3–5% disease-free survival benefit to treating the regional lymph nodes among appropriate breast cancer patients. Notably, despite treating the internal mammary nodes in both studies, the rate of cardiac adverse events was exceedingly rare (0.9% on MA.20) and was not significantly different in either study between those receiving radiation or not.

Thoracic radiotherapy for lung cancer has also been illustrative of the cardiac implications of radiotherapy. In the seminal RTOG 0617 trial of dose-escalation for unresectable stage III non-small-cell lung cancer (NSCLC), investigators evaluated whether a radiation dose of 74 Gy could improve disease control as compared to the prevailing 60 Gy standard dose [17]. To the surprise of many, the study revealed that the investigational 74 Gy conferred a potential decrement in survival, counter to the trial hypothesis and opposing the otherwise notable trends of improved disease control with higher doses in NSCLC. Much has since been written about this failure of dose-escalation, with many positing that higher doses do effect improved tumor control, but that an excess of mortality arises from the concomitant cardiopulmonary effects of radiation [18, 19].

Several studies have attempted to elucidate the underlying pathophysiology of radiation induced cardiac disease. In an autopsy series that included 27 cases [20], Veinot and Edwards identified pericardial injury in 70%, with effusion and tamponade in a subset. Similarly, radiation-associated valvular disease was identified in 71% of patients (mean dose 46 Gy), with 25 examined valves (8 aortic, 9 mitral, 5 tricuspid, and 3 pulmonary) all showing diffuse cusp or leaflet fibrosis without evidence of post-inflammatory change such as chronic inflammation or neovascularization, suggesting an alternate pathway to fibrotic injury from radiation. Perhaps most notably, 16 subjects had evaluable myocardium with 10 (63%) harboring interstitial fibrosis attributable to radiation injury, while 13 had evaluable coronary arteries with 2 young men (26 and 44 years old) showing significant narrowing via atherosclerosis or fibrointimal thickening attributable to radiation damage. Coronary disease in these two subjects was noted to be "disproportionately severe" in light of their non-radiation risk factors. Thus, radiation induced heart disease putatively affects every cardiac substructure, and subsequent studies have suggested that tissue fibrosis represents the unifying etiologic pathway [21].

Indeed, the implications of cardiac radiation exposure have now set the stage for a burgeoning industry of cardiac avoidance devices and techniques that are commonly used in clinical practice. Among these are prone immobilizers for breast cancer, allowing patients to be treated in the prone position as gravity is used to displace the target breast tissue away from the underlying heart (Fig. 22.2). The respiratory cycle can also be exploited to optimize cardiac positioning away from a nearby target. This approach uses respiratory gating, or the Deep-Inspiration Breath-Hold (DIBH) technique, whereby breathing is monitored via imaging or spirometry and radiation is delivered only during the most favorable anatomic phase of the respiratory cycle (Fig. 22.3). In breast radiotherapy, for example, treatment is often delivered during end-inspiration when the lungs are maximally inflated and the heart is displaced postero-inferiorly relative to the target internal mammary nodes which may otherwise be mere millimeters from the right ventricle during end exhalation (Fig. 22.4). These techniques, along with advanced planning modalities such as intensity modulated radiotherapy (IMRT) and volumetric modulated arc radiotherapy (VMAT) (Fig. 22.5), are routinely brought to bear in mitigating the cardiac and normal-tissue effects of radiation.

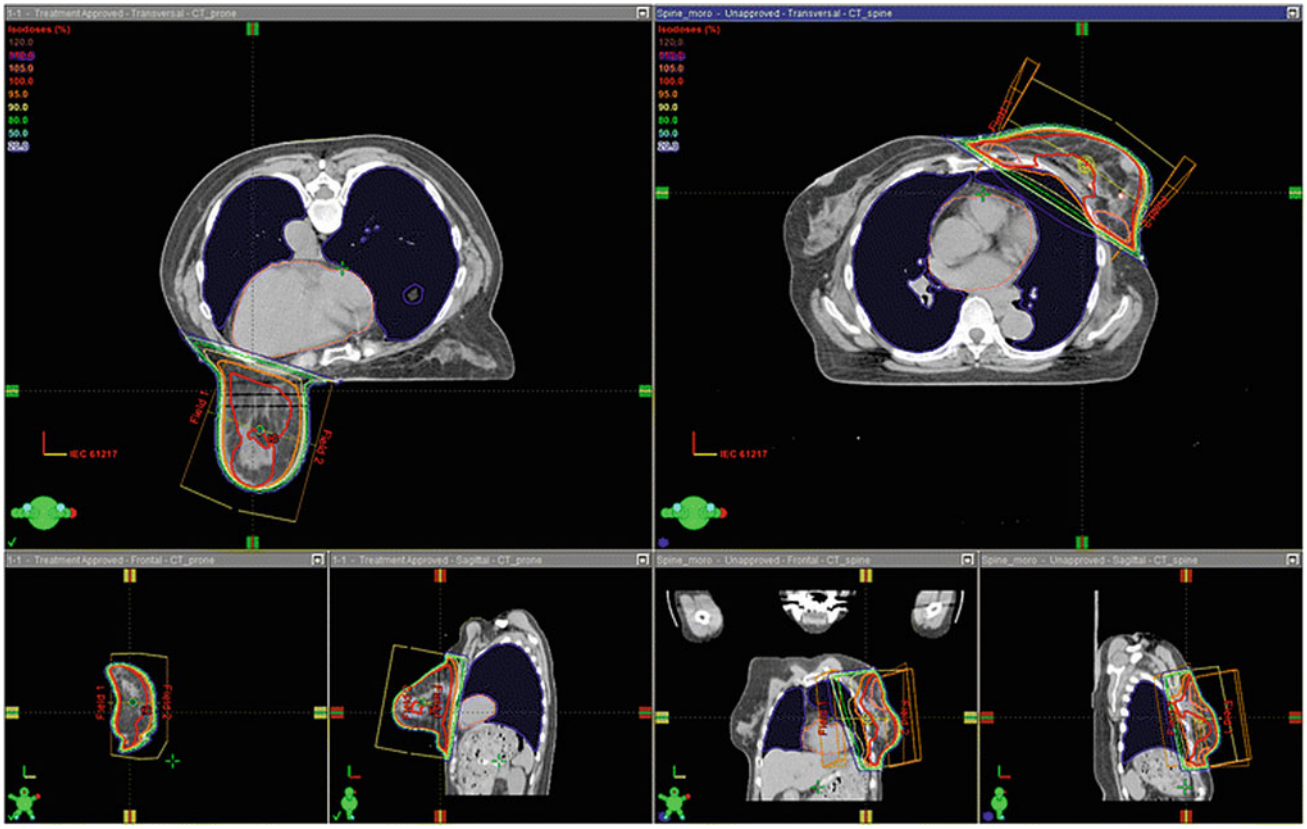

Fig. 22.2 Prone breast radiotherapy [22]. Typical dose distributions of a patients with a pendulous breast. For each patient, opposing tangential fields were set up to irradiate planning target volume in both supine and prone positions. (From Takahashi et al. [22]; Creative Commons Attribution 4.0 International License, https://creativecommons.org/licenses/by/4.0.)

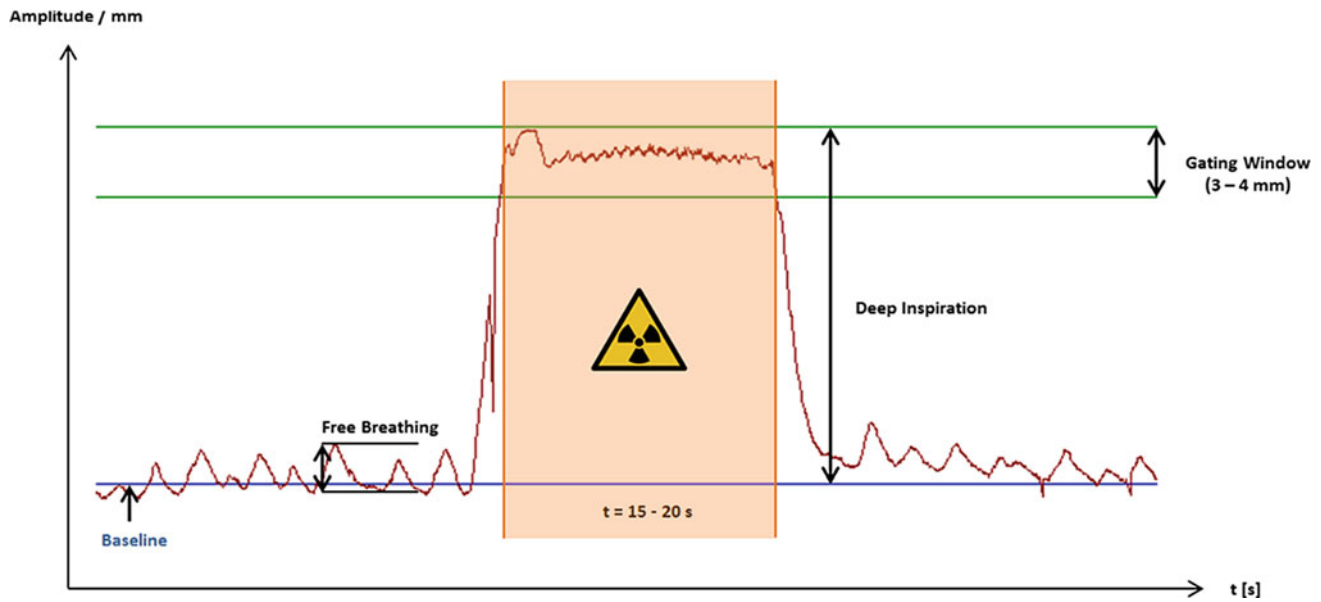

Fig. 22.3 Respiratory gating. The respiratory cycle is monitored using surface imaging and radiation is delivered during either deep-inspiration breath-hold (as below) or, alternatively, during any desired portion of the respiratory cycle. The beam can be automatically activated and deactivated as the surface anatomy enters or exists the specified "gating window" that corresponds to the desired respiratory phase. (From Schönecker et al. [24]; Creative Commons Attribution 4.0 International License, https://creativecommons.org/licenses/by/4.0.)

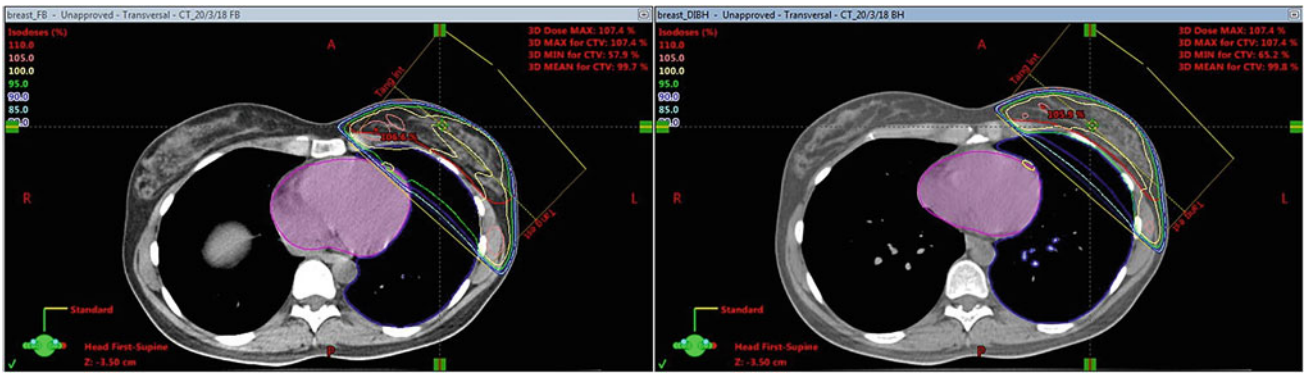

Fig. 22.4 Typical dose distributions from a free-breathing plan (left) and a deep-inspiration breath-hold (DIBH) plan (right). Note that neither the heart (magenta) nor the left anterior descending artery (yellow) is within the radiation fields in the DIBH plan. (From Aiello et al. [25]; with permission from Springer Nature.)

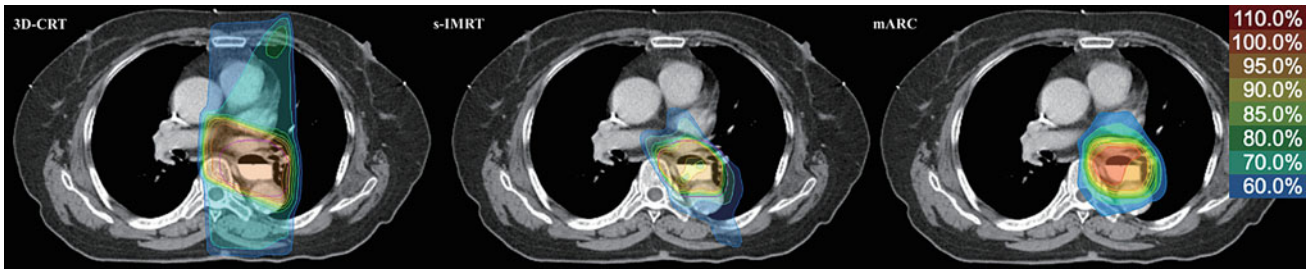

Fig. 22.5 Comparison of 3D, IMRT, and VMAT for the radiotherapeutic targeting of esophageal cancer. Note the extent of radiotherapy dose to adjacent structures in the 3D plan (using anterior and posterior beams) in comparison to the VMAT (mARC) plan using a modulated arc of radiotherapy. (From Choi et al. [26]; Creative Commons Attribution 4.0 International License, https://creativecommons.org/licenses/by/4.0.)

Thus, while there is no tumor that cannot be controlled with a sufficiently high dose of radiation, the countervailing sensitivity of adjacent structures may limit the feasibility of delivering an adequately ablative dose. The heart represents one such limiting organ, with potential for radiation injury to each cardiac substructure. As a result, contemporary radiation approaches employ combinations of advanced particle beams, novel beam shaping techniques, and patient positioning to limit cardiac toxicity while precisely targeting thoracic-based malignancies including tumors of the breast, lung, and mediastinum. Meanwhile, substantial efforts are underway to optimize prophylactic and therapeutic approaches to mitigate radiation-associated cardiac injury, and to prolonging survival via oncologic and cardiac approaches alike.

References

1. Röntgen W. Uber eine neue Art von Strahlen (On a new kind of rays). Vorläufige Mittheilung Aus den Sitzungsberichten der Würzburger Physik-medic Gesellschaft Würzburg: Stahel'sche K Hof und Universitätsbuchund Kunsthandlung; 1895. p. 137–47.
2. Curie P. Radioactive substances, especially radium. Nobel lecture 1905;6.
3. Ueyama T, Lécuyer C. Building Science-based Medicine at Stanford: Henry Kaplan and the Medical Linear Accelerator, 1948–1975. Devices and Designs: Springer; 2006. p. 137–55.
4. Pulsifer MB, Duncanson H, Grieco J, et al. Cognitive and adaptive outcomes after proton radiation for pediatric patients with brain tumors. Int J Radiat Oncol Biol Phys. 2018;102:391–8.
5. Pulsifer MB, Sethi RV, Kuhlthau KA, MacDonald SM, Tarbell NJ, Yock TI. Early cognitive outcomes following proton radiation in pediatric patients with brain and central nervous system tumors. Int J Radiat Oncol Biol Phys. 2015;93:400–7.
6. Cuzick J, Stewart H, Peto R, et al. Overview of randomized trials of postoperative adjuvant radiotherapy in breast cancer. Cancer Treat Rep. 1987;71:15–29.
7. Wallgren A, Arner O, Bergström J, et al. Radiation therapy in operable breast cancer: results from the Stockholm trial on adjuvant radiotherapy. International Journal of Radiation Oncology* Biology* Physics 1986;12:533–7.
8. Harris JR, Hellman S. Put the "hockey stick" on ice. International Journal of Radiation Oncology Biology Physics 1988;15:497–9.
9. Goyal G, Silberstein PT, Armitage JO. Trends in use of radiation therapy for Hodgkin lymphoma from 2000 to 2012 on the basis of the national cancer data base. Clin Lymphoma Myeloma Leuk. 2016;16:12–7.
10. Hull MC, Morris CG, Pepine CJ, Mendenhall NP. Valvular dysfunction and carotid, subclavian, and coronary artery disease in survivors of Hodgkin lymphoma treated with radiation therapy. JAMA. 2003;290:2831–7.

11. Applefeld M, Slawson R, Spicer K, Singleton R, Wesley M, Wiernik P. Long-term cardiovascular evaluation of patients with Hodgkin's disease treated by thoracic mantle radiation therapy. Cancer Treat Rep. 1982;66:1003–13.
12. Adams MJ, Hardenbergh PH, Constine LS, Lipshultz SE. Radiation-associated cardiovascular disease. Crit Rev Oncol Hematol. 2003;45:55–75.
13. Hancock SL, Donaldson SS, Hoppe RT. Cardiac disease following treatment of Hodgkin's disease in children and adolescents. J Clin Oncol. 1993;11:1208–15.
14. Darby SC, Ewertz M, McGale P, et al. Risk of ischemic heart disease in women after radiotherapy for breast cancer. N Engl J Med. 2013;368:987–98.
15. Whelan TJ, Olivotto IA, Parulekar WR, et al. Regional nodal irradiation in early-stage breast cancer. N Engl J Med. 2015;373:307–16.
16. Poortmans PM, Collette S, Kirkove C, et al. Internal mammary and medial supraclavicular irradiation in breast cancer. N Engl J Med. 2015;373:317–27.
17. Bradley JD, Paulus R, Komaki R, et al. Standard-dose versus high-dose conformal radiotherapy with concurrent and consolidation carboplatin plus paclitaxel with or without cetuximab for patients with stage IIIA or IIIB non-small-cell lung cancer (RTOG 0617): a randomised, two-by-two factorial phase 3 study. Lancet Oncol. 2015;16:187–99.
18. Cox JD. Are the results of RTOG 0617 mysterious? Int J Radiat Oncol Biol Phys. 2012;82:1042–4.
19. Thor M, Deasy JO, Hu C, et al. Modeling the impact of cardio-pulmonary irradiation on overall survival in NRG Oncology trial RTOG 0617. Clinical Cancer Research 2020.
20. Veinot JP, Edwards WD. Pathology of radiation-induced heart disease: a surgical and autopsy study of 27 cases. Hum Pathol. 1996;27:766–73.
21. Taunk NK, Haffty BG, Kostis JB, Goyal S. Radiation-induced heart disease: pathologic abnormalities and putative mechanisms. Front Oncol. 2015;5:39.
22. Takahashi K, Morota M, Kagami Y, et al. Prospective study of postoperative whole breast radiotherapy for Japanese large-breasted women: a clinical and dosimetric comparisons between supine and prone positions and a dose measurement using a breast phantom. BMC Cancer. 2016;16:757.
23. Hasson BF, Yeung D, Palta J. Bragg peak. In: Brady LW, Yaeger TE, editors. Encyclopedia of Radiation Oncology. Berlin/Heidelberg: Springer; 2013. https://doi.org/https://doi.org/10.1007/978-3-540-85516-3_657.
24. Schönecker S, Walter F, Freislederer P, Marisch C, Scheithauer H, Harbeck N, et al. Treatment planning and evaluation of gated radiotherapy in left-sided breast cancer patients using the CatalystTM/SentinelTM system for deep inspiration breath-hold (DIBH). Radiat Oncol. 2016;11:143. https://doi.org/10.1186/s13014-016-0716-5.
25. Aiello D, Borzì GR, Marino L, Umina V, Di Grazia AM. Comparison of deep inspiration breath hold and free breathing technique in left breast cancer irradiation: a dosimetric evaluation in 40 patients. J Radiation Oncol. 2019;8(1):89–96.
26. Choi KH, Kim J, Lee SW, Kang YN, Jang H. Dosimetric comparison between modulated arc therapy and static intensity modulated radiotherapy in thoracic esophageal cancer: a single institutional experience. Radiat Oncol J. 2018 Mar;36(1):63–70. doi: https://doi.org/10.3857/roj.2017.00241.

23 Cardio-Oncologists Perspective on the Cardiac Implications of Radiotherapy: Complex Cases of Radiation-Related Valvular and Vascular Disease

Maria Poltavskaya

Chest radiation therapy (RT) is an important cause of cardiovascular disease in patients treated for cancers including lung, esophagus, mediastinal tumors, and especially Hodgkin disease and breast cancer [1–3]. In patients with Hodgkin lymphoma radiation-induced heart disease (RIHD) can involve the pericardium, myocardium, valves, coronary arteries, aorta, and major arteries and becomes a leading cause of death during survivorship. RIHD is associated with 9.3–28 deaths per 10,000 patient-years [1] and the risk of heart failure is 4.9 fold higher than in the general population [2].

The risk of radiation cardiotoxicity depends primarily on chest irradiation from the anterior or left fields, cumulative dose, and the dose fractionation. It is not so much the total dose to the chest that matters but the volume of the heart that receives a sufficiently high dose [4]. Since the beginning of the so-called "modern era" of RT in 1985, the use of the latest technologies and conformal techniques with less radiation dose to the heart has resulted in a decrease in cardiovascular complications (see Chap. 22) [5]. The likelihood of RIHD increases in proportion to the time after RT. The prevalence of clinically relevant heart disease within 5–10 years after RT is 10–30% (often asymptomatic) [6] and after 40 years the incidence of various cardiovascular diseases increases to 50% [7]. RT potentiates the negative effect on the myocardium of chemotherapy drugs, such as anthracyclines [8].

There is evidence that the mechanisms underlying radiation injury of all cardiac tissues may be related to micro- and macrovascular damage. Early after the exposure to ionizing radiation endothelial cell hyperpermeability is observed with subsequent inflammatory response which promotes further deterioration. Microvascular damage results in reduction of capillary density driving myocardial fibrosis, diastolic dysfunction, and heart failure. Valve endothelial damage results in leaflet fibrosis, thickening, shortening, and calcification. Increased capillary permeability of the pericardium, thickening, and adhesions lead to effusions and constriction which contribute to diastolic dysfunction. Endothelial injury accelerates atherosclerosis resulting in endothelial dysfunction and coronary artery stenosis [9, 10]. Traditional risk factors such as smoking, diabetes, arterial hypertension, obesity, and hypercholesterolemia, significantly increase the risk of post-radiation coronary artery disease [2].

Radiation-induced pericardial disease can present as acute pericarditis with chest pain, friction rubs, pericardial effusions and later evolve into constrictive pericarditis. Management of acute pericarditis follows common guidelines and includes nonsteroidal anti-inflammatory drugs, colchicine, and sometimes reluctantly glucocorticoids. The approach to radiation related pericardial effusions does not differ from the approach to effusions of other etiologies. A malignant origin of the effusion should be excluded [11, 12]. Pericardiectomy may be considered for hemodynamically and clinically relevant constriction but early and late postoperative mortality is much higher than in constriction of other origins. The higher mortality may be explained by more extensive pericardial and mediastinal fibrosis, concomitant myocardial, valvular, and coronary impairment [13].

Myocardial fibrosis at advanced stages after radiation manifests as restrictive cardiomyopathy with symptoms of heart failure, diastolic dysfunction, preserved or moderately decreased ejection fraction, and abnormal myocardial strain [11, 14, 15]. The atrial and ventricular dimensions may be within the normal range. Management of heart failure in these patients with low cardiac output is directed at relieving symptoms. There is no evidence that ACE-inhibitors or beta-blockers are beneficial. They may be poorly tolerated and should be used with caution if at all. Cardiac

Electronic supplementary material
The online version of this chapter (https://doi.org/10.1007/978-3-030-70998-3_23) contains supplementary material, which is available to authorized users.

M. Poltavskaya (✉)
Department of Cardiology, Functional and Ultrasound Diagnostics, I.M. Sechenov First Moscow State Medical University (Sechenov University), Moscow, Russia
e-mail: m.poltavskaya@yandex.ru

R. M. Steingart et al. (eds.), *Atlas of Imaging in Cardio-Oncology*,
https://doi.org/10.1007/978-3-030-70998-3_23

transplantation can be considered for the management of heart failure due to radiation-induced end-stage cardiac disease [16].

Clinically relevant valvular disease is a rather late complication that usually manifests 10–20 years or more after mediastinal RT. The mitral and aortic valves are most commonly affected, and regurgitation is more common than stenosis [17]. Post radiation aortic valve disease can present as low-flow, low-gradient aortic stenosis [18]. When valve replacement is necessary, percutaneous approaches have become the methods of choice because the 30-day and long-term prognosis after open surgery is worse than in "conventional" cases because of severe aortic calcification and concomitant cardiac, mediastinal, and pulmonary disease [18, 19].

Coronary artery disease (CAD) may present with angina or acute coronary syndrome even in young patients without traditional risk factors [17]. At the same time significant coronary disease may be found in a third of asymptomatic patients screened by coronary angiography. Ostial and proximal coronary stenoses are typical after RT for Hodgkin disease [20]. The mid and distal segments of left anterior descending artery are most likely to be affected after left breast irradiation (see Chap. 24) [21]. Management of stable or acute CAD should follow the existing guidelines for conventional CAD.

All patients with a history of thoracic RT must be considered at high risk for cardiovascular disease and be followed by a cardiologist lifelong with regular screening with echocardiography and functional stress testing. Screening for and strict control of conventional risk factors is essential [11, 22].

23.1 Case 1. Aortic Stenosis with Low Ejection Fraction After Repeated Chemo- and Radiation Therapy for Left- and Right-Side Breast Cancer with Recovery After Transcatheter Aortic Valve Replacement (TAVR)

Key Points

- Unlike Hodgkin lymphoma, valve, and ostial coronary artery lesions are not typical after treatment of left breast cancer but they may be seen in patients who underwent "old radiation therapy" with radiation impact on a large heart volume
- Asymptomatic coronary artery disease (CAD) is often found in patients with radiation-induced valve disease and should be sought in all patients regardless of age. Concurrent myocardial and pericardial damage should also be considered.
- Common risk factors of atherosclerotic disease such as hypertension, dyslipidemia, smoking contribute to the risk of radiation-induced vascular and presumably valvular disease.
- Chest radiation is a major risk factor for cardiac surgery. That risk is underestimated by the commonly employed surgical risk scores. When feasible, in patients with radiation-induced aortic valve disease the decision is usually made in favor of TAVR which is probably nearly as effective as in "conventional" patients.

In 2016 a 55 y/o woman was admitted to the hospital with symptoms of congestive heart failure NYHA class IV: Dyspnea at rest, orthopnea, paroxysmal nocturnal dyspnea, extensive peripheral edema, cyanosis, hepatomegaly, and low effort typical angina. An aortic systolic murmur was present.

She was an ex-smoker, with a long history of arterial hypertension and obesity (body mass index of 32.7) and with recent onset diabetes. In 1987 she had undergone surgery, anthracycline-based chemotherapy, and radiotherapy for left-sided breast cancer, and in 2008—for right-side breast cancer. Heart failure and angina manifested in 2012 and worsened gradually. The patient received medical treatment with ASA, low doses of ARBs, beta-blockers, spironolactone, and diuretics.

Admission ECG in 2016 showed left ventricular hypertrophy. Echocardiogram revealed calcified tricuspid aortic valve with severe stenosis (aortic valve peak jet velocity of 405 cm/s, mean transvalvular gradient (ΔP) of 37 mm Hg, aortic valve area of 0.5–0.6 cm^2) and significant aortic regurgitation, mitral, and tricuspid regurgitation grade II, systolic dysfunction with ejection fraction (EF) of 20 to 25% and pulmonary hypertension (PAPS/PHT = 50) (Figs. 23.1 and 23.2, Videos 23.1 and 23.2).

CT scan performed as part of her preoperative evaluation showed calcification of the aortic valve and also of the right coronary artery (RCA) with a proximal stenosis and collateral distal flow (Fig. 23.3).

Coronary angiography confirmed the proximal occlusion of the RCA with collateral contrast filling. There were no indications for coronary intervention. Angina was considered related not to CAD but to severe aortic stenosis (Video 23.3).

The patient had left ventricular dysfunction presumably due to multiple contributing factors including severe aortic stenosis, myocardial ischemia, and radiation and anthracycline induced cardiomyopathy. She had a low EF, low mean ΔP and low flow according to velocity time integral (VTI) at the left ventricular outflow tract (LVOT) (stroke volume index (SVi) < 35 ml). Corrected by CT scan measurement of the LVOT the flow was redefined as normal with Svi

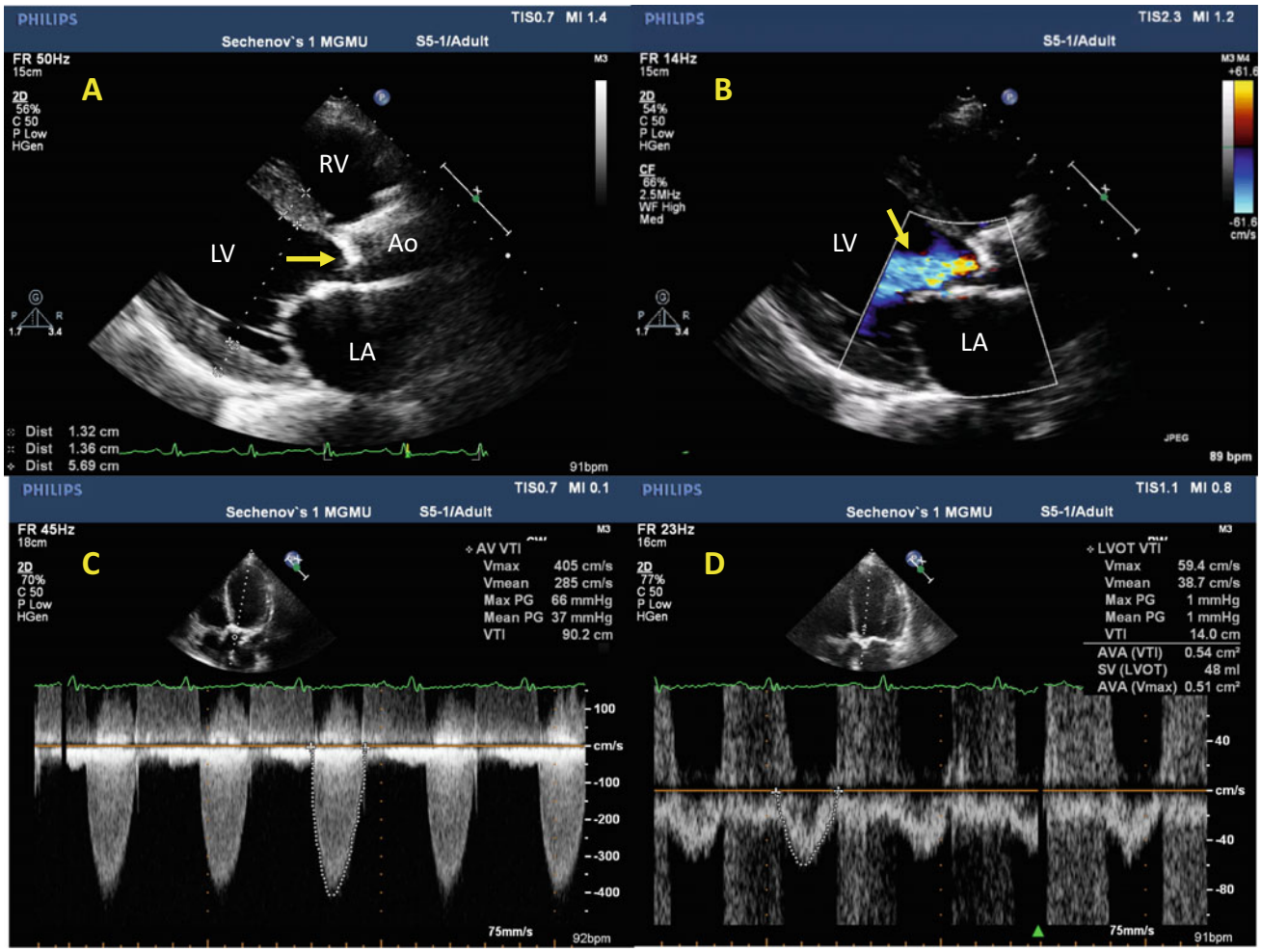

Fig. 23.1 Echocardiogram in 2016 before transcatheter aortic valve replacement (TAVR). **a** Thickening of aortic valve cusps (arrow) and annulus. Moderate LV hypertrophy. Parasternal long axis view. RV = right ventricle, LV = left ventricle, Ao = Aorta, LA = left atrium. **b** Color Doppler of aortic regurgitation. The arrow points at the moderate regurgitant jet. Parasternal long axis view. **c** Doppler echocardiography defining the severity of aortic stenosis. Maximal AV peak jet velocity (V_{max}) of 405 cm/s indicates severe stenosis. Mean transvalvular gradient of 37 mm Hg is classified as low gradient (<40 mm Hg) but it is underestimated because of low LV contractility. Apical view. **d** Doppler echocardiography at LVOT shows low VTI of 14 cm that corresponds with low stroke volume index (low flow stenosis). Aortic valve area (AVA) of around 0,5cm^2 indicates severe stenosis. Apical view. LVOT—left ventricular outflow tract. VTI—Velocity time integral

of > 35 ml. Together with high aortic V_{max} these findings were interpreted as a normal response to high afterload and improvement of ventricular function after relief of aortic stenosis could be expected [23].

The patient had strong clinical indications for aortic valve replacement. Surgical risk was estimated to be low according to the common scores: 3.56 by Euroscore and 1.9 by the society of thoracic surgeons (STS) score. Nevertheless, the Heart Team decided in favor of a transcatheter procedure taking into consideration the history of chest radiation which is a major risk factor for postoperative morbidity and mortality [24, 25]. The patient underwent TAVR with a biologic prosthesis. She recovered nicely with relief of heart failure and angina and in a year she was taken off diuretics. In 2019 she was seen for the management of high blood pressure and symptomatic runs of supraventricular tachycardia. There were no symptoms of heart failure or angina pectoris on treatment with ARB, beta-blocker, calcium channel blocker, low-dose thiazide, statin, clopidogrel, and oral antidiabetic drug. She had a normal systolic pressure gradient across the prosthesis and her LVEF had recovered to 56%.

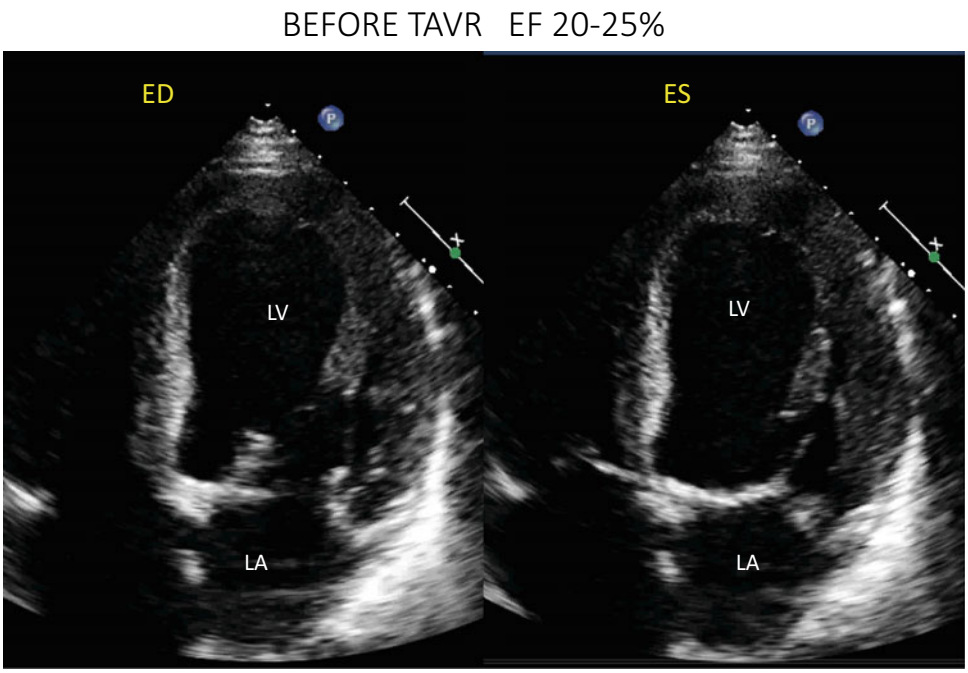

Fig. 23.2 Echocardiogram in 2016 before TAVR. End-diastolic (ED) and end-systolic (ES) images of LV illustrating low LV contractility. EF estimated under 20% and measured with the use of Simpson method 20–25%. EF—ejection fraction. LV—left ventricle

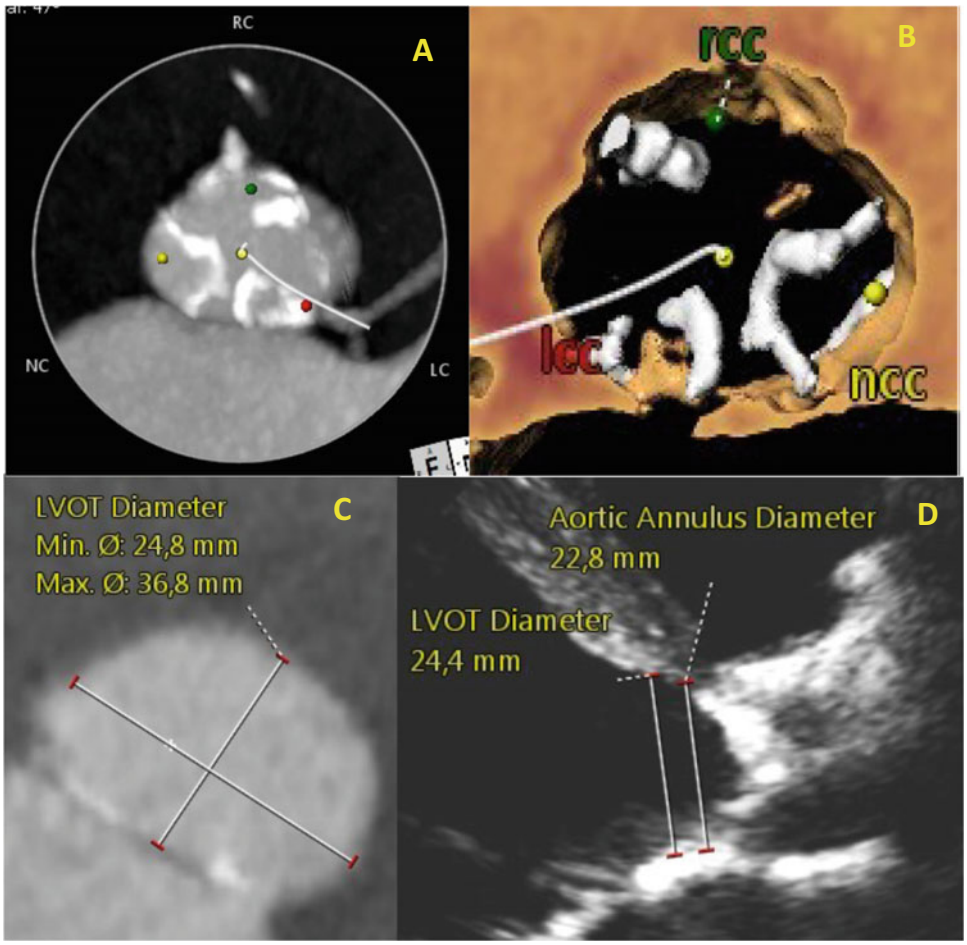

Fig. 23.3 CT scan in 2016 before TAVR. **a** and **b** CT images showing the tricuspid aortic valve with the marginal and basal calcification of the leaflets typical for radiation-induced valve disease. **c** Measurement of LVOT diameter by CT. CT planimetry is usually more accurate than the measurement based on echocardiography which can be hampered by calcification and by the shape of LVOT. The cross section of the LVOT is elliptical and even the minimal diameter is bigger than that measured by echo (**d**). That results in a larger estimated LVOT area and VTI. **d** Measurement of LVOT diameter with the use of echocardiography. CT—computed tomography. LVOT—left ventricular outflow tract. TAVR—transcatheter aortic valve replacement. VTI—Velocity time integral

23.2 Case 2. Radiation-Induced Coronary Artery, Thoracic Vascular Disease and Mitral Regurgitation with Heart Failure in a Hodgkin Lymphoma Survivor

Key Points

- In patients with a history of chest radiation therapy heart failure usually has a multifactorial origin with potential contributions from myocardial, pericardial, valvular, and coronary disease.
- Radiation-induced coronary artery disease (CAD) may manifest earlier than other cardiac lesions
- CAD associated with radiation therapy often has no or atypical symptoms and should be sought in all patients with other cardiac lesions regardless of age

In 2002–2003 at the age of 20 a women underwent chemotherapy (cumulative dose of doxorubicin—200 mg) and radiation therapy for Hodgkin lymphoma (total dose on all lymph nodes above the diaphragm—26 Gy, total dose on mediastinum and left hilum—up to 36 Gy, on right hilum—up to 36 Gy, on both supraclavicular fields—up to 30 Gy).

In January 2009 she had the onset of typical angina precipitated by the cold and exertion. With a diagnosis of "radiation-induced coronary inflammation" the patient was treated at a local hospital with glucocorticoids, antibiotics, beta-blockers, low doses of nitrates, and ACE-inhibitors but her condition deteriorated. With worsening angina and arterial hypotension she was transferred to a hospital with a cardio-oncology service. Coronary angiography showed 95% proximal left circumflex artery (LCx) stenosis, non-obstructive disease of the left anterior descending coronary artery (LAD), and intact right coronary artery (RCA). The patient underwent percutaneous transcatheter coronary angioplasty (PTCA) and drug eluting stent implantation with good clinical and angiographic result (Fig. 23.4, Video 23.4).

Echocardiography was also performed and it showed thickening of mitral valve leaflets, shortening of posterior leaflet with grade II to III mitral regurgitation, left atrial volume index (LAVI) of 33,7 ml/m^2, normal systolic and diastolic myocardial function, and no pulmonary hypertension.

Following the stenting procedure the patient participated in recreational sports continuing dual antiplatelet therapy (DAT), statin, and ivabradine for tachycardia. She did not tolerate beta-blockers because of symptomatic hypotension. A follow-up stress test months later revealed asymptomatic ST-segment depression suggestive of ischemia, but at a high workload. Because she was asymptomatic with excellent exercise tolerance repeat coronary angiography in consideration of a repeat coronary intervention was not deemed necessary.

In 2010 the patient experienced intermittent claudication of the left arm found to be due to left subclavian artery stenosis. Subclavian stenting was performed with good angiographic result and enduring clinical improvement (Fig. 23.5, Video 23.5).

In 2017 she experienced gradual worsening of exertional breathlessness, tachycardia, fatigue, with reduced exercise tolerance. There were several episodes of pulmonary edema precipitated by respiratory infections, physical or emotional strain, and anemia caused by menometrorrhagia. Diuretics were effective but the patient discontinued them because of fatigue. Echocardiography showed mitral regurgitation grade III, with moderate left atrial enlargement (LAVI of 38–40 ml) and pulmonary hypertension depending on diuretic therapy.

In 2019 the patient was admitted with worsening of heart failure and chest discomfort. Coronary angiography showed proximal and distal stent restenoses. PTCA was performed but stent implantation was deferred until the removal of the uterine polyp which caused the menometrorrhagia. After the intervention the symptoms did not resolve (Fig. 23.6, Video 23.6).

In May 2020 the patient was admitted with a non-ST-elevation myocardial infarction (NSTEMI) presenting with fatigue, breathlessness, and tachycardia. Coronary angiography showed subtotal LCx stent stenosis and 80% ostial stenosis of the LAD. The patient underwent crossover left main coronary artery (LMCA)-LCx and LMCA-LAD stenting and her symptoms improved significantly (Fig. 23.7, Video 23.7).

Three months later the patient was stable with moderate limitation of physical activity maintained on DAPT, statin, ivabradine, spironolactone, and daily low-dose torsemide. Echocardiography showed high-speed eccentric mitral regurgitation grade III. The LA enlargement is still moderate despite the long existing high grade MR, pulmonary hypertension is mild (estimated PAPs = 44 mm Hg). There is no evidence for mitral stenosis, other valvular impairment, significant myocardial, or pericardial disease (Fig. 23.8, Video 23.8).

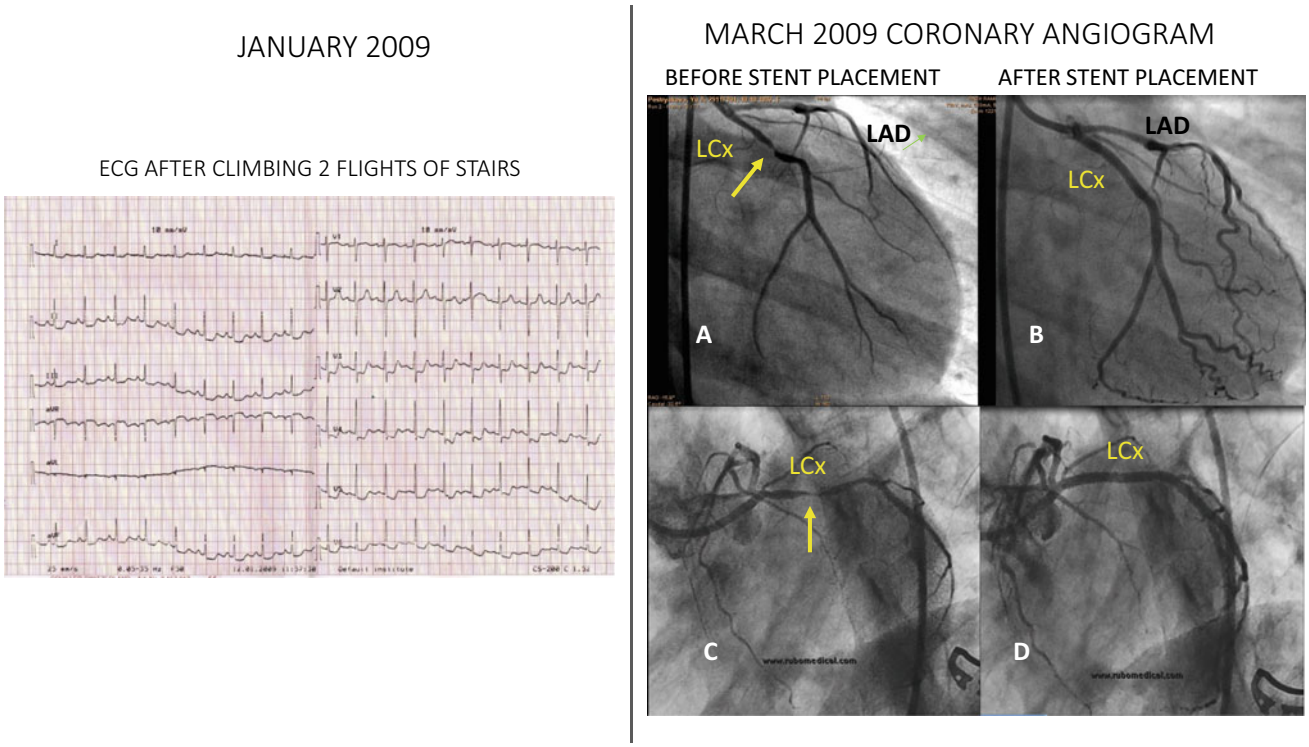

Fig. 23.4 Left panel, Electrocardiogram at first presentation of effort angina in 2009. It was recorded immediately after the patient climbed stairs in the outpatient clinic. ST-segment depression suggestive of ischemia is seen in multiple leads. Right panel, Coronary angiograms of left coronary artery at first presentation in 2009. **a** and **c** Two views before and stenting. *Arrows* indicate significant LCx stenosis. **b** and **d** Ater stent placement in LCx showing good coronary flow. LCx—left circumflex artery

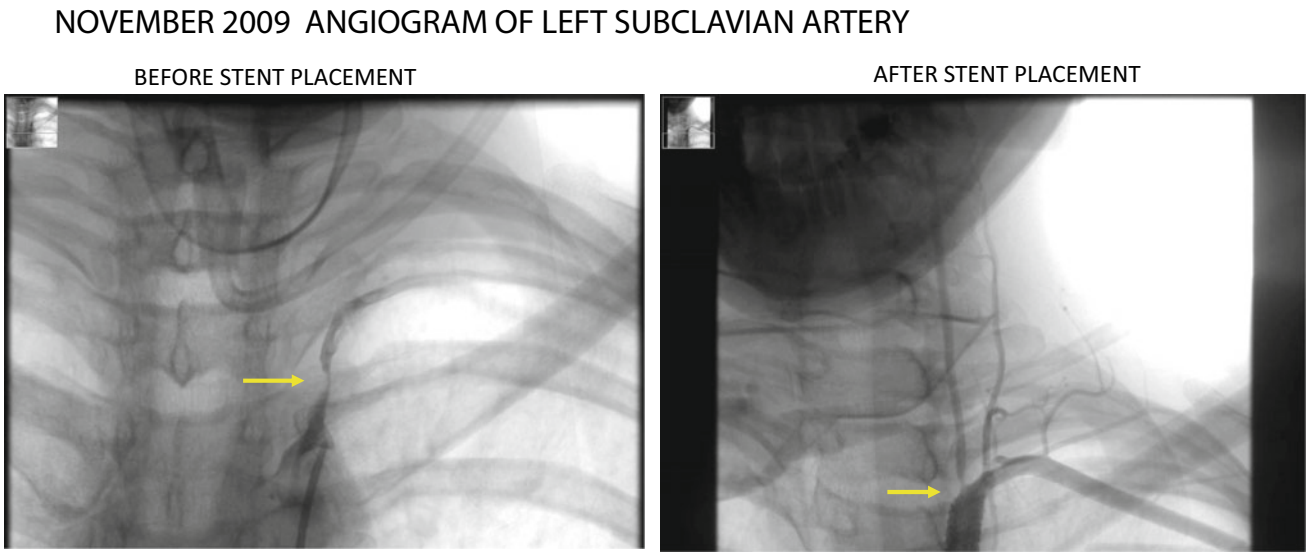

Fig. 23.5 Left panel, Angiogram of left subclavian artery performed after the onset of steal syndrome in 2010. The arrow points at severe artery stenosis. There are no visible branches of the artery due to the markedly reduced blood flow. Right panel, Angiogram of left subclavian artery after stenting. There are normal flow and contrast filling of the branches. The arrow points at the ostium of the vertebral artery that appears moderately narrowed (most likely as a consequence of radiation)

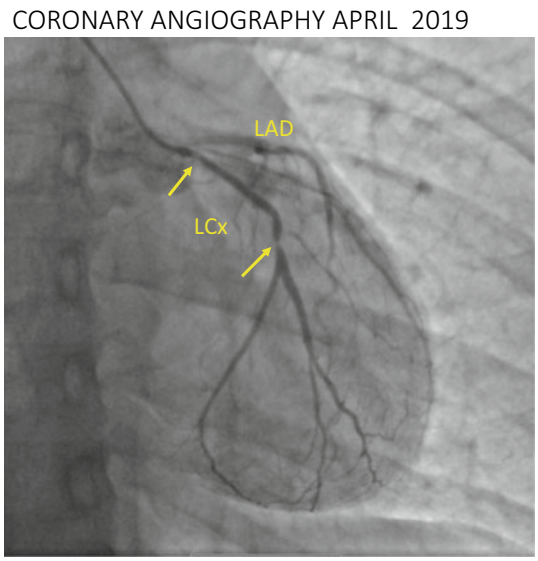

Fig. 23.6 Left coronary angiograms performed in May 2019 when the patient was admitted with worsening of heart failure and some chest discomfort not typical for angina (unlike the first presentation in 2009). Stenoses at the proximal and at the distal ends of the stent in LCx are clearly seen. LAD appeared normal. LAD—left anterior descending artery. LCx—left circumflex artery

Based on the patient's preferences, the marked improvement in her symptoms following coronary stenting, and the major risk of mitral valve surgery in the face of prior chest radiation, the decision was made not to perform mitral valve surgery. The very early experience with evaluating patients for MitraClip procedures suggests that the valve abnormalities associated with radiation therapy may not be well suited to this intervention, but further investigation is required for this and other percutaneous approaches to radiation related mitral valve disease. This patient's clinical course suggests that although the mitral valve disease was the main cause of her heart failure the severity of symptoms was dependent on precipitating factors, namely anemia, respiratory infections, and the NSTEMI she experienced. Management of the cardiovascular sequelae of cancer survivors, particularly those treated with combination therapies, demands careful attention to the multifactorial nature of their illness.

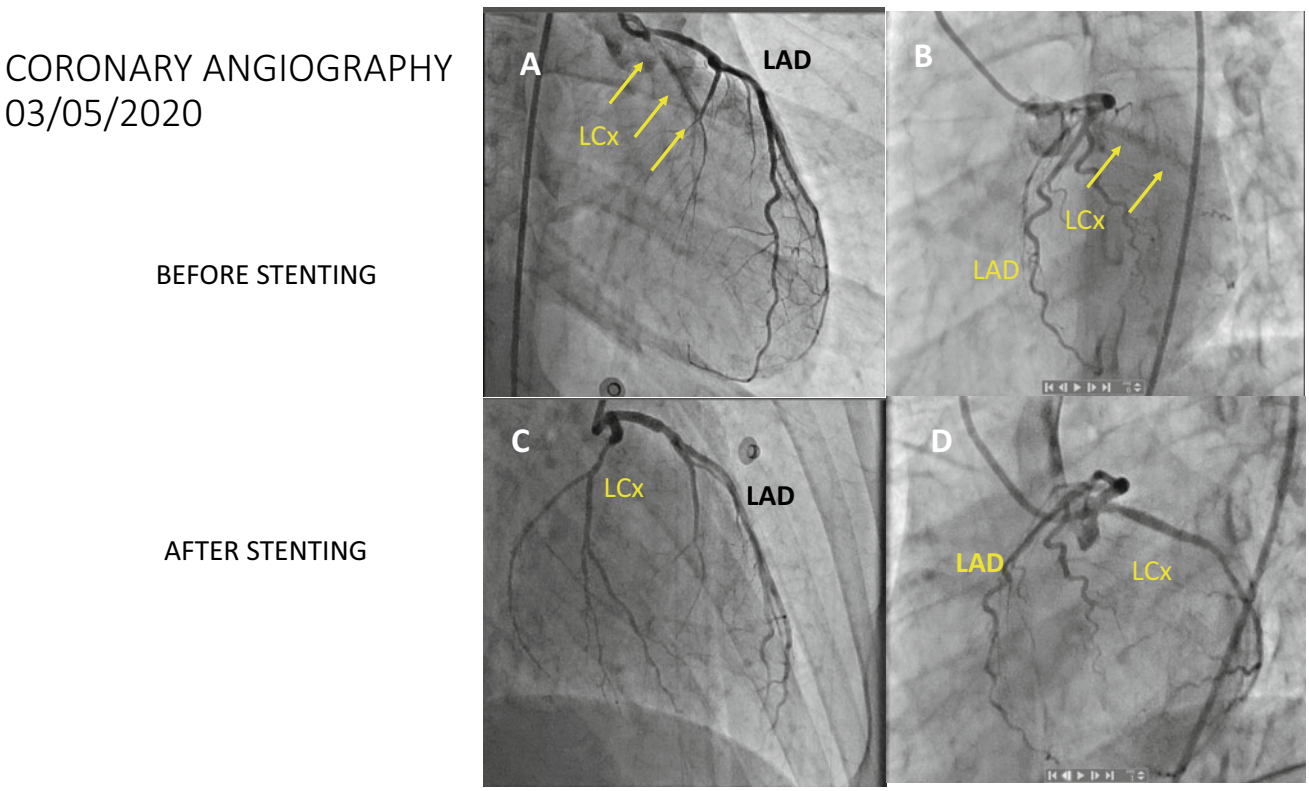

Fig. 23.7 Coronary angiograms performed in May 2020 at admission with diagnosis of non-ST-elevation myocardial infarction presenting with worsening of heart failure. **a** and **b** Two views of left coronary artery branches revealing subtotal LCx stent stenosis (arrows). LAD ostial stenosis was also recognized but it cannot be seen on these images. **c** and **d** 2 views of left coronary artery branches after terminal LMCA bifurcational stenting with good angiographic result. LAD—left anterior descending artery. LCx—left circumflex artery. LMCA—left main coronary artery

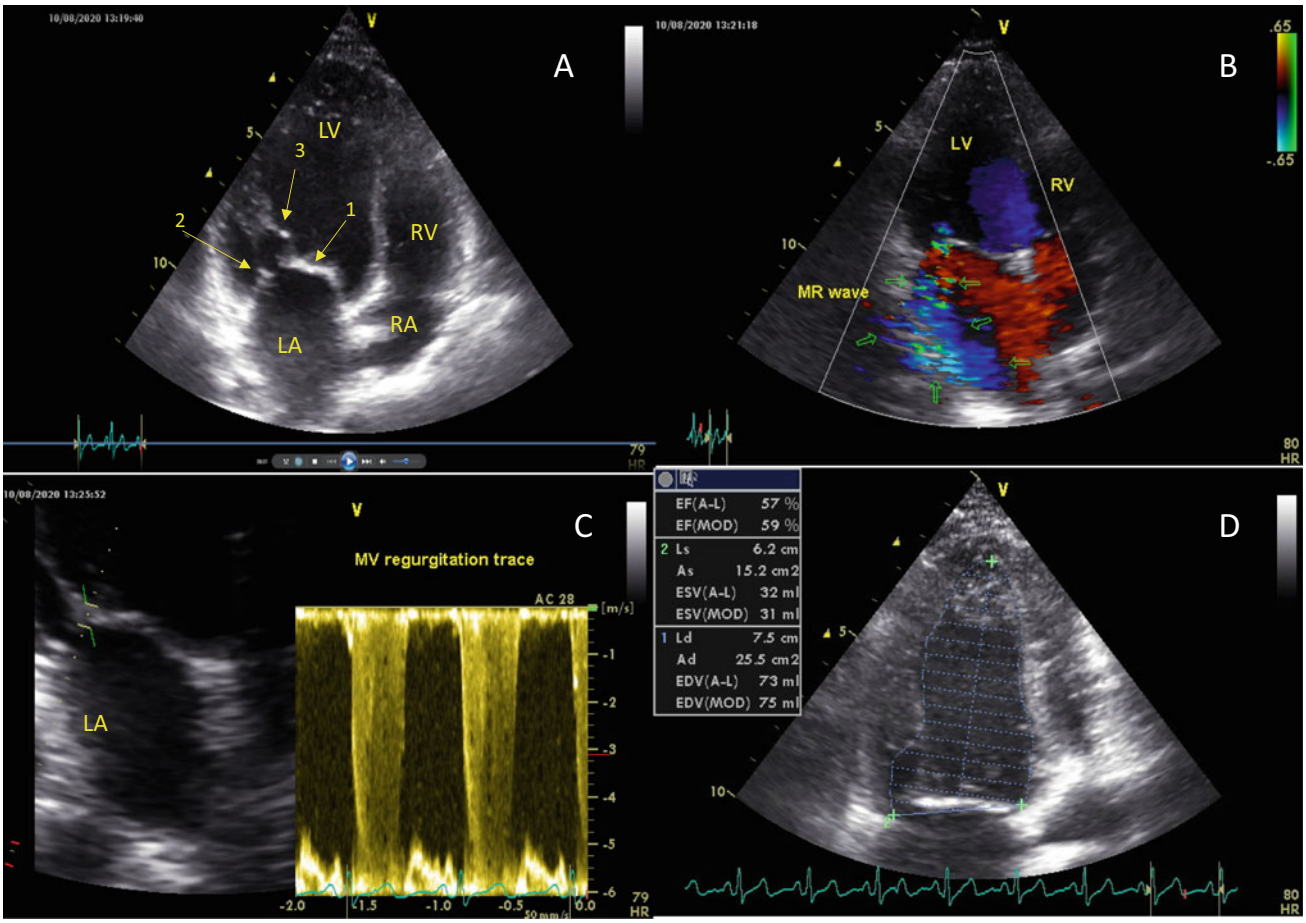

Fig. 23.8 Echocardiography after recent coronary intervention in August 2020. **a** four-chamber view showing mitral valve with thickening of anterior cusp (arrow 1), shortening of posterior cusp (arrow 2), and calcifications in subvalvular apparatus (arrow 3). **b** Color Doppler showing mitral regurgitation grade III. The arrows surround high-speed eccentric regurgitant jet area. **c** Doppler echocardiogram of high-speed jet of mitral regurgitation. **d** Two-chamber view: left ventricular ejection fraction measured with the use of Simpson method is 57%. LA—left atrium. LV—left ventricle, MR—mitral regurgitation, RA—right atrium, RV—right ventricle

References

1. Jaworski C, Mariani JA, Wheeler G, Kaye DM. Cardiac complications of thoracic irradiation. J Am Coll Cardiol. 2013;61:2319–28.
2. Aleman BM, van den Belt-Dusebout AW, De Bruin ML, van 't Veer MB, Baaijens MH, de Boer JP, Hart AA, Klokman WJ, Kuenen MA, Ouwens GM, Bartelink H, van Leeuwen FE. Late cardiotoxicity after treatment for Hodgkin lymphoma. Blood 2007;109:1878–86.
3. Darby SC, Ewertz M, McGalle P, Bennet AM, Blom-Goldman U, Bronnum D et al. Risk of ischemic heart disease in women after radiotherapy for breast cancer. N Engl J Med. 2013;368:987–98.
4. Borkenhagen JF, Bergom C, Rapp CT, et al. Dosimetric predictors of cardiotoxicity in thoracic radiotherapy for lung cancer. Clin Lung Cancer. 2019 Nov;20(6):435–41. doi: https://doi.org/10.1016/j.cllc.2019.05.014.
5. Taylor CW et al. Cardiac exposures in breast cancer radiotherapy: 1950's–1990's. Int J Radiat Oncol Biol Phys. 2007;69:1484–95.
6. Carver JR, Shapiro CL, Ng A, Jacobs L, Schwartz C, Virgo KS et al., ASCO cancer survivorship expert panel. American society of clinical oncology clinical evidence review on the ongoing care of adult cancer survivors: cardiac and pulmonary late effects. J Clin Oncol. 2007;25:3991–4008.
7. van Nimwegen FA, Schaapveld M, Janus CP, Krol AD, Petersen EJ, Raemaekers JM, Kok WE, Aleman BM, van Leeuwen FE. Cardiovascular disease after Hodgkin lymphoma treatment: 40-year disease risk. JAMA Intern Med. 2015;175:1007–17.
8. Meyer R, Gospodarowicz M, Connors J, et al., NCIC clinical trials group, eastern cooperative oncology group. ABVD alone versus radiation-based therapy in limited-stage Hodgkin's lymphoma. N Engl J Med. 2012;366:399–408.
9. Stewart F, Hoving S, Russell N. Vascular damage as an underlying mechanism of cardiac and cerebral toxicity in irradiated cancer patients. Radiat Res. 2010;174:865–9.
10. Yusuf S, Sami S, Daher I. Radiation-induced heart disease: a clinical update. Cardiol Res Pract. 2011;(317659):9. doi: https://doi.org/10.4061/2011/317659.
11. Lancellotti P, Nkomo VT, Badano LP, et al. Expert consensus for multi-modality imaging evaluation of cardiovascular complications of radiotherapy in adults: a report from the European association of cardiovascular imaging and the American society of echocardiography. Eur Heart J Cardiovasc Imaging. 2013;14:721–40.

12. Adler Y, Charron P, Imazio M, et al. 2015 ESC guidelines for the diagnosis and management of pericardial diseases: the task force for the diagnosis and management of pericardial diseases of the European Society of Cardiology (ESC) Eur Heart J. 2015 Nov 7;36(42):2921–64.
13. George TJ, Arnaoutakis GJ, Beaty CA, et al. Contemporary etioloigies, risk factors, and outcomes after pericardiectomy. Ann Thorac Surg. 2012;94:445–51.
14. Wethal T, Lund MB, Edvardsen T, et al. Valvular dysfunction and left ventricular changes in Hodgkin's lymphoma survivors. A Longitudinal Study. Br J Cancer. 2009;101:575–81.
15. Tsai HR, Gjesdal O, Wethal T, et al. Left ventricular function assessed by two-dimensional speckle tracking echocardiography in long-term survivors of Hodgkin's lymphoma treated by mediastinal radiotherapy with or without anthracycline therapy. Am J Cardiol. 2011;107:472–7.
16. Saxena P, Joyce LD, Daly RC, et al. Cardiac transplantation for radiation-induced cardiomyopathy: the Mayo Clinic experience. Ann Thorac Surg. 2014;98(6):2115–21.
17. Hull MC, Morris CG, Pepine cJ et al. Valviular dysfunction and carotid, subclavian and coronary disease in survivors of Hodgkin lymphoma treated with radiation therapy. JAMA. 2003;290: 2831–7.
18. Donnellan E, Griffin BP, Johnston DR, et al. Rate of progression of aortic stenosis and its impact on outcomes in patients with radiation-associated cardiac disease: a matched cohort study. J Am Coll Cardiol Img. 2018;11:1072–80.
19. Dolmaci OB, Farag ES, Boekholdt SM, et al. Outcomes of cardiac surgery after mediastinal radiation therapy: a single-center experience. J Card Surg. 2020 Mar;35(3):612–9.
20. Heidenreich PA, Schnittger I, Strauss HW, et al. Screening for coronary artery disease after mediastinal irradiation for Hodgkin lymphoma. J Clin Oncol. 2007;25:43–9.
21. Nilsson G, Holmberd L, Gamo H, et al. Distribution of coronary artery stenosis after radiation for breast cancer. J Clin Oncol. 2012;30:380–6.
22. Iliescu CA, Grines CL, Hermann J, et al. SCAI Expert consensus statement: evaluation, management and special considerations of cardiooncology patients in the cardiac catheterization laboratory (endorsed by the Cardiological Society of India, and Sociedad Latino Americana de Cardiologia Intervencionista). Catheter Cardiovasc Interv. 2016. https://doi.org/10.1002/ccd.26379.
23. Baumgartner H Chair, Hung J Co-Chair, Bermejo J, Chambers JB, Edvardsen T, Goldstein S, Lancellotti P, LeFevre M, Miller F Jr, Otto CM. Recommendations on the echocardiographic assessment of aortic valve stenosis: a focused update from the European association of cardiovascular imaging and the American society of echocardiography. Eur Heart J Cardiovasc Imaging. 2017 Mar 1;18(3):254–75. doi: https://doi.org/10.1093/ehjci/jew335.
24. Baumgartner H, Falk V, Bax JJ, De Bonis M, Hamm C, Holm PJ, Iung B, Lancellotti P, Lansac E, Rodriguez Muñoz D, Rosenhek R, Sjögren J, Tornos Mas P, Vahanian A, Walther T, Wendler O, Windecker S, Zamorano JL. ESC scientific document group. 2017 ESC/EACTS guidelines for the management of valvular heart disease. Eur Heart J. 2017 Sep 21;38(36):2739–91. doi: https://doi.org/10.1093/eurheartj/ehx391.
25. Donnellan E, Griffin BP, Johnston DR, et al. Rate of progression of aortic stenosis and its impact on outcomes in patients with radiation-associated cardiac disease: a matched cohort study. J Am Coll Cardiol Img. 2018;11:1072–80.

Radiation-Related Coronary and Conduction System Disease

24

Richard M. Steingart

Radiation therapy as primary or neoadjuvant/adjuvant therapy for cancer has cured disease, prolonged survival, and improved the quality of life of many cancer patients [1]. It is well known that there can be substantial adverse cardiovascular consequences to radiation therapy and therefore great effort has been expended to optimize efficacy while reducing the cardiovascular risk [2]. Despite those efforts, cardio-oncology clinicians frequently care for cancer survivors treated with radiation therapy, at risk for or presenting with clinically manifest coronary artery disease. There is much to be learned from our collective experience in treating these patients.

24.1 Case 1. Late-Onset Coronary Artery Disease After Radiation Therapy for Hodgkin Disease

Key Points

- Lifelong surveillance is difficult, and the fragmentation of resources between childhood and adult care systems imposes significant obstacles that the patient, oncologist, and cardio oncologist must overcome.
- Radiation coronary disease is progressive with an accelerated course after the initial clinical presentation.
- Diagnosis and management of radiation related coronary artery is complicated by the invariable presence of other radiation and non-radiation cancer related confounding factors.
- Frequent noninvasive testing, particularly serial rest and stress echocardiography is particularly helpful in sorting through the complex clinical course of these patients.

A 47-year-old woman had been treated for Hodgkin disease in 1982 at age 16 with mantle radiation and splenectomy. In 2010 she underwent thyroidectomy for radiation related thyroid cancer and started thyroid replacement therapy. A heart murmur was noted at that time. In 2012 she underwent bilateral mastectomies for radiation related ER + breast cancer and subsequently received 240 mg/m^2 adriamycin starting in January 2013. Echocardiogram just prior to adriamycin therapy showed EF 59%, thickened aortic valve, mild aortic regurgitation, and peak aortic velocity of 177 cm/s. Long-term tamoxifen therapy was begun. No further cardiac follow-up was undertaken.

She subsequently was treated by a rehabilitation medicine physician for a radiation fibrosis syndrome of the chest and neck and was referred to our cardiology clinic in the fall of 2013 for evaluation of a heart murmur amid complaints of mild dyspnea on exertion. During the cardiology consultation she was noted to have a systolic ejection murmur. A transthoracic echocardiogram showed normal systolic function, a thickened aortic valve with mild to moderate aortic regurgitation and stenosis. The EKG was normal (Fig. 24.1, Video 24.1).

Expert consensus recommendations call for screening for valvular and coronary artery disease after thoracic radiation exposures, the timing, and frequency of such screening dependent on the intensity of such exposure and concomitant therapies [3, 4]. The interval from 1982 to 2013 was clearly too long but not unusual. Hopefully with the emergence of cardio-oncology the importance of screening will find its way into routine practice. We were interested in exploring the clinical value of CT coronary angiography in cancer survivors [5]. Her CT coronary angiogram showed extensive

Electronic supplementary material
The online version of this chapter (https://doi.org/10.1007/978-3-030-70998-3_24) contains supplementary material, which is available to authorized users.

R. M. Steingart (✉)
Department of Medicine, Memorial Sloan Kettering Cancer Center, New York, NY 10065, USA
e-mail: steingar@mskcc.org

R. M. Steingart et al. (eds.), *Atlas of Imaging in Cardio-Oncology*,
https://doi.org/10.1007/978-3-030-70998-3_24

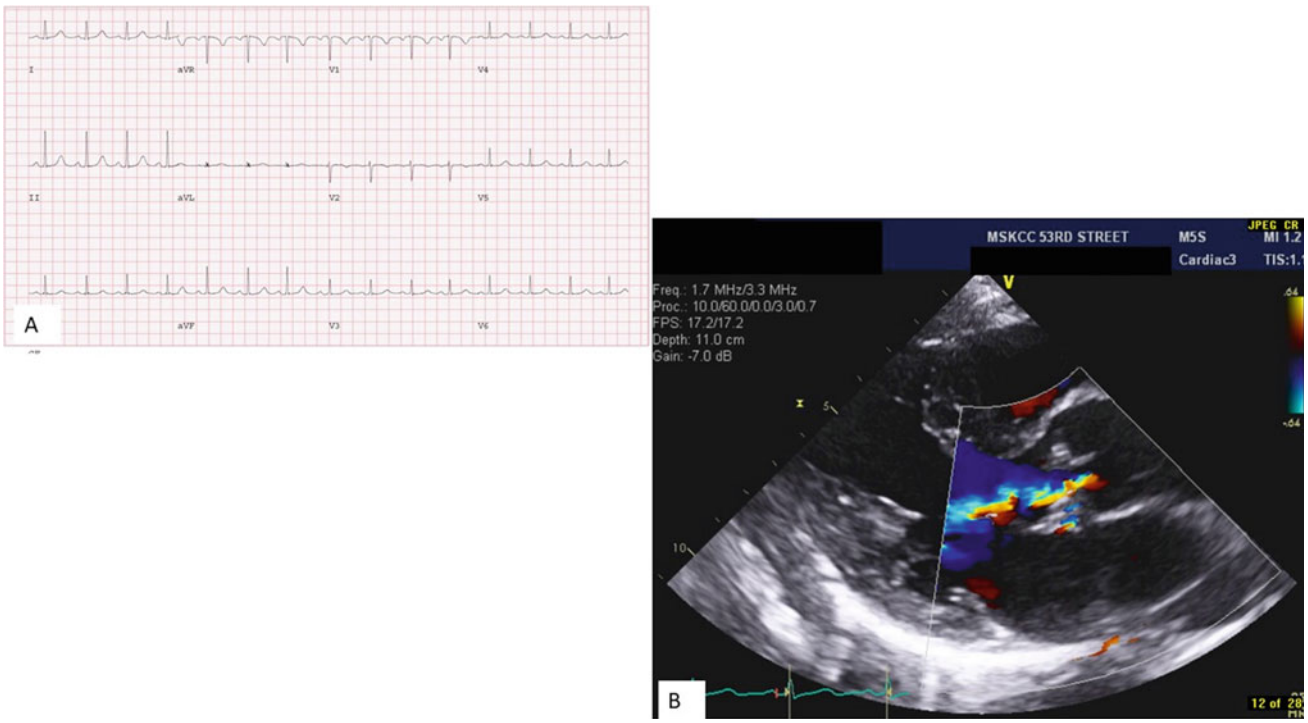

Fig. 24.1 **a** Normal baseline electrocardiogram at initial cardiology consultation. **b** Baseline echocardiogram at initial cardiology consultation showing calcified aortic valve and aortic regurgitation

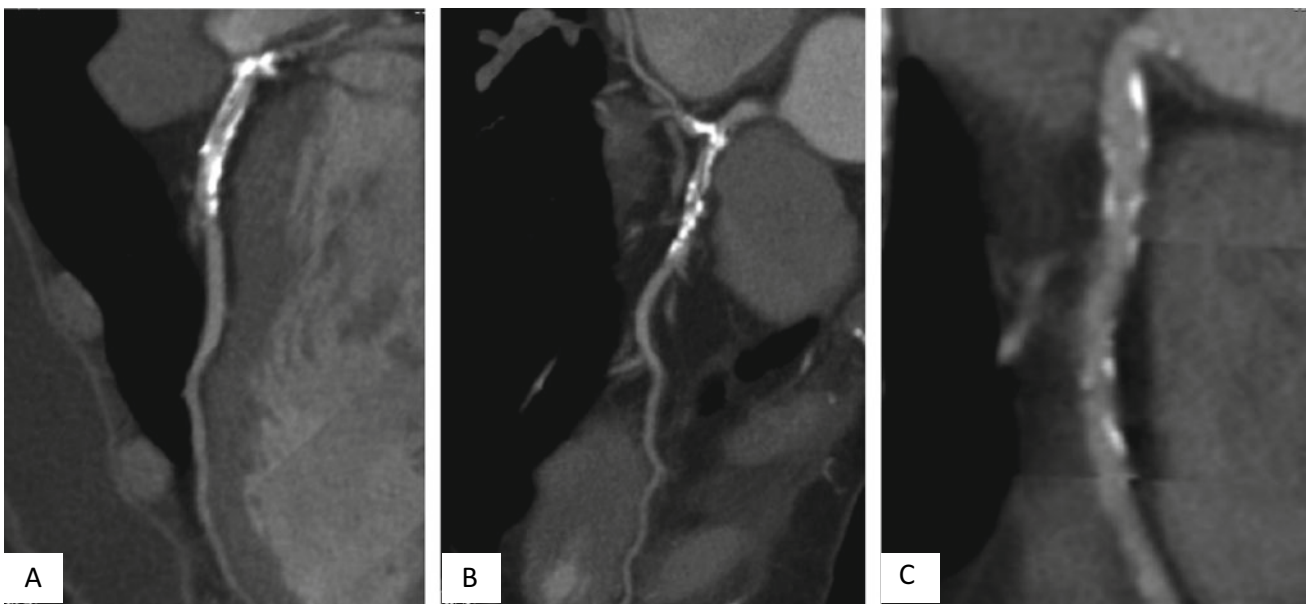

Fig. 24.2 CT coronary angiogram. **a** and **b** show calcification in the proximal left anterior descending and left circumflex coronary arteries. **c** shows more diffuse calcification in the right coronary artery. The plaques were interpreted as non-obstructive

coronary calcifications (Fig. 24.2) with non-obstructive coronary disease. Agatston calcium score 1004.

She was begun on low dose ASA and statin therapy. LDL fell from 130 to 70 mg/dl. To be more certain that the coronary and valvular disease were not contributing to her exertional symptoms she underwent stress echocardiography. Both the EKG and stress echo portion were negative for ischemia. Ventricular function improved with exercise.

Guidelines are less clear about the appropriate follow-up once coronary atherosclerosis is discovered in radiation

exposed cancer survivors. Certainly aggressive secondary preventive measures are indicated. It is our practice to carefully educate patients regarding signs and symptoms that would indicate worsening of the coronary atherosclerosis, ventricular function, and or valve disease and how to react to such indicators. We see radiation survivors with subclinical or clinically manifest cardiovascular disease in the clinic at least once or twice a year and have a low threshold for follow-up evaluations based on the clinical presentation. This can be challenging since as a consequence of radiation therapy (with or without chemotherapy and surgeries) there are frequently also abnormalities of the breasts, lung, pleura, pericardium, chest wall structures, skin, sensory, and autonomic nervous systems that can produce a constellation of confusing signs and symptoms. Further cardiovascular imaging is not uncommonly ordered, attempting to minimize testing risks including additional radiation exposure.

She did well while working as a teacher and exercising regularly in a modified cardiac rehabilitation program until 2016 when she developed the acute onset of dyspnea on exertion. She was diagnosed with a pulmonary embolism and was begun on full dose anticoagulation. Her dyspnea improved. At the time of the embolism she was being treated with Tamoxifen, and that combined with immunoglobulin therapy for an immunodeficiency syndrome could have predisposed her to thromboembolism. Tamoxifen was discontinued in favor of Lupron. At her urging, she later underwent oophorectomy and Lupron was discontinued.

Her dyspnea subtly returned a few months after the diagnosis of pulmonary embolism. She underwent an exercise nuclear stress test (Fig. 24.3).

The nuclear stress test showed transient ischemic dilation and a severe reversible inferior defect. Although the positive predictive value of nuclear stress testing after mediastinal radiation has been questioned in asymptomatic patients [6], exercise stress testing (with or without Lexiscan nuclear perfusion supplementation) can be a valuable tool in the decision for triage to cardiac catheterization and revascularization particularly in symptomatic patients. Her cardiac catheterization showed near total occlusion of the proximal right coronary artery along with significant obstruction of the left main coronary artery and the proximal left anterior descending coronary artery (Fig. 24.4). This distribution of lesions is characteristic of radiation related coronary disease [7]. She underwent staged stenting of the right coronary, left main, and left anterior descending coronary arteries. Exertional dyspnea and exercise tolerance improved as she participated in a cardiac rehabilitation program.

Overall patient outcome for both coronary stenting and coronary bypass surgery are probably less favorable for radiation survivors than for patients with classic coronary artery disease at least in part due to non-cardiac effects of radiation, the original cancer and non-cardiac late effects of cancer and its therapies as illustrated in our patient. Differences in the fundamental pathophysiology of the coronary lesions could also be playing a role (*see* Chap. 22) [8–12]. That said, coronary revascularization of radiation related lesions does improve exercise tolerance and overall quality of life. Extrapolating from the experience with "naturally occurring" coronary artery disease, coronary interventions for radiation related coronary disease likely prolong survival particularly in patients with left main or proximal obstructive left anterior descending coronary disease, severe or unstable ischemic symptoms and in the face of left ventricular dysfunction [8–12]. When coronary stenting is possible, it is preferred over bypass surgery because of the difficulties in surgical exposure, post-operative healing, and pulmonary function in the aftermath of radiation therapy [10].

Six months after the stenting procedure, the patient experienced a rather abrupt decline in exercise tolerance particularly noted with more vigorous exertion. During a treadmill exercise echocardiogram stress test ordered to investigate these complaints, she experienced the abrupt onset of exertional fatigue as the workload was increased. This duplicated her presenting complaint. While symptomatic, her exercise electrocardiogram demonstrated chronotropic incompetence with a sudden drop in her heart rate as the likely cause of her symptoms (Fig. 24.5 left panel).

At a submaximal heart rate, the immediate post-exercise echocardiogram showed an increase in the EF compared with baseline, a small regional wall motion abnormality and stable mild to moderate aortic stenosis and regurgitation (Videos 24.2 and 24.3).

Repeat cardiac catheterization showed that the coronary stents were patent. A rate responsive permanent pacemaker was indicated for symptom relief. Even this procedure had to be customized for this radiation treatment survivor due to anterior thoracic skin changes, muscle wasting, and difficulties with venous access. The rate responsive pacemaker was placed subcutaneously below the right axilla (Fig. 24.5 right panel). With that she was able to return to work and resumed her exercise regimen.

One year later she palpated a mass in the right axilla. Imaging revealed nodal and boney metastases. This lovely, courageous woman succumbed to widely metastatic breast cancer approximately 18 months after the discovery of her

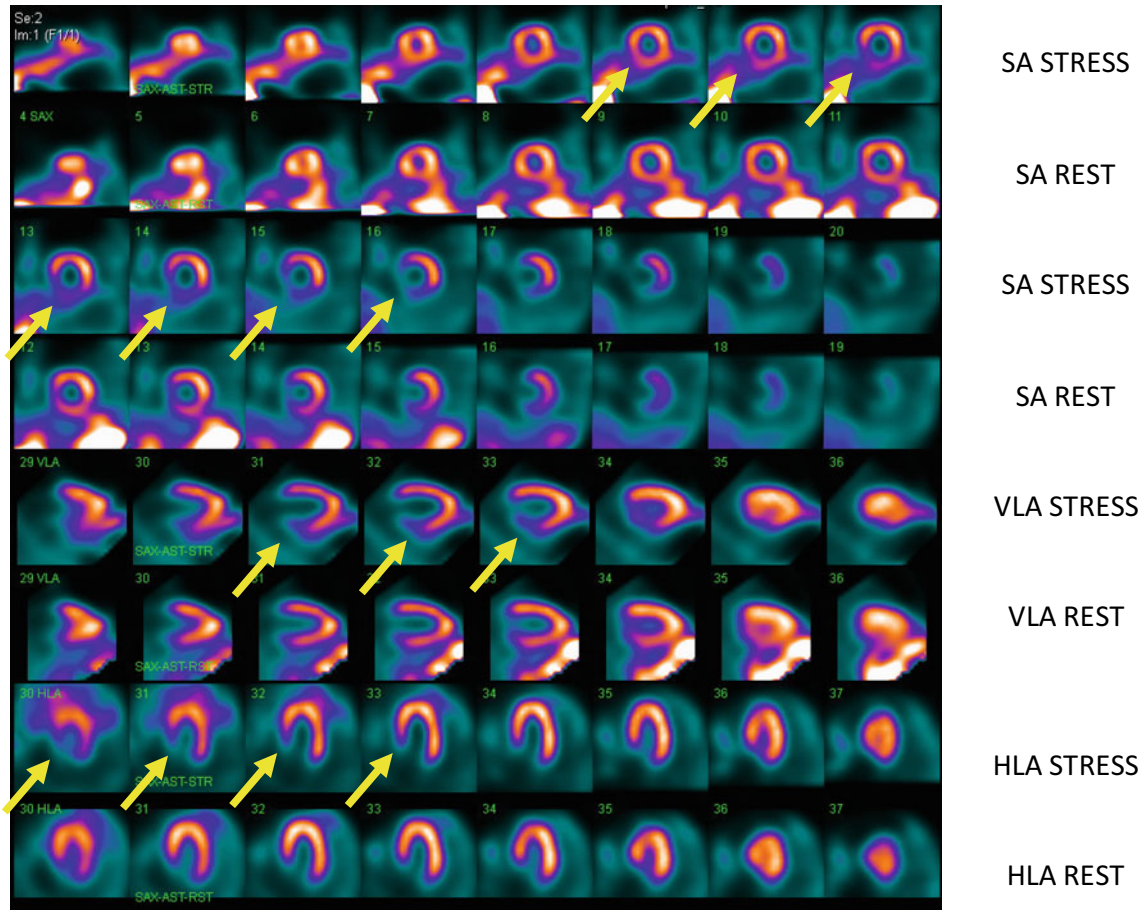

Fig. 24.3 Nuclear stress test. The arrows point to post-stress perfusion defects seen in multiple slices in three views with relative improvement to perfusion on the rest images below indicating a significant ischemic burden. Note the relatively larger cavity size on the stress images compared to rest, known as transient ischemic dilation, another indication that there is a significant ischemic burden. HLA, Horizontal long axis. SA, Short axis. VLA, Vertical long axis

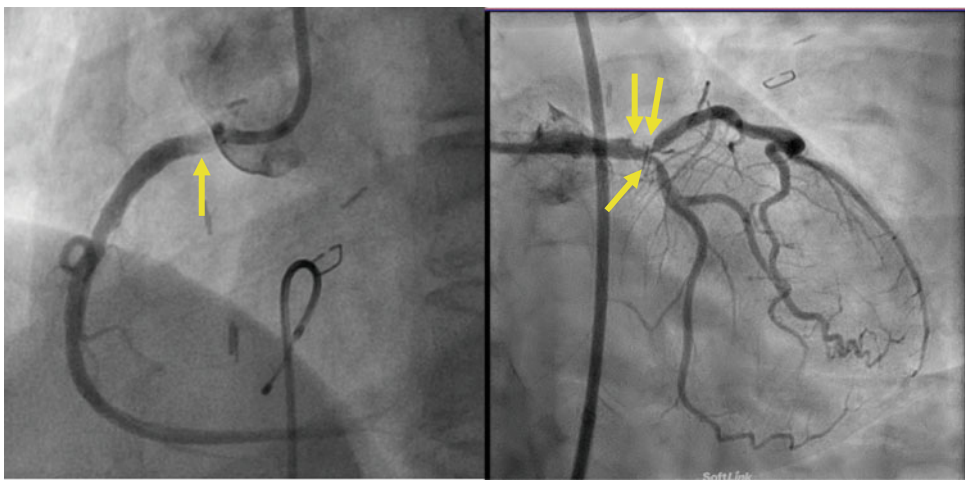

Fig. 24.4 Coronary angiogram. Left panel, Right coronary artery showing virtual total occlusion at the ostium. Right panel, >50% obstruction of the distal left main coronary artery (top arrow) leading into significant ostial lesions of the left anterior descending (2nd top arrow) and left circumflex coronary artery (bottom arrow)

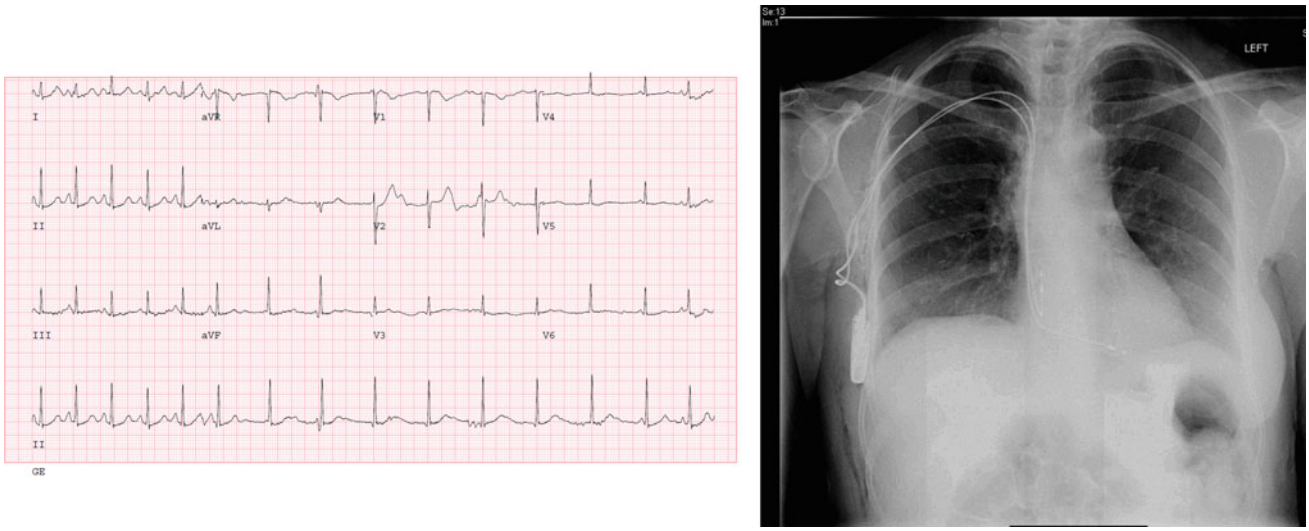

Fig. 24.5 Left panel, EKG during stress test done for return of symptoms following coronary stenting. Heart rate abruptly drops from 125 to 75 BPM coinciding with the patient's complaints of exertion related SOB and fatigue. Right panel, Rate response pacemaker had to be placed in the right axillary line due to radiation related skin and muscle changes and difficulties with venous access. With rate responsive pacing, exercise tolerance improved with disappearance of the bouts of acute onset exercise related fatigue and dyspnea

axillary mass. During the therapies for metastatic breast cancer, she had no further cardiac events.

24.2 Case 2. Coronary Artery Disease Associated with Radiation Therapy for Breast Cancer

Key Points

- For radiation doses traditionally used for left-sided breast cancer, there is no threshold effect between radiation dose and subsequent ASCVD.
- Atherosclerotic risk from radiation is proportionate to the dose to the heart and amplified by traditional cardiac risk factors .
- Risk-benefit discussions are key, especially with older women who have multiple cardiac risk factors .
- It is logical, but unproven, that aggressive management of risk factors for atherosclerotic disease will reduce the incidence of cardiac events following exposure of the heart and vasculature to radiation.

A 61-year-old woman with left-sided breast cancer underwent a wide local excision and sentinel lymph node biopsy on 7/13/2013. Past medical history was positive for obesity, sleep apnea, diabetes, hypertension, and hyperlipidemia. A preoperative nuclear stress test done at an outside institution in 2010 was reported as normal, done before lap band surgery.

Pathology from the breast surgery revealed 0.8 cm poorly differentiated invasive ductal carcinoma as well as ductal carcinoma in situ of high nuclear grade with a solid architecture. Margins were widely negative and none of the four sampled lymph nodes were involved with disease. Immunohisto-chemistry was ER/PR negative, HER-2 negative. Adjuvant chemotherapy treatment with cyclophosphamide, methotrexate, and fluorouracil was started 9/30/2013 and completed by April of 2014. Radiation therapy for locoregional control and breast cancer-specific survival was recommended but because of breast surgery wound infections, it was not started until 4/23/14 and then completed by 5/30/14. She received 15MV photons for a dose of 5000 cGy in 25 fractions. The treatment plan included a prone set up with opposed-tangential ports targeting the whole left breast. Considering the N0 clinical and pathological stage, nodal irradiation was not indicated nor was a boost dose to the lumpectomy cavity indicated because of her age over 60.

Two years later during evaluation for possible varicose vein surgery, she was noted to have a left renal mass on pelvic MRI. Biopsy revealed renal cell carcinoma. The General Internal Medicine service ordered a pharmacologic nuclear stress test and a resting echocardiogram for preoperative risk stratification because of her multiple risk factors , limited exercise tolerance, and dyspnea on exertion (Fig. 24.6, Video 24.4).

The evidence is compelling that there is a benefit of adjuvant radiotherapy in breast cancer in reducing local recurrences and deaths from cancer but there has been excess mortality from heart disease in some women administered radiation [13]. In the early trials, left-sided breast cancer radiation was associated with higher mortality from ischemic heart disease compared with right-sided cancer. The

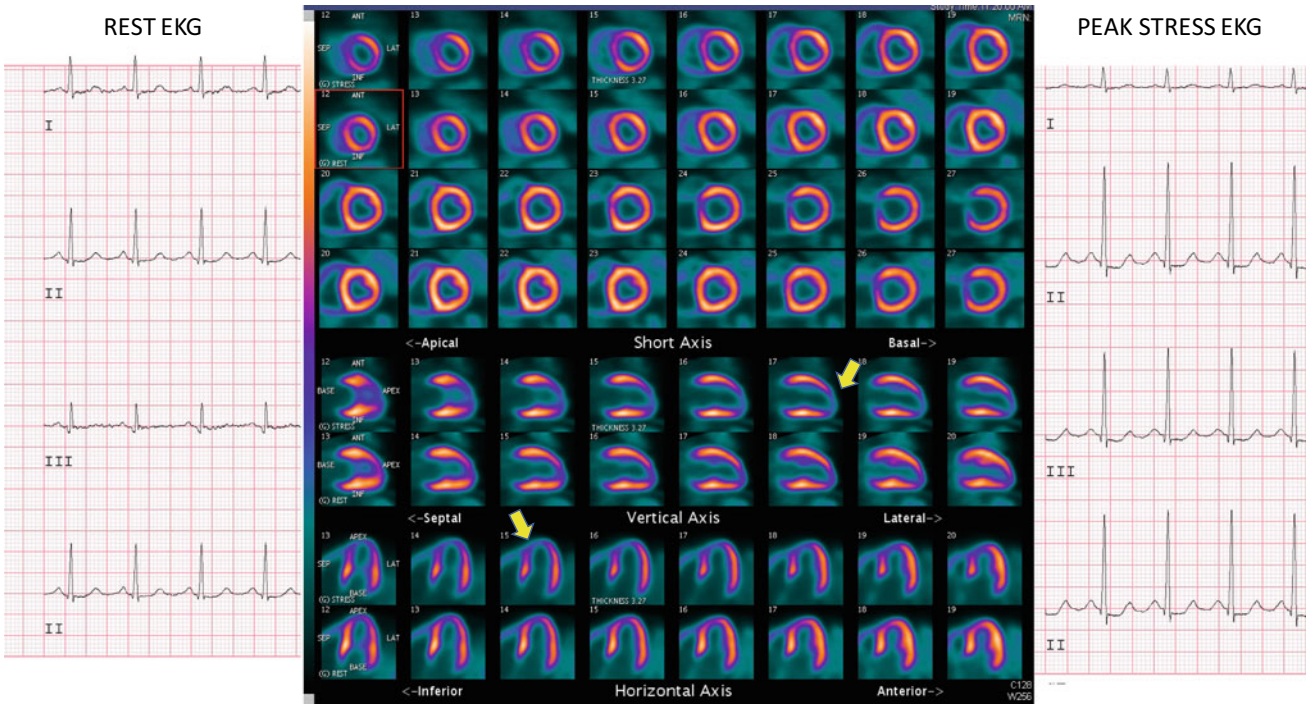

Fig. 24.6 EKGs and myocardial perfusion images from a pharmacologic PET stress test. Baseline EKG is normal, peak stress EKG shows horizontal ST-segment depression in the inferior leads. PET perfusion shows a reversible anterior apical and apical perfusion defect (arrows show the stress perfusion defect). The distribution of the perfusion defects is characteristic of mid-left anterior descending coronary artery disease after left-side breast radiation

coronary related mortality rates are probably lower with modern radiation methods (see Chap. 22). The pathophysiology of radiation-induced heart disease involves microangiopathy of the small vessels as well as macroangiopathy of the coronary arteries resulting in fibrosis of the myocardium, coronary artery disease, and eventually ischemic heart disease [14].

The landmark case-control study by Darby et al. [13] of major coronary events (i.e., myocardial infarction, coronary revascularization, or death from ischemic heart disease) in 2168 women who underwent radiotherapy for breast cancer between 1958 and 2001 in Sweden and Denmark prompted a re-examination of breast cancer treatments because of cardiovascular disease concerns, especially among women with multiple cardiac risk factors . In that study, rates of major coronary events increased linearly with the mean dose to the heart by 7.4% per gray with no apparent lower threshold. The increase started within the first 5 years after radiotherapy and continued into the third decade after radiotherapy. Women with preexisting cardiac risk factors had greater absolute increases in risk from radiotherapy than other women. To use an example from Darby's manuscript, a mean dose of radiation to the heart of 3 Gy in a 50-year-old woman with one or more cardiac risk factors would increase her risk of death from ischemic heart disease before the age of 80 years from 3.4 to 4.1% (an absolute increase of 0.7 percentage points), and it would increase her absolute risk of having an acute coronary event by the age of 80 years by 1.7% points. A mean dose of 10 Gy to her heart would result in radiation related risks that were higher. Although the risk grows to be considerable for a woman with multiple risk factors , the risk accumulates over many years and the large majority of women so exposed do not experience a cardiac event [12].

These revelations have catalyzed further efforts to develop radiation strategies that optimize breast cancer treatment while minimizing cardiac risks. Thus, although the field is changing, instituting best practice for a given patient is greatly challenging. That is, for our patient, did the benefit of RT exceed the cardiac risk, and what is the best approach to administering the radiation? At the start, cardiologists, oncologists, radiation therapists need to conference with the patient to promote understanding of all the options. Our patient was treated in 2014 with modern techniques. Yet the time course and location of the coronary stenoses found 2 years later are certainly consistent with radiation related coronary disease (Figs. 24.7 and 24.8).

A decision was made to manage the coronary disease medically with an aggressive secondary prevention regimen. She underwent an uncomplicated left nephrectomy.

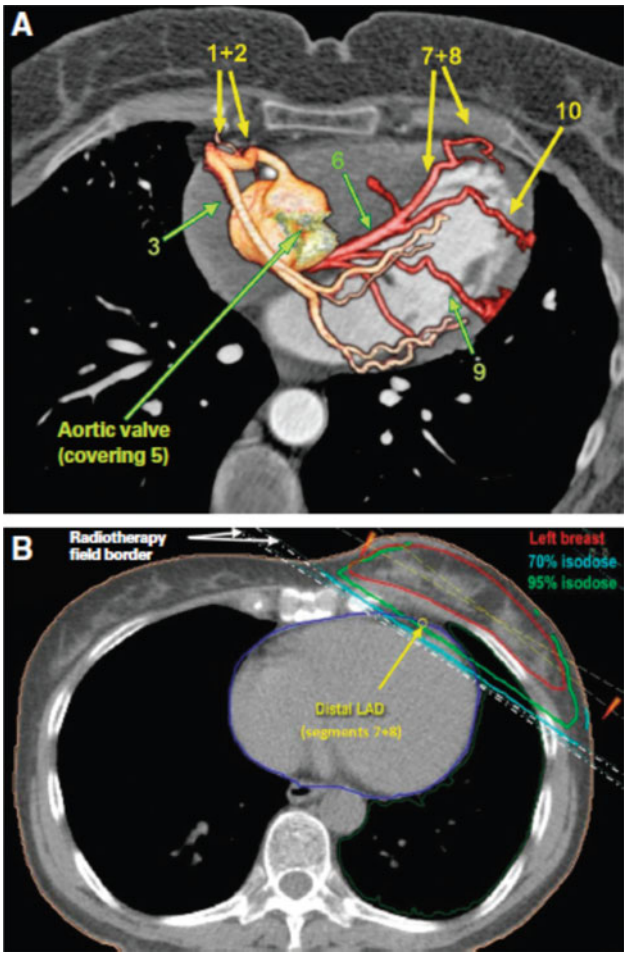

Fig. 24.7 **a** Coronary angiogram superimposed on computed tomography (CT) of heart illustrating anatomy of coronary arteries with branches of right coronary artery (orange) and left circumflex and left anterior descending (LAD) arteries (red); numbered arrows indicate segments. **b** CT dose-planned left tangential breast irradiation showing distal LAD (yellow circle) and radiation fields. (From Nilsson et al. [15], with permission from Wolters Kluwer.)

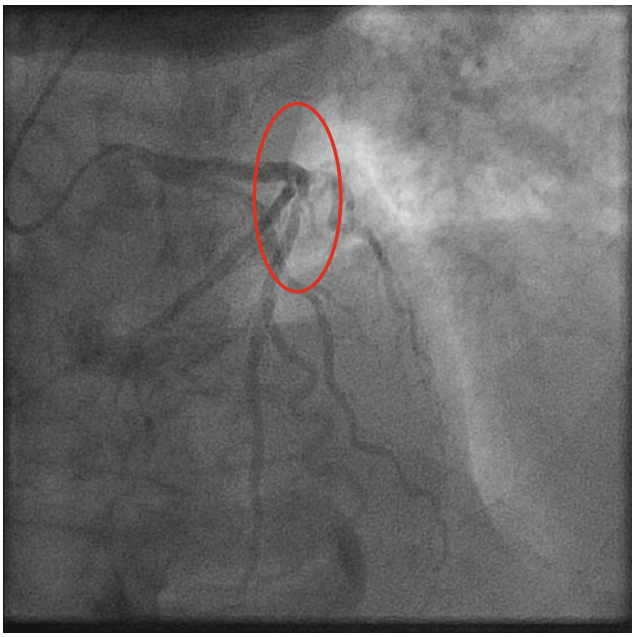

Fig. 24.8 Coronary angiogram showing lesion in the mid LAD of our patient following left breast radiation

References

1. Armenian SH, Armstrong GT, Aune G, Chow EJ, Ehrhardt MJ, Ky B, et al. Cardiovascular disease in survivors of childhood cancer: insights into epidemiology, pathophysiology, and prevention. J Clin Oncol. 2018;36(21):2135–2144. https://doi.org/10.1200/JCO.2017.76.3920. PMID: 29874141; PMCID: PMC6804893.
2. Cuomo JR, Javaheri SP, Sharma GK, Kapoor D, Berman AE, Weintraub NL. How to prevent and manage radiation-induced coronary artery disease. Heart. 2018;104(20):1647–1653. https://doi.org/10.1136/heartjnl-2017-312123. PMID: 29764968; PMCID: PMC6381836.
3. Chang HM, Okwuosa TM, Scarabelli T, Moudgil R, Yeh ETH. Cardiovascular complications of cancer therapy: best practices in diagnosis, prevention, and management: part 2. J Am Coll Cardiol. 2017;70(20):2552-2565. https://doi.org/10.1016/j.jacc.2017.09.1095. PMID: 29145955; PMCID: PMC5825188.
4. Childrens Oncology Group. Long-term follow up guidelines for survivors of childhood adolescent and young adult cancers, Version 5.0 Monrovia, CA: Children's Oncology Group; 2018. www.survivorshipguidelines.org.
5. Rademaker J, Schöder H, Ariaratnam NS, et al. Coronary artery disease after radiation therapy for Hodgkin's lymphoma: coronary CT angiography findings and calcium scores in nine asymptomatic patients. AJR Am J Roentgenol. 2008;191:32–7.
6. Heidenreich PA, Schnittger I, Strauss HW, Vagelos RH, Lee BK, Mariscal CS, Tate DJ, Horning SJ, Hoppe RT, Hancock SL. Screening for coronary artery disease after mediastinal irradiation for Hodgkin's disease. J Clin Oncol. 2007;25(1):43–9. https://doi.org/10.1200/JCO.2006.07.0805. Erratum in: J Clin Oncol. 2007;25(12):1635. PMID: 17194904.
7. Desai MY, Jellis CL, Kotecha R, Johnston DR, Griffin BP. Radiation-associated cardiac disease: a practical approach to diagnosis and management. JACC Cardiovasc Imaging. 2018;11(8):1132–1149. https://doi.org/10.1016/j.jcmg.2018.04.028. PMID: 30092970.
8. Reed GW, Masri A, Griffin BP, Kapadia SR, Ellis SG, Desai MY. Long-term mortality in patients with radiation-associated coronary artery disease treated with percutaneous coronary intervention. Circ Cardiovasc Interv. 2016;9(6):e003483. https://doi.org/10.1161/CIRCINTERVENTIONS.115.003483. PMID: 27313281
9. Wu W, Masri A, Popovic ZB, Smedira NG, Lytle BW, Marwick TH, Griffin BP, Desai MY. Long-term survival of patients with radiation heart disease undergoing cardiac surgery: a cohort study. Circulation. 2013;127(14):1476–85. https://doi.org/10.1161/CIRCULATIONAHA.113.001435. PMID: 23569119.
10. 10. Reed GW, Rossi JE, Masri A, Griffin BP, Ellis SG, Kapadia SR, Desai MY. Angiographic predictors of adverse outcomes after percutaneous coronary intervention in patients with radiation associated coronary artery disease. Catheter CardiovascInterv. 2019;94(3):E104–E110. https://doi.org/10.1002/ccd.28107. PMID: 30690850.
11. Hicks GL Jr. Coronary artery operation in radiation-associated atherosclerosis: long-term follow-up. Ann Thorac Surg. 1992;53

(4):670–4. https://doi.org/10.1016/0003-4975(92)90331-w. PMID: 1554280.

12. Desai MY, Windecker S, Lancellotti P, Bax JJ, Griffin BP, Cahlon O, Johnston DR. Prevention, diagnosis, and management of radiation-associated cardiac disease: JACC scientific expert panel. J Am Coll Cardiol. 2019;74(7):905–927. https://doi.org/10.1016/j.jacc.2019.07.006. PMID: 31416535.
13. Darby SC, Ewertz M, McGale P, Bennet AM, Blom-Goldman U, Brønnum D, Correa C, Cutter D, Gagliardi G, Gigante B, Jensen MB, Nisbet A, Peto R, Rahimi K, Taylor C, Hall P. Risk of ischemic heart disease in women after radiotherapy for breast cancer. N Engl J Med. 2013;368(11):987–98. https://doi.org/10.1056/NEJMoa1209825. PMID: 23484825.
14. Tapio S. Pathology and biology of radiation-induced cardiac disease. J Radiat Res. 2016;57(5):439–448. https://doi.org/10.1093/jrr/rrw064. PMID: 27422929; PMCID: PMC5045085.
15. Nilsson G, Holmberg L, Garmo H, Duvernoy O, Sjögren I, Lagerqvist B, Blomqvist C. Distribution of coronary artery stenosis after radiation for breast cancer. J ClinOncol. 2012;30(4):380–6. https://doi.org/10.1200/JCO.2011.34.5900. PMID: 22203772.

Radiation Injury to the Heart, Great Vessels, and Their Branches

25

Vera I. Potievskaya, Albert A. Akhobekov, Olga E. Popovkina, Elena V. Kononova, Dmitriy O. Nadinskiy, and Valeriy V. Kucherov

Key Points

- One of the most common indications for radiation therapy of the mediastinum is Hodgkin lymphoma [1].
- Hodgkin lymphoma is the most common malignancy in young patients with an estimated incidence of 3 cases per 100 000 population.
- Ten-year survival is more than 80% [2, 3].
- The incidence of coronary artery disease in patients with Hodgkin lymphoma 40 years after radiation therapy is approximately 60%. The risk of ischemic heart disease and myocardial infarction is 3.2-fold and twofold higher than in the general population, respectively [3, 4].
- Vascular disease is often insidious and delayed in onset, with precise prediction of the location and extent of clinically important vascular damage within the radiation field difficult.

25.1 Case 1: Radiation Injury to the Heart and Brachiocephalic Vessels

A 55-year-old patient was admitted to our clinic in 2018 with recurrent pneumonia and signs and symptoms of severe heart failure whose beginning was dated to six months earlier. Hodgkin lymphoma had been diagnosed in 1996 treated with radiation and chemotherapy. Sustained remission was achieved.

On presentation, ECG showed sinus rhythm at 77 bpm with ventricular extrasystoles, Q wave in III, and lateral ST-T changes (Fig. 25.1). Transthoracic echocardiography (TTE) revealed a dilated left ventricle (LV) with thrombosis of the apex of the LV, LV posterior and lateral wall akinesia and posteroseptal wall hypokinesia. The global contractility of the LV was reduced with LV ejection fraction (LVEF) of 30%. There was calcification of the aortic root and aortic cusps with valvular aortic insufficiency (2+) and aortic valve stenosis (peak gradient 35 mm Hg). There was mitral valve insufficiency 3+ and stenosis. The systolic pressure in the pulmonary artery was elevated at 50 mm Hg (Figs. 25.2, 25.3, 25.4 and 25.5).

Coronary angiography and angiography of the brachiocephalic arteries were performed. Right dominant coronary circulation, 55% stenosis of the left main coronary artery, 50% stenosis at the junction of the middle and distal left anterior descending artery. Total occlusion of the circumflex artery with post occlusion segment supplied through collateral vessels and long subtotal stenosis of the proximal segment of the first obtuse marginal branch were revealed. The right coronary artery was occluded at the ostium, and the post-occlusion segment is supplied through collateral

Electronic supplementary material
The online version of this chapter (https://doi.org/10.1007/978-3-030-70998-3_25) contains supplementary material, which is available to authorized users.

V. I. Potievskaya (✉) · E. V. Kononova
P. Hertsen Moscow Oncology Research Institute - branch of the National Medical Research Radiological Centre of the Ministry of Health of Russian Federation, 2nd Botkinsky Drive 3, Moscow, 125284, Russia
e-mail: vera.pot@mail.ru

E. V. Kononova
e-mail: elena24936@yandex.ru

A. A. Akhobekov
Clinical Hospital Lapino, 1st Uspenskoe Highway 111, Moscow Region, 143081, Russia

O. E. Popovkina · D. O. Nadinskiy · V. V. Kucherov
A. Tsyb Medical Radiological Research Centre - branch of the National Medical Research Radiological Centre of the Ministry of Health of Russian Federation, 4 Koroleva Street, 249036 Obninsk, Russia
e-mail: popovkinaoe@mail.ru

D. O. Nadinskiy
e-mail: dr.nadinskiy@gmail.com

V. V. Kucherov
e-mail: v.v.kucherov@gmail.com

R. M. Steingart et al. (eds.), *Atlas of Imaging in Cardio-Oncology*, https://doi.org/10.1007/978-3-030-70998-3_25

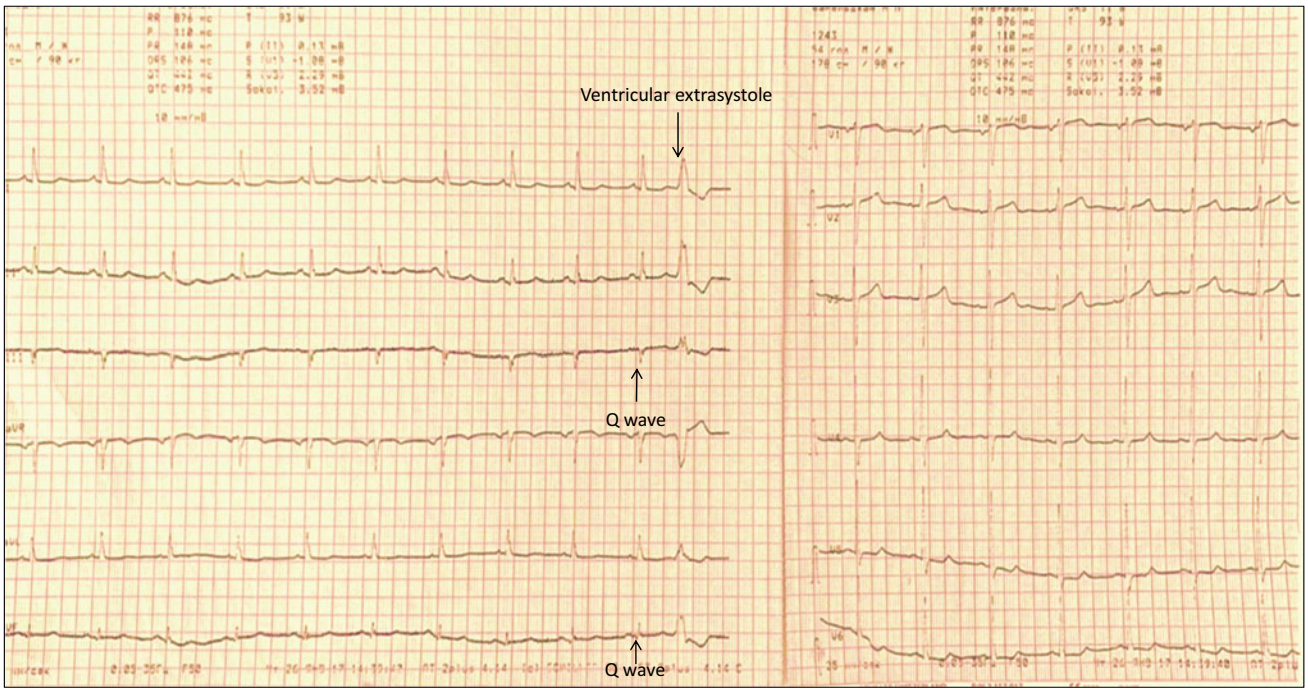

Fig. 25.1 EKG with inferior q wave. Ventricular extrasystole

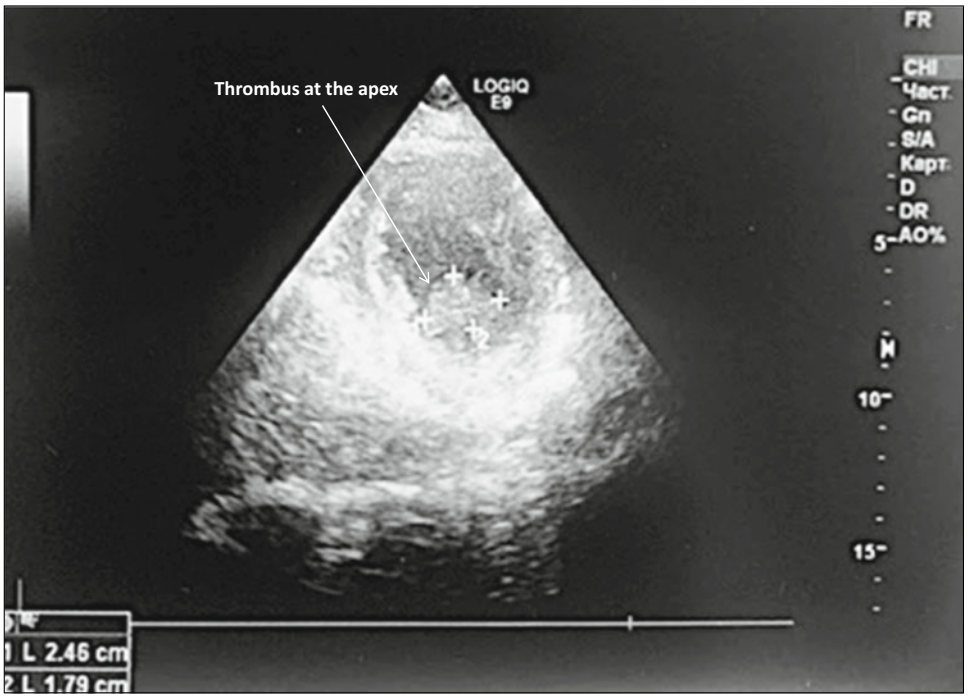

Fig. 25.2 Thrombus at the apex of the LV on transthoracic echocardiography

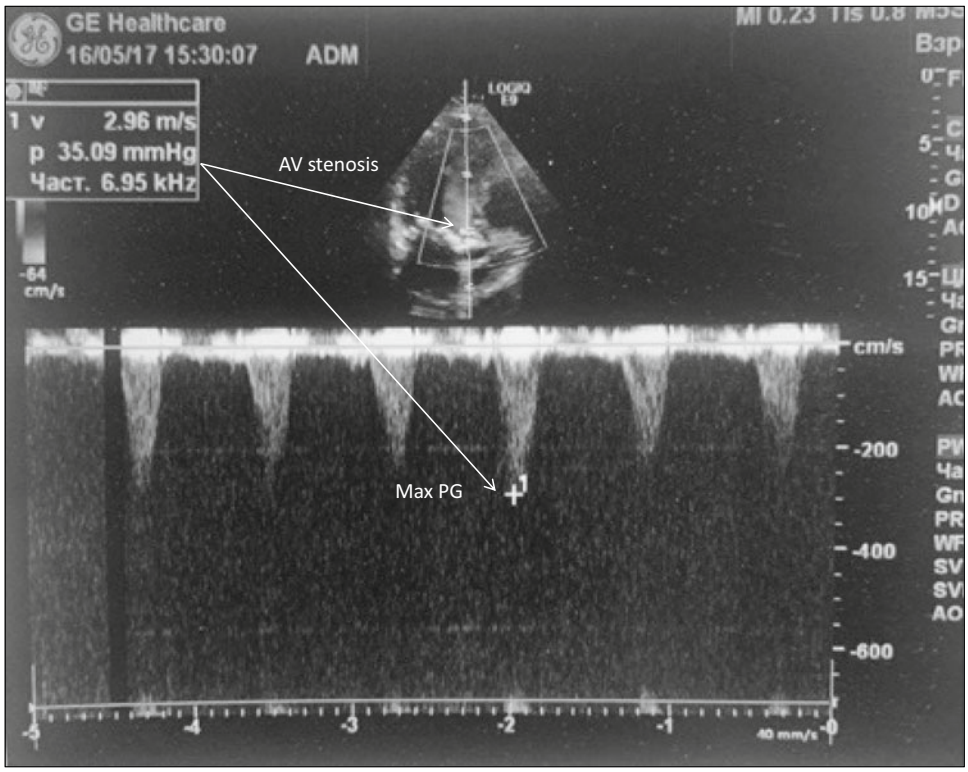

Fig. 25.3 Aortic stenosis on transthoracic echocardiography imaging and Doppler

Aortic regurgitation on color doppler transthoracic echocardiography .

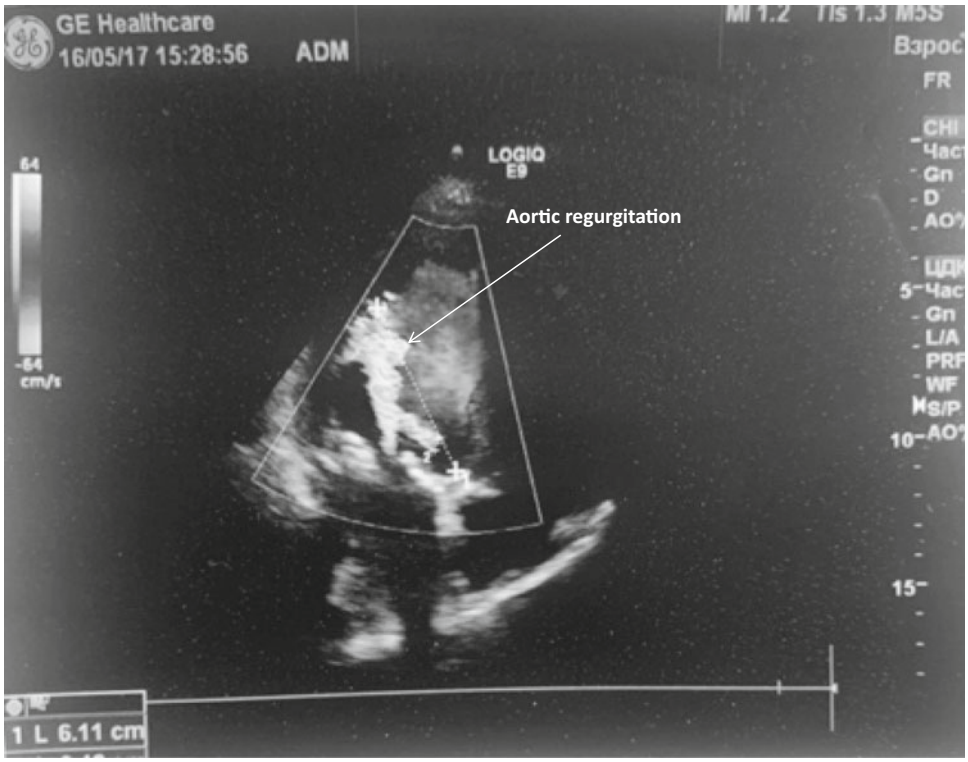

Fig. 25.4 Aortic insufficiency on color Doppler transthoracic echocardiography

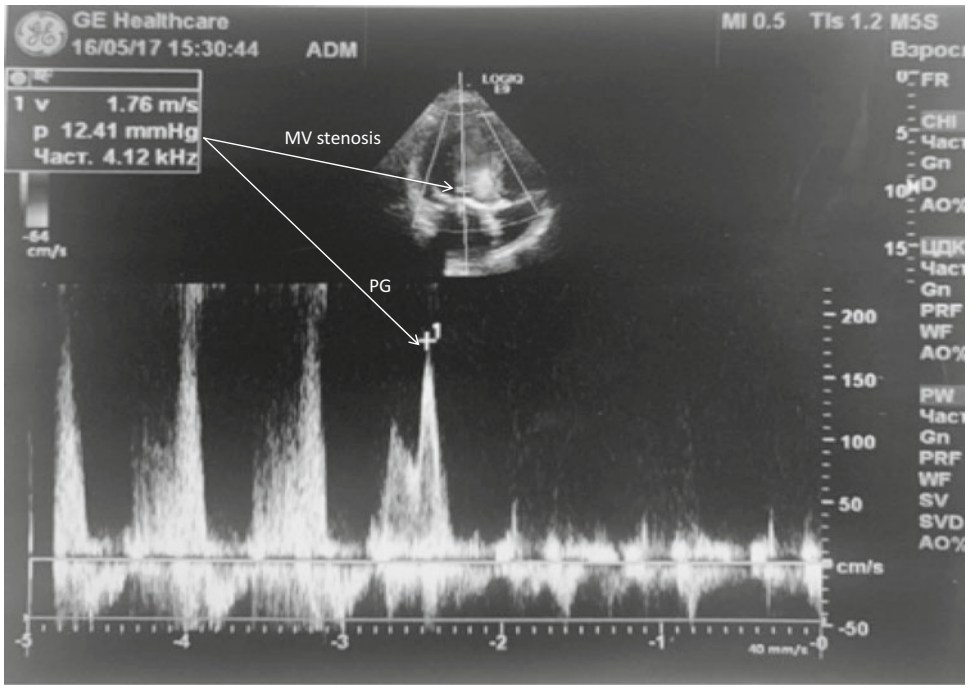

Fig. 25.5 Mitral stenosis. Transthoracic echocardiography

vessels. There was subtotal stenosis of the brachiocephalic trunk. Figs. 25.6, 25.7, 25.8 and 25.9; Videos 25.1, 25.2, 25.3 and 25.4.

Stenting of the brachiocephalic trunk was performed while stenting of the obtuse marginal branch and CX was attempted but unsuccessful.

The patient received guideline-directed optimal medical therapy for ischemic heart disease and heart failure, anticoagulation therapy for LV thrombus and significant improvement has been achieved. LVEF increased to 42%, and the degree of the mitral valve insufficiency decreased

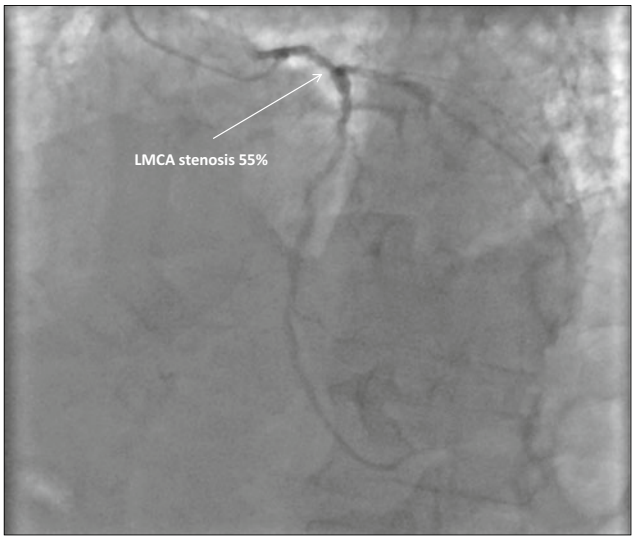

Fig. 25.6 LMCA stenosis 55%. Coronary angiography, LAO cranial view. LAO, Left anterior cranial oblique; LMCA, Left main coronary artery

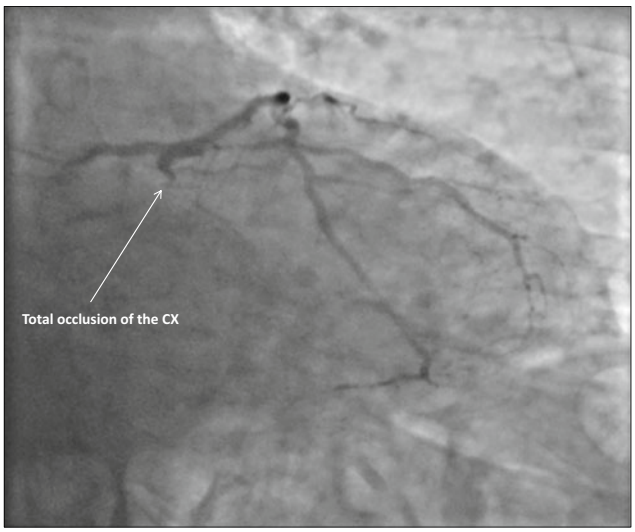

Fig. 25.7 Total occlusion of the CX. Obtuse marginal branch 1—subtotal stenosis. Coronary angiography, AP caudal view. AP caudal, Anterior–posterior caudal oblique; CX, Circumflex artery

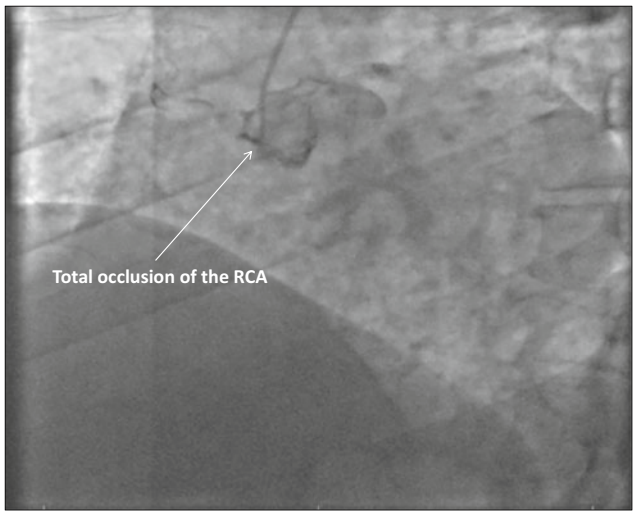

Fig. 25.8 Total occlusion of the RCA. Coronary angiography, LAO view. LAO, Left anterior oblique; RCA, Right coronary artery

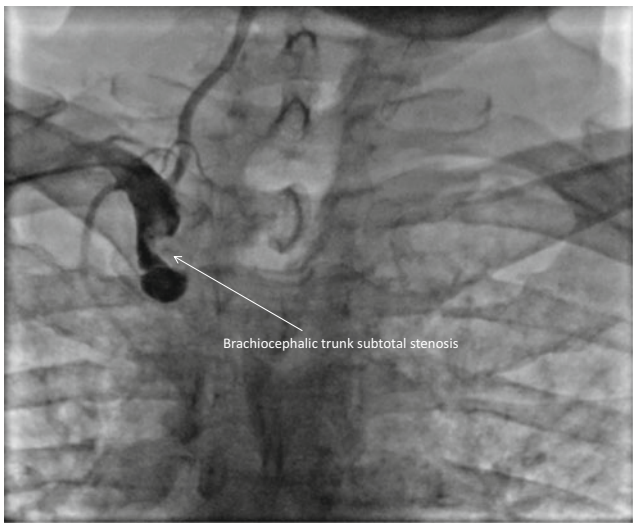

Fig. 25.9 Brachiocephalic trunk subtotal stenosis. Angiography

from 3+ to 2+; PA systolic pressure decreased from 50 to 41 mm Hg. A thrombus at the apex of the LV was resolved.

25.1.1 Discussion

This case illustrates an extreme degree of cardiac complications from chemotherapy and radiation for Hodgkin lymphoma becoming clinically manifest more than 20 years after the delivery of life-saving therapy. This patient had coronary artery disease, heart failure, myocardial infarction complicated by a thrombus at the apex of the LV, and damage to the aortic and mitral valves, and to the brachiocephalic artery.

It is possible but not clearly proven that earlier interventions in such a survivor using ACE inhibitors, ARBs, beta-blockers, statins, and antiplatelet drugs could prevent or at least delay the onset of these devastating complications. Too many survivors of childhood, adolescent or young adult cancers are "lost to follow up".

25.2 Case 2. Radiation Injury to the Carotid

A 55-year-old woman with the history of Hodgkin lymphoma underwent radiation therapy in 1991, including the mediastinal area and neck. She did have some risk factors for atherosclerosis—high blood pressure (BP) (max BP 210/100 mm Hg, regular home BP 140–150/90 mm Hg) and obesity (body mass index [BMI] is 35.1). She had no diabetes mellitus, never smoked, no family history of early heart disease, normal physical activity of daily living and acceptable level of total cholesterol of 5.23 mmol/l, low density lipoprotein levels (LDL) at 3.68 mmol/l, high density lipoprotein (HDL) at 1.2 mmol/l. Cardiovascular disease risk SCORE was 1–2%.

In 2006, she suffered a left-sided stroke and in 2012 had undergone stenting of a left-sided 75% stenosis of the internal carotid artery. Since that time she was treated with losartan 50 mg per day and 100 mg acetylsalicylic acid per day.

In 2016, a routine follow-up echocardiogram revealed mild aortic stenosis and regurgitation. In May of 2020 the patient underwent routine cardiology assessment prior to mastectomy for breast cancer. She complained of dyspnea during moderate physical exertion, more pronounced in the cold.

Duplex ultrasound demonstrated 45% stenosis of the subclavian artery, 25–30% stenosis in the stented internal coronary artery (ICA) (Figs. 25.10 and 25.11). Her ECG

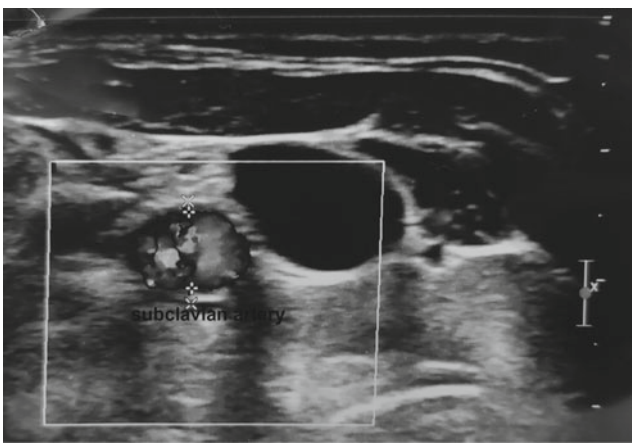

Fig. 25.10 Duplex ultrasound. 45% stenosis of the subclavian artery

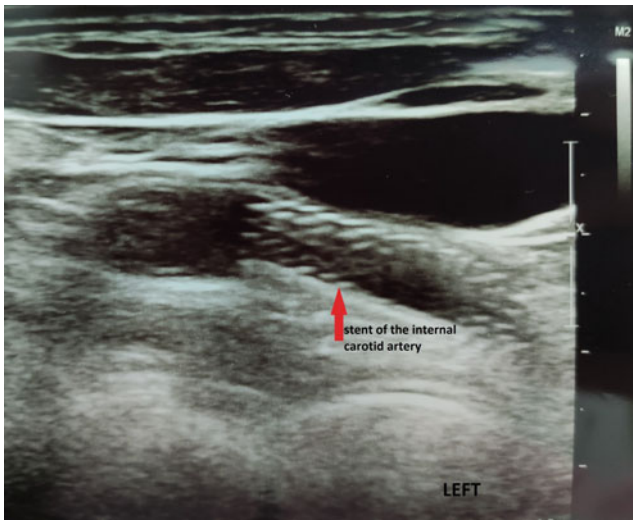

Fig. 25.11 Duplex ultrasound. 25–30% stenosis in the stented internal carotid artery

showed sinus rhythm with heart rate of 65 bpm, voltage criteria of left ventricular hypertrophy with secondary ST-T changes in left-sided leads. Echocardiogram reported normal ejection fraction of 64% (Simpson), normal local contractility, and previous aortic flow changes. Pre-test probability of obstructive coronary artery disease using standard criteria was only 9% [5], but due to the mediastinal radiation therapy almost 30 years ago an exercise electrocardiogram was performed to help assess the operative risk given her symptoms of dyspnea.

The exercise ECG revealed asymptomatic horizontal ST segment depression in leads II, III, aVF, V5-6 up to 1.5 mm at the first stage of Bruce protocol exercise test continued till 8 min at rest. BP response was normal (Fig. 25.12). This result was followed up with invasive angiography of the coronary arteries which revealed only minimal signs of atherosclerosis (Videos 25.5 and 25.6). One could have argued that for this symptomatic woman with hypertension, maybe LVH on EKG and low-to-intermediate pre-test probability of CAD, an imaging stress test was indicated rather than an EKG stress test. However, one of the problems in managing cancer survivors exposed to significant radiation is the often nonspecific nature of their symptoms, poor exercise tolerance and frankly imprecise methods by which to estimate their pre-test likelihood for CAD (5–7).

The patient was treated with azilsartan medoxomil/chlorthalidone 40/12,5 mg, bisoprolol 5 mg, amlodipine 5 mg, acetylsalicylic acid 75 mg, atorvastatin 40 mg. The BP decreased to normal values, the dyspnea disappeared and targeted values of LDL-C have been reached. Mastectomy was performed successfully.

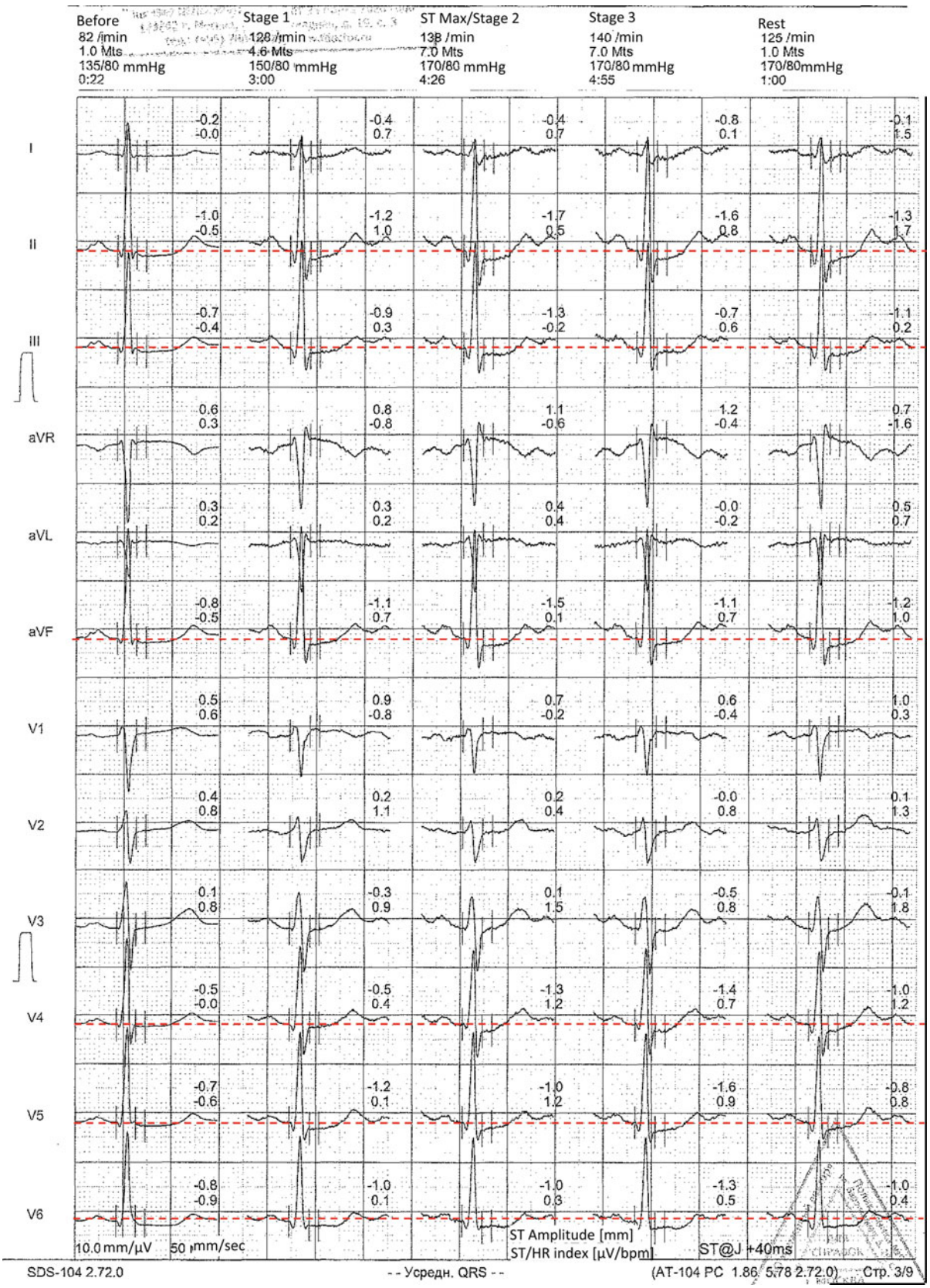

Fig. 25.12 The exercise ECG. Horizontal depression of the ST segment in leads II, III, aVF, V5-6 up to 1.5 mm from the first stage of the load up to 8 min of the rest

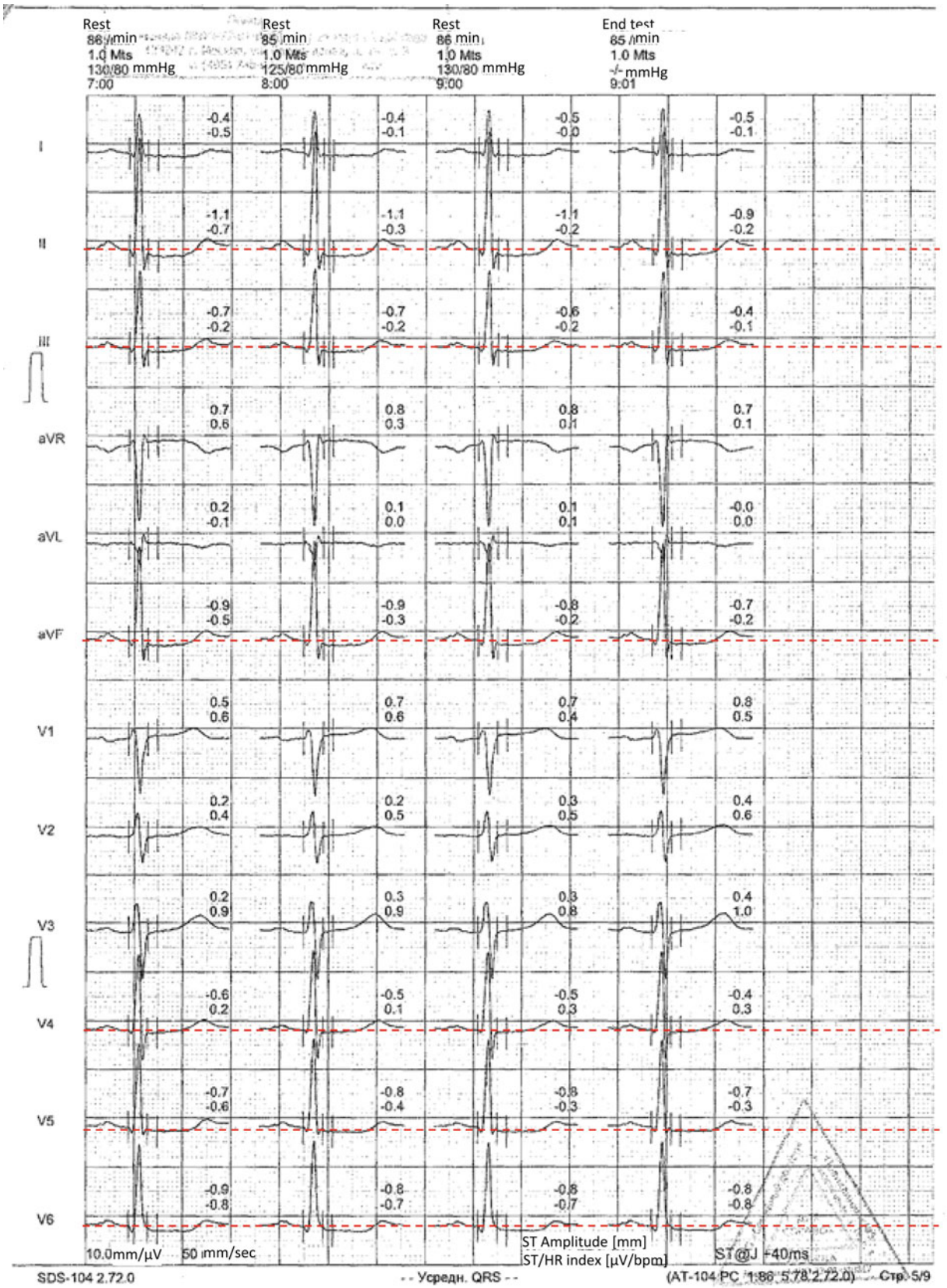

Fig. 25.12 (continued)

References

1. Liljegren G, Holmberg L, Bergh J, Lindgren A, et al. 10-Year results after sector resection with or without postoperative radiotherapy for stage I breast cancer: a randomized trial. J Clin Oncol. 1999;17(8):2326–9. https://doi.org/10.1200/JCO.1999.17.8.2326.PMID2326-2326.
2. Jaworski C, Mariani JA, Wheeler G, Kaye DM. Cardiac complications of thoracic irradiation. J Am Coll Cardiol. 2013;61:2319–28. https://doi.org/10.1016/j.jacc.2013.01.090.PMID24762470.
3. van Nimwegen FA, Schaapveld M, Janus CP, et al. Cardiovascular disease after Hodgkin lymphoma treatment: 40-year disease risk. JAMA Intern Med. 2015;175:1007–17. https://doi.org/10.1001/jamainternmed.2015.1180 PMID: 25915855.
4. Mousavi N, Nohria A. Radiation-induced cardiovascular disease. Curr Treat Options Cardiovasc Med. 2013;15:507–17. https://doi.org/10.1007/s11936-013-0259-0.
5. Diamond GA, Forrester JS. Analysis of probability as an aid in the clinical diagnosis of coronary-artery disease. N Engl J Med. 1979;300(24):1350–8. https://doi.org/10.1056/NEJM197906143002402 PMID: 440357.
6. Daniëls LA, Krol AD, de Graaf MA, Scholte AJ, Van't Veer MB, Putter H, et al. Screening for coronary artery disease after mediastinal irradiation in Hodgkin lymphoma survivors: phase II study of indication and acceptance. Ann Oncol. 2014;25(6):1198–203. https://doi.org/10.1093/annonc/mdu130 Epub 2014 Mar 31 PMID: 24692582.
7. Heidenreich PA, Schnittger I, Strauss HW, Vagelos RH, Lee BK, Mariscal CS, et al. Screening for coronary artery disease after mediastinal irradiation for Hodgkin's disease. J Clin Oncol. 2007;25(1):43–9. https://doi.org/10.1200/JCO.2006.07.0805.Erratum.In:JClinOncol.2007Apr20;25(12):1635 PMID: 17194904.

Cardiac Constriction and Restriction After Chest Radiotherapy for Hodgkin's Lymphoma and Breast Cancer

26

Marina V. Vitsenya, Alexandra V. Potekhina, and Jennifer E. Liu

Key Points

- Mediastinal irradiation can potentially affect all structures within the radiation field. Patients with radiation-induced heart disease (RIHD) may manifest inflammation, fibrosis, and calcification in varying degrees involving the pericardium, myocardium, great vessels, valves, coronary arteries, lungs, and diaphragm [1].
- Constrictive pericarditis can occur years after mediastinal radiotherapy. Although pericardiectomy is the definitive treatment, the short- and long-term post-surgical outcome is poor given the coexistence of other radiation-induced abnormalities such as premature coronary artery disease, valvular disease, and restrictive cardiomyopathy, as well as radiation-induced lung damage.
- Most patients with radiation-induced constrictive pericarditis will also have restrictive physiology as a result of radiation-induced myocardial fibrosis. Constrictive pericarditis and restrictive cardiomyopathy can be difficult to differentiate in patients with RIHD given their similar clinical presentations.
- Determining the predominant pathology of the clinical presentation is essential as treatment is different for each cardiac abnormality. Non-invasive multimodality imaging plays a major role in the evaluation of cardiac constriction and restriction in patients with RIHD.
- Standardized surveillance and screening have not been established given the protracted time course and the heterogeneity of the presentation among different individuals. Until further data become available, diligent assessment with follow-up testing dictated by patient risk profile and clinical suspicion is the best practice for the evaluation of the late cardiovascular (CV) effects of radiation.

A 51-year-old woman who was diagnosed with Hodgkin's lymphoma at age 26 (1995) and treated at that time with anthracycline-containing chemotherapy and radiation therapy to the chest, paraportal region and spleen (treatment doses not available). In 2011, she was diagnosed with synchronous bilateral T1N0M0 HER2 positive breast cancer. A single-stage bilateral mastectomy was performed, followed by the administration of adjuvant chemotherapy with paclitaxel and sequential targeted therapy with trastuzumab. The patient was asymptomatic until 2012 when palpitations and shortness of breath during exercise appeared. She underwent an echocardiogram which revealed normal-sized cardiac chambers with moderately decreased left ventricular ejection fraction (LVEF 40%) and mild pericardial effusion. Chest X-ray demonstrated pulmonary venous congestion and bilateral moderate hydrothorax. She was initiated on heart failure treatment, including beta blocker, angiotensin-converting enzyme inhibitor (ACEI), and diuretic therapy, which improved her symptoms. Trastuzumab was discontinued and replaced with an aromatase inhibitor.

Patient was lost to medical follow-up until 2018 when she presented with decompensated heart failure requiring hospital admission. Her NT-proBNP was 1764 pg/ml and 6-min walk distance was 166 m. She was also noted to have chronic kidney disease, stage 3b/4. Computed tomography scan of the lungs demonstrated post-radiation lung fibrosis as well as pericardial thickening, calcification of the coronary arteries, and aortic root (Fig. 26.1).

Electronic supplementary material
The online version of this chapter (https://doi.org/10.1007/978-3-030-70998-3_26) contains supplementary material, which is available to authorized users.

M. V. Vitsenya (✉) · A. V. Potekhina
National Medical Research Center of Cardiology, Russian Ministry of Health, Moscow, Russia
e-mail: marinavitsenya@gmail.com

A. V. Potekhina
e-mail: potehina@gmail.com

J. E. Liu
Department of Medicine, Memorial Sloan Kettering Cancer Center, New York, NY 10065, USA
e-mail: liuj1234@mskcc.org

R. M. Steingart et al. (eds.), *Atlas of Imaging in Cardio-Oncology*,
https://doi.org/10.1007/978-3-030-70998-3_26

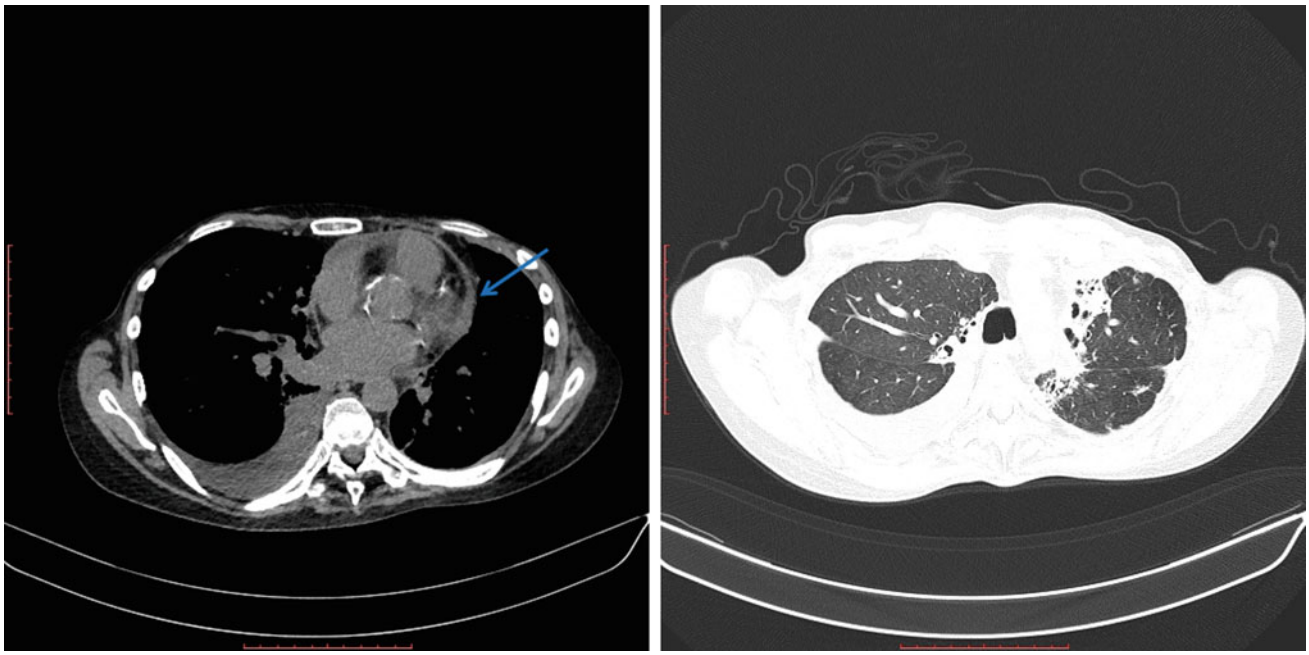

Fig. 26.1 Lung CT scans (Nov 2018) demonstrating post-radiation fibrosis - fibroatelectasis in the paramediastinal parts of lungs, traction bronchiectasis in the upper and middle lobes, lost volume of the left lung and right-sided hydrothorax (right panel), pericardial thickening (left panel, arrow), calcification of the coronary arteries and aortic root

Given her complex medical condition, she was transferred to Russian National Medical Research Center of Cardiology for further care. Due to her prior mastectomy and lung disease, the quality of her echocardiogram was technically difficult but the study showed normal-sized heart chambers and mildly reduced LVEF (46%) with a calculated cardiac index of 1.8 l/min/m2 and pulmonary artery systolic pressure (PASP) of 57 mm Hg. It also showed increased central venous pressure (plethoric inferior vena cava), aortic and mitral valve calcification with moderate regurgitations, and pericardial thickening with signs of both constrictive and restrictive heart disease (Videos 26.1 and 26.2; Figs. 26.1, 26.2 and 26.3). Cardiac MRI was not performed due to patient's claustrophobia. She was consulted by a multidisciplinary heart team to discuss the need for catheterization and the risk/benefit of possible pericardiectomy. The patient was deemed to be at very high risk for surgical treatment due to her chronic kidney disease, other radiation-induced heart diseases including heart failure with restrictive physiology, and post-radiation lung damage. A decision was made to continue medical treatment with loop diuretics, beta-blockers, and ACE inhibitors, which required careful titration due to systemic hypotension. During 15 months of follow-up, there was a slight improvement in exercise tolerance (6-MWD increased to 285 m) with no further hospitalization for heart failure exacerbation. The patient remained clinically stable in NYHA class II-III on medical management with carvedilol, fosinopril, furosemide, and rosuvastatin.

Pericardial disease is a frequent manifestation of RIHD. Acute pericarditis can occur early during treatment, which is generally benign and extremely rare with modern radiation techniques. Chronic, delayed pericardial effusion with and without constriction can occur in up to 20% of patients, frequently many years after treatment. Chronic pericardial inflammation causes fibrous thickening of the pericardium. The parietal surface is generally more damaged with replacement of pericardial fat by collagen. Constrictive pericarditis can present 10 or more years after mediastinal radiotherapy due to the development of a fibrotic and calcified pericardial sac. The clinical manifestation of constrictive pericarditis can range from a few non-specific symptoms to clinical heart failure. Medical management includes diuretics and beta blockers, though pericardiectomy

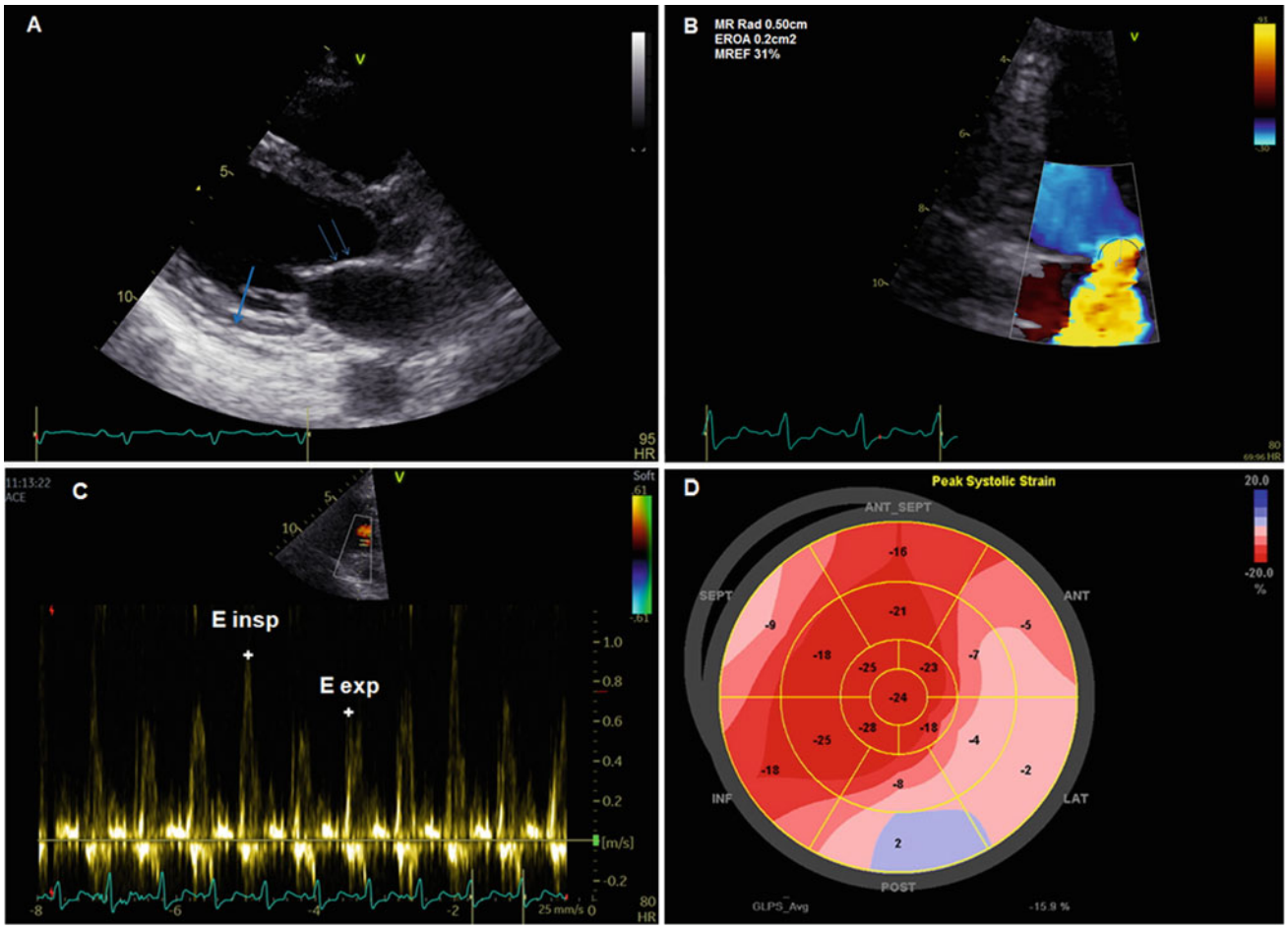

Fig. 26.2 **a** Parasternal long axis view demonstrating thickening of the pericardium (single arrow), normal-sized left ventricular chamber, mitral valve (MV) thickening (double arrow). **b** Moderate mitral regurgitation (regurgitant fraction of 31%). C. PW Doppler of the tricuspid inflow velocity with respiratory variation (>40%). D. Longitudinal strain depicted in bull's-eye map showing markedly reduced strain in the posterior LV wall with lesser reduction in the other segments

is the definitive treatment. However, patients with radiation-related constrictive pericarditis have worse early and late outcomes after pericardiectomy as compared to patients with idiopathic or infectious pericarditis due to the coexistence of other radiation-related cardiac lesions, including restrictive cardiomyopathy, premature coronary artery disease, and valvular disease, as well as post-radiation lung disease [2]. The predictors of poor overall survival after pericardiectomy include prior radiation, worse renal function, higher PASP, and abnormal left ventricular systolic function [3, 4].

Most patients with radiation-induced heart disease will have some degree of restrictive physiology due to the radiation-induced myocardial fibrosis which is commonly seen in autopsy series. Myocardial fibrosis can result in a wide spectrum of myocardial dysfunction ranging from asymptomatic mild diastolic dysfunction to severe restrictive filling with overt heart failure. Myocardial fibrosis is typically diffuse as a result of radiation-induced microvascular injury causing chronic ischemia in the myocardium and replacement of myocytes with fibrosis. It typically follows a restrictive cardiomyopathy phenotype with normal or low normal LVEF; however, regional wall motion abnormalities can be observed in the setting of concurrent radiation-induced coronary artery disease.

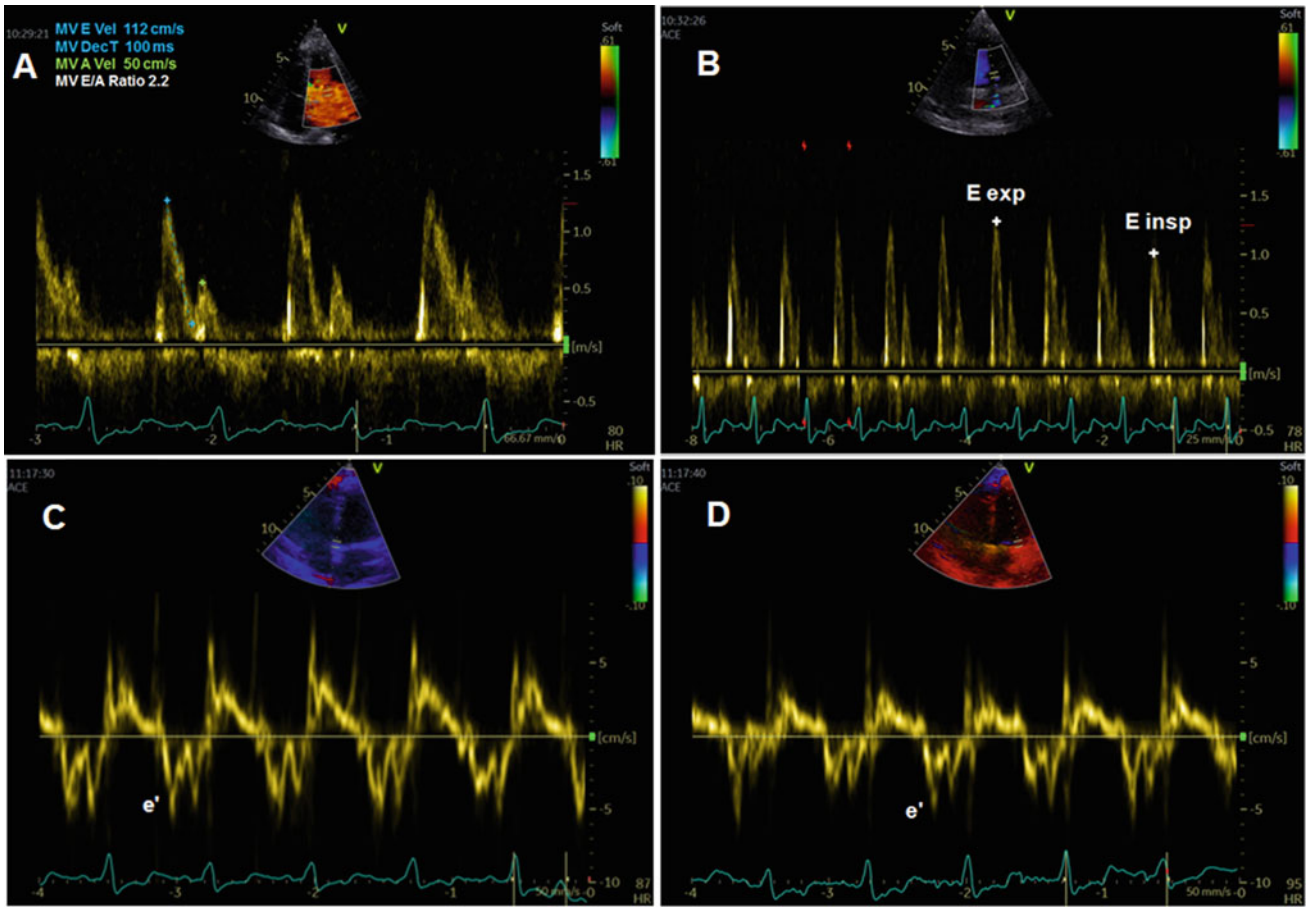

Fig. 26.3 **a** Doppler of the mitral inflow demonstrating E/A ratio 2.2 and MV deceleration time of 100 ms. **b** Mitral inflow velocity with respiratory variation of 15%. C, D. Doppler tissue imaging of medial (**c**) and lateral (**d**) e' velocity of 5 cm/s. The low annular velocities with increased E/e' of 20 are suggestive for concomitant restrictive cardiomyopathy which could explain the absence of annular reverses and less prominent mitral E inflow respiratory variation (<25%) in this patient with mixed cardiac pathology

Depressed LVEF with normal or dilated LV can occur when radiotherapy is co-administered with cardiotoxic chemotherapeutic agents such as anthracyclines or with high doses of radiation. Patients with radiation-induced myocardial fibrosis often present with impaired exercise capacity with chronic tachycardia while clinical heart failure is less frequent.

Multimodality imaging plays a major role in the evaluation of constrictive pericarditis and restrictive cardiomyopathy in RIHD. Differentiating the pathophysiology associated with each clinical entity can be challenging as they often coexist and share similar clinical presentations. However, determining which pathology dominates is essential given that treatment is different for each condition. Various imaging techniques can be utilized to identify key features for evaluation such as cardiac remodeling on echo and MRI, abnormal myocardial velocities and function on echo, pericardial pathology on CT and cMRI, and features of

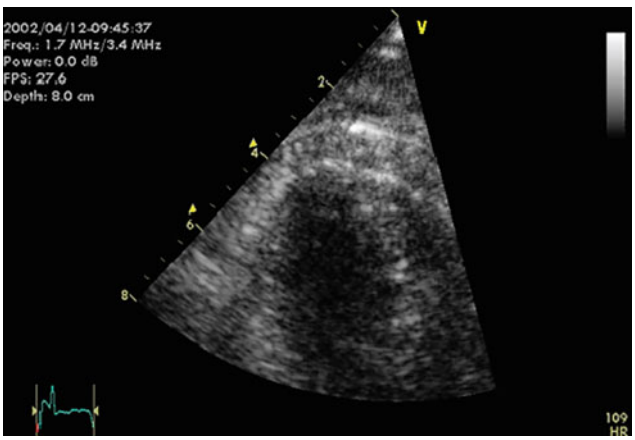

Fig. 26.4 Pericardial pathology in constrictive pericarditis. Common findings are fibrinous exudate and pericardial fibrosis that replace adipose tissue (arrow). Parietal pericardium is more involved than visceral pericardium

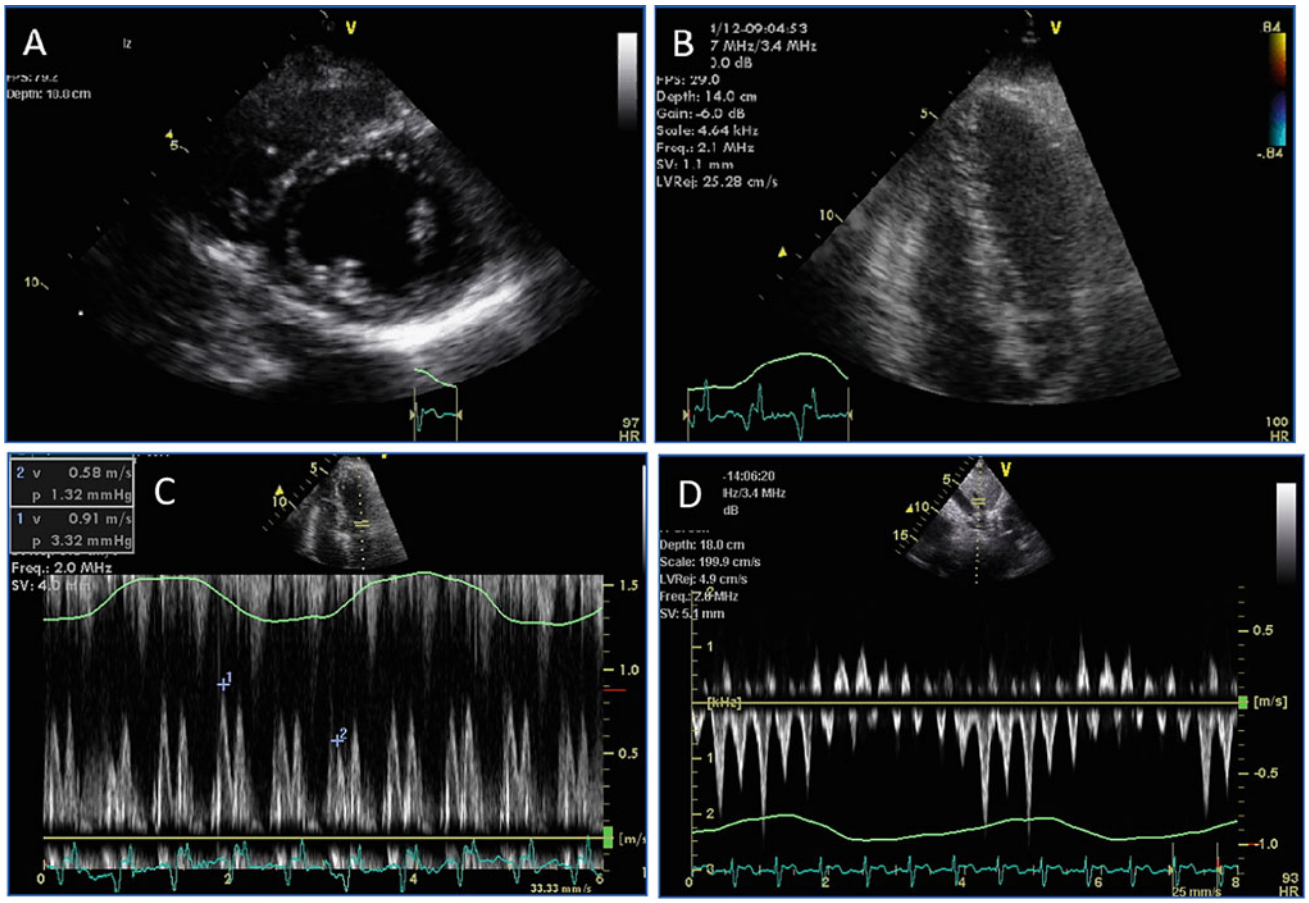

Fig. 26.5 Hemodynamics of constrictive pericarditis as a result of the dissociation of the intrathoracic and intracardiac pressures and exaggerated ventricular interdependence in diastolic filling. **a** Parasternal short axis view showing prominent septal bounce (see Video 26.3 left panel). **b** Apical 4 chamber view showing interventricular dependence and respirophasic variation of the interventricular septal motion (see Video 26.3 right panel). **c** Respirophasic variation of the transmitral inflow velocities with increase on expiration and decrease on inspiration. **d** Doppler of the hepatic venous flow with increase in flow reversal on expiration

constrictive physiology on echo and cMRI. But despite the armamentarium of imaging tests available, the diagnosis can still be elusive as patients with radiation-induced heart disease are often difficult to image due to chest wall deformities, lung disease, or breast prosthesis. Additional echo images illustrating radiation-induced constrictive pericarditis and restrictive cardiomyopathy are shown in Figs. 26.4, 26.5 and 26.6 and Videos 26.3 and 26.4.

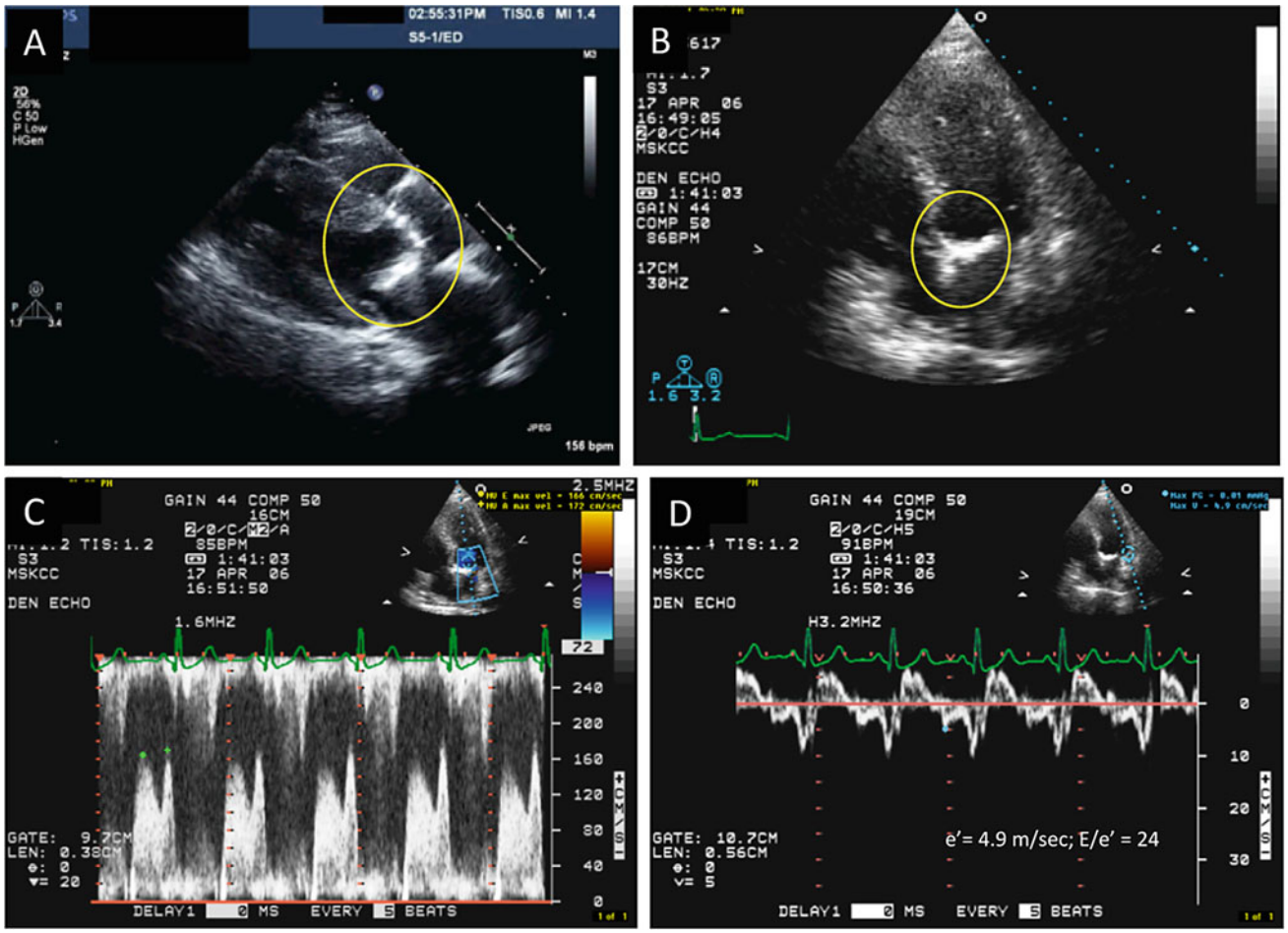

Fig. 26.6 Echo phenotype of radiation induced restrictive cardiomyopathy. **a** and **b** Small LV cavity size with low diastolic volume and low stroke volume (see Video 26.4). Other radiation induced cardiac abnormalities such as valvular disease often coexist as shown. **c** Pulsed wave Doppler of the mitral valve. **d** Tissue Doppler of the mitral annulus with low annular velocity. Increased E/e' suggestive of impaired LV compliance with elevated filling pressure is consistent with moderate diastolic dysfunction

References

1. Yusuf SW, Sami S, Daher IN. Radiation-induced heart disease: a clinical update. Cardiol Res Pract. 2011;2011:1–9.
2. Lancellotti P, Nkomo VT, Badano LP, et al. European Society of Cardiology Working Groups on Nuclear Cardiology and Cardiac Computed Tomography and Cardiovascular Magnetic Resonance, American Society of Nuclear Cardiology, Society for Cardiovascular Magnetic Resonance, Society of Cardiovascular Computed Tomography. Expert consensus formulti-modality imaging evaluation of cardiovascular complications of radiotherapy in adults: a report from the European Association of Cardiovascular Imaging and the American Society of Echocardiography. Eur Heart J Cardiovasc Imaging. 2013;14:721–40.
3. Bertog SC, Thambidorai SK, Parakh K, Schoenhagen P, Ozduran V, Houghtaling PL, Lytle BW, Blackstone EH, Lauer MS, Klein AL. Constrictive pericarditis: etiology and cause-specific survival after pericardiectomy. J Am Coll Cardiol. 2004;43(8):1445–52. https://doi.org/10.1016/j.jacc.2003.11.048.
4. Adler Y, Charron P, Imazio M, et al. European Society of Cardiology. 2015 ESC guidelines for the diagnosis and management of pericardial diseases: the task force for the diagnosis and management of pericardial diseases of the European Society of Cardiology (ESC). Endorsed by: the European Association for Cardio-Thoracic Surgery (EACTS). Eur Heart J. 2015;36:2921–64.

27 Onset of Heart Failure After Anthracycline Therapy in the Adult: Treatment and Expectations for Recovery

Marina V. Vitsenya, Alexandra V. Potekhina, and Olga V. Stukalova

Key Points

- High-dose anthracycline (AC) treatment and comorbid cardiovascular (CV) disease are well-known risk factors for AC-related cardiomyopathy. But cardiac dysfunction can develop after lower-dose AC treatment, particularly
  - if accompanied by radiotherapy where the heart is in the treatment field
  - in the presence of multiple CV risk factors
  - with sequential therapy with trastuzumab [1].
- AC-induced left ventricular (LV) dysfunction may be partially or completely restored during promptly initiated modern heart failure (HF) treatment, which is largely determined by the time elapsed from the end of chemotherapy [2].

27.1 Case Presentation

A 55-year-old woman underwent left mastectomy, adjuvant AC-based chemotherapy, radiotherapy, and hormonal therapy for breast cancer (cT1cN0M0, IA, RE 8, RP 8, HER2-negative) in 2017. Despite low preexisting cardiovascular risks (no hypertension, diabetes, smoking, body mass index 20 kg/m^2) she met criteria to be considered at some increased risk for developing cardiac dysfunction (lower-dose doxorubicin treatment 240 mg/m^2 in combination with left-sided radiotherapy). Echocardiogram before starting treatment reported as normal with ejection fraction (EF) 60%.

Fatigue, shortness of breath, and palpitations developed in April 2018. She was admitted to a local hospital in July 2018 with pulmonary edema, systemic hypotension, and sinus tachycardia. Echocardiography was reported to show diffuse left ventricular (LV) hypokinesis, EF 26%, moderately enlarged left-sided chambers, and moderate pulmonary hypertension. Coronary angiography revealed normal native coronary arteries. After recovery from this episode initial HF treatment was continued (metoprolol succinate, spironolactone).

She was referred to a cardio oncology center in Moscow in October 2018-NYHA Class III, blood pressure 90/60 mm Hg, HR 100 bpm, EF 19%, global longitudinal strain (GLS) _Avg -4.5%, severe left chamber enlargement (iLVEDV 88 ml/m^2), apical LV thrombosis, grade 3 diastolic dysfunction (MV E/A 3.3, E/e' 18), TR Vel 3.5 m/s (Figs. 27.1 and 27.2, Video 27.1). HF therapy was optimized and anticoagulation begun (metoprolol succinate, spironolactone, ivabradine, candesartan, warfarin).

November 2018-NYHA Class II, blood pressure 100/70 mm Hg, HR 90 bpm, EF 27%,GLS_Avg −8.0% (Fig. 27.3). Cardiac MRI demonstrated diffuse hypokinesis, EF 24%, no evidence of scarring or myocardial infiltration, no left ventricular thrombosis (Fig. 27.4, Video 27.2).

Candesartan was switched to sacubitril/valsartan (S/V).

Between November 2018 and May 2019, the therapy was gradually titrated with the escalation of S/V and de-escalation of ivabradine, and warfarin was discontinued.

May 2019 (S/V 400 mg, metoprolol succinate 25 mg per day, spironolactone 25, ivabradine 5)—NYHA Class I, blood pressure100/60 mm Hg, HR 52 bpm, EF 53%, GLS_Avg −16.9%, normal-sized left chambers (iLVEDV 54 ml/m^2), significant improvement in diastolic function

Electronic supplementary material
The online version of this chapter (https://doi.org/10.1007/978-3-030-70998-3_27) contains supplementary material, which is available to authorized users.

M. V. Vitsenya (✉) · A. V. Potekhina · O. V. Stukalova
National Medical Research Center of Cardiology, Russian Ministry of Health, Moscow, Russia
e-mail: marinavitsenya@gmail.com

A. V. Potekhina
e-mail: potehina@gmail.com

O. V. Stukalova
e-mail: olgastukalova@mail.ru

R. M. Steingart et al. (eds.), *Atlas of Imaging in Cardio-Oncology*,
https://doi.org/10.1007/978-3-030-70998-3_27

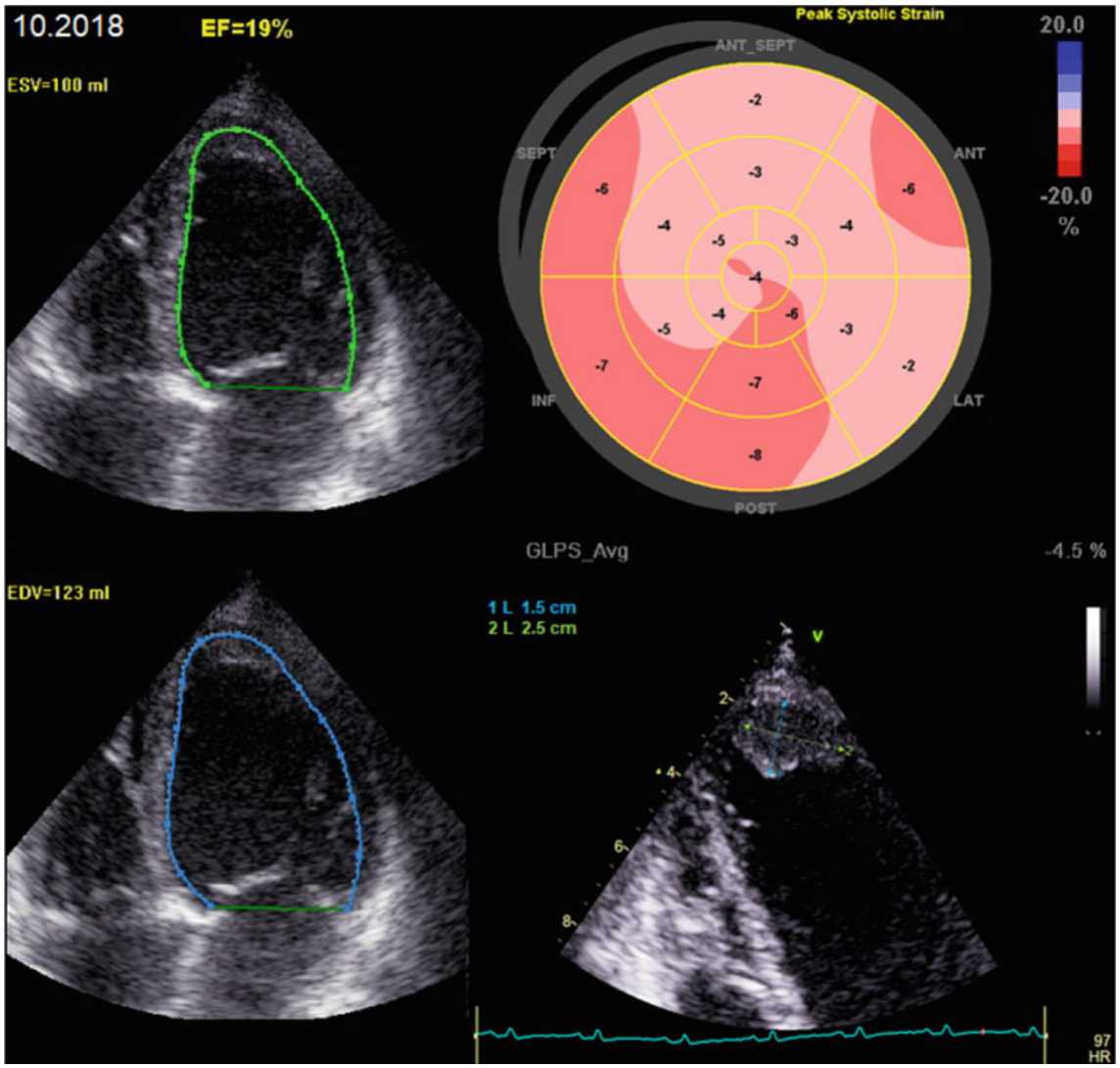

Fig. 27.1 Left panel: LVESV and LVEDV acquired from apical four chamber view during biplane evaluation demonstrating severe LV enlargement (iLVEDV 88 ml/m2) and LVEF reduction (19%) in October 2018. Right panel: Top—From that same evaluation, longitudinal echocardiography strain depicted in bull's-eye map showing diffuse reduction of strain (GLS_Av −4.5%). Bottom—LV apical thrombosis (marker)

(MV E/A 0.74, E/e' 6), TR Vel 2.4 m/s (Figs. 27.2 and 27.3, Video 27.3). Cardiac MRI confirmed cardiac functional improvement, EF 52% (Video 27.2).

The patient remains in NYHA Class I to the current day maintained on S/V 400 mg and metoprolol succinate 37.5 mg per day. Ventricular function remains in the mildly abnormal range (LVEF 50–52%).

27.2 Discussion

Since there are no controlled studies of specific medical approaches for HF associated with anticancer therapy, treatment of these patients follows generally accepted guidelines for therapy that was developed for HF caused by hypertensive or ischemic heart disease [3, 4]. This case illustrates several important points. HF can develop with relatively low doses of anthracyclines in patients without cardiovascular risk factors, particularly if the heart is exposed to radiation during or after the course of therapy [1]. Second, the timing of the onset of HF is variable. The cardiotoxicity of anthracyclines may be acute, early, or late. Acute toxicity, predominantly supraventricular arrhythmia, transient LV dysfunction, and electrocardiographic changes develop in 1% of patients immediately after infusion and is usually reversible; early-onset chronic, developing within 1 year, usually presenting as a dilated cardiomyopathy leading to HF; late-onset chronic, developing years, or even

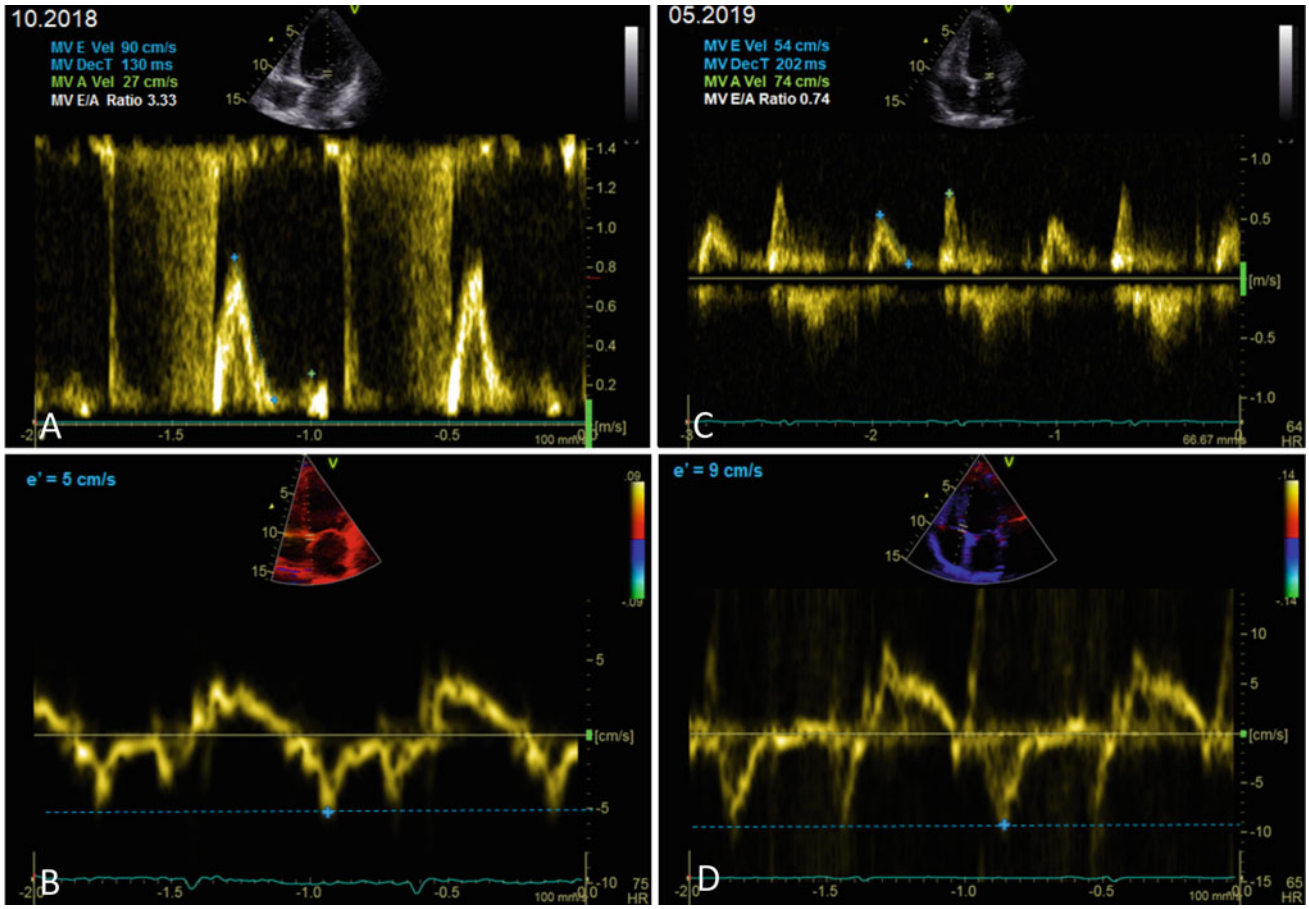

Fig. 27.2 Severe diastolic dysfunction in October 2018 with echo Doppler findings consistent with grade III diastolic dysfunction as characterized by high LV filling pressure with restrictive filling pattern. **a** Pulsed wave Doppler of mitral inflow with mitral E/A ratio of 3.3 and deceleration time of 130 ms. **b** Tissue doppler imaging of the mitral annulus with e' velocity of 5 cm/s E/e' of 18. Significant improvement of diastolic function in May 2019 with mitral E/A ratio 0.74 (**c**) and e' velocity 9 cm/s with E/e' ratio of 6 consistent with normal LV filling pressure (**d**)

decades, after the end of chemotherapy [4]. However, this classification has been challenged because rigorous monitoring during and after anthracycline therapy paints a different picture. Cardiotoxicity occurred in 9% of adults treated with anthracyclines, and its highest incidence (98%) was observed during the first year after the completion of chemotherapy [5]. Many affected patients may initially be asymptomatic, with clinical manifestations appearing only years later, often in the context of other triggering factors, indicating that anthracyclines may negatively affect compensatory mechanisms to cardiovascular stressors. But the current patient presented with HF well after the completion of therapy, with no clear additional precipitants such as sepsis, arrhythmia, or myocardial infarction.

And importantly, contrary to earlier teaching, AC-related HF can in fact be reversible, particularly if recognized soon after onset. The current patient responded very well to modern therapies including ivabradine and sacubitril/valsartan. It is important to again emphasize that careful surveillance of patients during and after treatment is required as LVEF recovery and cardiac event reduction may be achieved when cardiac dysfunction is detected early (<6 months from the end of chemotherapy) and modern HF treatment is promptly initiated [2, 5].

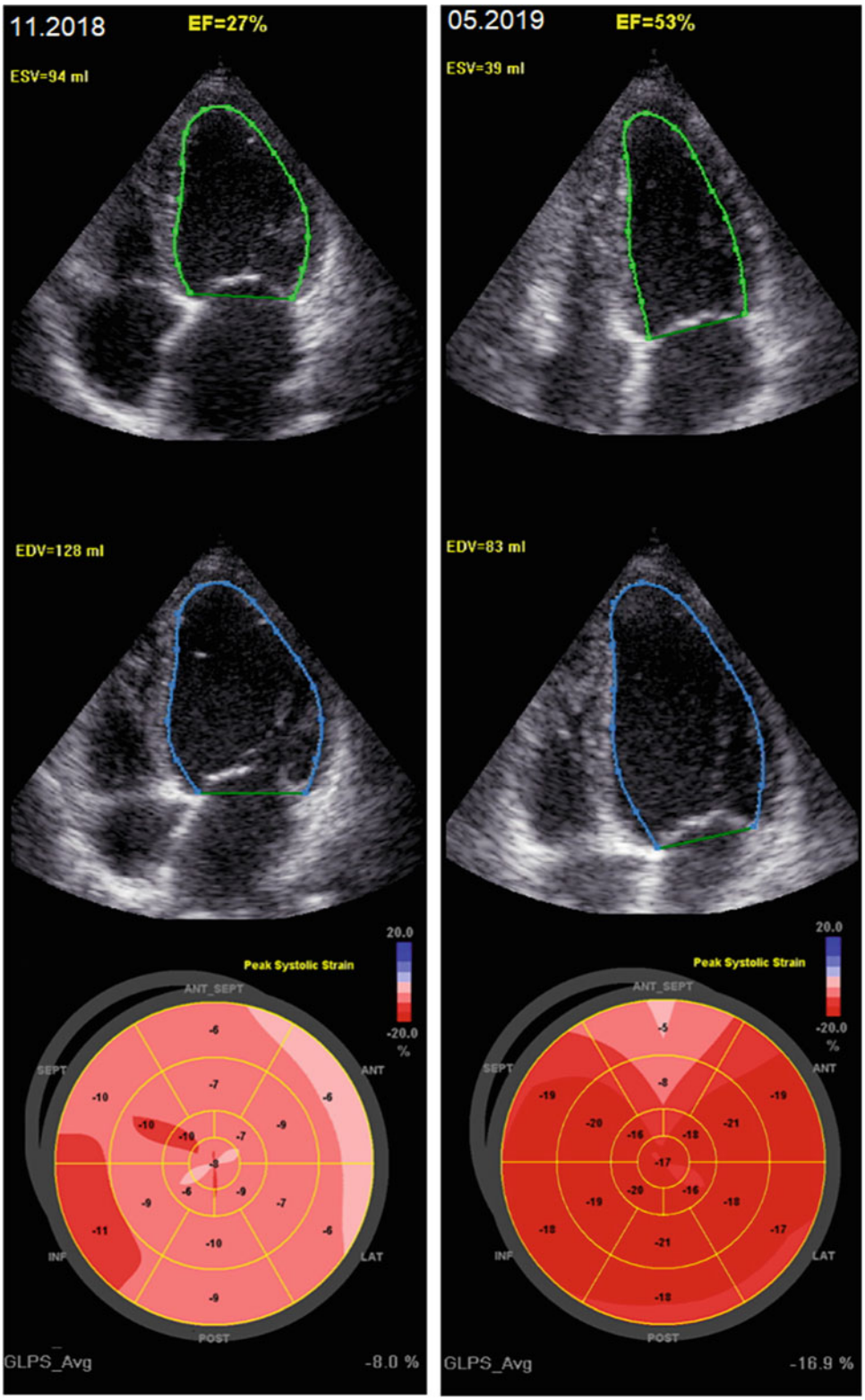

Fig. 27.3 Left panel: LV volumes and bull's-eye mapping of strain demonstrating partial improvement in LV systolic function (EF 27%) and strain values (GLS_Av −8.0%) in November 2018. Right panel: LV volumes and bull's-eye mapping of LS showing recovery of cardiac function in May 2019—iLVEDV 54 ml/m^2, EF = 53%, GLS_Av −16.9%

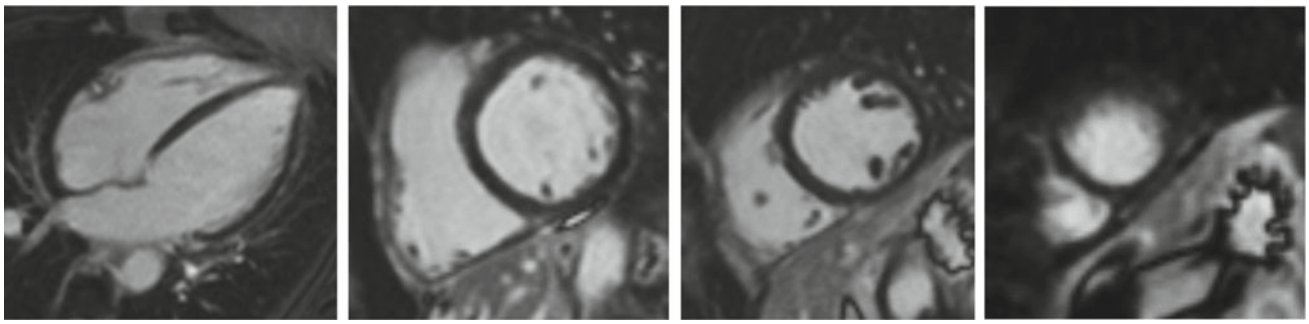

Fig. 27.4 Contrast cardiac MRI, LV 4-chamber long axis, LV short axes (basal, medium, apex levels), no late gadolinium hyperenhancement or scarring

References

1. Armenian SH, Lacchetti C, Barac A, et al. Prevention and monitoring of cardiac dysfunction in survivors of adult cancers: American Society of Clinical Oncology clinical practice guideline. J Clin Oncol. 2017;35:893–911.
2. Cardinale D, Colombo A, Lamantia G, et al. Anthracycline induced cardiomyopathy: clinical relevance and response to pharmacologic therapy. J Am Coll Cardiol. 2010;55:213–20.
3. Ponikowski P, Voors AA, Anker SD, et al. ESC Scientific Document Group. ESC Guidelines for the diagnosis and treatment of acute and chronic heart failure X “heart failure” . Eur Heart J. 2016;2016(37):2129–200.
4. Zamorano JL, Lancellotti P, Munoz DR, et al. 2016 ESC Position Paper on cancer treatments and cardiovascular toxicity developed under the auspices of the ESC Committee for Practice Guidelines. The Task Force for cancer treatments and cardiovascular toxicity of the European Society of Cardiology (ESC). Eur Heart J. 2016;37:2768–801.
5. Cardinale D, Colombo A, Bacchiani G, et al. Early detection of anthracycline cardiotoxicity and improvement with heart failure XE “heart failure” therapy. Circulation. 2015;131:1981–8.

Heart Failure in Long-Term Survivors of Childhood or Adolescent Cancers

28

Massimiliano Camilli and Giorgio Minotti

Key Points

- Ongoing cardiac surveillance is essential following treatment of childhood cancers.
- Too often patients are "lost to follow up" as they transition from childhood to adulthood.

28.1 Introduction

In contemporary oncology, several cautionary measures contribute to reduce the risk of on-treatment ventricular dysfunction and heart failure (HF). These measures include baseline evaluation of patient's cardiovascular characteristics, optimal treatment of comorbidities, and avoidance of unnecessary high cumulative doses of anthracyclines. That said, a risk of subclinical cardiotoxicity persists, especially if one appreciates that even low anthracycline doses can cause echocardiographic abnormalities that in the general population are known to progress toward systolic dysfunction and heart failure. The progression of subclinical cardiotoxicity toward clinically significant cardiac dysfunction is also promoted by cardiotoxic hits that occur after frontline treatment (second- or third-line treatments, chest radiation, and newly developing cardiovascular morbidities). It goes without saying that cancer patients should enter expert programs of cardiac surveillance but lessons from real life show that this surveillance strategy is not always doable or properly interpreted even in primary cancer centers. With the meritorious exception of patients followed within the framework of some US programs (Children's Oncology Group Study, Childhood Cancer Survivor Study, and BMT Survivor Study), and of some EU programs (primarily in the Netherlands), data from cancer survivors are not systematically retrieved. Many cancer survivors are left without a tailored surveillance. Subclinical cardiotoxicity can thus progress asymptomatically for years or decades, leaving cancer survivors exposed to the risk of sudden clinical symptoms. On the other hand, the last resort cardiologist who sees the symptomatic survivor often does not have access to the detailed oncologic history and is thus exposed to the challenge of treating advanced cardiac dysfunction while having to define on-the-fly customized treatment and follow-up modalities which may or may not best suit that patient. Describing this worst-case scenario is a good starting point with which to familiarize the reader with the entity of heart failure in long-term cancer survivors.

In childhood or adult cancer survivors the diagnosis of delayed cardiomyopathy should meet American Heart Association/American College of Cardiology criteria for cardiac compromise [1] and oncologic anamnestic information as described in reports or clinical practice guidelines from the International Late Effects of Childhood Cancer Guideline Harmonization Group [2] and the American Society of Clinical Oncology Survivorship Guidelines Advisory Group [3]:

1. Signs and/or symptoms:
   a. Dyspnea
   b. Orthopnea
   c. Fatigue
   d. Edema
   e. Hepatomegaly and/or rales

Electronic supplementary material
The online version of this chapter (https://doi.org/10.1007/978-3-030-70998-3_24) contains supplementary material, which is available to authorized users.

M. Camilli
Department of Cardiovascular and Pulmonary Sciences, Catholic University of the Sacred Heart, Rome, Italy
e-mail: Massimiliano.Camilli@unicatt.it

G. Minotti (✉)
Department of Medicine and Unit of Drug Sciences, Campus Bio-Medico University, Rome, Italy
e-mail: G.Minotti@unicampus.it

R. M. Steingart et al. (eds.), *Atlas of Imaging in Cardio-Oncology*,
https://doi.org/10.1007/978-3-030-70998-3_28

2. Or, in the absence of signs and/or symptoms:
   a. Ejection fraction $\leq 40\%$
   b. and/or fractional shortening $\leq 28\%$
3. History of:
   a. Anthracycline
   b. Anthracycline-trastuzumab
   c. Mitoxantrone
   d. Kinase inhibitors
   e. Chest radiation (particularly mediastinal or left-sided)
   f. Bone marrow transplant

Childhood cancer survivors carry a 5- to 15-fold higher risk of developing cardiomyopathy when compared with the general population [4]. The prevalence of cardiomyopathy averages 10% in adult cancer patients at one-year follow-up and slowly increases thereafter [5]. Cancer therapy-related delayed cardiomyopathy and heart failure (HF), usually but not always characterized by a reduced ejection fraction (HFrEF), is a complex entity that builds on multifactorial processes. The vast majority of information derives from survivors treated with anthracyclines or anthracycline-like drugs (e.g., mitoxantrone). The risk of anthracycline-related cardiomyopathy depends on lifetime exposure, with a cumulative dose of 400 mg/m^2 of doxorubicin equivalent being conventionally associated with 5% risk of HF in adults. However, children are inherently more vulnerable and may develop HF after exposure to significantly lower doses. Some adult patients may also develop HF after cumulative anthracycline doses that were thought to be safe [6]. Remarkable interpatient variability therefore occurs, which suggests that genetic predisposition may play a role. Single nucleotide polymorphism of genes involved in anthracycline distribution/elimination and bioactivation/detoxification have been invoked to explain why some patients are more vulnerable than others. An underlying familial cardiomyopathy may render patients more vulnerable to anthracycline toxicity [7]. That said, any childhood or adult cancer survivor with a history of ≥ 250 mg of doxorubicin/m^2 should receive survivor-tailored surveillance. This threshold is nonetheless an approximation; less than 250 mg of doxorubicin equivalent should warrant surveillance if the patient was also treated with chest radiation and/or other potentially cardiotoxic drugs [2, 3]. Other treatment-related procedures, most notably bone marrow transplant, introduce an additional risk of delayed cardiomyopathy [8].

Modifiable cardiovascular risk factors (hypertension, diabetes, dyslipidemia) represent additional variables to consider in the setting of delayed cardiomyopathy and HF. Approximately 80% of childhood cancer survivors develop at least one chronic condition by age 45. Fifty-year-old survivors may well develop multiple chronic conditions that overlap with and predispose to cardiomyopathy and HF [9]. In as much as chronic conditions develop and eventually surface as the survivor ages and no longer attends follow-up visits at the primary center where he/she was treated for cancer, an opportunity to intercept and aggressively treat cardiovascular morbidities is lost. As for adult cancer survivors, pre-existing comorbidities or unfavorable lifestyle play an intuitive role in increasing the risk of cancer treatment-related cardiovascular events. Despite that risk, the available evidence shows that cancer survivors tend to accumulate more comorbidities than seen in the general population [10]. Subclinical cardiotoxicity from anthracyclines may therefore deteriorate and progress to HF by conspiring with risk factors that mature after ending chemotherapy. Again, survivor-tailored surveillance should be warranted for at-risk patients, providing an opportunity for tailored pharmacologic treatment of risk factors. Thus, expert surveillance does not only serve to intercept signs and symptoms of a progressive deterioration of cardiac structure and function, but can also break the vicious cycle between cancer treatment-related and comorbidity-related cardiotoxicity. Lack of surveillance should therefore be considered as an independent risk factor of delayed cardiomyopathy and HF.

28.2 Clinical Case: Acute Heart Failure in a Seemingly Healthy Adult

28.2.1 Case Presentation

- 37-year-old Caucasian male admitted to the emergency department
- Complaint of progressively worsening dyspnea over two weeks
- Agitation, tachypnea, tachycardia, hypotension, oliguria, jugular distension, pulmonary rales.
- No apparent CV risk factor
- No familial history of cardiomyopathy and sudden death (confirmed by normal cardiologic assessment of parents and first-degree relatives).

28.2.2 Diagnostic Findings

- Chest X-ray: diffuse signs of alveolar pulmonary edema
- ECG: sinus tachycardia (125 bpm), nonspecific ST/T wave abnormalities in infero-lateral leads, no signs of acute myocardial ischemia (Fig. 28.1)
- Pulmonary computed tomography angiography: absence of pulmonary embolism
- Coronary angiography: absence of obstructive coronary artery disease (Fig. 28.2)

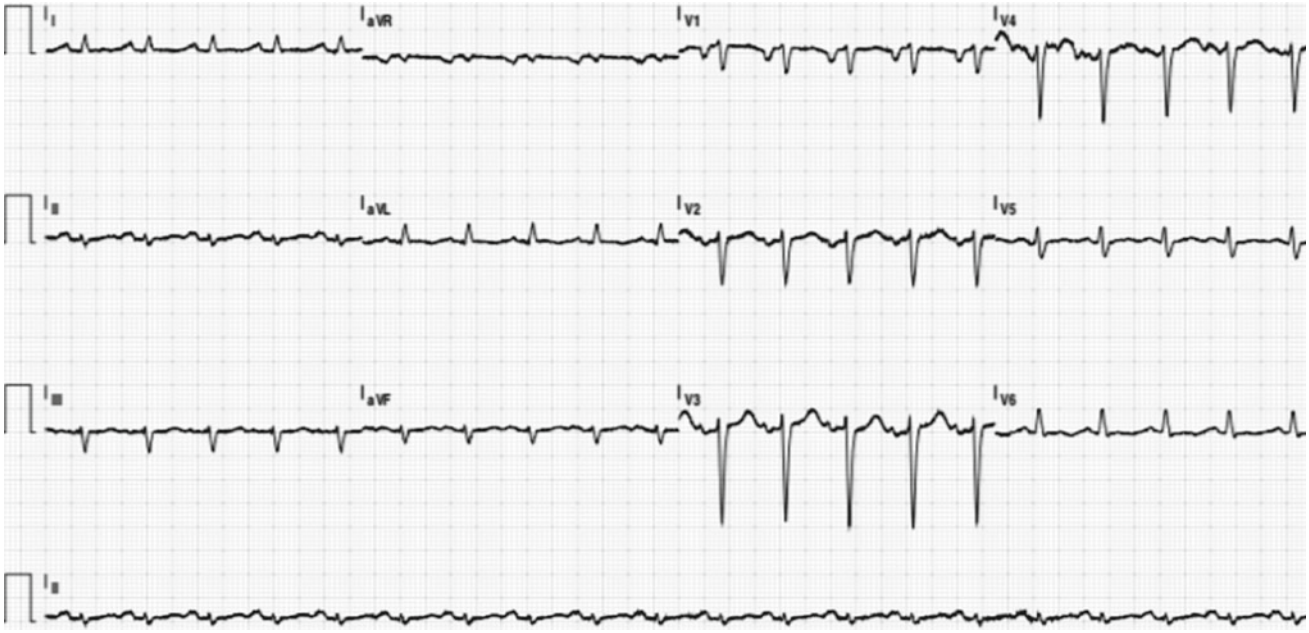

Fig. 28.1 ECG at admission. Sinus rhythm, tachycardia, non specific ST/T wave abnormalities in infero-lateral leads

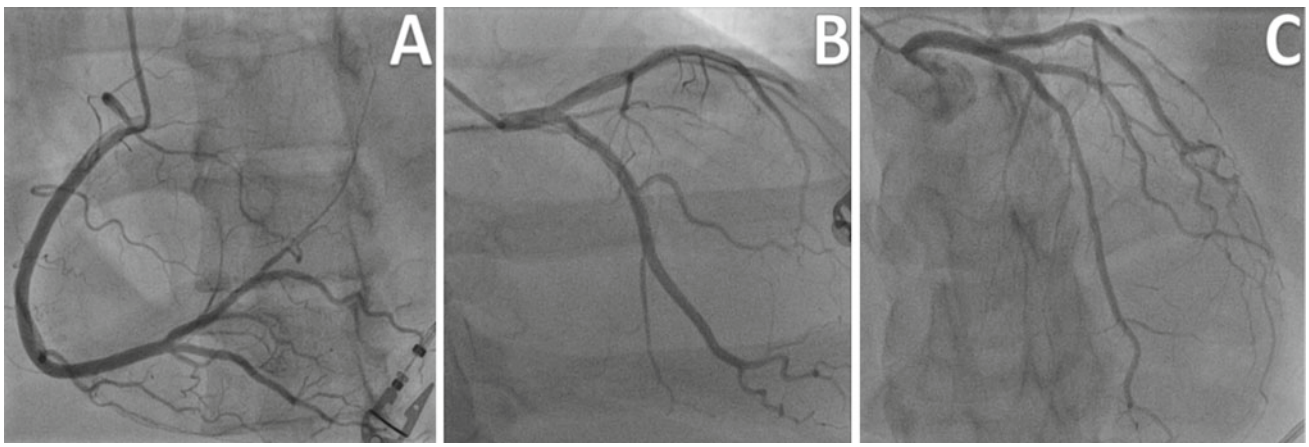

Fig. 28.2 *Coronary angiography*. Absence of stenosis in the right (**A**) and left (**B** and **C**) epicardial coronary arteries

- Trans-thoracic 2D echocardiography: Bi-ventricular severe systolic dysfunction (left ventricular ejection fraction [LVEF] 20%; tricuspid annular plane systolic excursion [TAPSE] 10 mm; right ventricular fractional area change [RVFAC] 26%; LV end systolic volume of 81 ml/m^2; global hypokinesia; reduced wall thickness; mild-to-moderate increase of left atrium volume (84 ml); moderate functional mitral and tricuspid regurgitation; and elevated estimated arterial systolic pulmonary pressure (65 mmHg) (Fig. 28.3)
- Cardiac magnetic resonance: Severe bi-ventricular dysfunction with diffuse reduction in cardiac mass and wall thickness; absence of late gadolinium enhancement (possible marker of fibrosis) or edema at T2-weighted sequences; absence of LV apical thrombus at early gadolinium enhancement sequences for microvascular obstruction (Fig. 28.4; Videos 28.1, 28.2 and 28.3)
- Laboratory: significantly increased NT-proBNP (16,000 pg/mL, institutional cut-off at 150 pg/mL); moderately increased troponin I (0.560 ng/mL, institutional cut-off at 0.04 ng/mL); normal C-reactive protein; bacterial, viral and immunologic panels negative for agents of acute myocarditis.

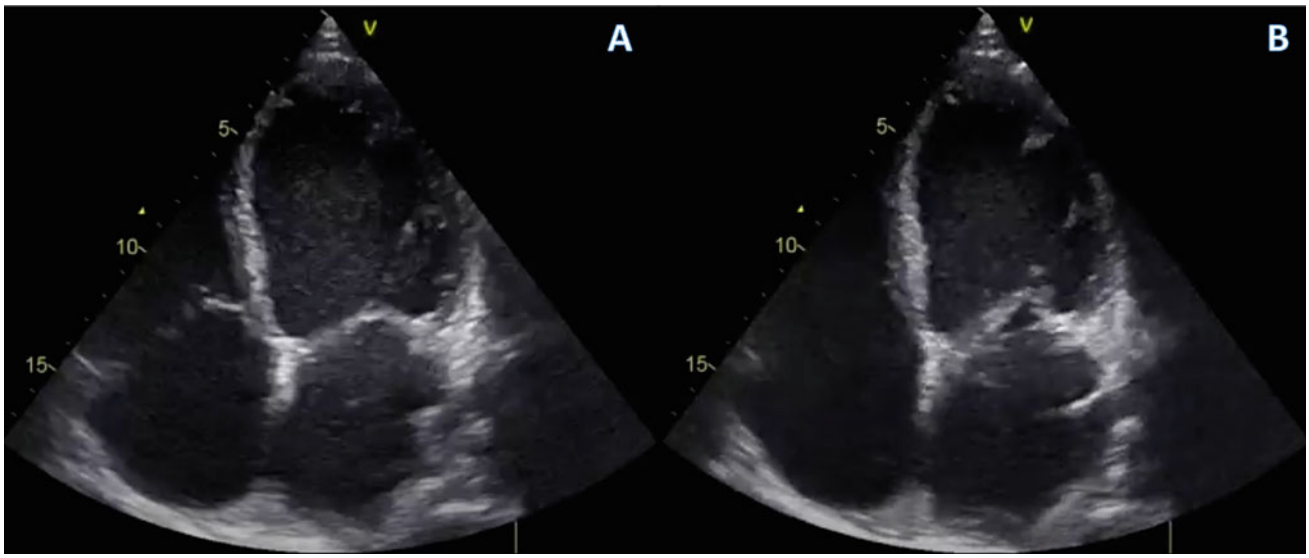

Fig. 28.3 *End diastolic and end systolic frames of trans-thoracic 2D echocardiography*. Main findings: severe left ventricular dilation, bi-ventricular dilation, severe systolic dysfunction (LVEF 20%, Tricuspid Annular Plane Systolic Excursion [TAPSE] 10 mm, Right Ventricular Fractional Area Change [RVFAC] 26%), global hypokinesia. **A** 4-chamber end diastolic volume; **B** 4-chamber end systolic volume

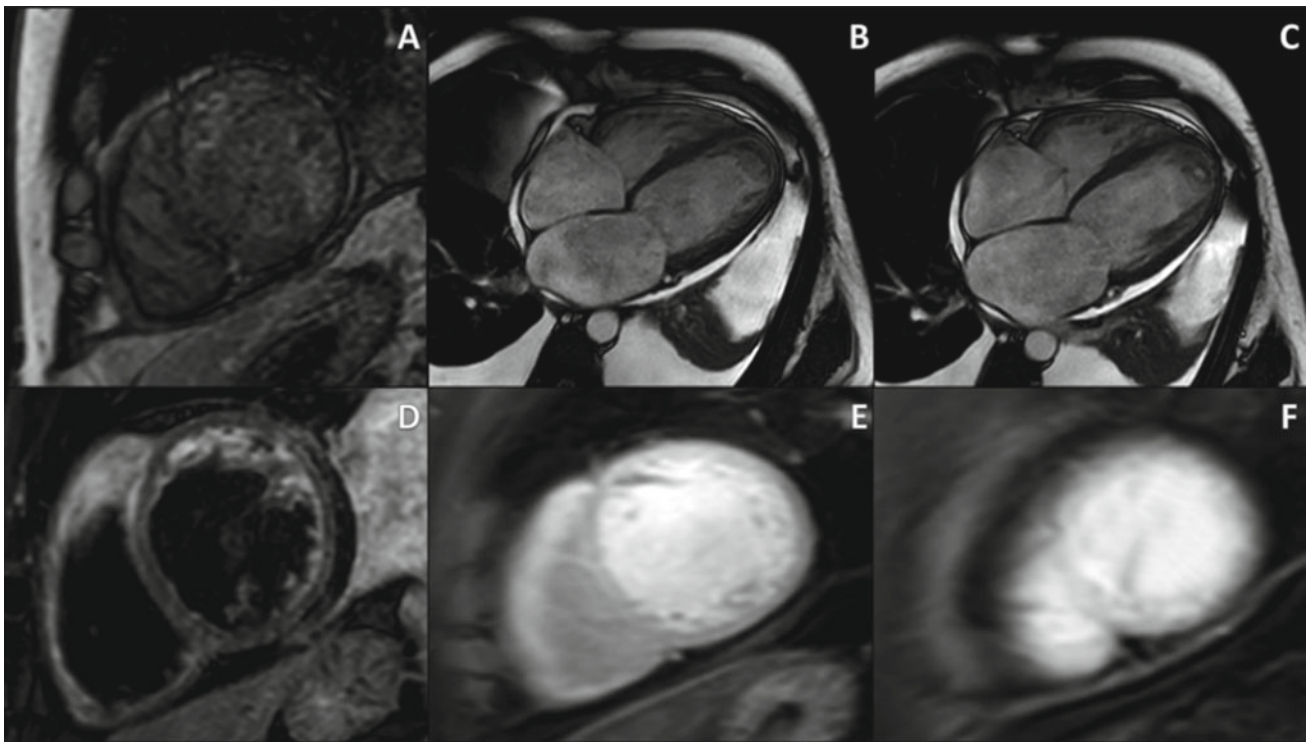

Fig. 28.4 *Cardiac magnetic resonance*. **A** (short-axis view) denotes absence of late gadiolinium enhancement; **B** (4-chamber view at end systole) and **C** (4-chamber view at end diastole) show significant bi-ventricular dysfunction, left ventricular dilatation and diffuse wall thinning; **D** (short-axis view) shows T2-weighted sequences without signs of myocardial edema; **E–F** (short axis view at mid-ventricular and apical level) show microvascular obstruction sequences with absence of LV apical thrombosis

28.2.3 Oncologic Anamnesis

Diagnostic findings ruled out most common causes of cardiogenic shock (acute coronary syndrome, Takotsubo syndrome, pulmonary embolism, viral or bacterial or autoimmune myocarditis, familial cardiomyopathy) . Anamnestic deepening therefore focused on patient's treatment for childhood cancer.

- Diagnosis of mediastinal diffuse large B cell non-Hodgkin lymphoma at the age of 8
- Frontline oncologic treatment with six cycles of CHOP regimen (cyclophosphamide/doxorubicin/vincristine/prednisone, cumulative doxorubicin dose of 300 mg/m^2)
- Tumor refractoriness
- High dose cytarabine and mitoxantrone as salvage therapy (mitoxantrone cumulative dose of 30 mg/m^2, corresponding to 300 mg of doxorubicin/m^2)
- Autologous stem cell transplantation as last treatment
- No chest radiation
- Patient's reporting of cardiac follow-up with transthoracic echocardiography until the age 23 (no records available, patient's reporting of normal findings)
- No cardiologic follow-up from the age of 23 to 37 when acute HF occurred.

28.3 Diagnosis of Cancer Treatment-Related Cardiomyopathy and Late Onset Heart Failure

On the basis of the patient's oncologic history, three major risks of cancer treatment-related cardiomyopathy were identified:

- High anthracycline cumulative dose (600 mg/m^2 [300 mg of doxorubicin + 300 mg of mitoxantrone])
- Bone marrow transplantation
- Lack of survivor-tailored surveillance over the last 14 years (as opposed to recommended lifelong surveillance with echocardiography for any survivor treated with $\geq$250 mg/m^2) [2]

It was therefore concluded that the patient carried a high risk of cancer treatment-related cardiomyopathy which progressed asymptomatically due to insufficient surveillance and eventually decompensated into acute HF.

28.4 Pharmacotherapy and Outcome

- Patient discharged after 12 days hospitalization (NT-proBNP at 2,880 pg/ml).
- Medical therapy: β blocker (carvedilol), potassium-sparing diuretic (canrenone), neprilysin inhibitor/angiotensin receptor blocker (sacubitril/valsartan at maximum tolerated doses of 49/51 mg bid).
- At three months follow-up: New York Heart Association functional class I; LVEF 45%, RVFAC 45%, mild mitral and tricuspid regurgitation at trans-thoracic echocardiography; NT-proBNP at 478 pg/mL.
- Similar echocardiographic findings at six months follow-up.
- Two years follow-up: Same findings as those at six months (Fig. 28.5) and Nt-proBNP at 120 pg/mL.

28.5 Conclusions

We summarized a case in which anthracycline cumulative dose, bone marrow transplantation, and lack of survivor-tailored surveillance conspired in exposing a childhood cancer survivor to the risk of chronic cardiomyopathy that acutely decompensated into HF 29 years after oncologic treatment. This is the most worrying scenario cardiologists may be faced with in the settings of cancer survivorship [11]. The prolonged absence of expert survivor-tailored cardiac follow-up allowed cardiomyopathy to progress asymptomatically.

The inexorable decrements of LVEF, changes in diastolic function, and myocardial strain could have easily been intercepted over the years had the survivor been assigned to a cardiology team conversant in cardiotoxicity from cancer drugs. Serial follow-up visits with echocardiography remain mandatory in these patients. On a different note, this clinical case shows that even the worst scenario can be satisfactorily managed with appropriate pharmacotherapy. Sacubitril/valsartan, which has improved medical therapy of HFrEF associated with hypertensive and atherosclerotic cardiovascular diseases, also presents valuable opportunities for patients with cancer treatment-related HF [11].

Video 28.1. Cardiac magnetic resonance (4-chamber view). Significant bi-ventricular dysfunction, left ventricular dilatation, diffuse wall thinning, moderate mitral regurgitation. RV, Right ventricle; LV, Left ventricle.

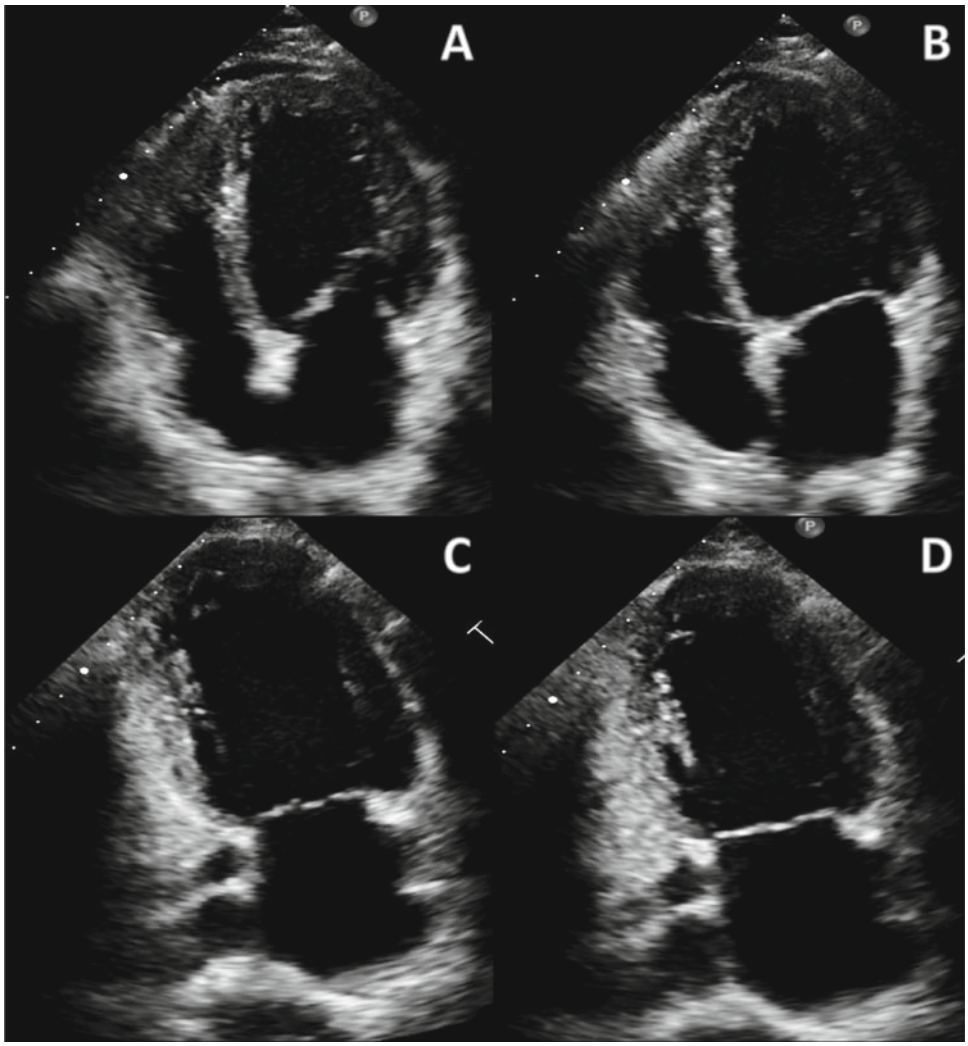

Fig. 28.5 *Echocardiographic findings at 2 years follow-up*. End diastolic and end systolic frames from the echocardiogram recorded at 6-months follow-up. Main findings: reduced left ventricular volumes, LVEF 45%, Tricuspid Annular Plane Systolic Excursion [TAPSE] 18 mm, Right Ventricular Fractional Area Change [RVFAC] 45%. Panel **A**: 4-chamber end diastolic volume; Panel **B**: 4-chamber end systolic volume; Panel **C**: 2-chamber end diastolic volume; Panel **D**: 2-chamber end systolic volume

Video 28.2. Cardiac magnetic resonance (short-axis view). Significant bi-ventricular dysfunction, left ventricular dilatation, diffuse wall thinning.

Video 28.3. Trans-thoracic echocardiogram (long-axis view) at 2 years follow-up. Improvement and stability in bi-ventricular systolic function and reduction of left ventricular volumes.

References

1. Hunt SA, Abraham WT, Chin MH et al. Focused update incorporated into the ACC/AHA 2005 guidelines for the diagnosis and management of heart failure in adults. A report of the American College of Cardiology Foundation/American Heart Association Task Force on Practice Guidelines Developed in collaboration with the international society for heart and lung transplantation. J Am Coll Cardiol. 2009;53:e1–90.
2. Armenian SH, Hudson MM, Mulder RL, et al. Recommendations for cardiomyopathy surveillance for survivors of childhood cancer: a report from the International Late Effects of Childhood Cancer Guideline Harmonization Group. Lancet Oncol. 2015;16:e123–36.
3. Armenian SH, Lacchetti C, Barac A, et al. Prevention and monitoring of cardiac dysfunction in survivors of adult cancers: American Society of Clinical Oncology clinical practice guideline. J Clin Oncol. 2017;35:893–911.
4. Smith LA, Cornelius VR, Plummer CJ, et al. Cardiotoxicity of anthracycline agents for the treatment of cancer: systematic review and meta-analysis of randomised controlled trials. BMC Cancer. 2010;10:337.
5. Cardinale D, Colombo A, Bacchiani G, et al. Early detection of anthracycline cardiotoxicity and improvement with heart failure therapy. Circulation. 2015;131:1981–8.
6. Salvatorelli E, Menna P, Chello M, et al. Modeling human myocardium exposure to doxorubicin defines the risk of heart failure from low-dose doxorubicin. J Pharmacol Exp Ther. 2017;362:263–70.
7. Garcia-Pavia P, Kim Y, Restrepo-Cordoba MA, et al. Genetic variants associated with cancer therapy-induced cardiomyopathy. Circulation. 2019;140:31–41.
8. Armenian SH, Sun CL, Shannon T, et al. Incidence and predictors of congestive heart failure after autologous hematopoietic cell transplantation. Blood. 2011;118:6023–9.

9. Howard E, Steingart RM, Armstrong GT, et al. Cardiovascular events in cancer survivors. Semin Oncol. 2019;46:426–32.
10. Jones LW, Haykowsky MJ, Swartz JJ, et al. Early breast cancer therapy and cardiovascular injury. J Am Coll Cardiol. 2007;50:1435–41.
11. Camilli M, Del Buono MG, Crea F, et al. Acute heart failure 29 years after treatment for childhood cancer. J Am Coll Cardiol Cardiooncology. 2020;2:316–9.

Health Care Disparities in Cardio-Oncology

29

Michelle N. Johnson

Key Points

- Black populations have higher prevalence of hypertension and diabetes and bear a disproportionate burden of cardiovascular disease. Blacks continue to have worse outcomes with the highest death rates and lowest survival from most cancers of any racial or ethnic group.
- Treatment is too often delayed such that both cancer and cardiovascular diseases are treated at a later stage.

Disparities between blacks and whites with respect to comorbidities, health outcomes and access to care have all been well documented. Black populations have higher prevalence of risk factors for cardiovascular disease, specifically hypertension and diabetes, and bear a disproportionate burden of cardiovascular disease [1, 2]. Differences in the incidence of disease and disease outcomes also exist in the arena of oncology where blacks continue to have worse outcomes with the highest death rates and lowest survival from most cancers of any racial or ethnic group [3–5]. Given that hypertension, diabetes and cardiovascular disease all increase the risk of cardiac complications from many forms of oncologic care, the question of whether this population also experiences disparate rates of cardiac complications from oncologic care and whether any such differences could contribute to the gap in cancer outcomes requires investigation.

The following cases illustrate examples of complications from chemotherapy, the impact of advanced cancer and heart disease at the time of presentation which required more potentially cardiotoxic treatment, and the impact of multiple cardiovascular comorbidities on the cancer treatment course.

29.1 Case 1

- Delay in definitive treatment.
- Cardiomyopathy and anthracyclines

A 45-year-old premenopausal black woman felt an axillary mass in February. She had last been seen by a physician some five years prior because her primary care a physician had retired. She presented for medical care and was referred for an ultrasound and bilateral mammogram at the end of April. Ultrasound revealed three masses.

She was referred for biopsy which revealed invasive ductal carcinoma ER 90%, PR 20%, HER2. PET-CT was performed in June and confirmed the presence of a 1.8 cm nodule in the left breast and two large left axillary lymph nodes.

The patient was seen by a surgeon for a second opinion in mid-August, six months after she had discovered the breast mass. She had had no interim interventions since her CT in June. Surgery was recommended and she underwent left partial mastectomy and axillary dissection with 3/17 nodes positive.

She had no history of HTN, NIDDM or CAD. Her pre-treatment echocardiogram was normal. She underwent treatment with dose dense doxorubicin, cyclophosphamide and Taxol, receiving a total of 240 mg/m^2 of doxorubicin. She received letrozole thereafter. She was followed for two years post treatment and then was lost to follow-up for two years. She then presented to an outside hospital with progressive shortness of breath.

Transthoracic echocardiogram (TTE) revealed severely reduced LV function with an ejection fraction of 17%, with grade III diastolic dysfunction (Fig. 29.1, Video 29.1). She was started on lisinopril and metoprolol. Subsequently lisinopril was changed to Entresto. She was referred for ischemia evaluation with PET/CT.

Electronic supplementary material
The online version of this chapter (https://doi.org/10.1007/978-3-030-70998-3_29) contains supplementary material, which is available to authorized users.

M. N. Johnson (✉)
Cardiology Service, Department of Medicine, Memorial Sloan Kettering Cancer Center, 1275 York Avenue, New York, NY 10065, USA
e-mail: Johnsom1@mskcc.org

R. M. Steingart et al. (eds.), *Atlas of Imaging in Cardio-Oncology*,
https://doi.org/10.1007/978-3-030-70998-3_29

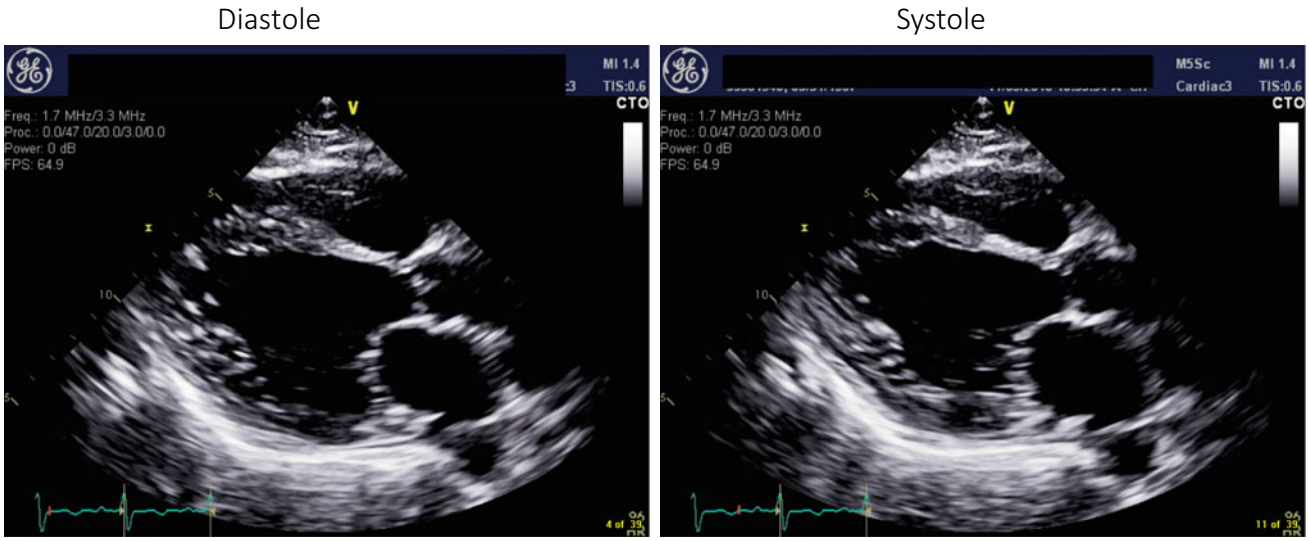

Fig. 29.1 Transthoracic echocardiogram (TTE) on presentation with dyspnea on exercise showing severely reduced LV function with an ejection fraction of 17%, with grade III diastolic dysfunction

PET scan showed a markedly dilated LV, with heterogeneous uptake of radiotracer, EF 22%, no evidence of myocardial infarct or stress-induced ischemia and a calcium score of 0 (Fig. 29.2). Her ejection fraction remained unchanged and it was recommended that she received an AICD. She expressed concerns about the invasive nature of this procedure and whether it would be visible to her employers and whether this would interfere with her ability to work. After several discussions on the topic she agreed to AICD placement.

Anthracyclines are among the best-studied oncologic agents with respect to cardiotoxicity. There are however limited data comparing the incidence of anthracycline (AC) induced cardiotoxicity (CT) by race/ethnicity. Among adult survivors of childhood cancers different rates of developing AC cardiomyopathy between blacks and whites have been documented [6]. Blacks had a relative risk of 1.7 of developing CT versus whites—with CT defined as congestive heart failure, decrease in ejection fraction prompting interruption of treatment, or sudden death felt to be due to cardiac causes. Other data supporting an increased risk in black Americans include a retrospective review of patients in a university registry where the rate of AC cardiomyopathy amongst these patients was three times higher than the generally stated rates. In addition, a meta-analysis supported the finding of increased risk in black Americans [7, 8]. Risk factors for AC cardiac toxicity include coronary artery disease and obesity [9]. Black Americans have higher rates of both risk factors than whites. Larger studies are needed to document rates of AC cardiotoxicity by race as well as the potential impact of aggressive risk factor modification at redressing any differences in outcomes.

Studies have shown improvement in outcomes with earlier detection of CT [10]. Whether there is role for increased surveillance in these high risk women also deserves evaluation. The black woman in this case was not undergoing routine mammography and detected her own tumor by self-examination, she had a relatively long delay between diagnosis and cancer surgery, and did not receive recommended post anthracycline cardiac monitoring. These factors are well-known contributors to worse cancer and cardiovascular outcomes in women with breast cancer, regardless of any yet to be discovered outcome differences based on race alone. It is important to note that this patient consented to aggressive guideline-directed medical therapy and AICD placement, a testimonial to the patient's improved health awareness and the effectiveness of committed health care providers working in a system that can deliver patient education and state-of-the-art therapies.

29.2 Case 2

- Impact of multiple cardiovascular comorbidities on treatment course
- Late stage of disease at the time of diagnosis.

A 52-year-old black male presented with a mechanical fall and hip fracture which was found to be a pathologic fracture. He was in acute renal failure with hyperkalemia, hypercalcemia and profound anemia on presentation. He was started on dialysis. Biopsy showed the fractures to be due to myeloma lytic lesions. He had good exercise capacity and no known cardiac history before starting chemotherapy. He

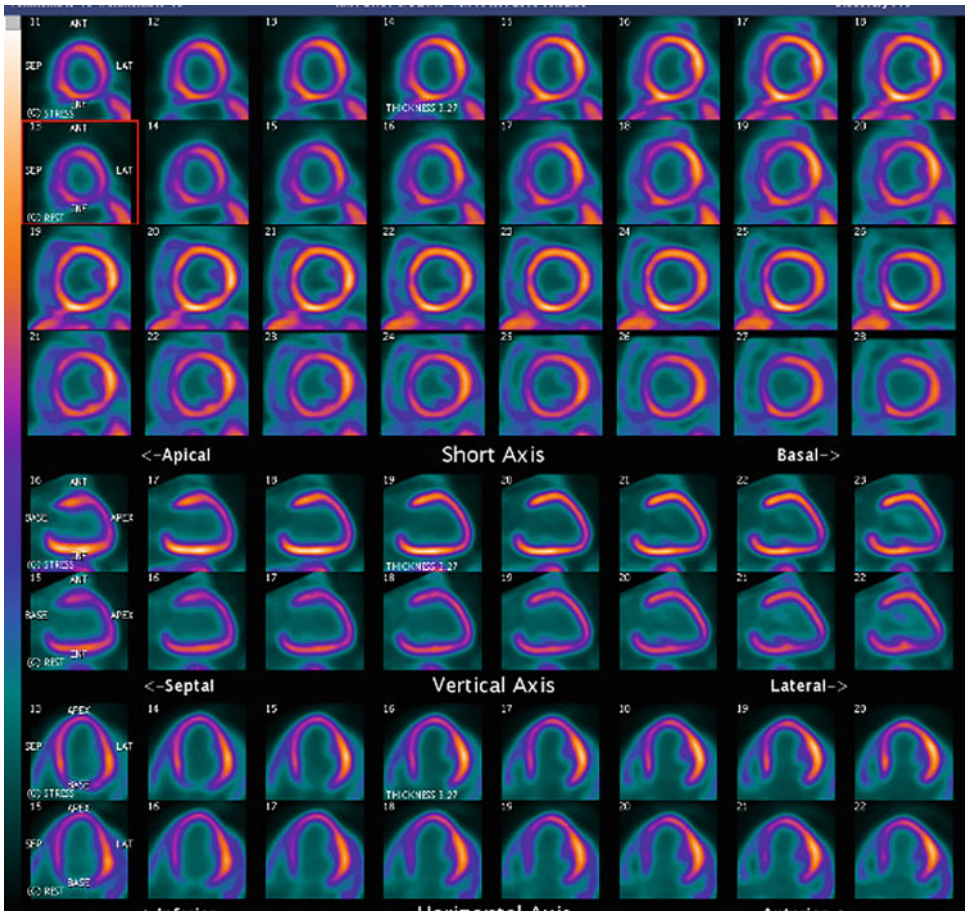

Fig. 29.2 Cardiac PET to assess for CAD. PET scan showed a markedly dilated LV, with heterogeneous uptake of radiotracer, EF 22%, no evidence of myocardial infarct or stress-induced ischemia. Calcium score of 0 on accompanying CT scan

reportedly had normal LV function, EF 75% on his pre-chemotherapy TTE. He received cyclophosphamide, bortezomib, dexamethasone for 1.5 cycles and was switched to carfilzomib, cyclophosphamide and dexamethasone. At this time he was diagnosed with hypertension and was treated with lisinopril. He then sought a second opinion. He was referred to cardiology for risk stratification for possible autologous stem cell transplant and had an ECG and echocardiogram performed.

He underwent CTA to evaluate for CAD (Figs. 29.3 and 29.4, Video 29.2).

CTA revealed non-obstructive CAD (Fig. 29.5); <50% obstruction in left anterior descending and right coronary arteries and non-luminal narrowing in left main.

He was deemed at increased risk for stem cell transplant given his CAD, renal failure and cardiomyopathy; however, given his young age and good functional capacity the decision was made to offer him transplant with dose-reduced cyclophosphamide. He had successful transplant but remained on HD with difficult-to-control hypertension.

Studies of multiple myeloma by race and ethnicity document later presentations and more advanced disease in blacks at the time of diagnosis [11]. Studies have also shown that black multiple myeloma patients are less likely to be deemed eligible for transplant. Treatment at NCCN centers is associated with a better prognosis [12]. The impact of cardiovascular comorbidities in black multiple myeloma patients is an area that deserves further investigation.

29.3 Case 3

- Multiple cardiovascular comorbidities and cardiovascular events interrupting the use of first-line agents for oncologic care
- Delay in diagnosis
- Late stage at the time of diagnosis increasing the need for adjuvant therapies with cardiotoxicities.

A 60-year-old black man with history of hypertension, obesity (BMI 45) and leiomyosarcoma referred for cardiac evaluation of newly diagnosed cardiomyopathy.

The patient was initially seen by his urologist for a lump in the scrotal wall. Over the subsequent six months the mass increased in size and there were also two additional lesions noted. He then had excision of the left scrotal lesion with

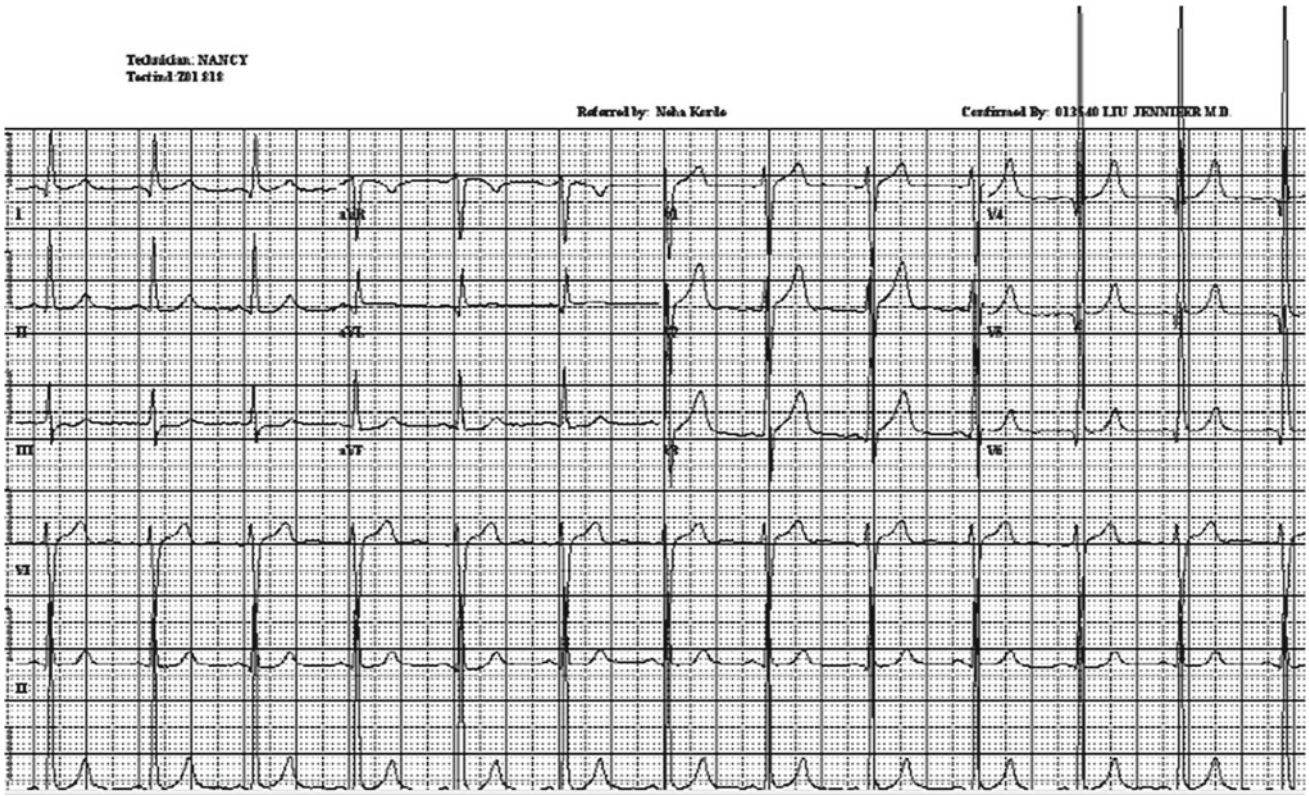

Fig. 29.3 ECG with LVH

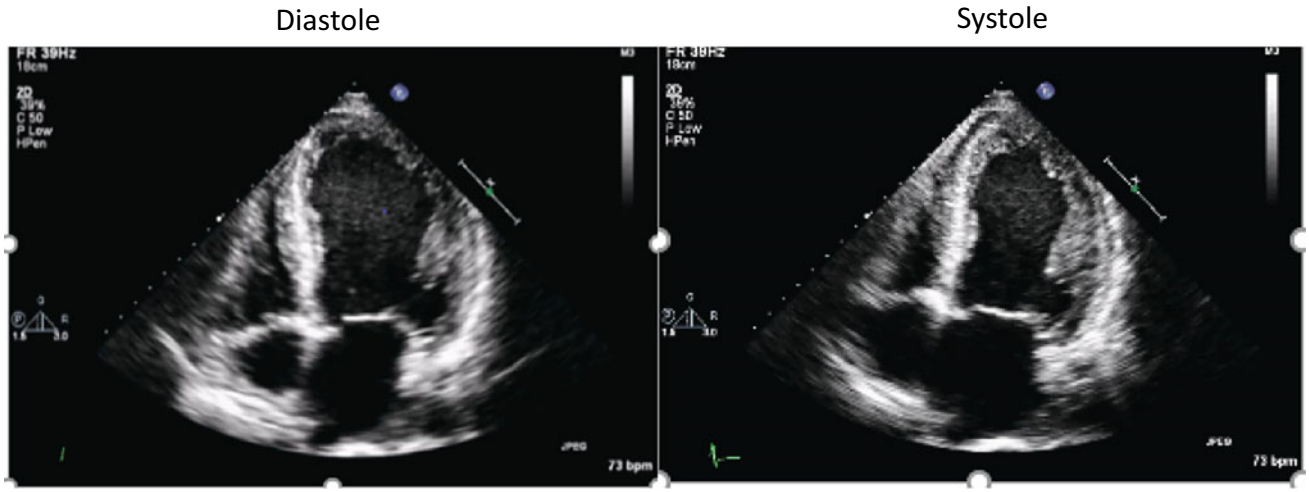

Fig. 29.4 TTE showed new mildly reduced LV function, concentric left ventricular hypertrophy EF 50%

pathology showing high-grade leiomyosarcoma. He had positive surgical margins and underwent re-excision and scrotal reconstruction with adjuvant external beam radiation treatment. Some months later chest X-ray showed new lesions, suggestive of metastatic disease. While waiting for biopsy he presented to an outside institution with blurry vision and difficulty with language comprehension. A CT of the head without contrast showed a non-hemorrhagic infarct involving the inferior left parieto-occipital junction with mild mass effect. He was evaluated by neurology and underwent brain MRI which confirmed CT finding and revealed no masses. He had an unremarkable CT angiogram

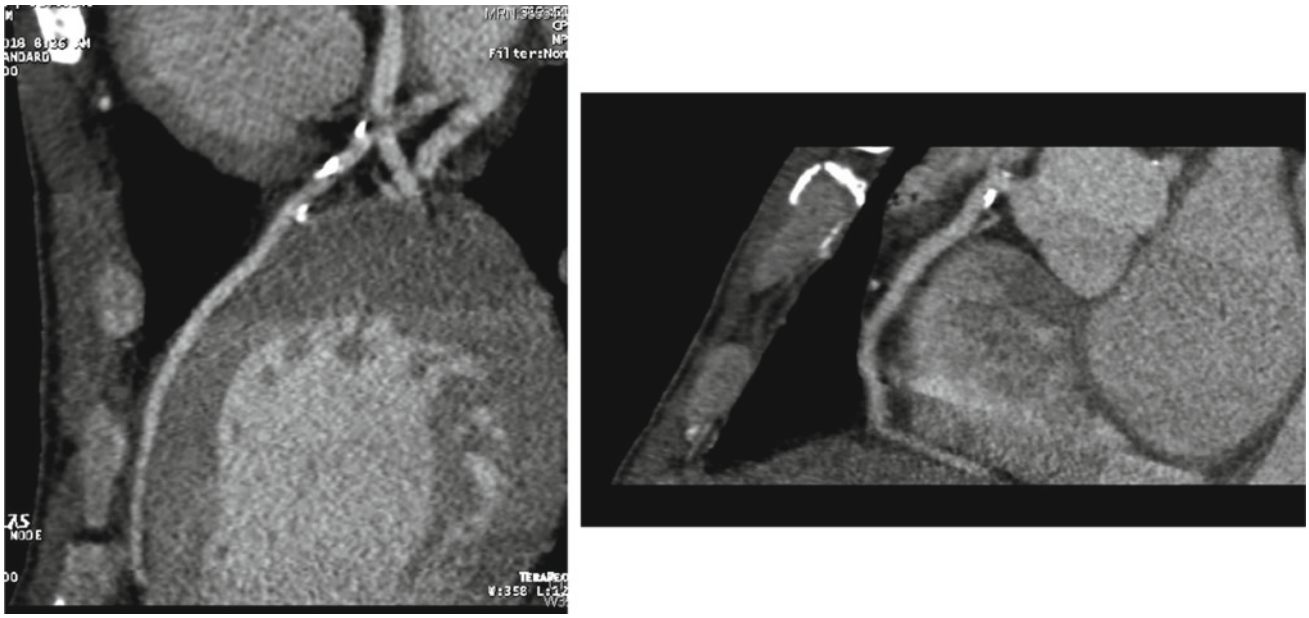

Fig. 29.5 CTA showing non-obstructive CAD

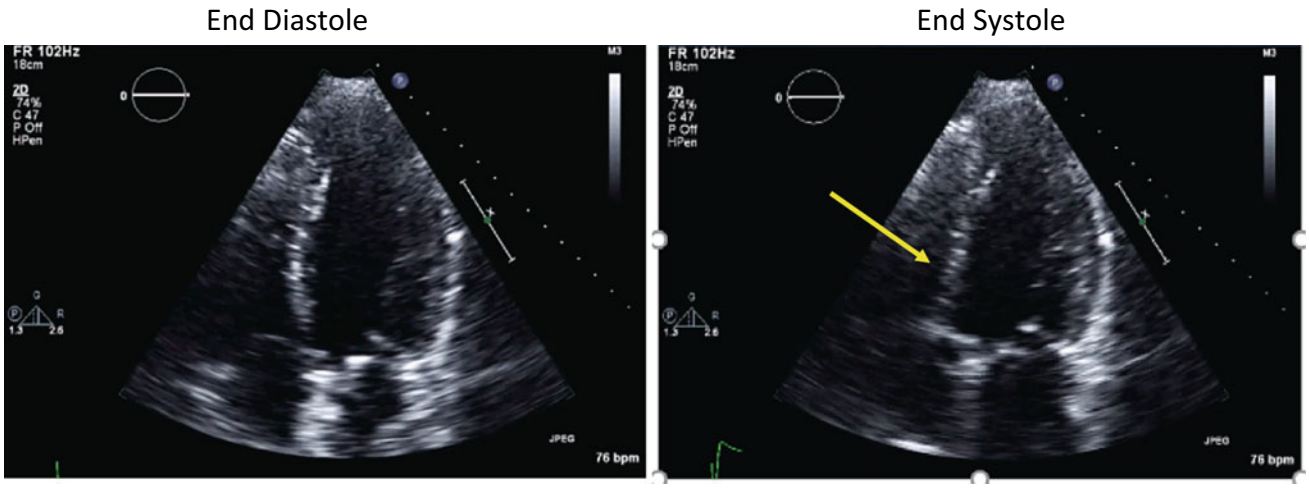

Fig. 29.6 TTE with EF of 40–45% with hypokinesis of inferior basal segment and anterior septum

of the neck and had a transesophageal echocardiogram which showed no evidence of clot but noted mild left ventricular dysfunction. The stroke was attributed to hypertensive vascular disease. He was discharged on ASA and carvedilol. He was seen by his oncologist who referred to cardiology for further cardiovascular management and assessment prior to gemcitabine and docetaxel therapy. He was referred for repeat evaluation of left ventricular function.

Transthoracic echocardiogram showed an EF of 40–45% with hypokinesis of inferior basal segment and anterior septum (Fig. 29.6). He was referred for ischemia evaluation with cardiac PET (Fig. 29.7).

Evaluation revealed moderately reduced left ventricular function with EF of 40–45% with mild global hypokinesia, possible septal infarct with no evidence of ischemia. Mildly dilated left ventricular size. Coronary calcium score was 1013.

He was started on guideline-directed medical therapy for LV dysfunction with ACEI and beta blockers in addition to his ASA and statin. He had subsequent improvement in EF to 50%. He was then started on trametinib but developed CHF with reduction in EF to 40%. He was treated with pazopanib which was interrupted due to development of hypertensive episodes. He had progression of disease at

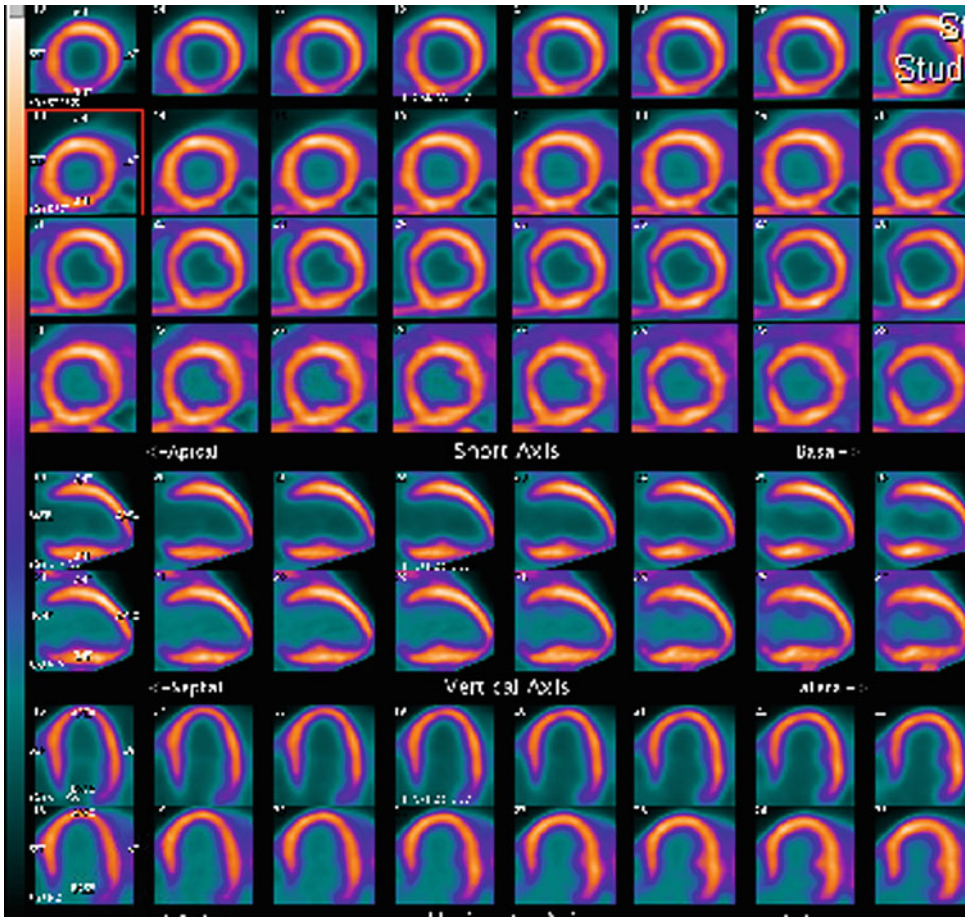

Fig. 29.7 Cardiac PET-moderately reduced left ventricular function, EF calculated at 40–45% with mild global hypokinesia and dilated thin walled left ventricle. Top row (s) stress, bottom row rest in three orthogonal planes. Maybe some subtle fixed defect consistent with an infarct in the septum which was suggested by hypokinesis on the echocardiogram, but no evidence for ischemia. There was evidence for atherosclerosis as indicated by the elevated coronary calcium score of 1013 on the accompanying CT scan

which point a conference was held involving the patient, oncology and cardiology services. Oncology recommended anthracycline therapy as the best agent for disease suppression. While he was deemed at increased risk of cardiac complications given his reduced EF, it was agreed to try a palliative course of anthracyclines with careful cardiac monitoring. He had no change in his EF but his malignancy proved unresponsive to this course of treatment. He ultimately succumbed to progression of disease.

These cases illustrate how cardio-oncological complications can occur in the setting of comorbidities such as hypertension, diabetes and coronary artery disease all of which have been associated with worse overall cancer survival [13, 14]. Differences in stage at diagnosis between blacks and whites have been repeatedly documented. Later stage disease in blacks translates to lower surgical cure rates for cancer and therefore may require more frequent use of neoadjuvant or adjuvant chemotherapy which increases risk of exposure to potentially cardio-toxic agents. In turn, later stage presentations require more complex decision-making and close communication among health care providers, the patient and his/her significant others. These already difficult decisions are made even more so by a lack of data specific to the black patient, adverse socioeconomic circumstances and by health care consumers who are often unfamiliar with and somewhat skeptical of the intentions of the health care system. Outcomes in cancer care have been shown to vary markedly based on where patients receive care. Issues of access may also impact cardio-oncologic sequelae from treatment. Differences in access cause disparate oncologic outcomes, and multiple studies have shown that equalization of access significantly reduces difference in outcomes [15].

Differences in referral patterns to practitioners versed in cardio oncology and to survivorship clinics may well follow the pattern of uptake of other new cardiovascular treatment developments, namely slower application to blacks than to whites. Difference in enrollment in clinical trials leads to an underestimation or under appreciation of cardiac complications in black patients [16]. Certainly, advancing health equity in cardio-oncology will require earlier and broader access for the black patient to investigations, diagnostics and therapeutics.

References

1. Mensah GA, Mokdad AH, Ford ES, Greenlund KJ, Croft JB. State of disparities in cardiovascular health in the United States. Circulation. 2005;111(10):1233–41. https://doi.org/10.1161/01.CIR.0000158136.76824.04 PMID: 15769763.
2. Safford MM, Brown TM, Muntner PM, Durant RW, Glasser S, Halanych JH, et al. REGARDS Investigators. Association of race and sex with risk of incident acute coronary heart disease events. JAMA. 2012;308(17):1768–74. https://doi.org/10.1001/jama.2012.14306. PMID: 23117777; PMCID: PMC3772637.
3. Aizer AA, Wilhite TJ, Chen MH, Graham PL, Choueiri TK, Hoffman KE, et al. Lack of reduction in racial disparities in cancer-specific mortality over a 20-year period. Cancer. 2014;120(10):1532–9. https://doi.org/10.1002/cncr.28617 Epub 2014 Feb 22 PMID: 24863392.
4. DeSantis CE, Miller KD, Goding Sauer A, Jemal A, Siegel RL. Cancer statistics for African Americans, 2019. CA Cancer J Clin. 2019;69(3):211–33. https://doi.org/10.3322/caac.21555 Epub 2019 Feb 14 PMID: 30762872.
5. Ward EM, Sherman RL, Henley SJ, Jemal A, Siegel DA, Feuer EJ, et al. Annual report to the nation on the status of cancer, featuring cancer in men and women age 20–49 years. J Natl Cancer Inst. 2019;111(12):1279–97. https://doi.org/10.1093/jnci/djz106. PMID: 31145458; PMCID: PMC6910179.
6. Krischer JP, Epstein S, Cuthbertson DD, Goorin AM, Epstein ML, Lipshultz SE. Clinical cardiotoxicity following anthracycline treatment for childhood cancer: the Pediatric Oncology Group experience. J Clin Oncol. 1997;15(4):1544–52. https://doi.org/10.1200/JCO.1997.15.4.1544 PMID: 9193351.
7. Hasan S, Dinh K, Lombardo F, Kark J. Doxorubicin cardiotoxicity in African Americans. J Natl Med Assoc. 2004;96(2):196–9. PMID: 14977278; PMCID: PMC2594938.
8. Lotrionte M, Biondi-Zoccai G, Abbate A, Lanzetta G, D'Ascenzo F, Malavasi V, et al. Review and meta-analysis of incidence and clinical predictors of anthracycline cardiotoxicity. Am J Cardiol. 2013;112(12):1980–4. https://doi.org/10.1016/j.amjcard.2013.08.026 Epub 2013 Sep 25 PMID: 24075281.
9. Scully RE, Lipshultz SE. Anthracycline cardiotoxicity in long-term survivors of childhood cancer. Cardiovasc Toxicol. 2007;7(2):122–8.
10. Cardinale D, Colombo A, Bacchiani G, Tedeschi I, Meroni CA, Veglia F, et al. Early detection of anthracycline cardiotoxicity and improvement with heart failure therapy. Circulation. 2015;131(22):1981–8. https://doi.org/10.1161/CIRCULATIONAHA.114.013777 Epub 2015 May 6 PMID: 25948538.
11. Ailawadhi S, Jacobus S, Sexton R, Stewart AK, Dispenzieri A, Hussein MA, et al. Disease and outcome disparities in multiple myeloma: exploring the role of race/ethnicity in the Cooperative Group clinical trials. Blood Cancer J. 2018;8(7):67. https://doi.org/10.1038/s41408-018-0102-7. PMID: 29980678; PMCID: PMC6035273
12. Ailawadhi S, Advani P, Yang D, Ghosh R, Swaika A, Roy V, et al. Impact of access to NCI- and NCCN-designated cancer centers on outcomes for multiple myeloma patients: a SEER registry analysis. Cancer. 2016;122(4):618–25. https://doi.org/10.1002/cncr.29771 Epub 2015 Nov 13 PMID: 26565660.
13. West DW, Satariano WA, Ragland DR, Hiatt RA. Comorbidity and breast cancer survival: a comparison between black and white women. Ann Epidemiol. 1996;6(5):413–9. https://doi.org/10.1016/s1047-2797(96)00096-8 PMID: 8915472.
14. Tammemagi CM, Nerenz D, Neslund-Dudas C, Feldkamp C, Nathanson D. Comorbidity and survival disparities among black and white patients with breast cancer. JAMA. 2005;294(14):1765–72. https://doi.org/10.1001/jama.294.14.1765 PMID: 16219879.
15. Fillmore NR, Yellapragada SV, Ifeorah C, Mehta A, Cirstea D, White PS, et al. With equal access, African American patients have superior survival compared to white patients with multiple myeloma: a VA study. Blood. 2019;133(24):2615–8. https://doi.org/10.1182/blood.2019000406. Epub 2019 Apr 19. PMID: 31003998; PMCID: PMC6566591.
16. Murthy VH, Krumholz HM, Gross CP. Participation in cancer clinical trials: race-, sex-, and age-based disparities. JAMA. 2004;291(22):2720–6. https://doi.org/10.1001/jama.291.22.2720. PMID: 15187053.

Cardio-Oncology Practice in the Community

30

Diego Sadler, L. Steven Zukerman, Lance Berger, Mahim Kapoor, Jacobo Kirsch, Kevin Leung, and Luis Hernandez

Key Points

There are currently 17 million cancer survivors in the United States [1]. Cancer patients have a 2–6 times higher cardiovascular mortality risk than the general population, and cardiovascular mortality is evident throughout the continuum of cancer care [2]. Furthermore, for those patients with effective cancer treatments and declining cancer mortality, cardiovascular disease management becomes critical to improve outcomes and reduce overall mortality [2,3]. Multiple factors result in decreased healthcare access and poor outcomes for these patients [4]. At the present time, cardio-oncology programs exist predominately in large, academic, quaternary institutions [5]. The American College of Cardiology's National Cardio-Oncology Survey [6] identified specific barriers which might limit the implementation of cardio-oncology programs, including: lack of funding, limited interest, lack of infrastructure, and lack of educational opportunities. Furthermore, cardiovascular testing indications that are not covered by medical insurance like post-radiation non-invasive cardiac testing for surveillance, biomarkers during chemotherapy treatment, and cardiac magnetic resonance used for early detection of cardiac effects of cancer-related therapies may present an additional obstacle to establishing cardio-oncology programs.

There is a need to improve access to care at the local, state, and national level. In Florida, we recently reported a practical model to start and maintain a successful cardio-oncology program without additional financial resources that can be reproduced in a variety of different practice settings to improve access to care [7]. Programs in the community can succeed by active participation and engagement with professional societies. We developed a collaborative program between the Florida Chapter of the American College of Cardiology and the Florida American Society of Clinical Oncology to assess the educational needs of both cardiologists and oncologists and subsequently developed educational materials to help bridge the identified knowledge gaps [8,9]. To further expand our access to care platform, we worked towards a large, multistate network that includes members from 19 ACC state chapters, 6 ASCO chapters, and 9 countries with International Cardio-Oncology Society (ICOS) affiliated chapters from both academic and private practice settings. This network is a platform for multiple current [10] and future collaborations. Different models have emerged to expand access to care in the community.

A practice model based in New Jersey has proposed protocols and algorithms for community-based cardio-oncology: Despite the obvious progress and growth of academic cardio-oncology, a significant majority of patients with cardio-oncology needs are served at smaller institutions in the community setting. The New Jersey model

Electronic supplementary material
The online version of this chapter (https://doi.org/10.1007/978-3-030-70998-3_30) contains supplementary material, which is available to authorized users.

D. Sadler (✉) · J. Kirsch · K. Leung · L. Hernandez
Robert and Suzanne Tomsich Department of Cardiovascular Medicine, Heart and Vascular Institute, Cleveland Clinic Florida, 2950 Cleveland Clinic Boulevard, Weston, FL 33331, USA
e-mail: sadlerd@ccf.org

J. Kirsch
e-mail: kirsch@ccf.org

K. Leung
e-mail: leungk@ccf.org

L. Hernandez
e-mail: hernanl@ccf.edu

L. S. Zukerman · L. Berger · M. Kapoor
Monmouth Cardiology Associates, 11 Meridian Road, Eatontown, NJ 07724, USA
e-mail: lsz1206@gmail.com

L. Berger
e-mail: lance.berger@monmouthcardiology.com

M. Kapoor
e-mail: mahim.kapoor@monmouthcardiology.com

R. M. Steingart et al. (eds.), *Atlas of Imaging in Cardio-Oncology*, https://doi.org/10.1007/978-3-030-70998-3_30

focuses on the following points to successfully evaluate and treat the cardio-oncology patient in the community:

The effective management of complex cardio-oncology cases can be quite challenging in both the academic and the community practice settings. Limited resources and lack of standardized protocols may pose additional obstacles. In this chapter, we present patients with complex cardiovascular issues related to cancer treatment where cardiovascular imaging was critical for diagnosis, treatment guidance, management, and monitoring. Patients from the Florida practice (Sects. 30.1, 30.2, 30.3 and 30.4) and the New Jersey practice (Sects. 30.5, 30.6, 30.7 and 30.8) are presented.

30.1 Case 1. Use of Cardiac Resynchronization Therapy To Improve Left Ventricular (LV) Systolic Function and Allow Initiation of Trastuzumab Therapy in a HER2 + Breast Cancer Patient with Non-ischemic Cardiomyopathy and Left Bundle Branch Block (LBBB)

- Patients with HER2 positive breast cancer with abnormal baseline LV function are at high risk for cardio-toxicity. A recent pilot study has shown the potential feasibility of trastuzumab therapy for asymptomatic patients with LV ejection fraction (LVEF) >40% when supported with cardioprotective treatment with carvedilol and ACE inhibitors [11].

  This is a 75-year-old woman with multifocal HER2neu 3 + breast cancer, with history of hypertension, diabetes, and non-ischemic cardiomyopathy as proven by cardiac catheterization in 2017. Baseline echocardiogram showed normal LV size with an LVEF of 30%. Cardiac MRI was consistent with a non-ischemic cardiomyopathy with no scar or late gadolinium enhancement (LGE) and dilated LV with LVEF 31%. Given her severely reduced LV systolic function, she was deemed high risk for neoadjuvant trastuzumab treatment. She was treated with carvedilol and ACE inhibitors and underwent a right partial mastectomy. She had no improvement in her LV systolic function despite guideline directed medical therapy with LVEF remaining at 30–35%. A very low global longitudinal strain (GLS) of 8.8% was also noted. She had a LBBB on the ECG. She underwent biventricular implantable cardioverter-defibrillator (ICD) insertion with cardiac resynchronization capability (CRT-D). Post-CRT-D echocardiogram, her LVEF improved to 44%. She was started on trastuzumab immediately after documentation of improvement of LVEF post-CRT-D. CRT-D interrogation showed 100% bi-V pacing. Echocardiogram after starting trastsuzumab showed a stable LVEF at 45%. This case shows a possible new approach with CRT-D to allow treatment with trastuzumab in patients with LBBB and non-ischemic cardiomyopathy (Figs. 30.1, 30.2 and 30.3, Videos 30.1 and 30.2).

30.2 Case 2. Patient with Multiple Myeloma, AL Cardiac Amyloidosis, Stem Cell Transplant, and Recurrent Disease

- Patients with multiple myeloma can present with co-existing cardiac AL amyloidosis. Management can be challenging, including various chemotherapy regimens, stem cell transplant, and immunotherapy. They do not respond to classic heart failure treatment medications like ACE inhibitors and beta blockers. Cardiac imaging and biomarkers are useful to assess prognosis, monitor disease progression, and treatment.

  This is a 70-year-old male presented with dyspnea and elevated kappa (17.8 mg/dL) and lambda (201 mg/dL) light chains diagnosed with monoclonal gammopathy, and bone marrow biopsy positive for multiple myeloma in early 2018. He had a troponin <0.01 ng/ml but elevated pro-BNP of 1178 pg/ml. Cardiac MRI showed circumferential myocardial thickening with mild global hypokinesis and patchy areas of persistent enhancement suggestive of infiltrative cardiomyopathy. Fat pad biopsy was negative for amyloid. Patient declined endo-myocardial biopsy. He continued treatment with cyclophosphamide, bortezomib, and dexamethasone. A clinical diagnosis of cardiac AL amyloidosis was made despite the negative fat pad biopsy based on the elevated pro-BNP, cardiac MRI, and an echocardiogram that showed a small LV, moderate left ventricular hypertrophy with "sparkling" appearance, and a normal LVEF = 74 ± 5% (2-D biplane) with Grade II left ventricular diastolic dysfunction. Reduced GLS of −11.1% with apical sparing pattern was highly suggestive of amyloidosis as was the EKG with low voltage QRS. He subsequently underwent stem cell transplant. He was treated with furosemide 40 mg and spironolactone 25 mg daily. His labs were notable for D-dimer 4520, pro-BNP 5663, and troponin 0.023. CT angiography was negative for pulmonary embolism. He had a favorable hematological response with monoclonal antibody therapy showing a progressive decrease of lambda light chains from 265 to 85 mg/dL, but he still had dyspnea on exertion on furosemide, spironolactone, and metolazone. Follow up echocardiogram showed moderate concentric LVH with mildly reduced LVEF 50% by 2-D, 48% by

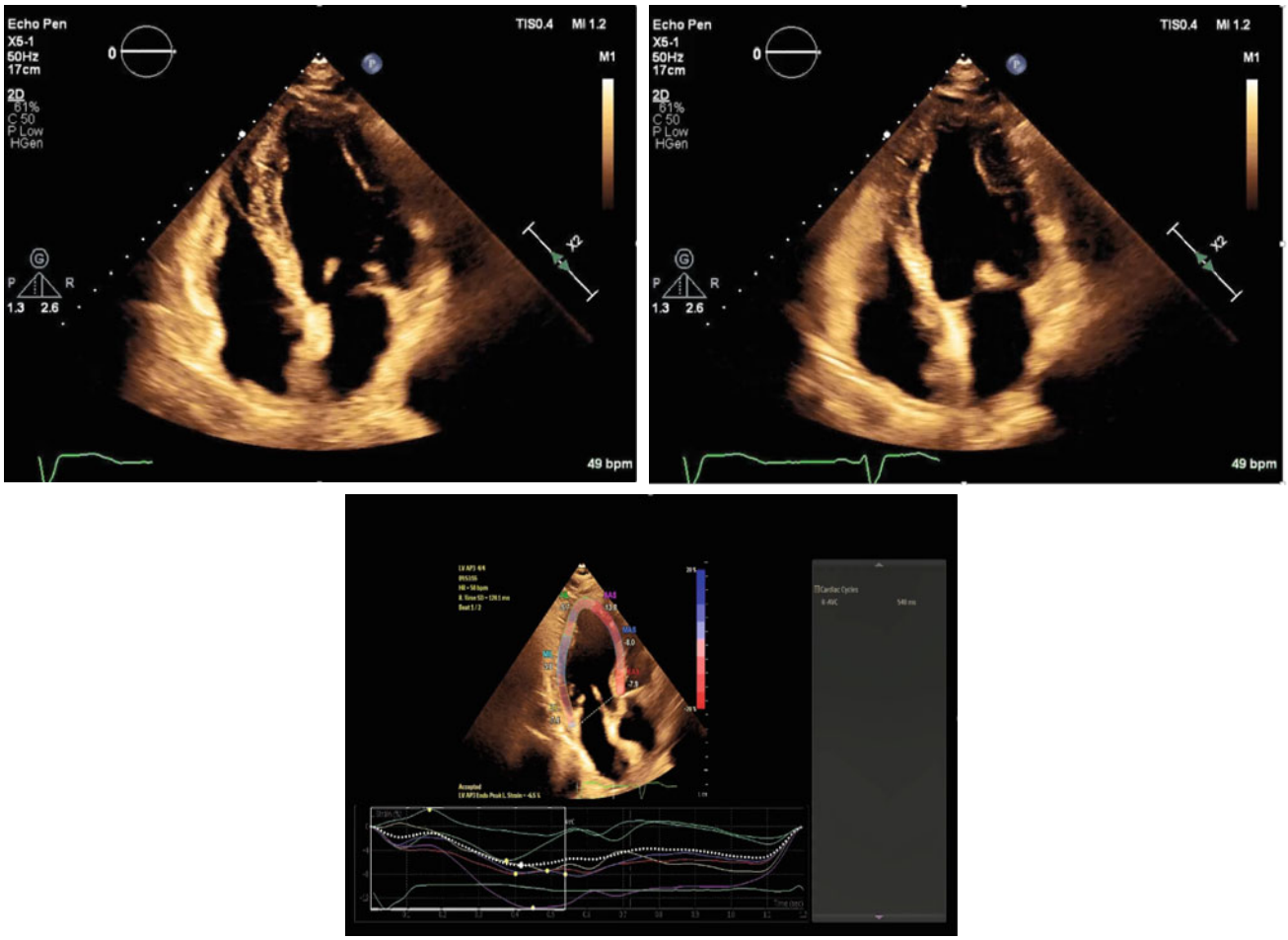

Fig. 30.1 Baseline echocardiogram (top): LVEF 30–35% with dyskinesis from LBBB in apical four-chamber views (end diastolic frame, left), and end systolic frame (right). Baseline global longitudinal strain (GLS) (bottom): Very low GLS of −8.8%. (apical three-chamber view)

3-D and reduced strain GLS −12.2%. This case illustrates the difficulties and challenges of cardiovascular management for these patients in spite of favorable hematological response (Fig. 30.4, Video 30.3).

30.3 Case 3. Thrombotic Complication of Ovarian Hyperstimulation in a Patient with Breast Cancer Followed by Cardiac Toxicity from Doxorubicin

- Young patients with breast cancer can undergo ovarian hyperstimulation and cryopreservation prior to initiation of chemotherapy for fertility preservation. This practice is associated with increased risk of thrombotic complications [12] and can become an additional cardiovascular risk to cancer-related treatment.

This is a 28-year-old female with Stage IIIB (cT2, cN3, cM0, G2, ER + , PR + , HER2-) right breast infiltrating ductal carcinoma. Her PET scan showed + FDG avidity in right breast, right axillary lymph nodes, and right internal mammary chain lymph nodes. She underwent ovarian hyperstimulation and next day was admitted with bilateral pleural effusions and right atrial thrombus, consistent with ovarian hyperstimulation syndrome. She started anticoagulation with intravenous heparin, subsequently switched to apixaban, and completed neoadjuvant treatment with dose dense AC (doxorubicin and cyclophosphamide) and subsequently underwent mastectomy. Echocardiogram post-ovarian stimulation prior to treatment: LVEF 50%, normal RV, right atrium with a partially mobile atrial mass attached to the posterior lateral free wall measured 1.43 × 1.34 cm, right ventricular systolic pressure of 43 mmHg. Cardiac MRI confirmed the 13 × 16 × 11 mm non-enhancing right atrial mass near the IVC connected to tip of the catheter

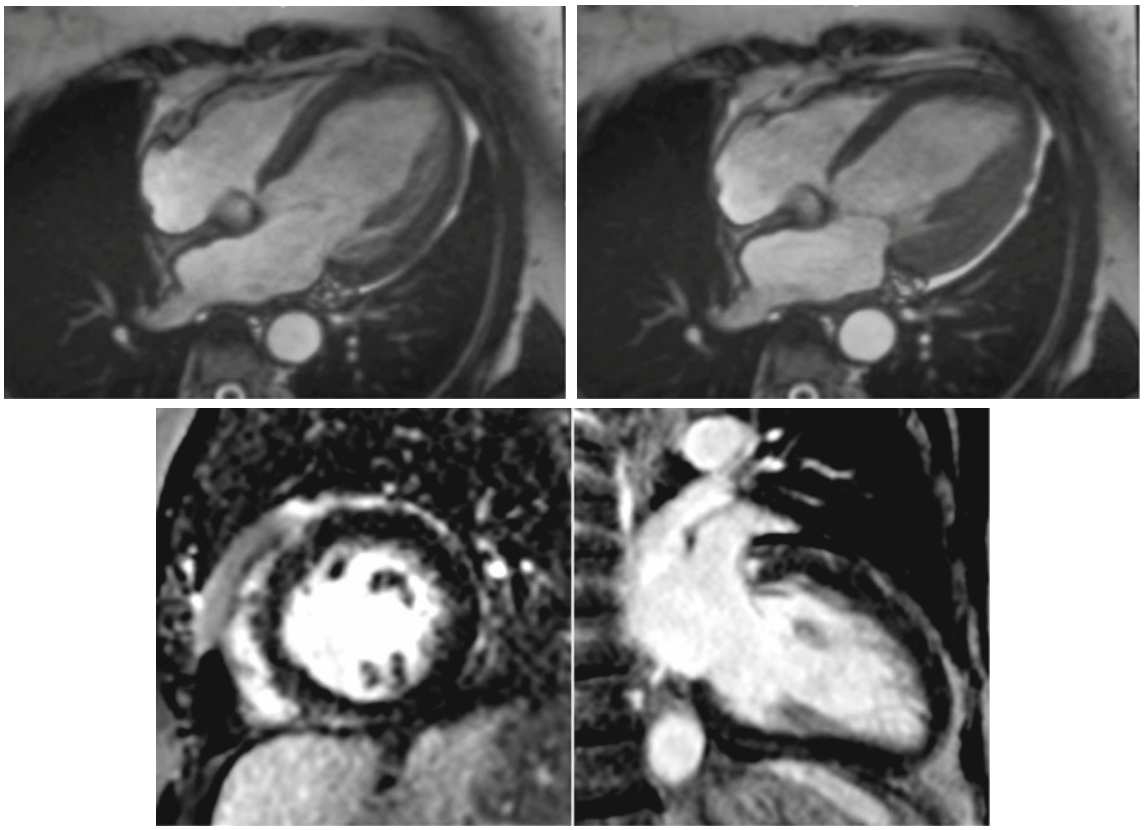

Fig. 30.2 Cardiac MRI: Top: Four-chamber balanced Steady-State Free Precession sequence: LV dilatation with moderate to severe global hypokinesis and septal dyskinesis. End diastolic frame (left) and end systolic frame (right) Bottom: Short Axis and two-chamber Phase-Sensitive Inversion Recovery sequence images (myocardial delayed enhancement imaging) showing appropriate nulling of the myocardial signal consistent with absence of underlying fibrosis, scar, or infiltrative process

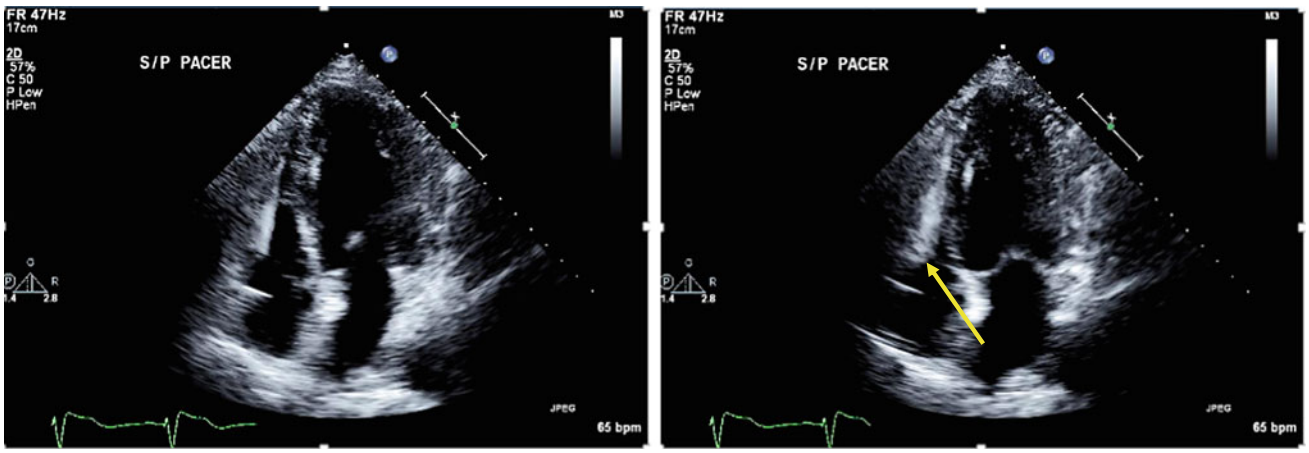

Fig. 30.3 LV Ejection fraction 44% post-CRT-D implantation seen in apical four-chamber view (left: end diastolic frame, right: end systolic frame). Pacemaker wire noticed in right ventricle (arrow)

consistent with a thrombus and normal LVEF with no pericardial effusion. After second dose of AC, LVEF decreased to 45% with mild global hypokinesis. She started low dose carvedilol for cardio-protection (limited by low blood pressure), had echo monitoring and biomarkers every 3–4 weeks. She received doses 3 and 4 of dose dense AC with off label dexrazoxane for cardiac protection and completed Taxol 12/12 prior to mastectomy. Post-treatment echocardiogram: LVEF 57% by 2-D, 50% by 3-D, GLS normal at −18.8%. Normal right

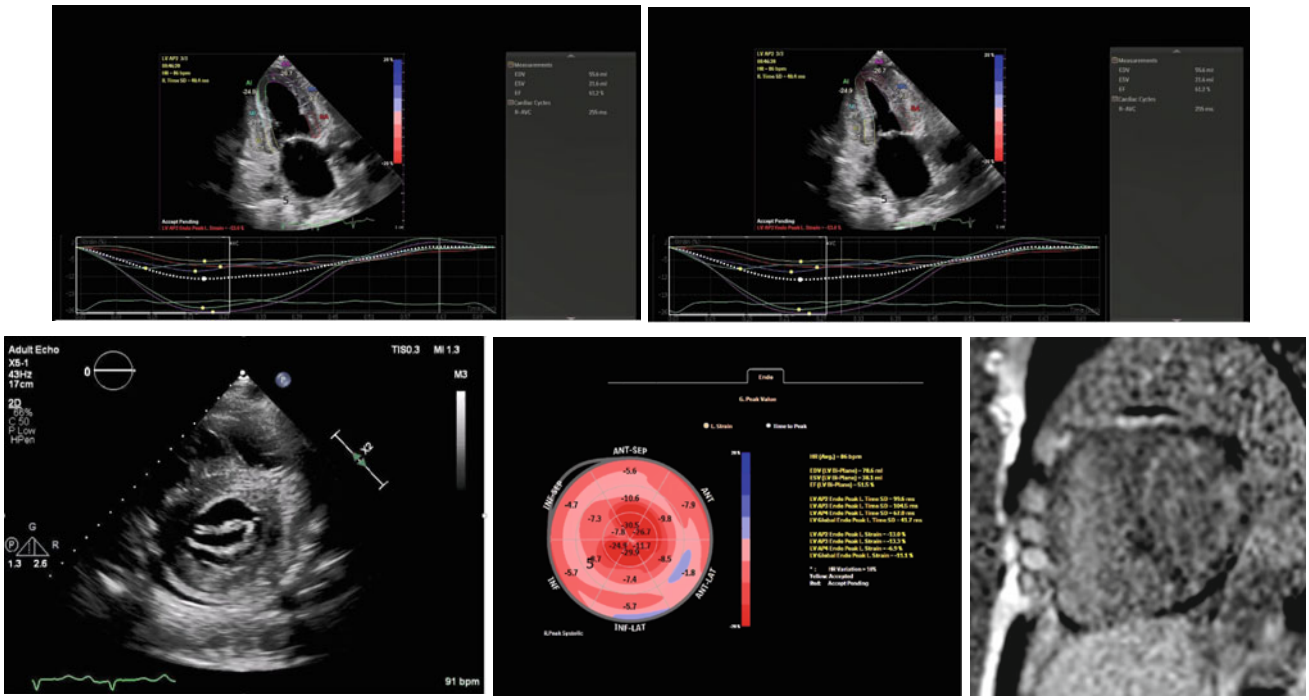

Fig. 30.4 Cardiac AL amyloidosis echocardiogram: apical two-chamber views end diastolic frame (top left) and end systolic frame (top right) and short axis view (bottom left): show moderate LVH with "sparkling" appearance, small LV cavity, EF 64%. Bottom center: Polar map illustrates reduced global longitudinal strain −11.1% with apical sparing pattern with reduced strain of basal segments and preserved strain at the apex, highly suggestive of cardiac amyloidosis. Bottom right: Cardiac MRI: Short Axis Phase-Sensitive Inversion Recovery sequence image (myocardial delayed enhancement imaging) shows diffuse poor nulling of the myocardial signal consistent with the presence of a myocardial infiltrative process

atrium. Right atrial thrombus was small, significantly improved compared to previous echocardiogram (Figs. 30.5 and 30.6, Videos 30.4 and 30.5).

30.4 Case 4. Check Point Inhibitor Myocarditis and Myasthenia Gravis in a Patient with Thymic Epithelial Tumor After Treatment with Pembrolizumab

- Pembrolizumab, an immune checkpoint inhibitor, is an IgG4 antibody that blocks interaction between programmed cell death protein 1 and programmed death-ligand 1. Myocarditis, an immune-related adverse event, has been reported in thymic epithelial tumors. Pembrolizumab has also been associated with development/exacerbation of myasthenia gravis (MG) [13].

A 70-year-old woman with metastatic thymic cancer presented to the hospital with shortness of breath, 21 days after initiation of pembrolizumab and was subsequently intubated due to respiratory failure. Her troponin levels were elevated with an electrocardiogram suspicious for myocardial infarction, but a coronary angiogram revealed normal coronary arteries and endo-myocardial biopsy confirmed the presence of myocarditis with lymphocytic infiltrates and myonecrosis. A dual-chamber pacemaker was placed due to complete heart block with asystole. Treatment was started with high-dose intravenous methylprednisolone and her cardiovascular status improved. However, the patient was unable to be weaned from mechanical ventilation and tested positive for acetylcholine receptor binding/blocking antibodies due to de novo MG. This case shows how pembrolizumab, a check point inhibitor is associated with increased risk of cardiovascular and neuromuscular adverse effects, particularly in patients with thymic epithelial tumors (Figs. 30.7, 30.8 and 30.9).

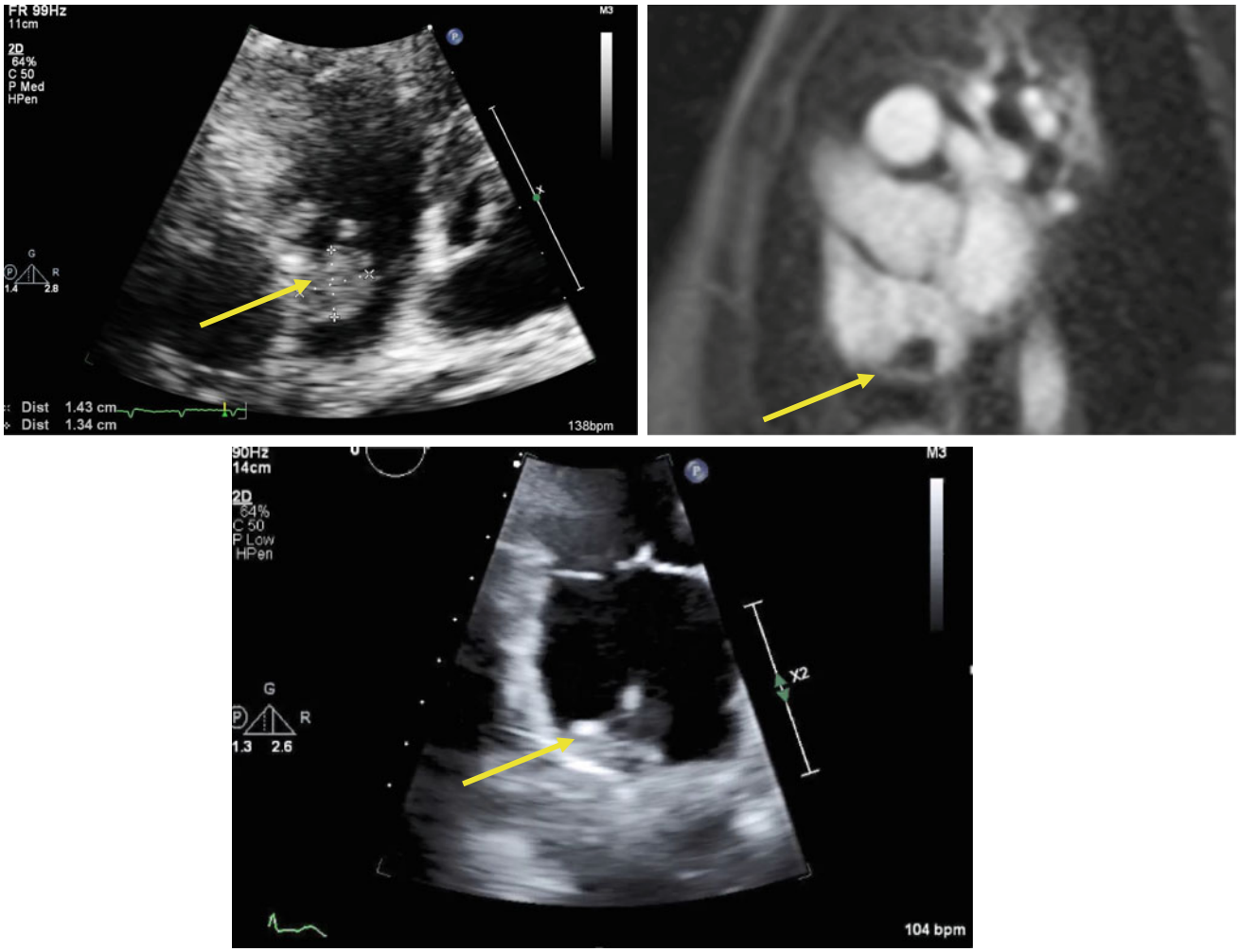

Fig. 30.5 Top left: 2-D echocardiogram shows rounded right atrial mass next to port catheter seen, measuring 1.43 × 1.34 cm in still image. Top right: MRI Short Axis Perfusion sequence during intravenous administration of contrast shows a non-enhancing hypo-intense mass in the right atrium Bottom: Resolving right atrial thrombus post-anticoagulation with apixaban

30.5 Case 5. Variant Angina and Coronary Vasospasm Due to Adjuvant Capecitabine (Xeloda) in Triple Negative Breast Cancer in the Absence Cardiovascular Risk Factors or Pre-existing CAD

- Capecitabine is an oral pro-drug of 5-fluoruracil (5-FU). While 5-FU is well known to cause endothelin-1 mediated endothelial dysfunction and subsequent coronary vasospasm, cases of variant angina associated with capecitabine therapy are less frequently described in the literature and under-recognized clinically.
- Shared decision-making is required to guide treatment. A trial of anti-anginal therapy can be utilized for mild cases, but termination of capecitabine is recommended for more severe cases.

A 52-year-old female without cardiovascular risk factors or cardiovascular disease was diagnosed with triple negative, stage 1 breast cancer. Pre-chemotherapy transthoracic echo (TTE) was normal, with EF 67% and GLS −24.8%. She underwent neoadjuvant chemotherapy with dose dense anthracycline, cyclophosphamide, and taxol (doxorubicin total dose 240 mg/m^2) followed by double mastectomy with negative lymph nodes. TTE 6 months post-anthracycline showed EF 66% and GLS −24.1%. Subsequently, she was treated with adjuvant capecitabine at 1000 mg/m^2 twice daily for 14 days every 3 weeks for 8 cycles. Since her first cycle of capecitabine, she noted exertional sub-sternal chest discomfort, burning quality, with radiation to the jaw, and relieved with rest. Her symptoms were present only when taking capecitabine and were not present in between cycles. Resting ECG was normal. Exercise ECG with myocardial perfusion imaging (in between capecitabine cycle) showed normal exercise capacity, no ischemic ST changes, and

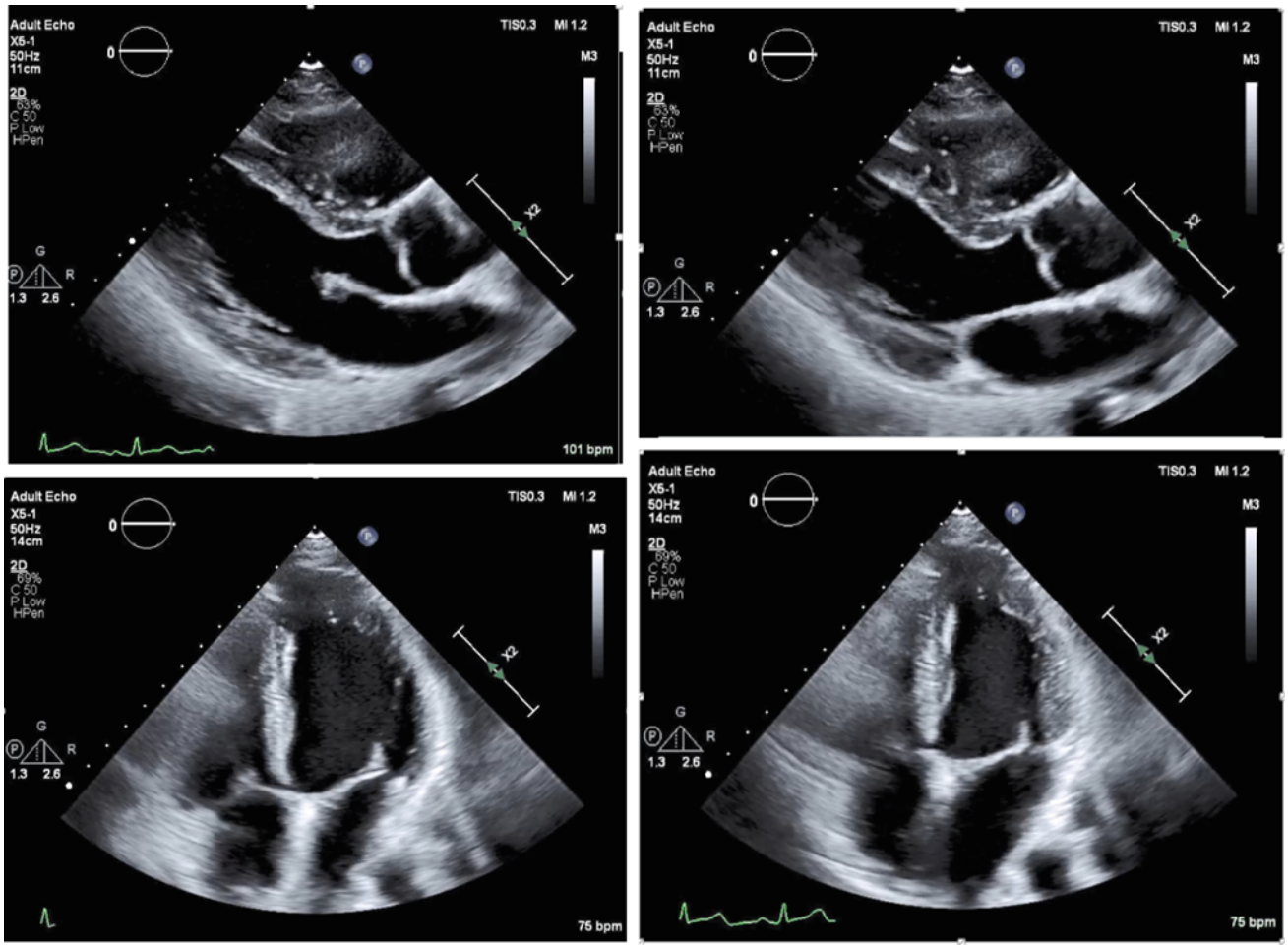

Fig. 30.6 Improved LV systolic function after cardioprotective strategy with carvedilol and dexrozaxane. LVEF 57% seen in parasternal long axis views (Top left: end diastolic frame; top right: end systolic frame) and apical four-chamber views (End diastolic frame bottom left; end systolic frame bottom right)

normal myocardial perfusion imaging. Given her typical angina despite normal exercise stress myocardial perfusion imaging, a coronary computed tomography angiogram (CCTA) was performed, which showed no coronary artery disease and a coronary artery calcium score of 0. The working diagnosis was vasospastic angina and amlodipine 5 mg daily and isosorbide mononitrate 30 mg daily were started which provided symptomatic relief with no further chest pain despite subsequent capecitabine dosing. Exercise testing in the midst of capecitabine dosing could have proven that ischemia was responsible for her chest pain but given her favorable clinical response to amlodipine and nitrates, this tact adds some small risk without clear clinical benefit. After discussion with her oncologist, capecitabine therapy was shortened to 6 cycles and anti-anginal medications were discontinued after completion of treatment. Patient remained asymptomatic on routine surveillance in survivorship clinic.

Capecitabine has been shown to be effective in prolonging disease-free survival and overall survival among patients with HER2 negative invasive breast cancer after neoadjuvant chemotherapy and standard surgery [14] and has therapeutic effects in a range of other cancers. Oral capecitabine is absorbed by the gastrointestinal tract and metabolized to 5-FU in vivo. The cardiotoxic effects of 5-FU (usually administered as IV infusion) are well described, but capecitabine induced vasospasm has only rarely been reported [15–18]. This case highlights the importance of awareness among community cardiologists and oncologists to recognize the lesser known side effects of common chemotherapeutic agents (Figs. 30.10 and 30.11).

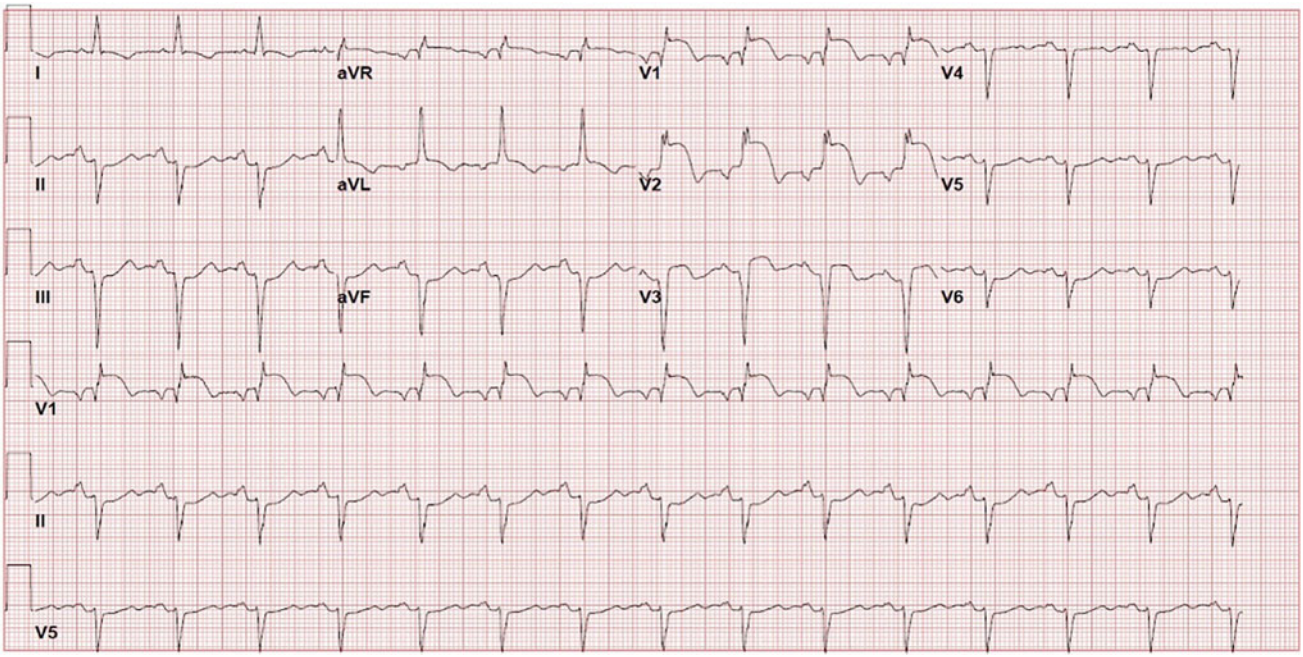

Fig. 30.7 Electrocardiography revealed a new right bundle branch block, with T-wave inversions in I and aVL, poor R-wave progression, ST elevation in precordial leads, and Q-waves in anterolateral leads, suggestive of anterior myocardial infarction (From Szuchan et al. [13]; with permission from Oxford University Press.)

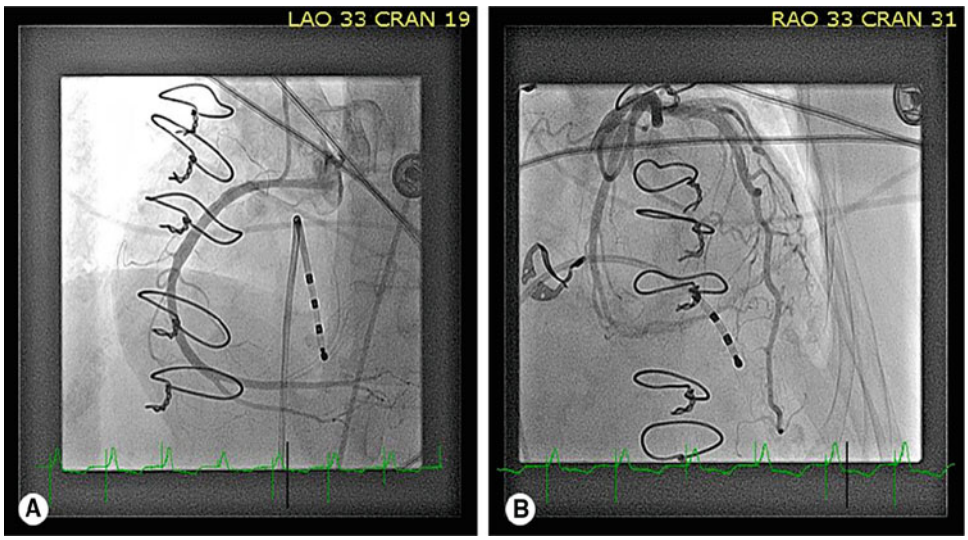

Fig. 30.8 Coronary angiography revealed normal coronary artery anatomy, as seen in left anterior oblique—cranial (**a**) and right anterior oblique—cranial (**b**) views (From Szuchan et al. [13]; with permission from Oxford University Press.)

30.6 Case 6. Radiation-Induced CAD and Aortic Stenosis

- Chest radiation, primarily when administered to patients with breast cancer or lymphoma, can result in severe proximal coronary artery disease (CAD) or valvular heart disease.
- Screening measures should be implemented in appropriate patients to evaluate for cardiovascular complications.

A 53-year-old man had a history of diabetes mellitus, hyperlipidemia, and Hodgkin's Disease diagnosed in 1985 (at the age of 18). He was treated with mechlorethamine hydrochloride, vincristine, procarbazine, prednisone (MOPP) and adriamycin, bleomycin, vinblastine, dacarbazine (ABVD) followed by radiation therapy to the chest. He was referred to a cardiologist in May 2014 after a systolic murmur was heard, and an echo at that time revealed mild aortic stenosis (AS). He was lost to follow-up until April 2018, at which time a repeat echo revealed moderate AS. An

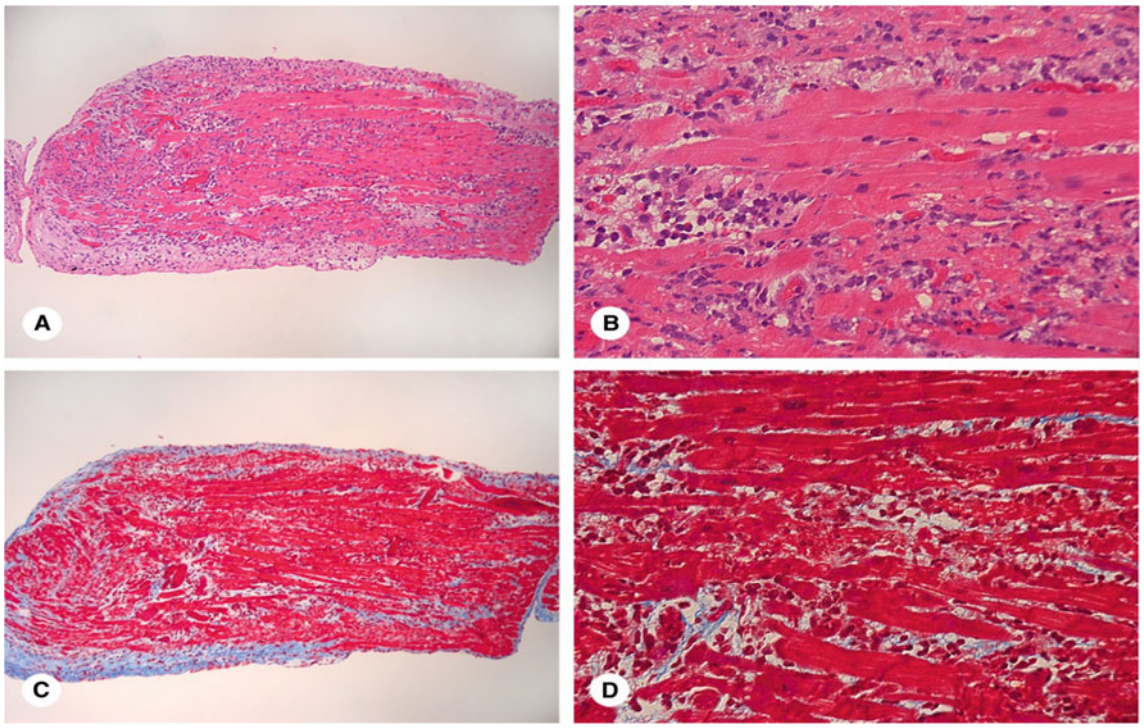

Fig. 30.9 Endomyocardial biopsy: **a** and **c** Light micrograph of a biopsy sample of myocardium. The endocardium surrounds the entire biopsy piece (blue fibrous tissue in c). The normal endocardium is seen in the right lower corner of the piece. The remainder of the endocardium is much thicker and shows mononuclear cells as well as spindle shaped cells (fibroblasts) indicating a repair process. The myocardium shows abundant inflammatory infiltrate as well as areas of interstitial fibrosis (blue stain in c). **b** and **d** Higher magnification shows the inflammatory infiltrates (predominantly lymphocytes and macrophages with a minor component of neutrophils and eosinophils) which encroach and separate the myocyte bundles. The interstitial fibrosis is more subtle but present (blue in d), indicating a repair process ongoing concomitantly with the inflammatory process (From Szuchan et al. [13]; with permission from Oxford University Press)

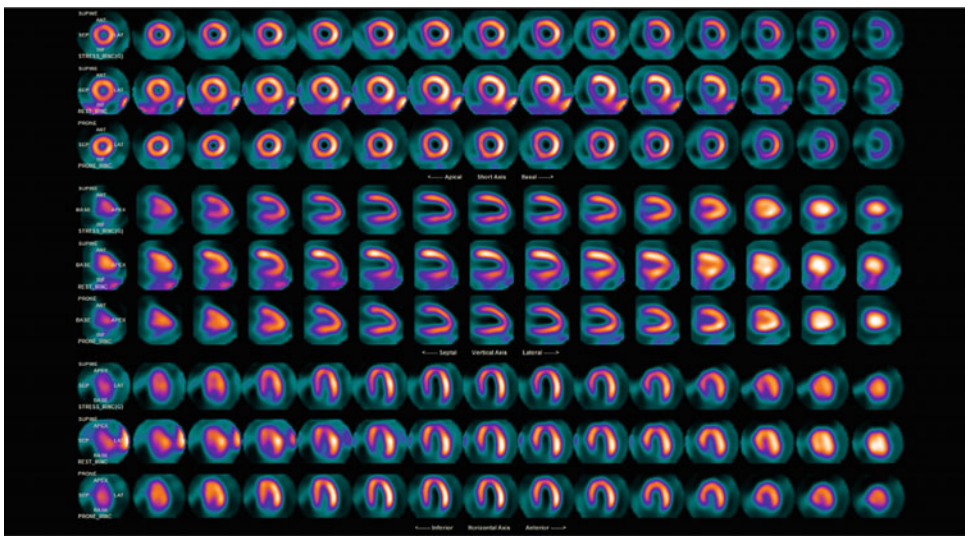

Fig. 30.10 SPECT (Single Positron Emitted Computed Tomography) images showing normal myocardial perfusion in all segments

echo in April 2019 was consistent with moderate-severe AS. In August 2019 he presented with dyspnea with minimal exertion and new T-wave inversions in the anterior leads. Right and left heart catheterization revealed moderate-severe AS (AVA 0.98 cm^2) (Fig. 30.12) and the LAD with 95% proximal stenosis (Fig. 30.13). The patient underwent successful DES-LAD in September 2019. He subsequently underwent TAVR for progressive symptomatic severe AS in March 2020.

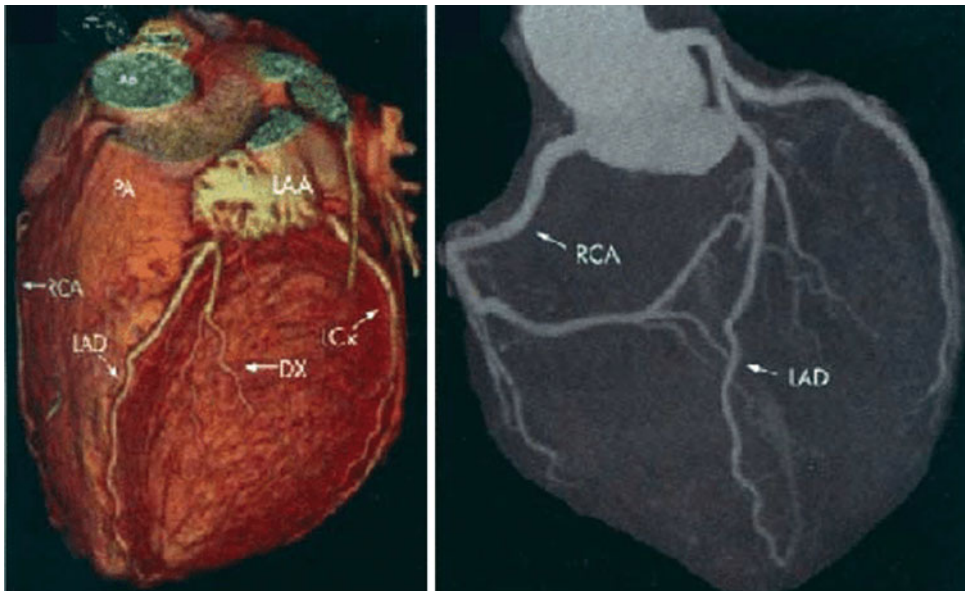

Fig. 30.11 Coronary Computed Tomography Angiogram (CCTA) reformatted images reveal normal coronary anatomy

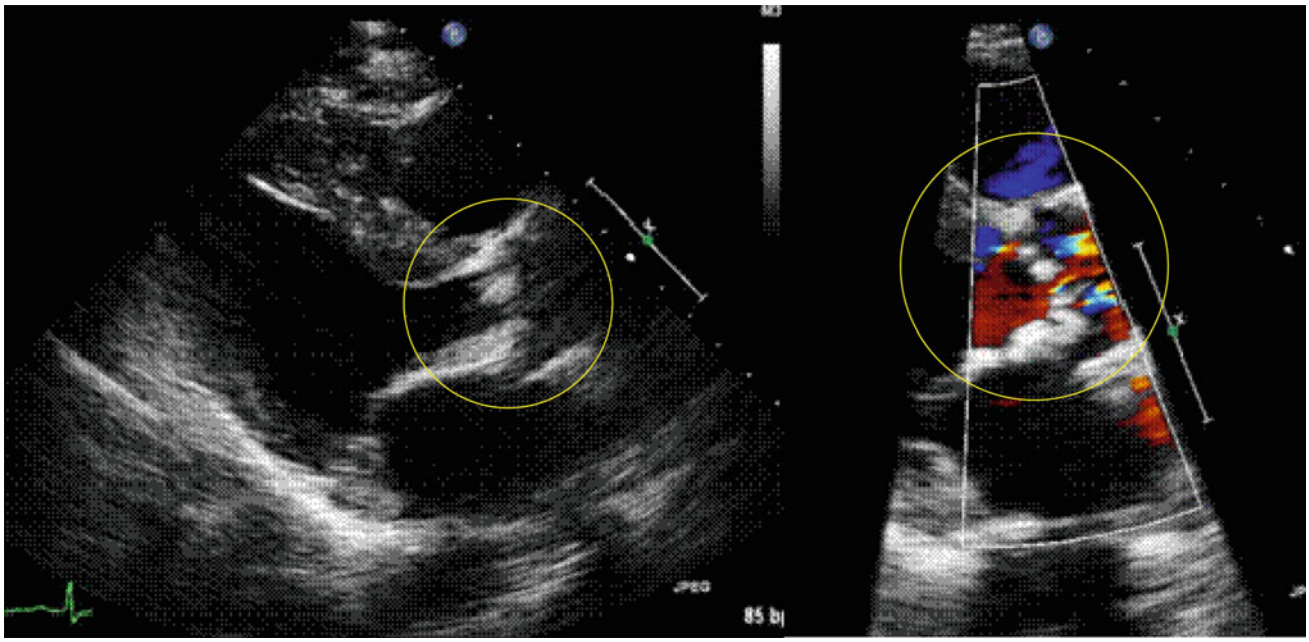

Fig. 30.12 TTE showing severe AS on imaging (left) and color doppler (right)

There is an increased risk of radiation-induced CAD in patients with Hodgkin's disease who were exposed to chest radiation at an age younger than 25 years old that further increases proportionally to total radiation dose and lack of cardiac shielding techniques [19]. Valvular heart disease is also seen after mantle radiation for Hodgkin's Disease, with aortic stenosis being the most common valvular abnormality [20]. The diagnosis of radiation-induced heart disease is most commonly made in the community setting, as this is usually identified at least 10–20 years following treatment. With the advent of TAVR, outcomes have been shown to be significantly better than SAVR [21]. This case highlights the need for long-term routine screening for radiation-induced heart disease (Videos 30.6 and 30.7).

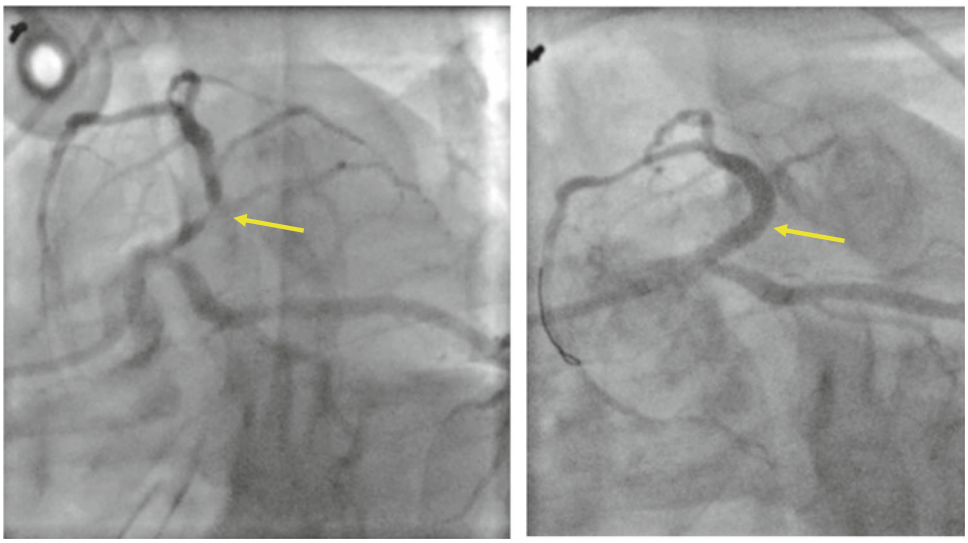

Fig. 30.13 Left, angiogram showing severe proximal LAD stenosis. Right, showing LAD stenosis status post-drug eluting stent placement

30.7 Case 7. Severe LV Dysfunction in a Patient with Breast Cancer and Cardiotoxic Chemotherapy Caused by Severe Multi-Vessel CAD

- Despite the known association of LV dysfunction and potentially cardiotoxic chemotherapy, comorbid multi-vessel CAD must be diagnosed and treated.

A 63-year-old female with a history of hyperlipidemia and diabetes mellitus was diagnosed with right breast cancer in October 2018. She underwent right breast lumpectomy and was staged and typed as T2N1 ICD ER + /PR + /HER2 + breast cancer. She was given Adriamycin and cyclophosphamide followed by paclitaxel (Taxol), (AC-T) followed by right chest radiation for 35 sessions. In March 2019 she was started on adjuvant Herceptin/Perjeta with an initial echo EF of 55–60%, GLS –19.6% (Fig. 30.14). In May 2019 her EF was 50–55%, GLS –18.1%. Her EF was similar in August 2019, but her GLS was –17.4%. Low dose carvedilol/valsartan was added. Prior to her next dose of Herceptin/Perjeta, an echo revealed LV EF of 40–45% with GLS –15.5%. Chemotherapy was held and a repeat echo now revealed LV EF 30–35% and GLS –11.8%. The patient was admitted to her local hospital with progressive dyspnea with minimal exertion, and diagnosed with acute systolic CHF. She was treated with IV diuresis with improvement in her symptoms, and an echo on 12/3/19 revealed LV EF 20% with a GLS of –7% (Fig. 30.15) Coronary angiography was completed on 12/16/19 with critical stenoses in the LAD, OM1, and possibly the RCA (Fig. 30.16) CABG surgery was considered, but given her comorbidities and condition, multi-vessel PCI was done. She underwent successful DES-LAD/OM1 and the RCA was found not to be significant by fractional flow reserve (FFR). Post-procedure TTE on 5/11/20 showed improvement with LV EF 50–55%, and GLS –17% (Fig. 30.17).

In this case, multi-vessel CAD was found to be the culprit for her left ventricular dysfunction, and revascularization led to the improvement of LV systolic function (Videos 30.7 and 30.8).

30.8 Case 8. Radiation-Induced Carotid Stenosis Detected on Routine Surveillance

- Patients with head and neck cancer treated with external beam radiation are at increased risk for developing radiation-induced carotid stenosis (RICS) and subsequent cerebrovascular events, events that carry high morbidity and mortality [21].
- Protocols for screening and monitoring for RICS in these high risk patients and referral for revascularization, when appropriate, are of paramount importance.

A 61-year-old male with head and neck cancer was treated with surgery, cisplatin, and radiation therapy 6 years ago. He was referred to a local cardiologist with expertise in cardio-oncology for risk factor management. Due to the prior neck irradiation, the cardiologist ordered a routine, screening duplex scan of his carotid arteries, which demonstrated a 20–39% stenosis in the right internal carotid

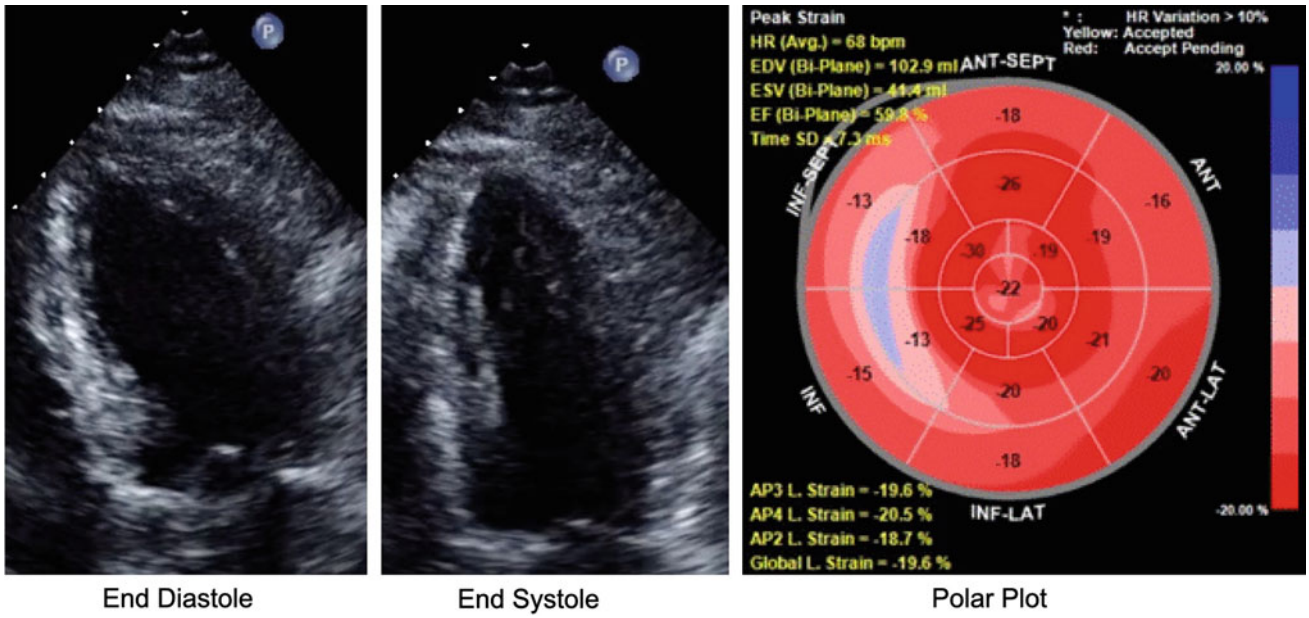

Fig. 30.14 Pre-chemotherapy TTE normal ejection fraction, global longitudinal strain, and polar plot

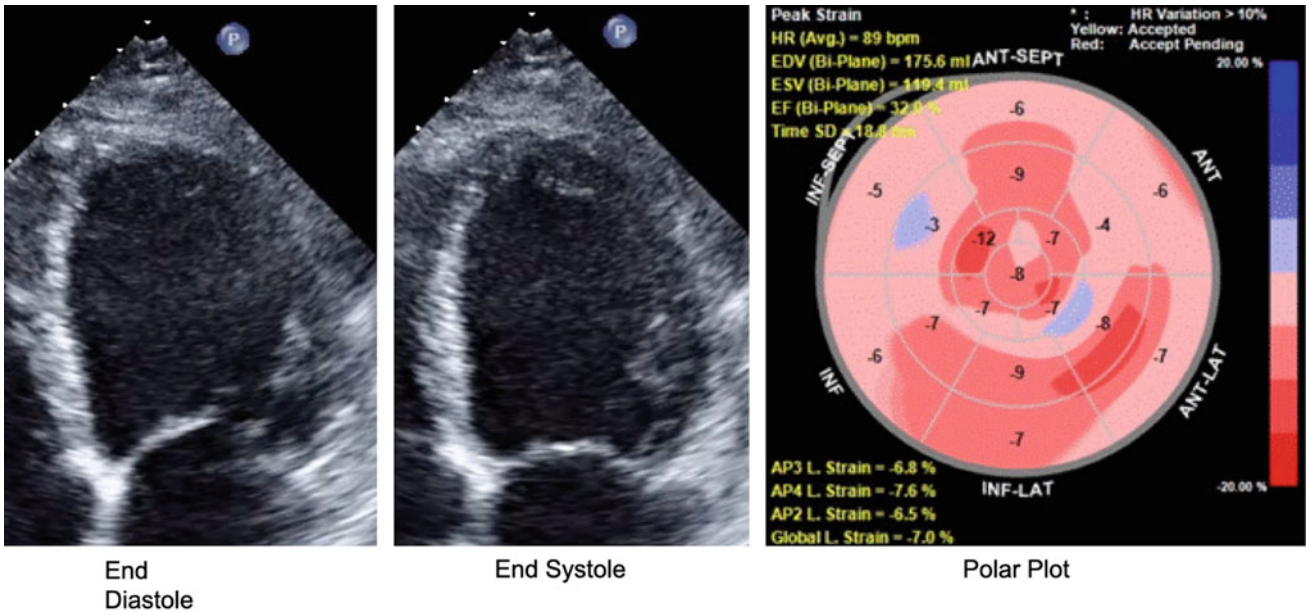

Fig. 30.15 Abnormal TTE with severely decreased ejection fraction, severely abnormal global longitudinal strain/polar plot

artery (ICA) and a 40–59% stenosis in the left ICA (Fig. 30.18). He was placed on a single antiplatelet drug and statin therapy, and routine, surveillance duplex sonography was recommended at 1–2 years interval. At the second surveillance duplex, there was a significant change with increased velocities (Fig. 30.19, Video 30.9) and disordered flow in the distal left ICA. A computed tomography angiogram (CTA) verified a critical (90%) stenosis (Fig. 30.20) and he was referred for carotid artery stenting. The patient obtained a number of opinions from different centers and elected to undergo carotid endarterectomy which was complicated by a stroke. He recovered with minor residual deficit and subsequent studies verified a complete occlusion of his left ICA (Fig. 30.21).

Patients with head and neck cancer treated with external beam radiation are at increased risk for developing radiation-induced carotid stenosis (RICS) and subsequent cerebrovascular events, with potential for significant

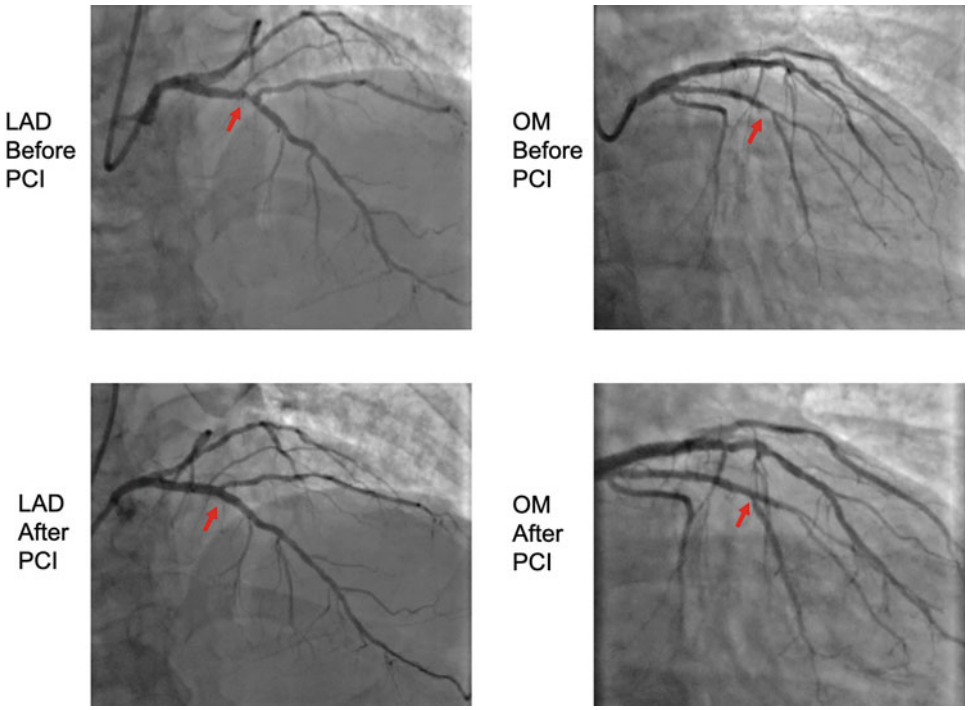

Fig. 30.16 Significant stenosis in proximal LAD and proximal OM1 pre- and post-percutaneous coronary intervention

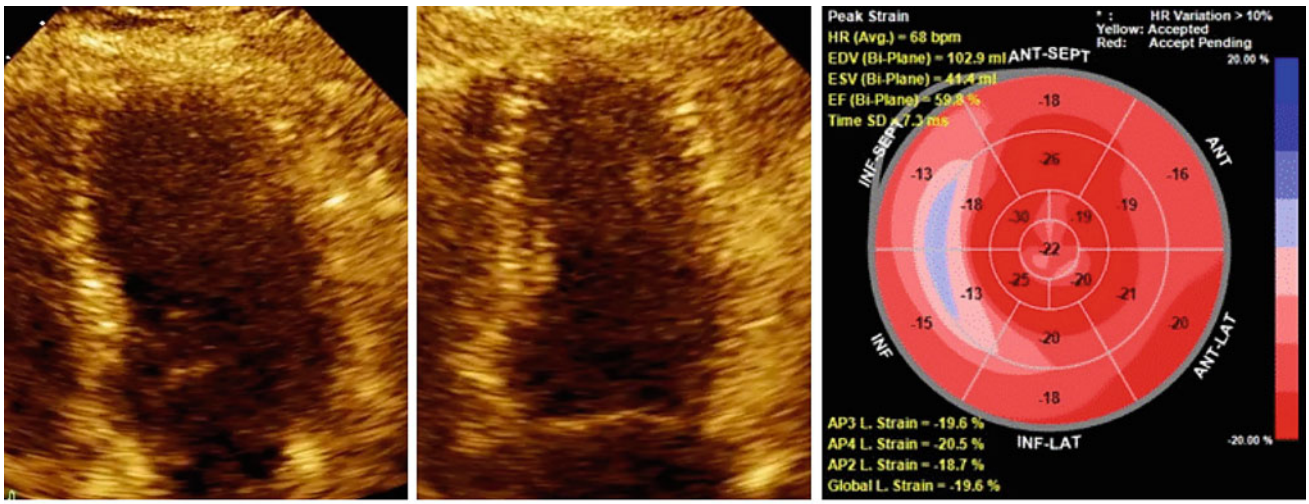

Fig. 30.17 Post-revascularization normalization of ejection fraction, global longitudinal strain, and polar plot

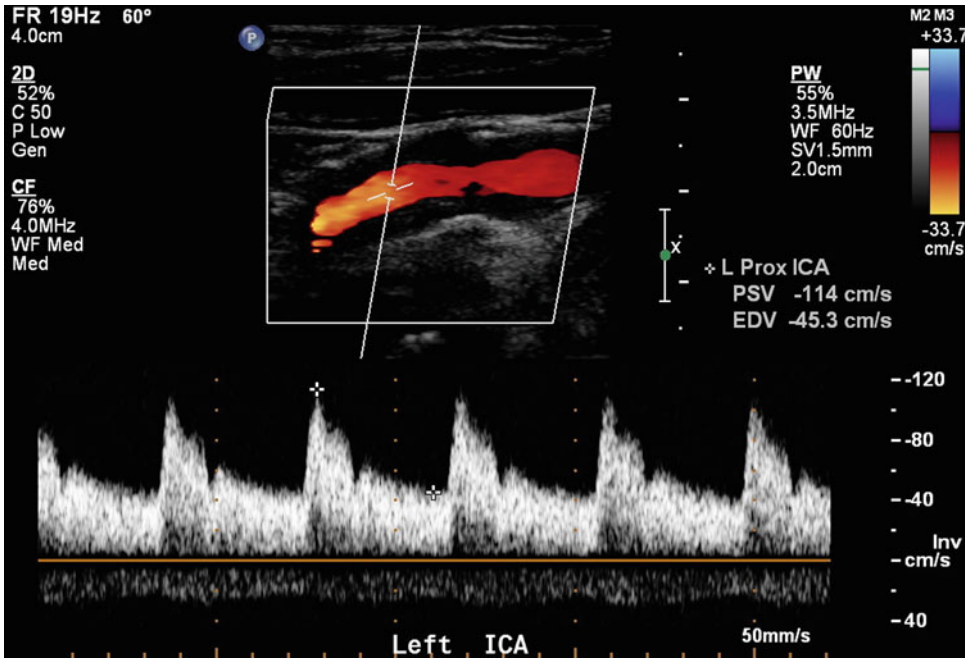

Fig. 30.18 Carotid Duplex showing moderate LICA stenosis

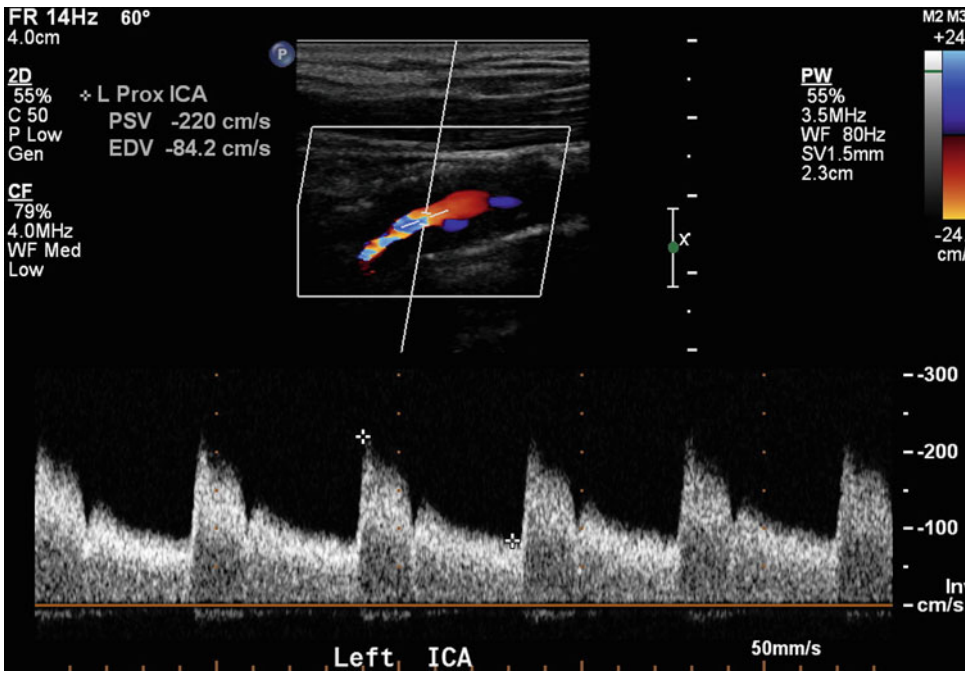

Fig. 30.19 Carotid Duplex showing worsening stenosis and higher velocities

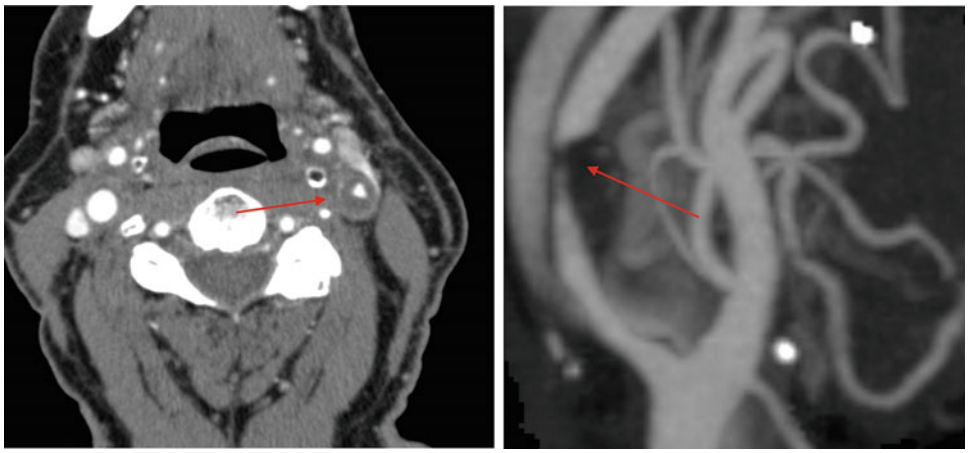

Fig. 30.20 CTA Neck showing greater than 90% LICA stenosis

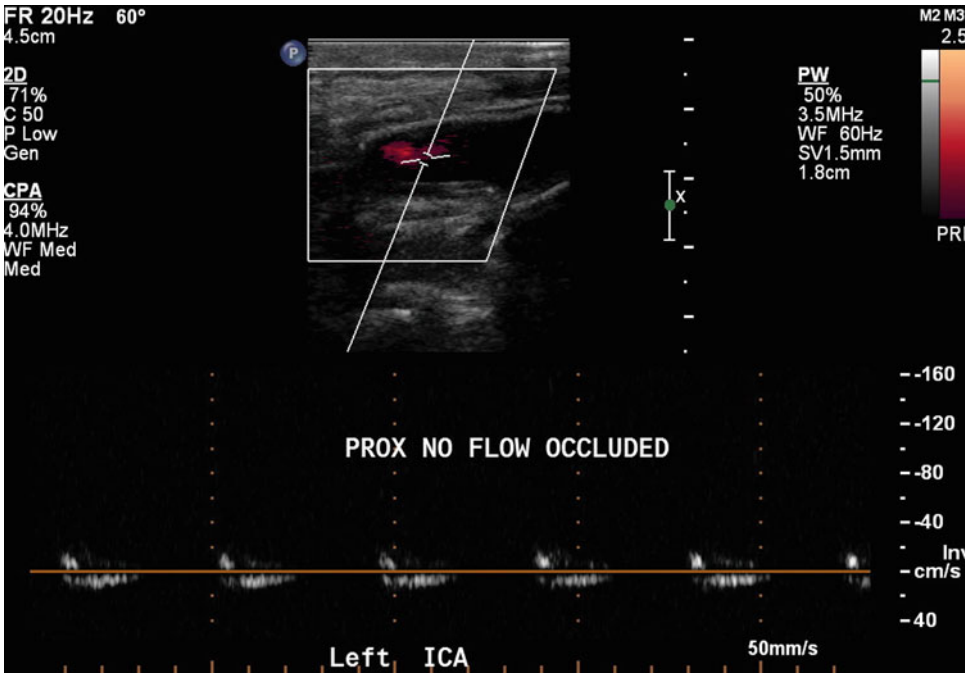

Fig. 30.21 Carotid Duplex showing occluded LICA

morbidity and mortality [22]. These patients may present innocuously to the community cardiologist, who must recognize the potential for delayed effects of radiation. Imaging with duplex sonography is the screening test of choice, commencing 3–5 years after treatment with radiation [23]. If a mild to moderate stenosis is discovered, surveillance should be considered thereafter at periodic intervals as the disease is different from standard atherosclerosis and can have a more aggressive course [24]. Surveillance should be carried out in a high quality, validated laboratory. If a severe stenosis is suspected, angiography (computed tomography, magnetic resonance, or digital subtraction) should be used to verify the findings. Although the data are scant with the use of statins, antiplatelets, and antihypertensives, it is prudent to engage in aggressive risk factors management. Patients with or without neurologic symptoms and a severe carotid artery stenosis should be considered for revascularization [24]. The standard management for carotid stenosis has been surgical carotid endarterectomy, an operative approach had been associated with higher complication rates, including wound complications and cranial nerve injuries [25]. Carotid artery stenting has been demonstrated to be equivalent to endarterectomy [26] and given the increased risks with open surgery in a radiated neck, it should be considered as an alternative in RICS.

References

1. Siegel RL, Miller KD, Jemal A. Cancer statistics. CA Cancer J Clin. 2018;68:7–30.
2. Herrmann J. From trends to transformation: where cardio-oncology is to make a difference. Eur Heart J. 2019;40:3898–900.
3. Sturgeon KN, Deng L, Bluethman SL, et al. A population based study of cardiovascular disease mortality risk in US cancer patients. Eur Heart J. 2019;40:3889–97.
4. Bluethmann SM, Mariotto AB, Rowland JH. Anticipating the "Silver Tsunami." Cancer Epidemiol Biomarkers Prev. 2016;25:1029–36.
5. Fradley MG, Brown AC, Shields B, et al. Developing a comprehensive cardio-oncology program at a cancer institute: the Moffitt experience. Oncol Rev. 2017;11:340.
6. Barac A, Murtagh G, Douglas P, et al. Health of patients with cancer and cancer survivors. JACC. 2015;65:2739.
7. Sadler D, Chaugalian C, Cubeddu R, Stone E, Samuel T, et al. Practical and cost effective model to build and sustain a cardio-oncology program. Cardio Oncol J. https://doi.org/10.1186/s40959-020-00063-x.
8. Sadler D, Fradley M, Ismail Khan R, Raez L, Bhandare D, Elson L, Perloff D, et al. Florida inter-specialty collaborative project to improve cardio oncology awareness and identify existing gaps. JACC Cardio Oncol.
9. Sadler D, Arnold A, Ismail-Khan R, Fradley M, Guerrero P et al. FCACC and FLASCO cardio oncology online educational platform. 2020. https://accfl.org/Cardio-Oncology.
10. Sadler D, DeCara J, Herrmann J, Arnold A, Ghosh A, Abdel-Quadir H, Yang E, Smith S, Ahter N, Leja M, Carvalho Silva C, Raikhelkar J, Brown SA, Dent S, O'Quinn R, Thuny F, Moudgil R, Raez L, Okwuosa T, Daniele A, Bauer B, Kondapalli L,Ismail-Khan R, Lax J, Blaes A, Nahleh Z, Elson L, Baldassarre L, Zaha V, Rao V, Sierra Lara D, Skurka K. COVID-19 pandemic and its impact on cardio oncology: results from the COVID-19 international collaborative network survey. JACC Cardio Oncol.
11. Lynce F, Barac A, Geng X, et al. Prospective evaluation of the cardiac safety of HER2-targeted therapies in patients with HER2-positive breast cancer and compromised heart function: the SAFE-HEaRt study. Breast Cancer Res Treat. 2019;175:595–603. https://doi.org/10.1007/s10549-019-05191-2.
12. Yechiel S, Schenker JG. Ovarian hyperstimulation syndrome and thrombotic events. Am J Rep Immun. 2014;6(72):541–8.
13. Szuchan C, Elson L, Alley E, Leung K, Nahleh Z, Sadler D. Check point inhibitor myocarditis and myasthenia gravis in a recurrent metastatic thymic carcinoma patient: a case report. Eur Heart J. 2020;4(3):1–8. https://doi.org/10.1093/ehjcr/ytaa051.
14. Masuda, et al. Adjuvant capecitabine for breast cancer after preoperative chemotherapy. NEJM. 2017;376:2147–59.
15. Golias et al. Acute presentation of vasospastic angina induced by oral capecitabine: a case report. J Med Case Rep. 2014;18.
16. Schnetzler B, Popova N, Collao Lamb C, Sappino AP. Coronary spasm induced by capecitabine. Ann Oncol. 2001;12:723–4.
17. Rizvi AA, Schauer P, Owlia D, Kallal JE. Capecitabine-induced coronary vasospasm: a case report. Angiology. 2004;55:93–7.
18. Aksoy S, Karaca B, Dinçer M, Yalçin S. Common etiology of capecitabine and fluorouracil-induced coronary vasospasm in a colon cancer patient. Ann Pharmacother. 2005;39:573–4.
19. Frederika A, et al. Cardiovascular disease after hodgkin lymphoma treatment. JAMA Intern Med. 2015;175(6):1007–17.
20. Hull MC, Morris CG, Pepine CJ, Mendenhall NP. Valvular dysfunction and carotid, subclavian, and coronary artery disease in survivors of hodgkin lymphoma treated with radiation therapy. JAMA. 2003;290:2831–7.
21. Zhang D et al. Outcomes of patients with severe symptomatic aortic valve stenosis after chest radiation: transcatheter versus surgical aortic valve replacement. J Am Heart Assoc. 2019;8e012110.
22. Cheng SW, Ting AC, Lam LK, Wei WI. Carotid stenosis after radiotherapy for nasopharyngeal carcinoma. Arch Otolaryngol Head Neck Surg. 2000;126(4):517–21. https://doi.org/10.1001/archotol.126.4.517. PMID: 10772307.
23. Xu J, Cao Y. Radiation-induced carotid artery stenosis: a comprehensive review of the literature. Interv Neurol. 2014;2(4):183–92. https://doi.org/10.1159/000363068. PMID: 25337087; PMCID: PMC4188157.
24. Brott TG, Halperin JL, Abbara S, et al. 2011 ASA et al guideline on the management of patients with extracranial carotid and vertebral artery. J Am Coll Cardiol. 2011;22,57(8):1002–44. https://doi.org/10.1016/j.jacc.2010.11.005.
25. Tallarita T, Oderich GS, Lanzino G, et al. Outcomes of carotid artery stenting versus historical surgical controls for radiation-induced carotid stenosis. J Vasc Surg. 2011;53(3):629–36.e1–5. https://doi.org/10.1016/j.jvs.2010.09.056. PMID: 21216558.
26. Gurm HS, Yadav JS, Fayad P, et al. Long-term results of carotid stenting versus endarterectomy in high-risk patients. N Engl J Med. 2008;358:1572–9.

Cardio-Oncology in the COVID-19 Era

31

Stephanie Feldman, Kristine Jang, Dylana Smith, and Robert S. Copeland-Halperin

Key Points

- Chest imaging in patients with COVID-19 share features that overlap with toxicities of radiation and immunotherapy.
- Lung cancer is prevalent among patients hospitalized with COVID-19.
- Abnormal troponin elevation occurs in COVID-19 and is associated with adverse outcomes.
- COVID-19 causes a systemic hyperinflammatory response. Vascular damage has been more pronounced in children.
- Both malignancy and COVID-19 infection are associated with hypercoagulable states.
- Atrial and ventricular arrhythmia occur frequently in critically ill patients with COVID-19.

31.1 Introduction

In December 2019, Wuhan city, the capital of Hubei province in China, became the center of an outbreak of pneumonia caused by the virus SARS-CoV-2, designated in February 2020 as coronavirus disease 2019 (COVID-19) by the World Health Organization [1]. This outbreak evolved into a global pandemic, with cases and deaths transforming the infection into a world health crisis. Cardiovascular disease and cancer are independently associated with increased risks for coronavirus infection and adverse outcomes from COVID-19 [2–4]. Patients with COVID-19 develop ischemic and non-ischemic myocardial injury, arrhythmias, and thrombotic complications through multiple overlapping mechanisms, which share features in common with complications of cancer therapies. Pericarditis, acute coronary syndromes, stress cardiomyopathy, myocarditis, atrial and ventricular arrhythmia, QT-interval prolongation, and right ventricular dysfunction reported in patients with COVID-19 bear a striking resemblance to potential cardiotoxicities of cancer therapies. Therefore, in cancer patients infected by SARS-CoV-2, cardiovascular complications have critical implications for ongoing cancer treatment [5–10].

31.2 Lung Imaging in Cancer Patients with COVID-19

Chest imaging is routine in the follow-up of patients with cancer, and findings consistent with COVID-19 infection occur frequently. Chest computed tomography is abnormal in > 85% of patients with COVID-19 [11]. Typical findings include subpleural and peripheral ground-glass opacification and consolidation. Lung involvement is bilateral in 75% of cases [12].

COVID-19 pneumonia shares common clinical, laboratory, and radiographic features with radiation and immunotherapy related pneumonitis [13]. Clinically, radiation pneumonitis typically presents with dyspnea and dry, non-productive cough, and with fever when severe. Symptomatic pneumonitis from radiation usually occurs within 3 months of the end of treatment, is more often unilateral, and its distribution corresponds to the radiation treatment field [14]. Elevated Westergren sedimentation rate (ESR),

Electronic supplementary material
The online version of this chapter (https://doi.org/10.1007/978-3-030-70998-3_31) contains supplementary material, which is available to authorized users.

S. Feldman · K. Jang · D. Smith
Memorial Sloan Kettering Cancer Center, 1275 York Avenue, New York, NY 10065, USA
e-mail: stephaniefeldman@gmail.com

K. Jang
e-mail: Jangk@mskcc.org

D. Smith
e-mail: Smithd8@mskcc.org

R. S. Copeland-Halperin (✉)
Department of Cardiology, Northwell Health (Zucker School of Medicine at Hofstra /Northwell), 270-05 76th Avenue, New Hyde Park, NY 11042, USA
e-mail: RCopelandHal@northwell.edu

R. M. Steingart et al. (eds.), *Atlas of Imaging in Cardio-Oncology*, https://doi.org/10.1007/978-3-030-70998-3_31

C-reactive protein (CRP), ferritin, and d-dimer, with normal procalcitonin, characterize both radiation pneumonitis and COVID-19 pneumonia. Lymphopenia, a hallmark feature of COVID-19, is also common following radiotherapy, as lymphocytes are relatively radiosensitive. Lymphocyte count reduction was reported in as many as 67% of patients with non-small cell lung cancer (NSCLC) undergoing chemoradiation [15]. On imaging, radiation pneumonitis appears as ground-glass opacities (GGO) initially, progressing to patchy areas of consolidation at its peak phase [14]. Pulmonary interstitial thickening characterizes both severe radiation pneumonitis and COVID-19. The incidence of immune-checkpoint inhibitor-related pneumonitis is 2.5–5% with anti-PD-1/PD-L1 monotherapy and 7–10% with combination therapy [16, 17], and may also exhibit radiographic features similar to COVID-19 pneumonia [18, 19].

The profound systemic inflammatory response that characterizes fulminant COVID-19 initially raised concern that immunotherapy would influence infection severity, but observations from cohorts of cancer patients with COVID-19 receiving immune-checkpoint inhibitors (ICI) did not indicate an association between the interval from last ICI administration and severity of COVID-19 illness [20, 21].

31.3 Myocardial Injury in COVID-19

Myocardial injury, defined by abnormal troponin elevation, occurs in approximately 20% of patients hospitalized with COVID-19 and is associated with pre-existing clinical cardiovascular disease, hypertension, diabetes, and cancer [22]. In a series of 52 patients with cancer and COVID-19, myocardial injury was evident in 15% [23]. Troponin release correlates with increased levels of systemic inflammatory markers and is associated with clinical deterioration, progressive respiratory failure, and mortality [22, 24]. In one report, among 671 patients hospitalized with COVID-19, elevated cardiac troponin-I predicted in-hospital mortality with an area under the ROC of 0.92 (95% confidence interval [CI], 0.87–0.96; sensitivity 0.86, specificity 0.86; $p < 0.001$) [25].

Myocardial injury in COVID-19 occurs through several mechanisms [5, 9, 10]. SARS-CoV-2 may cause direct myocardial damage with features of myocarditis [8]. Inflammation promotes coronary atherosclerotic plaque rupture, endothelial dysfunction, and activation of the coagulation cascade [6, 10]. Hypoxia, pulmonary edema, and augmented sympathetic tone create myocardial supply–demand mismatch and vascular and myocardial vulnerability [10]. Inflammatory cytokines associated with the systemic inflammatory response also cause apoptosis and necrosis of cardiac myocytes [26]. The systemic inflammatory syndrome mirrors cytokine storm and cytokine release syndrome in patients receiving novel cellular therapies such as chimeric antigen receptor T-cells [25]. Levels of inflammatory markers in serum correlate with the severity of illness and adverse outcomes [27]. C-reactive protein (CRP) is a particularly powerful prognosticator [15].

Electrocardiographic changes during COVID-19 infection consistent with ischemia in patients with or without occlusive epicardial coronary disease have been reported [6, 9]. Such electrocardiographic changes consistent with ischemia but without chemical evidence of myocardial injury or echocardiographic features of ventricular dysfunction have been reported most often in young adult patients [14, 28].

31.4 Coagulopathy and Thromboembolism in Patients with Cancer and COVID-19

Patients with cancer are at five- to sevenfold greater risk of developing venous thromboembolism (VTE) than the general population [29, 30], due both to the malignancies themselves and to the thrombogenic effects of some cancer therapies. Major venous and arterial thromboembolic events are also common in patients with COVID-19 and occur with greater frequency in those with concomitant cardiovascular disease [7, 31]. In a series of 198 hospitalized patients with COVID-19, 20% were diagnosed with VTE despite routine thromboprophylaxis [32]. Post-mortem studies give further insight into the hypercoagulability of these patients, with widespread pulmonary vascular thrombosis, microangiopathy, and occlusion of alveolar capillaries [29, 33].

Given these findings, there has been great interest in treating COVID-19 patients with higher dose ("intermediate") prophylactic anticoagulation and even full-dose systemic anticoagulation for prevention of VTE. Observational data from Wuhan and Spain suggest that treatment with systemic anticoagulation may be associated with lower mortality [34, 35]. In view of the lack of randomized trials and the high bleeding risk associated with systemic anticoagulation in critically ill patients, routine pharmacologic VTE prophylaxis is recommended in all patients hospitalized with COVID-19 without bleeding contraindication, rather than full-dose systemic anticoagulation for prophylaxis.

Some suggest intermediate-dose systemic anticoagulation (i.e., enoxaparin 0.5 mg/kg sc BID) for prophylaxis [7, 36, 37]. These recommendations may change as results emerge from ongoing randomized trials exploring anticoagulation in patients with COVID-19 [HEP-COVID (NCT04401293), CORIMMUNO-COAG (NCT04344756), IMPROVE (NCT04367831), COVI-DOSE (NCT04373707), A Randomized Trial of Anticoagulation Strategies in COVID-19 (NCT04359277), Safety and Efficacy of Therapeutic

Anticoagulation on Clinical Outcomes in Hospitalized Patients with COVID-19 (NCT04377997), Coagulopathy of COVID-19: A Pragmatic Randomized Controlled Trial of Therapeutic Anticoagulation Versus Standard Care (NCT04362085)].

Low molecular weight heparins (LMWH) are preferred over unfractionated heparin, oral anticoagulants, or platelet inhibitors in hospitalized patients with COVID-19 and have established safety and efficacy in patients with cancer. Current guidelines also recommend LMWH as the preferred agents in patients with cancer [38], but several recent trials found direct oral anticoagulants (DOACs) non-inferior [39–41]. In practice, vascularized tumors in the gastrointestinal or urinary tracts may increase the risk of bleeding with oral agents. Pancreatic cancer, associated with a higher risk of venous thromboembolism than other common cancer types, is one example [40]. When selecting an anticoagulant for a patient with active malignancy, it is important to consider pharmacodynamic interactions with chemotherapeutic agents (DOACs are metabolized by CYP3A4 or mediated by P-glycoprotein). Similarly, LMWH is the preferred VTE treatment in patients with COVID-19, in part because of limited interactions with other COVID-19 therapies, as well as administration in fixed dosage by intermittent subcutaneous injection, which reduces exposure of healthcare providers to the infectious milieu, and shorter duration of action, which facilitates interruption in case of bleeding or clinical decompensation necessitating urgent invasive procedures [7, 36, 37]. Thrombocytopenia and renal dysfunction, common in patients with COVID-19 and during cancer therapy, must also be considered in medical decision-making.

31.5 COVID-19 Cytokine Release and Systemic Inflammatory Syndrome

COVID-19 is characterized by a systemic hyperinflammatory response which correlates with organ dysfunction and adverse outcomes. Marked elevations in TNF-α, IL-1, IL-6, and IL-8 are present in patients with severe COVID-19 [42–44], and termed "cytokine storm." [45, 46]. Presentation of viral elements to the natural killer cells and CD8-positive cytotoxic T-cells usually leads to the death of the cells containing viral antigen. However, in COVID-19, interaction of the SARS-CoV-2 virus with these cells triggers increased activation of pro-inflammatory cytokines and chemokines which may foment unrestrained activation of the inflammatory system through positive feedback loops [47].

Similar unrestrained inflammatory activation characterizes the cytokine release syndrome which may complicate chimeric antigen receptor modified T-cells (CAR-T) cell therapy. CAR-T cell therapy involves harvesting T-cells from patient's serum and genetically modifying them by inserting the CAR gene [48–50]. These cells undergo in vitro proliferation and are infused back to the patient. CAR-T cells interact with the malignant or normal cells expressing the selected antigen, activating lysis of the target cells and cytokine secretion, one of the main mechanisms of adverse events. Cytokine release syndrome (CRS) occurs as a result of interferon–γ (INF-γ), soluble IL-2 receptor-α TNF-α, IL-6, Il-10, and inflammatory markers such as CRP and ferritin. Severe cases of CRS can lead to vasodilatory shock, disseminated, intravascular coagulation, hypoxia, and end-organ damage.

31.6 Arrhythmia in Patients with COVID-19

Both atrial and ventricular arrhythmias may be seen in patients with COVID-19 [51] . An early report from China reported an incidence of arrhythmias as high as 17% in hospitalized patients with COVID-19 and higher (44%) in patients admitted to the intensive care unit (ICU) [52]. An increased incidence of out-of-hospital cardiac arrests in Italy has been reported [53]. One review of 700 patients in the Philadelphia region described the rate of cardiac arrests as 11% in patients in an ICU. The majority of these cases were characterized by pulseless electrical activity or asystole; one patient had the torsade de pointes form of ventricular tachycardia [54]. The incidence of arrhythmia among patients with COVID-19 treated with hydroxychloroquine and azithromycin was 20.4% [55].

31.7 Vascular and Endothelial Dysfunction in COVID-19

SARS-CoV-2 mediates endothelial dysfunction through the release of vasodilatory substances, nitric oxide and prostacyclin, and vasoconstrictors such as angiotensin-II and endothelin-1, resulting in disruptions of vascular tone, thrombosis, and inflammation [11]. These effects of COVID-19 share features in common with vascular endothelial growth factor (VEGF) inhibitors and cases of ICI-related vasculitis. Monoclonal antibodies targeting the VEGF receptor are used in treating multiple solid tumors and are associated with hypertension and aortic dissection, stroke, and arterial and venous thrombosis mediated by effects on the vascular endothelium [56].

Immune-checkpoint inhibitors such as monoclonal antibodies against CTLA-4 (cytotoxic T-lymphocyte-associated protein 4) and PD-1 (programmed cell death 1) T-lymphocyte receptors have emerged as effective therapies against a variety of malignancies. Though rare, cases of

fulminant myocarditis garnered attention, in part due to high case mortality [57, 58], but vascular toxicity may also be seen [59–61]. The mechanisms of these adverse events remain incompletely understood but appreciation of the complex interplay of host immune-responses in COVID-19 may improve understanding of these rare but important adverse effects [59].

31.8 Clinical Cases

Despite numerous clinical observations, diagnosis and management of COVID-19 related heart disease in patients with cancer remains challenging. To date, no randomized studies are available. Furthermore, because of contagion, concerns about conservation of personal protective equipment, and the safety of patients and healthcare workers, information about the results of imaging and cardiac testing in patients with COVID-19 is limited.

31.8.1 Case 1: A Patient Receiving Immunotherapy for Lung Cancer Who Developed COVID-19

A 61-year-old man with metastatic non-small cell lung cancer and right-sided pleural effusion presented to the emergency department with shortness of breath, cough, and fever for 1 day. He received a second cycle of the programmed cell death protein-1 (PD-1) inhibitor pembrolizumab 5 days earlier. There was no significant hypoxemia at rest measured by pulse oximetry. Reverse transcription polymerase chain reaction (RT-PCR) testing for SARS-CoV-2 was positive. Serum troponin-I was 0.06 ng/mL (normal < = 0.02 ng/mL), decreasing on interval assessment. Computed tomographic radiography of the chest demonstrated features consistent with COVID-19, immune-checkpoint related pneumonitis, and progression of lung cancer. The patient remained clinically stable, without hypoxemia or fever during observation, and was discharged home with instructions for self-isolation. While ground-glass opacities seen on chest CT could have been caused by COVID-19, the presence of a large, chronic pleural effusion suggested symptoms were more likely explained by his underlying lung cancer. Pleural effusion and lymphadenopathy are less commonly from COVID-19 pneumonia. A pleural drainage catheter was subsequently placed with improvement in the patient's symptoms. He remains on pembrolizumab (Fig. 31.1).

- Chest imaging findings in patients with COVID-19 share features that overlap those associated with toxicities of radiation and immunotherapy for cancer.

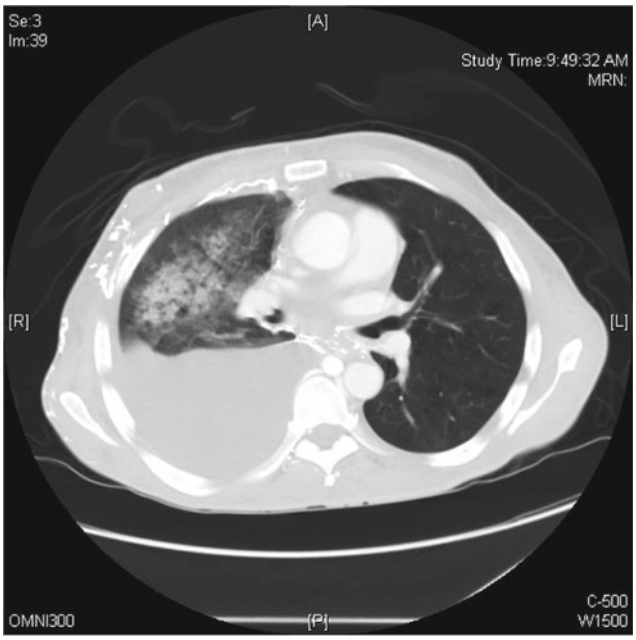

Fig. 31.1 Chest computed tomography in a patient with lung cancer receiving immunotherapy diagnosed with COVID-19. Salient findings include ground glass opacities; large right-sided pleural effusion; pericardial effusion

- Lung cancer is prevalent among patients hospitalized with COVID-19 [24, 26], explained in part by common demographic factors, such as older age and smoking.
- Myocardial injury, defined by abnormal troponin elevation, occurs in COVID-19 and is associated with adverse outcomes. Lower level, intermediate elevations of cardiac troponin can occur following immune-checkpoint inhibitor (ICI) treatment absent other signs/symptoms of myocarditis.
- An important clue in this case is the absence of significant hypoxia, which suggests the patient does not have severe lung involvement due to COVID-19.
- In patients with COVID-19 who do not develop respiratory failure, abnormalities on chest CT peak approximately 10 days after the onset of symptoms [62].

31.8.2 Case 2: Pacemaker Malfunction in a Patient with COVID-19 Receiving Immunotherapy for Lung Cancer

A 63-year-old woman with a history of atrioventricular conduction block, dual-chamber pacemaker implantation, and metastatic non-small cell lung carcinoma receiving treatment with carboplatin, pemetrexed, and pembrolizumab presented with fever, dyspnea, and cough. RT-PCR testing confirmed SARS-CoV-2 infection. During hospitalization,

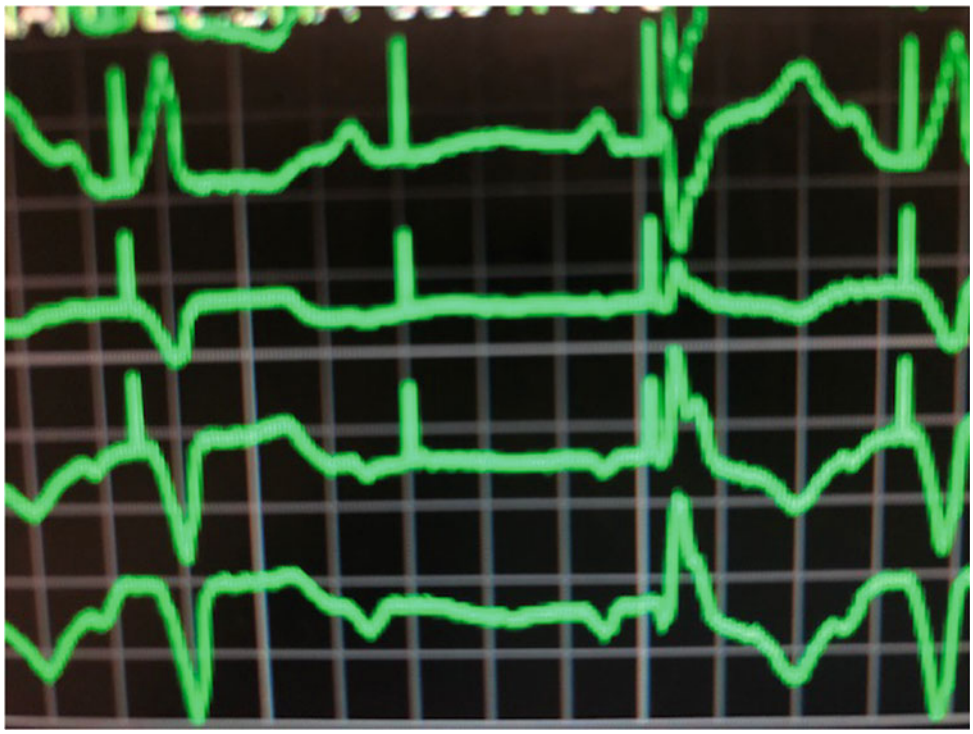

Fig. 31.2 Telemetry strip shows pacemaker with inconsistent capture

telemetric monitoring demonstrated loss of capture (Figs. 31.2 and 31.3). Serum electrolyte concentrations were normal. Serum Interleukin-6 concentration was markedly elevated, 116 pg/mL (ULN = 5 pg/mL). Interrogation of the pacemaker disclosed normal electrode impedance and generator energy. Output voltage and pulse width were increased to enable pacing. Due to worsening clinical status, patient and family wishes, she was transitioned to comfort-oriented care and died 6 days later.

- COVID-19 causes a systemic hyperinflammatory response characterized by marked elevations in inflammatory markers including TNF-α, IL-1, IL-6, and IL-8, which correlate with organ dysfunction and adverse outcomes.
- Similar inflammatory reactions may occur following ICI treatment and in the cytokine release syndrome, which may complicate chimeric antigen receptor (CAR) T-cell infusion therapy.
- Differential diagnostic considerations in this case, therefore, include ICI-related myocarditis as well as fulminant COVID-19.

31.8.3 Case 3. Acute Pulmonary Embolism (PE) and Right Ventricular Dysfunction in a Patient with Pancreatic Cancer and COVID-19

A 60-year-old man with pancreatic cancer on FOLFIRINOX (fluorouracil, leucovorin, irinotecan, and oxaliplatin) presented with fever, cough, and worsening dyspnea. Nasopharyngeal swab testing for SARS-CoV-2 infection by RT-PCR returned positive and he was hospitalized because of hypoxemia necessitating supplemental oxygen. Seven days later, he developed acute hypoxemic respiratory failure necessitating intubation and mechanical ventilation. The electrocardiogram showed sinus tachycardia with new right bundle-branch block (Fig. 31.4). Troponin-I peaked at 0.4 ng/mL (normal < 0.02 ng/ml). The plasma B-type natriuretic peptide level was 900 pg/mL (0–100 pg/mL). Point-of-care cardiac ultrasound (POCUS) demonstrated dilation of the right ventricle (RV) with focal akinesis of the free wall and preserved apical function suggesting acute PE despite thromboprophylaxis with enoxaparin (Figs. 31.5, 31.6 and 31.7). Because of his clinical instability and acute renal injury, he did not undergo confirmatory CT pulmonary angiography and was treated with low molecular weight heparin (1 mg/kg), which was continued upon discharge after a 28-day hospitalization.

This patient developed sinus tachycardia, a new right bundle-branch block, elevated troponin-I and BNP with evidence of RV dilation and dysfunction suggestive of a

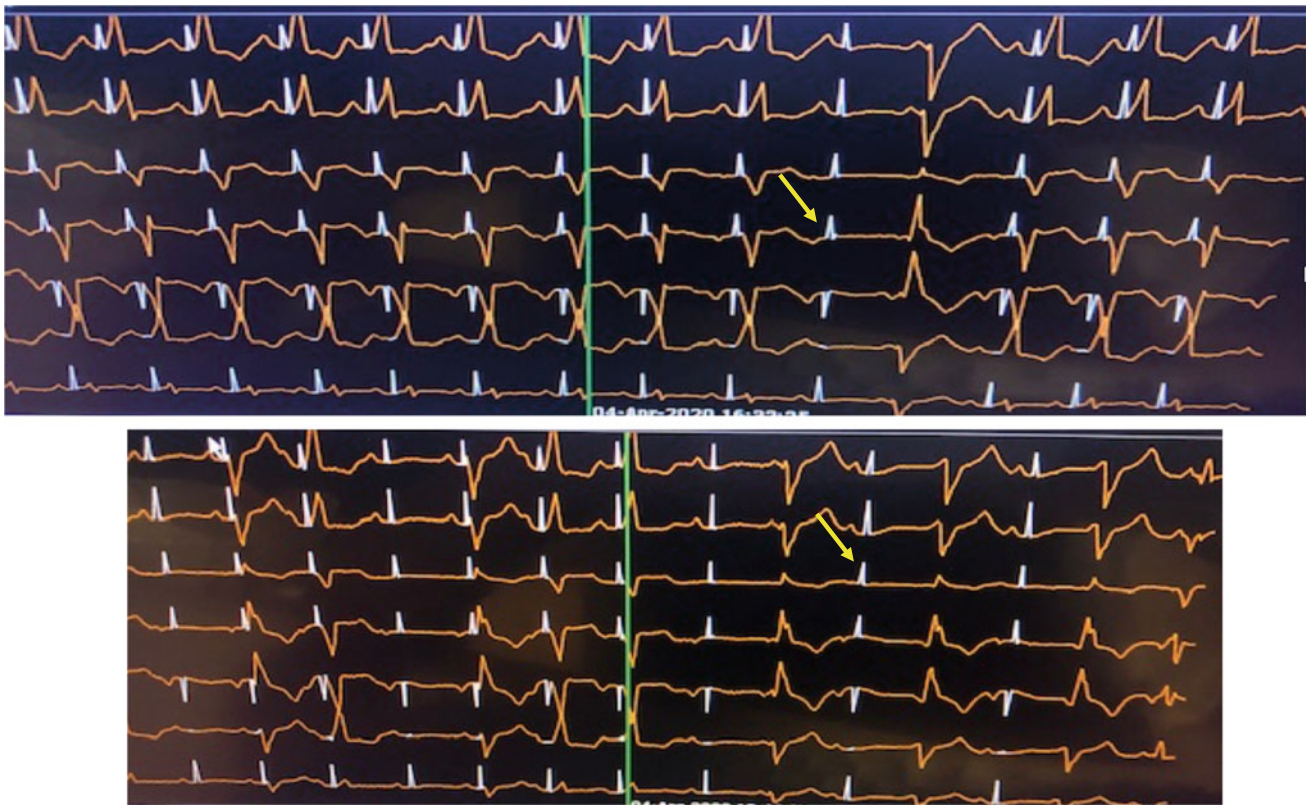

Fig. 31.3 Telemetric monitoring strips with arrows to some of the pacer spikes that failed to capture

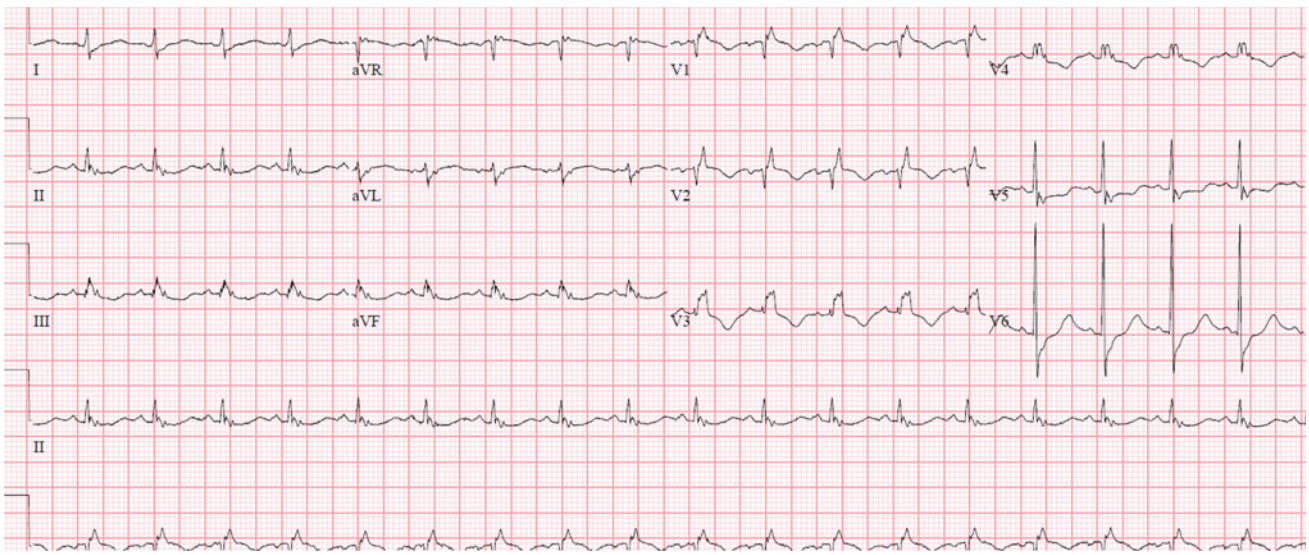

Fig. 31.4 ECG Sinus tachycardia with new right bundle-branch block

high-intermediate-risk PE [63]. These observations could also have been secondary to an alternative insult to the right ventricle by COVID-19. In 105 patients hospitalized with COVID-19 32 (31%) were found to have RV dilation (defined as basal diastolic right ventricular diameter exceeding 4.1 cm in the right ventricle-focused apical view and/or basal right to left ventricular diameter ratio of ≥ 0.9 in the apical 4-chamber view) [64]. RV dilation was strongly associated with in-hospital mortality. There is also evidence of RV dysfunction in patients who have recovered from

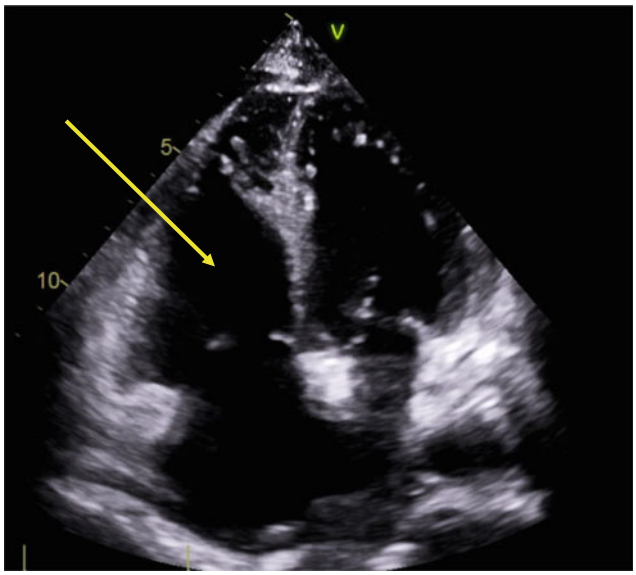

Fig. 31.5 Transthoracic echocardiogram: moderate RV dilation (arrow)

COVID-19. In a case–control study of 26 patients who recovered from COVID-19 and reported cardiac symptoms, fifteen (58%) had cardiac MRIs showing impaired RV systolic function [65]. The pathophysiology of the RV dysfunction is unknown, but hypothesized to be multifactorial secondary to thrombotic events, hypoxic vasoconstriction, cytokine milieu, and direct viral damage.

- Both malignancy and COVID-19 infection are associated with hypercoagulable states putting patients at increased risk of venous thromboembolism (VTE).
- Providers must consider drug interactions, thrombocytopenia, renal function, and optimum intensity and duration of anticoagulant therapy for VTE treatment in patients with malignancy and COVID-19.
- Both acute pulmonary embolism (PE) and COVID-19 infection may lead to RV dysfunction which can be identified by multiple imaging modalities.

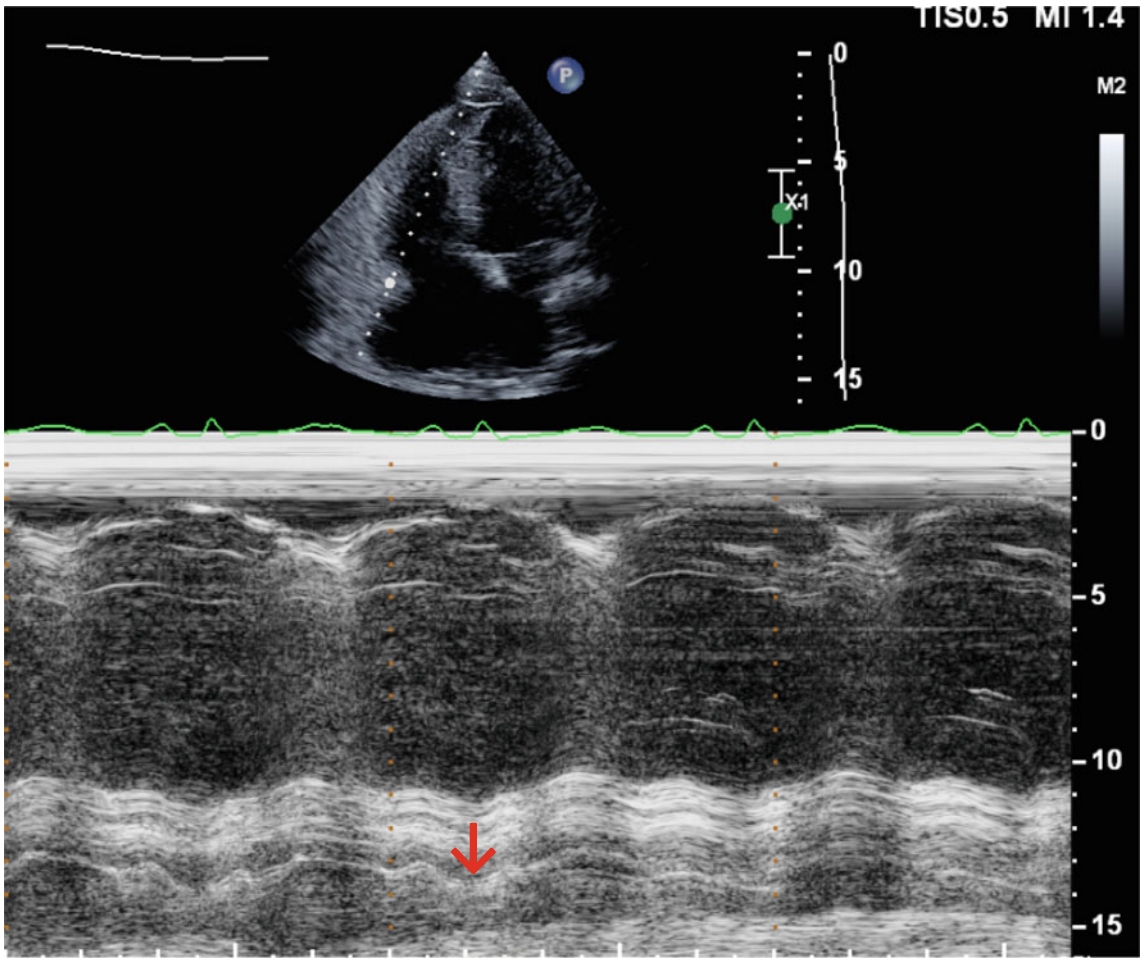

Fig. 31.6 Transthoracic echocardiogram: reduced RV function by tricuspid annular plane systolic excursion (TAPSE) red arrow

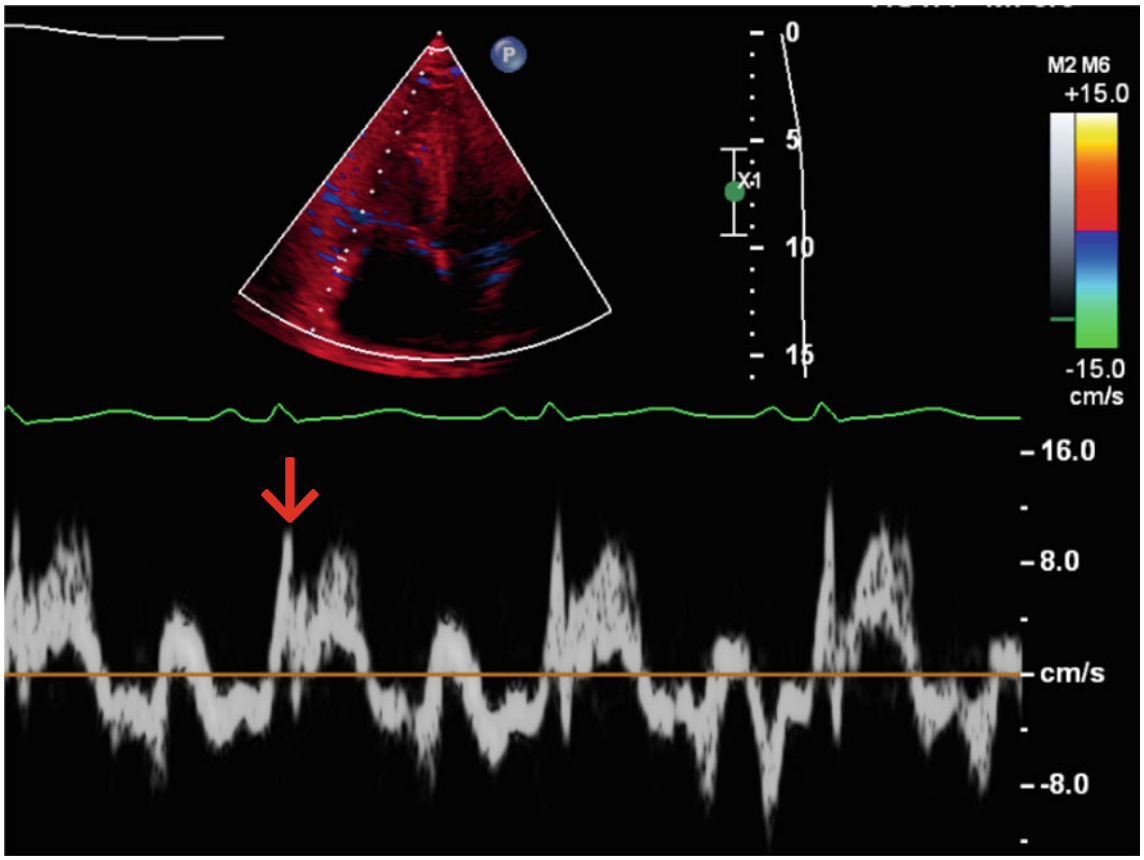

Fig. 31.7 Transthoracic echocardiogram: reduced RV systolic function by myocardial systolic excursion velocity (S') (arrow)

31.8.4 Case 4: Fatal Arrhythmia in a Critically Ill Patient with COVID-19

A 63-year-old woman with hypogammaglobulinemia on intravenous immunoglobulin (IVIG) secondary to follicular lymphoma (treated 3 years earlier with a combination of obinutuzumab, bendamustine, and atezolizumab) was admitted because of dyspnea, hypoxemia, and COVID-19. Her medical history was notable for coronary angioplasty and deployment of a drug-eluting stent 6 years before. Chest roentgenography revealed new bibasilar patchy airspace and reticular opacities. She was treated with antibiotics for pneumonia and with hydroxychloroquine. She developed progressive hypoxemic respiratory failure requiring intubation, mechanical ventilation, and prone positioning. She became acutely hypotensive and febrile to 104 °F. The electrocardiogram showed sinus tachycardia, ST-segment elevation in lead aVR, and diffuse ST-segment depressions. A POCUS showed normal LV systolic function without regional wall motion abnormalities. She developed wide-QRS tachycardia and increased vasopressor requirements. Troponin-I peaked at 0.19 ng/mL (normal < 0.02 ng/ml). Serum lactate was 7.3 mg/dL. Amiodarone was administered, but tachyarrhythmia recurred, progressing to asystole, and the patient died (Figs. 31.8, 31.9, 31.10, 31.11 and 31.12).

- Atrial and ventricular arrhythmia occur frequently in critically ill patients and are common in those with COVID-19.
- Mechanisms of arrhythmic complications include both direct viral effects and effects of potential therapeutics, such as hydroxychloroquine.
- Patients with cancer are exposed to additional agents associated with QTc prolongation and arrhythmia.

31.8.5 Case 5: A Young Man with an Intestinal Mass and a Multi-Organ Inflammatory Syndrome

A 19-year-old with a history of childhood asthma without recent exacerbation or current therapy presented with sudden onset of severe abdominal pain, nausea, vomiting, and high fever (103 °F for 3 to 4 days) during the initial surge of COVID-19 in New York City. He denied respiratory symptoms. A CT scan of the abdomen and pelvis with oral

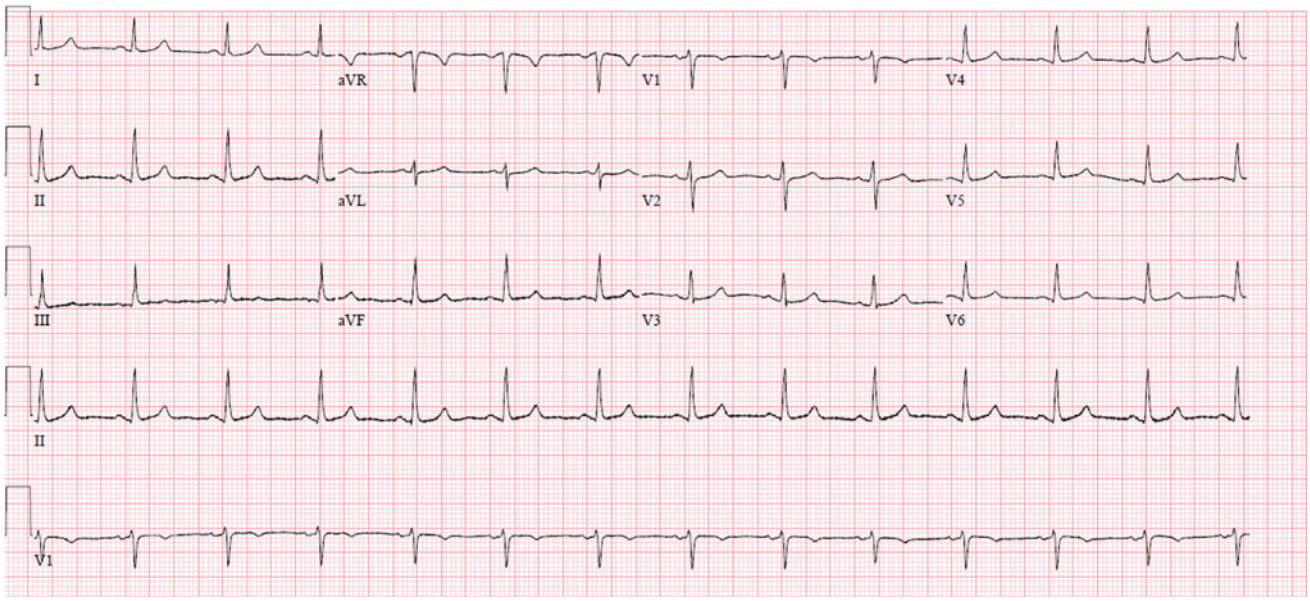

Fig. 31.8 Normal baseline ECG

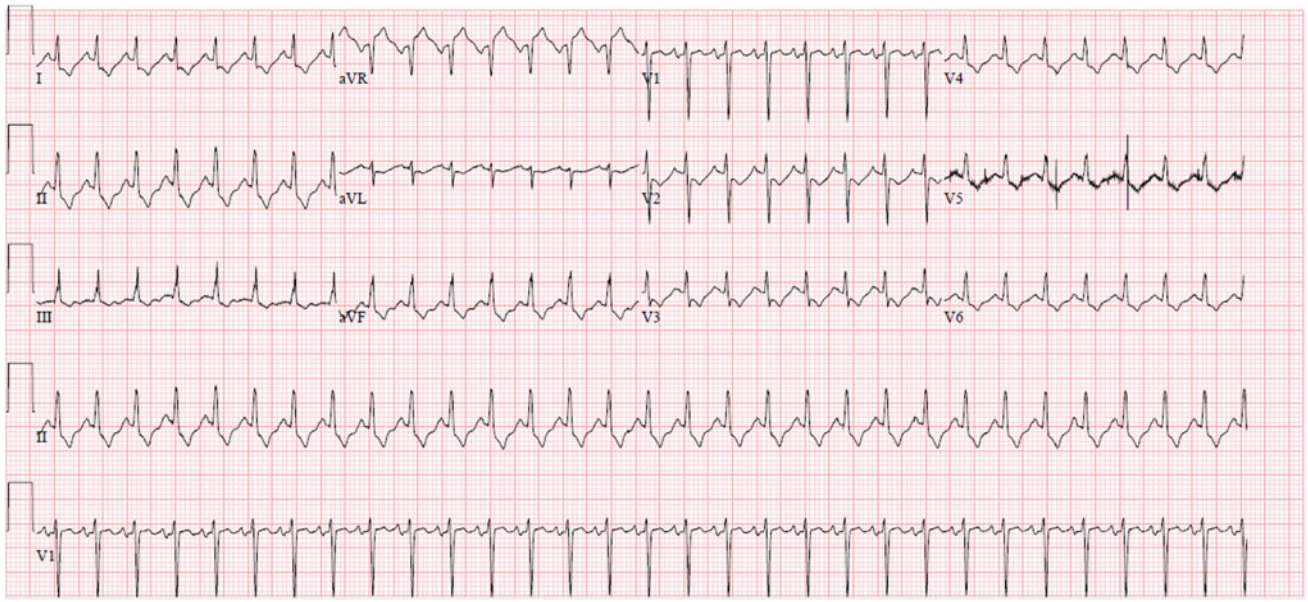

Fig. 31.9 Supraventricular tachycardia in a patient with COVID-19

and intravenous contrast and ultrasound examination of the gallbladder demonstrated cholelithiasis without cholecystitis. Empiric antibiotics were administered. The C-reactive protein level and ESR were markedly elevated. RT-PCR tests for SARS-CoV-2 PCR were repeatedly negative throughout the illness.

Magnetic resonance cholangiopancreatography (MRCP) revealed choledocholithiasis and inflammation of the ascending colon. Troponin T peaked at 261 ng/L (normal < 14 ng/L). The plasma NT-pro-BNP level was 5760 pg/mL (normal < 300 pg/mL). CT angiographic images are shown (Figs. 31.13 and 31.14). Echocardiography demonstrated severe left ventricular systolic dysfunction (ejection fraction 35%). He became hypotensive requiring vasopressors in the setting of rising inflammatory markers. Emergent exploratory laparotomy revealed bilious ascites and a hard mass in the ileocolic pedicle. Ileocolic resection was performed with ileostomy. Pathology of the surgical

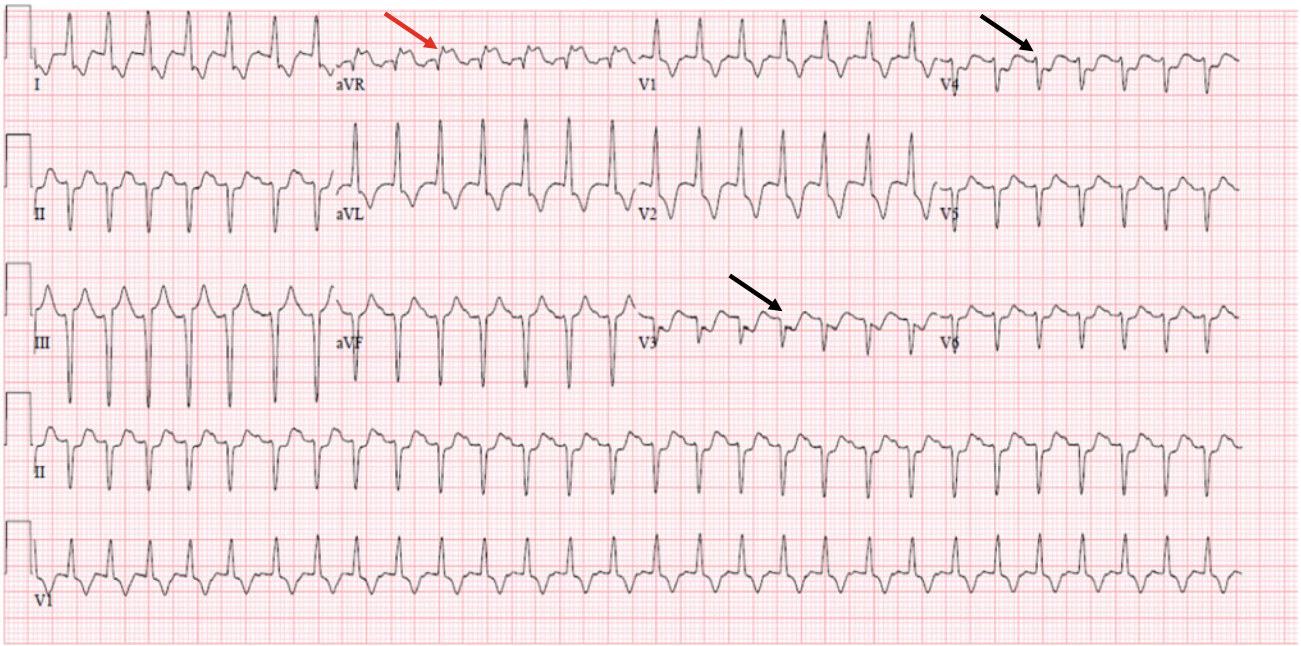

Fig. 31.10 Wide complex tachycardia, RBBB configuration, and ST-segment depression (black arrows) and elevation (red arrow) in patient with COVID-19

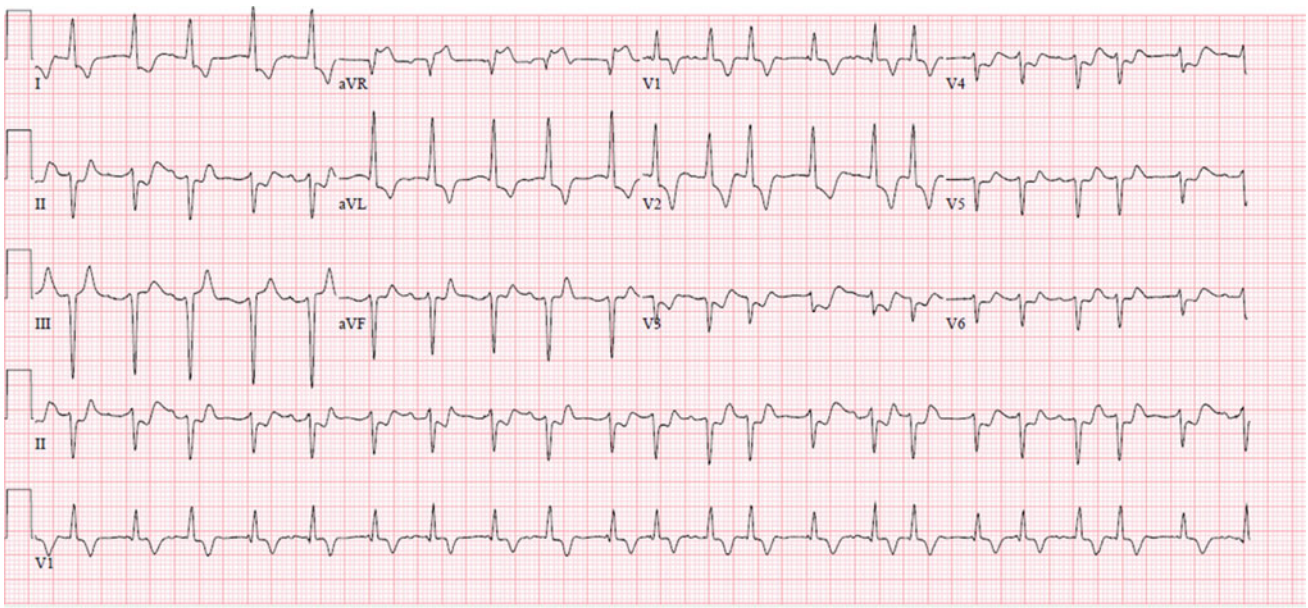

Fig. 31.11 Rhythm slows with irregularities. ST-segment changes persist

specimen demonstrated transmural fibrin thrombi and chronic inflammation of the wall of the small intestine with focal epithelial acute inflammation and reactive changes, mesenteric arteritis, and extensive necrosis of the lymph nodes. Inflammatory markers and troponin down-trended and ventricular dysfunction recovered. Antibodies to SAR-CoV-2 were subsequently detected in the serum (Figs. 31.13, 31.14, 31.15, 31.16 and 31.17; Videos 31.1, 31.2 and 31.3).

Kawasaki disease is an acute self-limiting, medium-vessel arteritis most common in children and affecting the coronary arteries in particular [66]. During the initial phase of

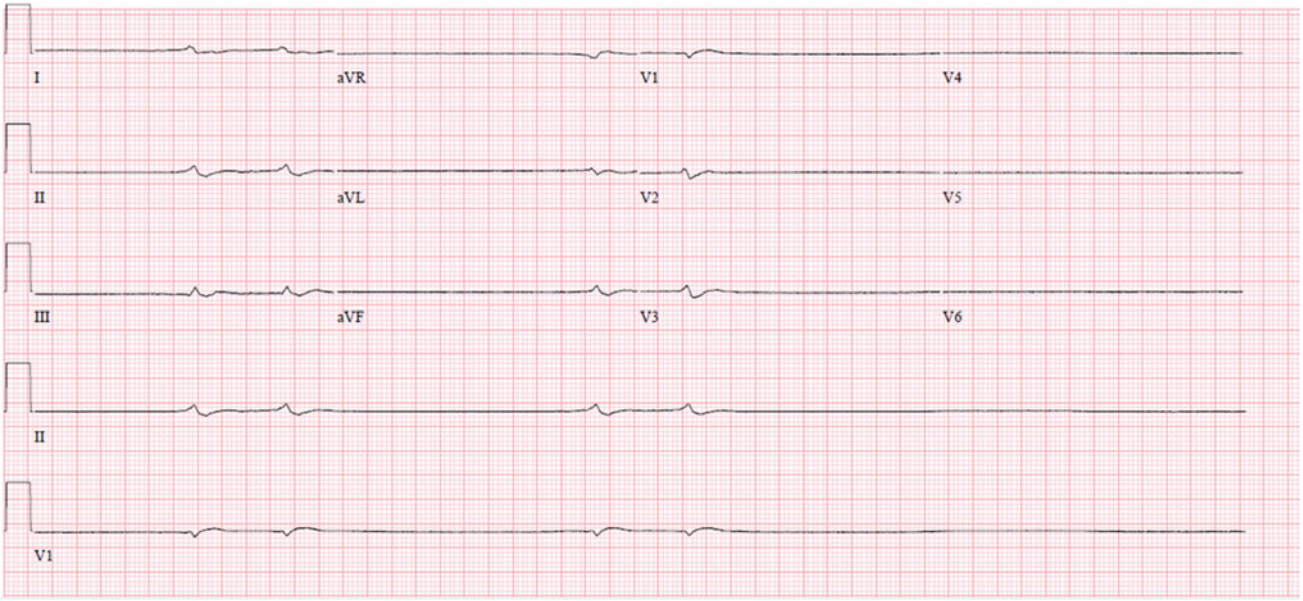

Fig. 31.12 Agonal rhythm

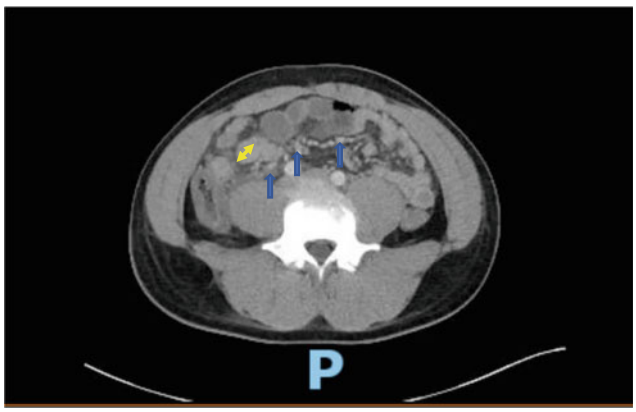

Fig. 31.13 CT angiogram of the chest, abdomen, and pelvis with abdominal slice showing ascending colitis, terminal ileitis and a mass (yellow arrow), mesenteric lymphadenopathy (blue arrows)

COVID-19 pandemic, a 30-fold increase in the incidence of Kawasaki-like disease in children was reported. Unlike classic Kawasaki disease, affected children were older and had multiple organ systems involved. They also exhibited lymphopenia, thrombocytopenia, and increased ferritin, typical of COVID-19. Importantly, many demonstrated serologic evidence of immunologic response to SARS-CoV-2. Subsequent reports of similar cases in the United States led to the designation multi-system inflammatory syndrome (MIS) [67]. Hallmark features include multi-organ system involvement, including gastrointestinal (92%), cardiovascular (80%), hematologic (76%), mucocutaneous (74%), and respiratory (70%) systems with corresponding elevation in multiple biomarkers of inflammation [67].

- Children with COVID-19 occasionally develop a systemic inflammatory syndrome in response to the infection
- Vascular damage has been more pronounced in children and a similar mechanism of adverse events has been reported with vascular endothelial growth factor (VEGF) inhibitors and immune-checkpoint inhibitors.
- Inflammatory masses may mimic tumors.

31.8.6 Case 6: Cardiomyopathy Following Anthracycline Chemotherapy in a Patient with COVID-19

A 72-year-old man with diffuse large B-cell lymphoma diagnosed in March 2020 was treated with reduced dose R-CHOP (Rituximab, Cyclophosphamide, Doxorubicin, Vincristine, and Prednisone). Before treatment, an echocardiogram in March showed normal left ventricular systolic function (ejection fraction >50%). He developed fever and cough in mid-April, after the first treatment cycle. Testing for SARS-CoV-2 by RT-PCR was positive. He recovered, but 4 weeks later repeat PCR testing for COVID-19 remained positive. In June, PCR testing results were negative. He resumed chemotherapy but developed fatigue and palpitations. A transthoracic echocardiogram (Figs. 31.18

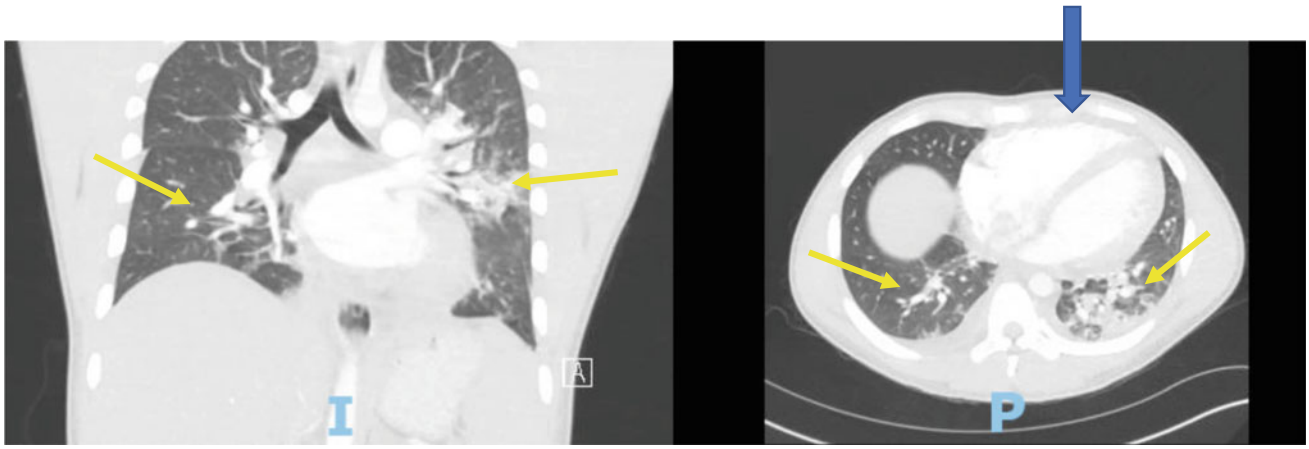

Fig. 31.14 CT angiography of the chest showing patchy opacities in bilateral lobes (yellow arrows) and new cardiomegaly (blue arrow)

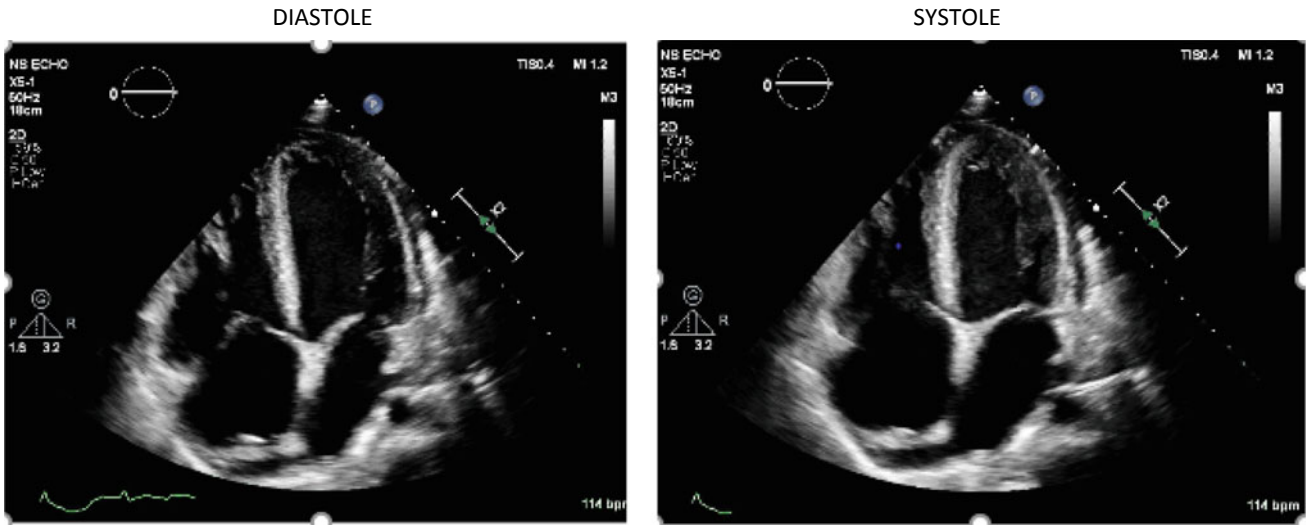

Fig. 31.15 Transthoracic echocardiogram shows global left ventricular hypokinesis with estimated LVEF of 35%. Apical four-chamber view

and 31.19; Videos 31.4 and 31.5) demonstrated global LV systolic dysfunction. The electrocardiogram showed sinus rhythm and premature atrial contractions, not significantly changed from prior tracings. Chest CT imaging during follow-up PET-staging demonstrated ground-glass opacities in the lungs (Fig. 31.20). Antibodies to COVID-19 remained undetectable 2 months later.

- Patients receiving anti-CD20 monoclonal antibodies such as rituximab may have an impaired immunologic response to COVID-19, characterized by failure to produce antibodies.
- Anthracyclines are associated with dose-dependent cardiomyopathy mediated by oxidative stress and impaired DNA repair mechanisms. Cardiotoxicity may be augmented by other factors, such as pre-existing heart disease, pregnancy, combination treatment with trastuzumab, and prior radiation.

Anthracycline chemotherapy, included in R-CHOP, is associated with dose-related cardiotoxicity, manifesting as reduced systolic function. Cardiotoxicity may develop at any dose, but more often occurs after doses >240 mg/m^2. Cardiomyopathy appears mediated in part by other risk factors, such as age, hypertension, trastuzumab therapy, and underlying heart disease. Whether illness with COVID-19 increases susceptibility to or augments toxicity is unknown.

Obinutuzumab and rituximab are monoclonal anti-CD20 antibodies used for leukemia and lymphoma targeting B-cells. Some observations suggest patients treated with these agents may have more severe infections from COVID-19 due to impaired immunogenic response including failure to produce

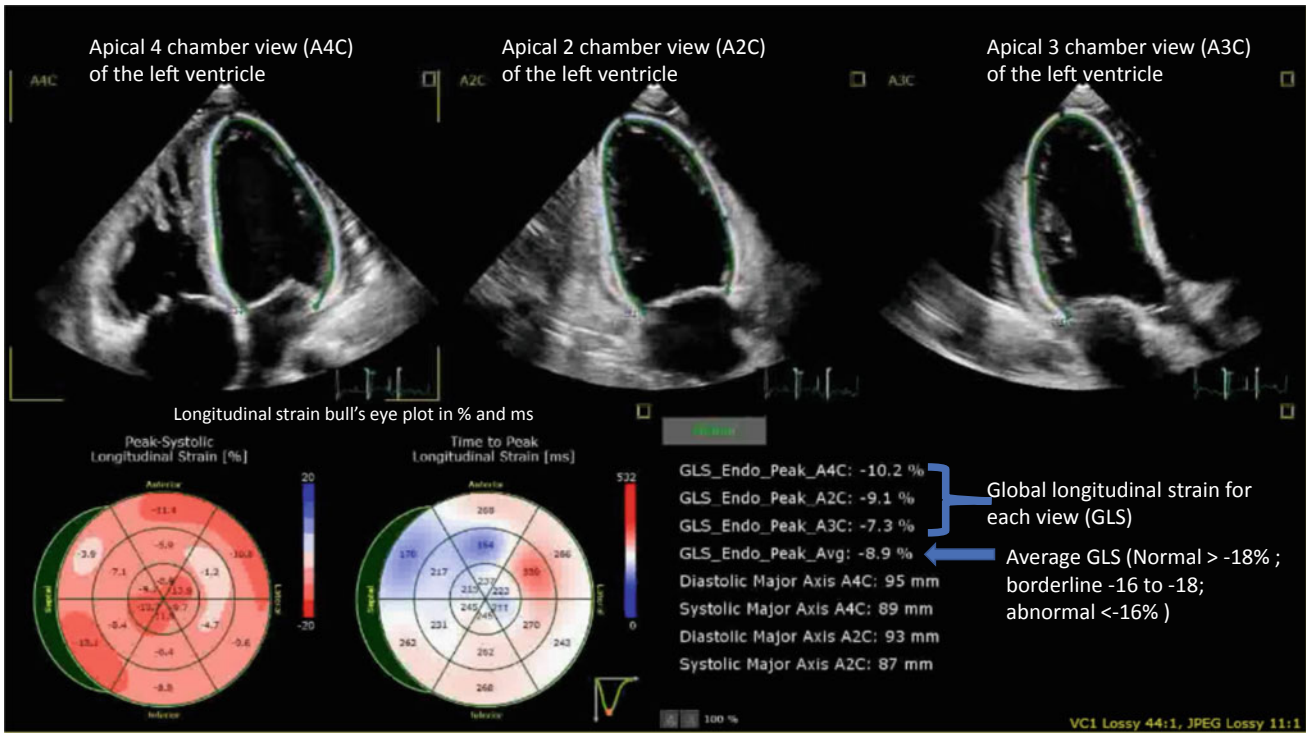

Fig. 31.16 Significantly reduced global longitudinal strain

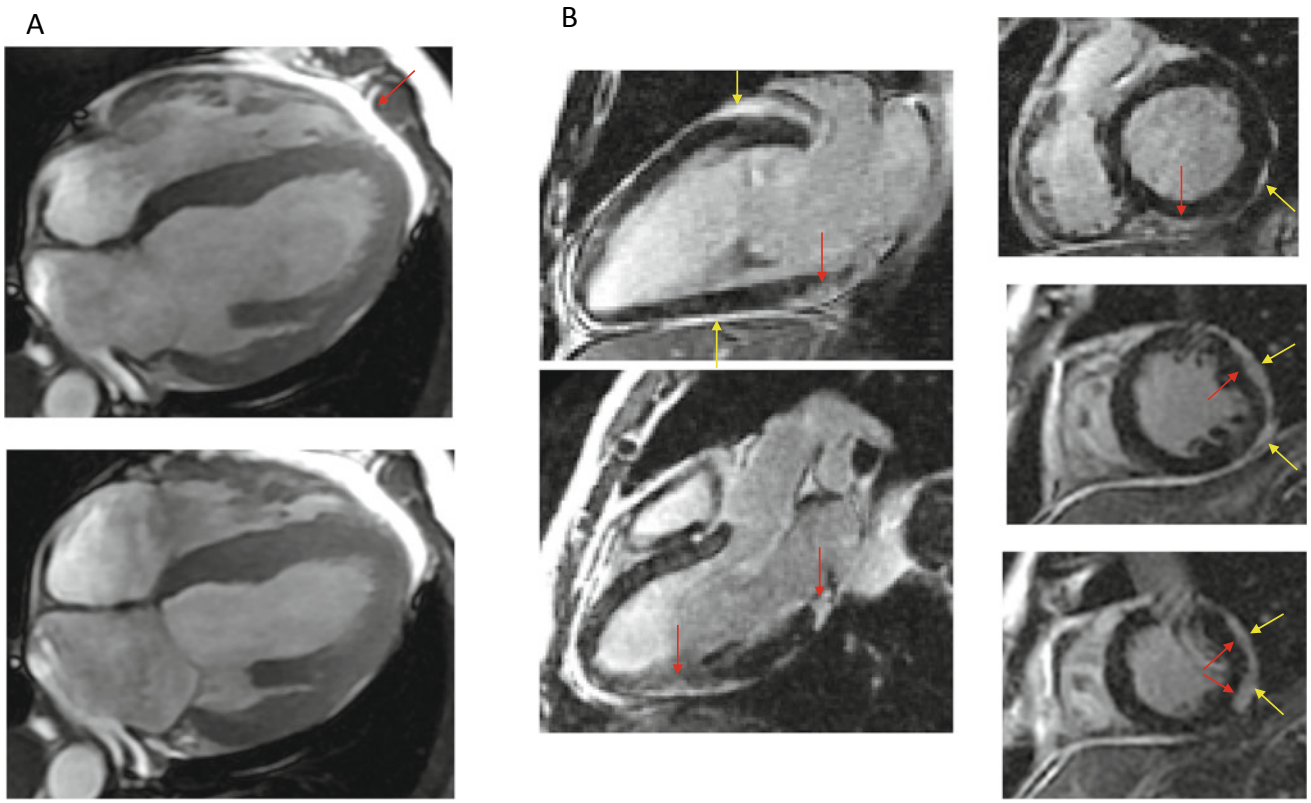

Fig. 31.17 Cardiac MRI of a different patient with COVID-19 showing myopericarditis. A, Still frames from cine-CMR in diastole (top) and systole (bottom) demonstrated moderately reduced global left ventricular systolic function (LV ejection fraction 37%), and pericardial effusion (red arrow). B, Late gadolinium enhancement CMR demonstrated myocardial enhancement in the epicardial aspect of the basal-mid inferior-inferolateral and apical lateral walls (red arrows), and circumferential pericardial hyperenhancement (yellow arrows), most consistent with myopericarditis

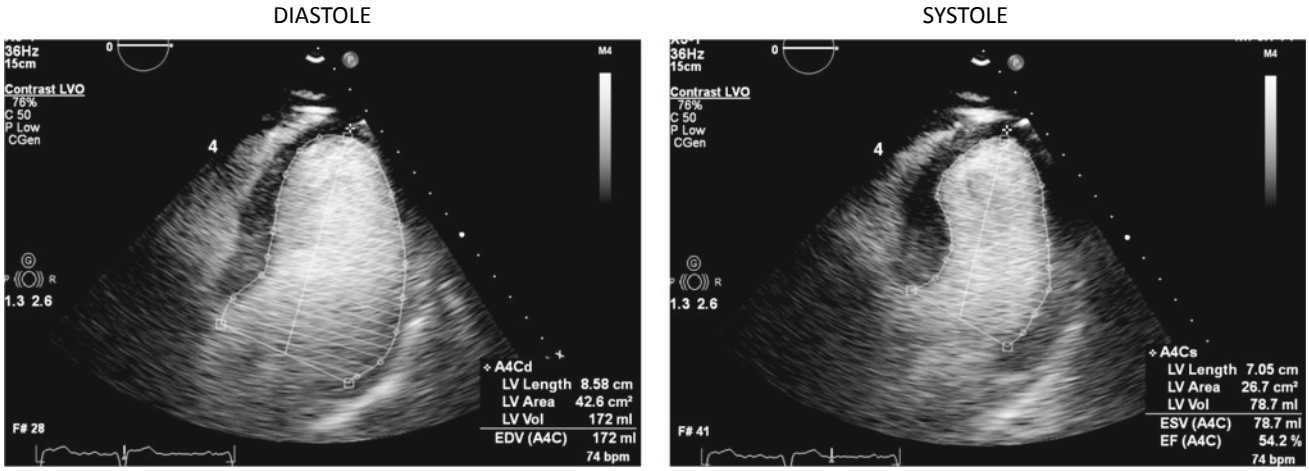

Fig. 31.18 Pre-treatment Echocardiogram in March 2020, EF was 54%, low normal

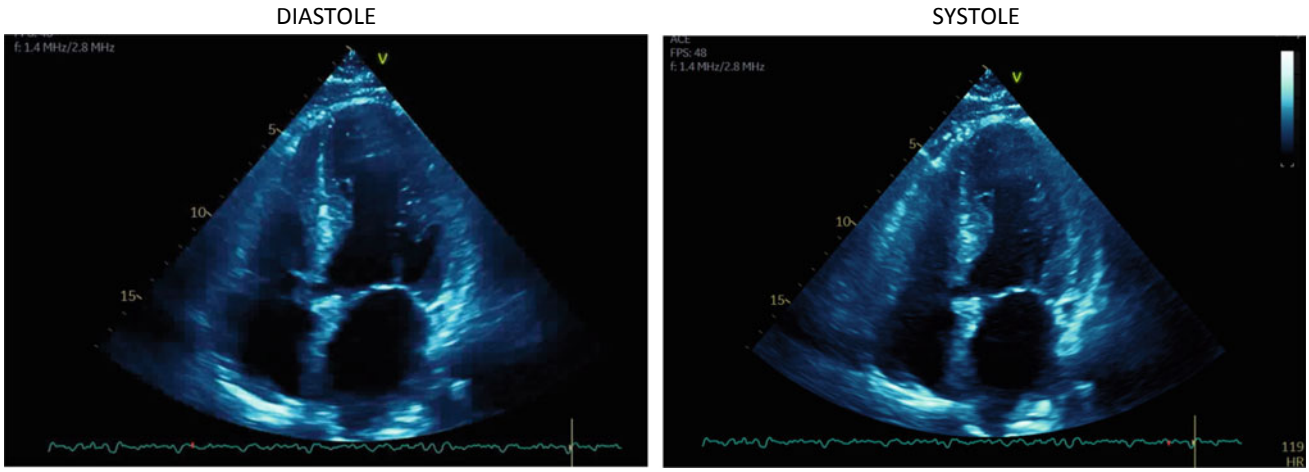

Fig. 31.19 Apical four-Chamber view, August, 2020, Ejection fraction = 30%

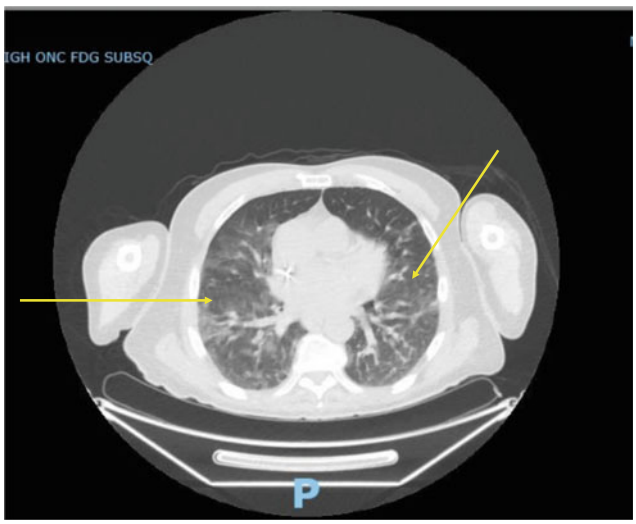

Fig. 31.20 This image demonstrates bilateral ground-glass opacities, which are nonspecific. In this post-COVID-19 patient with lymphoma and new cardiomyopathy, differential diagnosis includes infectious and inflammatory etiologies. There are no significant pleural effusions

antibodies after infection [68]. In contrast, organ transplant recipients seem not more commonly or severely affected by COVID-19 [69]. Immunosuppressive medications typically employed after organ transplantation, such as calcineurin inhibitors, act more selectively on T lymphocytes, with B-cell activity largely preserved.

References

1. WHO statement regarding cluster of pneumonia cases in Wuhan, China. 2020. https://www.who.int/china/news/detail/09-01-2020-who-statement-regarding-cluster-of-pneumonia-cases-in-wuhan-china.
2. Driggin E, Madhavan MV, Bikdeli B, et al. Cardiovascular considerations for patients, health care workers, and health systems during the COVID-19 pandemic. J Am Coll Cardiol. 2020;75:2352–71.

3. Ganatra S, Hammond SP, Nohria A. The novel coronavirus disease (COVID-19) threat for patients with cardiovascular disease and cancer. JACC CardioOncol. 2020.
4. Zhang J, Lu S, Wang X, et al. Do underlying cardiovascular diseases have any impact on hospitalised patients with COVID-19? Heart. 2020;106:1148–53.
5. Akhmerov A, Marban E. COVID-19 and the heart. Circ Res. 2020;126:1443–55.
6. Bangalore S, Sharma A, Slotwiner A, et al. ST-segment elevation in patients with Covid-19—a case series. N Engl J Med. 2020;382:2478–80.
7. Bikdeli B, Madhavan MV, Jimenez D, et al. COVID-19 and thrombotic or thromboembolic disease: implications for prevention, antithrombotic therapy, and follow-up: JACC state-of-the-art review. J Am Coll Cardiol. 2020;75:2950–73.
8. Inciardi RM, Lupi L, Zaccone G, et al. Cardiac involvement in a patient with coronavirus disease 2019 (COVID-19). JAMA Cardiol. 2020.
9. Kochi AN, Tagliari AP, Forleo GB, Fassini GM, Tondo C. Cardiac and arrhythmic complications in patients with COVID-19. J Cardiovasc Electrophysiol. 2020;31:1003–8.
10. Madjid M, Safavi-Naeini P, Solomon SD, Vardeny O. Potential effects of coronaviruses on the cardiovascular system: a review. JAMA Cardiol. 2020.
11. Varga Z, Flammer AJ, Steiger P, et al. Endothelial cell infection and endotheliitis in COVID-19. Lancet. 2020;395:1417–8.
12. Liang W, Guan W, Chen R, et al. Cancer patients in SARS-CoV-2 infection: a nationwide analysis in China. Lancet Oncol. 2020;21:335–7.
13. Ippolito E, Fiore M, Greco C, D'Angelillo RM, Ramella S. COVID-19 and radiation induced pneumonitis: overlapping clinical features of different diseases. Radiother Oncol. 2020;148:201–2.
14. Vidovich MI. Transient Brugada-like ECG pattern in a patient with coronavirus disease 2019 (COVID-19). JACC Case Rep. 2020.
15. Luo X, Zhou W, Yan X, et al. Prognostic value of C-reactive protein in patients with COVID-19. Clin Infect Dis. 2020.
16. Mehta V, Goel S, Kabarriti R, et al. Case fatality rate of cancer patients with COVID-19 in a New York hospital system. Cancer Discov. 2020;10:935–41.
17. Yang F, Shi S, Zhu J, Shi J, Dai K, Chen X. Clinical characteristics and outcomes of cancer patients with COVID-19. J Med Virol. 2020.
18. Russano M, Citarella F, Napolitano A, et al. COVID-19 pneumonia and immune-related pneumonitis: critical issues on differential diagnosis, potential interactions, and management. Expert Opinion Biol Therapy. 2020;20:959–64.
19. Yu J, Ouyang W, Chua MLK, Xie C. SARS-CoV-2 transmission in patients with cancer at a tertiary care hospital in Wuhan. JAMA Oncol: China; 2020.
20. Luo J, Rizvi H, Egger JV, Preeshagul IR, Wolchok JD, Hellmann MD. Impact of PD-1 blockade on severity of COVID-19 in patients with lung cancers. Cancer Discov. 2020;10:1121–8.
21. Wu Q, Chu Q, Zhang H, et al. Clinical outcomes of coronavirus disease 2019 (COVID-19) in cancer patients with prior exposure to immune checkpoint inhibitors. Cancer Commun (Lond). 2020;40:374–9.
22. Shi S, Qin M, Shen B, et al. Association of cardiac injury with mortality in hospitalized patients with COVID-19 in Wuhan. JAMA Cardiol: China; 2020.
23. Yang K, Sheng Y, Huang C, et al. Clinical characteristics, outcomes, and risk factors for mortality in patients with cancer and COVID-19 in Hubei, China: a multicentre, retrospective, cohort study. Lancet Oncol. 2020;21:904–13.
24. Guo T, Fan Y, Chen M, et al. Cardiovascular implications of fatal outcomes of patients with coronavirus disease 2019 (COVID-19). JAMA Cardiol. 2020;5:811.
25. Shi S, Qin M, Cai Y, et al. Characteristics and clinical significance of myocardial injury in patients with severe coronavirus disease 2019. Eur Heart J. 2020;41:2070–9.
26. Siddiqi HK, Neilan TG. COVID-19, Immuno-oncology and cardiovascular disease: viewpoint from the intersection. J Cardiovasc Transl Res. 2020;13:347–8.
27. Chen R, Sang L, Jiang M, et al. Longitudinal hematologic and immunologic variations associated with the progression of COVID-19 patients in China. J Allergy Clin Immunol. 2020;146:89–100.
28. Loghin C, Chauhan S, Lawless SM. Pseudo acute myocardial infarction in a young COVID-19 patient. JACC Case Rep. 2020.
29. Agnelli G, Verso M. Management of venous thromboembolism in patients with cancer. J Thromb Haemost. 2011;9(Suppl 1):316–24.
30. Sheth RA, Niekamp A, Quencer KB, et al. Thrombosis in cancer patients: etiology, incidence, and management. Cardiovasc Diagn Ther. 2017;7:S178–85.
31. Inciardi RM, Adamo M, Lupi L, et al. Characteristics and outcomes of patients hospitalized for COVID-19 and cardiac disease in Northern Italy. Eur Heart J. 2020;41:1821–9.
32. Middeldorp S, Coppens M, van Haaps TF, et al. Incidence of venous thromboembolism in hospitalized patients with COVID-19. J Thromb Haemost. 2020;18:1995–2002.
33. Lax SF, Skok K, Zechner P, et al. Pulmonary arterial thrombosis in COVID-19 with fatal outcome: results from a prospective, single-center, clinicopathologic case series. Ann Intern Med. 2020.
34. Ayerbe L, Risco C, Ayis S. The association between treatment with heparin and survival in patients with Covid-19. J Thromb Thrombolysis. 2020;50:298–301.
35. Tang N, Bai H, Chen X, Gong J, Li D, Sun Z. Anticoagulant treatment is associated with decreased mortality in severe coronavirus disease 2019 patients with coagulopathy. J Thromb Haemost. 2020;18:1094–9.
36. Barnes GD, Burnett A, Allen A, et al. Thromboembolism and anticoagulant therapy during the COVID-19 pandemic: interim clinical guidance from the anticoagulation forum. J Thromb Thrombolysis. 2020;50:72–81.
37. Moores LK, Tritschler T, Brosnahan S, et al. Prevention, diagnosis, and treatment of VTE in patients with coronavirus disease 2019: CHEST guideline and expert panel report. Chest 2020.
38. Lee AY, Levine MN, Baker RI, et al. Low-molecular-weight heparin versus a coumarin for the prevention of recurrent venous thromboembolism in patients with cancer. N Engl J Med. 2003;349:146–53.
39. Agnelli G, Becattini C, Meyer G, et al. Apixaban for the treatment of venous thromboembolism associated with cancer. N Engl J Med. 2020;382:1599–607.
40. Raskob GE, van Es N, Verhamme P, et al. Edoxaban for the treatment of cancer-associated venous thromboembolism. N Engl J Med. 2018;378:615–24.
41. Young AM, Marshall A, Thirlwall J, et al. Comparison of an oral factor Xa inhibitor with low molecular weight heparin in patients with cancer with venous thromboembolism: results of a randomized trial (SELECT-D). J Clin Oncol. 2018;36:2017–30.
42. Huang C, Wang Y, Li X, et al. Clinical features of patients infected with 2019 novel coronavirus in Wuhan, China. Lancet. 2020;395:497–506.
43. Qin C, Zhou L, Hu Z, et al. Dysregulation of immune response in patients with coronavirus 2019 (COVID-19) in Wuhan, China. Clin Infect Dis. 2020;71:762–8.

44. Xu Z, Shi L, Wang Y, et al. Pathological findings of COVID-19 associated with acute respiratory distress syndrome. Lancet Respir Med. 2020;8:420–2.
45. Mehta P, McAuley DF, Brown M, et al. COVID-19: consider cytokine storm syndromes and immunosuppression. Lancet. 2020;395:1033–4.
46. Soy M, Keser G, Atagunduz P, Tabak F, Atagunduz I, Kayhan S. Cytokine storm in COVID-19: pathogenesis and overview of anti-inflammatory agents used in treatment. Clin Rheumatol. 2020;39:2085–94.
47. Hu B, Huang S, Yin L. The cytokine storm and COVID-19. J Med Virol. 2020.
48. Brudno JN, Kochenderfer JN. Toxicities of chimeric antigen receptor T cells: recognition and management. Blood. 2016;127:3321–30.
49. Maude SL, Laetsch TW, Buechner J, et al. Tisagenlecleucel in children and young adults with B-cell lymphoblastic Leukemia. N Engl J Med. 2018;378:439–48.
50. Murthy H, Iqbal M, Chavez JC, Kharfan-Dabaja MA. Cytokine release syndrome: current perspectives. Immunotargets Ther. 2019;8:43–52.
51. Kochav SM, Coromilas E, Nalbandian A, et al. Cardiac arrhythmias in COVID-19 infection. Circulation: arrhythmia and electrophysiology. 2020;13.
52. Wang D, Hu B, Hu C, et al. Clinical characteristics of 138 hospitalized patients with 2019 novel coronavirus-infected Pneumonia in Wuhan, China. JAMA. 2020;323:1061.
53. Baldi E, Sechi GM, Mare C, et al. Out-of-hospital cardiac arrest during the Covid-19 outbreak in Italy. N Engl J Med. 2020;383:496–8.
54. Bhatla A, Mayer MM, Adusumalli S, et al. COVID-19 and cardiac arrhythmias. Heart Rhythm. 2020.
55. Rosenberg ES, Dufort EM, Udo T, et al. Association of treatment with hydroxychloroquine or azithromycin with in-hospital mortality in patients with COVID-19 in New York State. JAMA. 2020;323:2493.
56. Campia U, Moslehi JJ, Amiri-Kordestani L, et al. Cardio-oncology: vascular and metabolic perspectives: a scientific statement from the American heart association. Circulation. 2019;139:e579–602.
57. Campia U. Vascular effects of cancer treatments. Vasc Med. 2020;25:226–34.
58. Wang DY, Okoye GD, Neilan TG, Johnson DB, Moslehi JJ. Cardiovascular toxicities associated with cancer immunotherapies. Curr Cardiol Rep. 2017;19:21.
59. Daxini A, Cronin K, Sreih AG. Vasculitis associated with immune checkpoint inhibitors-a systematic review. Clin Rheumatol. 2018;37:2579–84.
60. Gambichler T, Strutzmann S, Tannapfel A, Susok L. Paraneoplastic acral vascular syndrome in a patient with metastatic melanoma under immune checkpoint blockade. BMC Cancer. 2017;17:327.
61. Laubli H, Hench J, Stanczak M, et al. Cerebral vasculitis mimicking intracranial metastatic progression of lung cancer during PD-1 blockade. J Immunother Cancer. 2017;5:46.
62. Pan F, Ye T, Sun P, et al. Time course of lung changes at chest CT during recovery from coronavirus disease 2019 (COVID-19). Radiology. 2020;295:715–21.
63. Konstantinides SV, Meyer G, Becattini C, et al. 2019 ESC Guidelines for the diagnosis and management of acute pulmonary embolism developed in collaboration with the European Respiratory Society (ERS): The Task Force for the diagnosis and management of acute pulmonary embolism of the European Society of Cardiology (ESC). Eur Heart J. 2019;41:543–603.
64. Argulian E, Sud K, Vogel B, et al. Right ventricular dilation in hospitalized patients with COVID-19 Infection. JACC Cardiovasc Imaging. 2020.
65. Huang L, Zhao P, Tang D, et al. Cardiac involvement in patients recovered from COVID-2019 identified using magnetic resonance imaging. JACC Cardiovasc Imaging. 2020.
66. Verdoni L, Mazza A, Gervasoni A, et al. An outbreak of severe Kawasaki-like disease at the Italian epicentre of the SARS-CoV-2 epidemic: an observational cohort study. The Lancet. 2020;395:1771–8.
67. Feldstein LR, Rose EB, Horwitz SM, et al. Multisystem inflammatory syndrome in U.S. children and adolescents. N Engl J Med. 2020;383:334–46.
68. Tepasse PR, Hafezi W, Lutz M, et al. Persisting SARS-CoV-2 viraemia after rituximab therapy: two cases with fatal outcome and a review of the literature. Br J Haematol. 2020;190:185–8.
69. Minotti C, Tirelli F, Barbieri E, Giaquinto C, Donà D. How is immunosuppressive status affecting children and adults in SARS-CoV-2 infection? A systematic review. J Infect. 2020;81:e61–6.

Acute Cardiac Care of Cancer Patients

32

Osnat Itzhaki Ben Zadok and Zaza Iakobishvili

Key Points

- With acute myocardial infarction, a concomitant cancer diagnosis is associated with a conservative medical management strategy and bears worse clinical outcomes compared to patients without cancer.
- Coronary syndromes in cancer patients are different from those in the general population, e.g., 5FU or post radiation.
- Pericardial tamponade may be the first presentation of previously unrecognized malignancies in about 7.5% of cases.
- Primary cardiac lymphoma accounts from 1 to 2% of all cardiac neoplasms and can present as acute right heart failure.

The majority of cardiovascular randomized controlled trials, which also serve the scientific basis for society guideline recommendations, exclude patients with cancer. Thus, even allegedly evidence-based management of a patient with an acute coronary syndrome or heart failure turns into a walk on unknown grounds when adding cancer to the equation. A recent cohort study of 6.5 million patients with a current or historical diagnosis of cancer found that a concomitant cancer diagnosis is associated with a conservative medical management strategy for acute myocardial infarction, and bears worse clinical outcomes, compared to patients without cancer [1].

Coronary syndromes in cancer patients are different from those in the general population. Taking a thorough history may prompt the early diagnosis of radiation-induced coronary artery disease. The management of acute coronary syndromes induced by chemotherapies such as 5FU is complicated by obstacles in diagnosis and treatment unique to those patients.

Heart failure in cancer patients may also manifest acutely and can include a wide spectrum of complications which include New-onset left/right ventricular dysfunction, acute pulmonary embolism, acute atrial/ventricular arrhythmias or large pericardial effusion, and tamponade. Management is often complicated by comorbidities, the need for further cancer treatments and drug-to-drug interactions.

Here, four cases of acute cardiac care of cancer patients are presented.

32.1 Case 1. Acute Myocardial Infarction in the Setting of Prior Thoracic Radiation

- Radiation therapy involving the heart is useful for the definitive treatment of localized tumors of the breast, lung, esophagus, and lymphomas, yet cardiac morbidity and mortality can counteract its beneficial effects.
- Modern techniques which include smaller fields, lower doses, breath-hold, IMRT, and protons have reduced cardiac exposure [2, 3].

A 42-year-old male patient, an active smoker, presented with an anterior ST-elevation myocardial infarction (MI) 23 years after receiving chemotherapy ("ABVD" treatment protocol: doxorubicin, bleomycin, vinblastine, and dacarbazine) and thoracic radiation (mantle radiation field) for childhood Hodgkin's lymphoma. Echocardiography on

Electronic supplementary material
The online version of this chapter (https://doi.org/10.1007/978-3-030-70998-3_32) contains supplementary material, which is available to authorized users.

O. Itzhaki Ben Zadok
Cardiology Department, Rabin Medical Center, 39 Jabotinsky Street, 49100 Petah Tikva, Israel
e-mail: osnat.itzhaki@gmail.com

Z. Iakobishvili (✉)
Department of Community Cardiology, Tel Aviv Jaffa District, Clalit Health Services, 15 Naomi Shemer St., 5840608 Holon, Israel
e-mail: zaza.iakobishvili@gmail.com

R. M. Steingart et al. (eds.), *Atlas of Imaging in Cardio-Oncology*, https://doi.org/10.1007/978-3-030-70998-3_32

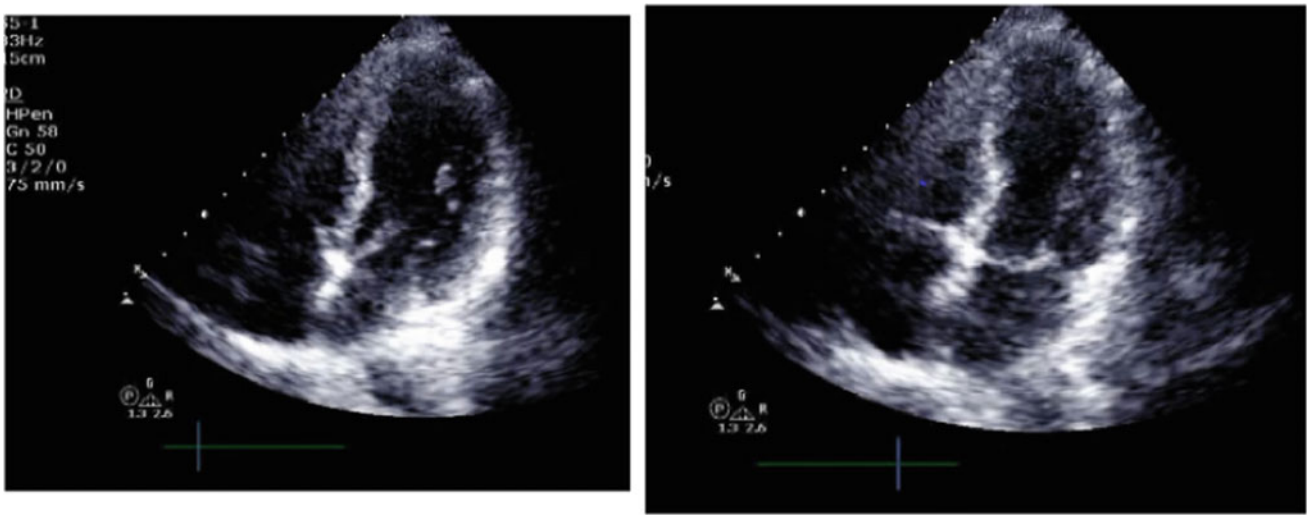

Fig. 32.1 Left and right panels showing diastolic and systolic images from echocardiogram at presentation. There is antero-apical hypokinesis and a moderately reduced left ventricular ejection fraction

presentation demonstrated antero-apical hypokinesis (Fig. 32.1, Video 32.1). Emergency angiography demonstrated occluded mid-distal left anterior descending artery and 95% stenotic lesion in the circumflex artery (Fig. 32.2, Video 32.2). Primary percutaneous intervention (PCI) was initially performed in the left anterior descending artery with a planned-staged procedure to the left circumflex artery (Fig. 32.3, Video 32.3). The patient was started on dual antiplatelet therapy with aspirin and prasugrel. The low-density lipoprotein cholesterol level on admission was 68 mg/dL. Extrapolating from the general coronary artery disease population, the patient was discharged on high-intensity statin therapy (atorvastatin 80 mg), bisoprolol 2.5 mg, and ramipril 2.5 mg OD. His left ventricular ejection fraction was assessed 8 weeks later on stress echocardiography as 40–45% at rest due to antero-apical akinesis. No ischemia was demonstrated on stress echocardiography and the planned revascularization of the marginal branch was canceled. Subsequently, due to complaints of lightheadedness and low blood pressure, ramipril and bisoprolol were stopped and he remains asymptomatic with excellent exercise capacity (13 METS on recent follow-up stress echocardiography). His LDL-C currently is in the range of 35–40 mg/dL (50% decrease according to STEMI guidelines) [4].

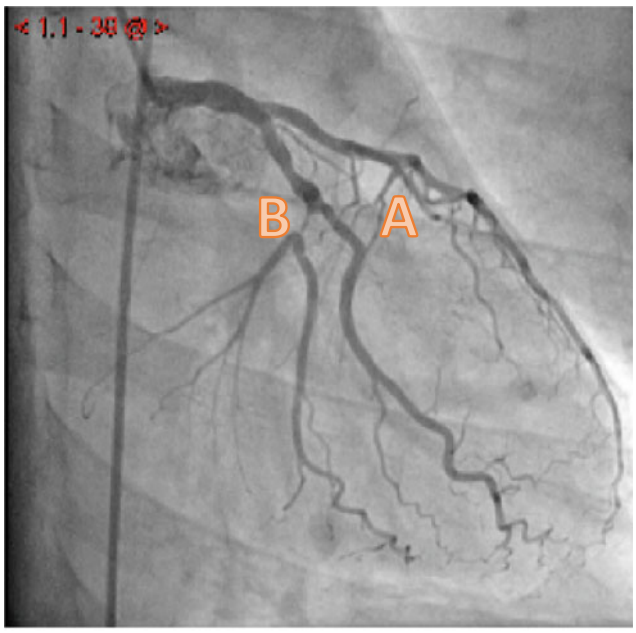

Fig. 32.2 Angiography, which was performed immediately on patient's presentation, showed occluded mid-distal LAD (**a**) and 95% stenotic lesion in the circumflex artery (**b**)

Clinical experience indicates that ST-elevation acute coronary syndromes late after radiation therapy can be effectively managed emergently with coronary stenting. However the published experience in this setting is limited. The efficacy of percutaneous coronary interventions for chronic presentations of radiation heart disease is somewhat better studied. The reader is referred to Chaps. 22 through 24 of this Atlas for a comprehensive look at the subject of radiation coronary disease.

32.2 Case 2. Cardiac Tamponade as the Initial Presentation of Lung Adenocarcinoma

- Pericardial tamponade may be the first presentation of previously unrecognized malignancies in about 7.5% of cases [5].

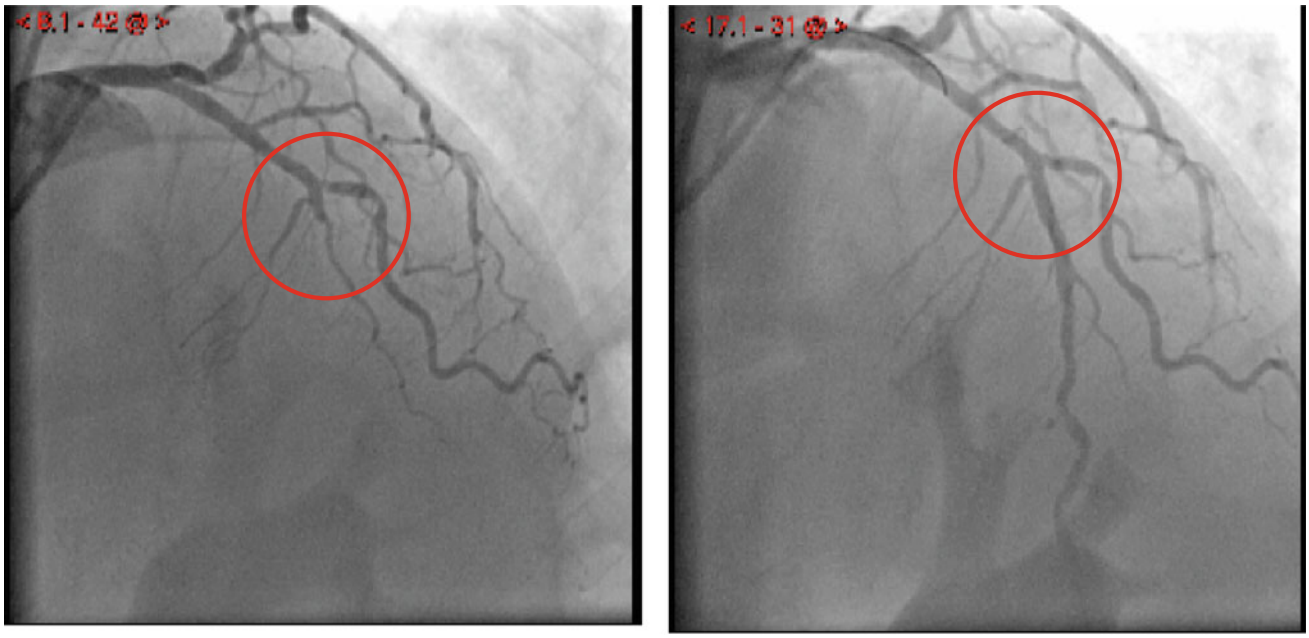

Fig. 32.3 The occluded LAD (left panel) was treated with primary percutaneous primary intervention (right panel) with restoration of flow

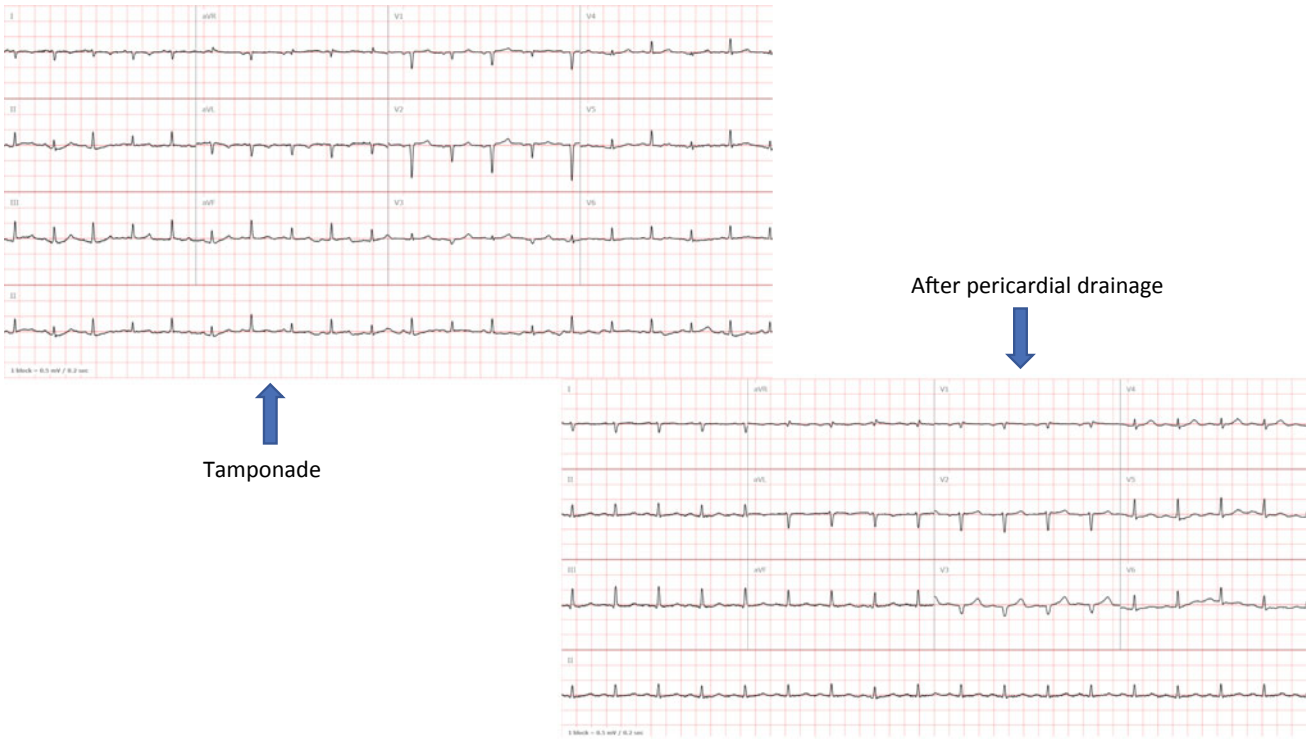

Fig. 32.4 Electrocardiogram on left performed on presentation demonstrating sinus tachycardia (110 beats/minute) and electrical alternans. Electrocardiogram on the right shows resolution of the alternans pattern after pericardial drainage

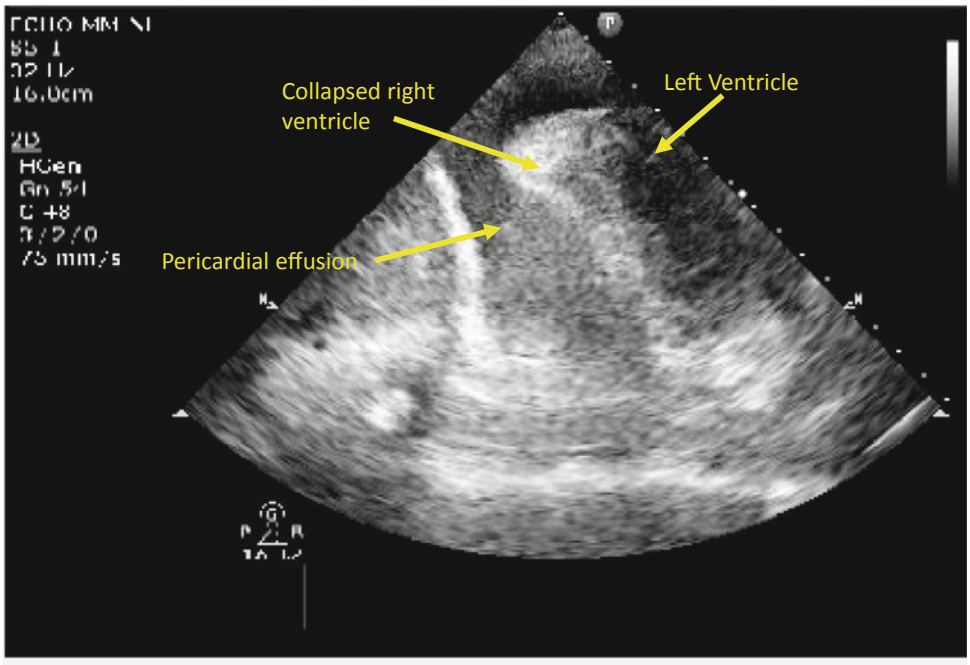

Fig. 32.5 Still frame from an echocardiogram showing large pericardial effusion, collapsed right ventricle, and small left ventricle consistent with tamponade

- During emergency pericardiocentesis it is imperative to send the fluid for cell block analysis to explore the genesis of the effusion [6].
- Despite the late stage of presentation (pericardial effusion in primary lung cancer is an indicator of stage IV disease) current oncology treatment (immunotherapy combined with chemotherapy) may significantly prolong overall survival and quality of life [7].

A 34-year-old woman with no known comorbidities presented to the emergency department with 10-day complaints of progressive dyspnea and orthopnea, as well as night sweats. Her physical examination revealed increased jugular venous pressure and her electrocardiogram (ECG) showed sinus tachycardia and electrical alternans (Fig. 32.4). Bedside echocardiography demonstrated large pericardial effusion with right ventricular collapse and a swinging heart (Fig. 32.5, Video 32.4). While awaiting pericardiocentesis which was scheduled to be performed shortly in the catheterization laboratory, the patient had hemodynamic collapse (systolic blood pressure was measured at 45 mmHg) necessitating immediate bedside sub-xiphoid pericardiocentesis. Blood pressure normalization and improved perfusion were noted after the initial drainage of 100 mL of pericardial fluid. A total of 250 mL fluid was drained over the following 24 hours. Two days later the patient underwent pericardial window surgery at which time pericardial and pleural biopsies were obtained. Pathologic evaluation demonstrated malignant cells of epithelial origin diagnosed as poorly differentiated lung adenocarcinoma. Notably, echocardiography soon after removal of the pericardial fluid demonstrated severe global left ventricular dysfunction which has been described after relief of cardiac tamponade (Video 32.5) [8]. Follow-up echocardiographic studies demonstrated improvement in LV systolic function (Video 32.5). The patient was treated with carboplatin-paclitaxel and pembrolizumab with excellent response. She now is maintained on pembrolizumab with good functional status and there has been no recurrence of the pericardial effusion during 2 years of follow-up. (*See* Chap. 21 on pericardial disease.)

32.3 Case 3. Acute Myocardial Infarction Presenting Concomitantly with Fluoropyrimidine-Based Chemotherapy

- Fluoropyrimidine-based chemotherapy is a possible trigger for coronary vasospasm and therefore for the development of type 2 myocardial infarction [9, 10].
- Little is known about re-challenge in patients who have had an acute coronary syndrome or have established coronary artery disease, although several protocols (mostly based on calcium-channel blockers and nitrates) have been proposed [11].
- In high-risk patients with suspected acute coronary syndrome and reasonable oncologic prognosis, urgent coronary angiography with possible coronary revascularization should be considered in a shared decision-making model (cardiology, oncology, patient) [12].

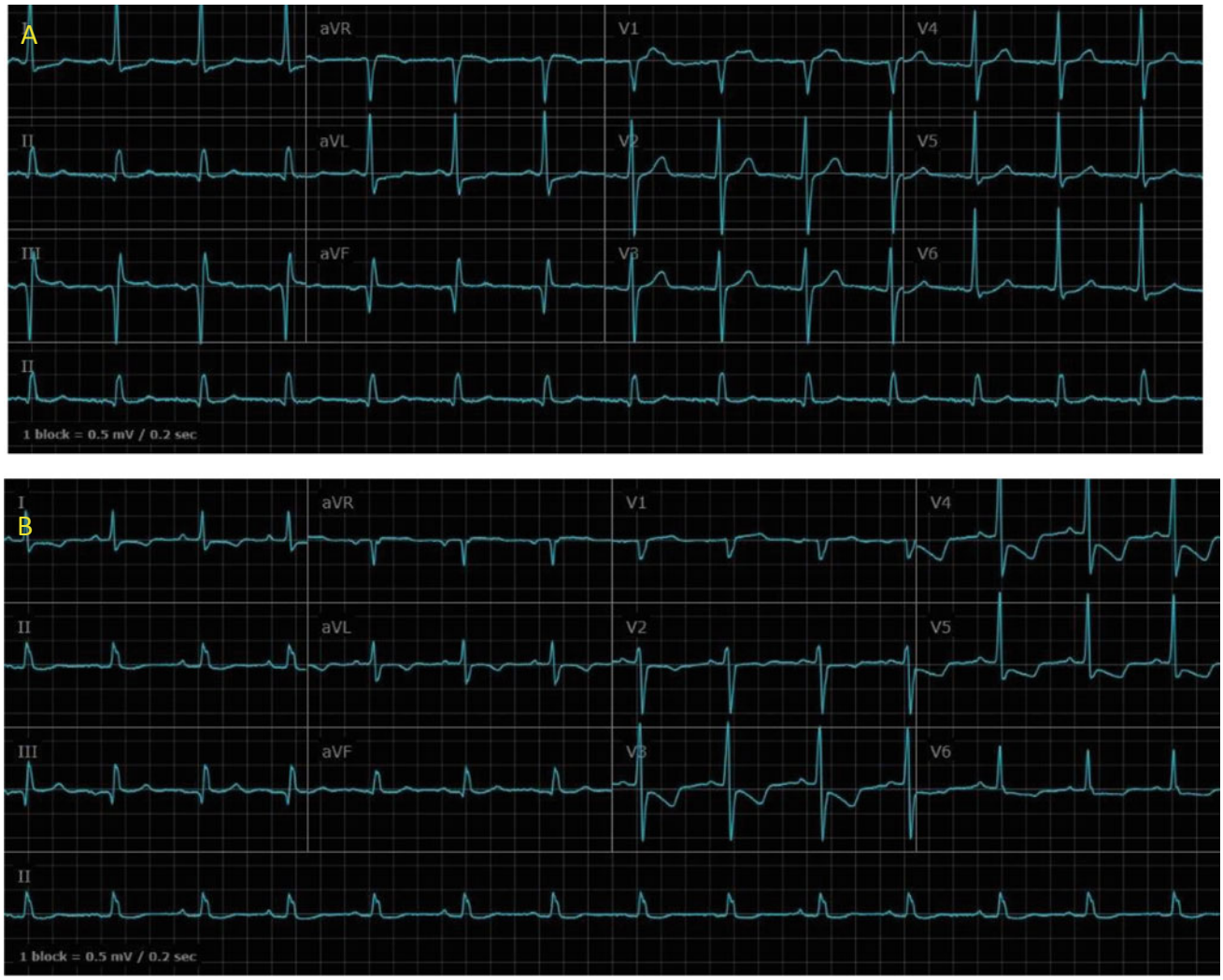

Fig. 32.6 **a** pre-chemotherapy electrocardiogram demonstrating slight ST-segment depression in lead I and AVL, with prominent Q-waves in diaphragmatic leads. **b** Electrocardiogram during chest pain presentation demonstrating lateral T-wave inversion (leads I, AVL, V4-6) and downsloping ST-segment depression (leads V3-6). Note that Q-wave is preserved only in lead III

A 66-year-old man who previously had a mechanical mitral valve replacement and known ischemic heart disease having undergone PCI to the right coronary artery (RCA) 10 years before his current presentation. The patient was recently diagnosed with rectal adenocarcinoma and neoadjuvant therapy with capecitabine (Xeloda) combined with focal radiation was initiated. During this therapy, he reported typical chest pain. Electrocardiogram demonstrated T-wave inversions in leads I and aVL, new from baseline (Fig. 32.6). Troponin-T was abnormally elevated (2,500 on 2 consecutive tests, normal laboratory range 0–14 ng/L) and echocardiography showed moderate to severe LV dysfunction (Fig. 32.7, Video 32.6). Severe three-vessel coronary artery disease was apparent on angiography with occluded proximal left anterior descending artery with tiny collaterals from the right system, tight stenosis of the large diagonal branch, and intermediate artery (Fig. 32.8). Provocative vasospastic tests were not performed. A presumptive diagnosis of vasospasm on the background of severe coronary disease was made resulting in type 2 myocardial infarction. After a thorough multidisciplinary discussion, the decision was made to revascularize the diagonal and intermediate arteries, as possible culprits and not to re-challenge the patient with fluoropyrimidine. The interventional coronary artery procedures were successful and the patient continues to be stable from a cardiac standpoint following the procedure. He was initiated on dual antithrombotic therapy (warfarin and clopidogrel) during this year without overt bleeding episodes. With

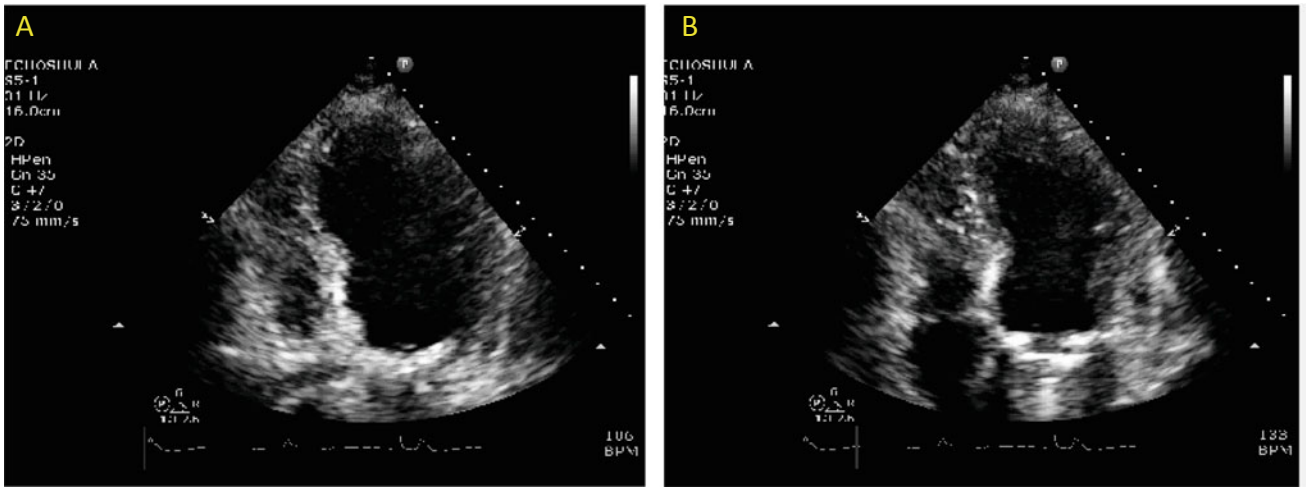

Fig. 32.7 Still frames from echocardiogram performed at presentation. **a** Diastolic image, **b** Systolic image. There is a large regional wall motion abnormality with depression of the ejection fraction

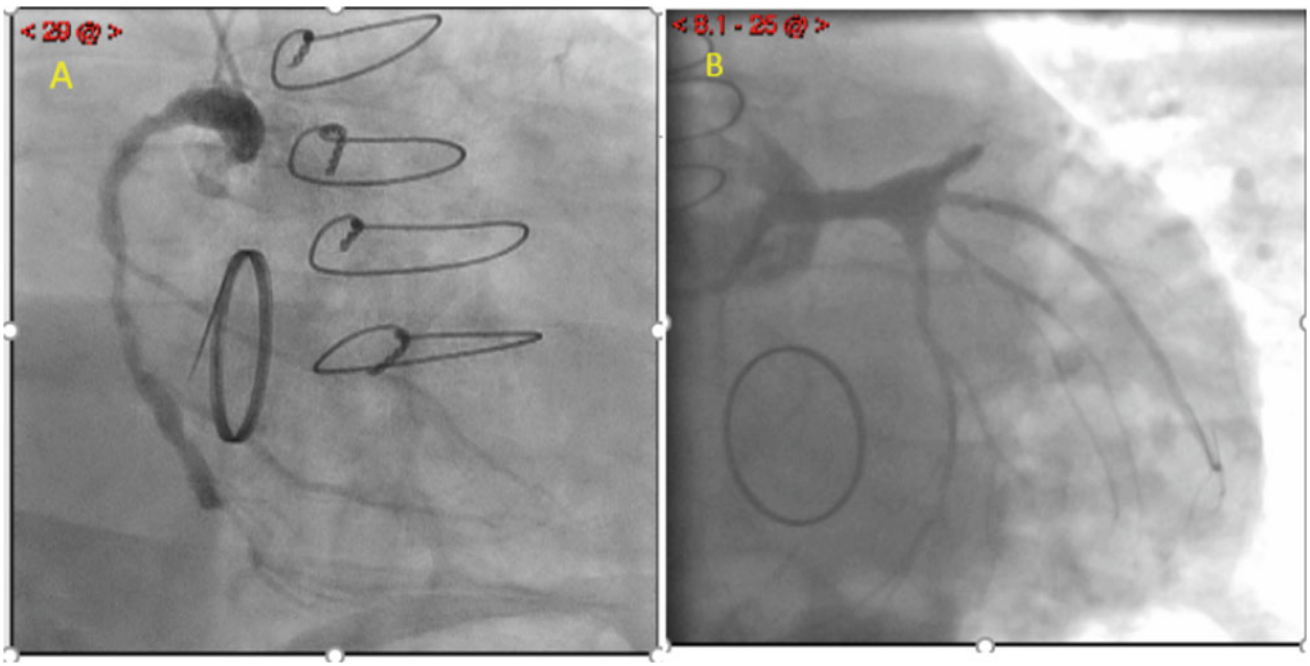

Fig. 32.8 **a** Right coronary artery injection demonstrating severe diffuse disease in the mid to distal vessel. **b** Left coronary artery injection with diffusely diseased intermediate branch and first diagonal artery. A non-dominant circumflex artery and proximal-mid LAD were occluded

the stability of his coronary artery disease, an alternate therapeutic approach to his cancer was discussed with the oncology team and the patient was advised to have potentially curative colorectal surgery, however, he refused. He is currently receiving warfarin, statins, and maximally tolerated guideline directed medical therapy for left ventricular dysfunction including sacubitril valsartan, bisoprolol, and spironolactone. His cancer remains under scrutiny by the oncology team. (*See* Chap. 11 on 5FU and its analogs).

32.4 Case 4. Right Ventricular Mass Presenting as Acute Right Heart Failure

- Cardiac neoplasms can be categorized according to their histological characteristics (benign or malignant) and their site of origin (primary or metastatic) [13].
- Primary cardiac lymphoma accounts from 1 to 2% of all cardiac neoplasms and is characterized by its ability to

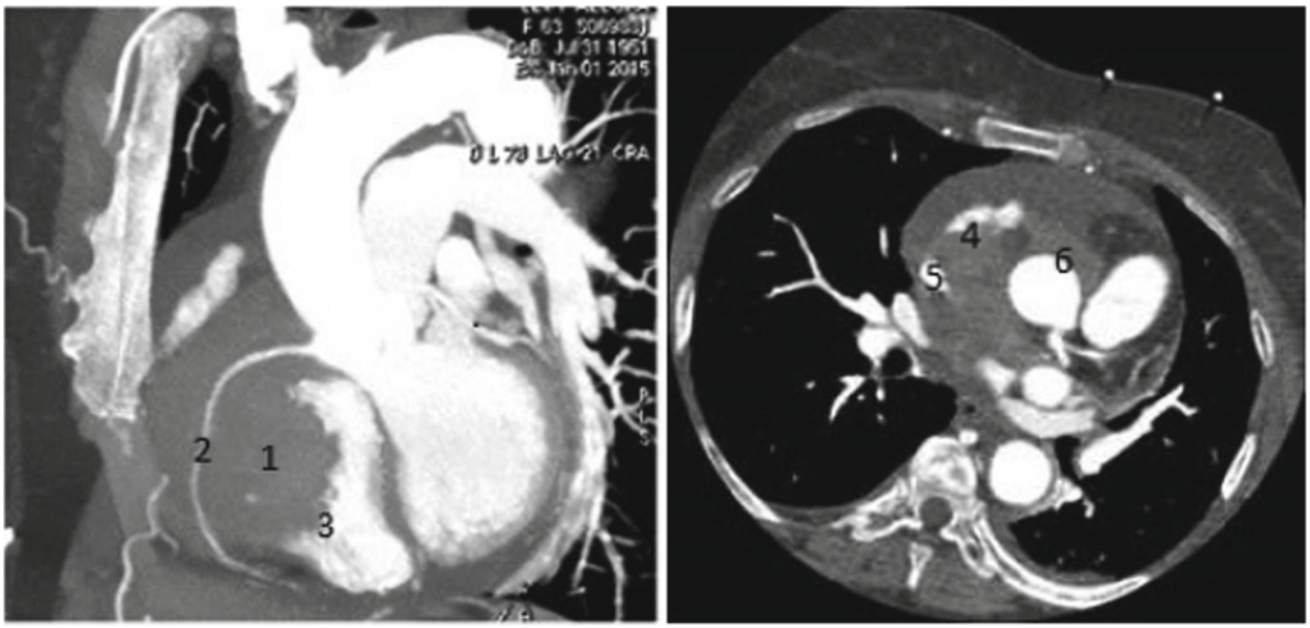

Fig. 32.9 Left and right panels, Cardiac computed tomography performed during patient's initial presentation demonstrating a homogenous mass involving the right ventricle. The mass dimensions were measured 85 mm * 53 mm * 90 mm. The mass is anterior to the atrioventricular groove encasing the right coronary artery but not narrowing it ("vessel-floating sign"). 1. Homogenous mass involving the right ventricle. 2. Encasing the right coronary artery but not narrowing it ("vessel-floating sign"). 3. Invades the right ventricle. 4. Invades the right atrium. 5. Involves the superior vena cava. 6. Involves ascending aorta and root

cross anatomic boundaries. Clinically, cardiovascular related symptoms develop either due to direct tumor extension or to tumor emboli [14].

A 63-year-old female patient, a former smoker, was admitted due to 2 weeks of progressive exertional dyspnea and cough. Chest CT demonstrated a mass in the right ventricle which extended to the right atrium and superior vena cava. Aortic root involvement was observed as well, yet with no extra-cardiac involvement (Fig. 32.9). The differential diagnosis of the right ventricular mass was cardiac sarcoma versus primary cardiac lymphoma. The latter was supported by the appearance of the "vessel-floating sign". This sign, which is highly specific to cardiac involvement in lymphoma, describes a mass which encases, rather than invading and narrowing the coronary arteries [15]. Moreover, the mass was characterized as homogenous which is also compatible with cardiac lymphomas. Echocardiography revealed a right ventricular mass interfering with tricuspid valve function (Fig. 32.10; Videos 32.7 and 32.8).

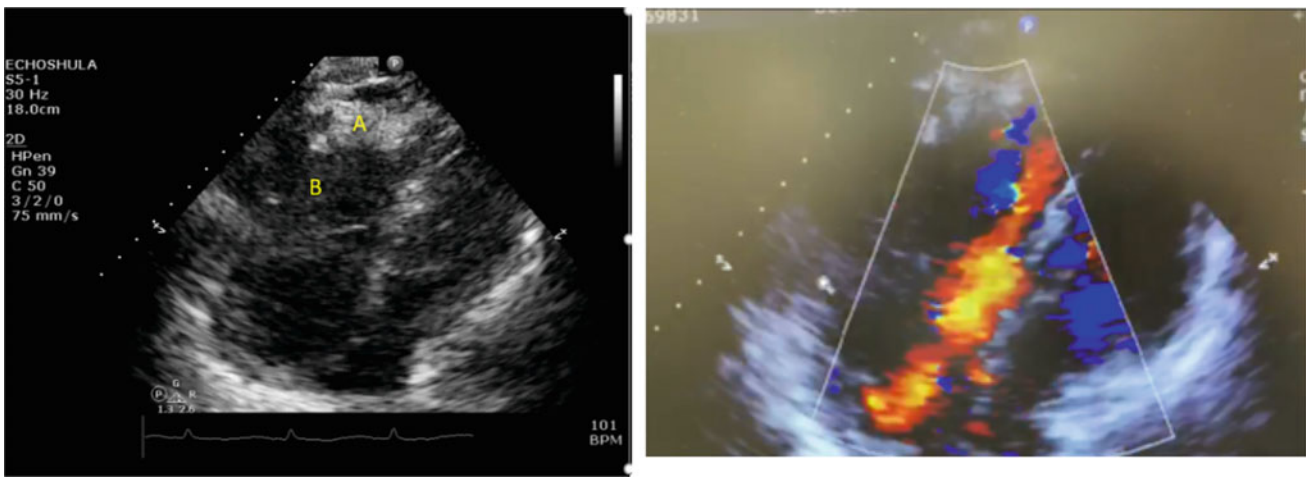

Fig. 32.10 Left panel, Echocardiogram frame showing a mass on the anterior aspect of the right ventricle (**a**) and the lateral aspect of the tricuspid valve ring (**b**). Right panel, The mass adversely affects the diastolic flow through the tricuspid valve illustrated by color doppler imaging

A biopsy by a mid-sternotomy incision was performed demonstrated non-Hodgkin's cardiac lymphoma. Chemotherapy based on R-CHOP protocol (rituximab-cyclophosphamide, hydroxydaunorubicin, vincristine, and prednisone) was initiated and was uneventful. During a one-year follow-up on echocardiography, no recurrence of intracardiac mass was observed. (*See* Chap. 16 on masses involving the heart and vasculature.)

References

1. Bharadwaj A, Potts J, Mohamed MO, Parwani P, Swamy P, Lopez-Mattei JC, et al. Acute myocardial infarction treatments and outcomes in 6.5 million patients with a current or historical diagnosis of cancer in the USA. Eur Heart J. 2020;41(23):2183–93.
2. Desai MY, Jellis CL, Kotecha R, Johnston DR, Griffin BP. Radiation-associated cardiac disease: a practical approach to diagnosis and management [Internet], vol. 11. JACC: Cardiovascular Imaging. Elsevier Inc.; 2018 [cited 2020 Sep 12], p. 1132–49. https://pubmed-ncbi-nlm-nih-gov.beilinson-ez.medlcp.tau.ac.il/30092970/.
3. Wennstig AK, Wadsten C, Garmo H, Fredriksson I, Blomqvist C, Holmberg L, et al. Long-term risk of ischemic heart disease after adjuvant radiotherapy in breast cancer: results from a large population-based cohort. Breast Cancer Res. 2020;22(1):1–9.
4. Ibanez B, James S, Agewall S, Antunes MJ, Bucciarelli-Ducci C, Bueno H, et al. 2017 ESC Guidelines for the management of acute myocardial infarction in patients presenting with ST-segment elevation. Eur Heart J. 2018;39(2):119–77.
5. Ben-Horin S, Bank I, Guetta V, Livneh A. Large symptomatic pericardial effusion as the presentation of unrecognized cancer: a study in 173 consecutive patients undergoing pericardiocentesis. Medicine (Baltimore). 2006;85(1):49–53.
6. Perek M, Tomaszewska I, Stefaniak S, Katynska IJM. Cardiac tamponade—unusual clinical manifestation of undiagnosed malignant neoplasm. Neoplasma. 2013;63(4):601–6.
7. Yang K, Li J, Bai C, Sun Z, Zhao L. Efficacy of immune checkpoint inhibitors in non-small-cell lung cancer patients with different metastatic sites: a systematic review and meta-analysis. Front Oncol. 2020.
8. Prabhakar Y, Goyal A, Khalid N, et al. Pericardial decompression syndrome: a comprehensive review. World J Cardiol. 2019;11:282–91.
9. Polk A, Shahmarvand N, Vistisen K, Vaage-Nilsen M, Larsen FO, Schou M, et al. Incidence and risk factors for capecitabine-induced symptomatic cardiotoxicity: a retrospective study of 452 consecutive patients with metastatic breast cancer. BMJ Open. 2016;6(10).
10. Peng J, Dong C, Wang C, Li W, Yu H, Zhang M, et al. Cardiotoxicity of 5-fluorouracil and capecitabine in Chinese patients: a prospective study. Cancer Commun (London, England) [Internet]. 2018;38(1):22. https://doi.org/10.1186/s40880-018-0292-1.
11. Clasen SC, Ky B, O'Quinn R, Giantonio B, Teitelbaum U, Carver JR. Fluoropyrimidine-induced cardiac toxicity: challenging the current paradigm. J Gastrointest Oncol. 2017;8(6):970–9.
12. Layoun ME, Wickramasinghe CD, Peralta MV, Yang EH. Fluoropyrimidine-induced cardiotoxicity: manifestations, mechanisms, and management. Curr Oncol Rep. 2016;18(6).
13. Poterucha TJ, Kochav J, O'Connor DS, Rosner GF. Cardiac tumors: clinical presentation, diagnosis, and management. Curr Treat Options Oncol. 2019;20(8):1–15.
14. Maleszewski JJ, Bois MC, Bois JP, Young PM, Stulak JM, Klarich KW. Neoplasia and the heart: pathological review of effects with clinical and radiological correlation. J Am Coll Cardiol [Internet]. 2018;72(2):202–27. https://doi.org/10.1016/j.jacc.2018.05.026.
15. Yoshihara S, Sugimoto Y, Matsunaga M, Suzuki S, Tanioka F. Coronary vessel floating sign in cardiac diffuse large B-cell lymphoma. Eur Heart J Cardiovasc Imag. 2020;21(2):233.

Index

R. M. Steingart et al. (eds.), *Atlas of Imaging in Cardio-Oncology*,
https://doi.org/10.1007/978-3-030-70998-3